SAFIR2014
The Finnish Research Programme on Nuclear Power Plant Safety 2011–2014

Interim Report

VTT

SAFIR2014

The Finnish Research Programme on Nuclear Power Plant Safety 2011–2014

Interim Report

Kaisa Simola (ed.)

SAFIR2014
The Finnish Research Programme on Nuclear Power Plant Safety 2011–2014
Interim Report

Abstract

The Finnish Nuclear Power Plant Safety Research Programme 2011–2014, SAFIR2014, is a 4-year publicly funded national technical and scientific research programme on the safety of nuclear power plants. The programme is funded by the State Nuclear Waste Management Fund (VYR), as well as other key organisations operating in the area of nuclear energy. The programme provides the necessary conditions for retaining knowledge needed for ensuring the continuance of safe use of nuclear power, for developing new know-how and for participation in international co-operation.

The SAFIR2014 Steering Group, responsible of the strategic alignements of the programme, consists of representatives of the Finnish Nuclear Safety Authority (STUK), Ministry of Employment and the Economy (MEE), Technical Research Centre of Finland (VTT), Teollisuuden Voima Oyj (TVO), Fortum Power and Heat Oy (Fortum), Fennovoima Oy, Lappeenranta University of Technology (LUT), Aalto University (Aalto), Finnish Funding Agency for Technology and Innovation (Tekes), Finnish Institute of Occupational Health (TTL) and the Swedish Radiation Safety Authority (SSM).

The research programme is divided into nine areas: Man, organisation and society, Automation and control room, Fuel research and reactor analysis, Thermal hydraulics, Severe accidents, Structural safety of reactor circuits, Construction safety, Probabilistic risk analysis (PRA), and Development of research infrastructure. A reference group is assigned to each of these areas to respond for the strategic planning and to supervise the projects in its respective field.

Research projects are selected annually based on a public call for proposals. Most of the projects are planned for the entire duration of the programme, but there can also be shorter one- or two-year projects. The annual volume of the SAFIR2014 programme in 2011–2012 has been 9,5–9,9 M€ Main funding organisations were the State Nuclear Waste Management Fund (VYR) with over 5 M€ and VTT with nearly 3 M€ annually. In 2011 research was carried out in 38 projects, and in 2012 the number of research projects was 42.

The research in SAFIR2014 has been carried out primarily by VTT. Other research organisations involved in research activities are Lappeenranta University of Technology, Aalto University, Finnish Institute of Occupational Health, Finnish Meteorological Institute, Finnish Software Measurement Association FiSMA, Fortum Power and Heat Oy, and Helsinki University. In addition, some subcontractors have contributed to the work in some projects.

This report gives an overview of the SAFIR2014 programme and a summary of the scientific and technical results of the research activities in 2011–2012.

Preface

The Finnish Nuclear Power Plant Safety Research Programme 2011–2014, SAFIR2014, is continuation to a series of government-led national NPP safety research programmes. Since 1989, the public nuclear safety research has been organised as national research programmes. First, the programmes were carried out separately in the fields of operational safety and structural safety, but since 1999 they were combined in a single programme. The annual volume of the research programme has grown from 3,6 in FINNUS programme (1999–2002) to nearly 10 M€ in SAFIR2014.

In accordance with the Finnish Nuclear Energy Act, the objective of the programme is to develop and maintain experimental research capability, safety assessment methods and nuclear safety expertise of Finnish nuclear power plants. More than half of the research programme funding is secured by a separate reserve of the State Waste Management Fund (VYR) which consists of annual fees collected from Finnish nuclear facility operators. The second major funding organisation is VTT with a share of nearly 30% of the programme volume.

The SAFIR2014 programme is divided into nine areas: Man, organisation and society, Automation and control room, Fuel research and reactor analysis, Thermal hydraulics, Severe accidents, Structural safety of reactor circuits, Construction safety, Probabilistic risk analysis (PRA), and Development of research infrastructure. Each of these areas comprise 2–8 research projects, and the total volume of research work in 2011–2012 was about 140 person years. Detailed research results are published in scientific journals, conference papers and research reports.

The programme management structure consists of the Steering Group, a Reference Group in each of the nine research areas, a number of ad hoc groups in various fields, and programme administration. The SAFIR2014 Steering Group consists of representatives of the Finnish Nuclear Safety Authority (STUK), Ministry of Employment and the Economy (MEE), Technical Research Centre of Finland (VTT), Teollisuuden Voima Oyj (TVO), Fortum Power and Heat Oy (Fortum), Fennovoima Oy, Lappeenranta University of Technology (LUT), Aalto University (Aalto), Finnish Funding Agency for Technology and Innovation (Tekes), Finnish Institute of Occupational Health (TTL) and the Swedish Radiation Safety Authority (SSM).

This report has been prepared by the programme management in cooperation with the project leaders and project staff.

More information on SAFIR2014 can be found on the programme website http://safir2014.vtt.fi/.

Contents

1. Introduction

Kaisa Simola

VTT Technical Research Centre of Finland
Tekniikantie 2, P.O. Box 1000, FI-02044 Espoo

Role of SAFIR2014 in Finnish nuclear safety research

The Finnish Nuclear Power Plant Safety Research Programme 2011–2014, SAFIR2014, is a 4-year publicly funded national technical and scientific research programme on the safety of nuclear power plants. The mission of the research programme is derived from the stipulations of the Finnish Nuclear Energy Act concerning ensuring and availability of expertise in nuclear safety. The objective of the SAFIR2014 is to develop and maintain experimental research capability, as well as the safety assessment methods and nuclear safety expertise of Finnish nuclear power plants, in order that, should new matters related to nuclear safety arise, their significance can be assessed without delay.

SAFIR2014 is continuation to a series of government-led national NPP safety research programmes. The programme is funded by the State Nuclear Waste Management Fund (VYR), as well as other key organisations operating in the area of nuclear energy. The annual funding of the SAFIR2014 programme is nearly 10 M€. Compared to the previous programme periods, the funding has significantly increased due to the Government decisions-in-principle confirmed by Parliament in 2010, since the VYR-funding is proportional to the nuclear power capacity, including planned capacity.

The planning period 2011–2014 for SAFIR2014 involves licensing processes for power plants that are in use and under construction, as well as overall safety evaluations related to licence terms. The construction works of the Olkiluoto 3 plant unit are proceeding, and the bidding and plant supplier selection phases of the Olkiluoto 4 and of the Hanhikivi 1 plant units are under way. These processes are reflected in many ways on national safety research. The Fukushima accident is also reflected in research activities.

The construction of new power plants in Finland increases the need of experts in the field, while the retirement of experts who took part in construction and operation of the existing plants is continuing. This calls for continuous education and

training, where research activities play an important role. The research programme serves as an important environment providing such long-term activity. Projects aim both at high-quality applied research and developing and maintaining basic know-how.

International co-operation is an essential part of the SAFIR2014 programme. Participation in OECD/NEA experimental and database projects is one of the key international activities. Further, international contacts include Nordic co-operation within Nordic Nuclear Safety research (NKS) and Nordic Thermal-Hydraulic Network (Northnet), and participation in other international experimental research programmes and various IAEA working groups. At European level, it is topical to establish modes of co-operation and joint programming in in the area of GenII and GenIII light water reactor safety, with the support of the next EU Framework Programme for Research and Innovation, Horizon 2020.

Besides research activities, the SAFIR2014 programme supports the development of research infrastructure in Finland. The existing experimental nuclear technology facilities and equipment, especially hot cell research capabilities, require renovation. Further, the thermal hydraulics experimentation facility needs updated instrumentation for producing measurement results suitable for validation of computational methods.

Figure 1. Organisations represented in the SAFIR2014 Steering Group.

The SAFIR2014 Steering Group consists of representatives of the Finnish Nuclear Safety Authority (STUK), Ministry of Employment and the Economy (MEE), Tech-

nical Research Centre of Finland (VTT), Teollisuuden Voima Oyj (TVO), Fortum Power and Heat Oy (Fortum), Fennovoima Oy, Lappeenranta University of Technology (LUT), Aalto University (Aalto), Finnish Funding Agency for Technology and Innovation (Tekes), Finnish Institute of Occupational Health (TTL) and the Swedish Radiation Safety Authority (SSM).

Research areas and projects

The areas of research and the research needs are described in the Framework Plan [1]. As these research needs are based on the knowledge at the time of making the framework plan, additional topics supporting the objectives of the research programme are included when needed by decisions of the Steering Group.

The SAFIR2014 research programme is divided into nine areas:

1. Man, Organisation and Society
2. Automation and Control Room
3. Fuel Research and Reactor Analysis
4. Thermal Hydraulics
5. Severe Accidents
6. Structural Safety of Reactor Circuits
7. Construction Safety
8. Probabilistic Risk Analysis (PRA)
9. Development of Research Infrastructure.

In 2011 research was carried out in 38 projects, and in 2012 the number of research projects was 42. In 2012 VTT was the responsible organisation of 35 research projects and the programme administration. Lappeenranta University of Technology was responsible of four projects, Aalto University of two projects and the Finnish Meteorological institute of one project. Seven projects were joint projects of two or more research organisations. Table 1 lists the projects in 2011–2012 with their participating organisations and volume.

Table 1. Projects in 2011–2012.

Project	Acronym	Participating organisations	Funding (k€) 2011–2012	Volume in person months
1 Man, Organisation and Society				
Managing safety culture through-out the lifecycle of nuclear plants	MANSCU	VTT	692	49
Sustainable and future oriented expertise	SAFEX2014	Aalto, TTL	206	22
2 Automation and Control Room				
Coverage and rationality of the software I&C safety assurance	CORSICA	VTT, FiSMA Ry	360	33
Human-automation collaboration in incident and accident situations	HACAS	VTT	451	32
Safety evaluation and reliability analysis of nuclear automation	SARANA	VTT, Aalto	799	68
Safety requirements specification and management in nuclear power plants	SAREMAN	VTT, Aalto	351	30
3 Fuel Research and Reactor Analysis				
Criticality safety and transport methods in reactor analysis	CRISTAL	VTT	522	40
Three-dimensional reactor anal-yses	KOURA	VTT	677	51
Development of Finnish Monte Carlo reactor physics code	KÄÄRME	VTT	413	31
Neutronics, nuclear fuel and burnup	NEPAL	Aalto	256	41
Extensive fuel modelling	PALAMA	VTT	745	59
*Radionuclide source term analysis	RASTA	VTT	61	6
4 Thermal Hydraulics				
Enhancement of safety evalua-tion tools	ESA	VTT	924	68
Experimental studies on con-tainment phenomena	EXCOP	LUT	545	45
OpenFOAM CFD-solver for nuclear safety related flow simu-lations	NUFOAM	VTT, LUT, Aalto, Fortum	351	42
Numerical modelling of conden-sation pool	NUMPOOL	VTT	236	18
Improvement of PACTEL facility simulation environment	PACSIM	LUT	97	8
PWR PACTEL experiments	PAX	LUT	661	58

Modelling of pressure transients in steam generators	SGEN	VTT	167	13
Uncertainty evaluation for best estimate analyses (In 2012: Application of best estimate plus uncertainty evaluation method)	UBEA (BEPUE)	VTT	195	19
5 Severe Accidents				
Core debris coolability and environmental consequence analysis	COOLOCE-E	VTT	363	28
Chemistry of fission products	FISKE	VTT	320	27
Thermal hydraulics of severe accidents	TERMOSAN	VTT	407	29
Transport and chemistry of fission products	TRAFI	VTT	688	66
* Reactor vessel failures, vapour explosions and spent fuel pool accidents	VESPA	VTT	145	14
6 Structural Safety of Reactor Circuits				
Environmental influence on cracking susceptibility and ageing of nuclear materials	ENVIS	VTT	1310	111
Fracture assessment of reactor circuit	FAR	VTT	505	34
Monitoring of the structural integrity of materials and compo-nents in reactor circuit	MAKOMON	VTT	431	29
RI-ISI analyses and inspection reliability of piping systems	RAIPSYS	VTT	307	21
Advanced surveillance technique and embrittlement modelling	SURVIVE	VTT	283	16
Water chemistry and plant oper-ating reliability	WAPA	VTT	336	28
* Fatigue affected by residual stresses, environment and thermal fluctuations	FRESH	VTT	155	11
7 Construction Safety				
Impact 2014	IMPACT2014	VTT	1008	60
Aging management of concrete structures in nuclear power plants	MANAGE	VTT, Aalto	403	21
Structural mechanics analyses of soft and hard impacts	SMASH	VTT	476	35
Seismic safety of nuclear power plants. Targets for research and education	SESA	VTT, Aalto, Univ. Helsinki	251	16

8 Probabilistic Risk Analysis (PRA)				
Extreme weather and nuclear power plants	EXWE	FMI	357	38
Risk assessment of large fire loads	LARGO	VTT	407	26
PRA development and application	PRADA	VTT, Aalto	455	39
* FinPSA knowledge transfer	FINPSA-TRANSFER	VTT	187	16
9 Development of Research Infrastructure				
Enhancement of Lappeenranta instrumentation of nuclear safety experiments	ELAINE	LUT	716	30
Renewal of hot cell infrastructure	REHOT	VTT	749	35
Administration				
Programme administration	ADMIRE	VTT	419	19
TOTAL			19384	1483

*) Projects started in 2012

Statistical information

In 2011 the volume of the SAFIR2014 programme was 9,5 M€ and 70 person-years. In 2012 the corresponding figures were 9,9 M€ and 70 person-years. The main funding organisations are the State Waste Management Fund (VYR) with a share of 55%, and VTT with a share of 29% of the total funding. Figure 2 shows the main funding sources in 2011–2012. The cost structure in 2011 is shown in Figure 3. By writing this, the cost structure breakdown was not available for 2012, but it is expected to be similar to 2011.
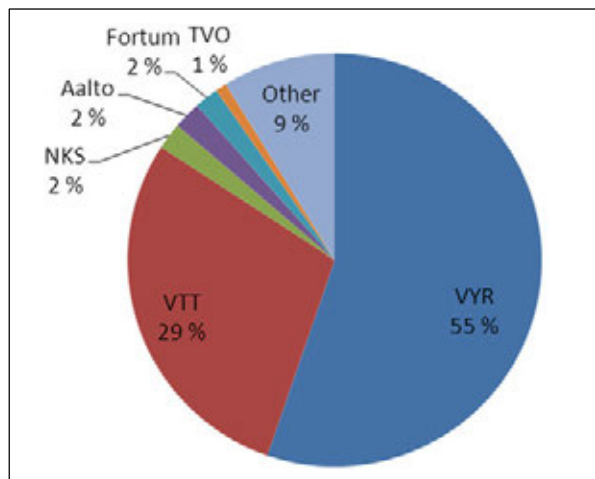
Figure 2. Main funding sources in SAFIR2014 in 2011–2012.
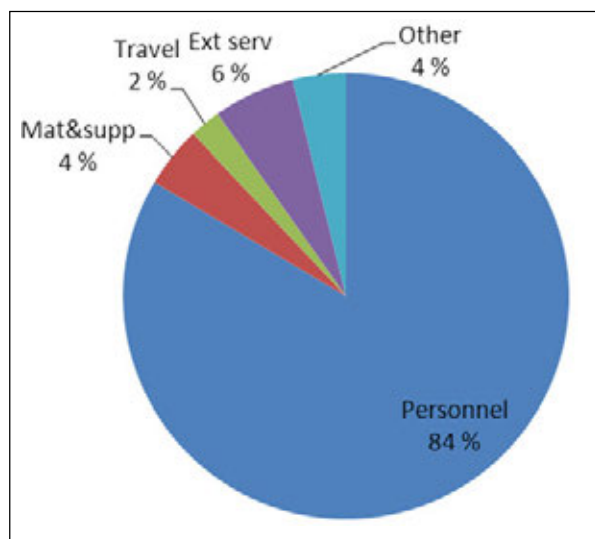
Figure 3. Cost structure in SAFIR2014 in 2011.

Figure 4 illustrates the VYR- and other funding by research areas in years 2011 and 2012. The distributions of total funding and person years in 2011–2012 by research area are presented in Figure 5.
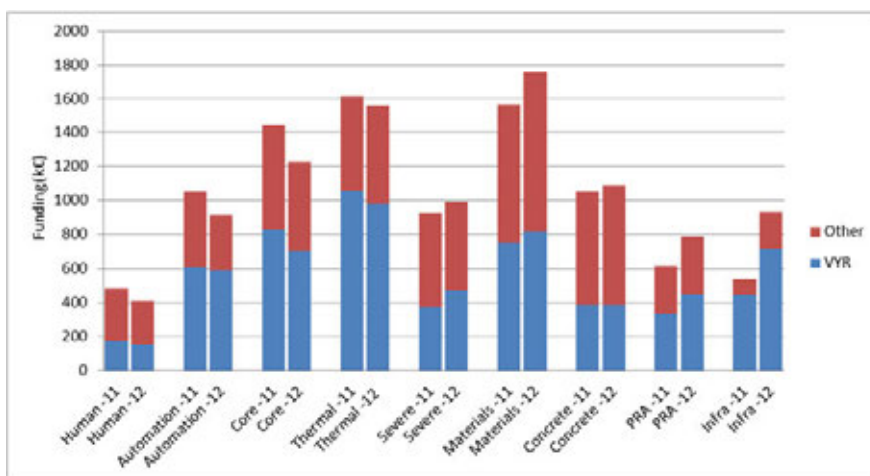
Figure 4. Distribution of funding in SAFIR2014 research areas in 2011 and 2012.
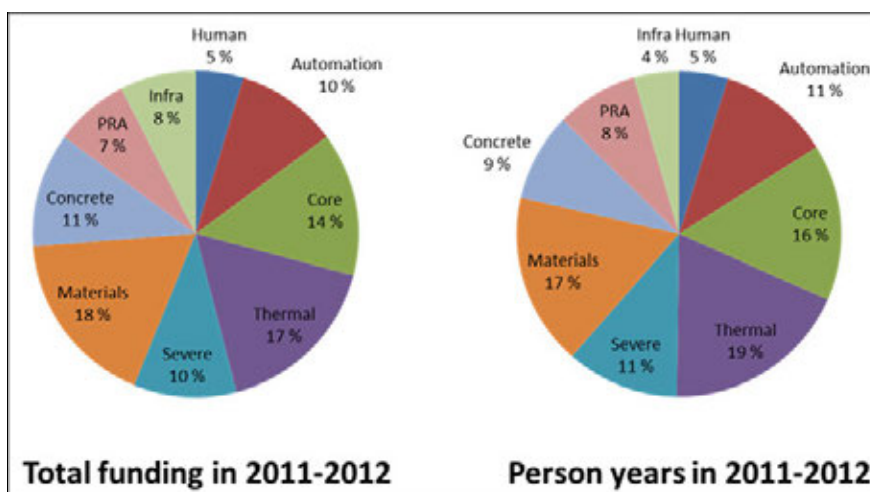
Figure 5. SAFIR2014 funding and person-years by research areas in 2011–2012.

In 2011, the research projects produced altogether 244 publications, and seven academic degrees were completed in the projects. More information can be found in the SAFIR2014 Annual Report 2011 [2]. Detailed statistical information on project year 2012 will be available in the SAFIR2014 Annual Report 2012.

Programme management

The SAFIR2014 programme is managed at three levels. At the highest level, the Steering Group is responsible of the strategic alignements of the programme. At the second level, Reference groups are responsible of the strategic planning and follow-up the progress of projects in their respective fields. Each research area has a Reference Group consisting of experts representing the nuclear utilities, the safety authority, and main research organisations. At the third level the projects are executed in the research organisations. Ad hoc groups can be formed to provide additional guidance and support for e.g. cross-disciplinary projects, or to stimulate communication between several projects and reference groups.

The director of the programme and the administrative organisation, VTT, is responsible of the administration of the programme. The administrative duties include the execution of Steering Group's decisions, follow up of projects, preparation of the annual plans (see e.g. [3, 4]) and reports at programme level, and organising the interim and final seminars. Further, the administrative organisation coordinates the annual call for proposals and the proposal evaluation process.

The Steering Group and the Reference Groups meet on a regular basis 4–5 times per year. The progress of projects is reported quarterly, and additionally annual plans are annual reports are published on the programme website http://safir2014.vtt.fi/. Detailed research results are published in scientific journals, conference papers and research reports.

Acknowledgements

The high quality scientific and technical work of all SAFIR2014 projects' personnel during these first two project years is highly appreciated. Special thanks are due to the project managers and their staff for providing the written contributions to this interim report.

The work of the persons in the Steering Group, Reference Groups and Ad Hoc Groups, carried out with the expenses of their home organisations, is acknowledged with gratitude.

References

1. National Nuclear Power Plant Safety Research 2011-2014. SAFIR2014 Framework Plan. Publications of the Ministry of Employment and the Economy, Energy and the climate 50/2010. http://safir2014.vtt.fi/docs/safir2014_framework_plan.pdf.

2. Simola, K. SAFIR2014 Annual Report 2011. Report VTT-03188-12. 120 p. + app. http://safir2014.vtt.fi/docs/SAFIR2014_Annual_Report_2011.pdf.

3. Simola, K. & Suolanen, V. SAFIR2014 Annual Plan 2011. Report VTT-R-03783-11. 34 p. + app. http://safir2014.vtt.fi/docs/SAFIR2014_AnnualPlan_2011.pdf.

4. Simola, K. & Suolanen, V. SAFIR2014 Annual Plan 2012. Report VTT-R-03343-12. 36 p. + app. http://safir2014.vtt.fi/docs/SAFIR2014_Annual_Plan_2012.pdf.

2. Man, Organisation and Society

2.1 Managing safety culture throughout the lifecycle of nuclear plants (MANSCU)

Pia Oedewald, Luigi Macchi, Elina Pietikäinen

VTT Technical Research Centre of Finland
Tekniikantie 2, P.O. Box 1000, FI-02044 Espoo

Introduction

Current theories of organisational safety emphasise that safety is more than absence of accidents and incidents (Woods & Hollnagel 2006; Reiman & Oedewald 2008). Safety can be viewed as organisational ability to succeed in varying conditions (Hollnagel et al. 2006). Thus, practical approaches to safety assessment and development should be based on understanding what constitutes the socio-technical *ability* to succeed in both normal and unexpected situations. Despite these theoretical statements safety management practices focus, for the most part, on failures (possibility of technical faults or human errors or organisational failure). Consequently, the view on the organisations ability to manage their operations may be biased since most of the time things do go right. To optimise the development of safety organisations should learn from normal, successful situations.

Modern industrial systems (such as NPP's) are so complex that all risks can never be anticipated and identified. Organisations' should not have a false conception of their ability to identify and control risks. Furthermore, in some cases the risk mitigation actions create new complexities in the organisation: the specific actions that aim to eliminate certain risks may create new challenges in other parts of the system. Therefore the latest safety theories, such as resilience engineering (Woods & Hollnagel 2006) emphasise that generic robustness and flexibility is important. This is, however, fairly contradictory to some of the safety management practices which aim at reducing variability of actions and introducing more rigorous ways of working (instead of flexibility).

The above described view on safety being organisational capability has been the basis of the organisational assessment approaches developed at VTT, namely

the CAOC (cf. Reiman & Oedewald 2007) and the DISC-model (cf. Oedewald et al. 2011, Macchi et al. 2011). These methods have been developed for assessing organisation's potential for safety. They aim at providing insights in the organisation's deeply rooted logics of action by analysing its culture. The focus is not solely on identification of weaknesses in the performance but rather in describing the reasons for success and occasional failures.

When VTT's research group has carried out organisational culture analysis and safety culture assessments in the nuclear industry they have paid attention to generic challenges which safety management should be able to tackle. These topics, which are discussed next, should be better incorporated into the safety culture models as well.

Research needs in the practical frameworks for safety culture and safety management

In the nuclear industry risk and quality management are very well established. Researchers have argued that sometimes this has led to a tendency to overemphasise the effectiveness of plans, rules and procedures in guaranteeing safety of the nuclear plants (Perin 2004). Nuclear industry culture has been described as "culture of control" (Perin 2004) where organisations and workers emphasise that risks are in control and they do not appreciate the inherent uncertainties. This has also been recognised by some of the Fukushima accident investigations (Epstein 2012; Diet 2012). In reality many activities in the nuclear industry, for example maintenance, design work, construction of new plants and emergency management involve dealing with unforeseen situations and performing underspecified work tasks (cf. Weick & Sutcliffe 2007, Reiman 2011, Oedewald et al. 2012, Grote 2012). In order to smoothly cope with these the culture of the organisation need to support flexibility and adaptability to some degree.

Many of the situations requiring flexibility and local adaptation are so typical and mundane that they are not reflected upon. In other words the actors do not pay any attention to the fact that they are doing ad hoc decisions or working without a specific instruction. It is everyday reality for example in the maintenance work that rules and instructions do not cover all circumstances thus the actions or decisions are based on worker or management expertise (Reiman 2011; Oedewald et al 2012). We state that safety management practices should not assume that all activities are – or could be – prescribed in a nuclear power plant. Instead, *safety management practices should support organisational mindfulness: vigilance and attentiveness to unexpected situations and means for coping with them in a flexible manner* (Weick & Sutcliffe 2007).

In order for the actions and decision to be safe they need to be *based on sound understanding of the possible risks and safety impacts of the decisions and actions.* Majority of everyday decisions are taken by the workers and their immediate supervisors and e.g. safety engineers or process experts are not necessarily involved in the decision making. It is important that those individuals who carry out

ad hoc decisions possess sufficient understanding of the possible safety impacts of the actions. Achieving and maintaining that understanding across the organisation is not self-evident, however. Partly this relates to very nature of nuclear hazards: the nuclear safety related risks are intangible and they realize infrequently thus not all workers really employ realistic understanding of e.g. radiation or core melt down related phenomena. Partly lack of understanding stems from the cultural assumption that not everybody needs to know the technical systems and their functionalities as long as they follow the rules and procedures. The hazards may also be considered distant due to multiple technical barriers and strict distribution of responsibilities among different actors. Further, some technical phenomena are rare, complex and hard to anticipate e.g. in the design stage.

We claim that safety culture models and safety management practices should not focus solely on attitudinal aspects (employees' and management attitudes towards safety) but include the knowledge component as well (see also Kirwan 2008). From practical perspective it is necessary to be able to identify whether the suboptimal decisions are due to "not caring" or "not understanding" because the corrective actions needed differ depending on the case. If the knowledge component is included in the safety culture models (as it is currently in the DISC model) it is not self-evident, however, how much systems understanding each actor should possess and what would be a meaningful way to deliver that kind of a knowledge. This is a topical question since the new power plant projects and modernisations of the operating units require such an amount of employees and services that it's necessary to utilise subcontractor companies and new workers with little or no previous experience in nuclear industry.

All in all, the question of *how to create safety culture in a supply chain or a network of organisations* is one of the practical challenges the power companies and regulators face at the moment. In modernisation or new build projects the work is typically carried out by a virtual organisation which consists of workers from multiple organisations. It is a temporary group with little shared history and thus little shared cultural norms and assumptions. Often these project organisations are multicultural (IAEA 2012). Safety management practices and safety culture models have their roots in single company context. Thus, it has not been easy for the practitioners to implement those in the networks of subcontractors. Especially the questions how to create sufficient understanding of the rationale behind the strict working practices and how to motivate the organisations to put effort in the nuclear specific requirements are challenging from the practical perspective. MANSCU-project has a hypothesis that concrete knowledge of the hazards, risks and safety significance related to the activities one is conducting is a key factor for creating such a motivation. It is an important factor also because in big projects adjustments are frequent: the work does not proceed exactly as planned and supervisors or workers make ad hoc decisions. On the other hand the (contractor) supervisors and workers are first-hand informants of possible quality problems and other safety worries. If they don't understand the safety significance of their observations they might not report them. Thus, understanding the hazards, risks and safety significance is one of the preconditions for organisational mindfulness.

However, even experienced and knowledgeable nuclear power organisations may have developed a culture where mindfulness towards the risks and preparedness for unexpected situations is inadequate. One of the mechanisms of drifting into failure is to take the past success as a guarantee of future success (Dekker 2011). It may lead to reduced vigilance towards weak signals of danger, overreliance of the competence in the organisation or overconfidence over the technical barriers and generic complacency in the organisation. This problem is usually discovered during accident investigations but little research has been carried out concerning the impacts of the safety management practices in fighting complacency and increasing mindfulness prior any visible problems.

The generic goals and research strategy of MANSCU-project

The generic objective of the MANSCU project (2011–2014) is to develop safety management approaches in such a way that they would better take into account the recent developments in safety science. MANSCU project focuses on three topics which are relevant practitioners in the Nordic nuclear industry as well as supports the theoretical development of the safety culture model VTT has created. Safety management approaches (such as rules and procedures, training, event investigation practices, safety culture evaluations and improvement programs, risk assessment and human performance programmes) should:

1) support the development of sufficient *understanding and knowledge of nuclear safety* and risks as well as nuclear industry specific working practice demands.

2) take into account the needs of *other contexts than the operating units*. Especially we focus on creating knowledge on how safety culture should be understood in a) design activities and b) complex networks of subcontractors. The networks and supply chains may be multicultural and interdisciplinary.

3) support *organisational alertness (mindfulness)* to new risks or other unexpected conditions which are based on either technical or social phenomena. It also means avoidance of complacency and constant effort of continual improvement.

The research strategy of MANSCU project is that in addition to the theoretical work case studies are carried out in Finland and Sweden. The case studies are designed based on interests of the power companies and regulators and thus, they are not directly structured according to the MANSCU-project generic goals. However, the purpose is that the practical case studies provide good material for gaining insights into the three above mentioned topics.

During 2011 and 2012 the case studies have focused in two distinct safety critical activities: maintenance (subtask MoReMo) and design (subtask DESIGN). The theoretical work which has been done parallel to the case studies has focused firstly, on creating a model on networked safety (e.g. design activities are typically carried out in a networked way). Secondly, we have aimed for exemplifying the

resilience engineering premises in practice in the maintenance related case studies. The DESIGN and MoReMo subtasks are described next.

Safety culture in the design process (subtask DESIGN)

It has been long acknowledged that safety culture needs to be taken into account and managed when operating and maintaining nuclear power plants. However, the fact that people taking part in designing the plants are also influenced by cultural issues has not been given much emphasis. As design flaws can contribute to serious nuclear power accidents, it is important to also start considering how safety culture affects the design activity and how the design work can be supported from this perspective. The DESIGN project is an opening to this complex and understudied research area. It aims at providing general understanding on design activities from safety culture perspective and mapping current cultural challenges and opportunities (Macchi et al. in progress). The DESIGN project has carried out interviews in Finland and Sweden and reviewed literature related to the topic. Here we present the key findings of the project so far.

Design is a practise that depends upon, integrates, and transforms heterogeneous domains of knowledge (Mark et al. 2007). Design products bridge functional knowledge and stakeholder power gaps across different social worlds (Mark et al., 2007). This is especially true in the nuclear power context where design requires highly specialised expertise and where the designed components come with several interfaces to other designed components. The design process in the nuclear industry is by nature a collective effort. No one individual designer alone can ensure that the designed end product is functional and safe and complies with regulatory requirements and design principles. Designing can be understood as a complex interaction and negotiation process between different experts and organisations (Table 1). Thus, when evaluating and improving safety culture in design, it is not enough to view safety culture only on an organisational level. Rather the whole organisational network should be taken as the unit of analysis.

Table 1. The roles of the various actors in the design process.

International organisation (e.g. IAEA, ISO, WANO, …)	National Regulator (STUK, SSM)
• Set guidelines • Set standards • Seek and disseminate best practices from National cases	• Set requirements to NPP • Inspect requirements fulfilment
Owner (E.On, Fortum Oyj, TVO Oyj)	**Design organisation (e.g. Fortum Technical support, AREVA, Siemens, Toshiba)**
• Set economical and temporal framework • Disseminate experiences from other plants	• Take requirements into account • Negotiate with NPP • Manufacture design
Operating organisation (NPP)	**Manufacturer**
• Set requirements to supplier/design organisation • Check fulfilment of requirements • Validation of design • Inspect design • Negotiate with suppliers • Verification of design • Primary review • Planning design • Implementing design • Operate the plant	• Manufacture design
	Implementing organisation
	• Take supplier's requirements into account • Manufacture design/components • Performs the construction work
	Technical support
Certifier	• Independent evaluation of design • Support design • Inspect design and report
• Certification of design and "stamp"	

What is good design safety culture like?

Design is inherently a dynamic, creative cognitive act. As Veland (2010) states, the designers in the nuclear industry need to "think on their feet" and immerse in active, flexible, reflective exploration of the problem space. From this it follows that in order to create safe and functional end-products it is not enough to provide strict guidelines and supervision. Rather, supporting safe design is about developing a balanced culture that – besides providing structures and rules – also supports creativity and participation in the work community.

Oedewald, Pietikäinen and Reiman (2011) have summarised qualities of good safety culture into three cornerstones of safe activities: mindset, understanding and organisational systems and structures (Figure 1). These criteria have been used as a foundation for evaluating safety culture at Nordic nuclear power plants (e.g. Oedewald et al. 2011). These criteria could also be utilised in understanding what good design safety culture is like. A good design safety culture means an informed culture (see also Reason, 1998), where all the relevant actors understand the hazards related to the activities and are able to see how their own work connects to the big picture. It also means that all the relevant actors consider nuclear safety an important aspect of their work, are motivated by it and take responsibility for the overall functioning of the plant in which the designed component will be used, not just their own work. This responsibility also needs to be taken in a long-term way as the designed components will often be used for decades. All the relevant actors also need to be mindful in their practices. That is, they need to be constantly aware of the possibility that something surprising will turn

up. There also need to be such systems and structures and resources in place that create good preconditions to work with good quality.
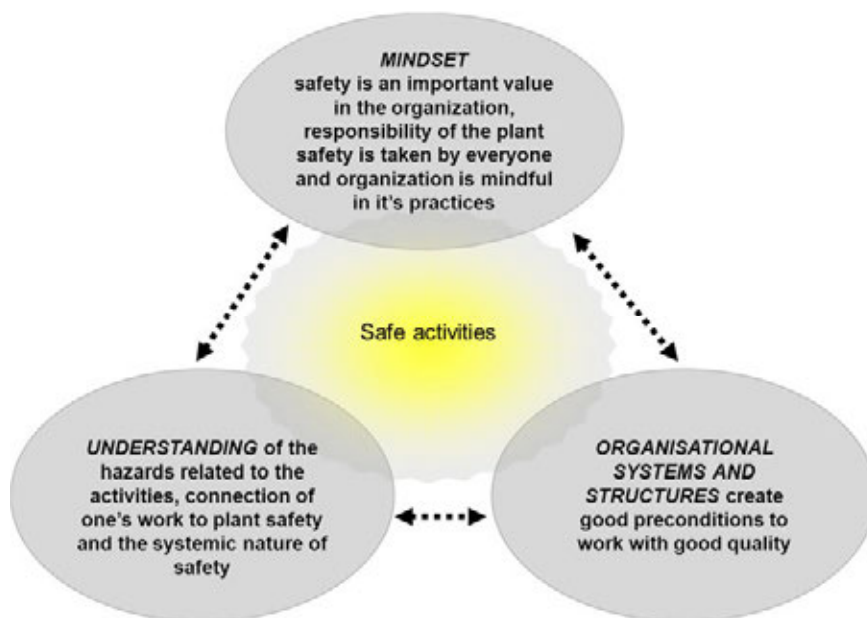
Figure 1. Cornerstones of safe activities (Oedewald et al. 2011).

As in the nuclear industry several organisations usually co-operate in the design process, it is important to consider how well the different organisational safety cultures interact (Figure 2). Safety emerges from these interactions. It is important for example to assess, whether the understanding concerning hazards and core task demands is the same in the different organisations and whether the organisations have compatible organisational systems and structures in place.

Current challenges in the design network from safety culture perspective

How well is the nuclear industry doing in these terms then? In the DESIGN project this issue was studied by interviewing people taking part in design activities in Finland and Sweden. The interviews revealed five main safety culture challenges relating to the interactions between the organisations in the design network.

First of all, safety is not always the first and most important guiding value in the design process. Rather the different actors involved in the design process – including the regulators – are constantly balancing between safety and economics in their work. There are commercial pressures between the organisations that may influence safety as well. For example, when making contracts with design organi-

sations, the power companies strive to make a good bargain. There is quite understandably a temptation not to start the bargaining with explaining all the safety requirements and possible risks and complexities that relate to the design work. However, if this is not done already in the contract phase, it may be difficult to make demands later in the design process.

Secondly, understanding the context where the designed end-product will be utilized may be difficult for the designers and this may lead to dysfunctional designs. It was mentioned by the interviewees that, for example some of the I&C designers have never been to an operating power plant and might thus not think of some relevant issues in their design work. Also, the interviewees pointed out that in some countries, the nuclear domain has been developed and in others recessed, so the level of designers' nuclear power specific expertise may vary depending on the country. It was considered important that power company's personnel who guide the design work have solid understanding on functioning of the plant and can communicate this understanding to the designers.

Thirdly, organisations do not always share the same safety philosophies and understand safety requirements in the same way. This is especially the case, if the organisations involved in design represent different national cultures – as is often the case in the nuclear industry. For example, it was mentioned in the interviews that the Finnish regulator emphasises the principle of continuous improvement much more than regulators in some other countries. If the designers don't understand this principle, they may not design enough buffers for the designed components. Also safety philosophies and understandings of the safety requirements may differ between operating organisations and design organisations. The interviewees also brought up that not only designers and operating personnel should understand the safety requirements, but the people doing the commercial contracts concerning the design process at the power companies as well.

Fourth, coordinating activities may be difficult between organizations that work according to different logics and understandings. For example, it is sometimes difficult to match the creative and iterative design process with the strict and ponderous regulatory process. These two sub processes of the wider design process seem to follow a different kind of time logics.

The fifth challenge that was found in the interviews related to distributing responsibilities and balancing roles between different stakeholders. For example, if the design activities are purchased from several subcontractors, who should manage the interfaces? Should the regulator inspect subcontractors that carry out the design work or only the power company who is the licensee and who purchases the design work from the design organisations? And how should regulators balance between inspection and giving improvement suggestions in the design process? On the other hand it is important for the regulators to stay in an independent evaluator role, which is their core task. However, how can they not interfere and suggest some directions for the companies when they evaluate the iterative step-by-step design process in all its stages and see the situation with outsiders' eyes? These challenges need to be solved or rather taken into account and continuously balanced between in everyday design activities.

In 2013 the DESIGN subtask will focus on testing and evaluation of the results of the work conducted in 2011–2012.

MoReMo subtask: Can resilience engineering approach help in managing safety in maintenance activities?

The MoReMo subproject describes maintenance organisations' practices in coping with underspecified, unanticipated multi-actor work tasks (Oedewald et al. 2012; Macchi et al. in progress, Axelsson et al. 2011). These situations are prone to so called human errors but in most cases the organisations cope well with them (Reiman 2011). The aim of the task is to come up with methods which help in modelling and managing these complex tasks in a systematic manner. The purpose is to find means to support flexible and adaptive work processes at the nuclear plants without sacrificing the safety of the decisions or the culture of complying with procedures.

MoReMo-project collected variety of data: field observations, interviews and documents concerning working practices during outages in three Nordic plants. Further observations of maintenance work during normal operations were done in one plant. In addition to that observations and interviews covered the field operator's work in one plant. The main goal was to identify what kinds of ad hoc adjustments are done, are there goal conflicts, are the adjustments good from the safety point of view or are some of them risky.

The observations and interviews confirmed the expectations that maintenance is an activity where tasks are underspecified and unexpected situations are part of everyday work. The unexpected situations we observed included following:

- the equipment the working group was using did not work and the working group had to find new equipment which postponed the task until the next day

- when a machine was opened for inspection a technical fault was identified which required consultation from a manufacturer abroad and which took many days

- work instructions were inaccurate a whole chapter was missing from the text

- a major overhaul and modification was scheduled to be carried out in a short timeframe during the outage which required new working arrangements: extra workers were borrowed from other unit and two shift system was implemented

- a newcomer was unsure how to use a computer program that was used in the testing and he was supported via telephone

- field operators struggled in finding the valves they were supposed to close in order to ensure isolation and maintenance working group fell behind the schedule

- field operators worked alone instead of working in pairs which is the norm

- a component was installed upside down during the overhaul which resulted in delays of start up after the outage

- recent modifications in the building have not been taken into account in the work planning and that caused challenges for the maintenance crew when they were lifting a big component

- when a system was opened the piping did not match with the drawings. The supervisor assumed that there is a mistake in the drawings rather than in the installation.

The above mentioned occurrences were considered fairly typical situations according to the interviews. The maintenance workers did not pay too much attention to these and seldom explicitly reflected the different options they had in the situations. For most of the occurrences there is no specific instruction on how to proceed; what is a good practice or risky behaviour in that kind of a situation. If these situations would have ended up in an unavailability of the technical system they would have been – most likely – labelled as human errors. If they do not result in any technical problems the actions taken are considered as normal organisational practice. From safety management perspective this kind of a hindsight approach is not fruitful. There should be means to identify adjustments points as they are happening and tools to evaluate the safety effects of the possible actions.

In order to come up with criteria for evaluating the working practices or ad hoc decisions the core task of maintenance during outages was modelled (Figure 2). The first basic assumption of the MoReMo analysis is that the adjustments that supervisors or workers do are acceptable if they aim to fulfil at least one of the demands set by the organisation's core task. Further, when ad hoc decisions are taken the workers should be sure that their actions do not compromise any of the core task demands.
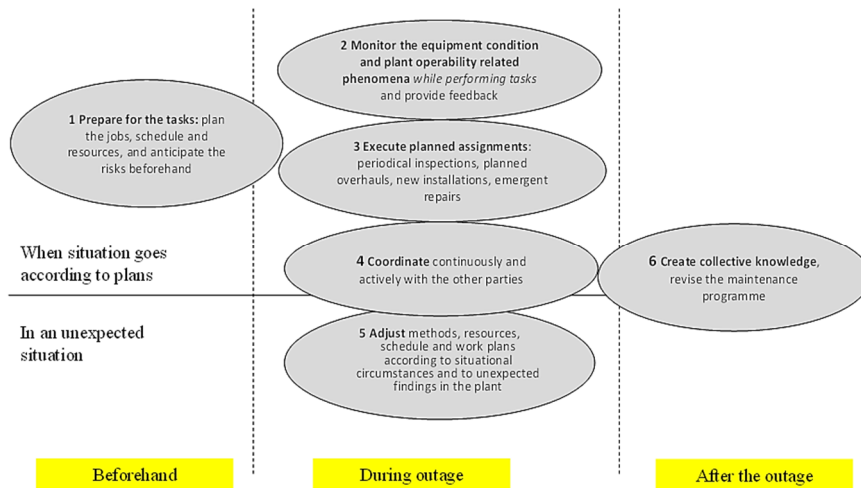
Figure 2. Maintenance during outages requires balancing between six different core task demands.

Some of the core task demands need to be fulfilled already before the outage starts, some after it has been completed. An important notion is that even though considerable efforts are put in preparation and the work tasks should proceed well in schedule and in predetermined order something unexpected always comes up. The workers and the organisation need to be able to switch from the "executing the plans" -mode to the "adjust methods, schedules etc." -mode. This switch should not, however, be carried out without taking the other core task demands into account: the major schedule needs to be respected, work needs to be coordinated and collective knowledge creation needs to take place after the outage.

The MoReMo research group modelled what kind of working practices would support the fulfilment of the outage core task. These are listed in Table 2.

Table 2. MoReMo study listed working practice demands which support fulfilment of maintenance core task during outage.

Involve different parties in the preparations	Identify the relevant expertise needed in the work	Utilise past experiences, screen documents etc.
Prepare for unexpected findings	Reserve slack resources	Analyse the nuclear safety significance of the work tasks beforehand and document that
Acquire tools, papers, spare parts etc. well beforehand	Pay attention to anything unusual even outside your work scope (walk eyes open)	Ask questions
Report findings and reward people from reporting	Participate to face to face forums where feedback can be given	Utilize of maintenance history database (or similar ICT system)
Check the plans, e.g. Pre-job-brief	Aim to accomplish the task, put effort in getting the work done, be active	Adhere to schedules, specifications of quality parameters, materials and tools, and specific instructions on conduct of work (if available)
Carry out readiness review	Take other's work task into account while performing yours	Learn to know others whose work task relate to yours
Explain what you are doing and what is relevant in it, make sure other stakeholder know the risks	Report progress and delays	Use multiple communication channels: phone calls, meetings, informal channels
Intervene and help out if other work groups are struggling with their work	Evaluate the safety impacts of any change in your work process	Be prepared to respond to local work scope circumstances
Analyse whether the preventive maintenance programme of each system is valid based on the information received during the outage	Analyse whether the maintenance instructions were sufficient and correct for the workers	Utilize the know-how of the shop floor personnel

However, there are other requirements to be fulfilled as well: organisational activities need to comply with generic safety culture norms. Thus we came up with an evaluation framework which on one hand evaluates whether the practice or ad hoc decision is done according to the core task demands and on the other hand whether the way it is carried out complies/violates the safety culture criteria (based on the DISC model, see Oedewald et al. 2011). The evaluation framework was used in judging various episodes that the MoReMo research group identified during the observations and heard during the interviews. Based on the evaluation framework we developed a first version of a checklist tool which might be useful for the power plant organisations. The checklist could be used for, first of all, helping the

maintenance organisation to pay attention to the fact that they do carry out lots of adjustments without paying too much attention to them. Secondly, when a situation which needs adjustment is recognised the checklist could help in evaluating whether the decision would be problematic in a long turn. Thus the checklist could serve as one practical safety management tool for supporting resilience in maintenance and outages.

The MoReMo subtask was finalised in 2012 but it is followed by a more specific study concerning safety management in maintenance. The new subtask for 2013–2014 is HUMAX. It reviews Human Performance tools that are used for reducing human errors in maintenance work. The aim is to find out:

- What are the expected benefits of human performance tools applied in nuclear power plant maintenance?

- What have the measurable benefits of human performance tools been so far in the plants (e.g. reduced number of failures, licensee event reports, and human errors)?

- How do maintenance personnel perceive the application and effects of human performance tools?

- What characterizes successful human performance tools and implementation processes?

- What aspects of maintenance work are most effectively met by use of human performance tools, and what could be solved by other socio-technical means?

References

Axelsson, C., Hildebrandt, M., Skjerve, A.-B. 2011. An interview study investigating efficiency-thoroughness trade-offs in maintenance work at a Nordic nuclear power plant. IFE/HR/F-2011/1516. Halden: Institute for Energy Technology.

Diet. 2012. The National Diet of Japan the official report of the Fukushima Nuclear Accident Independent Investigation Commission.

Epstein, S. 2011. A Probabilistic Risk Assessment Practitioner looks at the Great East Japan Earthquake and Tsunami. A Ninokata Laboratory White Paper. Tokyo Institute of Technology.

Dekker, S. 2011. Drift into failure. From hunting broken components to understanding complex systems. Farnham: Ashgate

Grote, G. 2012.Safety management in different high-risk domains – All the same? Safety Science, 50, 1983–1992.

Hollnagel, E., Woods, D.D., Leveson, N. (eds.). 2006. Resilience Engineering Concepts and Precepts. Farnham: Ashgate.

IAEA 2012. Safety Culture in Pre-operational Phases of Nuclear Power Plant Projects. Safety report series 74.

Kirwan, B. 2008. From Safety Culture to Safety Intelligence. In proceedings of Eurocontrol international conference. Bretigny 2008.

Macchi, L., Reiman, T., Pietikäinen, E, Oedewald, P. & Gotcheva, N. 2011. DISC model as a conceptual tool for engineering organisational resilience: Two case studies in nuclear and healthcare domains. In Proceedings of the 4th Symposium on Resilience Engineering. Sophia-Antipolis, France, June 8–10, 2011.

Macchi, L., Pietikäinen, E., Liinasuo, M., Savioja, P., Reiman, T., Wahlström, M., Kahlbom, U., Rollenhagen, C. Safety culture in design. (In progress.)

Macchi, L., Eitrheim, M., Gotcheva, N., Axelsson, C., Oedewald, P., Pietikäinen, E. Modelling resilience for maintenance and outage. Final report of Moremo project. (In progress.)

Mark, G., Lyytinen, K., Bergman, M. 2007. Boundary objects in design: An ecological view of design artifacts. Journal of the Association for Information System, 8(11), Article 34. http://aisel.aisnet.org/jais/vol8/iss11/34/

Oedewald, P., Pietikäinen, E., Reiman, T. 2011. A guidebook for evaluating organisations in the nuclear industry – an example of safety culture evaluation. SSM.

Oedewald, P. et al. 2012. Intermediate report of MOREMO: Modelling Resilience for Maintenance and outages. NKS-262 report. http://www.nks.org/scripts/getdocument.php?file=111010111128784

Perin, C. 2004. Shouldering Risks: The Culture of Control in the Nuclear Power Industry. University Press. Princeton, NJ.

Reason, J. 1998. Achieving a safe culture: theory and practice. Work and Stress, 12, 293–306.

Reiman, T. 2011. Understanding maintenance work in safety-critical organizations – managing the performance variability. Theoretical Issues in Ergonomics Science.

Reiman, T. & Oedewald, P. 2007. Assessment of Complex Sociotechnical Systems – Theoretical issues concerning the use of organizational culture and organizational core task concepts. Safety Science 45 (7), pp. 745–768.

Reiman, T., Oedewald, P. 2008. Turvallisuuskriittiset organisaatiot. Onnettomuudet, kulttuuri ja johtaminen. Edita. (In Finnish)

Veland, O. 2010. Design patterns in the nuclear domain: theoretical background and further research opportunities. OECD Halden reactor project. HWR-932.

Weick, K.E., Sutcliffe, K.M. 2007. Managing the unexpected – Resilient performance in an Age of Uncertainty. 2nd ed. John Wiley & Sons. Inc.

Woods, D.D., Hollnagel, E. 2006. Prologue: resilience engineering concepts. In: Hollnagel, E., Woods, D.D., Leveson, N. (eds.). Resilience Engineering. Concepts and Precepts. Ashgate, Aldershot.

2.2 Sustainable and future oriented expertise (SAFEX2014)

Krista Pahkin[1], Eerikki Mäki[2]

[1]Finnish Institute of Occupational Health
Topeliuksenkatu 41 a A, 00250 Helsinki

[2]Aalto University
Tuotantotalouden laitos, PL 15500, 00076 AALTO

Abstract

The Sustainable and Future Oriented Expertise (SAFEX2014), like the earlier Expert work in safety critical environment (SAFEX) project, aims to generate new knowledge on development of expertise and competence management on Finnish nuclear energy organizations. SAFEX2014 builds on research group's earlier findings of expert work and expertise development in nuclear energy industry. The importance of development of employees' expertise has been recognized widely in nuclear power industry organizations and e.g. in IAEA [1–4]. The aim of this study was to have a closer look of work engagement, which is an emerging occupational concept, and job-related factors behind it, and what is the role of work engagement on the development of expertise. The findings are based to the questionnaire survey carried out in six Finnish nuclear industry organizations (n = 770) in spring 2012.

The findings supported the earlier findings of job demands-job resources model and its effects on employees' well-being: the employees' motivation and well-being is based on good job-related resources. More over work engagement was connected to content of the work and engaged employees seemed to pay more effort to develop their own expertise. The results showed that good basics for work engagement and expertise development exists in the nuclear industry organizations, but at the same time there are demands, like work pressure, which could in the long run threaten the motivation path and employees' willingness to develop their own expertise.

Introduction

Development of employees' expertise is important in every expert organization. This is because of new technological opportunities, changes in organizational competence base, changes in markets, etc. In addition to these challenges the Finnish nuclear energy organizations will also face the challenges of many experienced experts retirement, and new plants start operating in few years. These reasons call for new experts and development of expertise within organizations. To be able to do this, nuclear power organizations must also have methods and practices that support expertise development and career development of experienced experts.

The findings of earlier SAFEX-project [5] have already shown that the development of individual expertise in the nuclear power industry is related to the content of work, the actions of the closest superior, the functionality of the work group, and to the way a superior takes into account the safety-critical aspects of the work. Expertise development is, however, long process [6] and extremely dependent on the individual employees themselves [7]. The SAFEX2014-project has continued to study the factors and practices aiming to support expertise development in the nuclear power industry. The aim of our study is to pay attention to the factors supporting individual employees' activity to develop own expertise.

Expertise is usually considered to include knowledge, skills and long experience on the specific technical or other domain. Moreover, strong motivation and independency are qualities often associated with experts and expertise. One factor, which also could be associated to expertise, is work engagement. Work engagement can be described as a positive state of emotional and motivational fulfillment at work, characterized by vigor, dedication, and absorption [8]. Vigor refers to high levels of energy and mental resilience while working, the willingness to invest effort in one's work, and persistence in the face of difficulties. Dedication is characterized by a sense of significance, enthusiasm, inspiration, pride and challenge. Whereas absorption refers to the sense of being fully concentrated and happily engrossed in one's work. Work engaged employees are known to be intrinsically motivated towards their work [9], they take initiative [10], and also show pursuit of learning [11]. Thus work engagement could be important in expert work

(such as work in nuclear energy industry), which is characterized by ability to solve problems and learn from them [12].

Since work engagement is one of the factors associated to the one's willingness to developed own expertise it is important to understand factors at work which can produce it. Several longitudinal studies have already shown that there are various job resources that have an impact on employees' well-being, their work engagement. Job resources are those physical, psychological, social or organizational aspects of the job (e.g. autonomy, feedback) which can help employees to achieve work goals, but also stimulate personal growth, learning and development, and work engagement. [13, 14]. Job demands, in the other hand, are factors (e.g. time pressure, emotional workload) at work which may lead to lower well-being, like burnout. (Figure 1) All of these are factors that can be found also in the safety critical organizations [15].
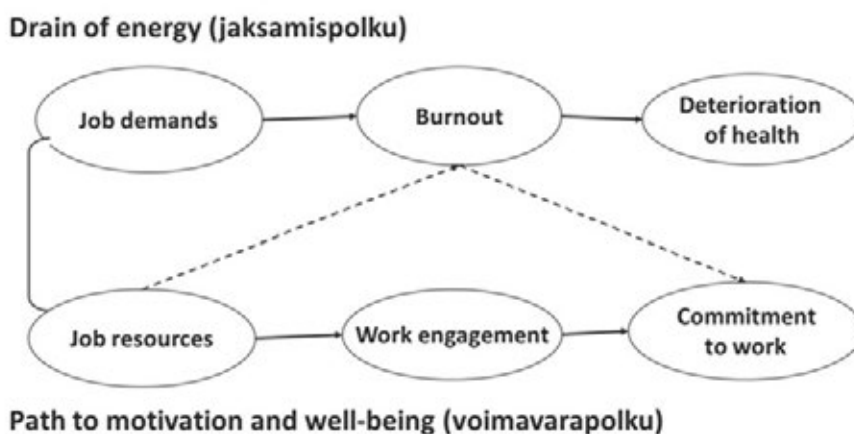
Figure 1. Job demands and resources model [14, 16].

The aim of this study is thus to find out:

1) If the job resources and demands differ among employees' who experience different level of work engagement?

2) What are the main resources behind work engagement in safety critical organizations?

3) What is the role of work engagement on the development of expertise?

Methods

In 2012, 770 experts from six Finnish nuclear industry organizations answered a questionnaire on the organizational practices and the improvement of expertise.

The content of the survey was same as in the earlier SAFEX –project [15], and the aim of the survey was to analyse and evaluate the content of learning organizations e.g. organization of work, actions of the supervisors, employees' well-being, motivation, work engagement and competence development of the experts.

In this study following variables were used:

> Own activity to develop expertise was measured with three questions, for example "*I have focused on developing my skills in accordance with the demands of the work*".

Work engagement was measured with three subscales (vigor, dedication, absorption) of the Utrecht Work Engagement [8]. Items of work engagement were rated on a seven-point scale ranging from 0 ("never") to 6 ("always"). Employees' were grouped into three group based on their work engagement:

- Group 1: those employees who seldom, only few times during a year, experience work engagement (low engagement, n = 39);

- Group 2: those employees who sometimes, once or twice during a month, experience work engagement (medium engagement, n = 183); and

- Group 3: those employees who often, weekly, experience work engagement (high engagement, n = 527).

Other sum scales used in the study were functionality of the work group, cooperation between work groups, actions of the supervisor, actions of the management, task and objectives, work load, opportunities to influence and develop. Work-related stress and job satisfaction was measured with single question. The format for answering most of the individual items was a Likert-type scale. Information on age (year of birth), gender and supervisory position were elicited with single questions.

All the sum scales were formed using factor analysis, and their reliability was assessed using Cronbach's alpha. Their internal consistency was satisfactory (<.70). Internal consistency of the activity to develop own expertise scale was 0.73 and of work engagement .94. Other methods used in the study were correlate and regression analyses.

Results

The results show that employees' whose work engagement is high (group 3), have more job-related resources compared to the other two groups but at the same time their job-related demands (work load) are as high as among the others (Figure 2). However, their well-being is better (they experience less stress). The results thus support the earlier findings of job demands-job resources model and its effects on employees' well-being: the motivation and well-being is based on good job-related resources.
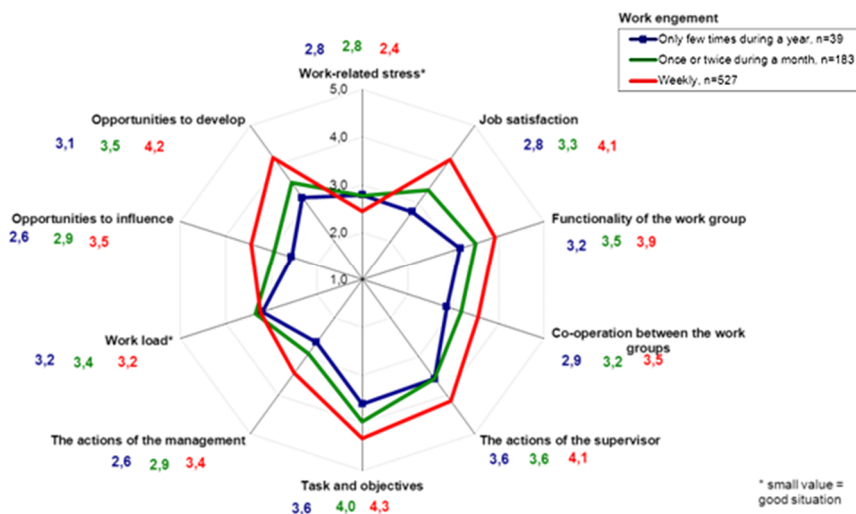
Figure 2. Job-related resources and demands based on the feeling of work engagement.

The further analysis showed that gender, age or supervisory position, were not connected to the work engagement. The strongest correlation was found between work engagement and content of the work (r = .52, p = .000). Work engagement correlated also with employees' activity to develop expertise (r = 0.45, p = .000). The correlations between work engagement and other studied variables (functionality of the work group, actions of the supervisor, actions of the management, task and objectives) varied between (r = 0.34–0.38, p = .000). The main variables (functionality of the work group, actions of the supervisor, actions of the management, task and objectives, content of the work, activity to develop expertise) used in the SAFEX-survey explained 31% of the employees' work engagement.

The results also revealed that 71% of those employees' who rarely (only few times a year) experienced work engagement (n = 39) also made very little effort to develop their own expertise. Whereas only 14% of those employees' who were highly engaged to their work (n = 527) made very little effort to develop their own expertise.

Conclusions

The results showed the meaning of good job-related resources to employees' well-being and to their work engagement. Furthermore, work engagement proved to be related to employees' own activity to develop their expertise. Therefore it is important that the nuclear industry organizations continue to pay attention to these factors and thus make sure that there is a good foundation for development of expertise available for all employees working in the organization. Since the content of

work is often described to be one of the main motivating factors for experts working in the sector, it is also important to make sure that it does not come too demanding.

References

1. IAEA NE Series No. NG-G-2.1: Managing human resources in the field of nuclear energy (2009).

2. IAEA-TECDOC-1510: Knowledge Management for Nuclear Industry Operating Organizations (2006).

3. IAEA-TECDOC-1399: The nuclear power industry's ageing workforce: Transfer of knowledge to the next generation (2004).

4. IAEA-TECDOC-1364. Managing human resources in the nuclear power industry: Lessons learned.

5. Pahkin, K., Leppänen, A., Mäki, E., Kuronen-Mattila, T., Järvenpää, E. 2011. Supervisor's role in knowledge management and expertise development. SAFIR2010 Seminar, March.

6. Kuronen, T., Säämänen, K., Järvenpää, E., Rintala, N. 2007. Hiljaisen tiedon säilyttäminen ja jakaminen ydinvoimalaitoksessa. Laboratory of Work Psychology and Leadership Report Series No. 1/2007. Espoo: Helsinki University of Technology, Department of Industrial Engineering and Management. (In Finnish)

7. Mäki, E., Kuronen-Mattila, T., Pahkin, K., Järvenpää, E., Leppänen, A. 2011. Expertise development in nuclear power industry. Project summary report. SAFIR2010 Seminar, March.

8. Schaufeli, W.B., Salanova, M., González-Roma, V., Bakker, A.B. 2002. The measurement of engagement and burnout: A two sample confirmatory factor analytic approach. The Journal of Happiness Studies, 3, 71–92.

9. van Beek, I., Taris, T.W., Schaufeli, W.B. 2011. Workaholic and work engaged employees: Dead ringers or worlds apart? Journal of Occupational Health Psychology, 16(4), 468–482.

10. Hakanen, J., Perhoniemi, R., Toppinen-Tanner, S. 2008. Positive gain spirals at work: From job resources to work engagement, personal initiative, and work-unit innovativeness. Journal of Vocational Behavior, 73, 78–91.

11. Sonnentag, S. 2003. Recovery, work engagement and proactive behavior. Journal of Applied Psychology, 88, 518–528.

12. Tynjälä, P. 1999. Konstruktivistinen oppimiskäsitys ja asiantuntijuuden edelly-tysten rakentaminen koulutuksessa. Teoksessa Oppiminen ja asiantunti-juus (Toim. Eteläpelto, A. & Tynjälä, P.) WSOY, Porvoo. (In Finnish)

13. Demerouti, E., Bakker, A.B., Nachreiner, F., Schaufeli, W.B. 2001. The job demands-resources model of burnout. Journal of Applied Psychology, 86, 499–512.

14. Schaufeli, W.B., Bakker, A.B. 2004. Job demands, job resources, and their relationship with burnout and engagement: a multisample study. Journal of Organizational Behavior, 25, 293–315.

15. Pahkin, K., Kuronen-Mattila, T., Mäki, E., Leppänen, A., Järvenpää, E. 2011. Asiantuntijatyö turvallisuuskriittisessä ympäristössä, SafeExpertNet 2007–2010. Työympäristön tutkimusraporttisarja 57, Työterveyslaitos, Helsinki. (In Finnish)

16. Hakanen, J. 2009. Työn imua, tuottavuutta ja kukoistavia työpaikkoja? – Kohti laadukasta työelämää. Työsuojelurahasto. (In Finnish)

3. Automation and Control Room

3.1 Coverage and rationality of the software I&C safety assurance (CORSICA)

Jussi Lahtinen[1], Lauri Lötjönen[1], Risto Nevalainen[2], Jukka Ranta[1], Timo Varkoi[2]

[1]VTT Technical Research Centre of Finland
Vuorimiehentie 3, P.O. Box 1000, FI-02044 Espoo

[2]Finnish Software Measurement Association FiSMA ry
Tekniikantie 14, 02150 Espoo

Introduction

There is a general need to perform qualification of I&C safety systems as effectively as possible, keeping still the necessary formalism and accuracy of the qualification. Early notification of potential problems is the most effective and proactive way to perform qualification. Good knowledge of nuclear standards, professional application of sophisticated methods and good ability to adopt novel technologies is essential for qualification.

In previous SAFIR2010 program we developed approaches to qualify and certify software intensive I&C systems for nuclear power plants. This work is continuing in current SAFIR2014 program, extending previous results for general evaluation for example in following topics:

- adequacy and relevance of process capability assessment in technical product evaluation,

- coverage and rationality of required development and assurance methods,

- certification and evaluation issues in using new technologies, for example FPGA,

- use of new standards in technical safety evaluation of nuclear I&C systems.

This article describes results from two first years of our CORSICA project. It is a partnership between VTT and FiSMA. FiSMA is responsible for process related topics, mainly the development of new process assessment model called Nuclear SPICE. Also integration of Nuclear SPICE with reliability and software quality concepts belongs to FiSMA. VTT is responsible for selected V&V methods in qualification, for example new kinds of review techniques. VTT has also worked with novel technologies, like FPGA and multicore platforms in nuclear power plants.

Use of evaluation concepts, methods and tools from other domains is also important in CORSICA, because nuclear power standards are not adequate alone for all qualification and certification needs. Experiments in pilot projects are also used to validate our results of CORSICA tasks.

Assessment of system/software development process with Nuclear SPICE

Main standard in functional safety is IEC 61508:2010 (3nd edition). It has seven parts. Software requirements are mainly in Part 3. [IEC 61508] The safety concept in IEC 61508 is called "safety related". In nuclear domain it would mean safety system in lower level safety class 3. Our concept "safety critical" in CORSICA means more or less the same.

Software standards in nuclear domain are IEC60880 [IEC 60880] for safety-critical software (Category A) and IEC 62138 [IEC 62138] for safety-related software (Category B and C). They can be classified as "second level" standards, referring directly to IEC 61513 [IEC 61513] but only indirectly to IEC 61508.

The standard IEC 61513 highlights the need for complete and precise requirements, derived from the plant safety goals. This standard is the highest I&C safety standard in the nuclear industry, giving requirements for I&C systems and providing also high level requirements for safety software.

The generic solution in process assessment is standard called "SPICE" as the brand name. It is currently in transition period from previous ISO/IEC 15504 (10 parts) into ISO/IEC 330xx series [ISO/IEC 330xx].

One major task in CORSICA has been to create an integrated family of methods to assess the degree of compliance with standards of system and software. SPICE provides a generic framework for this. By adding content and criteria from generic safety standards and from nuclear standards in Nuclear SPICE, a holistic method can be done to assess the process capability and compliance. This idea is presented in Figure 1.
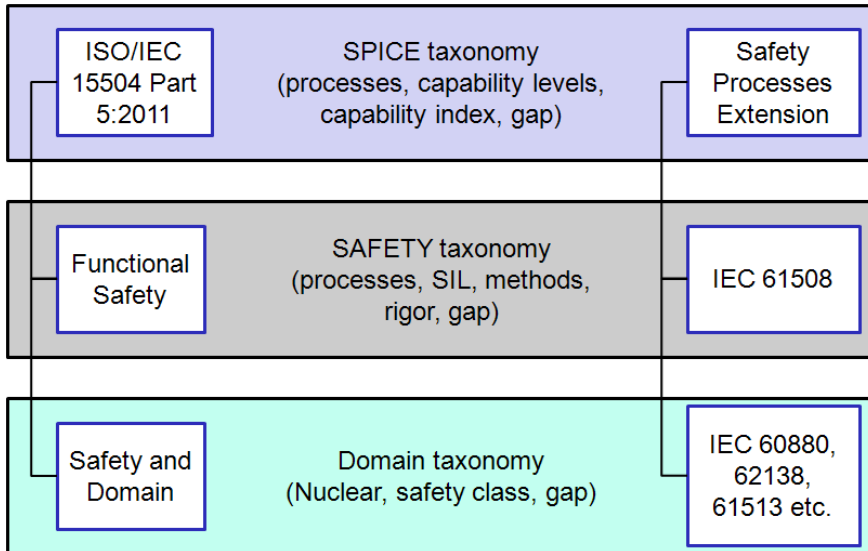
Figure 1. The integration layers of standards and criteria in Nuclear SPICE.

The main challenge is integration between layers. SPICE, IEC 61508 and IEC 60880 can be kept separate and leave space for ad hoc integration in each assessment and qualification case. Also deeper integration is made in small steps, for example by combining methods from IEC 61508 with processes from ISO/ISO 15504-5, the exemplar assessment model for software engineering processes.

The continuous development of the Nuclear SPICE framework produces a novel solution to a specific business need i.e. the need to assess processes that are used to develop software with utmost safety requirements. Further integration work will be done in 2013 for example with Common Position and new emergent YVL guidelines for I&C systems.

Altogether, FiSMA Association has published five reports about Nuclear SPICE topic in CORSICA project:

- FiSMA 2011-1: Nuclear SPICE PRM and PAM [FiSMA 2011-1].

- FiSMA 2011-2: S4N Assessment Process – Requirements for Nuclear SPICE assessment [FiSMA 2011-2].

- FiSMA 2012-1: Nuclear SPICE PAM for pre-qualification process assessment [FiSMA 2012-1].

- FiSMA 2012-2: Nuclear SPICE assessment process [FiSMA 2012-2].

- FiSMA 2012-3: Framework to evaluate software reliability based on Nuclear SPICE [FiSMA 2011-3].

FiSMA reports 2011-1 and 2012-1 are mainly process reference models (PRM) and process assessment models (PAM). The full Nuclear SPICE PRM and PAM are included in 2011-1 report. The second Nuclear SPICE model report 2012-1 (this report) is more detailed and is limited to pre-qualification in software intensive I&C systems mainly in Category A. It means more detailed mapping of Nuclear SPICE with IEC 61513 and IEC 60880. Many basic requirements of Nuclear SPICE are published already in model report 2011-1 and are not repeated in 2012-1.

The three other FiSMA reports are about the assessment process. Report 2011-2 is the set of requirements for assessment process to be compliant with previous and current requirements in ISO family of SPICE standards (mainly ISO/IEC 15504-5:2012 and DIS version ISO/IEC 33002). Report 2012-2 describes in detail an assessment process to meet the requirements specified in report 2011-1. The assessment process is intended for performing systems and software process assessment in highly safety-critical environments in nuclear industry domain. Report 2012-3 presents selected articles and assumptions related to software reliability, and defines a framework to support evaluation of risks for software reliability using process assessment (see more chapter 1.3).

Also some conference and journal articles and tutorials are made from Nuclear SPICE topic during years 2011 and 2012 [Varkoi 2013].

Software reliability and process assessment

Software reliability is often understood as a strictly quantitative property. For instance, Systems and software engineering vocabulary defines: the probability that software will not cause the failure of a system for a specified time under specified conditions [ISO/IEC 24765]. Sometimes software is considered to be a system component and the same, time-based, failure probability calculations are applied.

Many of the literature references for software reliability and safety rely on probabilistic models. It seems that the same approach that has worked with electromechanical systems is believed to be applicable to software. The nature of software as a design rather than a product is largely ignored – software reliability is still a difficult concept. On the other hand, most of the publications refer in some way to the development process as a factor of software reliability.

The focus of the software reliability related work at U.S. NRC seems to have changed throughout the years. Lawrence emphasizes software life cycle to improve safety and reliability [Lawrence, 1993]. Smidts bases his work on heavy measurement of the development process to predict operational reliability [Smidts, 2011]. Chu tries to apply quantitative methods to model software failures for probabilistic risk assessment (PRA) [Chu, 2011].

The work of Leveson sets reliability in totally new light when pursuing safety. Safety is seen in a wider perspective and the role of PRA is questioned. The relationship between reliability and safety is rejected. Leveson states that high reliability is neither necessary nor sufficient for safety; and that highly reliable software is

not necessarily safe, increasing software reliability will have only minimal impact on safety [Leveson, 2011].

Fenton uses probabilistic approaches to predict software defects and reliability. His work is focused on using Bayesian networks, but with a combination of both qualitative and quantitative measures [Fenton, 2008].

Nevertheless, all approaches take into account the development process as a source of risks. Quantification is viable when studying the software product in operation as a system element, while qualitative approach is preferable when evaluating software during development phases. Software reliability could benefit of software development process modeling and evaluation as a means to reduce software-related risks.

Reliability can be seen as a characteristic of dependability. IEEE defines dependability as follows: trustworthiness of a computer system such that reliance can be justifiably placed on the service it delivers [IEEE 982.1]. Reliability, availability, and maintainability are considered to be aspects of dependability.

From process assessment viewpoint, software product characteristics serve as assessment evidence of an existing process. Process assessments are by nature based on sampling, and thus do not provide adequate data for probabilistic analysis. Therefore a wider view of dependability, including reliability, is appropriate for process assessment. Process assessment models can be further developed to take into account safety requirements and to address dependability issues. Then, the qualitative aspect of software reliability can be addressed by process assessments.

Nuclear SPICE process and assessment models are developed based on ISO/IEC 15504 principles. ISO/IEC JTC1/SC 7 Working Group 10 develops 15504 set of standards into a new set of 33000 standards. In this development, a new concept of process quality has been introduced. Process quality is composed of quality characteristics, where the required set of characteristics depends on the applicable stakeholder needs and organization's business goals. In addition, process quality shall be measurable. Process quality, by definition, means the ability of a process to satisfy stated and implied stakeholder needs when used in a specified context. Process quality characteristic is a measurable aspect of process quality; or a category of process attributes that are significant to process quality.

In a process assessment, each process is evaluated using a set of process quality attributes. As a result, when achievement of attributes is evaluated, better understanding of process related risk is gained. In this project, we specified tentative sets of process quality attributes for process assessment in safety domain. The basic set includes attributes that meet the elementary requirements for trustworthy software development. One of the attributes is dependability.

Coverage and rationality of methods

Functional testing plays a major role in the V&V of safety critical software of instrumentation and control (I&C) in nuclear power plants (NPPs). Functional testing aims to check whether there are any program errors in meeting particular aspects

of the given specification and whether all specified requirements have been met. A test data set is derived from the specification and the software is regarded as a black-box without any need to look at inside the structure of the software. Tests are based on requirements and functionality.

However, functional testing has some challenges. Firstly, as a test is derived from the specification, it can only detect non-conformance to that specification, and cannot be used to prove software correctness. Thereby, evaluations of the specification, and the test plans derived from the specification, are as important as evaluation of the results of the functional testing. Several methods and techniques can be used for this purpose. The standard IEC 61508 gives recommendations on using different methods based on the system's safety integrity level. Grades of rigor are also attached to each method or technique. There are also techniques to confirm the credibility of the testing process and results. Software reviews, inspections and walkthroughs are techniques to be applied to any artefact of system and software. They do not require execution of software, and they are very effective technique for discovering errors.

The second challenge is that full test coverage with respect to completeness and correctness is practically impossible. Because of impossibility to evaluate comprehensively safety and reliability of software, we have to think of what is sufficient or reasonable. In specific and well-defined circumstances, it is possible to prune issues from comprehensive set of arguments and evidence and still maintain sufficient safety and reliability of software. There are rules for supporting the pruning: reliability and safety goals and operational profiles are commonly used. For example, safety requirements are specified related to a Safety Class or a safety integrity level, SIL; the higher the SIL, the greater the amount of required arguments and evidence. Operational profile is used by analysing the software environment to tell criticality and frequency of the use of the software. As pruning is necessary, we have to evaluate cost of achieving reliability goals and risk of not doing so.

Comparing U.S. NRC reactor trip software review process to the Finnish regulatory requirements

Nowadays, several instrument and control (I&C) systems have been accepted by the U.S. Nuclear Regulatory Commission (NRC) and offered to Finnish nuclear markets. Identifying the difference between the NRC and STUK regulatory requirements makes the approval of their systems easier. We have identified the main differences between the review process of the NRC and the Finnish regulatory requirements when a typical reactor trip software system is reviewed. The comparison of the review processes is documented in a research report [Harju, 2012].

The NRC-IEEE framework emphasises analysis and making of plans, whereas the STUK-IEC framework emphasises the management of requirements. In U.S., the result of the D3 analysis (diversity and defence-in-depth) has a more significant

effect on whether there should be diversity between two systems. In Finland, the requirement for independence or diversity between systems or subsystems is much more absolute. D3 analysis is needed to justify that systems credited in one defence-in-depth level are sufficiently independent of systems credited in the other levels.

Safety classifications of I&C systems are different in U.S and Finland. In U.S, there are one safety class and four echelons of defence, which are only conceptual. The NRC does not imply that these echelons of defence must be independence or diverse. In Finland there are two safety classes and absolute safety borders between systems which belong to different safety classes.

Even though the differences between requirements for independence and diversity are not especially significant in these two cases, the significant differences are in the implementation of backup systems. Where in the USA the backup system is allowed to be a non-safety software based system, in Finland the backup system has traditionally been a safety classified non-software based system.

The references to the software development standards differ between the two approaches. NRC refers to IEEE standards and has prepared several guidelines to interpreting these standards. STUK mainly refers to IEC 60880, and has added requirements to YVL guides about software development. However, both approaches do not deny using other standards than IEC and IEEE.

Reading techniques

In software development it is very useful to locate defects in the early phases of the development life-cycle. The cost of an error found in requirements specification is much less than an error that is found in the testing phase. The nuclear domain typically follows conservative life-cycle models that are quite inflexible, and this effect might be even greater when the development cycle is rigid.

Reviews and inspections are typically used to locate software defects in the early life-cycle phases. In an inspection, a group of people examine a software document such as a requirements specification or a design document, and try to find defects in the document using mainly their expert judgement. Some strategies for better defect detection in software inspection have been developed. The most effective strategies have been advanced reading techniques that are written for guidance or a procedure that the inspector should follow. Based on empirical research (see e.g. [Lahtinen, 2012a] for a survey), perspective-based reading techniques that utilize different reviewer roles have been most effective.

Many perspective-based reading techniques exist. One variant is Perspective-Based Reading (PBR). The idea in perspective-based reading is to examine a software artefact description from the perspectives of the artefact's stakeholders in order to identify defects. The reasoning behind this is that a document is probably of high quality when potential stakeholders that use the document cannot detect any defects in it. Perspective-based reading is typically performed by a team of reviewers. The reviewers focus on different aspects of the document. For example, one reviewer examines the document from a tester's perspective, one review-

er from the designer's perspective, and one reviewer from the user's perspective. The second key characteristic of the PBR method is the active role of reviewers in the inspection. The idea is that the reviewer creates a high-level version of a work product that the user would normally create from their perspective. The intention is that, by producing work products themselves, the reviewers obtain a more profound understanding of the system, and thus are able to detect more defects that are difficult to find and not just superficial errors.

We have applied the generic PBR ideas to the review of nuclear domain conceptual design plans, see [Lahtinen, 2012b]. A conceptual design plan is a high-level design document that is used as input when the detailed design of the system is made. We first analysed the development life-cycle and the use of the conceptual design plans by interviews. Based on this analysis we developed a review technique that consists of five different review perspectives. Separate review instructions (i.e. a scenario) were written for each perspective: an automation designer scenario, a control room designer scenario, an electrical designer scenario, a safety designer scenario, and a regulator scenario. The main novelty of the developed technique is that the reviewer can try to simulate the future work phases, and try to anticipate what kind of practical issues may not have been considered in the conceptual design phase.

One of the developed scenarios was tested to review a real conceptual design document. The review was performed by an automation designer working in the project organization related to the case study. The reviewer made nine findings using the technique. The developed method was considered to be effective, and the reviewer found several omissions and ambiguities in the reviewed document. In the reviewers own experience, the technique was helpful for finding defects and more effective than the technique usually used.

In conclusion, the more rigorous perspective-based review methods cannot completely replace the more traditional check-list based methods. However, the perspective-based reviews can be used to complement the existing review techniques where necessary.

Use of novel technologies in nuclear power plants

Interest in the use of field programmable gate array (FPGA) technology in nuclear power plant (NPP) automation has increased in recent years. The technology itself is not new and is widely used in other areas, such as telecommunication, but it is new in nuclear power generation and in particular in safety related systems. Old analogue and micro-controller systems are becoming obsolete and need to be replaced. At the same time, decisions on the technology to be used in new plants need to be made.

The experience of software-based systems is that demonstrating their reliability and safety in the licensing process is difficult and laborious. FPGAs are seen as an option that provides flexibility and capability similar to software but with a lower complexity, simpler system structure, and improved performance characteristics of

hardware. Many of the advantages come from having all functions implemented with dedicated hardware and no operating systems or similar layers of additional functionality or sources of interference between functions.

Cyber security issues are also considered to be lesser with FPGAs than with software because an FPGA can contain all of the memory and functions and it is difficult, or impossible for certain technologies, to alter it, for example, make the device run malware. Although the operational security is considered better, the development process may be more vulnerable to malicious acts due to the use of several software tools.

While there are advantages, there are also risks involved. The suitability, reliability, and possible problems of licencing a novel technology in the nuclear power generation domain all have uncertainties. Also the lack of harmonised guidance and regulations for FPGA-based systems in NPPs hinders the wider adoption of FPGA-based applications especially in safety-related systems. Work is being done for example by the IAEA to come up with a consistent guide to the development and use of FPGA-based systems in NPPs.

The FPGA device itself is a semi-conductor silicon chip with a regular array of transistors. As such it has no functions. The device can be configured (programmed), and in many cases re-configured, for a task after manufacture by configuring the connections between the components on the chip. This allows standardised mass production of the devices independent of the applications for which they are intended. This, in turn, provides advantages for the development process and manufacture as it makes them cheaper and more flexible.

Figure 2. An Actel FPGA device.

Application development based on FPGAs has much in common with software development. It is highly dependent on software tools, which can be sources of errors themselves but also create an illusion of simplicity by allowing easy construction of complex behavior. The initial stages of development are also rather similar in requirements specification, architectural design, and use of hardware description languages similar to programming languages.

The final product, however, is a hardware device without an operating system that would execute a program one step at a time. Instead, all operations run in parallel with separate hardware for each function. Thus, the last stages of application design have a much more hardware-oriented character, and they are similar to those found in integrated circuit design. The designer needs to take into account things such as the layout of transistors on the silicon chip, signal propagation and timing properties, and power consumption.

The risks associated with FPGAs and software-based systems have much in common. The correctness of the functioning may be difficult to prove due to com-

plexity of the system and the layers of design tools between the requirements specification and the final product. Because the technology is new in the nuclear power generation industry, there is little experience of what it is most suited for or how it should be implemented.

The work on bringing FPGAs into wider use in nuclear power plants is ongoing. There are already dozens of implemented systems in NPPs and new systems and platforms are under development. The focus is currently on replacing obsolete systems. Both analogue systems and microcontroller based systems have been replaced. One approach has been to emulate an old no-longer available microprocessor with an FPGA but otherwise retain the design.

In the first year (2011) of CORSICA project, a literature survey of FPGA technology and its current situation in the nuclear domain was conducted and a report published in the VTT Technology series [Ranta, 2011]. The report covers technological aspects, application design, reliability considerations, and the situation of currently existing FPGA based safety related systems.

In 2012 a case study was used to take a closer look at application design, implementation and verification. A logic circuit called the Stepwise Shutdown System (SWS) was implemented. The case study gave a good overview of the FPGA design process from the requirements to the actual programming and testing of the device. Although some comprehensive testing methods were developed, the analysis of the output-file data is still rudimentary. The design was successfully tested against the requirements specification, via both simulation and hardware testing, which was the main purpose of the testing in the case study. The case study is documented as a research report, see [Lötjönen, 2012].

In the future the SWS case study will be expanded to cover additional systems. These include multiple FPGAs running in parallel, additional external devices such as sensors and a serial connection between a PC and the FPGA to be able to do more comprehensive testing.

References

[IEC 61508] IEC 61508-3:2010, Functional safety of electrical/electronic/programmable electronic safety-related systems Part 3: Software requirements, IEC 2010.

[IEC 60880] IEC 60880:2006, Nuclear power plants – Instrumentation and control systems important to safety – Software aspects for computer-based systems performing category A functions. IEC 2006.

[IEC 62138] IEC 62138:2004, Nuclear Power Plants – I&C Systems Important to Safety – Software Aspects for Computer Based Systems Performing Category B and C Functions, 2004.

[IEC 61513] IEC61513 (FDIS 2011) Nuclear power plants – Instrumentation and control for systems important to safety – General requirements for system. IEC 2011.

[ISO/IEC 330xx] ISO/IEC 330xx, Information technology – Process assessment. Family of new standards for Process Assessment. ISO 2013.

[FiSMA 2011-1] FiSMA 2011-1: Nuclear SPICE PRM and PAM.

[FiSMA 2011-2] FiSMA 2011-2: S4N Assessment Process – rRequirements for Nuclear SPICE assessment.

[FiSMA 2012-1] FiSMA 2012-1: Nuclear SPICE PAM for pre-qualification process assessment.

[FiSMA 2012-2] FiSMA 2012-2: Nuclear SPICE assessment process.

[FiSMA 2011-3] FiSMA 2012-3: Framework to evaluate software reliability based on Nuclear SPICE.

[Varkoi 2013] Varkoi, T., Nevalainen, R., Mäkinen, T. Toward Nuclear SPICE – integrating IEC 61508, IEC 60880 and SPICE. Journal of Software: Evolution and Process (2013).

[ISO/IEC 24765] ISO/IEC/IEEE 24765:2010, Systems and Software Engineering Vocabulary.

[Lawrence, 1993] Lawrence, J. D. Software Reliability and Safety in Nuclear Reactor Protection Systems. 1993, NRC, CR6101.

[Smidts, 2011] Smidts, C. S. et al. A Large Scale Validation of a Methodology for Assessing Software Reliability. 2011, NRC.

[Chu, 2011] Chu T.-L. et al. Development of Quantitative Software Reliability Models for Digital Protection Systems of Nuclear Power Plants. 2011, NRC.

[Leveson, 2011] Leveson N.G. Engineering a Safer World: Systems Thinking Applied To Safety. 2011, MIT.

[Fenton, 2008] Fenton N., Neil M., and Marquez D.: Using Bayesian Networks to Predict Software Defects and Reliability. Proceedings of IMECHE 2008.

[IEEE 982.1] IEEE 982.1-2005, IEEE Standard Dictionary of Measures of the Software Aspects of Dependability.

[Lahtinen, 2012a] Lahtinen, J. 2012. Application of the perspective-based reading technique in the nuclear I&C context. CORSICA work report 2011. Espoo, VTT. 45 p. + app. 7 p. VTT Technology 9. ISBN 978-951-38-7621-0. http://www.vtt.fi/inf/pdf/technology/2012/T9.pdf.

[Lahtinen, 2012b] Lahtinen, J. 2012. Development of a review technique for conceptual design plans, VTT. 29 p. Research Report; VTT-R-08337-12. http://www.vtt.fi/inf/julkaisut/muut/2012/VTT-R-08337-12.pdf.

[Ranta, 2011] Ranta, J. 2011. Current state of FPGA technology in a nuclear domain, VTT Technology 10. Espoo, Finland.

[Harju, 2012] Harju, H. 2012. Planning a review process for software of reactor trip system. Supplementary requirements to U.S. NRC. Research Report VTT-R-06436-12. Espoo, Finland.

[Lötjönen, 2012] Lötjönen, L. 2012. FPGA Implementation of the Stepwise Shutdown System. VTT Research report. VTT-R-06053-12. Espoo, Finland.

3.2 Human-automation collaboration in incident and accident situations (HACAS)

Jari Laarni, Iina Aaltonen, Hannu Karvonen, Hanna Koskinen, Paula Laitio, Jari Lappalainen, Marja Liinasuo, Leena Norros, Paula Savioja, Mikael Wahlstöm

VTT Technical Research Centre of Finland
Vuorimiehentie 3, P.O. Box 1000, FI-02044 Espoo

Introduction

Effective and efficient functioning of the operating personnel plays a key role in the safe production of nuclear power. Currently, the general view is that the main objective in safety management is to ensure the resilient functioning of the whole sociotechnical system, especially during events that have some characteristics that are difficult to anticipate. Resilience at the operational level is mainly based on continuous and active monitoring of the power process and on regular training of personnel. More research is needed on how the resilient activities of control room (CR) crews develop during digital instrumentation and control (I&C) and CR upgrades in nuclear power plants (NPPs).

New safety automation with new emerging operating procedures (EOPs) and advanced safety human-system interfaces (HSIs) will change operator practices in accident situations. Operators have to successively monitor and operate several HSIs located in different places around the CR. New safety automation based on digital technology is also somewhat more complex on its architecture and functionality which may have an impact on automation skills and automation awareness. Apparently, the introduction of digital automation and HSIs has safety implications, and therefore new tools and practices are needed to help to manage possible problems caused by digital I&C systems.

Figure 1 portrays the main activities of the HACAS project in the program period of 2011–2014. The project focuses on studying how digital automation and CR upgrades affect resilient performance of CR personnel, and how humans and automation systems collaborate to accomplish safety and production goals of NPPs. Specifically, the project aims at gathering knowledge of control room operators' procedure usage and human-system interaction in accident management, with the aim to identify the operators' capabilities of supporting resilience of the entire system. The project also contributes to identifying Human Factors Engineering (HFE) considerations that are important in the selection of CR modernization strategies. In more focused studies the use of interactive large screen displays in process control is investigated. An important further task is to develop a new type of requirement-based validation approach for stepwise implementation of CR changes. In this connection, new ways of implementing risk assessment methods in the validation are also studied. The final issue under investigation is the effect of the operators' automation awareness on operator behaviour in incident situations. Methods and tools are developed for the evaluation of automation awareness and competence.

		2011	2012	2013	2014
TASK 1	**Operating procedures** in incident/accident management	Procedure guided activity	Procedure design	Procedure as a user interface	ConOps-based human-automation collaboration
TASK 2	**Human-system interface solutions** for supporting human-automation	Operator activities in accident management HSI design	HSIs in accident management	Accident management ConOps HSI design	
TASK 3	**Automation awareness (AA)** and its development and support	Concept definition Simulator environment design	Measurement of AA Simulator environment design	Automation competence and automation awareness Simulator tests	

Figure 1. Overall work plan of the HACAS project for 2011–-2014. Each year, special focus is placed on one of the three tasks (as depicted by the green background colour).

In 2011–2012, the research in the project has focussed on five main areas: First, we have studied the effect of routines of procedure usage on the management of severe accidents, the parallel use of EOPs and safety HSIs in accident management, and the procedure design process from the HFE perspective. Second, we have studied the effect of digital I&C systems on operator practices in accident situations. Third, we have identified challenges in the design of interactive large screen displays for the simulator environments. Fourth, we have prepared a literature review on operators' automation awareness and on the effect of automation complexity on automation awareness and automation skills. Fifth, we have designed an Apros-based simulation demonstrator for testing automation awareness in experimental settings.

The rest of this paper is organized as follows: we first present the modelling and analysis tools developed for the ecological investigation of activity, and after that, we present two examples of the application of the proposed framework.

Modelling and analysing operator work practices

Different approaches can be taken to analyze and model safety of complex sociotechnical systems, e.g., nuclear power plants. A typical approach has been to try to identify the sequence of events that has leaded to an accident. These kinds of linear or causal models have their problems, however, and there has been a shift in focus to investigate how safety can be supported and designed in different organizational levels.

In general, it has been suggested that systemic models are needed to identify different types of variance in the system's performance and analyze which variance is beneficial for adaptation and which leads to an uncontrolled situation [1]. In fact, according to the resilience engineering framework, one of the main research tasks in safety science is to identify manifestations of both possible resilient and threatening behaviours before any accident has occurred.

The approach to be described in the following has been developed in order to analyse operator practices from system resilience point of view. One of the key drivers in our work has been that operator practices and technologies used in work play an important role in the emergence of resilience. The main objectives are thus to support design of HSIs and develop concept of operations taking into account the requirements of different operational states. Methodologically, the approach can be considered as an ecological one, according to which the context in which activity takes place plays an important role in shaping human experience and action. Technologies are considered part of the environment but the mediating role of technologies and other artefacts in the human-environment interaction is acknowledged.

Steps of ecological analysis of practices

There are five main steps in the resilience-based analysis approach (Figure 2) that are next described, and some examples of their applications are provided (for a recent overview, see [2]). The steps have been presented in a particular order, but the analysis can be accomplished in the order most useful to each application case.
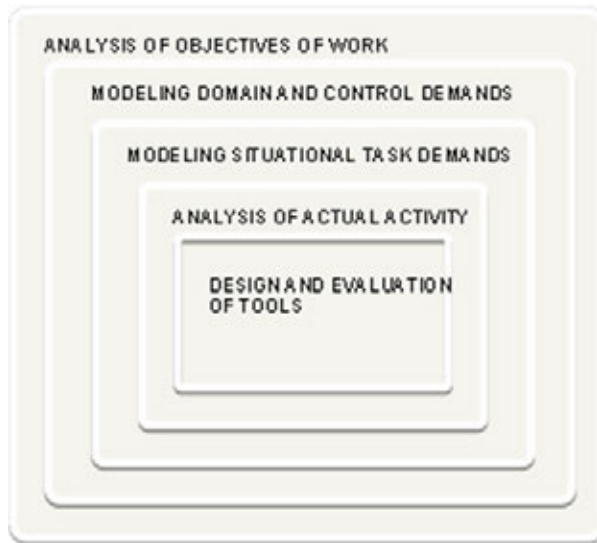

Figure 2. Overview of the ecological analysis of activity.

Firstly, it is possible to analyse the work system (illustrated in Figure 2 as the outermost ring) in order to identify the global tendencies of its development, and understand the demands that the optional, and possibly contradictory objectives put on the work organisation and its processes. Based on this kind of analysis, general hypotheses concerning the requirements for the control of the system can be formulated.

In the second step of analysis "Modeling domain and control demands" the attempt is to identify the core-task demands that the work puts on the actors. A modeling tool is used that identifies particular control demands typical of the domain with regard to three generic system features, i.e. *dynamicity*, *complexity* and *uncertainty* (DCU characteristics). The generic means of tackling these control demands on individual and team level are seen to call for three types of resources, i.e. *skills*, *knowledge* and *collaboration*. When connecting each of these resources with each of the control demands nine types of work demands, i.e., core-task demands emerge:

- Control of dynamicity involving
  - readiness to act in situation (skill-related)

- ▪ anticipation and identification of weak signals (knowledge-related)
- ▪ effective sharing of resources (collaboration-related)
- Control of uncertainty involving
  - ▪ flexibility and re-orientation (skill-related)
  - ▪ interpretation in action (knowledge-related)
  - ▪ dialogical communication (collaboration-related)
- Control of complexity involving
  - ▪ focusing on critical features (skill-related)
  - ▪ conceptual mastery of the domain (knowledge-related)
  - ▪ shared division of responsibility (collaboration-related).

The third step of analysis is called as "Modeling situation task demands". We have developed the so-called Functional Situation Model (FSM) method for concretising how the core-task demands portray in a particular temporally ordered process control situation. The FSM model provides both temporal and functional perspectives on a particular operational situation, and it can be used as a reference against which the actual operator behaviour can be analyzed. FSMs have been, for example, utilised in the validation of CR HSIs from the point of view of systems usability.

Our analysis of practices is based on comprehensive empirical data from the field or from simulated real-like situations. Interviews, observations of performance and process-tracing group discussions are used to reach an understanding of the details of the crew's performance. Out of these analyses of actions, and using the functional situation models, we then select episodes for further analysis. The fourth phase of the analysis is to identify a more generic pattern of behavior on the basis of the particular instance. We call these behavioural patterns *habits of action*, the content of which portray different aspects of activity, e.g. habits of searching information and habits of communicating with the crew. Habits of action may vary, reflecting different levels of interpretative power, i.e. there may be interpretative, confirmative or reactive reactions (for a theoretical basis of the classification scheme, see [3]). *Interpretativeness* is characterised by presence in the particular situation and questioning the observed phenomena and building expectations concerning the situation and future events. *Confirmativeness* means taking the situation for granted and acting in a predefined way; *reactiveness*, in turn, reflects passivity and lack of expectations concerning the situation. Their evaluation and classification are based on the objectives and actions connecting to them. Recently, this analysis approach has been applied in the analysis of operators' conceptions of procedure guidance in NPP process control [4].

The final step of analysis of practices is to study the relationship between operator behaviour and the used technologies. Three generic tool functions can be identified (Figure 3): The *instrumental function* is related to the effectiveness of the tool in its main purpose. The *psychological function* relates to the tool's role to shape human acting and to the need to design tools so that the tool-user system is as smooth as possible. By *communicative function* we mean that the tool enables collaboration and mediates shared forms of acting and thinking within the community of practice, and even wider. Tool usage needs to be evaluated not only with

regard to the performance outcome it enables, but also with regard to the practices it facilitates, and according to how promising the users think the tool is with regard to their needs and values. A three by three grid is formed out of these two dimensions, and as a result, nine different types of measures for the quality of "systems usability" emerge as shown in Figure 3. Using the metrics we may evaluate which tool functions are fulfilled best, and also identify whether the tool supports the pre-defined performance outcome, or whether it also has capabilities to facilitate interpretative practices and is experienced to provide added value for work in the future.

Figure 3. The Systems Usability Framework.

Two examples of the application of the analysis tools

Next, two examples are presented illustrating the application of the framework in the HACAS project to the analysis of the design process and to the modeling of operational scenarios.

Modelling the design process of the Virtual panel systems

Figure 4 shows how this kind of analysis can be used in the identification and tabulation of innovative features of so called "Virtual panel system", an interactive large screen display system that has been implemented into the Fortum Loviisa training simulator [5]. The first task was to define the work demands which should be supported by the designed technology. The work demands are characterised by the core-task demands and the generic tool functions of the technology. Systems usability is achieved when these demands are sufficiently fulfilled.

The model of the Virtual panel design is divided in two parts, i.e. *the Human System Interaction concept* and *the Interface.* Both of these are then portrayed in two ways, *the requirements* and *the solutions* which represent two levels of the design process. Requirement- and solution-level concepts and interfaces are then linked to some of the core task demands and tool functions that were described

above. HSI concept requirements are associated with training, process control, process monitoring and communication and collaboration; the interface requirements, in turn, set standards for monitoring and control of capabilities of the proposed system. The model suggests that the Virtual panel system can and should be evaluated in many levels of details, i.e., from its concept level requirements and solution point of view as well as the interface requirement and solution level.
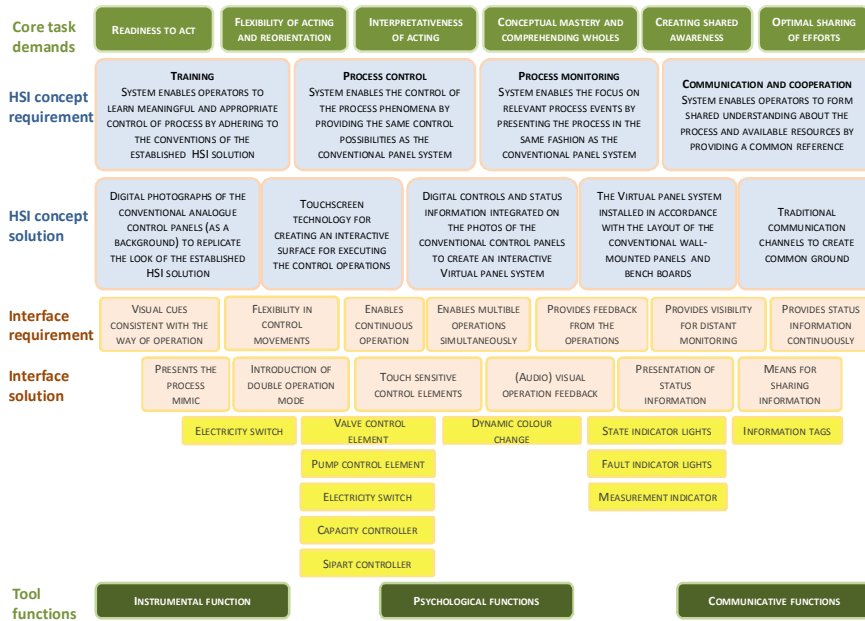

Figure 4. Model of the Virtual panel system design. The core task demands and the tool functions are portrayed by green boxes, HSI concept requirements and solutions by blue boxes and interface requirements and solutions by light orange boxes. [5]

Functional Situation Models in the analysis of operator practices

Functional situation models have been constructed for the analysis of simulated incident and accident scenarios. As mentioned above, FSMs provides two viewpoints to the modelled situation, chronological and functional (for more details, see [6]). These two dimensions define a two-dimensional space in which the most important operator actions and process phenomena are mapped.

In the chronological view the scenario (e.g., accident management following a simulated loss of coolant accident) is divided into different phases based on the goals of the operating activities. In the FSM the chronological phases are labelled according to the goals: detection, mitigation of effect, diagnosis, and stabilisation

of the process state. Although the four phases can be differentiated from each other, in real activity all the goals are somehow present simultaneously.

In the *detection phase* of a simulator run, the crew identifies some process events requiring operator actions. The process information presented to the operators is typically alarm information and notifications. This information enables the operators to understand the deviations in the process and to identify and explicate the initial events. In the *mitigation phase*, the operators' task is to alleviate the consequences of the failures. Some operating actions are tuned more towards mitigating the situation than monitoring the situation. In the mitigation phase, the operating actions that mitigate the process situation are mapped under the specific process information, and initial events of the detection phase that they are connected to. As the ultimate operating goal in an accident situation is to bring the process into a stable safe state, diagnostic actions are required from the operating crew. It is important to realise what the process situations are, in order to identify the required actions. In the *diagnosis phase* these actions are depicted in the model under the specific parameters of detection phase that they are related to. The *stabilisation phase* refers to the operating activities which aim at bringing the process into a safe and stable state. These actions are also connected to the relevant initial events.

A functioning sociotechnical system has the objectives of production, safety, and health [7]. These objectives form the basis of the functional view of the FSM (the three vertical paths in Figure 5). The most important items in the functional view are the critical functions of the process which are endangered in a specific situation. These functions can be, depending on the initial events, related to safety, production, or health. Typically, in a complex situation there are critical functions related to all of the above mentioned objectives which are endangered.

Operating activity, on a high level, is oriented towards maintaining the critical functions of the process. Thus, the operating actions required in the situation can be collated under general means to respond to the endangerment of the critical functions. This is depicted in the FSM by presenting a specific functional level in the model "functional means to respond". This level connects the individual operating actions to the critical functions. The relationship with the critical function level upward and with individual actions downward is of type means-ends, i.e., the operator actions are defined that are required for achieving the critical functions.

By connecting the individual level actions of the crew and the functional view to the situation, it is made explicit what is the meaning of each action in the wider context of the scenario. This important feature of the FSM enables the analysis of operating activity on the level of practice. In fact, we propose that this connection in action makes operating practice resilient in a situation.

In order to identify the critical functions in a situation it is important, first, to analyse the domain on a general level. We therefore consider the domain from the point of view of the three DCU characteristics that were introduced in 1.2.1. The core task of a work accomplished in a particular work domain is to take these characteristics into account in all situations. Coping with the DCU characteristics requires that the actors are capable and willing to mobilise resources related to

skills, knowledge and collaboration [8]. Resilience emerges from the ability of the actors to tackle the DCU features of a particular situation, and thus to fulfil the core task. Therefore, in Functional Situation Modelling the DCU features have to be considered, and the practices of tackling the situation are assessed with reference to managing the core-task demands.
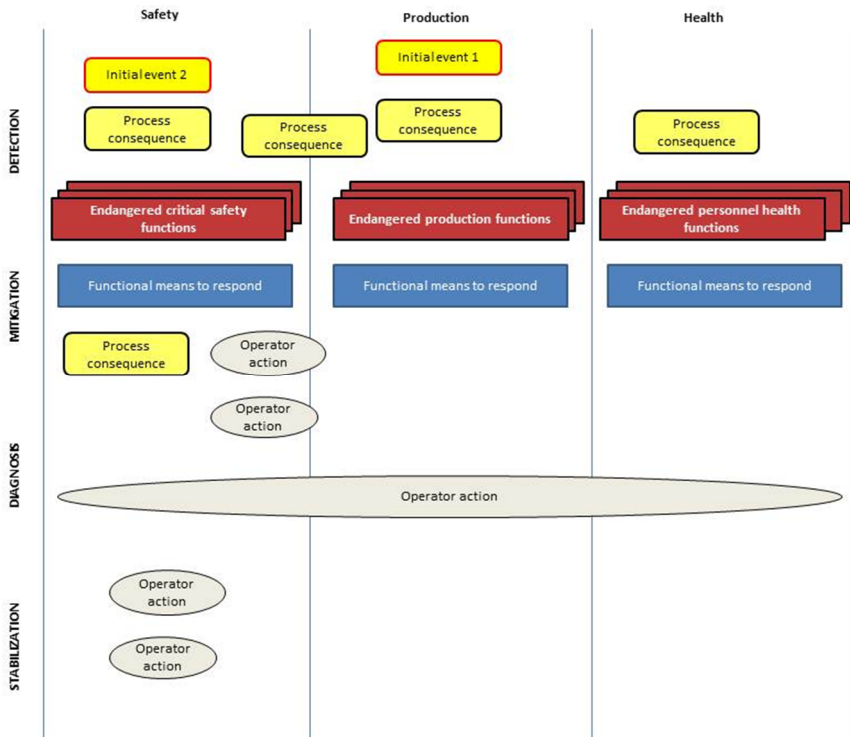

Figure 5. The general structure of a FSM. In modelling a scenario with a FSM, the boxes describing process events and information (yellow), critical functions (red), and operator actions (grey) are depicted connected to the critical functions and to the operative means to mitigate the functions (blue). The description is organised according to the chronological phases (detection, mitigation, diagnosing, and stabilization) according to the scenario in question. [6]

One of the strengths of FSMs is that they describe human activity in connection to the process system which is controlled by the automation and CR operators. By describing the functioning of this joint system the FSM connects the description of human activity and technical systems. The FSM also addresses the collaborative and distributed character of human activity. In the FSM model, activity is portrayed on the level of an operating crew but the actions of individual persons can also be depicted. Similarly, connections that exist between the actions of different individuals can be modelled. In complex work, cognition can be interpreted to be distrib-

uted among human actors, automation systems and for example operating procedures. In an FSM the role of each of these actors can be depicted in connection to the critical functions of the domain. We propose that the orientation of practice towards the critical functions of the domain makes the practice resilient.

Conclusions

Tools are needed for modelling and analysing HFE activities at different stages of the design process. For example, when conducting validation tests in the simulator, we have to model operator practices both before and after simulator runs. Before the test runs, the aim is to develop a conceptual basis for the assessment, and understand, analyze and describe the task-specific requirements for operator activity. If there are not detailed enough models of the tasks, it is not possible to attend to key activities during simulation runs and ask relevant questions during interviews and process-tracing group discussions. For example, the FSM provides the researchers a useful instrument to help to understand what is going on in the nuclear process system, and how the CR operators are expected to manage the situation. After the test runs, modelling tools are, in turn, needed for the organisation of test data and for the identification of important information. Several approaches to model and analyse HFE activities have been developed and used in the HACAS project.

The systems usability analysis tools has been applied for empirical evaluations of NPP CRs. In these studies we have found that performance-based criteria deliver important information of the tool's instrumental capabilities, and the practice-based and user experience-based measures are particularly valuable in informing of the tool capabilities with regard to the psychological and communicative functions. For example, we have found that the operators typically have some difficulties to utilize the features of the new digital HSIs, and we also have found clear differences in the use of process information among the teams. These results are important in judging the tool's capability to support resilience in the organisation.

References

1. Hollnagel, E., Woods, D.D., Leveson, N. (eds.). Resilience Engineering. Concepts and Precepts, Ashgate, 2006.

2. Norros, L. Analysis of work practices from the resilience engineering perspective. Nuclear Safety and Simulation, 3(4), 2012.

3. Peirce, C.S. The Peirce edition project. Introduction. In: T.P.E Project (Ed.), The Essential Peirce. Selected Philosophical Writings (Vol. 2, XVII-XXXVIII), Indiana University Press, 1998.

4. Norros, L., Liinasuo M., Savioja, P. Operators' conceptions of procedure guidance in NPP process control. (Submitted.)

5. Koskinen, H. Interactive Large Screen Displays in Process Industry. VTT, 2011.

6. Savioja, P., Norros, L., Salo, L. Functional situation models in analyses of operating practices in complex work. In: Proceedings of 30th European Conference on Cognitive Ergonomics, Edinburgh, UK, 29.–31.8.2012.

7. Vicente, K.J. Cognitive Work Analysis. Toward a Safe, Productive, and Healthy Computer-based Work, Lawrence Erlbaum, 1999.

8. Norros, L. Acting under Uncertainty, VTT, 2004.

3.3 Safety evaluation and reliability analysis of nuclear automation (SARANA)

Kim Björkman [1], Keijo Heljanko [2], Jan-Erik[1]Holmberg, Tuomas Kuismin [2], Jussi Lahtinen [1], Tero[1]Tyrväinen, Janne Valkonen[1]

[1]VTT Technical Research Centre of Finland
Vuorimiehentie 3, P.O. Box 1000, FI-02044 Espoo

[2]Aalto University
P.O. Box 11000, FI-00076 AALTO

Introduction

The general objective of the SARANA project is to develop methods and tools for safety and reliability analysis of digital systems and to utilize them in practical case studies. The project covers various topics and aims to build bridge between risk analysis and automation experts. SARANA provides guidelines to analyse and model digital systems in Probabilistic Risk Assessment (PRA) context, brings together deterministic and probabilistic analyses for safety assessment of plant designs, develops the reliability analysis tool YADRAT, develops an iterative and automatic algorithm for modular model checking of large systems, and develops more efficient methods for systematic model checking of asynchronous systems. This summary report introduces the on-going work and some of the intermediate results of the project.

Digital systems reliability

Reliability analysis of digital systems in PRA context

To assess the risk of nuclear power plant (NPP) operation and to determine the risk impact of digital systems, there is a need to quantitatively assess the reliability of the digital systems in a justifiable manner. The Probabilistic Risk Assessment (PRA) is a tool which can reveal shortcomings of the NPP design in general and PRA analysts do not have sufficient guiding principles in modelling particular digital components malfunctions [NEA/CSNI/R(2009)18].

OECD/NEA CSNI Working Group on Risk Assessment (WGRisk) has set up a task group, called DIGREL, to develop taxonomy of failure modes of digital components for the purposes of PRA. The taxonomy is aimed to be the basis of future modelling and quantification efforts. It will also help define a structure for data collection and to review PRA studies. DIGREL task has taken advantage from R&D activities, actual PRA applications as well as analyses of operating experience related to digital systems in the member countries. The taxonomy includes both protection and control systems of a NPP, though the primary focus is on protection systems. The taxonomy is organised hierarchically into the following levels (Figure 1): 1. the entire system (e.g reactor protection system), 2. a division (or channel), 3. I&C units, 4. modules, 5. basic components. A representative fictive digital protection system example has been developed to demonstrate the applicability of the taxonomy in the transparent manner. [NET-44-5-2012, PSAM11_10-Th4-1, PSAM11_10-Th4-3, NPIC & HMIT 2012_724]

Failure modes are defined functionally. At the system and division level, there are basically two failure modes: "failure to actuate the function" and "spurious actuation". At lower levels (I&C unit, module, basic component), it is relevant to consider more aspects of failure modes, i.e., the fault location (in which hardware or software module the fault is located), local effect, and detection situation. The combination of fault location, local effect, detection situation together with the fault tolerant design of the system are usually sufficient to determine the functional end effect, such as

- Loss of all functions (outputs) of the I&C unit,
- Loss of a specific function,
- Spurious function.

The above list is not exhaustive, and, e.g., for voting logics or in case of intelligent validation of input signals the functional end effect may be more complex (e.g. degraded voting logic). Anyway, the module level (both hardware and software) seems to be sufficient to analyse dependencies important to PRA, at least for protection systems.

In a Nordic activity parallel to DIGREL, a comparison of Nordic experiences and a literature review on main international references were performed [NKS-230]. The study showed a wide range of approaches and solutions to the challenges

given by digital I&C, and also indicated that no state-of-the-art currently exists. An existing simplified PRA model has been complemented with fault tree models for a four-redundant distributed protection system in order to study and demonstrate the effect of design features and modelling approaches. The model has been used to test the effect of common cause failure (CCF) modelling, fail-safe principle and voting logic. [Gustafsson 2012, NKS-261, NPIC & HMIT 2012_278]

Software failures are either omitted in PRA or modelled in a very simple way as a CCF related to the application software of the operating system. It is a difficult basis for the numbers used except the reference to a standard statement that a failure probability 10-4 per demand is a limit to reliability claims, which limit is then categorically used as a screening value for software CCF. Bayesian belief network (BBN) is a potential approach for the estimation of software reliability. Possible pieces for evidence to be used as input to the BBN model are operational experience or testing, software complexity analysis, V&V process quality. SIL [IEC EN 61508] may be used as a prior distribution. An advantage of BBNs is that they enable combining different types of evidence in the same model. [VTT-R-09293-11, PSAM11_10-Th2-2, PSAM11_10-Th2-4]
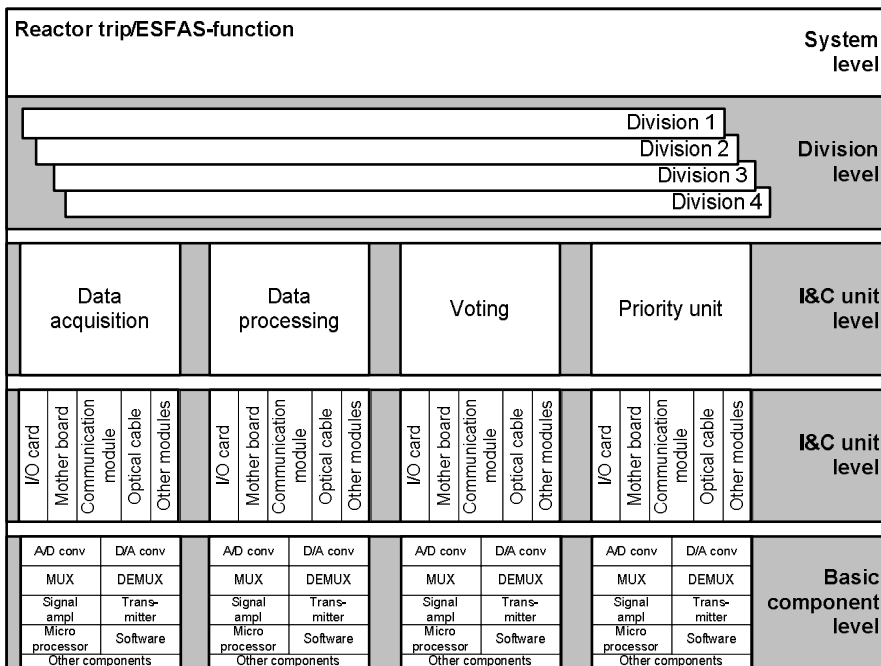

Figure 1. Structuring of the reactor protection system into different levels of details.

Reliability analysis of digital through dynamic flowgraph methodology

Dynamic flowgraph methodology (DFM) is an approach to modelling and analysing the behaviour of dynamic systems for reliability assessment and verification. In DFM models, the logic of the system is expressed in terms of causal relationships between the physical variables and the states of the system. The time aspects of the system associated with, e.g., the execution of control commands or the dynamics of the process are represented as a series of discrete state transitions and time delays.

DFM can be used to identify how certain top events (typically a system failure) may occur in a system. The result is a set of prime implicants that represents the system faults resulting from diverse combinations of software logic errors, hardware failures and adverse environmental conditions. A DFM analysis corresponds to a minimal cut set search of a fault tree, and prime implicants are similar to the minimal cut sets of fault tree analysis.

The YADRAT tool [Björkman et al. 2013], [PSA2011-80] developed at VTT is based on interpreting the DFM model as a Binary Decision Diagram. Figure 2 illustrates a simple YADRAT model. The objective is to develop a qualified tool for the reliability analysis of dynamic systems. YADRAT has been implemented in such a way that the DFM model can be translated into SMV (Symbolic Model Verifier) code that can further be examined with the formal model checking tool NuSMV.

An improved BDD based algorithm to solve prime implicants has been developed in the SARANA project, and a functionality to compute risk importance measures and to model common cause failures has been implemented [PSAM11_30-Th4-1]. After that, the BDD based algorithm to solve prime implicants has been enhanced improving both the memory consumption and computation times. With the optimization of the computation algorithm the memory consumption has decreased on average by 80% and the computation times have decreased on average by 90%. Also the functionality to compute risk importance measures and to model common cause failures has been improved. Additionally, an algorithm to compute the accurate top event probability has been developed.

The correctness of YADRAT has been analysed through several case studies. However, the analysed example systems have mainly been moderate sized systems. That is why one of the near future objectives is to perform a new case study to test how well DFM is suited for large systems and to test the scalability and usability of YADRAT to such systems. Another objective is to perform a comparison between the PRA software FinPSA and the YADRAT tool. The idea is to compare the benefits and limitations of both tools in modelling digital I&C systems and to compare the modelling effort and computational efficiency of the tools. A long term objective of the YADRAT development is to integrate it to FinPSA.
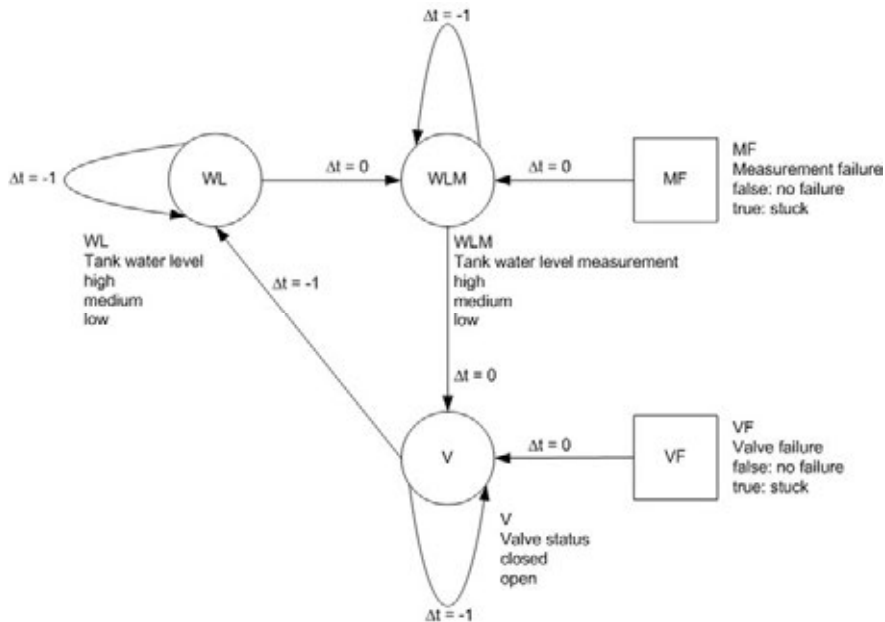
Figure 2. A simple YADRAT model [Björkman et al. 2013].

Model checking

Model checking is a computer-aided verification method developed to formally verify the correct functioning of a system design model by examining all of its possible behaviours. The models used in model checking are quite similar to those used in simulation, as basically the model must describe the behaviour of the system design for all sequences of inputs. However, unlike simulation, model checkers examine the behaviour of the system design with all input sequences and compare it with the system specification.

Formal analysis of large systems

Model checking has been successfully used to analyse individual functions of safety-critical I&C systems [Lahtinen et al. 2012]. However, it is often necessary to examine several functions simultaneously, because the functions may influence the same system parameters. A system may also have several redundant implementations, whose joint behaviour should also be covered. Applying the current model checking methods in a straightforward manner is not always possible in these large and complex systems, because the behaviour of the models becomes too rich (due to the state explosion problem).

The state space explosion can be controlled by creating more efficient modelling techniques. We have developed an iterative abstraction refinement technique for verifying large modular systems.
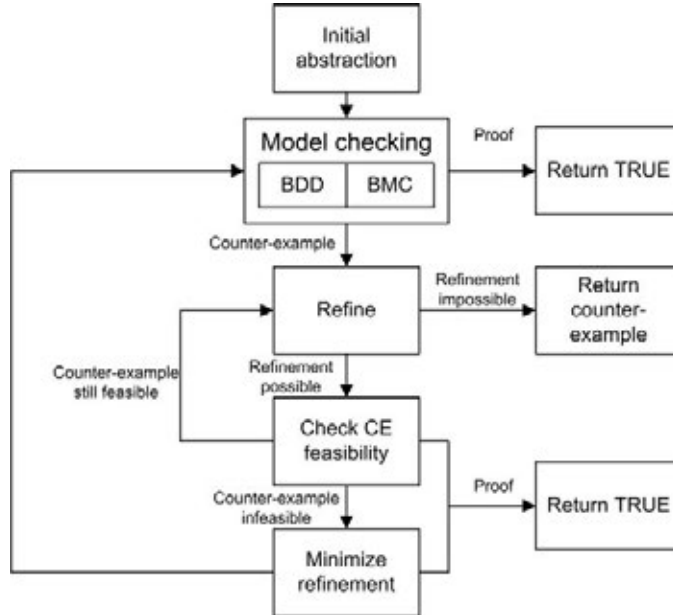

Figure 3. Overall algorithm for verifying large modular systems by model checking.

In our technique the system is divided into modules. Abstractions of the model are created by replacing a subset of the modules with non-deterministic interface modules. Iterative abstraction refinement is used to obtain a computationally manageable subset of the modules that is sufficient for proving the given formal specification. Our refinement procedure is based on traversing the dependency graph of the modules, and first finding some feasible refinement to the abstraction. The feasibility of the refinement can be checked rather quickly using a bounded model checking algorithm. After finding a suitable refinement, we use heuristics to minimize that refinement. In order to improve the performance of our technique we utilize two model checking algorithms in parallel. The overall algorithm is depicted in Figure 3.

We have applied the developed technique in the verification of an emergency diesel generator control system [MEMICS 2012]. The system is safety-critical, as emergency diesels are used e.g. in nuclear power plants to provide electricity in case of power failures. In order to compare our technique to traditional model checking methods, we tested randomly generated true state invariant properties on a model of the system using three different methods: BDD-based model checking, the k-induction method, and our verification technique. The results show that

for most of the properties our technique is able to find a proof more efficiently than the more traditional techniques.

System level interfaces and timing issues

In the earlier development of model checking methodology for nuclear I&C verification, the usual assumption has been that the analysed system is one fully synchronous entity through which all signals are able to traverse within a single system clock cycle. This assumption is good for performance, and often determines whether the model can be analysed with reasonable computational resources or not. However, for some systems the assumption does not hold. This is especially the case with distributed systems, where the subsystems employ different clocks and the signals do not always carry over from one part of the distributed system to another during a single clock cycle. Assuming synchronous behaviour can leave some errors undetected when verifying the model.

We study the analysis of timing in models by modelling them in two different ways, using two different model checking tools: NuSMV and UPPAAL. The NuSMV model checker is a free, open source tool that is initially designed for model checking hardware designs. It reads models that consist of a set of variables and rules that describe how their values can change from one state to the next. One of its strengths is that it can store a set of states as a single symbolic representation, potentially allowing efficient handling of very large state spaces. This technique is called symbolic model checking. The UPPAAL model checker is specialised to handle models with timing aspects. UPPAAL models contain timed automata, which resemble finite state automata, except that their behaviour can be influenced by clock variables. This is a natural way to measure time, because clock values are not limited to integers, and UPPAAL handles them efficiently. On the other hand, UPPAAL does not use symbolic model checking—all states of the model are stored separately in memory. Therefore big models may not be practical to check with it, since their state space will not fit into memory.

One of our main goals is to develop modelling techniques for asynchronous systems. A good modelling technique preserves the important aspects and behaviours of the system in the model, while omitting the unimportant details. It is necessary to include as little detail as possible so that the model checking tool will not run out of computational resources, but including too little detail makes it impossible to find faults in the system.

We have worked with a case study consisting of an asynchronous control circuit with both analogue and digital signals. We have modelled this system using both the UPPAAL model checker and the NuSMV model checker, using both the traditional timing assumptions and the more accurate asynchronous timing. The system was analysed with NuSMV and UPPAAL and both analyses took time less than 5 minutes. We were able to analyse the model in greater detail using the accurate timing model, while still keeping the model size small enough to fit into memory. The Figure 4 below presents an example of a timing problem that can

occur in circuit design. The behaviour of this circuit depends on how fast the components C and D react to their inputs. In an actual circuit designs such a pair of components needs to be directly connected to each other. Therefore spotting the timing issue would be very unlikely without automated analysis.
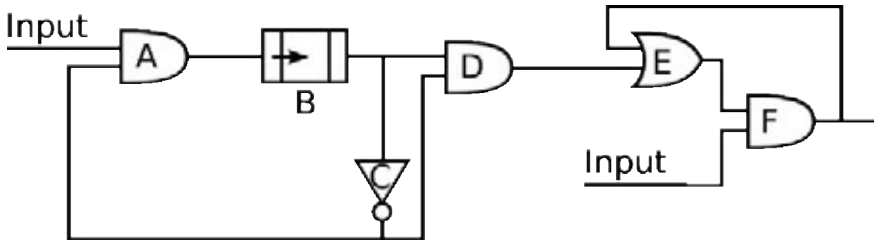

Figure 4. Timing problem in circuit design.

Architecture models and extended fault models

When analysing the fault tolerance of systems, the complex functioning (internal memories, timings) of digital I&C is typically not exhaustively considered. On the other hand, when the digital I&C systems are analysed through e.g. model checking, the architecture level failure assumptions, and effects of the different failures on the system level are not addressed. In order to combine these two approaches we have developed architecture level fault modules that can be used to extend traditional model checking models describing only the logical I&C functions. The idea is that in these it could be possible to analyse the exact behaviour of the plant under certain fault assumptions. The models could detect design errors in the system architecture, or logical I&C errors that together with a hardware failure or a common cause failure could cause an initiating event to develop into an accident.

Our fault modelling methodology has been developed using fictitious plant and I&C models. The purpose of the example models has been to demonstrate the fault modelling methodology. In the developed methodology, we have created separate fault modules that describe the information flow in the hardware, and effects of failures to that information. The hardware modules describe the behaviour of a group of hardware components and the information flows that exist between the components. These hardware fault models are then connected to traditional logical I&C modules. The fault models can include physical faults such as faults in telecommunication links, microprocessor faults, cable failures and electrical faults influencing all equipment in a cabinet. Common cause failures (CCFs) could also be postulated in such a fault model.

The most important problem in our examples has been that even a model of a simple system quickly becomes quite complex. In some cases it has been possible to separately verify the software functionality and after that verify the functionality of the hardware system (in specified failure conditions) assuming that the

software functions as specified. This so called assume-guarantee reasoning has a significant effect on the verification time of the system.

Model checking tool portfolio

An important question in employing model checking is the reliability of the tool: if the model checker says the system is correct, can we trust the result or is the model checker itself buggy? This concern is tried to be alleviated by creating an alternate model checking tool chain to analyse NuSMV models that does not share source code with the NuSMV code-base. This is possible by improving converters created for the Hardware Model Checking Competition (HWMCC). We aim at having an alternative model checking tool chain for verifying NuSMV models that do not share any tool source code base with NuSMV. This will allow for tool chain diversity when verifying NuSMV models, diminishing the reliance on the software quality (absence of bugs) of one tool (NuSMV) in trusting the model checking results. Figure 5 below illustrates the tools used when doing model checking without any code from NuSMV. The same model can then be given also to NuSMV for result comparison. If the results are same, it is very unlikely that both of them are wrong, and therefore confidence in that result is high.
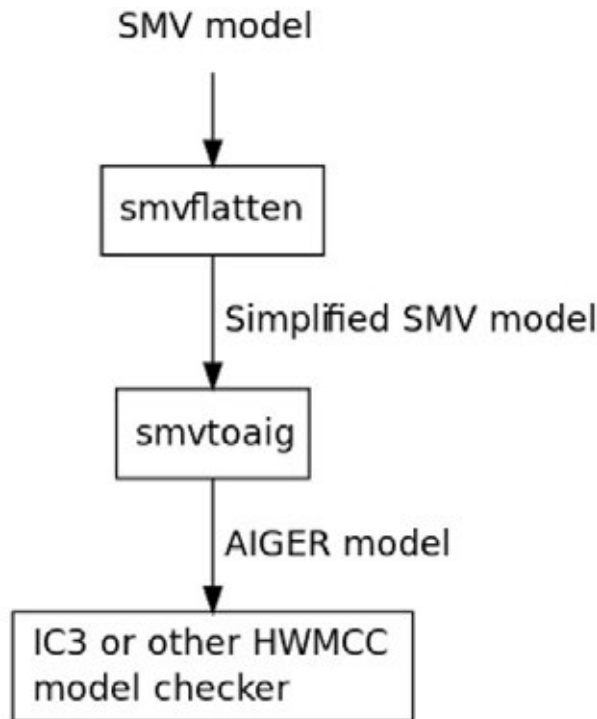

Figure 5. Tools used when doing model checking without any code from NuSMV.

The AIGER format is very low-level by design: the models consist of latches (i.e. memory elements) AND gates and NOT gates. Its purpose is to be a format into which any other hardware model can be converted. It is mainly developed for the HWMCC, and can therefore be used as a low level format that is understood by many model checking tools. Since many model checking tools are entered into the competition, it follows that many state-of-the-art tools support AIGER as an input format. Using AIGER as a back-end is useful in two ways: firstly it is an easy way to get the diversity in the tool chain, and secondly it enables using the best performing tools of each year's HWMCC.

The initial tool for converting NuSMV models into AIGER models only supported a small fraction of the NuSMV input language. We have added more support for the often used parts of the NuSMV input language. This includes arithmetic operations and handling of complex variable types like integer ranges. We have also tested the tool, and fixed many bugs. The fixes and improvements have been sent to the original author of the tool. The improvements to the converter tool have enabled model checking of actual case studies possible so that the only tools used are the improved converter and the IC3 model checker. The future objectives are to use the methodology in practical cases and continue the development.

Synthesis of different techniques and abstraction levels in nuclear I&C analysis

There are several techniques for analysing the safety of I&C systems in nuclear power plants, such as simulation, testing, PRA, and model checking. These techniques are utilized in different phases of the plant lifecycle and they consider various aspects of I&C safety on different abstraction levels. The problem observed is that basically each of the approaches requires its own model, modelling techniques and software tools, which are typically not directly compatible. They also have different objectives, different starting point, and they are used on different levels of detail. The connecting points between the techniques have been unclear, and it is not easy to use the results of one technique as an input for another.

To get an overview of the applicability of each technique, they are put in the same figure where the general I&C life cycle is on the top row (Figure 6). The life cycle is not extensive for all purposes but covers the most common phases where each technique can be utilized.

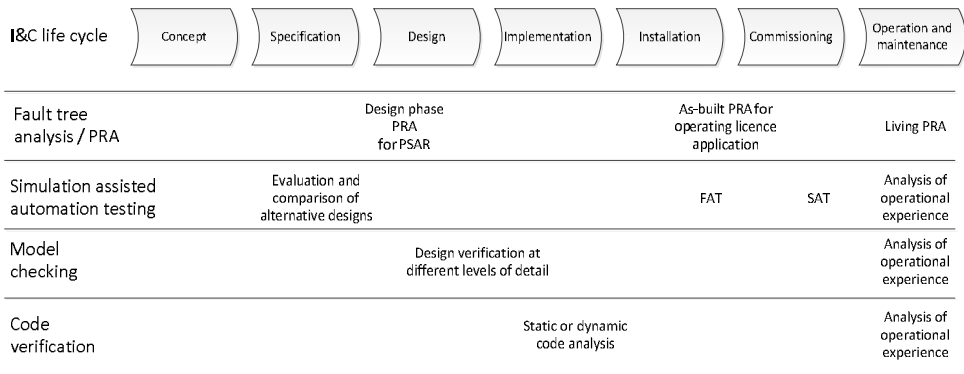| I&C life cycle	Concept	Specification	Design	Implementation	Installation	Commissioning	Operation and maintenance
Fault tree analysis / PRA			Design phase PRA for PSAR		As-built PRA for operating licence application		Living PRA
Simulation assisted automation testing		Evaluation and comparison of alternative designs			FAT	SAT	Analysis of operational experience
Model checking			Design verification at different levels of detail				Analysis of operational experience
Code verification			Static or dynamic code analysis				Analysis of operational experience

Figure 6. Verification methods and a generalised I&C life cycle.

Simulation and PRA treat the system on the highest abstraction levels of the methods in the figure and give least importance to the details. Of course, there are detailed failure probabilities behind PRA but the whole idea of PRA is not on the details. Typically PRA gets more detailed when the overall design process goes further. PRA is used e.g. to support safety analysis reports (Design phase PRA) and describing the reliability of the implemented system (As-built PRA). The term Living PRA refers to the continuously updated PRA which has the most relevant information of the plant. Also in simulation of automation, the details are not so crucial. For example in Apros simulator, the simulation model has dedicated modules representing common function blocks, but they do not necessarily contain exactly the same behaviour as the final implemented system.

Model checking goes more into details and strives for full coverage of the possible system behaviours per tested property. It mainly concentrates on rather small parts of the system to be analysed (especially I&C systems) because the state explosion problem limits the size of the systems that can be analysed. Typically, the analysed objects are function block diagrams, which are analysed on a very detailed level. However, model checking can also be used to verify designs on architectural level meaning that in addition to modelling the intended software function, also the hardware architecture of the system is taken into account. In such cases, the hardware is modelled as a set of individual components and elements through which the information flows. Hardware failures can be included in the model to induce alterations to the information flow. The intention is then to examine the effects of a set of hardware failures on the overall operation of the system. This type of modelling methodology will be developed further in the SARANA project. Model checking can also be used for verifying software code but so far it has mostly been out of the scope of SARANA.

References

[Björkman et al. 2013] Björkman, K. Solving dynamic flowgraph methodology models using binary decision diagrams. Reliability Engineering and System Safety 111(2013), 206–216. Doi:10.1016/j.ress.2012.11.009. (Article in Press.)

[Gustafsson 2012] Gustafsson, J. Reliability analysis of digital protection system of a nuclear power plant. Masters Thesis, Royal Institute of Technology, Stockholm. 2012.

[IEC EN 61508] Functional safety of electrical/electronic/programmable electronic safety-related systems, IEC 61508, International Electrotechnical Commission, Geneva.

[Lahtinen et al. 2012] Lahtinen, J., Valkonen, J., Björkman, K., Frits, J., Niemelä, I., Heljanko, K. Model checking of safety-critical software in the nuclear engineering domain. Reliability Engineering & System Safety, http://www.sciencedirect.com/science/article/pii/S0951832012000555?v=s5. ISSN 0951-8320, 10.1016/j.ress.2012.03.021. (Available online 2 April 2012.)

[MEMICS 2012] Lahtinen, J., Björkman, K., Valkonen, J., Niemelä, I. 2012. Emergency diesel generator control system verification by model checking and compositional minimization. Proceedings of 8th Doctoral Workshop on Mathematical and Engineering Methods in Computer Science (MEMICS 2012), Znojmo, Czech Republic, 25–28 October 2012. Pp. 49–60.

[NEA/CSNI/R(2009)18] Recommendations on assessing digital system reliability in probabilistic risk assessments of nuclear power plants, NEA/CSNI/R(2009)18, OECD/NEA/CSNI, Paris, 2009. http://www.nea.fr/nsd/docs/2009/csni-r2009-18.pdf.

[NET-44-5-2012] Authén, S., Holmberg, J.-E. Reliability analysis of digital systems in a probabilistic risk analysis for nuclear power plants. Nuclear Engineering and Technology 44(5), 471–482.

[NKS-230] Authén, S, Björkman, K., Holmberg, J.-E., Larsson, J. Guidelines for reliability analysis of digital systems in PSA context – Phase 1 Status Report, NKS-230 Nordic nuclear safety research (NKS), Roskilde, 2010. http://www.nks.org/scripts/pdfsearchbackend.php?Mode=getpdf&id=111010000275036&hash=055eaeac4b879aa3845cd9e798a899c7.

[NKS-261] Authén, S., Gustafsson, J., Holmberg, J.-E. Guidelines for reliability analysis of digital systems in PSA context – Phase 2 Status Report, NKS-261 Nordic nuclear safety research (NKS), Roskilde, 2012.

[NPIC & HMIT 2012_278] Holmberg, J.-E., Authén, S., Gustafsson, J. Nordic experience and experiments of modelling digital I&C systems in PSA. Proc. of the 8th International Topical Meeting on Nuclear Plant Instrumentation, Control and Human Machine Interface Technologies, NPIC & HMIT 2012, San Diego, 22–26.7.2012, American Nuclear Society, LaGrange, Park, Illinois, USA. Pp. 278–290.

[NPIC & HMIT 2012_724] Holmberg, J.-E., Authén, S., Amri, A., Sedlak, J., Thuy, N. Best practice guidelines on failure modes taxonomy for reliability assessment of digital I&C systems for PRA. Proc. of the 8th International Topical Meeting on Nuclear Plant Instrumentation, Control and Human Machine Interface Technologies, NPIC & HMIT 2012, San Diego, 22–26.7.2012, American Nuclear Society, LaGrange, Park, Illinois, USA. Pp. 724–732.

[PSA2011-80] Björkman, K., Karanta, I. A dynamic flowgraph methodology approach based on binary decision diagrams. Proceeding of International Topical Meeting on Probabilistic Safety Assessment and Analysis (PSA 2011), Wilmington, NC, 13–17 March 2011. American Nuclear Society. La Grange Park, Illinois, 60526 USA (2011). Pp. 267–278.

[PSAM11_10-Th2-2] Holmberg, J.-E., Bishop, P., Guerra, S., Thuy, N. Safety case framework to provide justifiable reliability numbers for software systems. Proc. of 11th International Probabilistic Safety Assessment and Management Conference & The Annual European Safety and Reliability Conference, 25–29.6.2012, Helsinki. Paper 10-Th2-2.

[PSAM11_10-Th2-4] Bäckström, O., Holmberg, J.-E. Use of IEC 61508 in Nuclear Applications Regarding Software Reliability. Proc. of 11th International Probabilistic Safety Assessment and Management Conference & The Annual European Safety and Reliability Conference, 25–29.6.2012, Helsinki. Paper 10-Th2-4.

[PSAM11_10-Th4-1] Holmberg, J.-E., Authén, S., Amri, A. Development of best practice guidelines on failure modes taxonomy for reliability assessment of digital I&C systems for PSA. Proc. of 11th International Probabilistic Safety Assessment and Management Conference & The Annual European Safety and Reliability Conference, 25–29.6.2012, Helsinki. Paper 10-Th4-1.

[PSAM11_10-Th4-3] Piljugin, E., Authén, S., Holmberg, J.-E. Proposal for the Taxonomy of Failure Modes of Digital System Hardware for PSA. Proc. of 11th International Probabilistic Safety Assessment and Management Conference & The Annual European Safety and Reliability Conference, 25–29.6.2012, Helsinki. Paper 10-Th4-3.

[PSAM11_30-Th4-1] Tyrväinen, T., Björkman, K. Modelling common cause failures and computing risk importance measures. In: The Dynamic Flowgraph Methodology, Proc. of 11th International Probabilistic Safety Assessment and Management Conference & The Annual European Safety and Reliability Conference, 25–29.6.2012, Helsinki. Paper 30-Th4-1.

[VTT-R-09293-11] Björkman, K., Bäckström, O., Holmberg, J.-E. Use of IEC 61508 in nuclear applications regarding software reliability, pre-study report. VTT-R-09293-11, VTT, Espoo, 2012.

3.4 Safety requirements specification and management in nuclear power plants (SAREMAN)

Teemu Tommila[1], Janne Valkonen[1], Mikko Raatikainen[2], Eero Uusitalo[2]

[1]VTT Technical Research Centre of Finland
Tekniikantie 2, P.O. Box 1000, FI-02044 Espoo

[2]Aalto University
School of Science, Department of Computer Science and Engineering
P.O. Box 15400, FI-00076 AALTO

Introduction

Requirements are a prerequisite not only for successful implementation but also for demonstrating the safety of nuclear power plant systems. However, requirements engineering is an abstract and multi-disciplinary area and widely considered as a challenge. Therefore, the SAREMAN project develops practices for requirements definition and management. Our approach is founded on well-defined models of both systems and engineering processes. From a consistent terminology we proceed to modelling and documentation methods, working practices and finally to utilization of information technology tools (Figure 1). The challenges in nuclear energy domain are similar to many other areas of industry. So, their standards and guidelines can be applied. Our focus on the safety of instrumentation and control

(I&C) systems and the early stages of design emphasises the multi-disciplinary nature of requirements engineering involving, for example, safety analysis, process engineering and human factors.
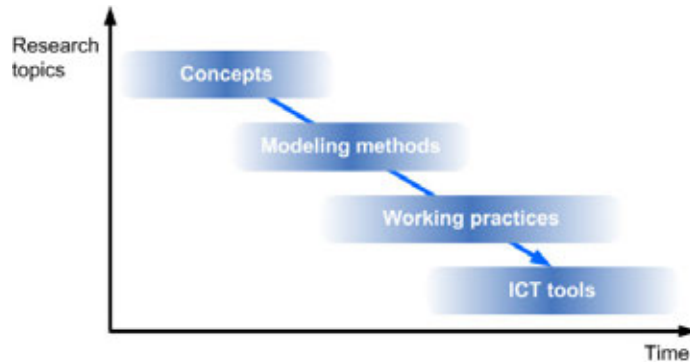

Figure 1. Overall work plan for the four-year period.

During the first project year 2011, we focused on terminology and recommendations for readable and unambiguous requirements. Related to the clarity of written requirements, we studied structured natural language requirements and in particular EARS, the Easy Approach to Requirements Syntax [1, 2]. Recommendations were collected for the key documents, e.g. the high-level Concept of Operations (ConOps) and the technical System Requirements Specification (SyRS). In 2012 the research focused on three areas: 1) traceability of design information; 2) guidance for requirements specifications; and 3) regulatory compliance and role of requirements in safety demonstrations.

The rest of this paper is organized as follows. First, Section "Requirements in systems modelling and design" the describes the main ideas that SAREMAN recommends for modelling requirements associated with a nuclear power plant and its systems. To present the more practical goals of the project, Section "Practices for requirements definition" discusses the role of requirement specifications and textual requirements in the design and licensing processes.

Requirements in systems modelling and design

As we claim below, requirements are *statements* about entities in the system of interest and its environment. To be able to express requirements in an unambiguous way, it is necessary to have a sound model of the system. In addition to the system, requirements often concern the processes of its development, operation and maintenance. Therefore, a pair of two models is needed, i.e. a *system model* and its *life-cycle model* [3].

Elements of the system model

Adopting the views of many international standards, we see *systems* as man-made, real-world entities consisting of, e.g., sub-systems, devices, structures, pieces of software and humans [4]. Figure 2 shows the main concepts in a class diagram with the UML notation (Unified Modeling Language). Systems perform various *activities*, such as producing energy or controlling process parameters. To do this, a system must be designed to have suitable capabilities, in particular *system functions*. The availability and service level depends on the current *operational state* and *operating mode* of the system. Activities can be performed by combining the capabilities of one or more redundant systems. In the early stages of design, only high-level concepts of these entities are outlined. However, they make it possible to express clearly the requirements for their properties, relationships and behaviour, for example, in the form of textual statements, tables or scenarios.
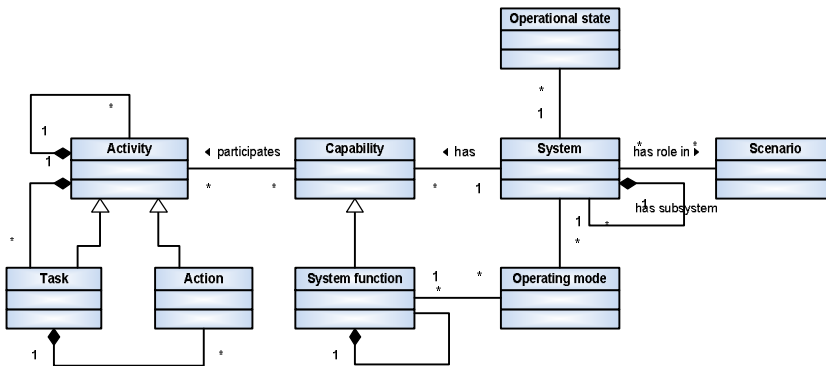

Figure 2. Modelling concepts for describing systems and their behaviour.

Elements of the life-cycle model

Life-cycle processes and models are discussed in many standards [4, 5]. It seems, however, difficult to find one widely accepted and conceptually sound model. In its widest sense, a life-cycle model describes

- technical and management processes to be carried out
- design artefacts and information flows between activities
- scheduling, phases and milestones
- participating organisations and their responsibilities
- practices, methods and tools to be applied.

Developing, operating and maintaining a system involves many activities carried out by various organisations. As we see it, the practices of system operation and

maintenance are part of the solution developed by designers. For example, operators are elements of the power plant system. Therefore, operation and maintenance are included in the system model. From the developers' viewpoint, our *project model* consists of consecutive *life-cycle phases* separated by decision gates, *milestones* (Figure 3). Parts of the project organisation participate in development activities and are responsible for certain areas of the system model. In a way, the project organisation is a "system" to which requirements can be attached. Therefore, different from *product requirements* concerning the system being developed, *process requirements* specify properties of the project organisation and its working practices.
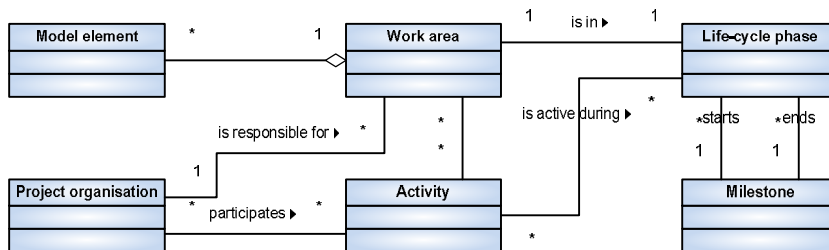

Figure 3. Elements of the project model.

Requirements and requirements engineering

Combining various standards and textbooks, we see *requirement* as a condition or capability that must be met or possessed by a system to satisfy a contract, standard, specification, or other formally imposed document [3]. A requirement expresses a mandatory feature without unnecessarily constraining the possible solutions. Requirements are found on all levels of detail and throughout the life-cycle. A specification on one level typically sets requirements for the next one.

Requirements are concerned with the communication between stakeholders. So, we understand a requirement as a *statement* of a stakeholder, e.g., a regulator, user or system architect, concerning a product or its development process. Statements are communicated in spoken form or coded as documents and drawings and delivered by a tool, such as e-mail or a shared design database. For successful communication, the interpretation should be easy and unambiguous. Design is iterative, and requirements are mixed with other types of statements, e.g. known facts and conceptual design solutions. Consequently, documents containing only requirements don't exist. To serve their purpose of communicating relevant information to the selected audience, documents must also describe the system environment and design solutions made so far.

Applying the ideas of the *speech act theory* [6], we see all pieces of design information as *statements*. In addition to requirements, engineers must express

current problems, facts, intentions and suggested design solutions. So, a good statement should indicate clearly, whether it is a soft goal, requirement, design constraint, an assumption or something else. Consistent use of words like "shall" and "should" are recommended for textual specifications. This is, however, not practical when system elements and functions are presented in graphical or tabular form, for example in the input-output list of an I&C system. Therefore, we model the communicative role of a statement as a separate attribute.

A key purpose of the *Requirements engineering* (RE) activity is to produce a consistent set of requirements that is then used in many other activities such as detailed design and test planning (Figure 4). RE contains two main activities, requirements definition and requirements management. *Requirements definition* includes discovering, analysing, documenting and validating and verifying the requirements. Analysis includes negotiation and prioritization processes that lead to a set of agreed requirements. Requirements definition also includes maintaining the traceability of requirements. *Requirements management*, in turn, can be seen as part of *configuration management*, e.g. identification and change control applied to requirements.
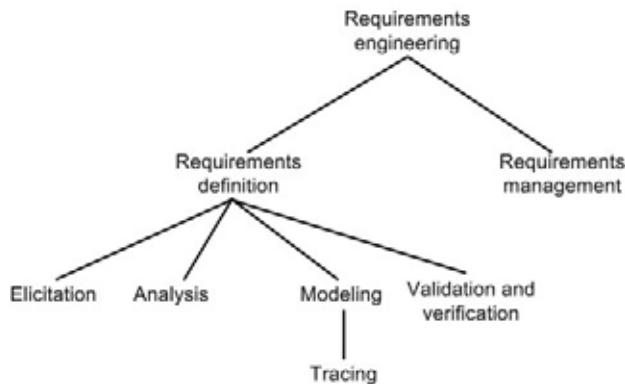

Figure 4. Main activities of requirements engineering.

In particular, it is important to create and maintain the *traces*, i.e. information that makes it possible to find out how and why requirements and design solutions have been derived from various information sources and what modifications have been made to them. Even if the idea is old, no single definition or a way to implement traceability can be found. Advanced traceability is rarely applied in the industry, due to its complexity and costs. Commercial software tools for requirements management and engineering provide some but fairly limited support for traceability. However, the issue is widely accepted as a critical one, and much research is going on around it, especially in the area of model-driven development.

Practices for requirements definition

The sections above imply that requirements can't be considered in isolation. Instead, requirements should be attached to an integrated system model continuously evolving during the iterative design process. Unambiguous concepts are needed for describing the system and expressing statements about its structure, functions and properties. In addition, SAREMAN looks for practical solutions based on the modelling principles and domain-specific terminology. Our plan is to summarise our research findings and lessons learned to a short guide intended to control engineers working in the nuclear domain. The sections below give some highlights of the work carried out so far.

Concept of Operations as a basis for requirements specification

We expect the nuclear industry to adopt in the future model-based design practices, where information is stored in computer databases and exchanged in standards-based formats. Nevertheless, traditional documents are also needed in most life-cycle stages and levels of plant hierarchy. Guidelines and standards describe various types of requirements specifications focusing on specific stakeholder viewpoints and levels of detail. The *User Requirements Specification*, *System Requirements Specification* and *Software Requirements Specification* are common examples.

Requirements definition is a multi-disciplinary activity. Requirements should be derived from identified hazards and the needs and features of various stakeholders and external entities that the system will interact with. In particular, we have studied the role of the *Concept of Operations* (ConOps) as a basis for conceptual design and high-level requirements definition. The idea was introduced in late 1980's and thereafter refined in many guidelines and standards, e.g. in [5]. The ConOps of a system is a high-level description of how the elements of the system and entities in its environment communicate and collaborate in order to achieve the stated goals of the system. As a result of conceptual design it is intended to communicate the overall system functions and properties among the user, regulator, developer and other stakeholders. Basically, a ConOps should contain the following information (on a suitable level of detail and to the extent known):

- overall goals and constraints of the (socio-technical) system
- the business or production processes to be carried out
- interfaces to external entities (e.g. company headquarters)
- elements of the system (technical systems, structures, human organisation)
- main functions the system and its elements
- operational states and operating modes, including abnormal situations
- allocation of responsibilities and tasks to the system elements
- operating scenarios (e.g. plant start-up)
- high-level user requirements (if not covered by the scenarios).

ConOps provides a basis for defining the more technical *system requirements* (Figure 5). The user requirements and the allocation of responsibilities, i.e. the degree of automation, determine the functional requirements of the I&C system, control room and human operators. With this allocation, also the performance requirements flow down to individual system elements.
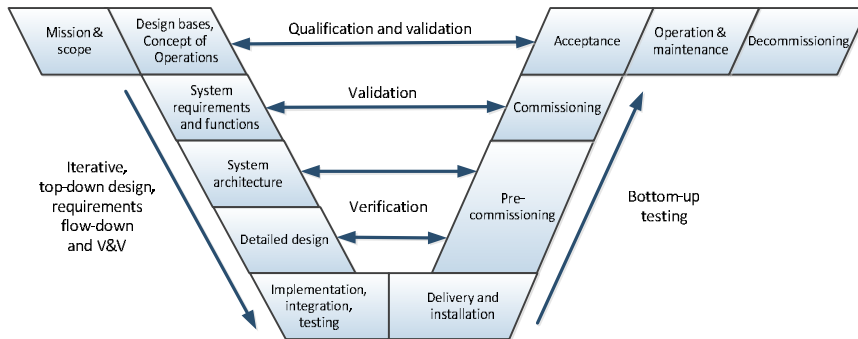

Figure 5. Position of ConOps in the system life-cycle.

The origin of ConOps is in systems engineering of complex, information-intensive systems. It has not been explicitly applied to nuclear power plants. However, corresponding elements can be identified in most Human Factors Engineering (HFE) guidelines, regulations and standards. For example, the preliminary and final *Safety Analysis Reports* (SAR) written by license applicants to demonstrate safety of a system requires both technical and human factors to be considered. To be a practical design artefact, ConOps should be adapted to the engineering and licensing processes applied in the nuclear domain.

Writing well-formed requirements

A good requirement is unambiguous, complete, verifiable and easy to understand [5, 7, 8]. A primary guideline is to use the word "shall" when expressing a textual requirement. In the one end, there are formal methods that try to make requirements unambiguous or even computer understandable. More practical approaches give guidance for well-structured natural language requirements. For example, Boilerplates [7] is a collection of templates for expressing requirements in natural language. Finally, there are general guidelines and relatively simple approaches similar to boilerplates such as EARS [1, 2], which gives only five generic templates. Despite the existing methods, industry experts are not necessarily well prepared for writing good requirements.

As a practical solution, we studied the feasibility of EARS in the nuclear domain, for example its overall applicability, required effort and training needs. We applied EARS in its original form as described in Mavin et al. [1, 2] at Rolls-Royce

Control Systems. EARS has been successfully applied to a variety of complex, safety-critical systems, including regulatory safety requirements. The method has been developed primarily for stakeholder requirements, as opposed to technical system requirements. The hypothesis of EARS is that a small set of simple requirement structures is an efficient and practical way to enhance the writing of high-level stakeholder requirements. One of the strengths of the approach is that the requirements remain in a form that is readable by anyone. Special training is not required, as opposed to formal methods. The results reported by Mavin et al. suggest that EARS can alleviate many problems with existing requirements, such as wordiness, complexity, untestability and ambiguity.

In EARS, the requirements are based on five sentence templates: ubiquitous requirements, event-driven requirements, state-driven requirements, unwanted behaviour requirements and optional requirements (Figure 6). Basic templates can be combined to create compound statements. Template types are identified by keywords 'when', 'while', 'if-then' and 'where'.

When existing requirements are restructured with EARS, one translation will often produce multiple EARS statements as the requirements become more atomic. Multiple iterations are usually needed to ensure consistency with the original requirements. Typically, there is no single correct way to apply the templates – there often are several alternatives, sometimes with subtly different implications with regard to the meaning. EARS does not impose a strict structure to any of the elements that are filled in. For example, the system response could include any number of responses, in sparse or great detail. This means that throughout the translation work, the characteristics of good requirements such as testability and unambiguity need to be considered.
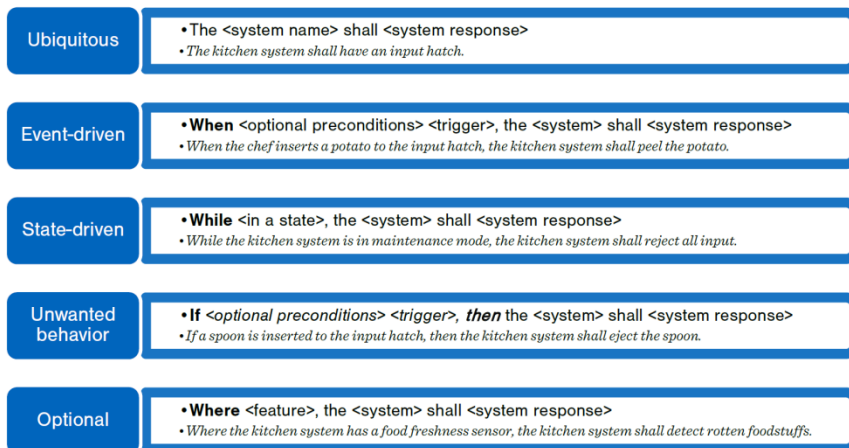

Figure 6. Sentence structures of the Easy Approach to Requirements Syntax (EARS).

In our study, we first applied EARS in an exploratory manner to see whether EARS is feasible to apply and whether the improvements are significant enough compared to the effort. The documents analysed were: 1) fragments from YVL 2.1, Safety Classification of Systems (currently in effect); 2) YVL B.1, Safety Design of a Nuclear Power Plant (draft L2); and 3) a generic requirements specification for rod control system upgrade [9]. The application of EARS to YVL 2.1 was not especially successful. The main reason was that it does not appear to be a requirements document per se. The application of EARS to the selected parts of YVL B.1 was more successful. The selected requirements were decomposed into atomic statements and translated into the EARS format in a single-pass manner. The difference of YVL 2.1 and YVL B.1 was noticeable, as the latter is constructed more carefully into single statements. This was one key factor that positively affected the feasibility of EARS in the case of YVL B.1. When interpreting and translating the requirements in YVL B1, it turned out that some assumptions had to be made about the original document. The assumptions made by the researcher were not always correct, partly due to the ambiguity of the sentences of YVL B.1 and partly due to the domain knowledge required. Finally, the application of EARS into functional [9] was successful. The original document contains properly expressed requirements and was relatively easy to restructure with EARS. In general, EARS appeared relatively lightweight in terms of effort and the learning required as compared to the benefits.

Secondly, on the basis of the encouraging results of the exploratory test, we applied EARS to the entire YVL B1. Non-requirements such as definitions, examples, and introductory texts were omitted. The rest was expected to be mostly requirements and was put into a table with columns for the original text, EARS formatted requirement and observations. The researcher used 130 hours in total for the EARS conversion, including the time spent for learning the EARS method. The data collected was categorized as characteristics pertaining to original YVL requirements. Of the 348 total YVL paragraphs, 324 paragraphs (93%) were considered to be requirements and were translated into EARS format, resulting in 900 atomic requirements. One observation was that the YVL requirements contained typically several requirements. For example, one long YVL requirement decomposed into 27 atomic EARS requirements. Of the 324 YVL requirements, 184 were well-formed but 140 had one or several issues, such as passive form or missing actor, poor use of terminology, or ambiguity in general. So, the study revealed that the interpretation of YVL is not always straightforward.

On basis of the experiences, we decided to construct a two-paged quick reference guide that summarizes EARS and some aspects of requirements engineering. The hand-out describes each of the EARS templates with examples and outlines the workflow for applying EARS. Additionally, the hand-out includes the general characteristics of a good requirement with brief explanations. Its length was intentionally limited to enable convenient use as a reference during daily work. The guidelines include also hands on training material that we tested with Master's thesis students at Aalto University.

Regulatory requirements and licensing

There is an increasing demand for the utilities to demonstrate the safety of their plants and systems throughout their life-cycle, not only with respect to regulatory requirements but beyond them by showing that all hazards have been adequately managed. In the nuclear field, *safety demonstration* is understood as a set of arguments and evidence elements which support a selected set of claims on the dependability – in particular the safety – of the operation of a system important to safety used in a given plant environment [10]. Structured approaches and tools exist to organise this information. On a generic level, *assurance case* is a reasoned, auditable artefact created to support (or challenge) its top-level claims [11]. Arguing through multiple levels of sub-claims, this structured argumentation connects the top-level claims to the evidence and assumptions. When the top-level claim is about safety, security, dependability, assurance cases are called *safety cases*, security cases, dependability cases, respectively.
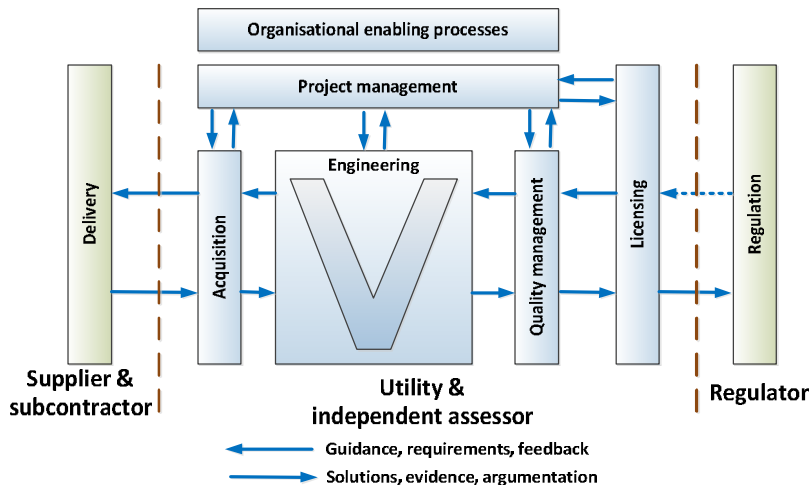

Figure 7. V-model embedded in the major life cycle processes.

We reviewed literature on licensing practices and safety demonstrations. On the basis of the review and discussions with domain experts, it seems that the current practices are not fully satisfactory. For example, requirements specifications, traceability and safety argumentation are not always clearly explicated. On the basis of these findings, the SAREMAN project plans to continue its work on clarifying the terminology and collecting guidelines for well-structured requirements. In addition, the processes, practices and documents needed in safety demonstrations and licensing will be studied (Figure 7).

References

1. Mavin, A., Wilkinson, P., Harwood, A., Novak, M. Easy approach to requirements syntax (EARS). In: Proceedings of 17th IEEE International Requirements Engineering Conference (RE'09). Pp. 317–322, 2009.

2. Mavin, A., Wilkinson, P. Big ears (the return of easy approach to requirements engineering). In: Proceedings of the 18th IEEE International Requirements Engineering Conference (RE'10). 2010. Pp. 277–282.

3. Tommila, T., Valkonen, J., Raatikainen, M. Conceptual model for safety requirements specification and management in nuclear power plants. Working report of the SAREMAN project.

4. ISO/IEC 15288. Systems and software engineering – rSystem life cycle processes. International Organization for Standardization (ISO), 2nd edition, 2008.

5. ISO/IEC 29148. Systems and software engineering – rLife cycle processes – Requirements engineering. International Organization for Standardization (ISO), 2011.

6. Searle, J., Vanderveken, D. Speech acts and illocutionary logic. In: Foundations of Illocutionary Logic, Cambridge University Press, 1985.

7. Hull, E., Jackson, K., Dick. J. Requirements Engineering. Springer-Verlag New York Inc., 2002.

8. Sommerville, I., Sawyer P. Requirements engineering: a good practice guide, John Wiley & Sons, 1997.

9. Requirement Specification for Rod Control System Upgrade: A Generic Specification for Westinghouse Pressurized Water Reactors. EPRI, Palo Alto, CA: 2000. 1000969.

10. Licensing of safety critical software for nuclear reactors – Common position of seven European nuclear regulators and authorised technical support organisations. 2010.

11. ISO/IEC 15026-2. Systems and software engineering – Systems and software assurance – Part 2.

4. Fuel Research and Reactor Analysis

4.1 Criticality safety and transport methods in reactor analysis (CRISTAL)

Karin Rantamäki, Petri Kotiluoto, Maria Pusa, Tom Serén

VTT Technical Research Centre of Finland
P.O. Box 1000, FI-02044 Espoo

Introduction

VTT has an extensive computer code system for stationary reactor physics calculations. Together with the dynamics codes it has to cover a wide range of applications dealing with both normal operation and transient conditions. In the analyses, the dynamics codes rely on input from stationary codes. In order to maintain a high level of competence in reactor safety analysis, it is important to keep up to date both the code system and the know-how about the codes.

Reactor physics is a base element in nuclear power safety. The expertise in the field is an important issue in order to ensure appropriate and adequate safety analyses. A lot of expertise at VTT has been lost during the last ten years. New researchers have joined the group but much effort and time is needed to train them into qualified reactor physicists. Consequently, the main aim of this project is to improve the knowledge in various fields of reactor physics.

The project has two major tasks and two smaller ones. The large ones where most of the work is done are calculation methods and criticality safety. The smaller ones are reactor dosimetry, and international co-operation including participation in training courses.

Most of the general reactor physics code work is done in the task calculation methods, which is divided into two parts: transport methods, and sensitivity and uncertainty analysis. The former covers a variety of tasks related to both the reactor itself and components outside the reactor. The duties range from cross section calculation of fuel assemblies to activation analysis of the pressure vessel. The main objective in this part of the project is to ensure a competent staff. Determination of the uncertainty of various parameters and their importance to the final re-

sults is necessary in order to understand the accuracy of computer codes. Tools for this purpose are created in the latter part.

Criticality safety is an important part in the fuel cycle. Especially as the enrichment of the fuel increases it has become more and more important. The expertise in this field has almost vanished from VTT and therefore special attention is needed to ensure the competency in this field. This has motivated the subtask of criticality safety in this project. In addition to the knowledge, special attention needs to be paid to the code system used in this field. It is extremely important that the criticality validation is brought to an appropriate level. This is an issue that has been neglected for several years. It is included as an important part in this subtask.

The third task is reactor dosimetry. As a small task, it has focused on updating the data and procedures. The analysing system depends very much on international development of cross section libraries and programs. Therefore, special attention is given to international collaboration in this task.

International co-operation involves work within AER and the OECD/NEA. The participation in the Nuclear Science Committee as well as the Working Party on Nuclear Criticality Safety and its expert groups is covered. The contribution has been especially strong in the Uncertainty Analysis in Modelling (UAM) group.

Calculation methods

The calculation methods used in the project cover a variety of computer codes. Some of them are self-made while most are commercial ones. The external codes include codes from the Studsvik Scandpower CMS-family [1], the SCALE-package [2] developed by ORNL and the DOORS-package [3]. Where possible, code development is performed also on commercial codes, like is the case with CASMO-4 [1]. The following subsections describe in more detail the applications of the codes within this project.

Applications of deterministic transport codes

Knowledge on basic reactor physics and reactor physics codes was enhanced by a study on the dependence of cross sections on various reactor parameters [4]. The study was performed using the deterministic lattice code CASMO-4/4E [1]. This also served in enlarging the user group of the CASMO-code. In the study itself, the basic reactor parameters, the fuel temperature, the moderator temperature and density, and the boron concentration were varied. Their effect on various cross sections was studied. The cross sections considerer were the diffusion coefficients, absorption cross sections and fission production rates for both the fast and thermal group, the transfer cross section from fast to thermal group, and the multiplication factor. The results obtained from the CASMO-calculations were compared to the polynomial fits used in the dynamics codes made at VTT. Within the parameter range the results behave roughly linearly. Consequently, it was concluded that the polynomial fits describe the system well enough.

Cross sections are used in the dynamics codes as source data. An increasing interest on cross sections is also shown by developers of system codes. Two-group cross sections have been produced for this purpose using CASMO. Earlier, the CAXMAN and CRFIT codes [5] have been written to extract the data from CASMO-output files and to process it into the format the core simulator HEXBU [6] or the dynamics code TRAB-3D [7] can read. In this work, a script was written that takes care of this calculation chain in the case of BWRs [8]. Since some features in the chain are specific to BWRs, a dedicated script was needed. The script uses given CASMO-inputs as a source and runs through the chain creating the needed inputs on the fly. As an outcome, it produces the material constants in the HEXBU-format. As a first application of this package, a cross-section set was prepared for the BWR stability benchmark studied in KOURA.

Deterministic radiation transport methods are often needed for out-of-core fluence calculations and deep penetration problems. In such cases, the Monte Carlo simulations are sometimes inefficient. In this study, the Olkiluoto BWR out-of-core fluence calculations were continued with the TORT 3D discrete ordinates code [9]. A large 3D geometry model for TORT of one quarter of the reactor with reflective boundaries was generated with BOT3P. Axially the model includes part of the steam separators, and extends radially to the outer surface of the concrete biological shield, which is 5.43 m from the centre of the core. The geometry is shown in Figure 1. The size of the computational TORT r-θ-z mesh was 382×364×129. The core region was divided axially into 10 layers, and the void fraction was taken into account in the homogenised material definitions. Control rods were modelled as separate regions. The fixed neutron source was based on a SIMULATE-3 power distribution of the Olkiluoto 1 cycle 10. The TOPICS-B code was used to generate the material-wise cross sections using BUGLE-96 cross section libraries. The TORT results were compared to earlier 2D DORT calculations. These Olkiluoto BWR TORT calculations were reported in the XV Meeting on Reactor Physics Calculations in the Nordic Countries in 2011 [10].

In addition, VVER-440 CB6 spent fuel final disposal benchmark [11] calculations have been carried out [12]. These benchmark calculations are divided into two parts: 1) decay calculations for the provided 29 time points from fresh fuel up to 1 000 000 years, and 2) criticality calculations at the corresponding time points using the fuel composition from the decay calculations. The decay calculations were performed with the point-depletion code ORIGEN-S. The geometrical model was created with BOT3P and material-wise cross sections with TOPICS-B using the BUGLE-96 cross section libraries. Multiplication factors were then calculated with TORT.

The major issue encountered in the CB6 benchmark calculations was that due to serious internal convergence problems of the TORT code, criticality eigenvalue results from several time points did not converge [12]. Some attempts were made to obtain a double precision version of TORT, claimed to solve these convergence problems [13], but without success. Therefore, only partial results were achieved [12]. Despite the difficulties, new experience on decay and 3D discrete ordinates radiation transport calculations has been gained, which was the main aim of this study.
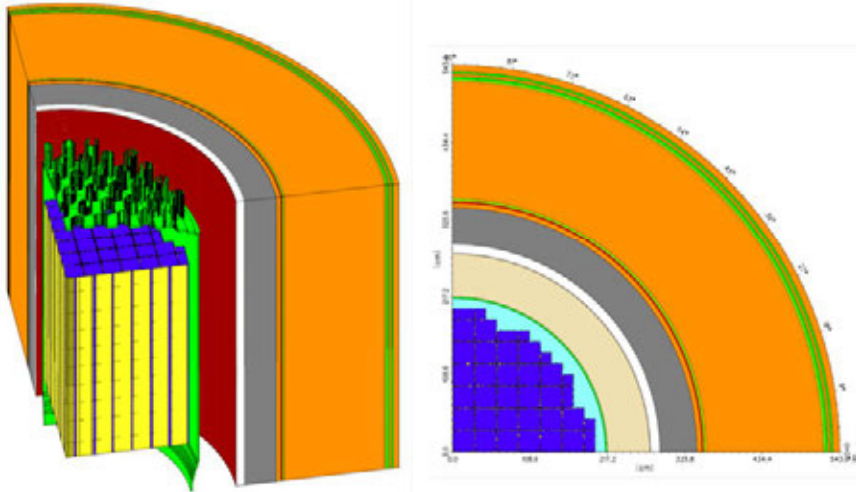
Figure 1. The 3D TORT model of the Olkiluoto BWR (left) with water regions and some homogenised core grid zones made transparent for better visualisation, and a 2D cut-image at the core height (right).

Sensitivity and uncertainty analysis

When uncertain parameters are used in a computation, the calculation results also contain uncertainty. In order to estimate the reliability of these calculations, it is necessary to develop uncertainty analysis methods that enable propagating the parameter uncertainty through the calculations.

In nuclear engineering calculations, the imprecision of neutron interaction data is believed to be one of the most significant sources of uncertainty. The goal of the UAM benchmark [14] launched in 2006 is to be able to propagate this uncertainty through coupled neutronics/thermal-hydraulics calculations. The first phase of the benchmark aims at propagating nuclear data uncertainty through fuel assembly calculations, which are used to produce homogenized data for the subsequent coupled calculations. The objective of the first phase can be considered ambitious, since the generally used fuel assembly codes did not have uncertainty analysis capabilities when the benchmark was started.

At VTT, the UAM benchmark was recognized as an opportunity to start developing an uncertainty analysis calculation system. The fuel assembly burnup calculation program CASMO-4 was chosen as the development platform for the first phase due to its role as a standard tool for lattice physics calculations at VTT.

In fuel assembly applications, the number of uncertain nuclear data is substantial, with tens of thousands of uncertain parameters for each calculation. This uncertainty is generally reported as covariance matrices that represent the second moment of the parameter's probability distribution. To illustrate the uncertainty

related to nuclear data parameters, Figure 2 shows the multi-group covariance matrix for the fission cross-section of ^{235}U.

Due to vast number of uncertain parameters, perturbation theory was chosen as the uncertainty analysis method for CASMO-4. In this framework, uncertainty is propagated in a deterministic manner by first computing the sensitivity profiles of the responses, and then approximating a linear relationship between the parameters and the responses. The sensitivity profile of a response is defined as a vector containing its relative derivatives with respect to all parameters of interest. In the context of CASMO-4, these parameters comprise of neutron cross-section values for each energy group. In perturbation theory, the sensitivity profiles are computed in an efficient manner by solving one generalized adjoint system for each response. This makes the approach computationally superior in comparison to statistical analysis. The drawback is that extensive code modifications are required.
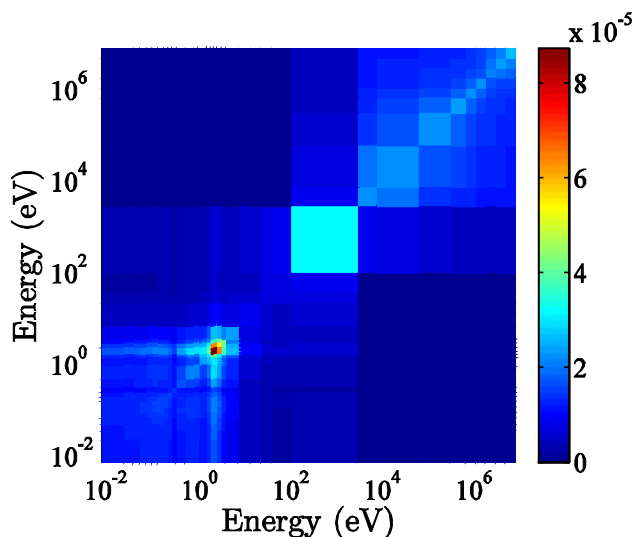

Figure 2. The relative covariance matrix of the ^{235}U fission cross-section taken from the SCALE 6.1 covariance library and modified to the 40 energy group structure of CASMO-4.

At first, classical perturbation theory was implemented in CASMO-4, which enabled the sensitivity analysis of the multiplication factor [15]. In addition, a covariance library was formed and connected with the code to allow uncertainty analysis. During the CRISTAL project, this methodology has been extended to responses that can be presented as reaction rate rations. This framework is called generalized perturbation theory (GPT) and it covers the homogenized assembly data that is passed on to the subsequent coupled neutronics/thermal hydraulics calculations. For the time being, homogenized two-group cross-sections have been considered as responses in the GPT setting. The work is reported in detail in Ref. [16].

Criticality safety

Criticality safety studies have been neglected during the past few years. Consequently, the augmentation of the knowledge base is the most important issue. Most criticality calculations have been done using the MCNP-code [17] although the in-house code Serpent [18] can also be used. The criticality safety validation was interrupted years ago until it has now been brought back. The following sections summarise the effort done in criticality safety during the first half of the programme.

General understanding of reactivity dependences

In order to increase the general knowledge and understanding in criticality, a study on the dependences of reactivity on various parameters was carried out [19]. The parameters of a VVER-440 assembly in an infinite storage grid were systematically varied. The calculations were performed with both MCNP and Serpent using the JEFF-3.1.1 cross section library. Additional MCNP calculations were done with the ENDF/B-VII library.

Altogether 20 parameters were varied most of which were geometry parameters. Material densities were also studied while compositions were only studied in a few cases. The variation of isotopic compositions was limited to the [234]U proportion in the fuel and the Hf or Nb concentration in cladding or shroud tube material. The enrichment of the fuel was obviously among the varied parameters.

In general the results were as expected. Many parameters have little or no effect on the reactivity as long as the parameter variation remains within a reasonable range. The largest effect was found with changes in the fuel enrichment and parameters related to moderation like assembly or rod pitch, moderator density or water level. Although many results were obvious, the study gave more confidence in how the various parameters affect reactivity. In addition to qualitative behaviour, the study also gave quantitative results.

The MCNP and Serpent results were in good agreement as in previous studies. This reassures the position of Serpent as an equally strong tool as MCNP in criticality calculations. However, a large difference of up to 700 pcm was observed between the two different cross section libraries. This difference was consistently seen in all calculations.

Criticality safety validation

Criticality safety validation is essential for criticality safety analyses. The objective of this validation is to find the bias of the calculation system, i.e. the calculation code including the cross section library, and the platform. It is extremely important to know this bias as it determines the extra safety margin needed due to the uncertainty of the calculation system. Criticality safety validation has to be done against critical experiments. The bias is defined by the amount the calculated results differ from the experimental ones.

Criticality safety validation needs a validation package. This package is basically a set of critical experiments modelled with the code that is used for criticality safety analyses. The cases included in the package should adequately cover the target to be analysed. In addition, the package has to be large enough to fulfil the requirements of the statistical analyses used to treat the results.

The assembling of such a package for the VVER-440 reactors was interrupted for over a decade. Now this effort has been reactivated. The evaluated benchmarks are picked from the International Handbook of Evaluated Criticality Safety Benchmark Experiments (ICSBEP Handbook) [20].

The work was started by reviewing the inputs of the cases chosen in the previous work. This initial set of inputs comprises 23 critical experiments from the ZR-6 reactor modelled with the MCNP-code. These inputs were revised and updated [21] to agree with the ICSBEP Handbook.

The initial set of modelled benchmarks was increased by 25 new cases from the LR-0 reactor [22]. This set includes fuel assemblies with enrichment of 3.6% and 4.4%. It covers assembly pitches from 18 to 19.25 cm. It also contains cases with and without absorbing elements around the assemblies. Figure 3 shows the geometry at the bottom of an assembly from this model.
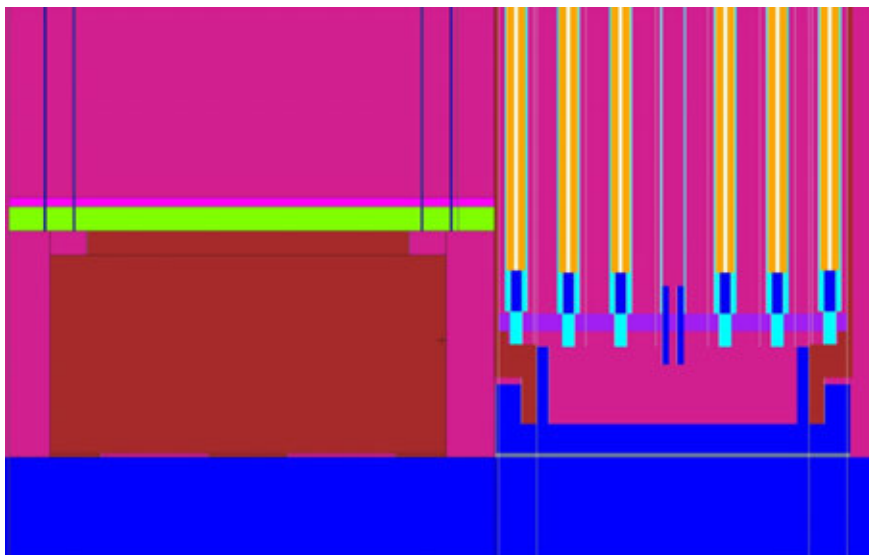

Figure 3. Geometry of the bottom of part of the LR-0 model for the validation package. The figure shows the bottom of the control cluster on the left and the nest and the base of the fuel assembly on the right.

The validation package now comprises 48 modelled critical benchmark experiments [23]. Thus the package is well on its way to its target which is 100 to 200 cases. However, no analysis on the cases has yet been done. The number of

cases has grown large enough for this to become possible. Therefore, also a script has been started. This script now only runs the calculations and collects the resulting k_{eff} -values. Eventually, this script should make the whole validation analysis and write a validation report automatically. The package should then be run for the specific code, library and platform combination on which the criticality safety analyses are to be made.

The validation process is a complicated one. To facilitate it and to accustom the current staff to the validation process an effort to write a Finnish validation guide was started. The intention of the work is to collect a "cook book" for the validation. The guide would thus describe the whole process as well as include tools needed to perform the analysis. It should also contain a simple example which can be used to verify the analysis process. However, by this time this guide has only been drafted [24].

Reactor dosimetry

A major part of the effort in 2011 was devoted to the 14th International Symposium on Reactor Dosimetry (ISRD). T. Serén was a member of the European organizing group (EWGRD). At the Symposium he chaired an oral session and a workshop. He was also a co-author of an oral presentation [25]. He further participated in the peer review of three papers presented at the Symposium.

Two major tasks were completed in 2012: an inter-laboratory "Round Robin" exercise involving precise activity measurements of samples prepared by SCK-CEN, Belgium, and preparation of a new basic cross section library based on the IRDFF library released by the IAEA in May-June 2012. The Round Robin exercise was proposed at the 14th ISRD and gained wide support. The exercise was launched in May 2012 with VTT as the first participant (apart from the organiser SCK-CEN). The samples were activated metallic foils of Ag, Co, Fe, Ti and Nb. Only the ^{94}Nb activity of the Nb samples was measured in this exercise since the counting of ^{93m}Nb requires destructive treatment.

The samples were weighed, measured and analysed at VTT immediately after arrival, and were promptly sent to the next participant. All samples were measured with a gamma spectrometer in standard, well calibrated geometry and analysed with the FitzPeaks program. To our knowledge, the samples have now been measured and reported by all participating laboratories. However, the results have not yet been compiled and compared. The results will be published in a report and presented at the next ISRD.

A "Master" cross section library in the SAND-II format (640 energy groups up to 20 MeV) has been prepared. This library is mainly based on the newly-released IRDFF library (in ENDF-6 format) with a few additional reactions of interest for dosimetry and isotope production, mostly taken from ENDF-B/VII. The cross sections are given in cm^2 and the uncertainty information in the form of relative uncertainties accompanied by a correlation matrix, mostly in a rather coarse group structure of just a few tens of groups. In cases where the original uncertainties were given in a very fine group structure, they have been condensed to the

BUGLE-80 group structure of 47 groups to save space. The "Master" library will be used to update the cross sections for the PREVIEW program and for the LSL-M2 adjustment program. Both of these use the BUGLE-80 group structure. Time and resources permitting, the 89-group cross section library for the NSVA-3 adjustment program will also be updated.

Summary

The CRISTAL project is an essential platform for educating new experts in the field of reactor physics. A wide range of codes and applications are dealt with. The expertise in the field has to be increased in order to ensure appropriate and adequate safety analyses where reactor physics is the basis. This is the most important objective of the project.

In addition to a knowledgeable staff, good enough coverage is needed on the code side. The project also tackles this issue. The codes have to be kept up to date as well as the understanding of them. In addition, their validation has to be brought to an appropriate level in accordance with international standards. This is an issue that has been neglected for quite some time.

In order to meet the above mentioned demands, the project was divided into two major tasks and two smaller ones. The larger ones covered calculation methods while the smaller ones dealt with reactor dosimetry and international co-operation. International co-operation is vital for improving the expertise since the resources of a single country are limited in this field.

The work done in the project has enabled the increase of general understanding of some basic reactor physics. Good examples are the studies on both cross section and reactivity dependences on various parameters. Both studies served their purposes of increasing the general understanding in the field. While perhaps not of strong scientific value, these studies were significant in the educational purpose. Also, the systematic approach was appreciated.

The inventory calculation study encountered some major obstruction as the code used in the work would not converge in all the cases. Although this prevented from obtaining appropriate results for part of the work, the study was useful. New experience on decay calculations and 3D discrete ordinates method was obtained. In any case, gaining experience was the main aim of this study although a successful study would have also provided experience in the subject.

Scientifically the most interesting work is the work on sensitivity and uncertainty analysis tools. The subject has become increasingly important as calculation tools and codes have improved. Calculations are made on more accurate geometries and with more sophisticated and accurate methods. As the calculation margins decrease, understanding the accuracy of the computer codes has grown increasingly important. The work done within this project has gained world-wide recognition.

Building a large enough validation package is a tedious work but of utmost importance in order to fulfil the criteria of international standards The validation package is well on its way as the work on it has been reactivated during this pro-

ject. Criticality safety validation has grown in importance as safety margins decrease. As the enrichment and burnup of the fuel increase, and when the use of burnup credit is enabled, the safety margins become smaller.

The project has been successful in its most important objective of increasing and ensuring the know-how in the field. The competency of the staff has increased during the work. However, a lot of work is still to be done in order to ensure high expertise needed for appropriate and adequate safety analyses.

References

1. Rhodes, J., Edenius, M. Studsvik Scandpower Report SSP-01/400 Rev 4, 2004 and Rhodes, J., Smith, K. and Edenius, M. Studsvik Scandpower Report SSP-01/401 Rev 2, 2004.

2. SCALE: A Comprehensive Modeling and Simulation Suite for Nuclear Safety Analysis and Design, ORNL/TM-2005/39, Version 6.1, ORNL, Oak Ridge, Tennessee, June 2011. Available from Radiation Safety Information Computational Center at Oak Ridge National Laboratory as CCC-785.

3. DOORS, One, Two- and Three-Dimensional Discrete Ordinates Neutron/ Photon Transport Code System, RSICC web page, http://www-rsicc.ornl.gov/codes/ccc/ccc6/ccc-650.html.

4. Räty, A., Rantamäki, K. VTT Research Report VTT-R-00457-12, Espoo. 2012.

5. Anttila, M. VTT Energy, Technical Report RDF-1/98, 1998, and Kaloinen, E. VTT Research Report VTT-R-03225-06, Espoo 2006.

6. Kaloinen, E. VTT Energy, Technical Report RFD 26/92, Espoo 1992.

7. Räty, H. VTT Research Report No VTT-R-04724-07, Espoo 22.5.2007.

8. Rantamäki, K., Räty, A. VTT Research Report VTT-R-00778-13, Espoo 2013.

9. Rhoades, W.A., Simpson, D.B. The TORT Three-Dimensional Discrete Ordinates Neutron/Photon Transport Code. ORNL/TM-13221 (October 1997).

10. Räty, A. Three-Dimensional Discrete Ordinates Calculations with TORT. in the XV Meeting on Reactor Physics Calculations in the Nordic Countries, Helsinki, Finland, April 12–13, 2011.

11. Markova, L. Specification for CB 6 Benchmark on VVER-440 Final Disposal. NRI, April 2010 http://www.oecd-nea.org/science/wpncs/buc/specificatio ns/CB6-VVER-Disposal-benchmark.pdf.

12. Räty, A., Kotiluoto, P. VTT Research Report. VTT-R-08653-12, Espoo 2013.

13. Bekar, K.B., Azmy, Y. M&C 2009 conference, Saratoga Springs, New York, May 3–7, 2009.

14. Ivanov, K., Avramova, M., Kodeli, I., Sartori, E. Benchmark for Uncertainty Analysis in Modeling (UAM) for Design, Operation, and Safety Analysis of LWRs. NEA/NSC/DOC(2007)23 (2007).

15. Pusa, M. Incorporating sensitivity and uncertainty analysis to a lattice physics code with application to CASMO-4. Annals of Nuclear Energy, 40(2012), 153–162.

16. Pusa, M. Perturbation Theory Based Sensitivity and Uncertainty Analysis with CASMO-4. Sci. Technol. Nucl. Install., 2012(2012). Article ID157029.

17. X-5 Monte Carlo Team, Report LA-UR-03-1987, Los Alamos National Laboratory (2003).

18. Serpent web page http://montecarlo.vtt.fi.

19. Viitanen, T., Rantamäki, K., Häkkinen, S., VTT Research Report VTT-R-00786-12, Espoo 2012.

20. LEU-COMP-THERM-015, International Handbook of Evaluated Criticality Safety Benchmark Experiments, NEA/NSC/DOC/(95)03/IV, Volume IV, OECD/NEA, 2009.

21. Juutilainen, P. VTT Research Report VTT-R-01123-12, Espoo 2012.

22. LEU-COMP-THERM-087, International Handbook of Evaluated Criticality Safety Benchmark Experiments, NEA/NSC/DOC/(95)03/IV, Volume IV, OECD/NEA, 2010.

23. Juutilainen, P. VTT Research Report VTT-R-00787-13, Espoo 2013.

24. Rantamäki, K., Juutilainen, P., Viitanen, T., VTT Research Report VTT-R-00976-12, Espoo 2012.

25. Thornton, D.A., Serén, T. et al. Dosimetry Assessment for the RPV and Core Barrel in UK PWR Plant. Proceeding of the 14th International Symposium on Reactor Dosimetry, Bretton Woods, New Hampshire, USA, May 22–27, 2011.

4.2 Three-dimensional reactor analyses (KOURA)

Ville Hovi, Anitta Hämäläinen, Mikko Ilvonen, Mikko Manninen, Jukka Rintala,
Hanna Räty, Elina Syrjälahti, Veikko Taivassalo

VTT Technical Research Centre of Finland
Tekniikantie 2, P.O. Box 1000, FI-02044 Espoo

Introduction

The fundamental objective of KOURA project is to have a truly independent transient calculation system, which can be utilized by the safety authority and other end-users for safety analyses that are independent from those of power plant designers and fuel vendors. One of the main objectives in this project is supplementing the code system with three-dimensional thermal hydraulics modelling. Other main objective during the first two years of the project has been the enhancement of VTT's boiling water reactor modelling capabilities.

3D Thermal hydraulics

The PORFLO code is a computational tool, developed at VTT, designed to analyse thermal hydraulic phenomena in multiphase flow problems related to nuclear power plant safety analysis. It is mainly targeted at applications where 3D phenomena may be significant but geometrical complexity does not allow for a CFD-style structure fitted grid all around the computational domain, e.g. fuel bundles, internal structures of reactor pressure vessels, steam generators and heat exchangers. Therefore, as the name PORFLO implies, the code utilizes the concept of porous medium to model structural features not represented explicitly in a computational mesh. In the porous medium approach, the fluid fraction of the total cell volume is defined as the porosity and the effects of the porous medium are modelled explicitly as source terms in the scalar transport equations that govern the fluid flow.

The new code version

A complete rewrite of the PORFLO code was done during 2011, in which two major improvements were introduced: the ability to handle unstructured meshes and parallelization. [1]

The previous PORFLO versions were based on a structured, rectilinear description of the solution domain, in which the geometrical information was described using porosity alone. This led to many difficulties when dealing with rounded shapes. With the new, unstructured version of PORFLO, it is possible to fit the grid to those structures that can be represented by an affordable number of cells, such as the cylindrical walls of the reactor pressure vessels and other components of the nuclear industry, and use variable porosity elsewhere when needed.

Together with the choice of a general data format, such as CGNS, the ability to handle unstructured meshes facilitates the comparison of results to other CFD codes, since the same mesh can be read to both code counterparts.

Parallelization of the code is based on a domain decomposition method and the use of MPI calls. Though the total cpu-time needed for a given simulation is not affected by parallelization, the wall-clock time is greatly reduced, which is a huge benefit when considering the coupled neutronics – thermal hydraulics solution, since the thermal hydraulics solution is significantly more cpu-intensive of the two.

Solution algorithm

The current solution method for the pressure-velocity coupling is the Phase-Coupled SIMPLE algorithm (PC-SIMPLE) [2]. The steps of the PC-SIMPLE algorithm are summarized below:

1. Solve momentum equations
2. Calculate face normal velocities (Momentum-interpolation)
3. Reconstruct volumetric fluxes
4. Solve pressure correction equations
5. Correct pressure and face normal velocities
6. Solve phase volume fractions
7. Reconstruct mass fluxes
8. Solve scalar equations
9. Repeat (from step 1) until convergence
10. If time-dependent, advance to next time step.

Turbulence modelling

The most widely used of the two equation models, the k-ε model developed by Launder and Spalding [3], has been implemented. From the perspective of the entire solution process this adds two scalar fields to the list of solved variables: these are the turbulence kinetic energy per unit volume (k) and its dissipation rate (ε). As a first approach the so called mixture model was chosen, in which the turbulence kinetic energy and turbulence dissipation rate are solved for the mixture of the two phases.

Once solved, the turbulent kinetic energy will affect many processes, most importantly the flow field through turbulent viscosity. Currently the predicted values of k and ε have been initially checked against Fluent and qualitative agreement has been found. For the time being, the model has appropriate source terms at known walls only, not in the porous medium.

Parallel computation

Parallelization of the code is based on a non-overlapping domain decomposition method, which bears resemblance to the Schur complement method. It is imple-

mented using Open MPI library calls (an open source implementation of the Message Passing Interface). The domain is divided into subdomains, one for each process. Each process works mainly on its own independent data block only to exchange data over the process interfaces. The coupling of the parallel processes is done at the level of the iterative solution of linear systems of equations. This ensures that the flow problem is exactly the same for both serial and parallel operation.

Two parallelized, preconditioned iterative linear solvers, both of which are Krylov subspace methods, are available for the solution of the linear systems of equations that arise during the solution process: the Preconditioned Conjugate Gradient method (PCG) for symmetric coefficient matrices (pressure correction equations) and the Preconditioned Bi-Conjugate Gradient Stabilized method (PBiCGStab) for non-symmetric coefficient matrices (all the scalar transport equations). The choice of the preconditioning method is currently limited to two: Incomplete Cholesky factorization (IC) and Symmetric Successive Over-Relaxation (SSOR). Both IC and SSOR can be used with the pressure correction and SSOR with the scalar transport equations.

PORFLO simulations

EPR Pressure vessel

The flow simulation for an EPR pressure vessel with the previous structured version of the PORFLO code demonstrates problems associated with structural meshes [4]. In a rectilinear grid, the description of curved and relatively small structures is inaccurate and unphysical results are developed. The performance of the new unstructured PORFLO was tested by performing a single-phase simulation for the EPR pressure vessel with a body-fitted mesh.

In the case considered, the total heating power of 3870 MW is assumed to be produced evenly by the fuel rods. The total mass flow rate of the coolant was chosen to be 22 200 kg/s and it is assumed to be divided evenly between the inlet nozzles. The feed temperature of the coolant is taken to be 296°C. The system pressure is assumed to be 15.8 MPa. As the heating power corresponds to 90% of the nominal heating power of the EPR and is evenly distributed, no significant vapour generation is expected to occur and the single-phase simulation is justified.

By utilizing symmetry of the pressure vessel, the computational domain covers only a quarter of the pressure vessel. A mesh consisting of about 250 000 hexahedral and tetrahedral cells was created for the computational domain (in Figure 1). Only the main components are represented as such in the mesh. For the smaller structural components, the porous medium description is applied. The volume for fluid flow in each cell was determined by assigning a proper value for the porosity. The pressure drop in porous zones is modelled by the inertial loss coefficient.

Symmetry boundary conditions are imposed at the symmetry planes. At the walls associated to porous fluid zones, free slip (no friction) boundary conditions are applied. The other walls are considered no-slip (zero velocity) boundaries.
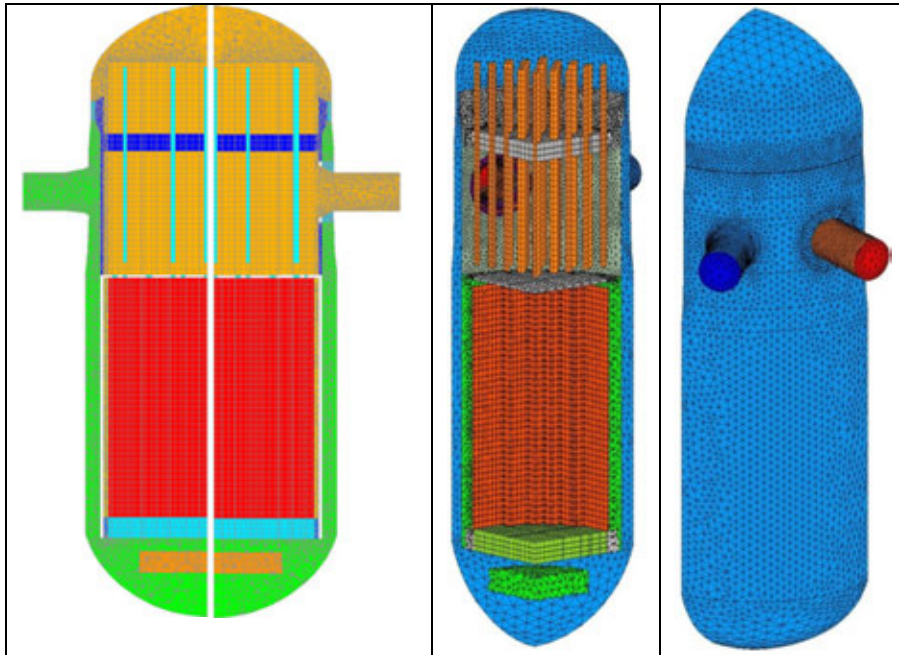
Figure 1. Visualizations of the unstructured mesh for an EPR pressure vessel.
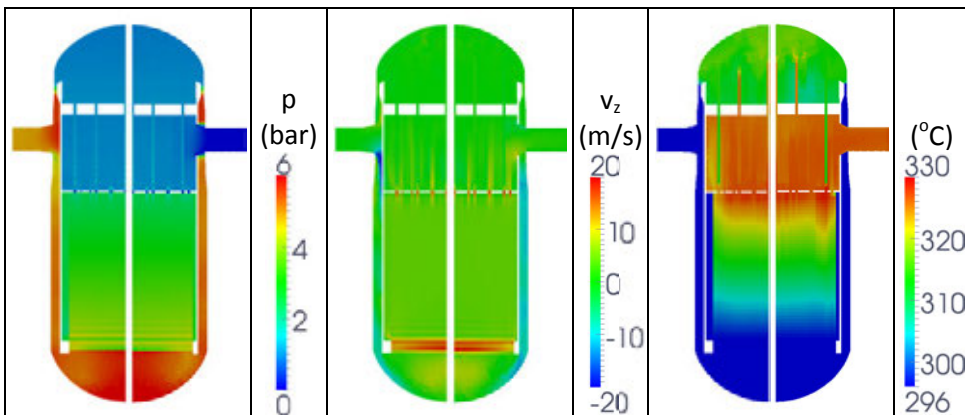

Figure 2. Pressure, vertical velocity and temperature on the planes of the inlet and outlet nozzles computed with the PORFLO code for the unstructured mesh of an EPR pressure vessel.

The standard kε turbulence model is employed to model the influence of flow turbulence. At this stage, the balance equations for k and ε include no additional

correction terms for the porous zones mainly because no general, widely accepted closure models exist for these terms [5].

In order to reduce computing time, constant values for the density, viscosity, thermal conductivity and specific heat of the water are assumed. Since the maximum temperature is expected to be about 328°C, values for the temperature of 312°C are used in the simulation.

Figure 2 shows contour plots for the pressure, vertical velocity and temperature. Analysing the flow field, we can conclude that the flow pattern is expectable: The liquid flows down between the core barrel and the pressure vessel walls, up through the fuel assemblies and through the pattern of the control rod assemblies towards the outlet nozzles. According the simulations, a small portion (about 0.7%) of the coolant flows directly through the upper support plate to cool the upper head. In the columns for the inner control rod assemblies, the liquid flows upward whereas in the outer ones the flow is downward. The leakage directly to the outlet nozzle is about 0.6% of the total flow. Although the pressure loss over the core (about 2 bar) is close to the design value, the total pressure loss over the whole pressure vessel is larger than the design value [6]. The too large total pressure drop is caused mainly by the coarse mesh. The tetrahedral cells are relatively large especially in the downcomer and outlet nozzle area. In addition, the mesh is not dense enough to reproduce the flow in the holes in the upper core plate. Large changes in the porosity are computationally challenging and cause the non-smoothness of the results shown in Figure 2.

Simulations in an EPR fuel assembly

The unstructured version of the PORFLO code was applied to simulate the thermal-hydraulic phenomena in an EPR fuel assembly. The computational domain covers vertically the length from the lower face of the lower support plate to the upper face of the upper core plate. Horizontally, the computational domain covers the whole area reserved for each fuel assembly in the core (215.04 mm x 215.04 mm). As the EPR possesses an open core, in the simulation the fuel assembly is hydrodynamically assumed to be in an infinite fuel bundle matrix and symmetry at the vertical boundaries can be assumed (i.e. no flow through the vertical boundaries). The computational domain was discretised with hexahedral cells (68 000 = 18 x 18 x 209). For each cell, the porosity was assigned to describe the space available for fluids.

The water mass flow of 87.1 kg/s is assumed to flow upward through the four holes in the lower support plate. The temperature of the feed water is assumed to be 296ºC. No steam is assumed to be in the feed water. The total heating power was distributed evenly among the fuel rods for their active length of 4200 mm. For each cell, the heating power was obtained by multiplying the total heating power of the whole assembly by the ratio of the volume of the (active) fuel rods in the cell to the total volume of the fuel roads. Two cases with the total heating power of 18.2 and 26.0 MW were computed.

Figure 3 shows the liquid temperature (scale 296–346.5ºC) and void fraction (scale 0–0.13) for the 26.0 MW case on a vertical cross-section plane. The high peak value in the void fraction close to the top is related to the numerical difficulties in case of large porosity steps. More results are presented in [7].

The simulations has several limitations and simplifications: dimensions especially for the end pieces are evaluated from pictures and are thus inaccurate, the mesh is too coarse to reproduce details of flow, constant values were used for densities and viscosities, inaccuracies in the models for the flow resistance, ignoring the turbulent velocity fluctuations and consequently the turbulent mixing phenomena, and the total heating power is divided evenly for the (active) fuel rods. Moreover, the current results are computed with a development version of the unstructured PORFLO which it is not fully debugged. Therefore, the current results should not be considered as an analysis of thermo-hydraulic phenomena in an EPR fuel assembly and they have limited value from the safety assessment point of view.

Reactor dynamics

BWR

Reactor dynamics of boiling water reactors have been modelled at VTT with the TRAB3D [9] code, which includes a three-dimensional nodal model for the core, coupled to parallel one-dimensional hydraulics channels and radial heat transfer in the fuel and cladding. TRAB3D includes also models for the rest of the BWR pressure vessel thermal hydraulics using one-dimensional channels, as well as models
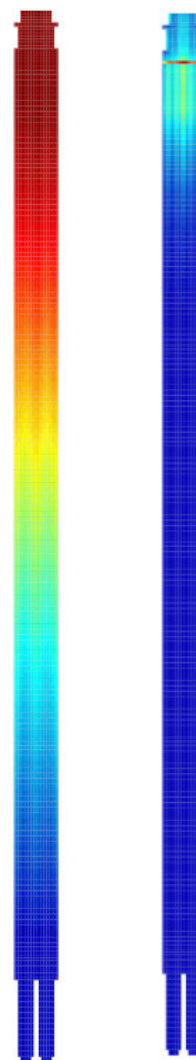

Figure 3. Liquid temperature (left) and void fraction (rigth) in EPR fuel assembly with PORFLO.

for steam lines, pumps and control systems. TRAB3D is designed especially for Olkiluoto type of BWR reactors, and its modelling capabilities in thermal hydraulics are intended to transients with upwards flow in the reactor core. The internal coupling of TRAB3D 3.0 with the system code SMABRE 6.0 [10] replaces all the hydraulics modelling in TRAB3D with models of SMABRE, while heat transfer is calculated optionally with either code. With SMABRE it is also possible to model all the automation and process components and systems in nuclear plants. The internal coupling of the codes extends the modelling capabilities transients with reversed flow in a flow channel, and the coupled code is more versatile for modelling of different types of reactors.

Development of the coupling of the codes continued up to the end of the previous SAFIR 2010 project, mainly focusing on PWR reactors. In the present KOURA/SAFIR2014 project the focus has been on the validation of the coupling, as well as on the features of BWR reactors. Furthermore, first steps have been taken with the intention to coupling of the TRAB3D neutronics with the 3-D thermal hydraulics code PORFLO utilizing the experience of the TRAB3D-SMABRE-coupling.

Successful calculation of the flow reversals have been demonstrated for the HPLWR-core, which has also downwards flows in the core in its nominal state, and for the EPR with quite an extreme test case [11, 12].
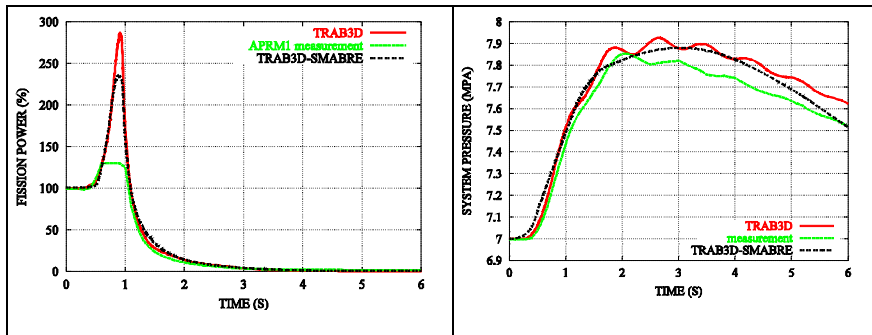

Figure 4. Measured and calculated reactor power and system pressure with TRAB3D and TRAB3D-SMABRE in Olkiluoto 1 overpressurization transient 1985.
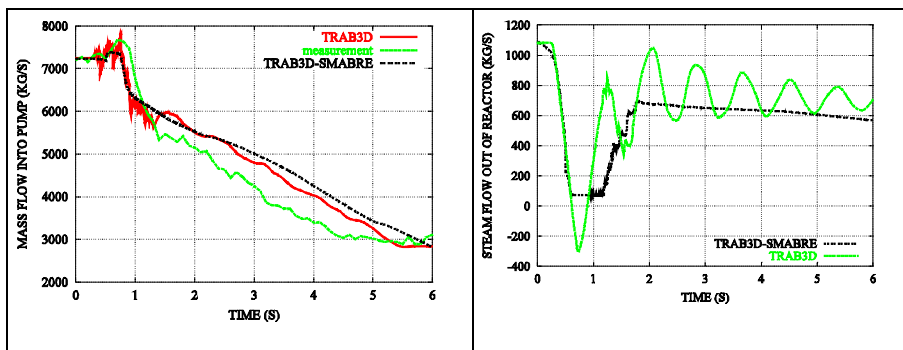
Figure 5. Measured and calculated pump mass flow and total steam line mass flow out of reactor pressure vessel with TRAB3D and TRAB3D-SMABRE in Olkiluoto 1 overpressurization transient 1985.

Validation of the internal coupling was initiated with code-to-code comparisons. Along with the devel-opment of the coupling, the disturbances from the load rejection test of 1998 at Olkiluoto 1 were used as separate test cases and compared against TRAB3D results, but the transient has not been calculated as a whole yet. The features needed for the pressurized water reactor were tested using the pump seizure of an EPR, against the parallelly coupled TRAB3D-SMABRE version in which SMABRE models the coolant circuit outside reactor core. The latest validation efforts concern the Olkiluoto 1 overpressure transient from 1985, earlier calculated as part of the validation of TRAB3D [11], and an EPR control rod ejection case.

The Olkiluoto 1 overpressure transient of 1985 was initiated by a malfunction in the pressure controller, resulting in fast closing of the turbine valves. This was followed by a rapid increase in reactor pressure, causing the collapse of voids in reactor core and a fast power increase. Recirculation pump trip and reactor scram (as well as the Doppler effect) terminated the power excursion, while the pressure was decreased with the opening of the relief valves. The results of the standalone TRAB3D and internally coupled TRAB3D-SMABRE calculations of the overpressure transient have been compared against measurements in the Figure 4 and Figure 5 for the fission power, reactor pressure, main circulation flow and steam flow out of the reactor. Qualitatively these first results of this fast BWR transient agree quite well both between the codes and with the measured values.

Calculation of the overpressurization transient helped to localize the submodel in the code which has caused trouble in the development: the radial fuel rod model had been erroneously implemented from TRAB3D to SMABRE, and these calculations have been for now carried out with a simpler average fuel rod model of SMABRE. For the recirculation pumps the homologous pump model of TRAB3D is used, instead of the simpler model of SMABRE. Another known defect in the coupled model can be seen in the behaviour of pressure and steam flow: steam line dynamics is still missing from the steam line description of SMABRE. With steam line dynamics the increase in pressure is sharper, and results in a more pro-

nounced fission power peak. The height of the actual peak is not known, as the measurements stop at about 130% of the nominal power.

Due to the erroneous fuel rod model the other validation case, control rod ejection in an EPR reactor, was also calculated with the average fuel model of SMABRE. The control rod ejection causes a sharp power increase and a sharp power decrease due to the Doppler feedback. While using the average fuel rod model in SMABRE, the height of the power peak is nearly identical in the results of the parallelly and internally coupled code versions (Figure 6).

Future work on the internal coupling consist of identifying and rectifying the errors in the radial fuel model of

Figure 6. Calculated fission power peak in EPR control rod ejection with internally and parallelly coupled TRAB3D-SMABRE.

SMABRE, as well as testing the so far unused option of the fuel rod calculation in the TRAB3D instead of SMABRE. Steam line dynamics need also to be included, either by modifying SMABRE or including the TRAB3D model in the coupling. More studies are also needed for some oscillations appearing in PWR cases with reversed core flows. The results of the validation cases performed up to now are promising but still new cases should be studied.

OECD/NEA launched new boiling water reactor benchmark in 2011. The benchmark is based on the stability event at the Oskarshamn-2 nuclear power plant in February 1999. VTT participates in the benchmark with the aim of challenging and enhancing its BWR modelling capabilities, with special emphasis on deepening the expertise on BWR phenomena and further training of reactor dynamics specialists on using TRAB3D for BWR analyses. In this benchmark it is possible to validate TRAB3D against plant data and other codes, and to deepen the knowledge on stability analysis. Creation of a new model from scratch is laborious, but a very useful lesson in the modelling of boiling water reactors.

Figure 7. Geometry of TRAB3D circuit model for Oskarshamn-2.

In 2012 the TRAB3D model for Oskarshamn-2 plant has been constructed [14]. Main difference to the TRAB3D's usual BWR application, Olkiluoto power plant, is that pumps are located to external recirculation lines. An overview of the geometry of the
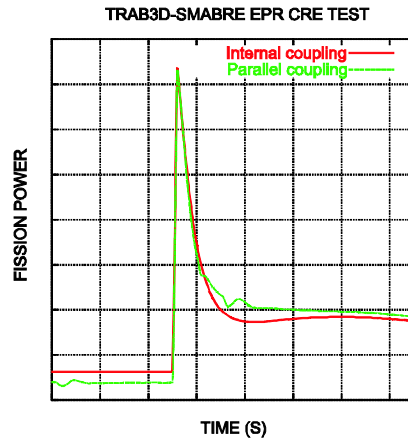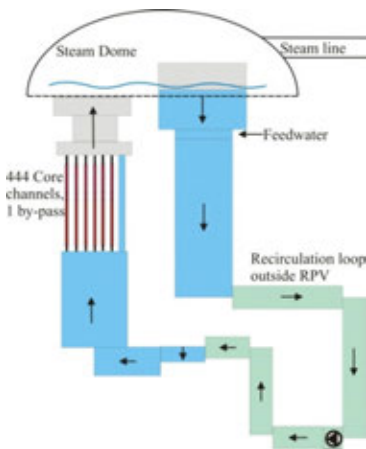
circuit model is shown in Figure 7. According to the steady state calculations, TRAB3D is capable to model this kind of recirculation line geometry. The cross section data has been modified in co-operation with CRISTAL project to the format that can be used in TRAB3D. Some of the fuel properties have not been delivered to the participants, and thus actual transient has not been calculated yet. Modelling of the transient has been tested with separate models and with the Olkiluoto data. The actual benchmark exercise will be calculated in 2013.

Neutronics

Currently the nodal codes used at VTT, HEXBU-3D, HEXTRAN, TRAB3D and APROS calculate only the nodewise power distribution. However, more accurate safety analyses and modern thermal hydraulic solvers, such as PORFLO, require a pinwise power distribution. A method for pin power reconstruction, which can be used in a manner of routine in nodal code calculations, is an essential developments step in road of enhancing the safety analysis methods.

On the base of the literature review, it was concluded that the previous work in the area of pin power reconstruction at VTT is the best starting point for the current project [15, 16]. Previously a first version of an external code for pin power reconstruction has been developed and tested with some relatively simple test cases. The method is based on combining the homogeneous power distribution by a nodal code and a heterogeneous power distribution, which is achived by using pre-calculated intranodal power distributions. This is an effective and relatively accurate method, which is commonly used in different nodal codes around the world.

After choosing the method, the work in the project has concentrated on taking the old reconstruction code in the use again and getting to know to the code to understand its construction and operational principles. Use of the code has been started by very basic testing, because the code had thus far been used only for some test calculations by its original developer. This approach has turned out to be beneficial.

The code has now been taken into the use by first compiling it with the currently used compiler. Further, its basic functioning has been tested in small parts, subroutine by subroutine to understand their operation and check their correct operation. The second main task has been a taking into use the option in TRAB3D, which provides the additional output for the pin power reconstruction. The next step in the project is to perform a first new full test calculation, where the data is obtained by a new TRAB3D calculation, while thus far the code testing has been performed by old data files. Further, a full size reactor core test case with accurate comparison data (e.g. by Monte Carlo codes) is essential for testing of the method.

International co-operation and QA

International co-operation

Participation in the OECD Nuclear Energy Agency (NEA) working groups and benchmarks is one of the most important ways of validating the methods and codes used in reactor analysis. This project includes the participation in the meetings of the NEA Working Party on the Scientific Issues of Reactor Systems (WPRS), which is responsible for the organization of the reactor dynamics benchmarks among other activities and included participation to the work of Nuclear Science Committee (NSC) in 2011. In the frame of the KOURA project VTT has participated in the OECD/NEA BWR stability benchmark (O2) and Uncertainty analysis benchmark series (UAM)

The cooperation and information exchange on VVER safety within the AER framework together with other countries that use VVER reactors has been continued. Conference papers have been presented in AER symposium [17, 18]. Project has also included participation to FJOH summer school and to the international scientific workshop on reactor dynamics and safety. Workshop focused on stability analysis. Work done in the project has been presented also in ICONE-20 conference [8].

Quality assurance and documentation

One aim of the project is to maintain and improve usability of the code system. Reactor dynamic codes TRAB3D, HEXTRAN and SMABRE have been transferred to Linux environment, and in that connection several deficient and non-standard features of the source code have been replaced. Branched versions of reactor dynamics codes, especially TRAB3D versions used in internal and parallel couplings with SMABRE, have been merged with the stand-alone TRAB3D. TRAB3D-SMABRE has been modified for the further coupling with the PORFLO code.

Usability of the code system has been improved also by documenting the codes and analysis methods developed in the predecessors of SAFIR2014. [19]

Summary

During first two years of SAFIR2014 program, VTT's reactor dynamic code system has been further developed and validated.

The computational capabilities of the new unstructured PORFLO code were tested and demonstrated by simulating the thermal-hydraulic phenomena in an EPR pressure vessel and fuel assembly. A body-fitted unstructured mesh created for the EPR pressure vessel demonstrates the benefits of the unstructured grid arrangement over rectilinear meshes in case of complex geometries. Simulation results are mainly expectable. Still some unphysical results in the vicinities of large porosity steps remain for future examination and improvement. On a whole, the

simulation results obtained assure that the new PORFLO version is able to discretise computational domains utilizing unstructured meshes as an input, to build up discrete algebraic equations for the conservation equations and to solve the resulting set of equations. Nevertheless, due to several significant simplifications and limitations, the value of the current results is limited from safety assessment point of view.

The validation of the internal coupling of TRAB3D with SMABRE has been started against the stand-alone TRAB3D and against measurements from the plant transients in the Olkiluoto power plant. Validation calculations have revealed deficiencies in certain submodels. For that reason also PWR validation cases have been recalculated with the internally coupled TRAB3D-SMABRE using submodels congruent with the parallelly coupled code. The results of the validation calculations are promising but still new cases should be studied. The errors found in the fuel rod model should be corrected, and TRAB3D's steam line dynamics need to be included into the internally coupled code.

Improvement of the neutronics model of the reactor dynamic codes by pin power reconstruction has begun. International co-operation has been continued by active participation to the work of AER and OECD/NEA, including participation in the Oskarshamn-2 BWR stability benchmark with the TRAB3D code.

References

1. Hovi, V. New PORFLO version with unstructured mesh and parallelization. VTT Technical Research Centre of Finland. Research report VTT-R-01143-12, 2012.

2. Vasquez, S.A., Ivanov, V.A. A phase coupled method for solving multiphase problems in unstructured meshes. In: Proceedings of ASME FEDSM'00: ASME 2000 Fluids Engineering Division Summer Meeting. Boston, Massachusetts, June 11–15, 2000. Pp. 743–748.

3. Launder, B.E., Spalding, D.B. The Numerical Computation of Turbulent Flows. Computer Methods in Applied Mechanics and Engineering 3(1974), 269–289.

4. Hovi, V., Ilvonen, M. The 3D two-phase porous medium flow solver PORFLO and its apllications to VVER SG and EPR RPV. In SAFIR 2010 Final report. VTT, 2011. VTT Research notes 2571. Pp. 160–170.

5. Mathey, F. Macroscopic Turbulent Models for Heat and Mass Transfer in Catalyst Reactors. AIP Conf. Proc. 1453, 2012. Pp. 121–126.

6. UK EPR. 2012. PCSR – Sub-chapter 4.4 – Thermal and hydraulic design. UKEPR-0002-044 Issue 04.

7. Hovi, V., Taivassalo, V., Ilvonen, M., Manninen, M., Takasuo, E. EPR-related applications of the PORFLO code on rectilinear and unstructured meshes. VTT Technical Research Centre of Finland. Research report. VTT-R-01142-12, 2012. 53 p.

8. Takasuo, E., Hovi, V. and Ilvonen, M. Applications and Development of the PORFLO 3D Code in Nuclear Power Plant Thermal Hydraulics. In: Proceedings of ICONE-20. Anaheim, California, USA, July 30 – August 3, 2012. Paper ICONE20-54161.

9. Kaloinen, E., Kyrki-Rajamäki, R. TRAB3D, a new code for three-dimensional reactor dynamics. In Proceedings of ICONE-5, Nice, France, May 26–30, 1997.

10. Miettinen J., Hämäläinen A. Development and Validation of the Fast Running Thermohydraulic Model SMABRE for Simulator Purposes. In Proceedings of ICONE-8. Baltimore, USA, April 2–6, 2000.

11. Seppälä, M., Hämäläinen, A., Daavittila, A. High Performance Light Water Reactor Transient Analysis with Neutronics Feedback using TRAB3D and SMABRE Codes. In Proceedings of ICAPP '10, San Diego, CA, USA, June 13–17, 2010. Paper 10103.

12. Hämäläinen, A., Räty, H. The internally coupled TRAB-3D 3.0 and SMABRE 6.0 codes. VTT Technical Research Centre of Finland. Research report VTT-R-00523-11, 2011.

13. Daavittila, A., Kaloinen, E., Kyrki-Rajamäki, R., Räty, H. Validation of TRAB-3D against Real BWR Plant Transients. In: International Meeting on "Best-Estimate" Methods in Nuclear Installation Safety Analysis (BE-2000). Washington, D.C., USA, 12–16 November, 2000 [CD-ROM]. La Grange Park: American Nuclear Society, 2000. ISBN 0-89448-658-6.

14. Syrjälahti, E. TRAB-3D model of the Oskarshamn-2 plant for OECD/NEA-O2 benchmark. VTT Technical Research Centre of Finland. Research report VTT-R-00713-13, 2013.

15. Rintala, J. Selection of the method for pin power reconstruction. VTT Technical Research Centre of Finland. Research report VTT-R-01163-12. 2012.

16. Mattila, R. Pin power reconstruction module for TRAB-3D nodal code. Technical Research Centre of Finland/Helsinki University of Technology, Master's thesis, 1999.

17. Rintala, J. Overview of the validation of the new 3-D neutronics model in Apros. In: Proceedings of the twenty-first Symposium of AER, Dresden, Germany, September 19–23, 2011.

18. Syrjälahti, E. Characterization of a representative VVER-440 fuel rod with the statistical ENIGMA. In: Proceedings of the twenty-second Symposium of AER, Pruhonice, Czech Republic, October 1–5, 2012. Pp. 721–734.

19. Räty, H. User's manual for hot channel analyses with the one-dimensional reactor dynamics code TRAB. VTT Technical Research Centre of Finland. Research report VTT-R-01166-12. 2012.

4.3 Development of a Finnish Monte Carlo reactor physics code (KÄÄRME)

Jaakko Leppänen, Maria Pusa, Tuomas Viitanen, Ville Valtavirta

VTT Technical Research Centre of Finland
Tekniikantie 2, P.O. Box 1000, FI-02044 Espoo

Introduction

The continuous-energy Monte Carlo method is widely used in nuclear and radiation transport applications, mainly because of its inherent capability to model complicated systems without major approximations. The method can be characterized as a brute-force simulation technique, well suited to linear problems that can be divided into a number of well-defined sub-tasks. For particle transport applications this implies simulating the motion of individual neutrons or photons through a process of random walk from one interaction to the next. The laws of physics for the simulated particles are represented by probability distributions, derived from theoretical nuclear models and experimental data, from which the outcome of each interaction is randomly sampled. When the process is repeated for a very large number of particle histories, detailed stochastic estimates for various physical quantities can be collected from the simulated events using statistical methods. The simulation requires a lot CPU time, which is one of the factors limiting the physical scale of the applications.

Monte Carlo method in reactor physics

Traditional Monte Carlo applications in nuclear engineering include criticality safety analyses, radiation shielding and dosimetry calculations, detector modeling and the validation of deterministic transport codes. The common factor in all cases is

the need to model the geometry and the interaction physics to within maximum accuracy, often regardless of the computational cost. Despite its versatility, however, the method has not been widely used for modeling operating nuclear reactors. The reason for this is not so much the difficulty of the neutron transport problem alone, but rather the fact that the fission chain reaction is so strongly coupled to heat transfer and coolant flow.

The solution of the coupled problem requires various approximations, which divide the calculation chain into multiple parts. The full-scale simulation of an operating reactor is traditionally based on few-group nodal diffusion methods, which provide sufficient accuracy for most design and safety analyses, with a low-enough computational cost for performing iterations between neutronics and thermal hydraulics. The preceding part of the calculation chain is focused on producing the input parameters for the simulator calculation through a procedure called homogenization, which essentially means reducing the level of detail in geometry and interaction physics, while preserving the reaction rate balance at the macroscopic scale. In addition to the neutron transport and the thermal hydraulics solutions, additional methods are needed for simulating the isotopic and mechanical changes in the materials as the fuel is burnt.

Moving from deterministic transport methods to Monte Carlo simulation brings a whole new range of possibilities in reactor analysis. The geometry description is inherently three-dimensional, and complicated structures can be modeled without major approximations. Neutron interactions are handled at the microscopic level, using the best available knowledge on the underlying physics. The calculation scheme is not subject to applications-specific limitations, and the same code and interaction data can be applied to any fuel or reactor type. Nevertheless, the method also has its drawbacks and limitations. The simulations are extremely computing-intensive, and statistical accuracy is basically a function of the overall running time. Combining continuous-energy Monte Carlo to deterministic transport methods is not always straightforward, and extending the scale of the simulations from pin- and assembly- to full-core level is not fully established, and may yet result in unexpected challenges.

The Serpent code

There are two ways in which continuous-energy Monte Carlo simulations can be brought into the reactor analysis calculation chain:

1) Use of Monte Carlo codes for producing input parameters (homogenized group constants) for deterministic reactor simulator calculations

2) Multi-physics simulations, in which a Monte Carlo neutron transport code is used as the neutronics solver of the calculation scheme and directly coupled to CFD or system scale-thermal hydraulics or a fuel performance code.

The first approach can be considered more viable, taking into account the limitations of the currently available computational resources, and it is also the idea that

originally inspired the development of the Serpent code. The work started at VTT Technical Research Centre of Finland in 2004, under working title Probabilistic Scattering Game, or PSG [1]. The code was specifically designed and optimized for assembly-level reactor physics calculations. This was considered a somewhat novel idea at the time, since most of the widely-used general purpose Monte Carlo codes lacked the capability to generate all group constants needed for simulator calculations. The name was later changed to Serpent, and the applications have considerably diversified along with code development and the growing user community. Even though KÄÄRME is the first project in the series of national SAFIR programmes exclusively devoted to the development of the Serpent code, it can be considered direct continuation to the work carried out in previous EMERALD and TOPAS projects in the first and second SAFIR programmes.

The first publicly distributed version of Serpent 1 was released at the OECD/NEA Data Bank in May 2009, and RSICC distribution in North America began a year later, in March 2010. The code is still under development, and new versions are distributed directly to registered users. A website containing the best and the most up-to date description of the Serpent code, including an input manual and a complete list of related publications, is set up at http://montecarlo.vtt.fi. An interactive php-based discussion forum for Serpent users can be found at http://ttuki.vtt.fi/serpent/.

Project goals

The calculation methods in Serpent 1 were developed over a relatively short time period, without really considering how the program structure should look as a whole. The result of this "live-and-learn" approach was that new calculation routines were constantly being added on top of existing source code, making the implementation of new capabilities increasingly complicated. In addition to the problems with maintainability, it became clear that certain choices regarding optimization between memory usage and performance made it impossible to extend the scale of burnup calculations beyond the fuel assembly level. The excessive memory usage also became a major limitation for parallel calculation, which was relying on a distributed-memory approach using the Message Passing Interface (MPI).

In order to keep up with the needs of the growing user community and computer development heading more and more in the direction of multi-core CPU's, computer clusters and massive parallelization, it was decided to re-write the entire source code. The development of a new version, Serpent 2, began in September 2010, and the work forms the major part of the KÄÄRME project. The main goals can be summarized as:

1) Extending burnup capability from 2D assembly level problems to full-core calculations involving over 100,000 depletion zones, without any limitations in parallelization

2) Developing new methods for reactor analysis and supporting long-term goals aiming at the coupling of Serpent into multi-physics calculation schemes

3) Establishing and maintaining a wide international network of Serpent users, and contributing to education of new experts in Finland and abroad.

The fulfillment of these goals is addressed in the following sections. It should be noted that in addition to the development of the new code version, an important and significant, although somewhat less interesting part of the project involves maintaining the publicly distributed Serpent 1.

Current status

The first half of the four-year KÄÄRME project has focused on parallelization and the fundamental transport and burnup capabilities of the Serpent 2 code. A beta-version was made available to registered users in January 2012, and most of the capabilities in Serpent 1 are now available in the new version. A significant effort was put to re-writing the parallelization routines based on a hybrid OpenMP / MPI approach, which has practically removed the previous limitations regarding the utilization of available computational resources (see Figure 1).
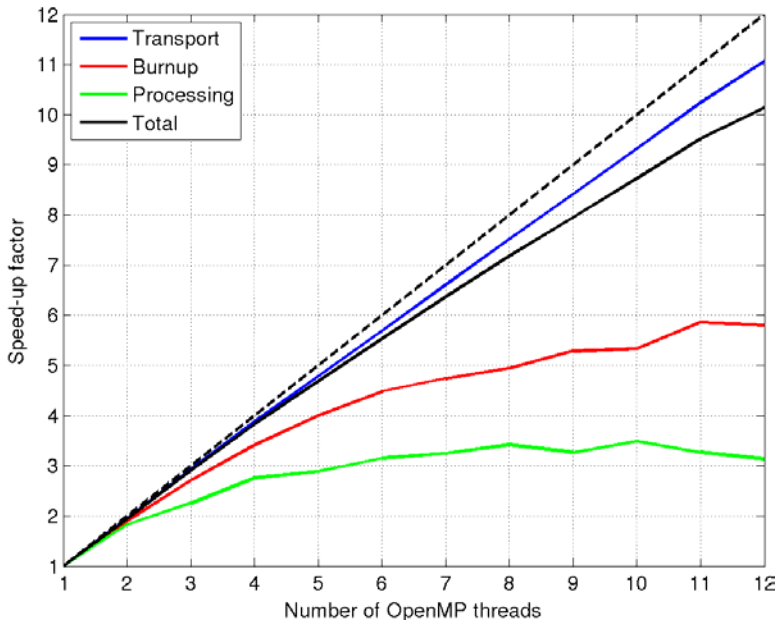

Figure 1. The results of an OpenMP parallel scalability test for Serpent 2, involving a 2D assembly-level BWR burnup calculation. Most of the CPU time is contributed to the transport routine, which scales reasonably well up to 12 CPU cores. The ideal linear scalability curve is plotted with a dashed line.

The problems with excessive memory usage were solved by introducing different optimization modes for small and large burnup calculation problems [2], and test calculations have shown that Serpent 2 can now handle over 120,000 depletion zones in a high-performance PC workstation or computer cluster. Since group constant generation and assembly-level burnup calculations remain among the most important user applications, the methods developed for increasing the performance at the cost of computer memory by the use of unionized energy grid and pre-calculated material cross sections [3] were kept in the higher optimization modes. In practice, any Serpent 1 calculation can be run using Serpent 2 with equal performance and no limitations regarding parallelization.

Serpent 2 also serves as the main platform for developing new features and capabilities. New methods for reactor analysis include advanced time-integration methods for burnup calculation [4, 5], developed in collaboration with the NEPAL project, and homogenization in leakage-corrected critical spectrum in collaboration with the Helmholtz-Zentrum Dresden-Rossendorf (HZDR) in Germany [6, 7]. Other improvements include new detector capabilities and visualization tools (see Figures 2 and 3). The development of a photon transport simulation mode has been started, and in the long run, some significant effort will be devoted to coupling Serpent with thermal hydraulics and fuel performance codes. Many of the calculation methods supporting these goals share common interests with the KÄÄRME project.
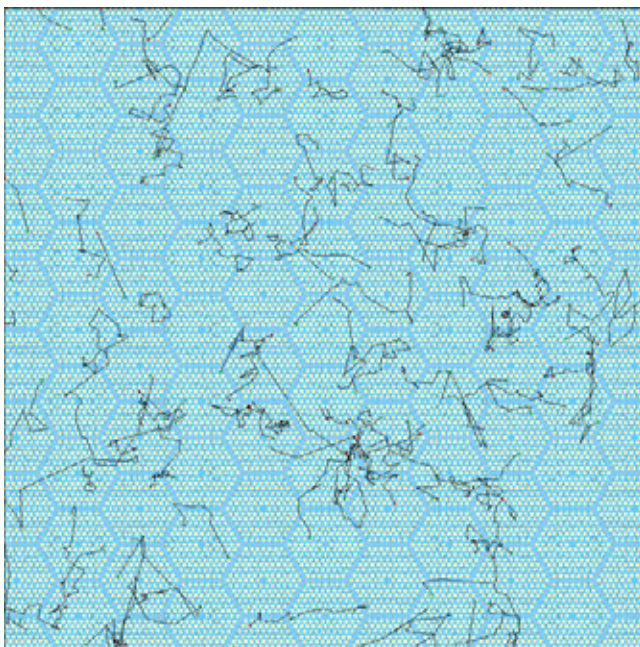

Figure 2. Simulated neutron tracks in a VVER-440 fuel assembly lattice. The track plotter is a new feature in Serpent 2, developed for visualizing source distributions and the random walk of neutrons and photons.
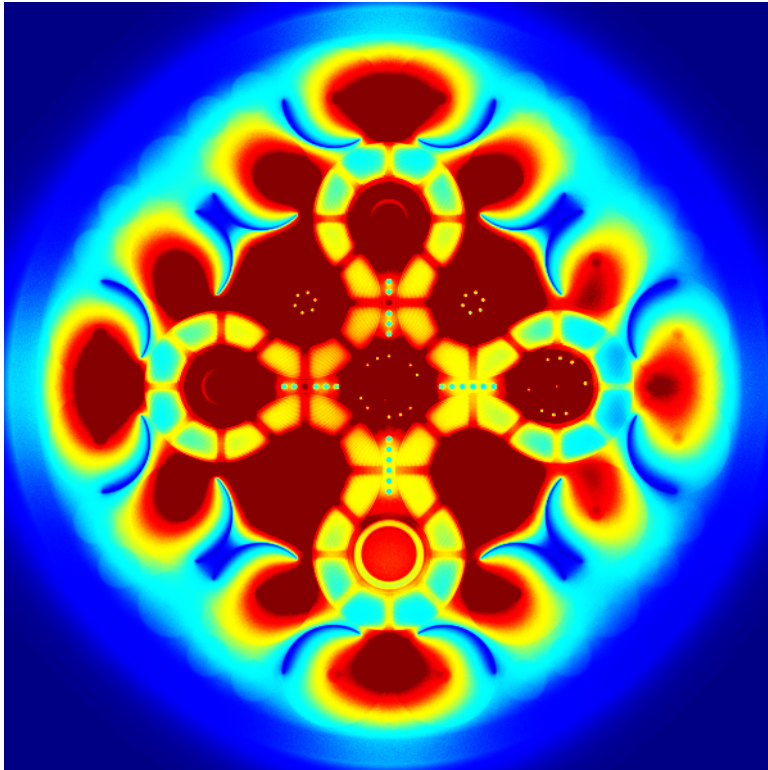
Figure 3. Neutron density distribution in the ATR reactor operated at Idaho National Laboratory (INL) in the U.S. The figure is generated by Serpent 2, using a collision flux detector with a 1/v response function.

International user community

By the end of January 2013, there were 212 registered users for the publicly distributed Serpent 1 in 86 universities and research organizations in 27 countries around the world. The beta-testing group for Serpent 2 consisted of 88 users. The applications range from group constant generation and assembly-level burnup calculations to modeling of complicated research reactor cores. Examples of user experience can be found in Serpent progress reports [8–10].

Communication with the Serpent user community is maintained by e-mail and using the discussion forum. Seminars and invited lectures have been given in various universities and research organizations, such as Massachusetts Institute of Technology (MIT), University of California, Berkeley and Idaho National Laboratory (INL) in the U.S, Seoul National University in Korea and Culham Centre for Fusion Technology (CCFE) in the UK. The first international Serpent user group meeting was organized with Helmholtz-Zentrum Dresden-Rossendorf (HZDR) in Germany,

in September 2011. The two-day event brought together 30 Serpent users from 15 organizations around the world. The second meeting was held a year later in Madrid, Spain. The meeting program was extended from two to three days, and the number of participants grew to 40. The next international meeting is planned to be held in the U.S. in 2013.

Education of new experts

By 2013, the Serpent team at VTT has grown to 4 scientists, three of which are developing the code as a part of their doctoral studies. Some of the work has already been published in scientific journals and presented at international conferences [11–16]. Related work outside the scope of the KÄÄRME project involves three more doctoral students at VTT and three in Finnish universities. Over the years, Serpent applications have provided topics for several M.Sc. and B.Sc. theses and other student projects.

The KÄÄRME project has educational value at the international level as well, since the typical Serpent user is a graduate or undergraduate student who is using the code for academic research. More than half of the 86 user organizations are universities, but due to the lack of more detailed figures it is not possible to estimate the number of on-going Serpent-related thesis projects worldwide. The code has also been brought to class room at least at the Royal Institute of Technology (KTH) in Sweden, UC Berkeley and Texas A&M in the U.S. and the École Polytechnique de Montréal in Canada. The educational use of Serpent is expected to increase in the future.

Future plans

The main focus in the development of Serpent 2 has moved from improved parallelization and completing the fundamental calculation routines to entirely new applications. Important topics for the remaining two years include:

1) Completing the photon and coupled neutron / photon transport simulation modes for gamma heat deposition and radiation shielding applications

2) Developing improved methodology for assembly- and core-level fuel cycle analyses

3) Continuing work on the built-in temperature feedback routine and external coupling to fuel performance codes.

Some of this work has already been started in collaboration with the NEPAL and PALAMA projects in SAFIR-2014 [17–18]. The calculation methods developed within the KÄÄRME project also support the long-term goals related to multiphysics applications [19], studied within the framework of the Academy of Finland Numerical Multi-Physics (NUMPS) and the EU High-Performance Monte Carlo Reactor Core Analysis (HPMC) projects.

Summary and conclusions

The KÄÄRME project continues the development of the Serpent Monte Carlo reactor physics burnup calculation code, started at VTT in 2004, and mainly funded from the previous SAFIR research programmes. The work is currently focused on a new version, Serpent 2, which extends the field of applications from assembly-level to full-core calculations. After the first half of the project is completed, the new code version is considered ready for a beta-testing phase, which was gradually began in January 2012. The second half will concentrate on entirely new features and capabilities, and the public distribution of Serpent 2 is scheduled for 2014. The KÄÄRME project also supports the long-term goals of Serpent development, aiming at multi-physics applications involving couplings to thermal hydraulics and fuel performance codes.

The Serpent code has gathered an international and constantly growing user community consisting of over 200 users in 86 organizations and 27 countries around the world. Maintaining this network is an important goal in the KÄÄRME project. Forms of collaboration include direct communication with code users, participating in international conferences and organizing annual user group meetings in changing locations. So far the collaboration has been extremely fruitful, benefiting both parties. Feedback from Serpent users is valuable for the development work, and the code provides a versatile tool for research and education of a new generation of experts.

References

1. Leppänen, J. Development of a New Monte Carlo Reactor Physics Code. D.Sc. Thesis, Helsinki University of Technology. VTT Publications 640, 2007.

2. Leppänen J., Isotalo, A. Burnup Calculation Methodology in the Serpent 2 Monte Carlo Code. In Proc. PHYSOR-2012. Knoxville, TN, 15–20 April, 2012.

3. Isotalo, A., Aarnio, P. Higher order methods for burnup calculations with Bateman solutions. Ann. Nucl. Energy 38(2011), 1987–1995.

4. Leppänen, J. Two Practical Methods for Unionized Energy Grid Construction in Continuous-Energy Monte Carlo Neutron Transport Calculation. Ann. Nucl. Energy 36(2009), 878–885.

5. Isotalo, A., Aarnio, P. Substep methods for burnup calculations with Bateman solutions. Ann. Nucl. Energy 38(2011), 2509–2514.

6. Fridman, E., Leppänen, J. On the Use of the Serpent Monte Carlo Code for Few-group Cross Section Generation. Ann. Nucl. Energy 38(2011), 1399–1405.

7. Fridman, E., Leppänen, J. Revised Methods for Few-Group Cross Section Generation in the Serpent Monte Carlo Code. In Proc. PHYSOR-2012. Knoxville, TN, 15–20 April, 2012.

8. Leppänen, J. Serpent Progress Report 2009. VTT Technical Research Centre of Finland. VTT-R-01296-10, 2010.

9. Leppänen, J. Serpent Progress Report 2010. VTT Technical Research Centre of Finland. VTT-R-01362-11, 2011.

10. Leppänen, J. Serpent Progress Report 2011. VTT Technical Research Centre of Finland. VTT-R-05444-12, 2012.

11. Pusa, M., Leppänen, J. Computing the Matrix Exponential in Burnup Calculations. Nucl. Sci. Eng. 164(2010), 140–150.

12. Pusa, M. Rational Approximations to the Matrix Exponential in Burnup Calculations. Nucl. Sci. Eng., 169(2011), 155–167.

13. Pusa, M., Leppänen, J. An Efficient Implementation of the Chebyshev Rational Approximation Method (CRAM) for Solving the Burnup Equations. In Proc. PHYSOR-2012. Knoxville, TN, 15–20 April, 2012.

14. Viitanen, T., Leppänen, J. Explicit treatment of thermal motion in continuous-energy Monte Carlo tracking routines. Nucl. Sci. Eng., 171(2012), 165–173.

15. Viitanen, T., Leppänen, J. Explicit Temperature Treatment in Monte Carlo Neutron Tracking Routines – First Results. In Proc. PHYSOR-2012. Knoxville, TN, 15–20 April, 2012.

16. Viitanen, T., Tulkki, V. Combining Reactor Physics and Fuel Performance Calculations. In Proc. TopFuel 2012. Manchester, UK, 2–6 September, 2012.

17. Valtavirta, V. Designing and implementing a temperature solver routine for Serpent. M.Sc. Thesis, Aalto University, 2012.

18. Viitanen, T. Serpent-ENIGMA – Combining Monte Carlo Reactor Physics with Fuel Performance. VTT Technical Research Centre of Finland. VTT-R-06265-11, 2011.

19. Leppänen, J. Viitanen, T., Valtavirta, V. Multi-physics Coupling Scheme in the Serpent 2 monte Carlo Code. Trans. Am. Nucl. Soc. 107 (2012) 1165–1168.

4.4   Neutronics, nuclear fuel and burnup (NEPAL)

Pertti Aarnio[1], Jarmo Ala-Heikkilä[1], Aarno Isotalo[1], Markus Ovaska[1] Antti Rintala[1],
Ville Valtavirta[1, 2], Risto Vanhanen[1]

[1]Aalto University School of Science
P.O. Box 11000, FI-00076 AALTO

[2]Current affiliation: VTT Technical Research Centre of Finland
Tekniikantie 2, P.O. Box 1000, FI-02044 Espoo

Introduction

The Fission and Radiation Physics Group at Aalto University School of Science concentrates on developing calculation methods for reactor physics, modeling basic physical and chemical phenomena in nuclear fuel, and researching new fuel cycles and next generation nuclear reactors. The activities seamlessly combine education and research of nuclear engineering. The essential field of know-how of the group covers physics-based analyses and numerical computation.

The behavior of high-burnup fuel in a quasi-stationary situation mainly depends on the mechanical strength of the cladding and its ability to transfer heat to the coolant. The characteristics of fuel pellets are described on the basis of empirical data. Reliable modeling outside of the normal operating parameters necessitates thorough understanding of the phenomena and their modeling in a mesoscopic scale. Behavior of a porous, chemically complex medium in a radiation field is a challenge to model. Besides mechanical strength the composition of nuclear fuel is important to know for radioactivity analysis methods and disposal of spent nuclear fuel.

Accurate methods for burnup calculations

A group of methods for burnup calculations solves the changes in material compositions by evaluating an explicit solution to the Bateman equations with constant microscopic reaction rates. This requires predicting representative averages for the one-group cross-sections and flux during each step, which is usually done using zeroth and first order predictions for their time development in a predictor–corrector calculation.

In one of our papers (Isotalo, Aarnio, 2011a) we present **the results of using linear, rather than constant, extrapolation on the predictor and quadratic, rather than linear, interpolation on the corrector**. Both of these are done by using data from the previous step, and thus do not affect the stepwise running time. The

methods were tested by implementing them into the reactor physics code Serpent[1] and comparing the results from four test cases to accurate reference results obtained with very short steps. Linear extrapolation greatly improved results for thermal spectra and should be preferred over the constant one currently used in all Bateman solution based burnup calculations. The effects of using quadratic interpolation on the corrector were, on the other hand, predominantly negative, although not enough so to conclusively decide between the linear and quadratic variants.

When material changes in burnup calculations are solved by evaluating an explicit solution to the Bateman equations with constant microscopic reaction rates, one has to first predict the development of the reaction rates during the step and then further approximate these predictions with their averages in the depletion calculation. Representing the continuously changing reaction rates with their averages results in some error regardless of how accurately their development was predicted. Since neutronics solutions tend to be computationally expensive, steps in typical calculations are long and the resulting discretization errors significant.

In another paper (Isotalo, Aarnio, 2011b) we present a simple solution to reducing these errors: the depletion steps are divided to substeps that are solved sequentially, allowing finer discretization of the reaction rates without additional neutronics solutions. This greatly reduces the discretization errors and, at least when combined with Monte Carlo neutronics, causes only minor slowdown as neutronics dominates the total running time.

Substeps, as well as the higher predictor and corrector orders, were implemented to the release branch of Serpent starting from version 2.0. The results are, however, not Serpent specific and could be applied to other codes using similar methods.
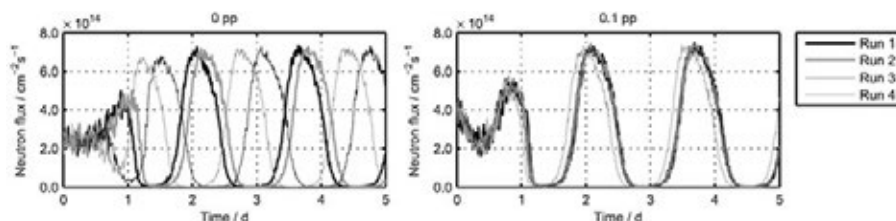

Figure 1. Neutron flux in one end of a symmetric (0 pp) and a slightly asymmetric (0.1 pp) pin cell from four identical runs without equilibrium xenon. Oscillations emerge despite extremely short 15 min steps, demonstrating that stabilization is required. (Isotalo et al., 2013)

Existing Monte Carlo burnup codes suffer from **xenon driven spatial oscillations large geometries** (Isotalo et al., 2013). Since the accurate solutions to the simulation models for many of these geometries oscillate, simply reducing step lengths, or solving the model better, would not work in a general case. When using predic-

---

[1] Up-to-date documentation on Serpent: http://montecarlo.vtt.fi

tor-corrector methods these oscillations can be difficult to detect as they can happen between the predictor and corrector, instead of subsequent steps, which makes the usually collected results look stable.

Forcing xenon and flux to a mutual equilibrium offers a simple solution to these oscillations. Since the equilibrium calculation can be integrated to normal Monte Carlo neutronics, it has only a minor effect on running times and can be used with any burnup calculation algorithm. Furthermore, at least the equilibrium iteration algorithm of Serpent can significantly improve flux convergence in large geometries with high dominance ratio.

Oscillations driven by fuel burnup still arise if too long steps are used, but unlike xenon oscillations, these only occur with long steps, allowing calculations to be performed with reasonable step lengths. This is a major improvement, especially in cases where stable solutions simply could not be obtained without the equilibrium method. It is important to remember that while the equilibrium xenon treatment allows stable solutions to be obtained for any model, the equilibrium levels are only as accurate as the model they have been calculated for.

In connection with burnup studies, we derived **a formalism to order nuclides by their importance to a given quantity of interest** (Vanhanen, 2012). A quantity can be any result of any linear effect of nuclides. Linear effects yield quantities that depend linearly on the amounts of nuclides, such as decay heat emission rate, spontaneous fission rate and neutron balance rate. Non-linear effects yield quantities such as effective multiplication factor and detectability of nuclides, and depend non-linearly on the amounts of nuclides.

The formalism can be used in identification of important minority and majority nuclides for any application. Application-specific criteria must be expressed as quantities of interest for which effects must be derived. This part remains to be an art. The formalism can be used to order nuclides by their importance to selected quantities of interest. Another art is to judge which nuclide is the last important one for a quantity; any nuclide with less importance is not important.

Temperature distribution in a fuel pellet and coupling it to neutronics

We developed **an external temperature solver for a fuel pellet**, named Thermosss, and coupled it to Serpent in the burnup calculations (Valtavirta, 2011). For the burnup calculations the fuel pins were divided into rings. Material compositions and heat production in each ring were obtained from Serpent. They were utilized to first calculate the local heat conductivity and then solve the steady-state radial heat conduction equation analytically in each ring. The outer temperature of the cladding was used as a boundary condition. Since local heat conductivity is dependent on the solved temperature distribution, iterations were made in calculating the heat conductivity and the accurate temperature distribution until self-consistence was obtained.

Using this code, we estimated the errors that result from using a homogenized temperature for gadolinium doped fuel pins rather than a more realistic multi-temperature profile. The first case focused on an infinite square lattice of EPR pins, where a Gd-doped pin was surrounded by eight non-doped pins. Comparisons were done at burnups ranging from 0 to 60 MWd/kgU, showing different trends for different temperature homogenization methods. The most accurate results were obtained from Rowlands' chord-averaging that was also the only method that stayed on the conservative side, i.e., overpredicting the reactivity rather than underpredicting it.

The second case was set to assess the errors made in assuming a bundle-wide homogeneous temperature in a Loviisa-type VVER-bundle containing six Gd-doped pins. Differences began to show at burnups of 20 MWd/kgU and higher. The results of the VVER-case state that even though the volume average temperature of the gadolinium doped pins reaches the homogenized temperature at a certain burnup, the difference between the cases only continues growing at an accelerated pace. One cannot thus justify using a homogenized temperature on the basis that the average temperature of the Gd-pins will reach it eventually.

We concluded that while the effect of temperature homogenization on the neutronics of the system is very subtle, it results in clear differences in the burnup calculations. The differences are explained by changes in the material compositions due to the temperature related changes in cross-sections.

The effect of the accuracy of the temperature profile inside a fuel pin on the results of burnup calculations was investigated in another study (Rintala, 2012). The case study was an infinitely long EPR-type fuel pin in an infinite two-dimensional lattice. The studied results were the reactivity, the two-group macroscopic fission and neutron capture cross sections and the nuclide composition of the system. These results calculated with different numbers of discrete volume averaged temperature zones in the fuel pin were compared with those calculated with the most accurate temperature profile, consisting of 32 temperature zones. The total burnup of the system varied from 0 to 60 MWd/kgU.

The reactivity of the system was smaller with less accurate temperature profiles, but the errors decreased close to zero with high burnups. The errors of the macroscopic two-group fission cross sections for the fast and thermal group increased as burnup increased with less accurate temperature profiles. The neutron capture cross sections tended to stay higher with less accurate temperature profiles over all burnups.

The amounts of the studied nuclides were overpredicted with less accurate temperature profiles, not including the amount of ^{238}U, which was underpredicted. The errors either increased with increasing burnup or stayed at an almost constant value. The errors of all of the studied results were at their highest when using only one temperature zone, and they tended to halve each time the number of temperature zones were doubled. Because of the clear differences in the results, especially in the nuclide compositions of the fuel, the correct temperature profile should be taken into account when doing reactor calculations.

Figure 2. The rod-wise volume averaged temperatures at the top-left quadrant of a 17x17 PWR fuel assembly. The red squares contain Gd-doped UO_2 rods and the black squares instrumentation and guide tubes. (Valtavirta, 2012)

The studies were continued with a Master's thesis **aiming to design and implement a temperature solver routine for the Serpent code** (Valtavirta, 2012). The routine is used in conjunction with the on-the-fly Doppler processor already found in Serpent 2 to provide high resolution temperature discretization with minimal memory usage. This leads, however, to a significant increase in the computation time needed for simulations.

The new routine addresses the radial heat transfer in fresh 2D pin-geometries. The consideration of 3D-problems and addressing the effect of the burnup on the problem are, however, deemed to be realistic directions of future development for the routine. Likewise, the temperature distribution could also be solved for non-pin-like geometries as long as certain simplifications such as symmetry considerations can be applied.

A thorough literature review was made for choosing default internal material property correlations for the routine and an integral comparison was performed against the fuel code Femaxi-6. The correspondence between the results was found to be good.

Two assembly level calculations verified the capability of the code to handle problems while monitoring various fuel pins of different compositions. The simulations also gave quantitative results on the differences between using the temperature feedback system and a single homogeneous volume-averaged temperature for the fuel part of the bundle combined with Doppler pre-processing.

Joint modeling of thermal creep and fission gas diffusion in nuclear fuel

The microstructure of nuclear fuel changes significantly during reactor operation. As fuel undergoes fission, heat and fission products are released. Since oxide fuels have low heat conductivity, the center of a fuel pellet becomes hotter than the outer region. An uneven temperature distribution causes radial fragmentation during early stages of a fuel pellet's lifetime. Thermal creep due to thermal stress leads to further microcracking over time.

In addition to thermomechanical effects, fission products play an important role in the fuel's microstructural evolution. Stable gases, such as several isotopes of xenon and krypton, make up a significant portion of all fission products. Gas atoms diffuse inside the pellet, and eventually form bubbles both within grains (intragranular) and grain faces (intergranular). The formation of bubbles increases the fuel's porosity, causing swelling and lowering the fuel's thermal conductivity. Gas released from the fuel mixes with the fill-gas (pressurized helium) in the pellet-cladding gap, decreasing thermal conductivity between the pellet surface and cladding. The behavior of fission gases is an important safety issue, since they can potentially cause the fuel assembly to overheat, or lead to pellet-cladding interactions due to swelling. Economically it makes sense to use fuel up to higher burnups, but the amount of fission products increases with burnup as well.

Gas diffusion and thermal creep are coupled together. Both gas bubbles and microcracks make the fuel more porous over time. This can affect the rate of gas release due to gas diffusion occurring through pore networks in addition to atomistic diffusion. There is evidence of fission gas release via coalescing gas bubbles along the grain boundaries. The goal of this subproject is to combine porosity formation from thermal creep fracture and gas accumulation to the diffusion of generated gas within a fuel pellet.

We are developing **a computational model for simulating the microstructural evolution of nuclear fuel** (Ovaska, 2013). The model includes damage accumulation from thermal creep deformation and from fission gas buildup within the pellet. Damage accumulation is linked with increasing porosity of the fuel, as microcracks and gas bubbles are formed. Diffusion of fission gases is simulated from the viewpoint of percolation theory: gas flows through interlinked pores, and can only reach the surface of the pellet through continuous pore pathways.

Currently, the basic components of the model have been implemented into a computer code and tested. Preliminary results demonstrate how gas diffusion is affected by local porosity. When the average porosity is lower than the percolation threshold, only a small fraction of gas generated near the edges of the system is released. Most of the gas is trapped in the inner parts, from where there are no open pathways to the surface. Once the average porosity is increased over the critical threshold, most of the generated gas is released.

The next step is to modify some parts of the model. Simultaneous time evolution of porosity and the gas inventory should be implemented, so that porosity is direct-

ly linked to the amount of gas. A realistic value for the critical porosity and other simulation parameters should also be determined. It will be interesting to see how different rates of damage accumulation from creep and radiation damage, together with a pore closure mechanism, will affect the dynamics of the gas in the system.
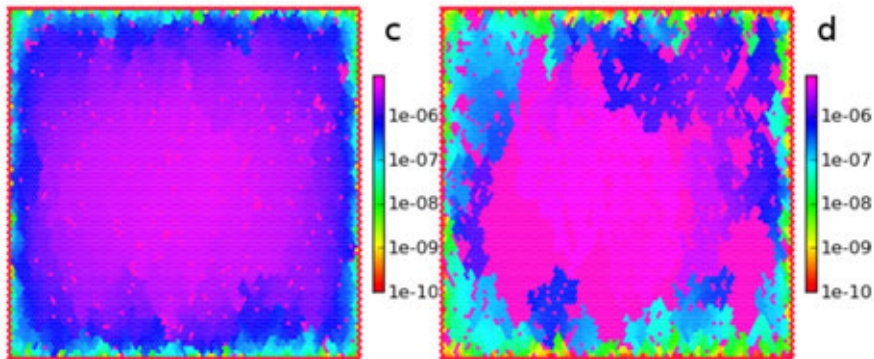

Figure 3. Steady state gas concentration profiles at two percolation thresholds, 0.0975 and 0.10. The average porosity in both cases is 0.10 with a maximum local deviation of 0.01. (Ovaska, 2013)

Conclusions

The most important result of the NEPAL project is education of new experts on nuclear engineering and the sustainable recruiting of new students to an academic research and education environment at Aalto University. The project will produce a number of Doctoral, Master's and Bachelor's theses in close collaboration with VTT, STUK and the power companies. The aim is to do our share in reaching the goals that were set in the report of the Committee for Nuclear Energy Competence in Finland (MEE, 2012).

Acknowledgement

References

Isotalo, A.E., Aarnio, P.A. Higher order methods for burnup calculations with Bateman solutions. Annals of Nuclear Energy 38, 1987–1995 (2011a).

Isotalo, A.E., Aarnio, P.A. Substep methods for burnup calculations with Bateman solutions. Annals of Nuclear Energy 38, 2509–2514 (2011b).

Isotalo, A.E., Leppänen, J., Dufek, J. Preventing xenon oscillations in Monte Carlo burnup calculations by enforcing equilibrium xenon distribution. Submitted to Annals of Nuclear Energy (2013).

Ministry of Employment and the Economy. Report of the Committee for Nuclear Energy Competence in Finland, Energy Department Report 14/2012.

Ovaska, M. Joint modelling of thermal creep and fission gas diffusion in nuclear fuel. Aalto University Technical Report FF-2013-01.

Rintala, A. Effect of temperature discretization on the results of neutronics calculations. Bachelor's thesis, Aalto University School of Science, Aug 9, 2012.

Valtavirta, V. Effect of temperature homogenization on neutronics calculations of Gd-doped fuel, Aalto University Special Assignment / Tfy-56.5111 Advanced Energy Technologies, Oct 7, 2011.

Valtavirta, V. Designing and implementing a temperature solver routine for Serpent. Master's thesis, Aalto University School of Science, Sep 1, 2012.

Vanhanen, R. Selection criteria for important minority nuclides. Aalto University Technical Report FF-2012-01.

4.5 Extensive fuel modelling (PALAMA)

Asko Arffman, Anitta Hämäläinen, Timo Ikonen, Seppo Kelppe, Joonas Kättö, Anna Nieminen, Jan-Olof Stengård, Elina Syrjälahti, Ville Tulkki, Tuomas Viitanen

VTT Technical Research Centre of Finland
Tekniikantie 3, P.O. Box 1000, FI-02044 Espoo

Introduction

Reactor fuel, as regards both its construction and materials, is a product under continuous development. The progress largely stems from expectations on efficiency, particularly through striving for higher fuel discharge burnups. Expected revisions of the regulatory guides will set new limits for acceptable ranges of fuel use and improved models and codes are required for assessments.

The investigation into the effects of increasing burnup has been ongoing for years with strong ties to experimental work performed at the OECD Halden Reactor Project. Methods for statistical approach at steady state conditions have been

created but need to be implemented to the latest code versions. A statistical tool for transient analysis was created during SAFIR2010, but a verification of its capabilities remains. In-house development of the ENIGMA fuel behaviour code continues. Active collaboration tasks with the PNNL regarding the FRAPCON/ FRAPTRAN code line, as well as with the IRSN and the SCANAIR RIA code are ongoing. These tools need to be developed and validated further while their areas of application are concurrently widened.

The general goal of PALAMA project is to develop and maintain competence and tools required for independent nuclear fuel behaviour assessment in both normal operation and accident conditions. The upcoming update to the regulatory guides creates a need to better understand, describe and model phenomena related to increasing burnup and the statistical nature of the fuel rod behaviour. Investigation into so-called design extension conditions requires fuel behaviour studies broadened towards areas such as thermal hydraulics, reactor dynamics and severe accidents. The increasing volume of Finnish nuclear power production induces new challenges as the load following operation may be required and its effects to the fuel performance must be understood. The fuel performance codes need to be systematically validated, and the creation of a framework for such a purpose is one of the goals of the project.

The scope of PALAMA as presented in this report is divided between the basic fuel behaviour of Section "Fuel behaviour" addressing issues of improved fuel performance modelling, statistical analysis of Section "Statistical analysis" relating to development and use of various statistical tools and methods, multiphysics work discussed in Section "Multiphysics" where links to other related fields, such as reactor physics are discussed, and work done on validation and international benchmarking described in Section "Validation and Benchmarks".

Fuel behaviour

SCANAIR

The SCANAIR code, developed by the Institut de Radioprotection et de Sûreté Nucléaire (IRSN), is designed for modelling the behaviour of a single fuel rod in fast transient and accident conditions during a reactivity initiated accident (RIA) in PWR. In SCANAIR, the available fuel material properties and the thermal-hydraulics model are for PWR fuel and coolant conditions, respectively, but the code does not have similar models for BWR to be applied in BWR RIA, the rod drop accident (RDA). Thus, the code lacks material properties of Zircaloy 2 (Zry-2) which is the cladding material in BWR fuel rod. Up until now, the only Zry-2 models implemented into the code have been the laws for yield stress (YS) and ultimate tensile stress (UTS) of irradiated cladding from a bibliographic study, and the laws have not been validated with SCANAIR.

As a development work of SCANAIR, new YS and UTS laws were fitted based on PROMETRA (French cladding mechanical properties test programme) tests

and implemented into SCANAIR. Comparative simulations with the new and old laws were conducted by applying the code to LS-1 and FK-1 tests performed in NSRR facility in Japan.

The Zry-2 PCMI failure criterion was also addressed: a criterion based on Critical Strain Energy Density (developed by EPRI) was applied with the FK test series (11 tests on BWR fuel performed in NSRR) which were simulated with SCANAIR using the new UTS correlation. The results were found to be in alignment with those gained by EPRI using the FALCON code. The thermal hydraulic model of SCANAIR for NSRR conditions (room temperature, atmospheric pressure, zero flow) was deduced to be adequate to model the worst initial condition for an RDA, cold zero power (CZP), but it should be kept in mind, however, that the boiling curve in SCANAIR has been fitted based on tests with fresh and pre-oxidized fuel and may therefore give inaccurate results for the temperatures of irradiated fuel.

The failure predictions based on the SCANAIR calculations of SED were found to be very sensitive to the gap size calculated by the irradiation code (FRAPCON). Compared to the source of uncertainty resulting from that, the new YS and UTS correlations have only a minor significance to the failure predictions. Despite the uncertainty resulting from the gap size, Zry-2 cladding failure predictions based on SCANAIR calculation of SED and EPRI's CSED criterion were found to give good results.

The development of SCANAIR for BWR applications continues with an attempt to extend the thermal hydraulics modelling of SCANAIR beyond CZP conditions.
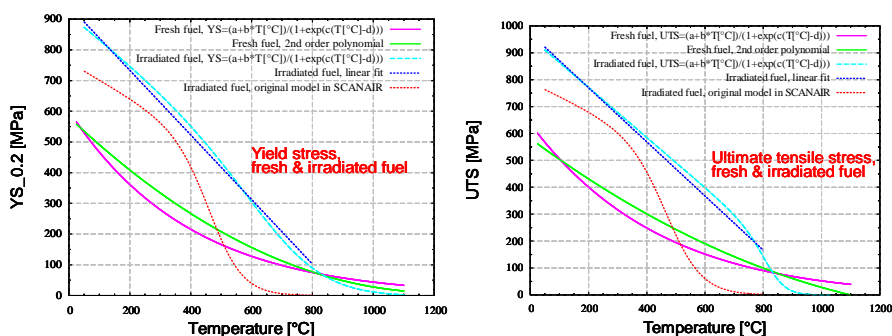

Figure 1. $YS_{0.2}$ and UTS of fresh and irradiated Zry-2. Different correlations were tried in order to find the best match to the measurements.

Gadolinia fuel

Fuel pellet deformation and heat transfer of gadolinium-doped fuel rods differs from behaviour of pure UO2 fuel rods. Several gadolinium bearing VVER, PWR and BWR fuel rods irradiated in three different experiments in the Halden reactor were modelled with the ENIGMA code. Simulation results were compared to in-pile measurements.

Densification effect at low burnup is weaker in the gadolinium-doped fuel rods as in the UO2 fuel. On the base of measurements, dependence of gadolinium content was added to the densification model of the ENIGMA code. The model damps down the densification effect when gadolinium content increases.

Results revealed also that fuel swelling parameters used for UO2 fuel in the ENIGMA overestimate swelling. Different swelling parameter values were studied and lower value was suggested for the modelling of gadolinium-doped fuel. Testing of different fuel conductivity models and radial power profile models revealed that models developed for gadolinium-doped fuel rods in the SAFIR2010/POKEVA project improve also modelling of the fuel pellet deformation.

Cladding creep

High temperatures and stress differential across the cladding wall causes the cladding tubes to plastically deform during its reactor life. This slow plastic deformation is called creep, and it is often separated into primary and secondary creep. Primary creep acts right after the stress change, and the secondary creep is the steady phase after the primary creep has actualized. Creep caused by static stress is relatively straightforward, but transient stress brings additional complications. Conventionally the stress changes are modelled assuming the strain hardening rule. However, the observations on the primary creep behaviour made in Halden experiments with on-line measurements do not support such assumption. The experimental results, however, are not sufficient for implementation to the simulation codes, as they do not provide information on how to deal with constantly changing stress levels. A way of implementing both the results of the Halden tests and the strain hardening behaviour of zirconium alloy in a creep model was developed in PALAMA. The model is based on the assumption of a dynamical internal stress state on which the cladding has relaxed. The primary creep induced by the stress change is then based on the difference between this internal state and the cladding stress.

New phenomena of interest

Finnish future nuclear reactors and new regulatory guides introduce conditions and challenges that have not been in the focus previously. New nuclear capacity combined with the planned wind power production would make a load following operation of NPPs a possibility. New regulatory guides allow fuel rod internal overpressure, as long as lift-off is avoided. This brings new requirement to the analysis codes, as the rod behaviour must be understood in such an off-normal situation better than before. Also, as severe accidents are a separate field of study, there exists a gap between the disciplines that should be bridged. All these subjects have been studied under PALAMA to gain better understanding of the phenomena involved.

Statistical analysis

Numerical analysis

At VTT, the statistical analysis of steady-state fuel behaviour has been done using primarily two fuel performance codes, ENIGMA and FRAPCON. To facilitate the statistical simulations, VTT has maintained two branches of the FRAPCON code. The main branch is up-to-date with the current FRAPCON distribution, but is not capable of performing statistical analysis on its own. The other branch, while having the statistical analysis functions, contains other features that have become obsolete. To make maintaining and updating the codes easier, merging of the two branches was considered necessary. This work has been started by developing a script, which performs the statistical simulations by running the main branch version of the FRAPCON code. The script can be easily extended to include more features, specifically the statistical simulation options of the secondary FRAPCON branch. Thus, updating two separate code versions should not be necessary in the future. The script has been documented and tested.

In addition, a novel statistical method, the so-called Sobol' variance decomposition, was employed in the uncertainty and sensitivity analysis of the FRAPCON-3.4 code. A benchmark steady-state case was studied with both conventional correlation methods and with the variance decomposition technique. It was shown that the variance decomposition method performs better in the case where the model has strong interactions between the uncertain input variables. For example, in the case of the gap width and gap conductance, these non-additive interactions can account for a significant amount of the output uncertainty. This result highlights the importance of considering case-appropriate uncertainty and sensitivity measures in the analysis of fuel performance codes.

Rod initialization at burnup

Properties of the gas gap of a fuel rod have a remarkable effect on the heat transfer from the fuel pellet to the coolant and thus the behaviour of the whole reactor. In VTT's reactor dynamic codes TRAB-3D, HEXTRAN and TRAB, heat transfer in a gas gap is usually characterized by some temperature dependent curve that is given as input data. Reactor dynamics calculation starts from some pre-defined initial state and typically in gas gap properties burnup is taken into account in a rather simple way, e.g. by using different curves for fresh, one, two and three year old fuel assemblies. The aim of this work was to determine the properties of gas gap of a "representative fuel rod" at various points of its reactor life and thus improve the description of fuel rods in reactor dynamic codes.

A VVER440 fuel rod was modelled with the statistical ENIGMA code by using a artificial power history with uncertainties. Relationships between different input and output variables were studied. As a result, width of the gas gap was chosen to be represented as a function of burnup. A set of 100 ENIGMA runs was calculated

several times, e.g. with different range of varied parameters. A curves describing fuel pellet outer radius and cladding inner radius were fitted to the calculation results of ENIGMA runs. Fitting was made to properties of the rods at a cold state and a operation conditions were modelled by adding thermal expansion to the model. With this kind of a model, also behaviour during the transient can be modelled, if the data is utilized in reactor dynamic codes.

As a result a crude model for width of the gas gap was found. The next phase is to study how this kind of a simple model works in reactor dynamic analysis and to test the model for some transient in the reactor dynamics codes together with KOURA project.

In this connection statistical version of ENIGMA code was renewed with similar approach as described above for FRAPCON.

Multiphysics

Serpent-ENIGMA

A new coupling code for performing combined fuel performance and reactor physical calculations was created. The code couples the reactor physics code Serpent with the steady-state fuel performance code ENIGMA. The new code uses ENIGMA to model the dynamical behaviour of the fuel, i.e. changes in the fuel dimensions and temperature distribution. This information is forwarded to Serpent, which is responsible of the burnup and power distribution calculations. The radial power distribution data is returned to ENIGMA to be utilized by its power depression routines. The coupling provides for detailed temperature and geometry modelling in a burnup calculation. Hence, it can be utilized to examine the errors originating from the usual approximation of stationary thermo-mechanical properties of the fuel. The new code can also be used in the verification of models and input parameters of a fuel behaviour code.
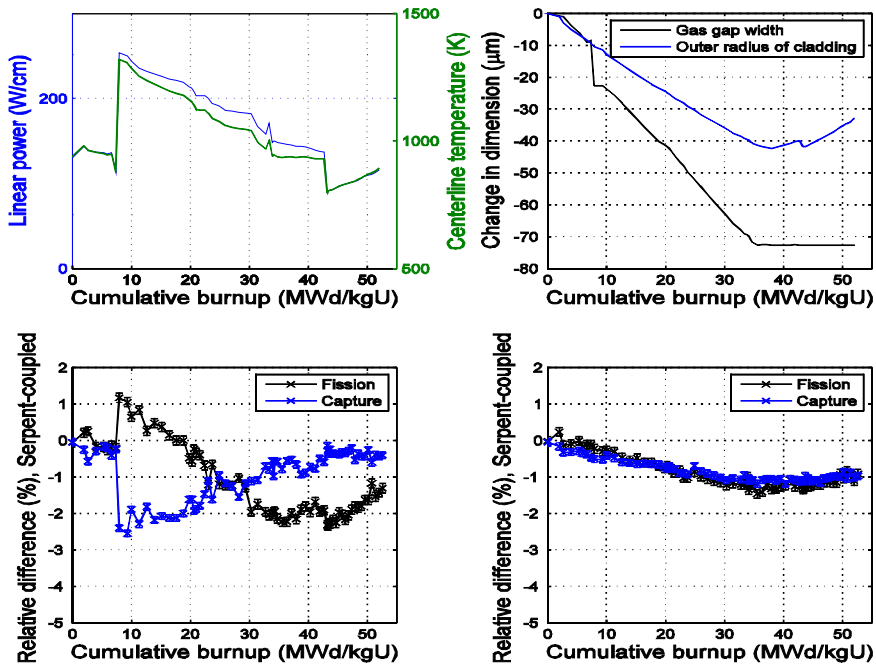
Figure 2. (Up, left) The given linear power and the calculated centreline temperatures of the FUMEX PWR. (Up, right) The corresponding changes in the dimensions of the fuel rod. (Down) Difference in homogenized cross-sections between the fully (geometry & temperature) coupled and standalone neutronis simulation are presented in the left plot and the effect of the changing geometry (temperature constant) is shown on the right.

FRAPTRAN-GENFLO

In the Safir10/POKEVA and Safir14/PALAMA projects, VTT has developed a new method for statistical analysis of fuel failures in accident conditions. The VTT approach applies neural networks and methods developed for uncertainty and sensitivity analyses.

According to the VTT method for evaluating fuel failures in accidents starts with 59 system code simulations of the accident with varying global parameters in the input deck. The results are applied as boundary conditions for FRAPTRAN-GENFLO analysis where the number of failed fuel rods is calculated. The FRAPCON code calculates the burnup dependent and fuel manufactory parameter dependent data into a restart file used in FRAPTRAN. The rest of the local parameters are varied in the FRAPTRAN-GENFLO analysis. Instead of calculating all the rods, a method using neural networks has been applied, where only part of the rods are analysed. The final objective of the project is to find out the number of

failed fuel rods in a LBLOCA accident, but also applicability of the VTT method and the adequacy of the boundary conditions from the system code analysis are tested.

Most recently, the variation of global and local parameters has been deliberated, new features of the boundary conditions have been included in the GENFLO code, and prerequisites for the whole calculation system in a LBLOCA application have been studied. Several APROS LBLOCA analyses for EPR were used as testing material. Both 1-D or 3-D neutronics were tested and the number of the core fluid channels was varied. In conclusion, the target of more stable FRAPTRAN-GENFLO runs with the complete boundary conditions has been met.

Simple rod model

The development of a fuel performance model and interface for multiphysics applications has been started. The model computes the solution of the fuel rod thermal and mechanical behaviour, using a library of material correlations and user-supplied boundary conditions. The model is in many parts based on the FRAPCON and FRAPTRAN codes, although some phenomena are described with further simplified sub-models. The main purpose of the model is to provide a realistic description of the fuel rod behaviour to thermal hydraulics and neutronics codes used at VTT, with increased performance and flexibility compared to existing fuel performance codes.

Validation and benchmarks

Validation tools development

Validation of a model is an essential part of any model development, and for that reason a new validation system for models in ENIGMA Fuel Performance Code was developed. The validation system consists of three parts. The first part is the validation code called Simulation Performance Analysis Code for ENIGMA (SPACE). The second part is a database that contains all the measurement and input data. The third part of the system are different MATLAB routines that are used to graphically illustrate the SPACE output. The development of the validation system started in 2011, and since then two versions of the code have appeared. The latest version of the code appeared in June 2012.

The main idea of the SPACE code is to allow the user to compare two different versions of ENIGMA. The other version should include the model to validate, while the other version includes the reference models. SPACE runs these two versions of ENIGMA, and prints the simulation results of both the new model and the reference model. Also measurement data is printed. This allows the user to see how different models affect different quantities. The order of superiority between the models is based on average relative errors of simulated values. When new ENIGMA models are developed, the SPACE code is a useful tool to compare the new model to older models.

An essential part of the validation system is a database, that includes all the measurement data and ENIGMA input data. At the moment the database contains input and measurement data for little over hundred fuel rods. Most of the measurement data is for fission gas release (FGR). In future there are intentions to grow the size of the database.

In model validation it is often useful to illustrate the simulation results graphically. By doing so it is easier to detect for example systematical errors in the models. This is why different MATLAB routines were developed to further analyse the output of the SPACE code. One example of a MATLAB figure illustrating SPACE output is presented in Figure 3, where simulated FGRs are plotted as a function of measured FGR. The blue circles present simulated FGR according to a reference model, while the red stars present simulated FGR according to a new model.
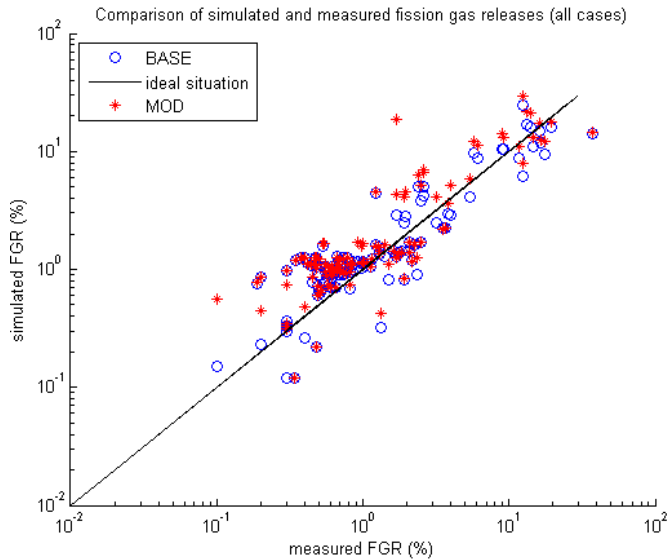
Figure 3. MATLAB figure of the SPACE output. Simulated FGRs are plotted as a function of measured FGR.

Benchmarks

To find out the state-of-the-art of reactivity initiated accident (RIA) fuel performance modelling, it was recommended in OECD/NEA Workshop "Nuclear Fuel Behaviour during Reactivity Initiated Accidents" held in Paris in 2009, that an RIA fuel codes benchmark exercise would be organized as an activity of the Working Group on Fuel Safety (WGFS) of NEA. The preparation the of benchmark specifications was coordinated by IRSN and Japan Atomic Energy Agency (JAEA), and it is participated by 17 institutions from 14 countries. The benchmark started in 2011

and the final report will be ready in 2013. VTT participates to the benchmark with the IRSN-developed SCANAIR code (V6.6).

In the benchmark, four distinct RIA tests are simulated. With the SCANAIR simulations, convergence problems were often encountered in thermal-mechanical iterations. The plenum temperature model of SCANAIR was found not to work as it should when the cladding outer temperature was prescribed. Despite the challenges, all the calculation cases could be finalized.

As findings of the benchmark simulations, some lacks in the results of the base irradiation initialization made with the ENIGMA code were pointed out: some FGR data produced by the VTT-developed ENIGMA-SCANAIR interface module was found non-realistic, and the oxide layer thicknesses calculated by ENIGMA (with the default parameters) were consistently underestimated. The user effect was also one of the subjects to be quantified in the benchmark; it was discovered that the SCANAIR results delivered by IRSN, VTT, SSM and CIEMAT were quite close to each other.

The benchmark continues with the preparation of the final report which includes all the contributions by the participants. Due to the large scattering in the results of different codes, this benchmark is planned to be continued in the near future.

VTT participated in the IAEA Coordinated Research Programme FUMEX-III that took place 2008–2011, first part of SAFIR2010 project POKEVA and then with PALAMA. FUMEX-III had over 30 participants using various fuel behaviour codes, and the benchmark cases ranged over a wide variety of cases and topics of interest. A state of the art review of VTT's fuel performance code ENIGMA and a Licentiate of Technology thesis was prepared as a part of VTT's benchmark work.

OECD Benchmark for Uncertainty Analysis in Best-Estimate Modelling (UAM) benchmark consists of three phases, out of which the first, neutronics calculations, has nearly finished by 2013. The second phase, announced in the UAM-5 workshop in 2011, is to include an exercise focusing on fuel behaviour modelling. Thus far these benchmark have been participated in and VTT has contributed to the definition of the fuel exercise. The work done on uncertainty and sensitivity analysis in PALAMA is the basis of VTT participation. The workshop is also appropriate venue for presenting and getting feedback on cross-disciplinary studies such as the representative rod model and Serpent-ENIGMA coupling.

Project publications

Arffman, A., Rintala, J. 2011. Statistical Analysis of Fuel Failures in Accident Conditions. 2011 Water Reactor Fuel Performance Meeting, Chengdu, China, Sept. 11–14, 2011.

Arffman, A. 2011. Recent RIA and LOCA Analyses Performed at VTT Using Fuel Performance Codes SCANAIR and FRAPTRAN-GENFLO. IAEA Technical Meeting on Fuel Behaviour and Modelling Under Severe Transient and LOCA Conditions, Mito, Ibaraki-ken, Japan, Oct. 18–20, 2011.

Arffman, A. 2012. WGFS RIA fuel codes benchmark – simulations with SCANAIR: fresh fuel case 562-12 and revision of some previous results. VTT Research Report VTT-R-03294-12. 27 p.

Arffman, A. 2012. Evaluation And Adaptation Of The RIA Code SCANAIR For Modelling BWR Fuel and Conditions – Vol. 1. VTT Research Report VTT-R-06561-12. 33 p.

Arffman, A. 2012. WGFS RIA fuel codes benchmark – simulations with SCANAIR: CIP0-1, CIP3-1, VA-1 and VA-3. VTT Research Report VTT-R-00246-12. 32 p.

Arffman, A., Alain M., Vincent, G. 2012. Evaluation and Adaptation of the RIA Code Scanair for Modelling BWR Fuel and Conditions. TopFuel2012, Manchester, United Kingdoms, Sept. 3–6, 2012.

Hämäläinen, A. 2012. Preparations for applying statistical method for resolving fuel failures. VTT Research Report VTT-R-00635-12. 15 p.

Ikonen, T. 2012. Variance decomposition as a method of statistical uncertainty and sensitivity analysis of the fuel performance code FRAPCON-3.4. VTT Research Report VTT-R-07723-12.

Ikonen, T. 2013. FINIX – rFuel behavior model and interface for multiphysics applications – Code documentation for version 0.13.1. VTT Research Report VTT-R-00730-13.

Kelppe, S., Klecka, L., Tulkki, V. 2011. ENIGMA modeling of IFA-610 overpressure series. Enlarged Halden Programme Group Meeting 2011, Sandefjord, Norway, Oct. 3–6, 2011.

Kelppe, S. 2012. HRP Lift-off Experiment Summary Part 2 PIE. VTT Research Report VTT-R-01954-12.

Kelppe, S. 2013. Load following in LWRs and related fuel behaviour issues. A Review. VTT Research Report VTT-R-00726-13.

Kättö, J. 2011. ENIGMA-polttoainekoodin WHITE4- ja NFI-lämmönjohtavuusmallien vertailu SPACE-ohjelmalla. VTT tutkimusraportti VTT-R-05921-11. 37 p. (In Finnish)

Kättö, J. 2012. The SPACE Code Users Guide. VTT Research Report VTT-R-04093-12.

Manngård, T., Massih, A., Stengård, J.-O. 2011. Evaluation of Halden IFA-650 loss-of-coolant accident experiments 2, 3 and 4, Quantum Technologies AB Report TR11-006V1. 36 p.

Manngård, T., Stengård, J.-O., Jernkvist L., 2013. Evaluation of Halden IFA-650 loss-of-coolant accident experiments 2, 3, 4, 5, 6 and 7. Enlarged Halden Programme Group Meeting 2013, Gol, Norway, March 10–15, 2013.

Nieminen, A. 2012. Overview on fuel behaviour under accident circumstances, VTT Research Report VTT-R-01675-12. 23 p.

Syrjälahti, E. 2011. Characterization of a representative VVER-440 fuel rod with the statistical ENIGMA. VTT Research Report VTT-R-08464-11. 18 p.

Syrjälahti, E. 2012. Modelling of gadolinium-bearing fuel rods with ENIGMA. VTT Research Report VTT-R-08525-12.

Tulkki, V. 2011. VTT ENIGMA Calculations for FUMEX-III CRP, VTT Research Report VTT-R-08459-11. 47 p.

Tulkki, V. 2011. Development of VTT ENIGMA creep models. Enlarged Halden Programme Group Meeting 2011, Sandefjord, Norway, Oct. 3–6, 2011.

Tulkki, V. 2011. Review of the Fuel Performance Code ENIGMA. Licentiate's Thesis, Aalto University School of Science, 19 August 2011. 74 p.

Tulkki, V. 2012. Analysis of cladding creep and lift-off behaviour. VTT Research Report VTT-R-08519-12.

Tulkki, V., Ikonen T. 2013. Implementation of model for primary creep derived from Halden experimental results. Enlarged Halden Programme Group Meeting 2013, Gol, Norway, March 10–15, 2013.

Viitanen, T. 2011. Serpent-ENIGMA – Combining Monte Carlo Reactor Physics with Fuel Performance. VTT Research Report VTT-R-06265-11. 23 p.

Viitanen, T., Tulkki, V. 2012. Combining reactor physics and fuel performance calculations. TopFuel2012, Manchester, United Kingdoms, Sept. 3–6 2012.

4.6 Radionuclide source term analysis (RASTA)

Anna Nieminen, Antti Räty, Ville Tulkki

VTT Technical Research Centre of Finland
Tekniikantie 3, P.O. Box 1000, FI-02044 Espoo

Introduction

Nuclear fuel accumulates all kinds of radioactive nuclides during the irradiation. While the actinides can be claimed to be unwanted side product of the process, without the fission products there would be no power produced in the reactor. The other side of the coin are the dangers these radioactive nuclides pose to people and environment should they be released, whether it would happen during a reactor accident or after years of interim storage or millennia of repository life. For safety analysis knowing and understanding the source term is important, and while different disciplines of safety analysis do address nuclear fuel in various forms and scale, the approaches are by necessity often very different. In the work performed in one-year project RASTA the tools of reactor physics, fuel behaviour and severe accident analysis are investigated in order to find ways to synergise between strengths of different disciplines. Individual investigations are described also to serve as a reference of the use of the tools and the viewpoint utilized by different disciplines, as it is well recognized that the first obstacle to fruitful co-operation is the one's inability to understand the mental framework and assumptions of the experts of other fields.

Long-term activity inventory calculations have been performed extensively with code ORIGEN-S both internationally and in the VTT. The calculated inventories from ORIGEN can be used as input for various accident analysis tools which make assumptions regarding distribution and behaviour of different radionuclides. The development of Monte Carlo based reactor physics calculation tool Serpent has given a tool to do these calculations with more spatial precision, thus enabling investigations in the scale of the fuel rod.

Fuel behaviour codes traditionally track only fission products that may affect rod integrity, in other words stable noble gases and in some cases iodine. The focus of the analysis has been the failure of the rod, not the subsequent release. Especially in the final repository assessments the similarity and differences between the behaviour of noble gases and the radionuclides have been investigated, but so far very little actual modelling has been performed.

The research of severe accident in-vessel phenomena have recently focused at VTT on core degradation and coolability. This approach has not enabled detailed analysis on radionuclide release. The integral codes only assume, that the radionuclide source term is initiated by diffusion from fuel grains, which does not take pre-existing radionuclide deposits or radically modified fuel structure into account.

This model is assumed to give incorrect estimations in the case of slowly progressing accidents.

One of the focus areas of the work done in RASTA is the effect of increasing burnup, subsequent formation of high burnup structure (HBS) and its effect on the radionuclide release. As the Finnish utilities have gained permission to increase discharge burnup from the old 45 MWd/kgU, the highest power rods are well within the burnup region where HBS begins to form, and its effect should be determined.

Results of the work performed

In the course of the work done in RASTA several separate tasks were performed, as reported in [1]:

- Activity inventories were calculated for a PWR rod for a burn-up of 51.22 MWd/kgU with point-depletion code ORIGEN-S. The calculation also included a cooling (decay) period of 10 000 years. For reference, the same case was calculated with Monte Carlo code Serpent. The main difference between the methods is that as a point-depletion code ORIGEN-S does not provide information on the distribution of nuclides within a rod, while Serpent model used divided the rod into 15 axial rings. Effect of different cross section libraries was studied with Serpent using four different libraries.

- Amount of readily released nuclides during accident or in repository were studied by literature survey as well as by implementing the ANSI/ANS-5.4 recommended models into VTT's fuel behaviour code ENIGMA. The limitations of these models were discussed as well as the effect of high burnup structure which is not taken into account by the models that are based solely on conventional fission gas release models. Effect of environment to the actual release was briefly discussed.

- State of the art of the severe accident analysis regarding radionuclide release was examined. The various radioactive nuclides were listed and their behaviour in case of severe accident was detailed. Example code runs with ASTEC were performed, with an attempt to simulate also the effect of the high burnup structure.

Some findings of the project team:

When discussing the effect of burnup to the amount of releasable radionuclides the most important effect comes from the increasing inventory. While some of the nuclides reach a stable level early on during the irradiation, others keep accumulating during the whole irradiation period. The relative fraction of short-lived radionuclides which are released after rod failure in handling-type accidents can be assumed to be fairly stable, as long as the fuel temperature has been that of the usual operation. The fractional amount of longer-lived isotopes that should be in the free volume is assumed to be linearly related to traditional FGR, but even that varies over a

batch of rods. Traditionally high burnup structure is not taken into account (Table 1), but depending on the accident scenario or repository lifetime assumptions it could be justified in some cases, as the potential increase in fast released fraction is large.

Table 1. Assumptions made in various models on nuclide release.

			Diffusion in matrix				Inventory includes		
	Half-life	Grain release model	Diffusion rate based on	Diffusion rate I/Xe	Diffusion rate Cs/Xe	Grain boundary release	gap	grain boundary	HBS
ANS/ANSI-5.4	short	Model developed from Booth	Noble gases	Precursor effect	Precursor effect	Interlinkage threshold	Yes	No	No
	long	Correlated to FGR	Noble gases	1	2	As per FGR	Yes	No	No
Repository	long	Correlated to FGR	Noble gases	1	1/3	GB included in IRF	Yes	Yes	Varies
MELCOR	N/A	Evaporation	N/A	N/A	N/A	N/A	N/A	N/A	N/A
ASTEC	N/A	Model developed from Booth	Iodine	1	2	Instant release limited by evaporation rate	Yes	Yes	No

The amount of inventory residing in HBS is not straightforward to determine from e.g. burnup alone (Figure 1). While it probably would be possible to determine rim inventories to specific nuclides parametrically, the ability of MC neutronics simulations to provide spatial nuclide distributions provide sufficient information for such analysis. This is assuming HBS inventory is relevant, as it appears to be in LOCA accident scenarios. For repository analysis the jury is still out, and the early effect may be vanishingly small for full-blown severe accident scenario.
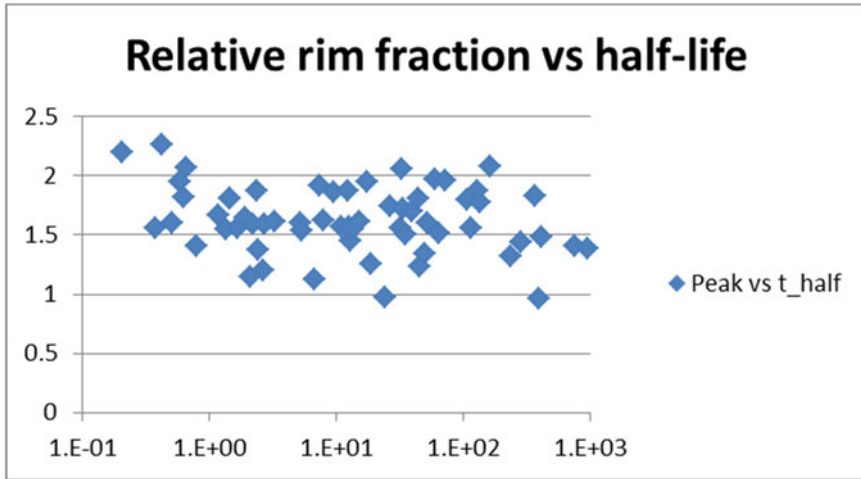
Figure 1. Relative rim nuclide density (to pellet average nuclide density) of various nuclides plotted as a function of their half-lives (in years).

ANSI-5.4 standard provides guidelines for radionuclide release from the fuel. The standard has several limits to its applicability, especially the limit to sudden temperature increase as well as demand that no oxidation takes place. Temperatures that are high for reactor conditions are discussed in the RASTA final report, especially regarding HBS effect, and severe accident conditions have a part of the report of their own. The oxidation of the fuel is taken into account in ASTEC fuel models and should model development for scenarios where fuel oxidation is important, such as operation with defective fuel, those models would be a logical place to start. Also, ANSI-5.4 is based on the measurements of Kr-85m, and other radioisotopes are connected to that with some correcting factors. Therefore it should be noted that while the different cross-section libraries that are commonly used produce very similar results for isotope compositions, the very Kr-85 yield is different depending on the library used (Figure 2).
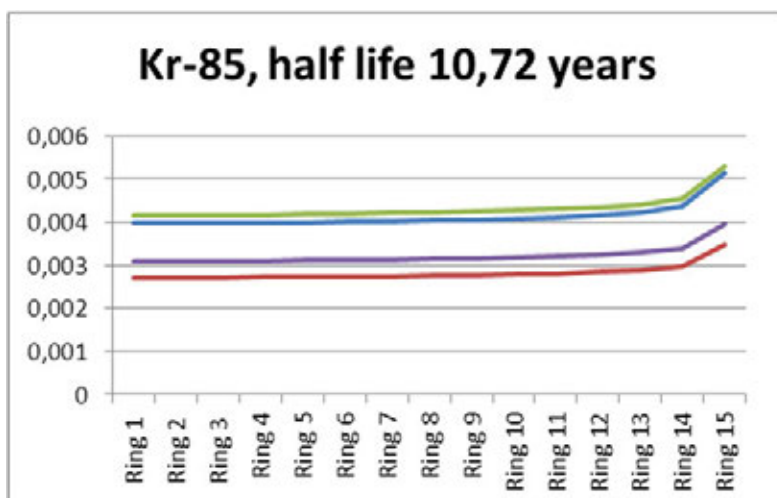
Figure 2. Kr-85 inventory along radial cross.section, simulated with different cross-section libraries (lines: green JEFF-2.2, blue JEFF-3.1, violet ENDF/B-7.2, red ENDF/B-6.8).

The literature on accident analysis contradicts the assumptions made for repository analysis on some issues, such as the rate of diffusion of several key radionuclides (Table 1). As these are related to chemical characteristics of the fission products and not methodology, they should be ultimately unified according to the best understanding.

As the severe accident analysis codes focus on the situations where the fuel melts, the early release from (relatively) intact fuel is hardly a focus for them. As it is, the radionuclide release from the fuel is not very rigorously modelled in e.g. MELCOR. ASTEC has its own model for fuel grains, which works but is known not to predict all the dynamics of radionuclide release (Figure 3). HBS is supposed to be modelled as small separate grains, which has implications to early interpretation of the HBS behaviour. However, as the HBS appears to release gases at high temperature transients, the model is somewhat justified, even if not necessarily mechanistic. As it is the HBS portion of the fuel could be modelled with some difficulty, unfortunately it would appear that the ASTEC model for grain release is either not functioning or just does not affect the end result much. Also the gap inventory, which in theory could also be used to model the HBS as clad failure might happen only after HBS burst, is vented at the beginning of the simulation regardless of the temperature in ASTEC.
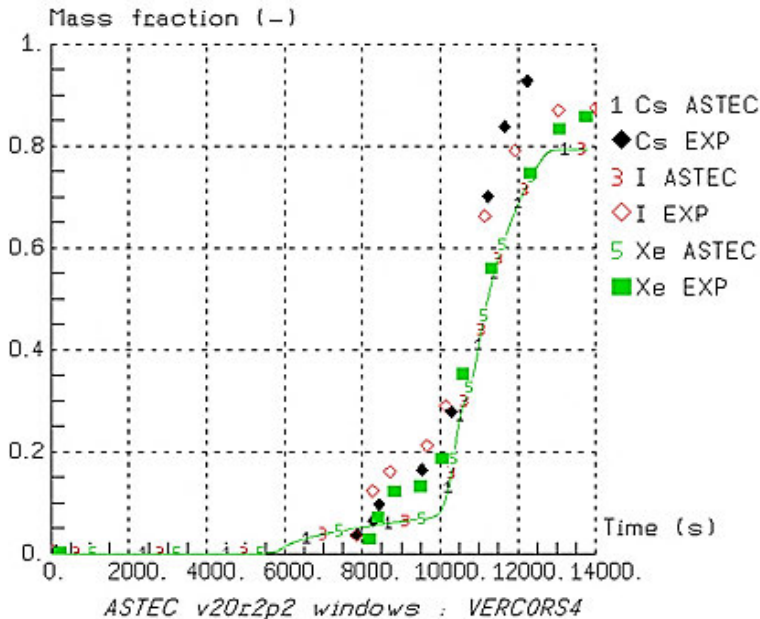
Figure 3. The release rate of caesium, iodine and xenon in VERCORS4 experiment, both experimental and ASTEC simulations. Some discrepancies can be seen in dynamics between simulated and measured behaviour.

Future work

While the combining of the different fields as they currently are is challenging, there are some possibilities to synergy in specific cases. Using reactor physics tools capable of spatial discretization is necessary for determining the HBS inventory. Fuel performance studies can provide insight how the HBS should be modelled in severe accident codes, however the end effect is probably very small considering the energetic nature of the postulated accidents in these scenarios. Nuclide release in severe accidents is affected by fuel oxidation, which is not taken into account by ANSI/ANS-5.4 but could be important in some cases, and as such following the example of severe accident models would benefit the development of fuel performance code models.

References

1. Nieminen A., Räty A., Tulkki V. 2013. Radionuclide source term analysis. VTT Research Report VTT-R-00647-13.

5. Thermal Hydraulics

5.1 Enhancement of safety evaluation tools (ESA)

Ismo Karppinen, Seppo Hillber, Pasi Inkinen, Sampsa Lauerma, Joona Kurki,
Jarno Kolehmainen, Ari Silde, Risto Huhtanen

VTT Technical Research Centre of Finland
Tekniikantie 2, P.O. Box 1000, FI-02044 Espoo

Abstract

The main objectives of the project are to develop and validate calculation methods for safety evaluation of nuclear power plants. Both thermal hydraulic system analysis codes and CFD calculations are used in the analysis and their usability is studied and enhanced. Participation in international OECD/NEA research projects and Nordic co-operation are included in the project. An important objective is also to educate young experts in thermal hydraulics.

The project is divided in two main tasks: 1) validation of system analysis codes and 2) validation of containment analysis methods. In the former task APROS and TRACE codes are validated with both separate effect and integral tests taking in account the phenomena important for the new plant concepts offered to TVO and Fennovoima. In the latter task both lumped parameter (LP) and CFD codes are used. As a result of the project both the safety authority and the utilities will get better validated tools for safety analysis and design evaluations.

Validation of system analysis codes

A systematic and thorough validation of codes is a prerequisite for their use in safety analysis and in planning new experiments. Calculation of the validation cases and analysis of the results is also an effective mean to educate young experts. The thermal hydraulic system analysis codes APROS and TRACE have been validated with experimental data from Lappeenranta University, EU and OECD research programs. Participation in EU and OECD research programs trains young experts also in international co-operation.

Validation of APROS with condenser experiments

Most of the new power plant concepts offered to TVO and Fennovoima have passive condenser systems, operation of which is based on natural circulation. The ability of APROS code to simulate behaviour of those condensers was tested by calculating NOKO [1] and PANDA PCC experiments [2]. The German NOKO experiment facility is a model of the passive emergency condenser of the Kerena plant concept (Figure 1), but quite similar condensers with horizontal heat exchangers are used also in other power plant designs.
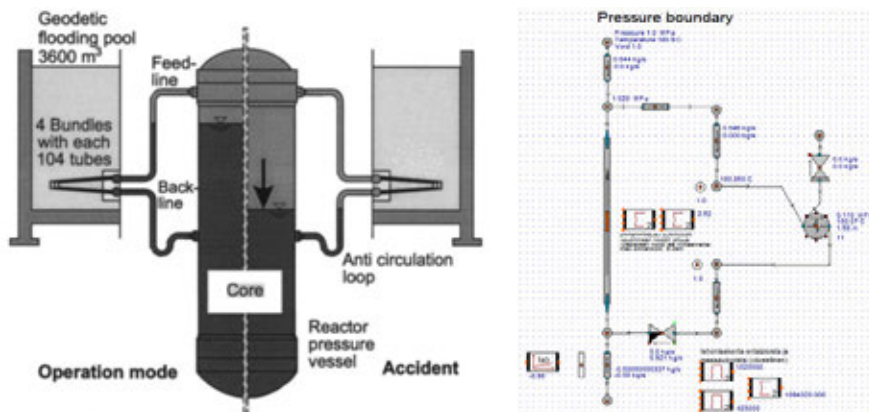
Figure 1. Principal diagram of Emergency Condenser and APROS model of NOKO experiment.

Measured [3] and calculated condenser performance was compared in 10 different operation conditions using 3 alternate condensation correlations available in APROS code. The results show reasonable agreement with the experiments although the comparison to the data suggests that there may be some over prediction of heat transfer in some of the simulated cases with the default correlation (Shah). On the basis of APROS calculations Nusselt model for condensation is recommended for this kind of condensers (Figure 2).

Test	Primary side		Secondary side
	pressure [MPa]	water level [m]	temperature [ºC]
EU1M3	0,98	3,66	66,10
EU1M4	1,00	2,49	88,00
EU3M2	3,02	4,83	63,20
EU3M3	3,01	3,64	101,70
EU3M4	3,01	2,47	111,00
EU4M1	3,01	4,85	105,10
EU5M2	7,07	5,89	44,60
EU5M4	7,07	3,58	111,00
EU5M6	7,06	1,29	117,00
EU6M2	7,07	4,42	113,50
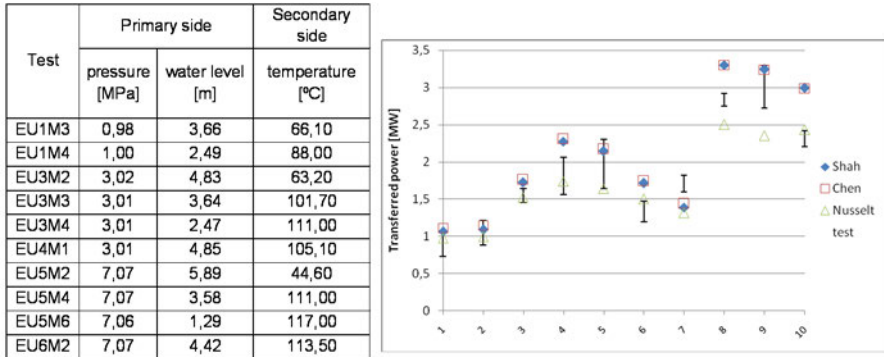
Figure 2. Calculated and measured heat transfer in NOKO experiments.

PANDA facility is a large scale containment test facility located at Paul Scherrer institute in Switzerland. A set of isolation condenser (IC) tests [4] were simulated with APROS using both a detailed model of the IC heat exchanger (Figure 3) and a heat exchanger process component available in APROS. Both modelling approaches gave the same results. The tests and simulations were run at 3, 6 and 9 bar pressure ranges so that each range had a pure steam test along with three tests with different amounts non-condensable gas mixed in the steam flow. Suitability of three different interfacial heat transfer correlations was evaluated. Chen and Nusselt correlations produced results that are very close to each other but also in a reasonably good agreement with the test results. Shah correlation, however, produced a considerably lower heat transfer rate (Figure 4). The Shah correlation is developed for general interfacial heat transfer and seems not suit in this case, where liquid film is attached on the tube wall and has relatively low velocity and hence low Reynolds number. Interfacial heat transfer in Shah correlation depends on Reynolds number.
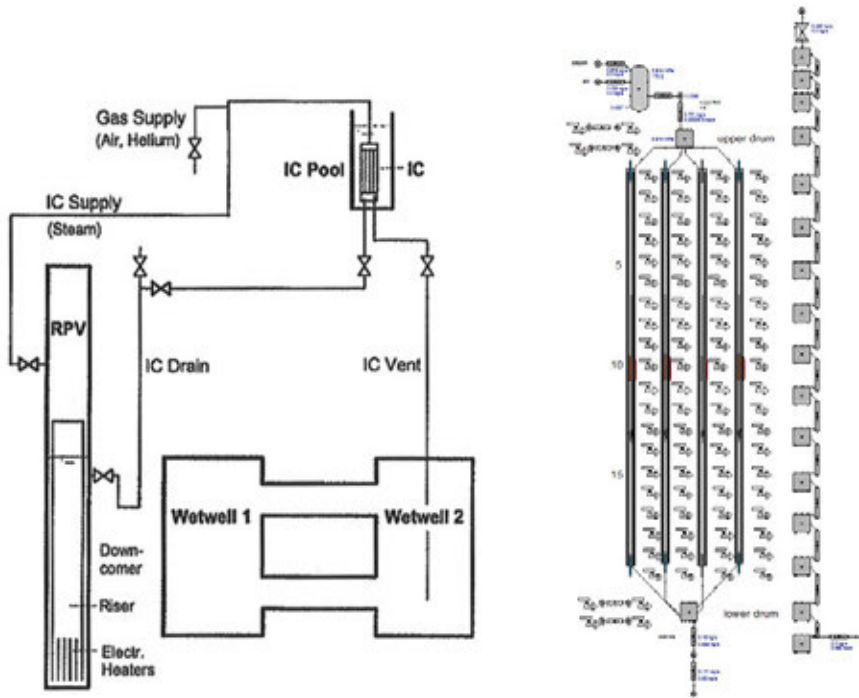
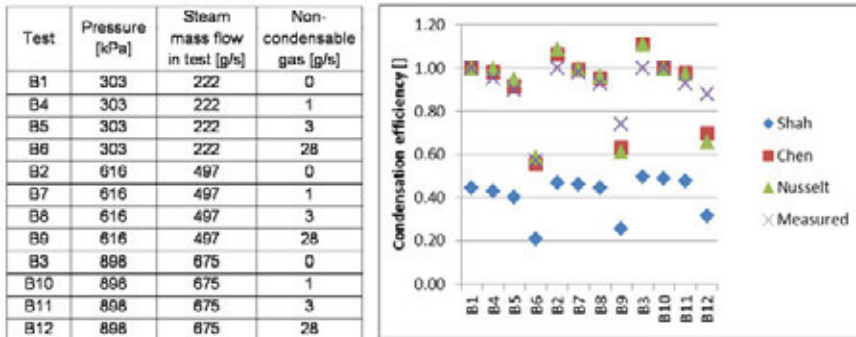**Figure 3.** The PANDA facility in the test configuration and the detailed APROS model of the condenser.

Test	Pressure [kPa]	Steam mass flow in test [g/s]	Non-condensable gas [g/s]
B1	303	222	0
B4	303	222	1
B5	303	222	3
B6	303	222	28
B2	616	497	0
B7	616	497	1
B8	616	497	3
B9	616	497	28
B3	898	675	0
B10	898	675	1
B11	898	675	3
B12	898	675	28

Figure 4. Measured and calculated condensation efficiencies in PANDA IC tests.

Validation of APROS with PACTEL steam generator test

Heat transfer degradation in horizontal steam generator due to non-condensable gas was studied in PACTEL experiments NCg-1, NCg-3, NCG2-04 and NCG2-05. The tests were modelled with APROS to validate the heat transfer models of the code [5] (Figure 5). Stepwise injection of non-condensable gas decreased heat transfer in the steam generator and consequently system pressure increased after each injection [6]. Measured and calculated pressures, Figure 6, 7show good agreement between calculation and the experiment.
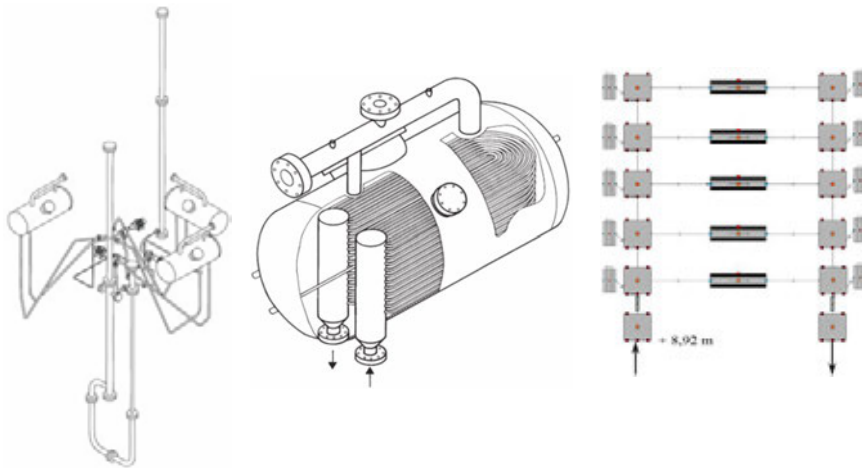
Figure 5. PACTEL facility, steam generator and APROS model of the steam generator.
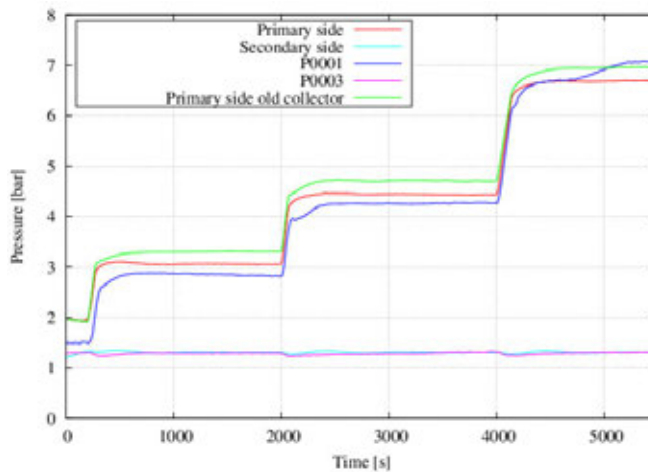
Figure 6. Measured (P0001, P0003) and calculated pressures in PACTEL NCG2-04 experiment.

Validation of APROS and TRACE with ROSA/LSTF experiments

OECD/ROSA-2 Test 3 was simulated and analysed using system codes APROS and TRACE [7]. The TRACE model utilized 3D vessel component, which usability was studied by calculating ROCOM mixing tests [8]. The experiment described a hot leg small break loss-of-coolant accident with a break size equivalent to 1.5% [9]. The test consisted of high pressure transient and conditioning before the low pressure transient phases to better compare the experimental results with the similar counterpart test performed with PKL III test facility. Especially primary circuit cooling through secondary-side depressurization and the response of core exit temperature to the generation of superheated steam was studied.

The nodalizations of the models are presented in Figure 7. Both models predicted reasonably well the major events of the ROSA-2 Test 3. Most of the major experimental findings were observed in the simulation; especially the high pressure phase in general was quite well reproduced by both codes. Some differences were also observed in comparison to the experiment, which could be partially resolved by refining the model nodalization. For example, during the low pressure phase TRACE reproduced most of the events slightly later, whereas APROS reproduced them too early.
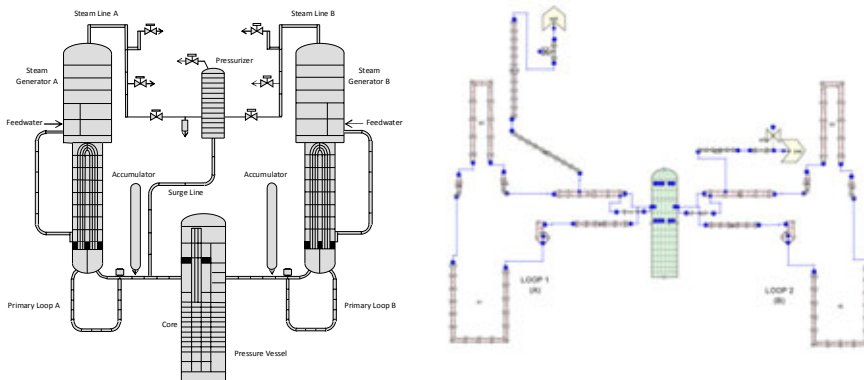
Figure 7. ROSA/LSTF model nodalizations in APROS (left) and TRACE (right).

Comparison of core exit temperature and maximum cladding temperature is presented in (Figure 8). The relation between the temperatures is quite well reproduced by both codes in the high pressure phase although slightly underestimated. In low pressure phase the simulated temperature is even more underestimated by APROS. This could probably be addressed by creating a more detailed model of the core and the measurement system used for defining the core exit temperature.

147
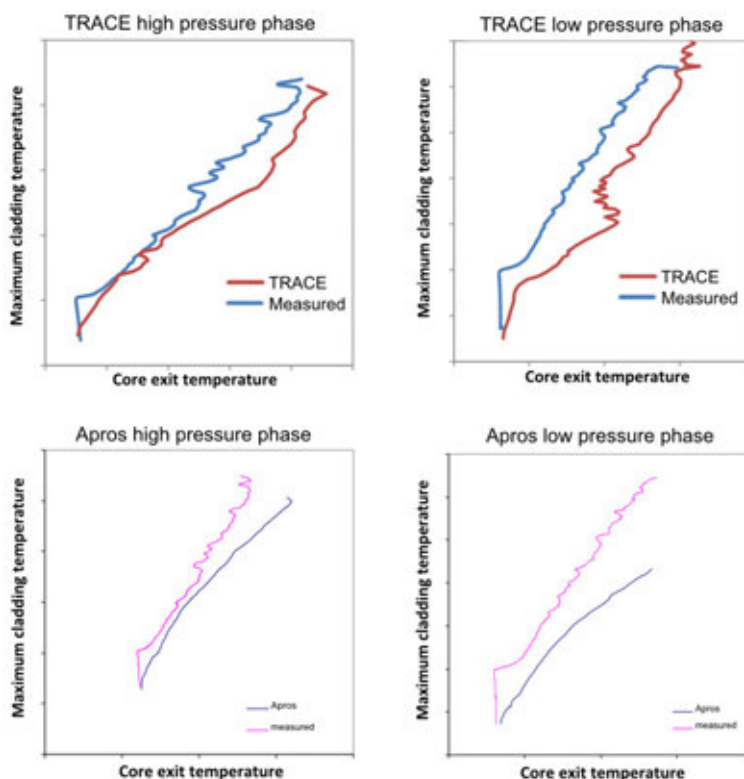
Figure 8. Comparison of core exit temperature and maximum cladding temperature in low and high pressure transient phases.

Validation of containment analysis methods

Generic Containment Benchmark

A Generic Containment Benchmark exercise was organised in the frame of the European Network of Excellence SARNET2 (Severe Accident Research Network) [10, 11]. Within the exercise, a comparison of results of complex code systems, containing the interaction of many single models, describing the different physical phenomena and technical systems, is performed. In total, 14 European organisations applying 10 different, the most common lumped parameter (LP) codes, such as MELCOR, ASTEC, COCOSYS, APROS, WAVCO, CONTAIN, SPECTRA, ECART, FUMO, GOTHIC, were contributing to this activity. VTT participated in the all benchmark steps with the APROS containment code. Some of the participating organisations used the same code and the code version. The benchmark basic nodalization was developed for a German pressurized water reactor (PWR) with

1300 MW$_{el}$, provided by GRS (Figure 9). All participants tried to build-up an identical nodalization concept/simulation model.

In the frame of the initial benchmark step, 'Generic Containment-run-0' [10], a simple test-case, i.e. only the containment thermal hydraulics of the in-vessel phase of a small break loss-of-coolant accident (SB-LOCA) was simulated and compared. The subsequent step run-1 aimed on the simulation of severe accident conditions where hydrogen and carbon monoxide and dioxide (products of core concrete interactions) were released to containment [11]. In the last step (run-2), the Generic Containment was applied as a basis for testing different passive auto-catalytic recombiner (PAR) modelling approaches, where a PAR system consisting of 57 AREVA type PARs, has been modeled. The Generic Containment nodalization was similar in all phases of the benchmark exercise.
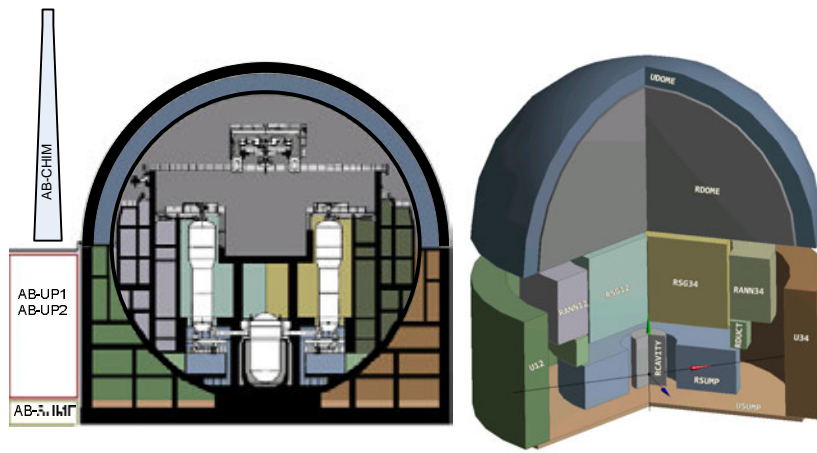
Figure 9. Nodalization for the German pressurized water reactor containment [10].

The basic recombiner model of APROS is based on Canadian type of recombiner manufactured by AECL. A new correlation for the AREVA type of PARs has been implemented in APROS [12, 13, 14] and used in the General Containment Benchmark. The APROS simulation results of dome pressure, gas temperature, hydrogen concentration and recombination rate are compared with the mean values and standard deviation band of the other calculations in Figure 10 and Figure 11. The APROS results were well within the deviation band. Similar trend was observed in all important target variables compared. One observation of the benchmark was that there were differences between some calculation results, even if the same computer code with similar nodalization were used.
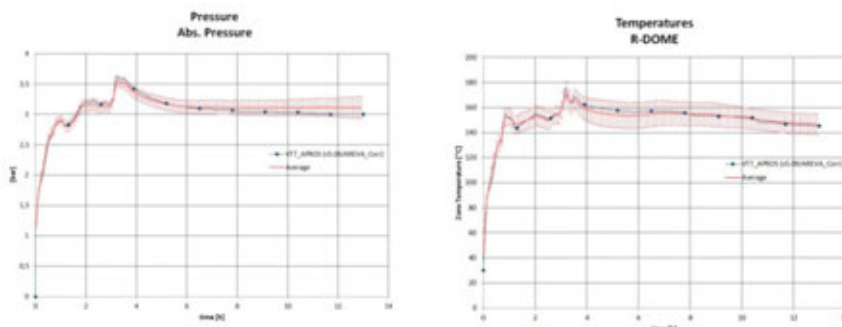
Figure 10. Calculated dome pressure and gas temperature of APROS compared to the mean values and standard deviation band of the other calculations in SARNET Generic Containment benchmark.
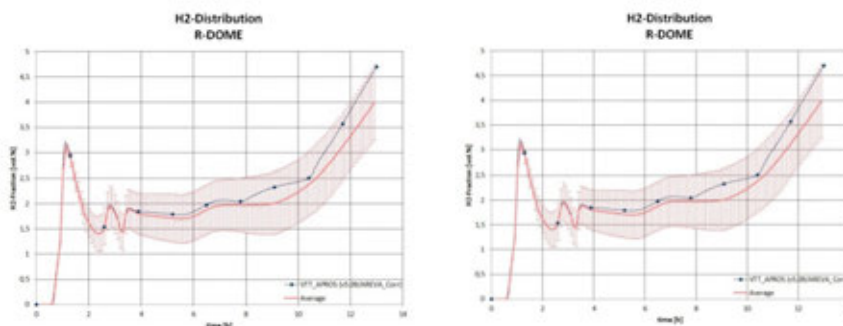

Figure 11. Dome hydrogen concentration and recombination rate of APROS compared to the mean values and standard deviation band of the other calculations in SARNET Generic Containment benchmark.

SARNET elementary spray benchmark

A single droplet heat and mass transfer tests conducted at IRSN CARAIDAS facility (SARNET spray benchmark) [15] was calculated using the APROS containment code and Fluent CFD code [16, 17]. Both evaporation and condensation cases were studied. The main goal of the work was to validate the containment spray heat and mass transfer models of APROS and to verify that the droplet models in Fluent are suitable for modelling containment spray. The absolute initial pressure in the tests was in the range of 1 to 5.4 bar, the initial gas temperature was ranging from 20 to 142°C and the relative humidity from 3 to 87%. Monosized spray drops (standard deviation lower than 10 μm) were generated in the top of the facility. Since the test facility (height 5 m, diameter 0.6 m) was well mixed, the space of the test facility was modeled in APROS by a single adiabatic node.

150

As an example of calculated cases, evaporation of a droplet is presented as a function distance from the spray nozzle (Figure 12). Sensitivity analysis and different modelling options were studied with both codes. Generally speaking, the drop size predicted by APROS at two different levels during the drop fall agreed well with the measurements. The results indicated that the drop size in the weak evaporation cases was slightly over predicted i.e. the evaporation rate was under predicted, but the simulated drop size was only about 10 µm or less above the upper error band of the measurements. The final drop size was predicted consistently by the simplified and detailed spray model options. This indicates that the use of the model option of simplified spray for fast speed simulations and simulator purposes can be justified.
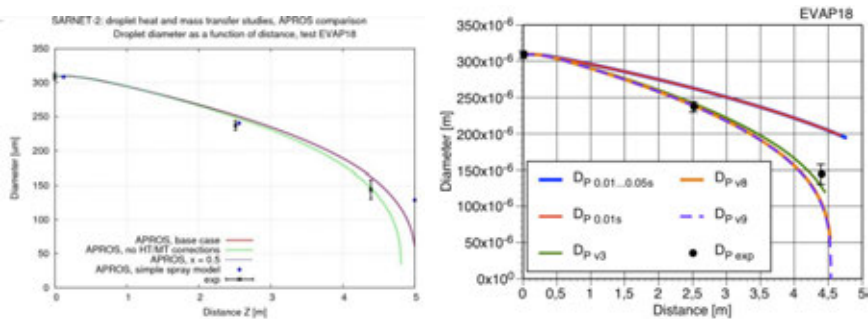
Figure 12. Calculated droplet size evolutions with APROS (left) and Fluent (right) and measured droplet diameters in test EVAP18 with different modelling options.

Calculation of THAI test TH24

VTT participated in blind and open calculations of German THAI experiment TH24 with the Fluent CFD code and the APROS lumped parameter (LP) containment code. Experiment TH24 was intended to investigate the dissolution of a steam layer subject to natural convection in the atmosphere of the THAI test vessel [18]. Conventionally, CFD simulation tools are used to solve complicated natural circulation and gas stratification phenomena. However, during the last few years LP containment models has been used more and more in modeling gas stratification phenomena e.g. APROS LP containment model has been applied in modelling MISTRA and PANDA experiments. During these activities, a "pseudo 3-D" LP nodalization concept has been developed and tested. The blind calculation of TH24 gave a great opportunity to utilize this experience and to test the LP nodalization concept in simulation of stratification and natural circulation phenomena without knowing the experimental results beforehand.

The main component of the THAI facility is a cylindrical steel vessel of 9.2 m height and 3.2 m diameter, with a total volume of 60 m³ (Figure 13) [18]. the vessel space is subdivided by an open inner cylinder and a horizontal separation plane in the annular region with vent openings. These internal structures were

removable in test TH24. The outer cylindrical wall has cooling/heating jackets subdivided in three vertical sections. The entire vessel is thermally insulated. The experimental procedure of the transient phase of TH24 was as follows: 1) heating the lower and middle vessel mantle and cooling the upper mantle, 2) when the temperature at the heated mantles has reached 100°C, the heating power is reduced and regulated to keep a level of 100°C, 3) start of the steam injection to build up a stable steam-air stratification in the upper plenum, and 4) observation of the stratification dissolution process due to convection flows. The transient phase took place at 3287 s.

In the APROS model (totally 140 nodes); the vessel was divided into 28 vertical node levels (Figure 13). Each node level was further divided horizontally into 5 nodes forming so called "pseudo 3-D" nodalization. The steam injection zone had an own 8-node nodalization.
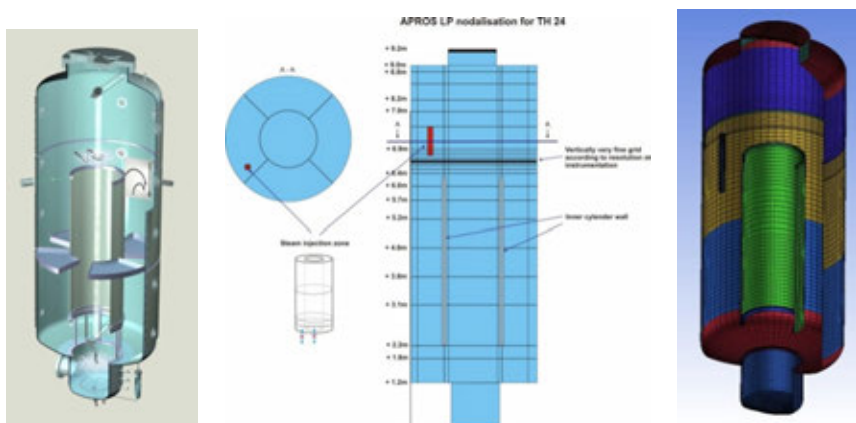
Figure 13. THAI test facility (left) [17]. APROS (middle) and Fluent (right) nodalizations for TH24.

Preliminary results of the benchmark show that main features of the simulated field distributions are qualitatively comparable to the measured data. This is shown by both CFD and LP models (Figure 14 and Figure 15). The pressure increase is qualitatively well simulated by most LP and CFD models, but quantitative comparison indicates that there is still a need for further model improvements [18]. It was found that APROS LP code could simulated the steam stratification with a very good quality as well as the mixing of the steam until t = 700 s. The fact that the later mixing occurs quicker than in the experiment, is most likely due to an over prediction of the convective loop.
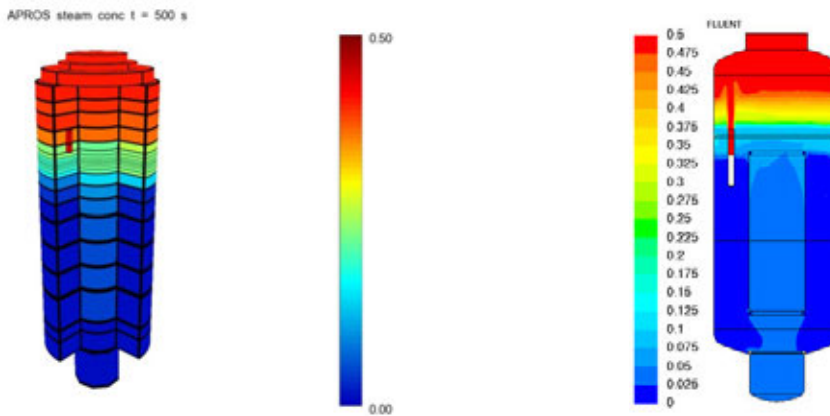
Figure 14. Steam molar fraction at t = 500 s calculated by APROS (left) and Fluent (right) codes.
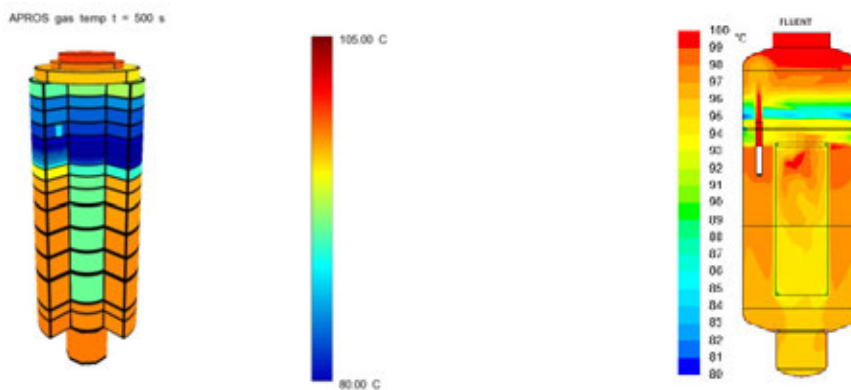

Figure 15. Gas temperature at t = 500 s calculated by APROS (left) and Fluent (right) codes.

References

1. Hillberg, S. Simulation of NOKO emergency condenser EU experiments with APROS. VTT-R-06319-11.

2. Hillberg, S. PANDA steady state isolation condenser experiments with APROS. VTT-R-01259-12.

3. Krepper, E., Schaffrath, A. 1999. Numerical simulation of the emergency condenser of the SWR1000. Kerntechnik 64.

4. Dreier, J., Aksan, N., Aubert, C., Fischer, O., Lomperski, S., Huggenberger, M., Strassberger, H.-J. 1998. Panda Test Results and Code Assessment for Investigations of Passive Heat Removal from the Core of a BWR. 6th International Conference on Nuclear Engineering, ICONE-6463.

5. Kolehmainen, J. Simulation of the PACTEL non-condensable gas experiments NCG-1, NCG-3, NCg2-04 and NCg2-05 with APROS 5.11.02. VTT-R-07223-12.

6. Purhonen, H., Puustinen, M. 2001. Integral System and Horizontal Steam Generator Behaviour in Non-condensable Gas Experiments With the PACTEL Facility. Lappeenranta.

7. Inkinen, P., Lauerma, S. ROSA-2 Test 3 Simulation with TRACE and Apros. VTT-R-01120-12.

8. Kurki, J. Simulation of ROCOM Test 2.1 with APROS and TRACE, VTT-R00417-12. (Restricted)

9. Takeda, T., Ohtsu, I., Nakamura, H. LSTF Test of CET Performance During PWR Hot Leg Small-Break LOCA and RELAP5 Analysis. NURETH-15, Pisa, Italy, May 12–15, 2013.

10. Kelm, St. et al. Generic Containment. A first step towards bringing (European) containment simulations to a common level. 5th European Review Meeting on Severe Accident Research (ERMSAR-2012). Cologne, Germany, March 21–23, 2012.

11. Kelm, St. et al. Generic Containment, a Detailed Comparison of Containment Simulations Performed on Plant Scale. To be presented in the 15th International Topical Meeting on Nuclear Reactor Thermalhydraulics, NURETH-15, Pisa, Italy, May 12–15, 2013.

12. Silde, A. Modelling of passive autocatalytic hydrogen recombiner (AREVA type) in the APROS Containment code. VTT Research Report VTT-R-07488-12. 10.12.2012.

13. AREVA: Passive Auto-Catalytic Reconbiners, Tec-Sheet, 2011. http://us.areva.com/home/liblocal/docs/Solutions/literature/G-008-V1PB-2011-ENG_PAR_reader.pdf.

14. AREVA: Recombiner modelling on GASFLOW for APR application. Presentation in SARNETworkshop 23./24..6.2005. Framatome ANP GmbH NGPS4.

15. Malet, J. et al. Spray Model Validation on Single Droplet Heat and Mass Transfer for Containment Applications – SARNET-2 Benchmark, NURETH14-255, Toronto Ontario Canada, September 25–30, 2011.

16. Silde, A. Validation of containment spray modelling of APROS on single droplet heat and mass transfer tests. VTT Research Report VTT-R-08953-11. 31.1.2012.

17. Huhtanen, R., Kyttälä, J. Verification of a droplet evaporation and condensation model on Fluent. VTT-R-00095-12. (Restricted)

18. Freitag, M. Comparison Report for Blind Simulations of THAI Test TH24 (CV5) "Dissolution of Steam Stratification by Natural Convection". Report no. 150 1361 – TH24 – VB. Becker Technologies GmbH, Eschborn. Draft Aug. 2012. (To be published.)

5.2 Experimental studies on containment phenomena (EXCOP)

Markku Puustinen, Jani Laine, Antti Räsänen, Vesa Tanskanen, Lauri Pyy

Lappeenranta University of Technology
Skinnarilankatu 34, P.O. Box 20, FI-53851 Lappeenranta

Introduction

The main goal of the EXCOP project is to gather an extensive experimental database on condensation dynamics, heat transfer and structural loads in a suppression pool environment to be used for testing and developing computational methods used for nuclear safety analysis, such as Fluent, NEPTUNE_CFD, TransAT, GOTHIC, APROS and TRACE. The behaviour at the blowdown pipe outlet during air/steam discharge still needs to be investigated experimentally in more detail to improve simulation models. The PPOOLEX test facility at Lappeenranta University of Technology (LUT), including models of the Boiling Water Reactor (BWR) drywell and wetwell compartments and withstanding prototypical system pressure, has been used in the experiments. During the first two years of the project direct-contact condensation (DCC) at the vicinity of the blowdown pipe outlet, the effect of a blowdown pipe collar and stratification/mixing during a long-lasting steam discharge condition have been studied.

To achieve to above mentioned goals sophisticated measuring solutions i.e. a Particle Image Velocimetry (PIV) system and a modern high speed camera have

been installed to the PPOOLEX facility in 2011–2012. With these devices development of flow fields at the vicinity of the blowdown pipe outlet and macroscopic interfacial area related to the increase and collapse of steam bubbles can be investigated. Furthermore, novel gradient heat flux sensors are being used for determining local heat fluxes through the blowdown pipe. The applicability of the experiment results for the validation of CFD, lumped parameter and structural analysis codes increases considerably as a result of these improvements in instrumentation.

Networking among international research organizations has been enhanced via participation in the NORTHNET framework and NKS/ENPOOL project. Analytical and numerical work of Kungliga Tekniska Högskolan (KTH) has been combined to the EXCOP, ELAINE, NUMPOOL and ESA projects of SAFIR2014. The EXCOP project has also a connection to the nuFoam project of SAFIR2014, where PPOOLEX data on DCC is used for the validation of an OpenFOAM-solver.

This paper shortly introduces the PPOOLEX test facility, summarizes the main results of the PPOOLEX experiments and related research in 2011–2012, presents an example of numerical simulations and finally concentrates on the findings of the stratification/mixing experiments in more detail.

PPOOLEX facility

The PPOOLEX facility consists of a wet well compartment (condensation pool), dry well compartment, inlet plenum and air/steam line piping. An intermediate floor separates the compartments from each other but a route for gas/steam flow from the dry well to the wet well is created by a vertical blowdown pipe attached underneath the floor.

The main component of the facility is the ~31 m3 cylindrical test vessel, 7.45 m in height and 2.4 m in diameter. The test facility is able to withstand considerable structural loads caused by rapid condensation of steam. The removable vessel head and a man hole in the wet well compartment wall provide access to the interior of the vessel for maintenance and modifications of internals and instrumentation. The dry well is thermally insulated. A sketch of the test vessel is shown in Figure 1.
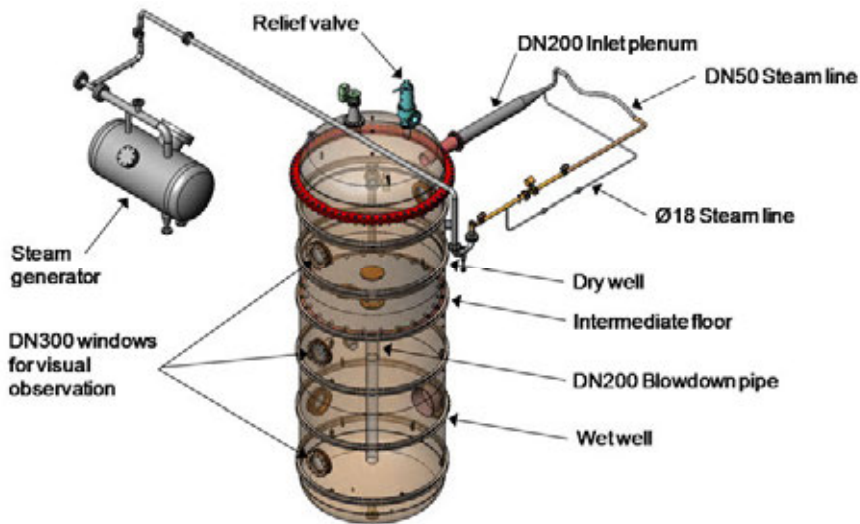
Figure 1. PPOOLEX test facility.

Steam needed in the experiments is produced with the nearby PACTEL [1] test facility, which has a core section of 1 MW heating power and three horizontal steam generators. Steam is led through a thermally insulated steam line from the PACTEL steam generators to the test vessel. Accumulators connected to the compressed air network of the lab can be used for providing non-condensable gas injection. The DN200 blowdown pipe is positioned inside the pool in a non-axisymmetric location, i.e. the pipe is 300 mm away from the centre of the condensation pool.

The applied instrumentation depends on the experiments in question. Normally, the test facility is equipped with several thermocouples for measuring steam, pool water and structure temperatures and with pressure transducers for observing pressures in the dry well, inside the blowdown pipes, at the condensation pool bottom and in the gas phase of the wet well. Steam flow rate is measured with a vortex flow meter in the steam line. Additional instrumentation includes, for example, strain gauges on the pool outer wall and valve position sensors. In order to gain CFD grade measurement data of rapid steam condensation processes sophisticated instrumentation techniques has to be used. Therefore, a Particle Image Velocimetry system and an up-to-date high speed camera have been added to the PPOOLEX facility in 2011–2012. National Instruments PXIe PC-driven measurement system is used for data acquisition. The system enables high-speed multichannel measurements.

Research program in 2011–2012

The backbone of the EXCOP project in 2011–2012 has been the different kind of experiments with the PPOOLEX test facility. These have included experiments on thermal stratification/mixing, direct contact condensation and the effect of a blowdown pipe collar. CFD calculations of selected previous POOLEX experiments and studies on the PCCS behaviour have supplemented the EXCOP research effort.

Experiments with a blowdown pipe collar

The shape and geometry of the blowdown/vent pipe outlet designs are known to have a significant effect on structural loads experienced by submerged condensation pool structures. A series of steam discharge experiments with a scaled collar model attached to the blowdown pipe outlet of the PPOOLEX facility was carried out [2]. Additional pressure sensors were installed inside the pipe in order to get high resolution data of the movement of the condensation front. A high speed camera was positioned towards the interior of the blowdown pipe with the help of a viewing window installed to the bottom segment of the pool.

The measured pressure loads inside the blowdown pipe, below the pipe and at the pool bottom indicated no minimizing effect due to the collar. Between the reference and collar experiments there was no clear difference in the maximum amplitude of registered pressure loads. Also the piezoelectric pressure sensors at the blowdown pipe outlet gave no indication of any beneficial effect of the collar if the measured maximum amplitude of the dynamic pressure component is considered. However, due to larger than desired amount of non-condensables among the flow no definitive conclusions on the effect of the collar on loads experienced by submerged pool structures can be drawn on the basis of these experiments since non-condensables strongly diminish condensation loads. Figure 2 shows the dynamic pressure component at the blowdown pipe outlet during the collapse of a steam bubble.
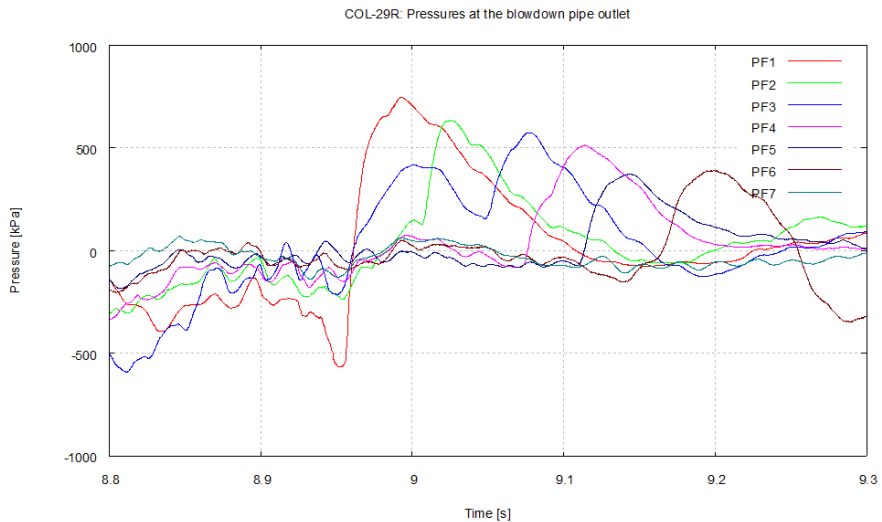
Figure 2. Dynamic pressure component at the blowdown pipe outlet during the collapse of a steam bubble in a collar experiment.

Preliminary PIV tests

A Particle Image Velocimetry measurement system was installed to the PPOOLEX facility at the end of 2011 for capturing the details of DCC related phenomena. The idea is to get CFD grade measurement data for verification/validation of numerical models.

The main objective of the first PIV tests was to gather information about the functioning of the experimental setup and about suitable measuring parameters such as the amount of seeding material and correct time delay between laser pulses [3, 4]. For seeding glass hollow spheres with a mean diameter of 11 µm were used. The used laser sheet thickness was 7 mm.

The measurement series included eight independent measurements with changing values in the pulse delay and mass flow rate of blowdown steam. The objective was to achieve a steady state steam/water-interface at the exit of the pipe.

In some occasions a need for masking out some parts of the raw images is necessary. For example, there can be a high reflection from a shiny surface that can affect the PIV processing. With a geometrical mask an area which will be masked out can be drawn on the raw image and then applied to every raw image so that the same area is always masked out. In PPOOLEX, for example, the area of the blowdown pipe outlet may have to ne masked out.

In the measurements it was found out that there was some fluctuation in the velocity field when the steam/water-interface was at the exit of the blowdown pipe. Condensation of steam in the vicinity of the pipe exit caused these fluctuations. A strong constant outflow was usually followed by a strong constant inflow towards

the pipe exit. Between these two phases the velocity field was rather stable and the movement was from the centreline of the pipe exit towards the outer edge. In this middle phase the velocities were relatively small compared to the stronger outflow and inflow phases.

From the set of 1000 velocity field images analysed in total 85 images were characterized by a relatively strong outflow from the blowdown pipe exit. Figure 3 presents the averaged velocity field from this period with a background image of the cameras. The outline of the pipe exit is highlighted with orange dots. Due to the geometrical masking some velocity information is lost in the top left corner below the pipe exit as well as in the top right corner next to the pipe wall. The reference vector with the value of 0.01 m/s is shown in the top left corner. The background colour refers to the out-of-plane velocity component and the scale is on the right side of the figure. In Figure 3, the average velocities vary roughly from 0.01 m/s to 0.001 m/s. The time intervals between the corresponding phases were alternating from 0.2 seconds to 3.2 seconds. The maximum duration of the strong outflow phase was 0.8 seconds.
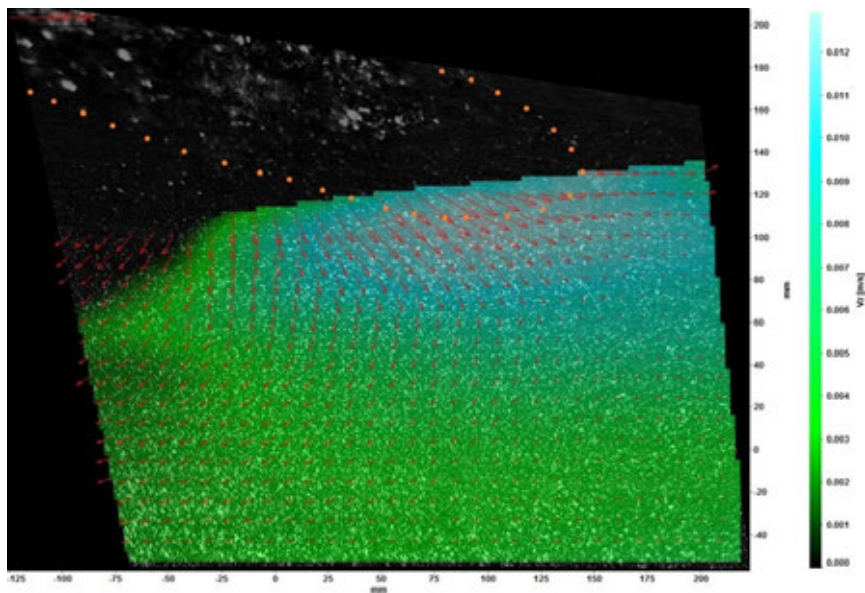
Figure 3. Averaged velocity field of a strong outflow phase with a background image. The outline of the blowdown pipe exit is highlighted with orange dots.

Experiments in the PPOOLEX facility form a very challenging environment for the use of the PIV measurement system but already these preliminary tests have shown that reasonably good results can be obtained. The biggest restriction for the future studies in PPOOLEX with PIV is the facility itself. A fully free positioning of the PIV system is out of the question because there are limitations for the

amount of viewing windows that can be installed to PPOOLEX. When experiments are performed in harsher environment, e.g. the mass flow of steam is high enough to cause chugging phenomenon at the pipe exit, the use of laser-induced fluorescence (LIF) should be considered. By using a fluorescent dye as a tracer and filters that filter out the wavelength of the laser, the possible steam bubbles that reflect the laser light can be filtered out. The density of the used seeding material was close to the water density and in the experiments the seeding followed and reflected well the fluctuations caused by condensation of steam. In this respect the physical properties of the used seeding material were ideal.

Studies on Passive Containment Cooling System

The passive containment cooling system (PCCS) is a system that passively removes heat from the containment to the liquid pool surrounding the PCCS heat exchangers. In addition to cooling it also has an important role in mitigating the offsite dose by retention of a fission product release in the containment. The possibility of using PPOOLEX as a host facility in PCCS experiments in order to gain data for the validation of severe accident code MELCOR was examined and modifications needed for the PPOOLEX facility were evaluated. The main benefit of using the PPOOLEX facility comes from an easy opportunity to create and control boundary conditions needed in the experiments. In discussions with modellers from VTT the horizontal PCCS design used in the ABWR concept was ranked as the most interesting case to be studied. A scaled PCCS condenser model of the type used in ABWRs was designed and constructed in 2012 (Figure 4) [5]. The systems for aerosol feeding and for measuring the deposition of aerosols in the condenser tubes are to be designed in cooperation with VTT.

Figure 4. PCCS model next to the PPOOLEX host facility.

Simulations of POOLEX experiments

The NEPTUNE CFD recalculations of the POOLEX STB-31 experiment (steady steam/water-interface experiment) confirmed the earlier results [6]. The Hughes-Duffey condensation model overestimated the condensation rate by one order of magnitude whereas the Lakehal et al. (2008b) condensation model predicted the condensation rate very accurately. The Coste-Lavi´eville model predicted condensation rates close to the rates of the Lakehal et al. condensation model.

The NEPTUNE CFD simulations of the POOLEX STB-28 experiment (chugging condensation mode) using a 2D-axisymmetric geometry were started (Figure 5 and Figure 6) [7]. The condensation models of Hughes-Duffey and Lakehal et al. 2008 were compared. Initial 2D results indicate that the Hughes-Duffey condensation model predicts clearly higher condensation rates than the model of Lakehal et al. 2008. Furthermore, both models indicate lower condensation rates than observed in the experiment. However, when the interface was initialized to a high enough level inside the pipe, the vigorous initial penetration of it into the pool water created a turbulent wake which invoked chugging due to the improved heat transfer rate by increased turbulence production. The initiated chugging state was then self-sustaining. In that case the condensation models of Hughes-Duffey and Coste-Lavi´eville predicted realistic chugging behaviour whereas the model of Lakehal 2008b still underestimated the condensation rates.
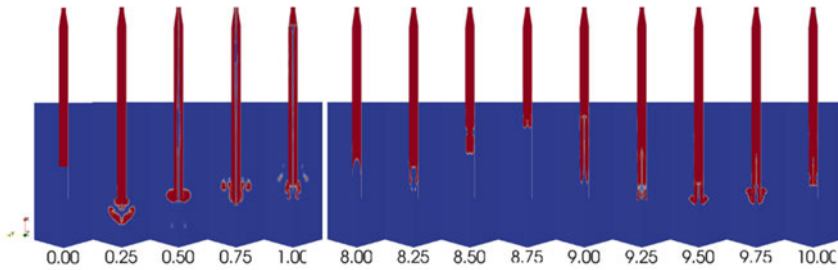
Figure 5. Volume fraction of steam during the first and last seconds of simulation in a 2D-axisymmetric NEPTUNE CFD simulation of the STB-28-4 blowdown using the Hughes-Duffey condensation model.
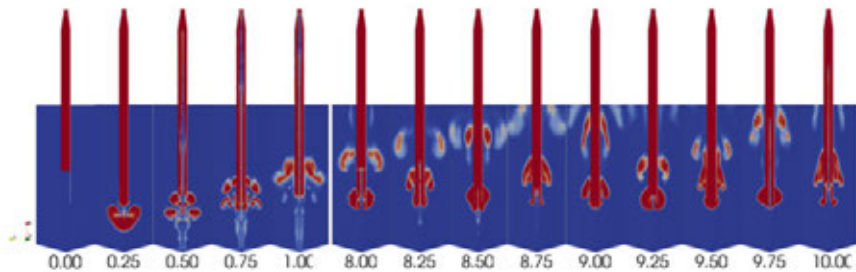

Figure 6. Volume fraction of steam during the first and last seconds of simulation in a 2D-axisymmetric NEPTUNE CFD simulation of the STB-28-4 blowdown using the Lakehal '08b condensation model.

Stratification and mixing experiments

In case of small steam flow rates, thermal stratification could develop above the blowdown pipe exit and significantly impede the pressure suppression capacity of the condensation pool. The pressure of containment, which is determined by the temperature of free surface of water pool in the wetwell, will increase with development of thermal stratification and cause safety concerns in the containment.

Experimental studies have shown that once steam flow rate increases significantly, momentum introduced by the steam injection and/or periodic expansion and collapse of large steam bubbles due to DCC can destroy stratified layers and lead to mixing of the pool water. However, accurate and computationally efficient prediction of the pool thermal-hydraulics with thermal stratification, mixing, and transition between them, presents a computational challenge, because the DCC, which dominates such phenomena during the steam injection, is not fully understood and cannot be modelled correctly [8].

KTH is developing and implementing the Effective Heat Source (EHS) and Effective Momentum Source (EMS) models in GOTHIC code. To provide necessary data for the development of the models, a series of experiments in the PPOOLEX facility at LUT was carried out in the framework of SAFIR2014 and NORTHNET RM3 programs [9].

A fine resolution both in space and time for detection of the dynamics of free water surface in the blowdown pipe is needed to get an accurate estimation of the frequency and amplitude of oscillations for the assessment of the effective momentum. This was achieved with an extensive net of measurements added into the blowdown pipe before the experiments.

Thermal stratification

In the beginning of the experiments the wet well pool was filled with isothermal water. During the small steam flow rate period temperatures below the blowdown pipe outlet remained constant while increasing heat-up occurred towards the pool surface layers indicating strong thermal stratification. Figure 7 shows the development of vertical temperature profile of pool water above and below the blowdown pipe outlet elevation.
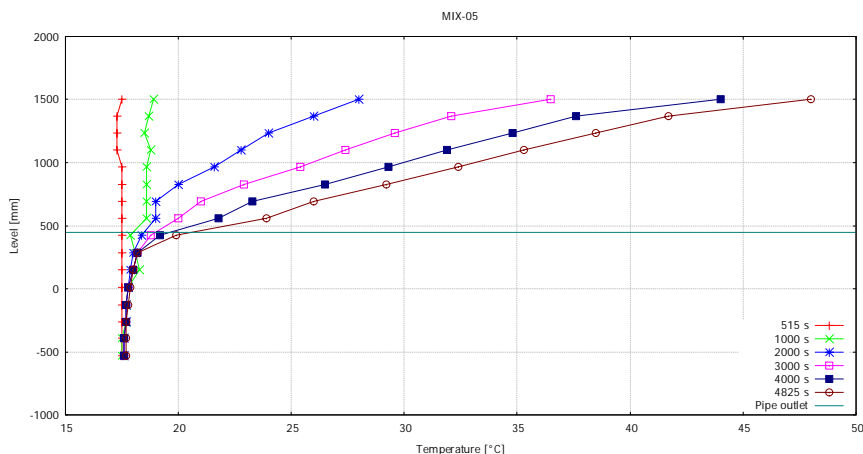

Figure 7. Development of vertical temperature profile of pool water during the stratification period.

Mixing by chugging

As the experiments proceeded to the mixing period the steam mass flow rate was rapidly increased to get the steam/water-interface moving up and down inside the blowdown pipe and to totally mix the condensation pool water inventory. Typically the prevailing condensation modes were *steam condensation within vents or*

blowdown pipes and *chugging* [10]. Depending of the used steam flow rate and the degree of thermal stratification of the pool water it took 150–500 s to achieve total mixing of the pool volume.

Two experiments were extended beyond the total mixing phase without reducing the steam discharge rate. As the pool water temperature increased above 50°C the water inventory began to staritfy again. This restratification continued until the experiments had to be stopped due to reaching the temperature limit of certain test facility structures. The different phases of the experiment can be clearly distinguished from the temperature and steam flow rate curves in Figure 8. The initial heat-up and non-condensable gas blowdown period lasts for about 500 seconds, the stratification period is between 500 and 2700 seconds, the mixing and temperature increase period between 2700 and 3500 seconds and finally the restratification period from there until the end of the experiment.
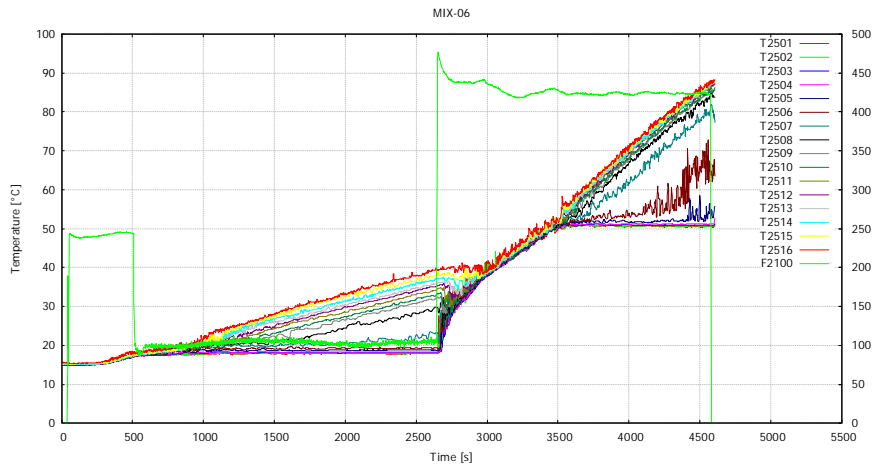

Figure 8. Different phases of a stratification/mixing experiment in the PPOOLEX facility.

For the estimation of the momentum source, which affects the intensity of mixing, the details of the movement of the steam/water-interface inside the blowdown pipe have to be known. The experiments revealed that during the mixing period the steam/water-interface oscillated up and down inside the blowdown pipe with amplitude of 29–999 mm and frequency of 0.6–1.82 Hz depending on the used steam flow rate and prevailing pool water temperature. Figure 9 presents how this movement was captured with the help of temperature measurements in the beginning of the mixing period.
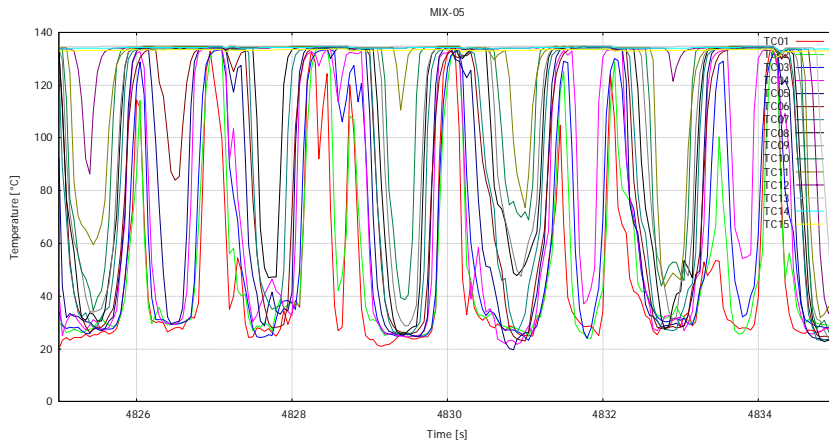
Figure 9. Oscillating behaviour of steam/water-interface during the mixing phase as registered by temperature measurements inside the blowdown pipe.

References

1. Tuunanen, J., Kouhia, J., Purhonen, H., Riikonen, V., Puustinen, M., Semken, R.S., Partanen, H., Saure, I., Pylkkö, H. General Description of the PACTEL Test Facility. Espoo: VTT. 1998. VTT Research Notes 1929. ISBN 951-38-5338-1.

2. Puustinen, M., Laine, J., Räsänen, A. PPOOLEX Experiments with a Blowdown Pipe Collar. Lappeenranta University of Technology, Nuclear Safety Research Unit, Research Report EXCOP 1/2011. Lappeenranta 2012.

3. Pyy, L. Utilization of Particle Image Velocimetry in PPOOLEX Condensation Experiments. Master's thesis, Lappeenranta University of Technology. 2012.

4. Puustinen, M., Pyy, L., Purhonen, H., Laine, J., Räsänen, A. First PPOOLEX Tests with the PIV Measurement System. Lappeenranta University of Technology, Nuclear Safety Research Unit, Research Report EXCOP 2/2011. Lappeenranta 2012.

5. Purhonen, H. Passive Containment Cooling System Experiments: Preliminary Design of the PCCS Test Facility. Lappeenranta University of Technology, Nuclear Safety Research Unit, Research Report EXCOP 3/2011. Lappeenranta 2011.

6. Tanskanen, V. CFD Modelling of Direct Contact Condensation in Suppression Pools by Applying Condensation Models of Separated Flow. Acta Universi-

tatis Lappeenrantaensis 472, Lappeenranta 2012. Diss. Lappeenranta University of Technology. ISBN 978-952-265-221-8, ISBN 978-952-265-222-5 (PDF), ISSN 1456-4491.

7. Tanskanen, V., Jordan A. Validation of Condensation Models against POOLEX STB-31 and STB-28 Experiments. Lappeenranta University of Technology, Laboratory of Nuclear Engineering, Research Report EXCOP 4/2011. Lappeenranta 2012.

8. Li, H., Villanueva, W., Kudinov, P. Effective Models for Prediction of Stratification and Mixing Phenomena in a BWR Suppression Pool. Royal Institute of Technology (KTH). Division of Nuclear Power Safety, NORTHNET Roadmap 3 Research report. Stockholm 2012.

9. Laine, J., Puustinen, M., Räsänen, A. PPOOLEX Experiments on the Dynamics of Free Water Surface in the Blowdown Pipe. Lappeenranta University of Technology. Nuclear Safety Research Unit, Research Report EXCOP 2/2012. Lappeenranta 2013.

10. Lahey, R. T., Moody, F. J. The Thermal-Hydraulics of a Boiling Water Reactor. American Nuclear Society, Illinois. 2nd edition. 1993.

5.3 OpenFOAM CFD-solver for nuclear safety related flow simulations (NUFOAM)

Juho Peltola[1], Juhaveikko Ala-Juusela[2], Tomas Brockmann[2], Karoliina Ekström[3],
Jarto Niemi[1], Giteshkumar Patel[4], Timo Pättikangas[1], Timo Siikonen[2],
Vesa Tanskanen[4], Timo Toppila[3]

[1]VTT Technical Research Centre of Finland
P.O. Box 1000, FI-02044 VTT, Finland

[2]Aalto University
P.O. Box 11000, FI-00076 AALTO, Finland

[3]Fortum Power and Heat Oy
P.O. Box 100, FI-00048 Fortum, Finland

[4]Lappeenranta University of Technology
P.O. Box 20, FI-53851 Lappeenranta, Finland

Abstract

OpenFOAM is a popular open source computational fluid dynamics source code library. In this project, solvers based on the library have been used to simulate single phase flow in fuel rod bundles and a T-junction. Simulation results were submitted to the blind OECD/NEA MATIS-H fuel rod bundle benchmark. A modified solver has been developed for simulation of subcooled nucleate boiling and tested against experimental data and results of alternative CFD codes. The same solver has also been modified and tested for simulation of direct contact condensation.

Introduction

In the field of nuclear safety analysis, Computational Fluid Dynamics (CFD) has become an increasingly popular tool for thermo-hydraulic investigations. There are several suitable, commercial and open-source, CFD-codes available, but in recent years an open-source CFD-library called OpenFOAM has been gaining popularity worldwide. It is developed by OpenCFD Ltd. (ESI Group) and distributed by the OpenFOAM Foundation The code has originated in Imperial College London during the early 1990's and was published as open-source in 2004.

Compared to commercial solvers, the benefits of an open source CFD code are transparency, infinite customizability and lack of licensing fees, which brings the cost structure of massively parallel computation down to a feasible level. Compared to other open source CFD codes, the benefits of OpenFOAM® are a large, active and growing user base, modern approach to mesh handling with unstructured and

polyhedral meshes, parallelization and an object oriented code structure that makes it fast and easy to implement new models and solvers in the top level code.

Distinct drawbacks of OpenFOAM are the lack of public, formal documentation and – partially because of the previous point – a very steep learning curve. Generally it can also be said that many of the features of OpenFOAM represent the state-of-the-art, but often lack the polish to directly apply them to practical engineering problems. In this project we try to alleviate these drawbacks from the perspective of nuclear safety analysis to make OpenFOAM a practical tool for these applications. Initial work was carried out in 2010 by validating turbulent near-wall treatments in pipe flows, developing a version of two-phase solver that is suitable for dispersed bubbly flows and by participating in the OECD/NEA T-junction benchmark.

OpenFOAM and OpenCFD are registered trademarks of OpenCFD Ltd. (ESI Group) and this project has not been endorsed or approved by OpenCFD Ltd.

Main objectives

The main aim of the project is to validate OpenFOAM® as a tool for nuclear safety related simulations. An application oriented approach for validation is used. The first goal is to be able to simulate transient single-phase flows and heat transfer in a complex geometry, especially in the fuel assembly and its head parts, more accurately using efficient parallel computing. As a result, we expect to have more detailed understanding of the coolant mixing and the results can be used e.g. in verifying safety issues when increasing the burn up of the fuel.

Another branch of the project is to adapt and extend OpenFOAM® two-phase flow capabilities for nuclear safety analysis applications, specifically to two-fluid turbulent gas-fluid flow simulations with heat transfer, boiling and condensation. The validation results and lessons learned in the single-phase tasks are applied in two-phase solver development. In this project, the goal is to successfully simulate subcooled nucleate boiling in a PWR fuel rod bundle and direct contact condensation (DCC) in a suitable test case.

An important goal of the project is also to strengthen the Finnish CFD community in the field of nuclear safety and to participate in Northnet and other international cooperation.

Simulation of single phase flows

The work on single phase simulations has been carried out at Aalto University and Fortum. Fortum took part in the MATIS-H benchmark, simulating a horizontal fuel rod bundle with a spacer grid utilizing RANS turbulence modelling. The main emphasis of Aalto University has been on the VVER-440 fuel rod bundle, which has been simulated with different turbulence modelling approaches, including more advanced approaches like Large-Eddy Simulation (LES) and Detached-Eddy

Simulation (DES). A new inflow boundary condition was implemented that is able to generate the transient turbulent inflow that is required in LES and DES simulations.

OECD/NEA MATIS-H Benchmark

OECD/NEA MATiS-H benchmark (Measurement and Analysis of Turbulent Mixing in Subchannels – Horizontal) was a blind CFD benchmark exercise, where the flow in a cold rod 5x5 fuel bundle with a spacer grid is solved. The test facility, MATIS-H, is located at the Korea Atomic Energy Research Institute (KAERI) in Daejeon, South Korea. The test participants were given details of the test geometry and operating conditions. Based on that the velocity components, turbulent intensity and vorticity information inside the fuel rod and in the vicinity of the spacer grid was simulated. Fortum contributed in the benchmark by calculating the test case with OpenFOAM 2.1.0.

The mesh of CFD model was created using ANSYS Gambit 2.4.6. The mesh contained 14 million cells of which 87% were hexahedral and 13% tetrahedral. The case was calculated using different solvers and turbulence models and for comparison, the case was also calculated using commercial CFD code ANSYS Fluent 13.0. The computation mesh is presented in Figure 1.
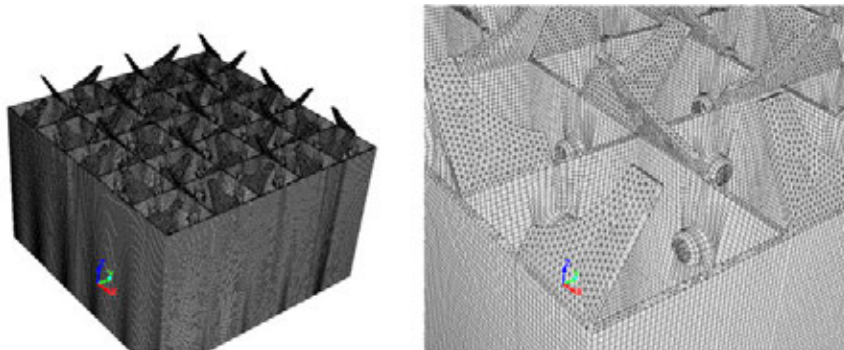

Figure 1. Computation al mesh at the surface of spacer grid in the MATIS-H simulations. Whole spacer grid (left) and one mixing vane (right).

The results of the different simulations were compared against the experimental data from a test without a spacer grid available for participants, as presented in Figure 2. The κ-ε turbulence models in Fluent and OpenFOAM seemed to give quite coherent results, whereas the Reynolds stress model in Fluent differed to some extent. The κ-ε model results gave good agreement with the experiment. The Fluent steady state and time dependent results were identical. In OpenFOAM, the SimpleFoam (steady state) and PimpleFoam (time dependent) results were very similar as well. After comparisons of the different cases, the OpenFOAM – SimpleFoam – κ-ε results were chosen as those to be submitted to the benchmark organisers.
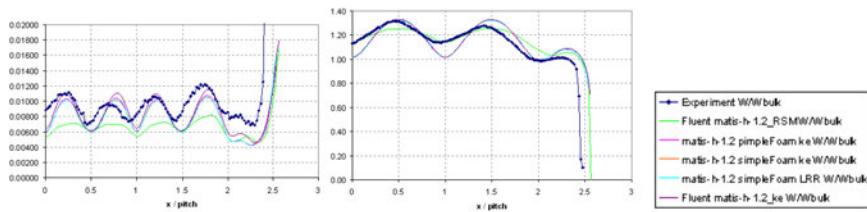
Figure 2. Flow inside the MATIS-H fuel rod bundle without a spacer grid. Turbulent kinetic energy k on the left and scaled axial velocity component w/w_ave on the right. Measurement line was in the middle between the fuel rods.

Summary of the results of all participants was presented in OECD/NEA & IAEA workshop CFD4NRS-4 in September 2012. The total of 25 participants had submitted simulation results. Commercial codes CFX, STAR-CCM+ and Fluent were used by the most participants, only one had used OpenFOAM code. Different approaches were used for the turbulence modelling; LES, hybrid approaches, RSM and RANS with SST k-ω or k-ε. Our results were selected as the "best estimations case of k-ε turbulence model", and the most of the main flow features were presented satisfactory by our simulation. As a feedback for the NuFoam project is that it was clear that the OpenFOAM is as good as any CFD code for this kind of CFD simulations.

VVER-440 fuel rod bundle

Simulations of VVER-440 fuel rod bundle were continued by applying OpenFOAM and FinFlo CFD-codes to isothermal one spacer grid interval models. OpenFOAM RANS simulations were carried out with traditional 30 degree sectional models as well as a single sub-channel model. The standard k-epsilon, SST k-omega and Launder-Gibson Reynolds stress models are applied to include the turbulent effects. All RANS simulations share similarities with earlier simulations, showing sharp peaks in velocity distributions above the spacers which hold fuel rods. A large velocity peak also tends to appear above the 'O'-shape sub-channel, which is not there in the measured flow distributions. The Reynolds stress turbulence model predicted stronger vorticity structures in the sub-channels than the two-equation models.

Initially, a single spacer interval DES simulation was done with the FinFlo-code by applying the SST k-omega turbulence model. The simulation gives some time varying flow patterns, but otherwise the results are close to the RANS results which were used as an initial guess. Large-scale turbulent fluctuations did not appear. Initial full rod length RANS simulations were also calculated with the FinFlo-code. In coarser grid level simulation, velocity distributions along the measurement line are not totally periodic from spacer to spacer. On denser grid level, the flow develops gradually along the flow axis (Figure 3) and the additional velocity peaks are similar to the periodic single spacer interval simulations.
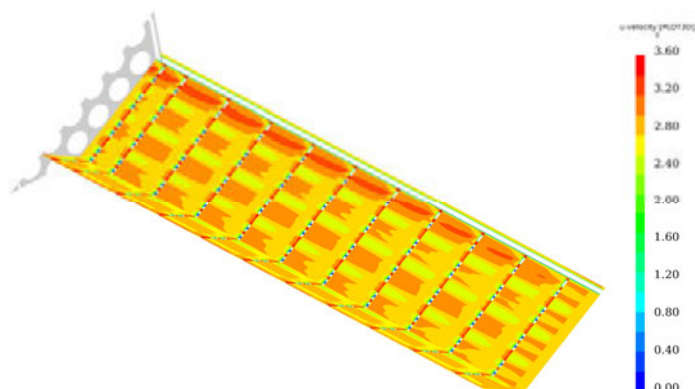
Figure 3. Velocity distributions in denser full-rod-length RANS simulation. FinFlo-code and SST k-omega turbulence model. Geometry is scaled for visual purposes.

Revised single sub-channel simulations were done by applying the RANS, LES and DES turbulence modelling approaches with OpenFOAM (Figure 4). The model is reduced to minimal size in order to save precious computational time while studying the turbulent behaviour. It was important as well to avoid excessive computational difficulties related to the complexity and size of the computational grid. The simulations were carried out with coarse meshing near the walls. The LES/DES grid had to be fine enough to capture the large-scale turbulent behaviour, which requires significantly more cells than RANS simulations. The RANS simulations using a 0.39 million cells grid lasted 15 hours on wall clock and the LES and DES simulations on 2.9 million cells grid 14 days. Mean flow passes the model 7 times during the simulation time. In the DES and LES simulations, SST-SAS and self-implemented version of dynamic Smagorinsky turbulence models were applied respectively (Menter & Egorov, 2009; Piomelli & Liu, 1995).

Static inflow conditions are often inadequate in time dependent LES and DES simulations, where transient large-scale-eddies are resolved time-accurately. In order to make realistic LES and DES simulations of turbulent flows, it is necessary to describe properly the incoming turbulent flow. In this work a pre-processing utility was developed to create synthetic flow fluctuations on boundary surfaces of OpenFOAM simulations. The fluctuating velocity components are based on sums of Fourier series to include the energy spectrum between the smallest and largest resolvable scales. In present work, the fluctuations are isotropic and seldom an accurate representation of actual flow conditions. Regardless, the method as demonstrated in channel flow of Figure 5 is a useful way of initialising turbulent flows without lengthy transitional phases (Davidson, 2007).
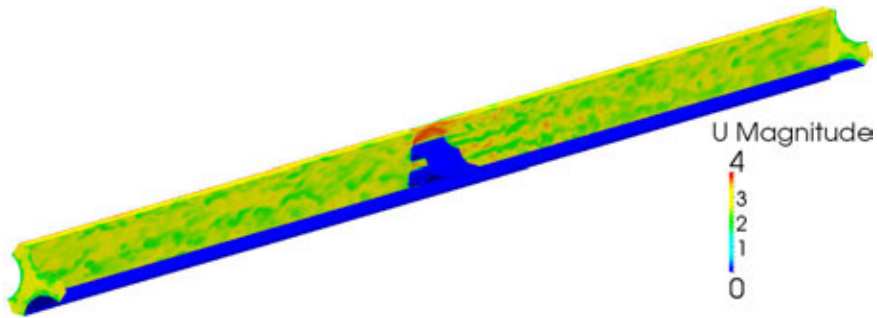
Figure 4. Velocity distributions in the single sub-channel DES simulation. SST-SAS turbulence model. Periodic boundary conditions.
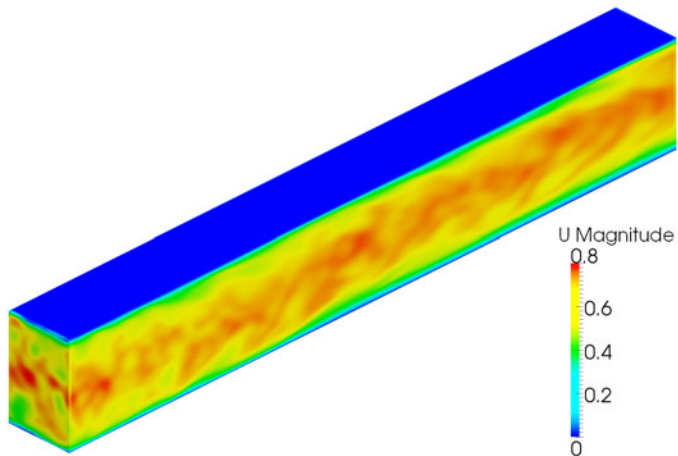

Figure 5. Velocity distributions in a channel flow LES simulation with isotropic synthetic turbulent inflow. Dynamic Smagorinsky turbulence model. $Re_b = 2800$.

Two-phase solver development

In two phase flows, the work in the project is more oriented towards code development simply because the present publicly available OpenFOAM solvers are not capable of simulating two-phase flows with boiling and condensation. The development effort of the main solver and simulations of subcooled nucleate boiling has been done at VTT. LUT has concentrated on adapting the solver for simulations of direct contact condensation and relevant test simulations.

The two-phase solver is based on OpenFOAM 1.7 solver called twoPhaseEulerFoam. Several modifications and enhancements have been implemented to make it suitable for these kinds of simulations. Turbulent dispersion and wall lubrication forces have been added and bubble specific interfacial force models for

drag and lift forces have been implemented. Models have been implemented for bubble induced turbulence and turbulence response coefficient. The transport equations have been modified to allow non-uniform material properties and mass transfer between the phases. Support for user selectable bubble diameter models has been added.

To include the heat transfer solution, specific enthalpy transport equation have been added for both phases. Interfacial heat transfer between the phases is modeled with a two-resistance model and includes optional interfacial thermal phase change. To model the nucleate boiling on the walls, an implementation of the so-called RPI wall boiling model has been included. Moreover, LUT have implemented two DCC models in the two-phase solver. The first model is the surface renewal model of Hughes and Duffey (1991) and the other one is the surface divergence model of Lakehal et al. (2008). The initial validation of implemented DCC models were performed by considering CFD calculations of the STB-31 experiments which was related to steam discharge into sub-cooled water. These experiments were carried out with a scaled down condensation pool test facility (POOLEX) at LUT.

Subcooled nucleate boiling

In the initial isothermal test simulations of 2010, the results of the two-phase solver were compared to experimental results on vertical bubbly flows from the literature. Since the addition of heat transfer, the main test cases have been DEDALE (EDF, Grossete, 1996) and DEBORA (CEA, Manon, 2000) experiments as well as the latest addition, OECD/NRC PSBT steady single-channel benchmark.

In the DEBORA simulations, two experiments of subcooled nucleate boiling in a vertical R-12 pipe flow were successfully simulated with the newly developed solver (Peltola, Pättikangas, 2012). The results were compared to experiments and simulations carried out with the commercial CFD solver ANSYS FLUENT 14. Overall, the twoPhaseNuFoam simulation results compared well with both experiments and FLUENT results, but the twoPhaseNuFoam k-ε turbulence model proved to be highly sensitive to vapor volume fraction in the near-wall grid cells. At higher volume fractions, the turbulent kinetic energy in the bulk flow decreased dramatically, which led to under-prediction of turbulent dispersion and diffusion of heat.

Because of the sensitivity of the k-ε turbulence model, an alternative k-ω SST model was implemented in the solver. In the initial testing it has proved much more predictable than the k-ε model, providing a more stable platform for development of other sub models. In the present solver, the k-ω SST is the default turbulence model.

While all the previous test cases were vertical flows in circular pipes, the PSBT single-channel benchmark introduces a more complex geometry. The Figure 6b shows a cross-section of the channel. It is a cross shaped channel with heaters in the rounded corners. The end walls of the cross are adiabatic.

The combinations of sub models used in the simulations were similar to those used by Frank et al. (2011) in their benchmark simulations: k-ω SST turbulence mode, algebraic bubble diameter model, with and without non-drag interfacial force models. The vapor forms on the four heated walls and is pushed towards the edges of the channel by the lift force. The condensing vapour warms the adiabatic corners of the channels. This slows the condensation rate and by the end of the channel allows build-up of vapour in these corners.

Direct contact condensation

After successful implementation of DCC models to the solver code, the STB-31 steam discharge experiment was selected for the CFD simulations. The POOLEX test facility is an open cylindrical pool (5.0 m in height and 2.4 m in diameter), modeling the condensation pool of a BWR. In these experiments, the vertical blowdown pipe (inner diameter 214.1 mm) was thermally insulated to prevent condensation on the pipe inner wall. The direct-contact condensation phenomenon took place only at the steam-water interface near the pipe outlet due to very low steam flow rates. The steam-water interface remained steady close to the pipe outlet. For further information of the STB-31 experiment, see Laine and Puustinen (2006a).

In this work, the numerical calculations have been performed with 2D wedge-axisymmetric grid. The height of the domain was set to 2.63 m in this grid. By using this height, the initial surface of the water could be set on the upper edge of the domain. Moreover, the lower conical part of the vessel was truncated off at 0.8 m from the mouth of the pipe. The radius of the domain was set to 1.2 m, which is the mean radius from the center of the blowdown pipe to the wall of the condensation pool, because in the POOLEX test facility the blowdown pipe was not exactly at the center of the pool. These simplifications should have negligible effect on the results. By imposing these simplifications, it is possible to avoid the free air surface at the top and the conical shape of domain at the bottom part.
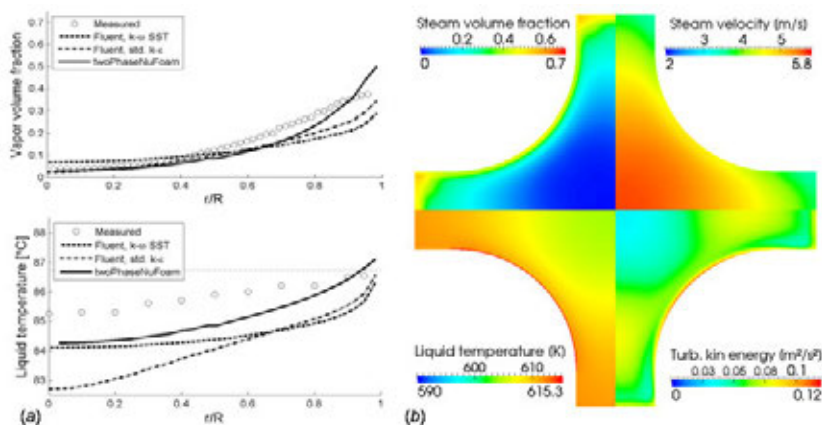
Figure 6. Subcooled nucleate boiling: a) Radial liquid temperature and vapour volume fraction profiles of DEBORA5 test case with the *k-ε* turbulence model. b) Contours of volume fraction, gas velocity, temperature and turbulent kinetic energy from a coarse mesh simulation of PSBT 1.2011 sub channel benchmark with active non-drag interfacial force models.

The grid was made by rotating a 2D-grid around the axis of rotation to create an angular dimension of thickness of a single cell. The angle between the front and the back face was 1 degree. The grid contains total 14240 cells (14050 hexahedral and 900 prismatic cells) which was more refined at the pipe tip region in order to study DCC of steam in that region.
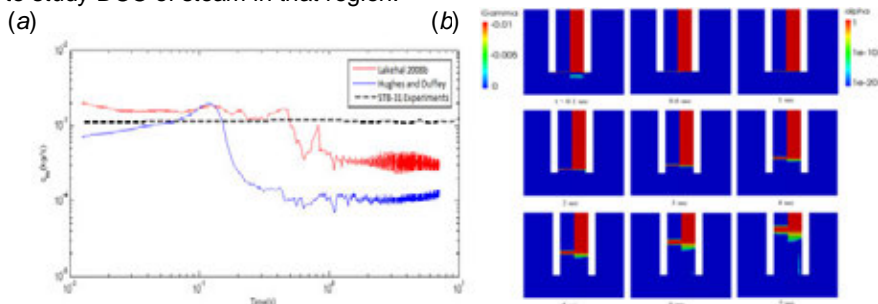

Figure 7. a) Condensation mass flow rate predictions of the Hughes-Duffey and the Lakehal 2008 models versus the STB-31 experimental data. b) Instantaneous profiles of interfacial mass transfer rate (left part) and volume fraction (right part) of the gas phase during of the simulation.

Figure 7a displays the condensation mass flow rate predictions of both models versus the STB-31 experimental data. Figure reveals that at the early phase of the simulations, the both models tend to predict relatively similar condensation mass flow rates as in the experiment. However, the both models start to underpredict the

condensation rate after certain period simulated. The Hughes-Duffey model under-estimates the DCC rate almost an order of magnitude while the Lakehal 2008b model yields 50% less condensation mass flow compared to the experiment.

Figure 7b demonstrates the instantaneous profiles of interfacial mass transfer rate (the left part) and volume fraction (the right part) of the gas phase during of the simulation with the Lakehal 2008b model. Relatively similar trends of both fields have been observed also in the Hughes-Duffey model. The steam-water interface is sharp due to the dense grid at the beginning of simulation. After some seconds it spreads due to the courser grid in the pipe. However, these simulations were quite unstable. Still more work is needed to be done regarding the stability of calculations.

Summary and conclusions

OpenFOAM based solvers have been tested in different nuclear safety related single- and two-phase flows. In single-phase flows the solvers have been demon-strated to be relatively mature, with results mostly comparable with other CFD codes. There is still work to be done for ex. in investigation of turbulent near wall treatment in complex geometries, efficient mesh generation and general usability, but the solvers could be applied to practical problems. In the OECD/NEA MATIS-H blind benchmark the OpenFOAM results submitted by Fortum were selected as the "best estimations case of k-ε turbulence model".

Simulations of two-phase flows with boiling and condensation require much more development. Existing OpenFOAM two-phase solver has required significant development effort to allow simulation of such cases. The capability has been tested in several different experimental cases. In most of them, the results of the newly developed solver have been comparable to those published in literature or obtained with other CFD codes. However, there is still a lot work to be done to improve usability, stability and efficiency of the solver as well as to improve model-ling of material properties and bubble size distributions. Not to mention the need for better multiphase closure models, that is common to all CFD codes.

References

Davidson, L. Using Isotropic Synthetic Fluctuations as Inlet Boundary Conditions for Unsteady Simulations. Advances and Applications in Fluid Mechanics 1(1), 1–35, (2007).

Frank, Th., Reiterer, F., Lifante, C. Investigation of the PWR subchannel void distribution benchmark (OECD/NES PSBT benchmark) using ANSYS CFX. NURETH-14, Canada, (2011).

Grossetete, C. EDF, ISSN 1161-0611, (1996). 289 p.

Hughes, E.D., Duffey, R.B. Direct Contact Condensation and Momentum Transfer in Turbulent Separated Flows. International Journal of Multiphase Flow, 17(5), 599–619.(1991).

Lakehal, D., Fulgosi, M., Yadigaroglu, G. DNS of Condensing Stratified Steam Water Flow. ASME J. Heat Transfer, 130, 021501–10.(2008).

Laine, J., Puustinen, M. Condensation Pool Experiments with Steam using Insulated DN200 Blowdown Pipe. Research Report POOLEX 3/2005, Lappeenranta University of Technology.(2006).

Manon, E. Ph.D. Thesis, Ecole Centrale Paris, (2000).

Menter, F.R., Egorov, Y. DESider: Notes on Numerical Fluid Mechanics and Multidisciplinary Design). (2009).

Peltola, J., Pättikangas, T. Development and validation of a boiling model for OpenFOAM multiphase solver. CFD4NRS, Daejeon, South Korea, (2012).

Piomelli, U., Liu, J. Large-eddy Simulation of Rotating Channel Flows Using a Localized Dynamic Model. Phys. Fluids 7(4), April (1995).

5.4 Numerical modelling of condensation pool (NUMPOOL)

Timo Pättikangas, Jarto Niemi, Antti Timperi, Michael Chauhan

VTT Technical Research Centre of Finland
P.O. Box 1000, FI-02044 Espoo

Introduction

In boiling water reactors (BWR), the major function of the containment is to protect the environment if a loss-of-coolant accident (LOCA) should occur. The containment is designed to accommodate the loads generated in hypothetical accidents, such as sudden rupture of a main steam line. In such an accident, a large amount of steam is suddenly released in the containment. An essential part of the pressure suppression containment is a water pool, where condensation of released steam occurs.

In a BWR, the pressure suppression containment typically consists of a drywell and a wetwell with a water pool. In a hypothetical LOCA, steam and air flow from

the drywell through vent pipes to the wetwell, where the outlets of the vent pipes are submerged in the water pool. When steam flows into the water pool, so-called chugging effect may occur, which means periodic formation and rapid condensation of large vapour bubbles at the vent outlets. The rapid condensation of the vapour bubbles may induce significant pressure loads on the structures in the pressure suppression pool and on the containment.

In the NUMPOOL project, computational fluid dynamics (CFD) simulations of chugging are performed by using the Euler-Euler two-phase model of the commercial ANSYS Fluent code. Experiments performed with the PPOOLEX facility [1] at the Lappeenranta University of Technology are modelled. The direct-contact condensation in the water pool is modelled with user-defined functions implemented in the ANSYS Fluent code.

During the discharge of steam into the condensation pool, the rapid condensation of large vapour bubbles may induce significant pressure loads on the pool structures. The collapse of a vapour bubble and the loads are modelled with the ABAQUS Finite Element Method (FEM) code. The Eulerian method is used for taking into account the toroidal shape of the bubble, the vent pipe and the finite pool geometry. For scaling analysis, the effect of system size on the loads is first studied. Calculations are then performed for the PPOOLEX experiment COL-01, where fairly large pressure loads were measured.

The pressure suppression pools of boiling water reactors (BWRs) typically have a large number of vent pipes. Experiments have shown that the pressure loads originating from different vent pipes are slightly desynchronized [1, 2]. The desynchronization reduces the overall pressure load compared to the case in which the chugging occurs simultaneously in all vent pipes. The experimental results for desynchronization are studied and applied to a model of a BWR containment.

CFD modelling of experiments with parallel vent pipes

The PPOOLEX facility is a pressurized cylindrical vessel with a height of 7.45 meters and a diameter of 2.4 meters [1]. The volume of the drywell compartment is 13.3 m^3 and the volume of the wetwell compartment is 17.8 m^3. Steam is blown into the drywell compartment via a horizontal DN200 inlet plenum. In the PAR-10 experiment, the interaction of two parallel vent pipes was studied. In the following, chugging is discussed, which occurred in a late stage of the experiment.

In the beginning of the CFD simulation, the temperature of the gas in the drywell was 140°C and the pressure was 2.89 bars. The temperature of the water pool in the wetwell was 43°C. The mass flow rate of vapour into the drywell was 0.523 kg/s and the temperature of the vapour was 155°C.

In Figure 1, condensation of a vapour bubble in the CFD simulation is illustrated at one instant of time. Formation of bubbles at the outlets of two vent pipes is seen in Figure 1(a). The interphasial area concentration between liquid-water and vapour is shown in Figure 1(b). The interphasial area and the volumetric heat transfer coefficient determine the condensation rate that is shown in Figure 1(d).
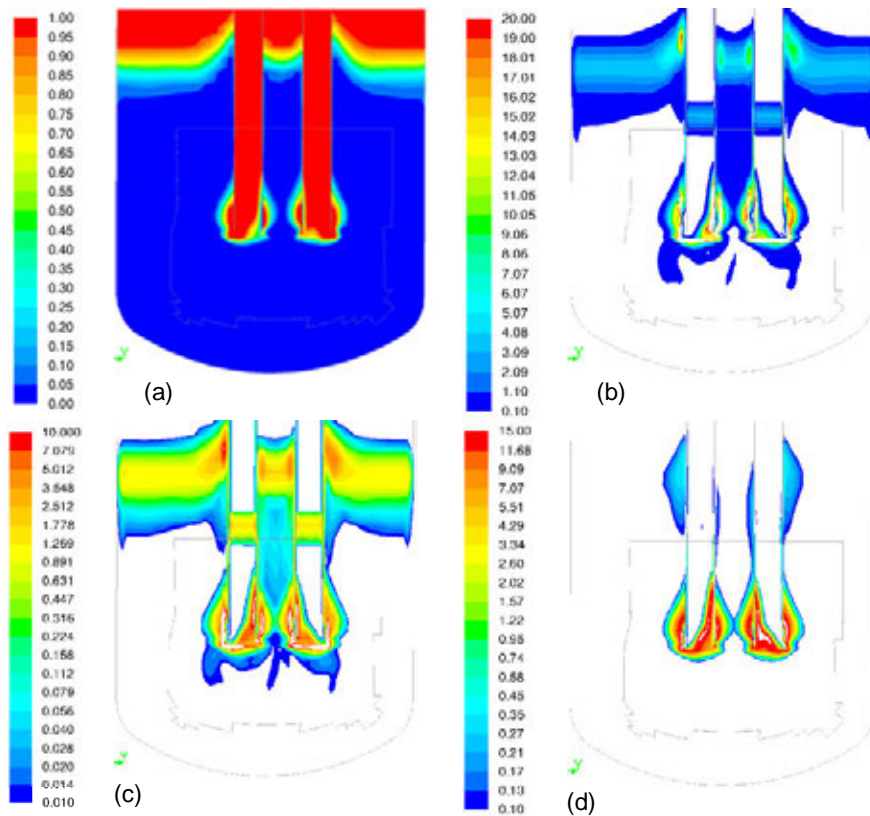
Figure 1. Direct-contact condensation of a vapour bubble in the water pool: (a) Volume fraction of vapour. (b) Interphasial area concentration (m^{-1}). (c) Volumetric heat transfer coefficient (MW/m^3K). (d) Condensation rate (kg/m^3s).

Pressure loads due to collapsing vapour bubble

The Eulerian method of ABAQUS was used for analysing the bubble collapses in simplified cases. In this method, the numerical mesh is fixed and the material flows through the mesh which is in contrast to the Lagrangian description used commonly for structural calculations.

A toroidal bubble at the vent pipe outlet is shown for the experiment in Figure 2. Collapses of spherical bubbles were analysed analytically and numerically in 1D in earlier work, and hence main characteristics of the spherical and toroidal cases were first compared. For the spherical cases, effective bubble radii were used which results in same bubble volumes as for the toroidal cases.

Effect of system size on the bubble collapse time and on the amplitude and width of the pressure pulse is shown in Figure 3. The water initial pressure was set

to 1 bar. For determining the pressure pulse properties, a small amount of air was assumed in the bubble by setting the initial pressure of air to 2000 Pa. Firstly, the collapse times are approximately equal for both bubbles in spite of their differing shapes. The collapse time depends linearly on the bubble size also for the toroidal bubble. Secondly, the pressure amplitude measured at corresponding locations is constant, which is consistent with the earlier 1D calculations. Thirdly, as for the collapse time, the pulse width also depends linearly on the system scale. Dimensional analyses were also performed for the collapse time and for the pressure pulse, confirming the scaling properties obtained numerically.
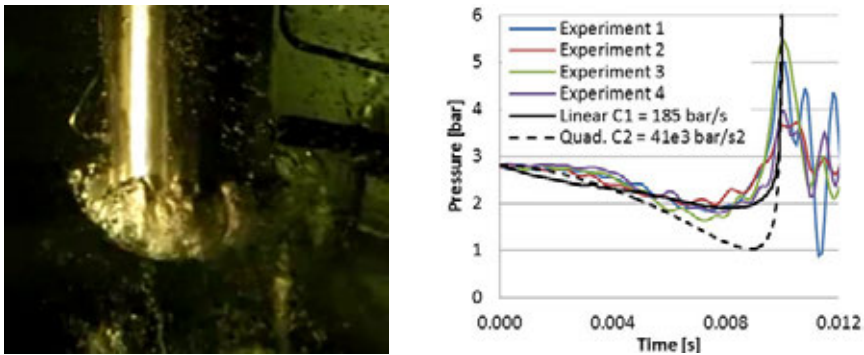

Figure 2. Steam bubble just before the collapse in PPOOLEX experiment COL-01 and the pressure signals near the vent pipe outlet.
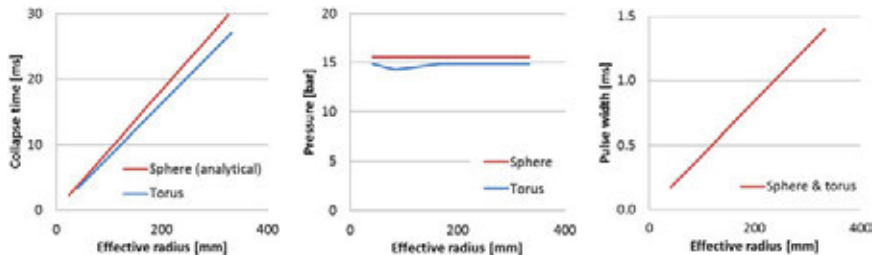

Figure 3. Bubble collapse time and pressure amplitude and pulse width as functions of effective radius. An effective radius of 83 mm corresponds to the experiment.

Comparison with the experiment showed that while the collapse time is reproduced quite well, the calculated pressure peak is about an order of magnitude too high and too sharp. One possible reason for this is that there may be a significant amount of steam left in the bubble in the important final phase, which could soften the water-hammer considerably. The possible rise of steam pressure in the final phase could not be taken into account in the present calculations.

For studying the effect of finite condensation rate on the low-pressure phase of the collapse, we used linear and quadratic pressure differences [3]: $\Delta p = C_1 t$ and

$\Delta p = C_2 t^2$. The pressure difference is $\Delta p = p_0 - p_B$, where p_0 is pressure in the wetwell gas space and p_B is pressure in the bubble. Calculated pressures near the pipe outlet are compared against the experiment in Figure 2 for cases where the constants C_1 and C_2 have been set to give the correct collapse time. Overall, the linear case is closer to the experimental data. For the quadratic case, the pressure difference becomes too high in the late phase, although the early phase is better represented than in the linear case.

FEM analysis of a BWR containment

The behaviour of a pressure suppression containment of a BWR is studied with the help of experiments performed with the PPOOLEX facility. The focus was on the experiment PAR-10, in which steam is discharged through two parallel blow-down pipes into the condensation pool filled with sub-cooled water. The aim was to study, how the desynchronization of the chugging events between different vent pipes affects the loading.

The desynchronization of chugging between two pipes was studied by examining the measured pressures in pipe 1 and pipe 2. Times of underpressure peaks were carefully determined from both pipes. Chugging phase is distinguishable in most pressure peaks. It is characterized by pressure decrease, meaning that the bubble is collapsing. This phase is followed by sudden increase in pressure, resulting from the rapid deceleration of the water volumetric flow.

From the measured data, 58 pairs of events were selected for the statistical determination of the desynchronization time. An example of desynchronized chugging events is presented in Figure 4(a), where the desynchronization time is determined as the time difference between peak underpressures. The standard deviation of desynchronization time for PAR-10 experiment was determined to be 13,6 ms. Kukita and Namatame [2] have studied desynchronization in a full-sized seven-vent-system of JAERI test facility [4]. In their study, the standard deviation of desynchronization time was found to be 42 ms for chugs that caused pool boundary load amplitudes greater than 10 kPA. The average time between chugging events in experiment PAR-10 was determined to be 1.75 s and 2 s in JAERI, whereas the duration of the pressure pulses were determined to be less than 0.01 s in experiment PAR-10 and 0.15 s in the JAERI experiment. The number of vent pipes in JAERI test facility is seven and pipe outer diameter is 0.6 m, whereas in PPOOLEX test facility, the corresponding values during experiment PAR-10 are 2 and 0.2 m. Distance between the two pipes in PPOOLEX facility is 0.5 m. In JAERI test facility, the distance between the vent pipes varies, the minimum distance being 1.2 m and maximum 4.7 m.

During 2011, a FEM model of the containment was utilized in the attempt to model the effect of desynchronization. The computations were carried out using implicit dynamics and modal dynamic analyses in ABAQUS [5]. As mentioned by Björndahl and Andersson [6], the speed of sound in the water may vary from 450 m/s to 1280 m/s. This affects the acoustic pressure loading caused by chug-

ging. Hence three different cases were considered were the speed of sound in the water in cases 1, 2 and 3 are 500 m/s, 1000 m/s and 1491 m/s, respectively. The standard deviation determined by Kukita and Namatame [2] was assumed to be more representative for BWR containment with 16 blowdown pipes, than the standard deviation determined in the two-vent pipe test PAR-10. Thus a normal distribution with standard deviation of 0.042 s was created, and out of this distribution, sixteen initiation times were determined using Matlab's random-function. Loads were determined using volume acceleration in ABAQUS. The shape of the volume acceleration was determined from a representative chugging event in experiment COL-01, but the length was scaled up to match the length of a representative chugging event in the seven-vent test reported by Kukita and Namatame [2] and amplitude was set to equal one.
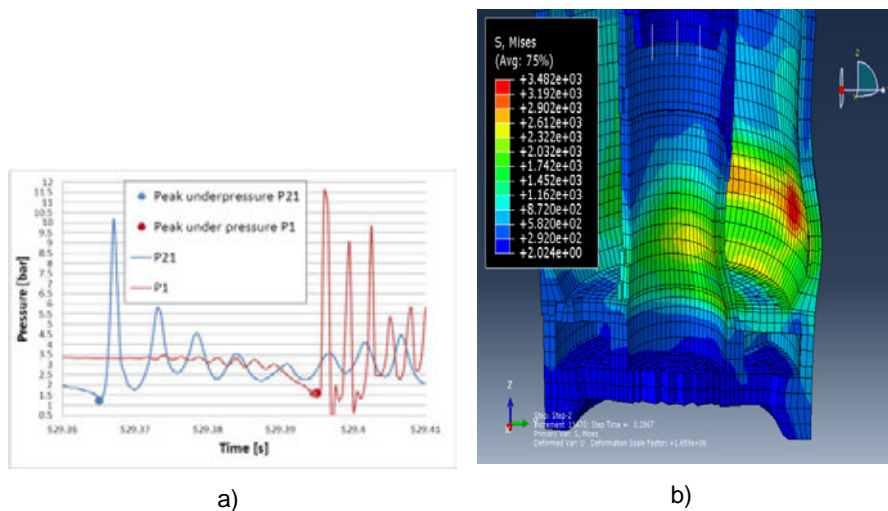

a)   b)

Figure 4. (a) Example of a case where desynchronization time between chugging events could be determined. The blue and red dot indicate the time of peak under pressure. (b) Vertical cross-section of the containment at the time of occurrence of maximum von Mises stresses at the pool boundary in case 1.

The results showed that highest von Mises stresses occurred with the highest speed of sound in the water. The second highest stresses were obtained when the speed of sound in the water had the lowest value (500 m/s). However, in this case there is a delay between the load event and structural response, thus the other chugs also affect the load, and the location experiencing the maximum stresses and the time of occurrence become more difficult to predict. A vertical cross-section of the whole containment model is presented in Figure 4(b).

As the desynchronization time varies between events, multiple chugging events with varying desynchronization time should be considered in order to get more realistic picture of the loads. Therefore, simplified model geometry was created

and analyses were performed using explicit dynamics. This enabled the computation of structural response during multiple (100) chugging events experienced by a single pipe (altogether $16 \times 100 = 1600$ events) within a reasonable time. The same standard deviation of 0.042 s was assumed for the desynchronization time and 1600 initiation times were determined from normal distribution using a random-function. Time period between chugging events experienced by a single vent pipe was assumed to be approximately 2 s. A case with chugging occurring simultaneously at every 16 vent pipes was considered for comparison. In both considered cases, the speed of sound in the water was 1491 m/s. The maximum von Mises stress was found to be 49% higher in the case, where chugging occurred simultaneously in every vent pipe, compared to the case, where the desynchronization was taken into account. The maximum stress occurred at the outer wall of the containment, approximately at the same height in both cases.

Summary and discussion

The CFD simulation performed for the PPOOLEX experiment PAR-10 show some differences compared to the experiment. In the simulation, the period of chugging is shorter than in the experiment and the condensation in the simulation is weaker than in the experiment. The differences between the simulation and the experiment are probably caused by three main reasons. First, the heat transfer coefficient between liquid water and vapour may be too small. Second, the calculated interfacial area between the phases may be too small. Third, in the experiment one can see that mixing is rapidly increased on the interface of the vapour bubble when it starts collapsing at the vent outlet. This is not yet modelled properly.

The rapid collapse of a vapour bubble was analysed with the Eulerian model of ABAQUS. Collapses giving the largest loads in the experiment COL-01 were analysed. The calculated pressure peaks were clearly too high and sharp, even though the collapse time was correct. Although the calculations could not predict the peaks correctly, they were suitable for fitting the pressure variation inside the bubble to the measured low-pressure signal near the bubble. Constant, linear and quadratic pressure variations were applied. The linear and quadratic variations produced fairly realistic results; the linear case was overall in better agreement with the experiment. Effect of the system size on the bubble collapse time and on the pressure peak was examined numerically and by dimensional analysis, both showing same scaling properties. These results are used for further studies of the scaling of the experiments to full-scale in future.

The desynchronization of chugging events in the two vent experiment PAR-10 was studied. Statistical distribution of desynchronization was determined from the measured pressure data and compared to results obtained in a seven vent pipe experiment found in literature. The standard deviation of the desynchronization times was found to be 13.6 ms in this experiment.

The response of BWR containment during desynchronized chugging events and with varying speeds of sound was numerically computed using direct time

integration and modal dynamics procedure. Desynchronization between chugging events was taken into account by determining individual times of initiation of chugging for each pipe. Normal distribution with zero mean value and standard deviation of 42 ms was created and out of this distribution sixteen initiation times were determined using a random-function. In addition to time and magnitude, the location of maximum stresses also changed with speed of sound. In order to get more realistic picture of the loads caused by the chugging events, a simplified model geometry was created and computation for 1600 chugging events, 100 per vent pipe, was carried out using explicit dynamic analysis. A case, where chugging occurred simultaneously, was computed for comparison. The results showed that the maximum von Mises stress was 49% higher, when chugging occurred simultaneously in every vent pipe, compared to the case, where the desynchronization was taken into account.

Acknowledgement

References

1. Puustinen, M., Laine, J., Räsänen, A. 2011. Multiple blowdown pipe experiments with the PPOOLEX facility. Lappeenranta University of Technology, Nuclear Safety Research Report CONDEX 2/2010. 28 p. + app. 8 p.

2. Kukita, Y., Namatame, K. 1985. The vent-to-vent desynchronization effects on LOCA steam condensation loads in BWR pressure suppression pool. Nuclear Engineering and Design 85, 141–150.

3. Giencke, E. 1981. Pressure distribution due to a steam bubble collapse in a BWR pressure suppression pool. Nuclear Engineering and Design 65, 175–196.

4. Namatame, K. et al. 1980. Full-Scale Mark II CRT Program: facility description. Japan Atomic Energy Research Institute, JAERI-M 8780.

5. ABAQUS, Analysis User's Manual, Dassault Systèmes. Providence, RI, Version 6.10–2. 2010.

6. Björndahl, O., Andersson, M. 1998. Globala vibrationer vid kondensationsförlopp i wetwell orsakade av LOCA i BWR-anläggningar. Swedish Nuclear Power Inspectorate, SKI Report 99:3, Stockholm. 81 p.

5.5 Improvement of PACTEL facility simulation environment (PACSIM)

Juhani Vihavainen

Lappeenranta University of Technology
Skinnarilankatu 34, 53850 Lappeenranta

Introduction

The main objective of the PACSIM project has been to improve the simulation environment of the PACTEL facility with the TRACE thermal hydraulic code. The Finnish Radiation and Nuclear Safety Authority, STUK, has required an independent tool to support safety and licensing analysis and decided to use the TRACE code. The use of the TRACE code enhances the preparedness to give analysis support and improves education in computational thermal hydraulics. This project aimed to develop a complete PACTEL model and use the model for validation calculations at Lappeenranta University of Technology (LUT). PACSIM project started at 2008 and was completed at 2012 and hence has been operating during SAFIR2010 and SAFIR 2014 research programmes. The TRACE code has been used for preparation of PACTEL facility model with horizontal steam generator and also for preparation of PWR PACTEL model with vertical steam generator. Various validation cases have been modeled and calculated. The validation cases in the frame of SAFIR2014 programme consisted of two Primary-to-secondary side leakage experiments (PSL) and one Anticipated transient without scram (ATWS) experiment. The results of these validation cases are summarizes here. The validation knowledge covering the whole PACSIM project has been also summarized in separate report. The results of PACSIM project has been and will be also utilized in PAX SAFIR2014 project, where PWR PACTEL model has been used and developed further.

Trace model of the PACTEL facility

According to the Code Applications and Maintenance", CAMP-program agreement USNRC has provided the TRACE thermal hydraulic code and Symbolic Nuclear Analysis Package (SNAP) graphical user interface to the use of the partners. Hence, TRACE code (currently version 5.0 Patch 3) has been implemented at LUT as well as the newest version of the SNAP package (version 2.2.1).

The TRACE model of the PACTEL facility has been prepared at LUT (Figure 1) The model was constructed from scratch and aiming to cover finally all main parts of the primary and secondary sides of the facility. The modeling of PACTEL facility with TRACE code resembles the guidelines adopted in RELAP5 modeling for PACTEL.
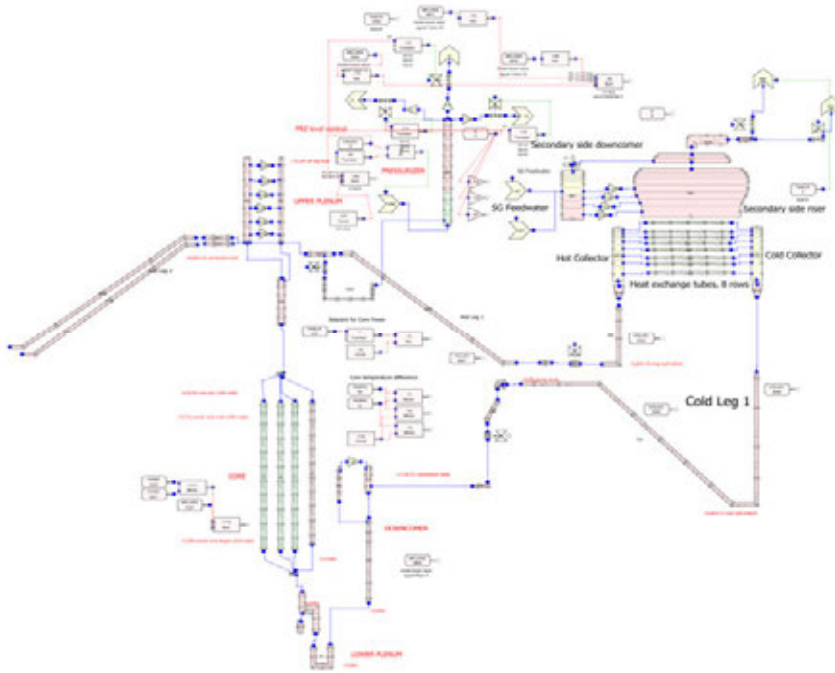
Figure 1. TRACE/SNAP modeling of PACTEL facility for calculations of ATWS-32 experiment. Loop one fully visible.

During the model construction and validation processes 15 PACTEL experiments were calculated in the PACSIM project. The recent experiments chosen for the validation calculation were PSL-10, PSL11 and ATWS-32 experiments in the PACSIM project during the SAFIR2014 programme. The objectives of the experiments are presented in the Table 1. The main focus in selection of these experiments was to enlighten the VVER-specific features like loop seal effect.

Table 1. PACTEL experiments calculated with the TRACE code.

EXPERIMENT	BREAK SIZE/TYPE	OBJECTIVES AND CONDITIONS FOR THE EXPERIMENT
PSL-10	Ø 5.5 mm	Steam generator collector rupture, original construction, flow area not reduced
PSL-11	Ø 2.5 mm	Steam generator collector rupture, new construction, reduced flow area
ATWS-32	No Break, inventory reduction through pressurizer relief valves	Simulation of control rod withdrawal from the core, power feedback

PSL-10 and PSL-11 experiments

Two experiments were carried out. In the first experiment (PSL-10) the original construction was used as a reference for the second experiment. The second experiment (PSL-11) focused on effect of the new construction. The experiment procedures were based on the current regulations for operator actions during a state of emergency in the Loviisa nuclear power plant. The experiments focused on reducing the primary pressure and temperature with fast cooling according the regulations for operator actions so low that the primary pressure stays below the opening pressure of the steam generator safety valve and the boiling margin in the core is more than 20°C.

In each experiment all three steam generators were used, two intact and one broken steam generator. The intact steam generator steam lines were coupled. The main isolation valves in the primary circuits were presumed to be stuck open, which prevented the broken loop isolation. The pressurizer spray and the accumulators were used in all the experiments. Due to different collector construction in PACTEL, the uppermost heat exchanging tube row was chosen as a break location.

The experiments began with a 1000 s steady-state period. The transients were started by opening a break valve in a heat exchanging tube of the broken loop steam generator. Using volumetric scaling to the full-scale break sizes, break size Ø 5.5 mm in PSL-10 and Ø 2.5 mm in PSL-11 was chosen. Simulating scram the core power was decreased from 1 MW to 344 kW when the collapsed level in the pressurizer reached 2.8 m. After that the core power followed the decay heat power. When the pressurizer collapsed level reached 2.3 m the pressurizer heaters were switched off, the main circulation pumps started to coast down and the high pressure injection was initiated.

In PSL-11 the process was slower and the actions did not begin until after 40 s from the core power reduction. The temperatures on the primary side decreased because of the core power reduction and the HPI. The decreased loop flow reduced the heat transfer between the primary and the secondary side of the facility. Then, the steam generation rate on the secondary side decreased. The secondary side pressure dropped until the pressure control system totally closed the control valve of the secondary side.

In PSL-10, the safety valve of the broken steam generator cycled few times and released secondary side inventory to the atmosphere. In the experiment the safety valve of the broken steam generator was simulated by using the control valve. The planned setpoint values were 30% open at 48 bars and at 47 bars closed. Unfortunately exact recordings of the timing and opening of the valve were not available from the experiment. In PSL-11 the safety valve openings did not occur. The spikes in primary side pressure in PSL-10 were results of the pressurizer spray system operation.

The accumulator injection was turned off in PSL-10 at 2030 s. In PSL-11 they did not inject at all because the boiling margin in the core was more than 10°C when the injection was supposed to begin. The high pressure injection was

stopped at 2670 s in PSL-10 and in PSL-11 170 s earlier to prevent losing steam volume in the pressurizer. When pressure in the intact steam generators was below 30 bar, the flow area of the relief valve was reduced.

ATWS-32 Experiment

The PACTEL experiment chosen as validation case was ATWS-32, transient without scram experiment. The intention was to challenge the code and increase the degree of difficulty in every new calculation case. The experiment simulated the control rod withdrawal from the core when the core was initially operating with low, almost zero power. The core power was then promptly increased to the maximum value. Special core power feedback control system was developed, which could respond to the changes in core void fraction. Only limited emergency systems were available. The aim of the experiment was to study slow steam compression and overall behavior of the facility. The experiment was performed with all three loops running.

The experiment began with a 1000 s steady state period. The facility was operating with 1% core power (about 50 kW). After 1000 s, the core power was raised quickly to maximum available power (about 1000 kW) and the steam generator feedwater injection rate was set to 1.25 l/min in each steam generator. The feedwater injection rate corresponded to the capacity of one emergency feedwater pump in Loviisa NPP. Automation controlled the pressurizer heaters. When the water level in any steam generator was reaching 54 cm, the main circulation pumps began to coast down. The operation of the pressurizer safety valves was simulated at first with two on/off valves (Ø3 mm). Soon it was found that the capacity of the valves was not enough to keep the primary pressure below maximum primary pressure of the PACTEL facility. In ATWS-32 experiment three valves were used; two Ø3 mm valves and one Ø17 mm valve. The small diameter valves simulated the pressurizer safety valves while the large capacity valve operated as a pressure cut-off valve. It did not counterpart in the power plant.

After 1000 s, the core power feedback was modeled also. When the main circulation pumps coasted down and the heat exchanging tube layers in the steam generators uncovered steadily, energy transport from the core to the steam generator decreased. This caused the primary pressure increases and the pressurizer safety valves to open. When voiding in the core increased enough, the core power control value decreased below the maximum available core power. Then the primary system began to oscillate. One cycle took 10–15 s. Because of the time constants of the core power control system, there was 5–8 s delay between the set point and the measured core power. This is about half of the whole cycle. So, the core power was all the time in the phase where it amplified the primary system oscillation process. Oscillations continued to the end of the experiment.

Calculation of PSL-experiments

The PACTEL experiments PSL-10 and PSL-11 simulating the primary to secondary leakage (Figure 2) were calculated using the TRACE code model. The break diameters were 5.5 and 2.5 mm. The emergency core cooling systems were in use. Some model changes and improvements were introduced concerning steam generator behavior. For example, it was necessary to restrict the inner circulation of the horizontal steam generator to model the pressure behavior more precisely. The overall behavior could be modeled satisfactorily, even though some discrepancies appeared. Especially, in experiment PSL-10 the valve operations concerning the broken steam generator had significant effect on the overall behavior of the calculations. After several test calculations appropriate valve operation settings were achieved.
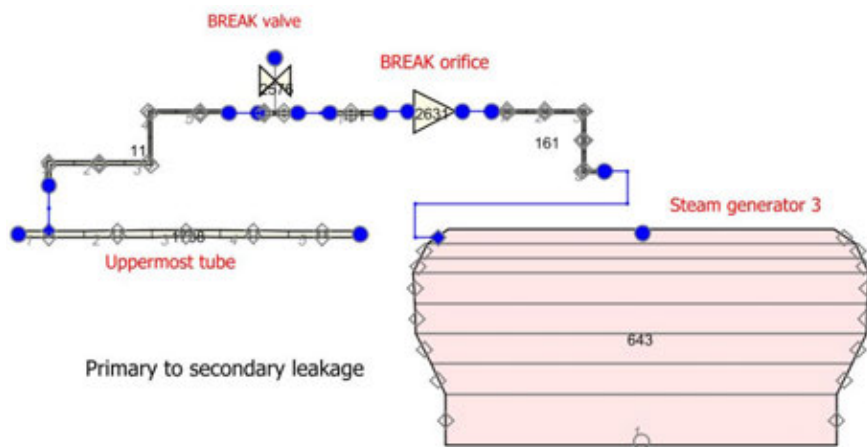

Figure 2. TRACE/SNAP primary to secondary side leakage model used for calculations of PSL-10 and PSL-11 experiments.

In calculation of PSL-11 the primary side pressure was not decreased as expected. Some improvement could be implied by modifying the break loss coefficient. However, this modification could not make the calculated results good enough. Then the HPI flow was decreased to achieve better results for primary side pressure and pressurizer collapsed level. The changes that had to be made for the HPI mass flow fell even beyond the error margins and thus mass flow rates were unrealistic.

The calculation results indicated that inventories were not in balance between primary and secondary sides. Precise analysis of propagation of primary and secondary side inventories in experiment would have been necessary. Another reason for this odd behavior is probably the heat loss relations between upper

plenum and pressurizer. More thorough sensitivity analysis would have been necessary also for assessing the effect of break setup.

Calculation of ATWS-32 experiment

The PACTEL experiment ATWS-32 was modeled and calculated using the TRACE code. The experiment was simulating the control rod withdrawal from the core, when the core was operating with almost zero power. A prompt power excursion to the maximum value was introduced, which caused pressure increase and intensified heat transfer to the secondary side and thus decreasing collapsed level in the steam generators. According to the procedure no emergency core cooling systems were in use. Only fixed rate feedwater in every steam generator was set in operation.

Some model changes and improvements were introduced to the TRACE calculation model. The additional pressure relief valves were modeled with similar setup to the experiment. The core power in the calculation was set as boundary condition according to the averaged measurement data values. The power feedback according to the core voiding was not coded to the calculation model.

The overall behavior could be modeled satisfactorily until the moment, when flow stagnation took place in the experiment. This event was not found in the TRACE calculation. This discrepancy caused that the rest of the calculation results were not fully comparable with the experiment. The pressurizer relief valve operations were significantly driving the events during the experiment. Despite of the anomalies the calculated overall natural circulation flow rate appeared to agree rather well with the experiment value.

The PACTEL experiment ATWS-32 was modeled and calculated using TRACE code. The experiment was simulating the control rod withdrawal from the core, when the core was operating with almost zero power. A prompt power excursion to the maximum value was introduced, which caused pressure increase and intensified heat transfer to the secondary side and thus decreasing collapsed level in the steam generators. According to the procedure no emergency core cooling systems were in use. Only fixed rate feedwater in every steam generator was set in operation.

Some model changes and improvements were introduced to the TRACE calculation model. The additional pressure relief valves were modeled with similar setup to the experiment. The core power in the calculation was set as boundary condition according to the averaged measurement data values. The power feedback according to the core voiding was not coded to the calculation model.

A reason for odd behavior is probably the heat loss relations between upper plenum and pressurizer. More thorough sensitivity analysis would have been necessary to study the effect of heat losses.

Related publications

1. Tuunanen, J., Kouhia, J., Purhonen, H., Riikonen, V., Puustinen, M., Semken, S., Partanen, H., Saure, I., Pylkkö, H. General description of the PACTEL test facility, 1998. VTT, Espoo. VTT Tiedotteita – Research Notes 1929. 35 p. + app. 74 p. ISBN 951-38-5338-1; 951-38-5339-X.

2. TRACE V5.435 User's Manual. Volume 1: Input Specification. Pdf documentation published by NRC.

3. TRACE V5.0 USER'S MANUAL, Volume 2: Modeling Guidelines, pdf documentation published by NRC.

4. Vihavainen, J., Riikonen, V., Kyrki-Rajamäki, R. TRACE code modeling of the horizontal steam generator of the PACTEL facility and calculation of a loss-of-feedwater experiment. Annals of Nuclear Energy 37(2010)11, 1494–1501.

5. Vihavainen, J. Validation report 1.2a: Calculation of PACTEL pressure loss experiments with the TRACE code. 2009, Lappeenranta University of Technology, LUT Energy, Laboratory of Nuclear Engineering, PACSIM 2008. P. 24.

6. Vihavainen, J. Validation report 1.2b: Calculation of PACTEL heat losses with TRACE code. 2009. Lappeenranta University of Technology, LUT Energy, Laboratory of Nuclear Engineering, Research Report, PACSIM 2008. P. 13.

7. Vihavainen, J., Riikonen, V., Puustinen, M., Kyrki-Rajamäki, R. Modeling of the PACTEL Facility and Simulation of a Small Break LOCA Experiment With the TRACE V5.0 Code. The 14th International Topical Meeting on Nuclear Reactor Thermalhydraulics, NURETH-14, Toronto, Ontario, Canada, September 25–30, 2011. CD publication, art nro. 463.

8. Vihavainen, J. Validation report: Calculation of PACTEL experiments SBL-31, SBL-33 and IMPAM VVER T2.3 (IMP06) with the TRACE code. 2011. Lappeenranta University of Technology, Lappeenranta, SAFIR2010, The Finnish Research Programme. P. 31.

9. Riikonen, V., Kouhia, V., Vihavainen, J. Study of flow reversing in vertical heat exchange tubes. PAX 4/2011. 2011. Lappeenranta, Research Report, Lappeenranta University of Technology, Nuclear Safety Research Unit. 14 p. + app. 8 p.

10. Vihavainen, J. Validation report: Calculation of PACTEL experiments PSL-10 and PSL-11 with the TRACE code. 2012. Lappeenranta University of Technology, Lappeenranta, SAFIR2014 research report. P. 25.

11. Vihavainen, J. Validation report: Calculation of PACTEL experiment ATWS-32 with the TRACE code. 2012. Lappeenranta University of Technology, Lappeenranta, SAFIR2014 research report. P. 10.

5.6 PWR PACTEL experiments (PAX)

Vesa Riikonen, Virpi Kouhia

Lappeenranta University of Technology
Skinnarilankatu 34, P.O. Box 20, FI-53851 Lappeenranta

Introduction

Traditionally the experimental work in Finland has focused on the horizontal steam generators. The new EPR type nuclear power plant under construction in Olkiluoto, Finland, contains vertical steam generators. Hence, the PWR PACTEL facility with vertical steam generators was constructed and taken into operation in the PAOLA project in 2009 to fulfil the new research needs.

The objective of the SAFIR2014 PAX project is to utilize the PWR PACTEL test facility in an effective way in nuclear safety research in Finland and internationally. The first step was the PWR PACTEL international benchmark calculation exercise in the SAFIR2014 PAX project [1] in 2011. Seven organizations from five countries participated in the benchmark. The exercise offered a unique opportunity to test the best practices and solutions in modelling and analysing tasks as well as a possibility to increase knowledge about the interpretation of test results.

The PWR PACTEL facility was accepted to the OECD/NEA PKL Phase 3 project [2] in 2011. The first PWR PACTEL experiment in the project was planned in 2012 and it will be carried out in the beginning of 2013. It is a supplement experiment for the PKL 'Cooldown under Natural Circulation Conditions in Presence of Secondary side Isolated Steam Generators' experiment. The second PWR PACTEL experiment in the project will be a station blackout related experiment and planned for year 2014. The last experiment is still undefined.

In the PAX project several other experiments have been carried out also. These tests focused on supporting the earlier characterizing experiments, on experimentally verifying the flow reversal in the steam generator tubes, and on studying the U-leg draining.

One of the main goals of the PAX project is also to validate the PWR PACTEL model for APROS and TRACE codes. Analyses with thermal hydraulic computer codes are also an essential part of the experiment preparation.

The knowledge on two-phase flow behaviour would increase if measured data of the void fraction in the secondary side of steam generators was available. This kind of data would be useful in the computer code validation and analysis. Anyhow, such experimental data is not currently available. Furthermore, especially in vertical steam generators the measuring of the void fraction is extremely challenging e.g. due to the triangle array of the tubes. Possibilities of measuring the void fraction in the secondary side of vertical steam generators were studied in the PAX project also. Possibilities of using different measuring and instrumentation systems as well as using separate effects test facilities was studied to find a solution for this problem [3].

PWR PACTEL facility

The PWR PACTEL [4, 5] test facility is designed and constructed to be utilized in the safety studies, especially related to the thermal-hydraulics of PWRs with EPR type vertical steam generators. PWR PACTEL consists of a reactor pressure vessel model, two loops with vertical steam generators, a pressurizer and emergency core cooling systems (ECCS), see Figure 1. A significant design and construction basis of the facility is the utilization of some parts of the original PACTEL facility [6, 7], i.e. the pressure vessel model, pressurizer and ECCS. Hence, the facility core parts are not direct models of the reference EPR core. The new loops and steam generators of EPR style construction enable the PWR and EPR related experimental research.
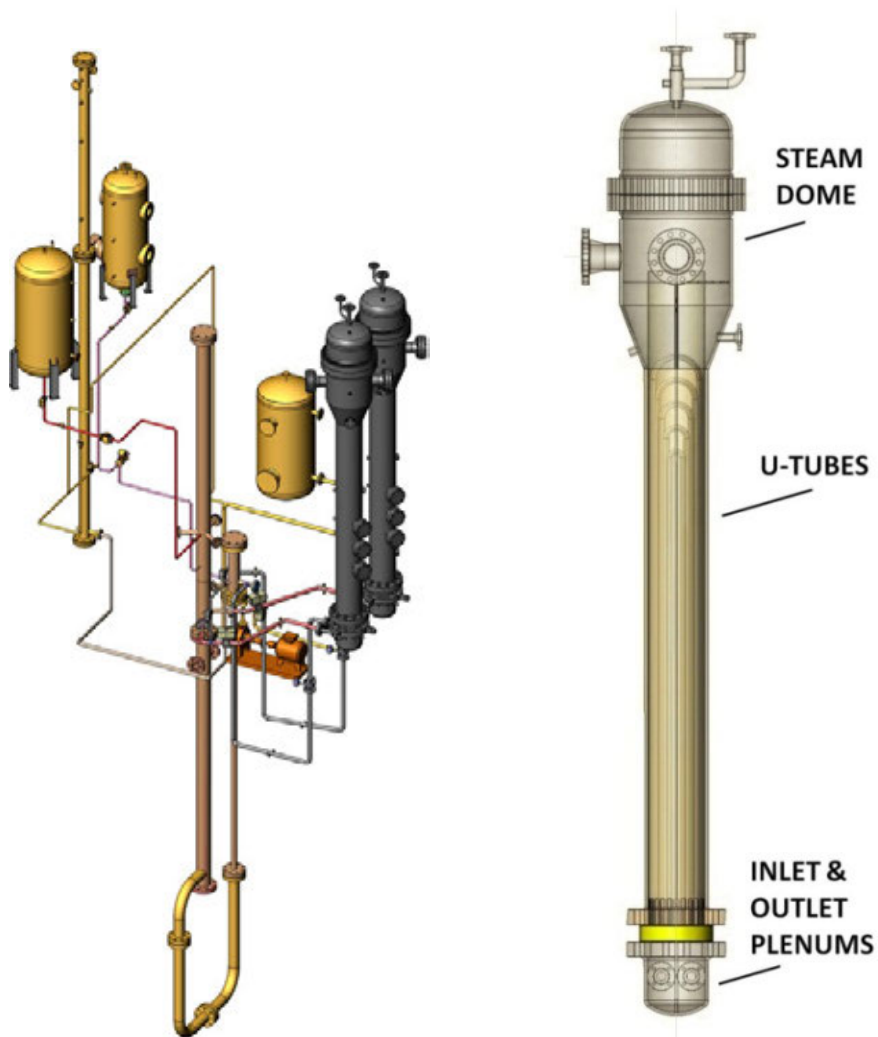
Figure 1. PWR PACTEL facility and general view of the steam generators.

The pressure vessel model in PWR PACTEL comprises a U-tube construction modelling the downcomer, lower plenum, core and upper plenum. The core rod bundle consists of 144 electrically heated fuel rod simulators arranged in three parallel channels. The core can be powered by a maximum of 1 MW electric power supply. The ECCS of PWR PACTEL includes high and low pressure pumps and two separate accumulators for the injection of water to the system.

The main focus with the PWR PACTEL design is set on the new construction of the primary loops and steam generators. The set-up is designed to allow the simulation of the main PWR and EPR features and the studying of loop and steam

generator behaviour in particular. Both primary loops simulate one reference EPR loop. The heat transfer area of the steam generator U-tube bundles and the primary side volume of each steam generator are scaled down with a ratio of 1/400 compared to the reference steam generator. The inner diameter of the steam generator U-tubes in PWR PACTEL is the same as in the EPR steam generator. The secondary sides of the steam generators include a downcomer, a riser and steam dome volumes as well as feed water injection systems. The riser and downcomer parts are also divided into hot and cold sides. There are altogether about 250 temperature, pressure and differential pressure measurement transducers especially attached to allow deeper analysis of the steam generators.

Benchmark

The PWR PACTEL benchmark exercise was organized in Lappeenranta by Lappeenranta University of Technology. The benchmark consisted of a blind and an open calculation phase. Seven organizations from the Czech Republic, Germany, Italy, Sweden and Finland participated in the benchmark exercise, and four system codes were utilized in the benchmark simulation tasks. Two workshops were organized for launching and concluding the benchmark, the latter of which involved presentations of the calculation results as well as discussions on the related modelling issues.

The chosen experiment for the benchmark was a small break loss of coolant accident experiment which was performed to study the natural circulation behaviour over a continuous range of primary side coolant inventories. For the blind calculation task, the detailed facility descriptions, the measured pressure and heat losses as well as the results of a short characterizing transient were provided. For the open calculation task part, the experiment results were released.

Experiment

The SBLOCA experiment SBL-50 was chosen to be the PWR PACTEL benchmark experiment. This experiment was performed earlier to study the natural circulation behaviour over a continuous range of primary side coolant inventories [8]. Both primary loops were utilized during the experiment. The core power was set to 155 kW, and the primary and secondary side pressures were initially set to 75 bar and 42 bar, respectively. The SBL-50 experiment was started by maintaining a steady state operation at full inventory for 1000 seconds to establish initial condition settings.

The actual transient started when the pressurizer heaters were switched off and the pressurizer was isolated. These actions were followed by the opening of the break in the cold leg 2 between the loop seal and the downcomer to produce a slow inventory loss. An orifice plate (Ø1 mm with sharp edge, about 0.04% of the PWR PACTEL cold leg cross sectional area) was used to simulate the break size and to control the loss rate. The experiment was concluded when the top of the

core dried out and some of the measured core cladding temperatures exceeded the value of 350ºC. No other pre-planned actions were taken during the experiment than maintaining the secondary side water level through an addition of feed water. The benchmark experiment involved also an unintentional quasi steady state period that was actually thought to bring more challenge to the benchmark calculations. The break valve closed because of a failure in the valve control mechanism at the time when the primary system had about 53% of its inventory left. The incident was discovered and fixed about 20 minutes later.

The loop flow was a single phase liquid flow and nearly constant in the inventory range of 75–100%, see Figure 2. For inventories below 75%, the collapsed water level in the upper plenum was below the hot leg elevation and at the same time the mass flow rate increased. Therefore, two phase flow prevailed. The loop flow rate experienced its maximum value when the mass inventory was about 70%. As the inventory was reduced further, the flow rate declined. Heat transfer from the primary side to the secondary side at inventories below about 50% was mainly controlled by the boiler condenser or reflux condensation mode. The loop flow rate was quite low because of the high energy transfer efficiency of this mode.
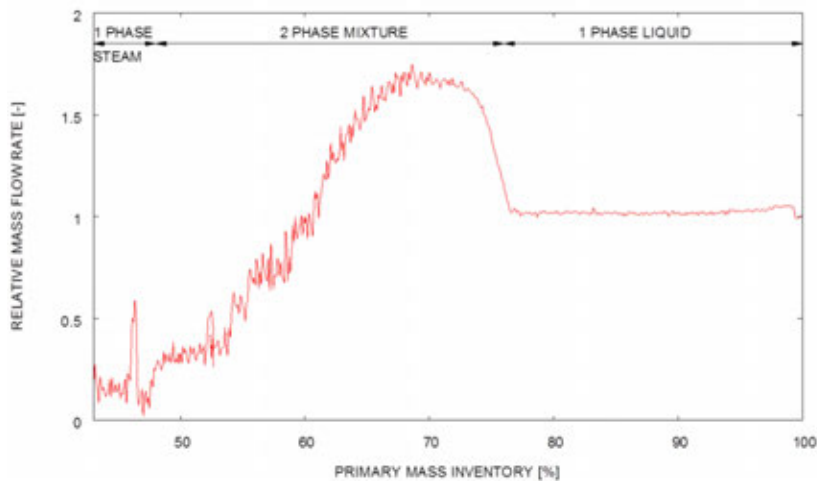

Figure 2. Measured loop flow rate as a function of the primary mass inventory in the PWR PACTEL benchmark experiment.

Benchmark calculations

The benchmark exercise began with the blind calculation phase which included the facility modelling task and the blind simulation of the benchmark experiment. The earlier measured pressure and heat losses of the facility were provided for the participants. In addition, the results of a short characterizing transient were made available to be utilized already within this first phase of the exercise. Also a written

short description report on the initial general conditions of the experiment and operational actions during the experiment was provided for the blind calculation case. Still, no experiment result data on the benchmark experiment itself were made available at this first stage.

After the blind simulation results and short notes from the participants were delivered to the organizers, the actual experiment result data was released for the participants. This launched the second calculation phase of the benchmark, i.e. the open calculation task. The results of the blind calculations and the analysis of the experiment data, after receiving it for the open calculation case, inspired the participants into several actions to improve the simulation models and calculation of the transients. The blind and open calculation results are presented in the benchmark summary reports [9, 10].

Found issues

The general system behaviour of the facility and different phases of the particular transient were relatively successfully simulated whether the core channels or the steam generator U-tubes were lumped together or modelled more separately in smaller groups. The general trends of the overall system behaviour of the simulations were not strongly dependent on the level of the model details in that perspective. Of course, when the reversed or stagnant flow inside the steam generator heat exchange tubes was to be studied in particular, these issues could not be predicted with an averaged lumped U-tube bundle model.

On the basis of the second workshop presentations, the delivered results, and the descriptions of the participants, it can be concluded that the accuracy of the simulation models improves remarkably when the pressure and heat loss information is provided and carefully taken into account in the models. The heat losses in the upper plenum were revealed to have a strong effect on the primary side behaviour in this kind of long transient. A more detailed adjustment of the pressure losses along the facility resulted in a better simulation of the flow distribution.

Sometimes it is impossible to present the real temperature behaviour with only one calculated temperature, e.g. in case when there is a change from sub-cooled via saturated to superheated conditions. Certainly the temperature sensors give no direct information on the phase of the measured flow. One has to be careful when interpreting both experimental data and simulation results individually as well as when comparing them with each other. Conclusions of the real physical conditions in the facility made on the basis of temperature measurements must be treated with extra caution.

The amount of non-condensable gases in the primary side caused discussion and seems to be an issue that needs further studies. The correct use of the models for critical flow, condensation and CCFL and the appropriate user chosen values of the parameters connected to the use of those models were also widely discussed. It was seen, that the values recommended in the code manuals did not suit well in this test in some parts of the facility models and some parameters had

to be tuned by hand. Sensitivity studies were performed to gain information on parameters affecting the transient simulation progression. There is also a need for user guidelines or for a collection of best practices in modelling for system codes that could be utilized when different types of transients and situations are to be analysed.

Other experiments

Experiments at low pressures

Various SBLOCA experiments have revealed a strong dependence of natural circulation behaviour on the primary coolant inventory. Natural circulation in test facilities is characterized by three distinct modes: single phase flow for a near maximum primary inventory, two phase circulation for intermediate inventories, and reflux condensation or a boiler condenser mode for low inventories. Transitions between these flow types are usually relatively smooth. Very low mass flow rates are observed for the reflux condensation and boiler condenser modes, but the energy transport is still sufficient to provide core cooling. To observe the natural circulation flow behaviour under quasi steady state conditions over a range of primary side inventory levels at a low pressure two stepwise inventory reduction experiments (SIR-32 and SIR-33) [11] were performed with the PWR PACTEL facility.

The ROSA/LSTF experiments have revealed the system wide oscillation with the mass inventories between 40% and 50%, a characteristic C-shape vertical temperature distribution in the steam generator secondary side, and a "stagnant two-phase stratification" at low pressures [12]. These phenomena were not observed in the PWR PACTEL SIR experiments. In the PWR PACTEL SIR experiments only one steam generator was used. That might have had an effect on the system behaviour. The power level in the SIR experiments was lower than in the ROSA/LSTF experiments and the internal circulation in the steam generator secondary side was therefore also smaller. The EPR features and others differences in the construction of the PWR PACTEL compared to the ROSA/LSTF facility might also have had effect on the results.

Flow reversing in vertical heat exchange tubes

Four steady state experiments (RF-01, RF-02, RF-03, and RF-04) [13] were carried out to experimentally verify the flow reversal in the steam generator tubes for single phase liquid flow. In the first experiment air was discovered in the heat exchange tubes of one steam generator. It showed that it is impossible to distinguish the flow stagnation caused by air in the tube from the possible reversed flow from a uniform temperature distribution. With the new differential pressure measurements between the inlet and outlet plenum and with the new temperature measurements in the steam generator plenums the non-uniform flow character-

ized by the coexistence of the normal and reversed flow was observed directly in the experiments for single phase liquid flow (Figure 3).

From the measured data was estimated that the flow reversed in about 30% of the heat exchange tubes. According to these experiments the amount of tubes where flow was reversed is independent of the secondary side conditions. The location of the hot leg connection has an effect on the flow reversing in the heat exchange tubes.

Two secondary side pressure transients were conducted after the RF experiments for the SAFIR2014 SGEN project to be used in CFD modelling.
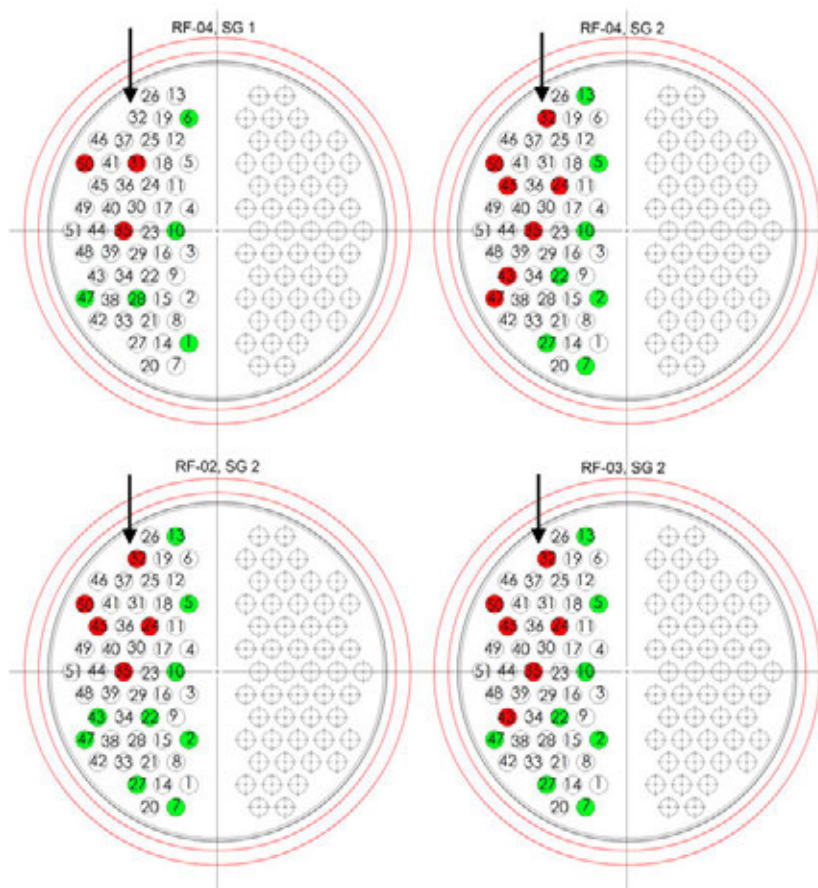
Figure 3. Flow direction in the instrumented heat exchange tubes of the steam generators in the RF-02, RF-03, and RF-04 experiments. Tubes having normal flow (from hot plenum to cold plenum) are marked with green colour and tubes where the reversed flow is possible according to the measurements with red colour. The flow direction from the hot leg is indicated with an arrow.

Loop seal experiments

The U-leg draining phenomenon is well known and it has been observed on different test facilities. EPR type nuclear power plant analyses have shown that the peak cladding temperature depends not only on the core uncover depth and duration but also on the number of U-legs drained. The U-leg draining phenomenon is mainly driven by the size and location of the break.

A series of experiments (LSC-01, LSC-02, and LSC-03) [14] were proposed by TVO to validate the EPR FSAR analyses, to determine the effect of break size on U-leg draining during intermediate break loss-of-coolant-accident conditions and to test the suitability of the PWR PACTEL facility for the U-leg draining studies. Both loops and the pressurizer were used in the experiments. Two emergency core cooling systems were also used. An orifice plate was used to simulate the break size and to control the loss rate. Parameter values, boundary conditions as well as initial break sizes for the experiments were chosen based on the results of the pre-test calculations with TRACE.

In the experiments both U-legs opened but as soon as one U-leg was opened, the pressure difference across the U-leg that was the main driving force leading to clearing was strongly reduced, and the second U-leg did not remain open (Figure 4 and Figure 5). The U-leg that remained open was not always the same in the experiments. In these experiments the effect of break size on U-leg draining could not be verified as the safety limit for heater rod temperature was exceeded in one experiment and it had to be terminated too early. Despite of this these experiments showed that the PWR PACTEL facility is suitable for U-leg draining studies with some limitations characteristic to the facility. The experiments also showed that small breaks can be more serious for the core than bigger ones and confirmed the results of EPR analyses.

The simulations of the LSC-03 experiment were performed with the APROS and TRACE codes. The U-leg draining was visible in both simulations.
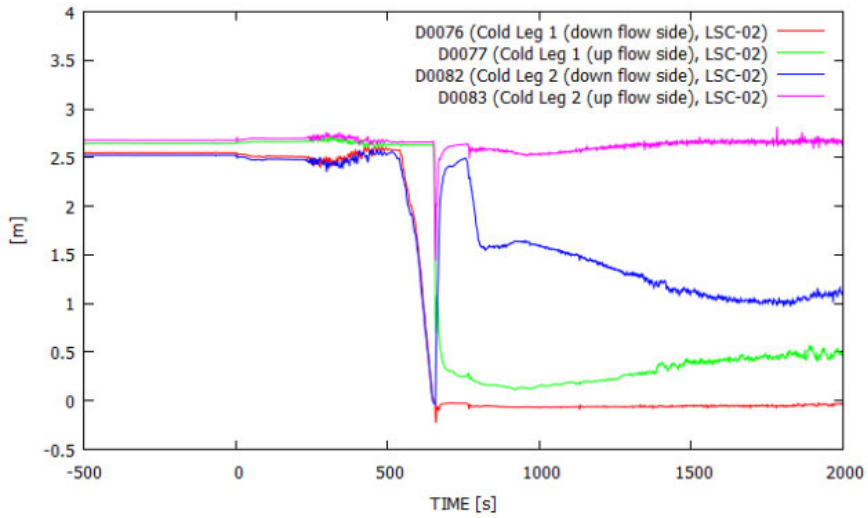
Figure 4. Collapsed water levels in cold U-legs in the LSC-02 experiment.
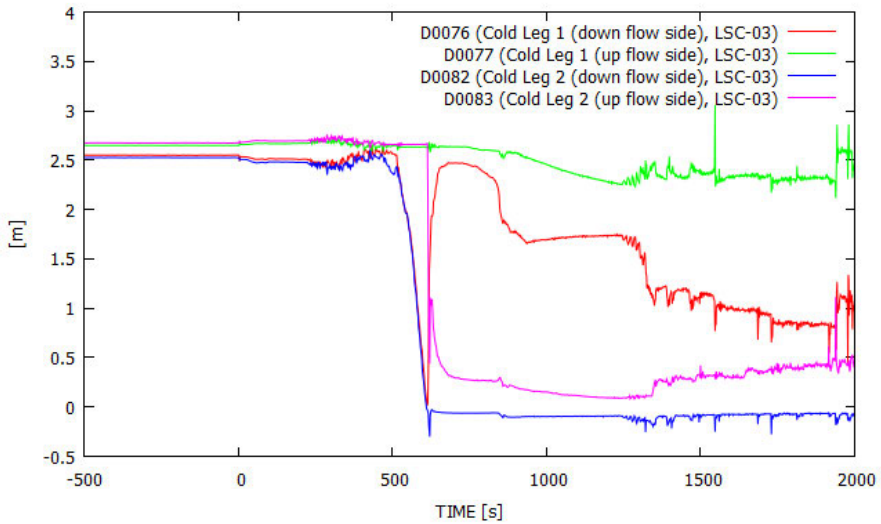

Figure 5. Collapsed water levels in cold U-legs in the LSC-03 experiment.

References

1. Kouhia, V., Riikonen, V., Kauppinen, O.-P., Purhonen, H., Austregesilo, H., Bánáti, J., Cherubini, M., D'Auria, F., Inkinen, P., Karppinen, I., Kral, P., Peltokorpi, L., Peltonen, J., Weber, S. Benchmark Exercise on SBLOCA

Experiment of the PWR PACTEL Facility. Article offered in January 2013 to be published in journal Annals of Nuclear Energy.

2. OECD/NEA PKL-Phase 3 Project. http://www.oecd-nea.org/jointproj/pkl-3.html. (Accessed 3.1.2013).

3. Telkkä, J. Aukko-osuuden mittausmenetelmien kartoitus PWR PACTEL -koelaitteiston pystyhöyrystimen sekundääripuolella, Diplomityö, Lappeenrannan teknillinen yliopisto, LUT Energia, Lappeenranta, 2012.

4. Riikonen, V. et al. General description of the PWR PACTEL test facility. Research Report, Lappeenranta University of Technology, Nuclear Safety Research Unit, YTY 1/2009. Lappeenranta, 2009.

5. Kouhia, V. et al. PACTEL and PWR PACTEL Test Facilities for Versatile LWR Applications. Integral Test Facilities and Thermal-Hydraulic System Codes in Nuclear Safety Analysis, Science and Technology of Nuclear Installations, vol. 2012, Article ID 548513, 2012. Doi:10.1155/2012/548513.

6. Tuunanen, J. et al. General description of the PACTEL test facility. VTT Research Notes 1929. VTT Technical Research centre of Finland, Espoo, 1998. ISBN 951-38-5338-1.

7. Purhonen, H. et al. PACTEL integral test facility – Description of versatile applications. Annals of Nuclear Energy 33, Issues 11—12, August 2006, Elsevier 2006. ISSN 0306-4549, Doi: 10.1016/j.anucene.2006.05.011. Pp. 994–1009.

8. Riikonen, V. Natural Circulation Experiments with PWR PACTEL Facility. Technical Report, Lappeenranta University of Technology, Nuclear Safety Research Unit, YTY 3/2010. Lappeenranta, 2010.

9. Riikonen, V., Kouhia, V. Summary Report of PWR PACTEL Benchmark Experiment Blind Calculations. Research Report, Lappeenranta University of Technology, LUT Energy, Nuclear Safety Research Unit, PAX 1/2011. Lappeenranta, 2011.

10. Riikonen, V. and Kouhia, V., Summary Report of PWR PACTEL Benchmark Experiment Open Calculations. Research Report, Lappeenranta University of Technology, LUT Energy, Nuclear Safety Research Unit, PAX 2/2011. Lappeenranta, 2011.

11. Riikonen, V., Kouhia, V. PWR PACTEL experiments at low pressures. Research Report, Lappeenranta University of Technology, LUT Energy, Nuclear Safety Research Unit, PAX 3/2011. Lappeenranta, 2011.

12. Yonomoto, T. ROSA/LSTF Experiments on PWR Natural Circulation and Validation of RELAP5/MOD3.3, Japan Atomic Energy Research Institute, IAEA's Second Research Coordination Meeting on the CRP on Natural Circulation Phenomena, Modelling, and Reliability of Passive Safety Systems that Utilize Natural Circulation, Oregon State University, Corvallis, Oregon, USA, 2005.

13. Riikonen, V. et al. Study of flow reversing in vertical heat exchange tubes. Research Report, Lappeenranta University of Technology, LUT Energy, Nuclear Safety Research Unit, PAX 4/2011. Lappeenranta, 2011.

14. Riikonen, V., Kouhia, V., Kauppinen, O.-P. Loop seal experiments with PWR PACTEL. Research Report, PAX 1/2012, Lappeenranta University of Technology / Nuclear Safety Research Unit, Lappeenranta, 2012.

5.7 Modelling of pressure transients in steam generators (SGEN)

Timo Pättikangas[1], Ville Hovi[1], Jarto Niemi[1], Timo Toppila[2]; Tommi Rämä[2]

[1]VTT Technical Research Centre of Finland
P.O. Box 1000, FI-02044 Espoo

[2]Fortum Power and Heat Oy
P.O. Box 100, FI-00048 FORTUM

Introduction

Steam generators are used in pressurized water reactors to convert water of the secondary circuit into steam. Most western reactors employ vertical steam generators, where the heat transfer tubes are arranged vertically, parallel to the flow of the mixture of water and steam rising between the tubes on the secondary side. Examples of such an arrangement are the steam generators of the European Pressurized Reactor (EPR) and the steam generators of the PWR PACTEL experimental facility [1]. In the eastern VVER-440 reactor, the heat transfer tubes are arranged horizontally. Therefore, the rising steam flows perpendicular to the primary tubes.

In the SGEN project, three-dimensional computational fluid dynamics (CFD) models are developed for simulations of secondary sides of steam generators. The models are applied to experimental devices and to steam generators of nuclear power plants (NPPs). The steam generators of NPPs have thousands of primary tubes. Therefore, it is not possible to model them in detail in three-dimensional calculations, but some approximative approach has to be used. In the following, the geometry of the secondary side is described by using the so-called porous media model, where the flow resistance caused by the primary tubes on the secondary side is described with experimental correlations. The heat transfer from the primary tubes is modelled with source terms of enthalpy. A similar approach has previously been applied to VVER-1000 steam generators by Stosic and Stevanovic [2].

The flow in the primary circuit is solved with the Apros system code [3] and the outer wall temperatures of the primary tubes are interpolated into the CFD mesh. The heat transfer from the primary to the secondary side is included in the boiling model implemented in the ANSYS Fluent CFD code. In addition, the drag forces and the heat and mass transfer between vapour and liquid-water are implemented in Fluent by using User Defined Functions (UDFs). In order to model transient situations, wall condensation model and proper steam tables were also implemented in Fluent by using UDFs.

In the following, the porous media model is briefly described. Then, simulations performed for the PWR PACTEL test facility located at the Lappeenranta University of Technology are discussed. Results on the modelling of a natural circulation stationary state experiment are presented. Application of the model to the steam generator of the VVER-440 nuclear power plant is then presented. Finally, the results are briefly discussed.

Steam generator model

The CFD model is based on the basic conservation laws of mass, momentum and energy for the vapour and the liquid-water phases. The model equations are written in the form used in the Euler-Euler two-phase model of the commercial CFD code ANSYS Fluent version 14.0 [4]. An earlier version of the model is presented in ref. [5].

Conservation of mass of phase q can be written as

$$\frac{\partial}{\partial t}\left(\gamma \alpha_q \rho_q\right) + \nabla \cdot \left(\gamma \alpha_q \rho_q \mathbf{v}_q\right) = S_{\mathrm{mass},q} \tag{1}$$

where γ is porosity, α_q is the volume fraction, ρ_q is the density and $\mathbf{v}_q$ is the velocity of phase q. Porosity, γ, is defined as the fluid fraction of total volume, i.e., the fraction available for liquid flow on the secondary side. Therefore, $1 - \gamma$ is the volume fraction of the primary tubes. Indices $q = 1$ and $q = 2$ stand for the liquid and vapour phases, respectively. The sum of volume fractions is $\alpha_1 + \alpha_2 = 1$. Evaporation and condensation are described with the source term $S_{\mathrm{mass},q}$.

Conservation of momentum of phase q is

$$\frac{\partial}{\partial t}\left(\gamma\alpha_q\rho_q\mathbf{v}_q\right) + \nabla\cdot\left(\gamma\alpha_q\rho_q\mathbf{v}_q\mathbf{v}_q\right) = \mathbf{S}_{M,q} \tag{2}$$

The source term $\mathbf{S}_{M,q}$ on the right-hand side contains interphase momentum transfer, lift force and virtual mass force. In addition, it includes the gravitation and the flow friction caused by the primary tubes, which is modelled by using the experimental correlations of Simovic et al. [6].

Conservation of energy is

$$\frac{\partial}{\partial t}\left(\gamma\alpha_q\rho_q h_q\right) + \nabla\cdot\left(\gamma\alpha_q\rho_q\mathbf{v}_q h_q\right) = S_{E,q} \tag{3}$$

where h_q is the specific enthalpy of phase q. The source term $S_{E,q}$ on the right-hand side includes the interphasial heat exchange and the heat source from the primary tubes. The surface heat transfer is modelled by using the Thom pool boiling correlation. The mass transfer between the phases is included in equation (1) as source and sink terms. The drag and the heat and mass transfer terms have been implemented by using User Defined Functions in the Fluent code.

ANSYS Fluent version 14.0 does not have proper steam tables which are essential when pressure transients in steam generators are modelled. Therefore, steam tables of the Apros code were implemented in Fluent by using the user-defined real gas model of Fluent. In pressure transients, the heat capacity of the solid structures is important. Therefore, the wall condensation model developed earlier for containment analysis [7] has been adapted in the steam generator model.

Modelling of a PWR PACTEL steam generator

A CAD model of a steam generator of the PWR PACTEL facility is shown in Figure 1(a). The steam generator consists of a riser tube in the middle, a downcomer surrounding the riser tube and a steam dome on the top. The lower part of the riser has been divided into hot and cold sides by a divider plate. The downcomer is also divided into hot and cold sides, which are connected to the hot and cold sides of the riser at the bottom. The primary side of the steam generator consists of 51 U-tubes, which are connected to the hot and cold collectors at the bottom of the steam generator.

The main features of the circulation in the secondary side are as follows: the mixture of water and vapour rises upwards through the riser tube into the steam dome, where the vapour is separated. The liquid flows downwards from the steam dome to the hot side of the downcomer and finally to the hot side of the riser tube at the bottom. Feed water is injected into the top part of the cold side of the downcomer, where it flows downwards to the cold side of the riser tube.

The surface mesh of the CFD model is illustrated in Figure 1. The outer surface of the steam generator is shown in Figure 1(b) and the riser tube separating the downcomer and the riser is shown in Figure 1(c). The feed water manifold near the top part of the riser tube is also visible. The horizontal plate between the downcomer and the steam dome has holes, which allow circulation from the steam

dome to the hot side of the downcomer. Some water also leaks from the steam dome to the cold side of the downcomer.
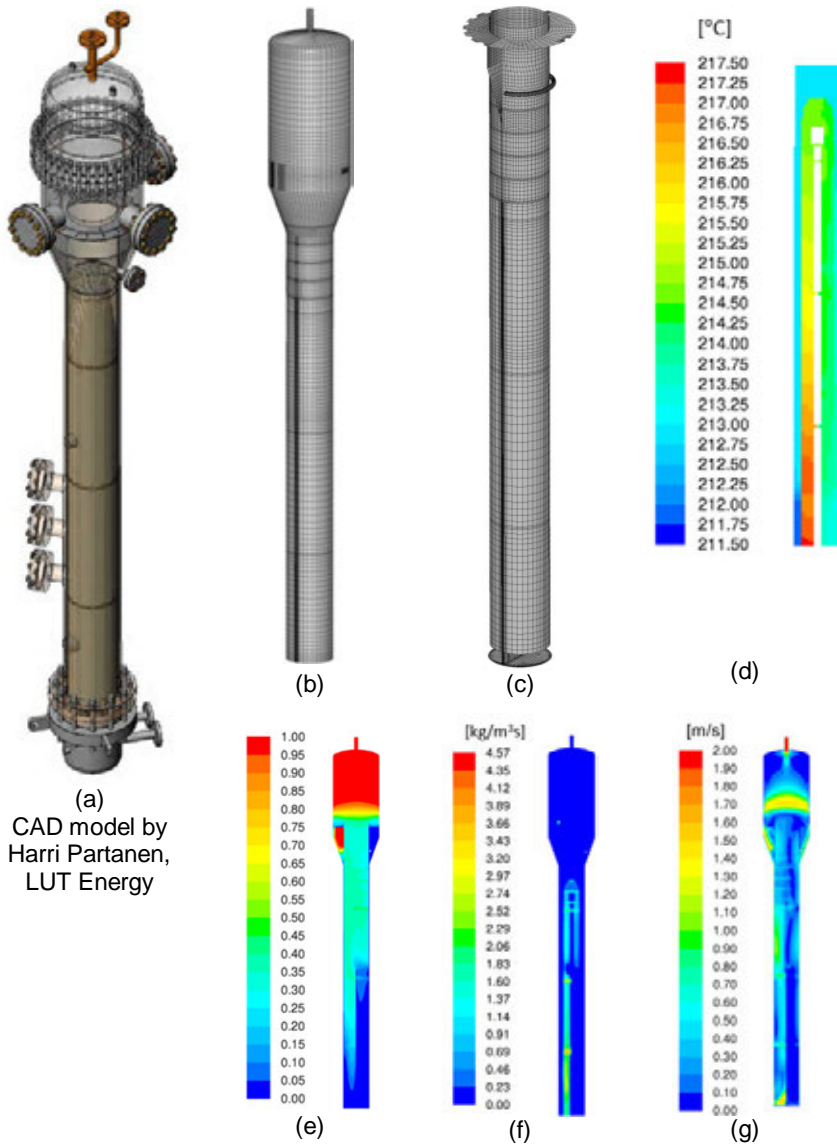

Figure 1. CFD modelling of the PWR PACTEL steam generator: (a) CAD model of the steam generator, (b) surface mesh of the outer wall in CFD model, (c) surface mesh of the riser tube, (d) outer wall temperature of the primary tubes, (e) void fraction on the secondary side, (f) steam generation rate and (g) magnitude of the velocity of liquid water.

The natural circulation stationary state experiment NC-10 performed with the PWR PACTEL steam generator has been simulated. In the experiment, the primary side coolant entered the steam generator at the temperature of 279°C and left at 216°C. The mass flow rate in the primary circuit was 1.1 kg/s and the pressure was 75 bars. About 335 kW of power was transferred to the steam generator. On the secondary side, the collapsed level was kept constant at 3.7 m. The mass flow rate of the feed water injection was 125 g/s at a temperature of 20°C. The secondary side pressure was 20 bars.

The outer wall temperatures of the primary tubes were first resolved with a detailed Apros model of the primary circuit. The temperatures were interpolated to the porous media region of the CFD mesh, which describes the primary tubes. The resulting temperature distribution is shown in Figure 1(d), where the hot collector is on the left-hand side. Note that the flow in the longest tubes is reversed, i.e., in the natural circulation conditions the flow direction is from the cold to the hot collector.

The void fraction is shown in Figure 1(e). The void fraction is much larger in the hot riser than in the cold riser, where almost no vapour exists. Some water rises into the steam dome, where it returns mainly to the hot side of the downcomer. Strong condensation of vapour occurs in the cold side of the downcomer because the cold feed water is injected there. Therefore, the water level rises to the level of the horizontal plate separating the cold downcomer from the steam dome. The strong boiling on the hot side of the riser is also evident in Figure 1(f), where the vapour generation rate is shown

The magnitude of the liquid velocity is shown in Figure 1(g). Large flow velocities can be seen above the plate separating the steam dome from the downcomer. In addition, large velocities are found in the region, where flow enters from the hot side of the downcomer to the hot riser.

In Figure 2(a), the calculated liquid temperatures are compared to the measurements in the experiment NC-10. The calculated values are very close to the measurements except in the measurement point 5, where the calculated temperature is somewhat higher than the measurement. This measurement point is located in the region of a steep temperature gradient, which is caused by cold feed water flowing from the cold side of the downcomer into the riser.

In Figure 2(b), the calculated internal circulation on the secondary side is illustrated. The main circulation is from the hot riser to the steam dome, where the liquid returns to the hot downcomer and flows back into the hot riser. Some flow also occurs between the hot and cold downcomer through narrow gaps, which are connecting them.
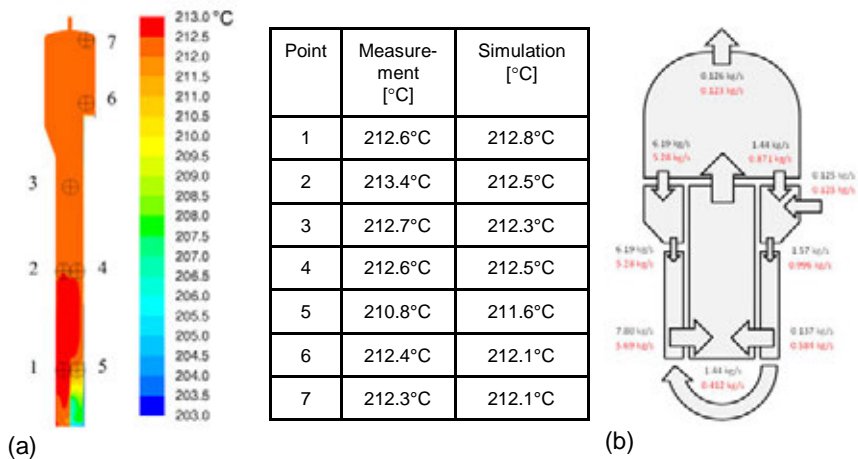
Figure 2. (a) Calculated liquid temperature in the NC-10 experiment compared to the measurement (table). (b) Internal mass flow rates obtained from the CFD calculation (black numbers) and Apros calculation (red numbers).

Modelling of a VVER-440 steam generator

The horizontal steam generator consists of hot and cold collectors, tube bundles supported by thin support plates and steam drier above the bundles. The primary circuit consists of more than 5 000 tubes that are connected to the hot and cold collectors. The geometric model of the Loviisa VVER-440 steam generator with computational mesh is presented in Figure 3(a). The computational mesh containing 140 000 cells consists mostly of hexahedral cells.

The feed water injection is the flow inlet boundary of the model and it is located above the tube bundles. The flow outlet boundary is set by the secondary side pressure at the top of the model. The primary tube temperatures were simulated with detailed steam generator model of the Apros system code [3], where both primary and secondary sides of the steam generator were modelled, and then interpolated to the Fluent mesh where the tube bundles were modelled as porous media, Figure 3(b).
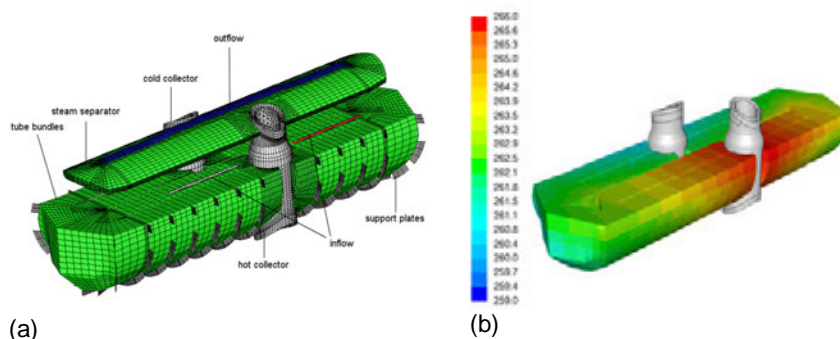
(a) (b)

Figure 3. (a) Geometric model of the inside parts of the VVER-440 steam generator and computational mesh. (b) Temperatures [°C] on the outer walls of the primary pipes interpolated to the Fluent mesh.

In the operational state, the primary side water is at the pressure of 124 bars. Approximately 1400 kg/s water flow enters the primary tubes of the steam generator at the temperature of 300°C and leaves at the temperature of 266°C. Secondary side of the steam generator is at the pressure of 45.3 bars. Feed water injection is 140 kg/s at the temperature of 257°C. Thermal power produced is approximately 250 MW. In Figure 4, is presented the operational state of the steam generator. Void fraction and the location of the water level are in the operational state are presented in Figure 4.

(a) (b)
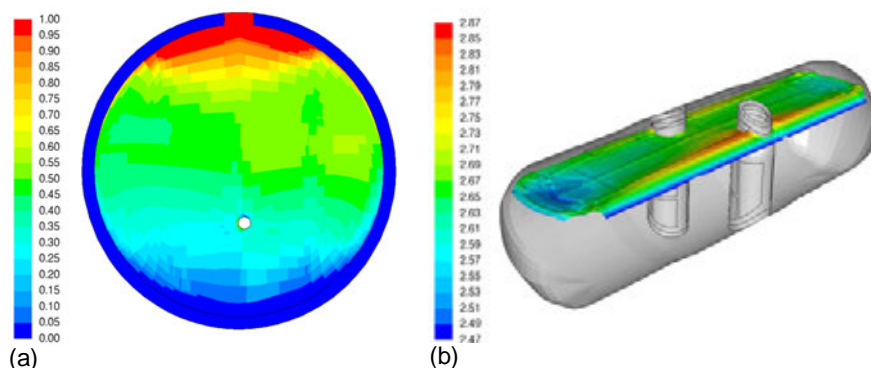
Figure 4. (a) Void fraction on the secondary side of the steam generator. (b) 70% vapour level in the secondary side of the steam generator.

According to the void fraction, Figure 4(a), water rises almost to the outflow level in the middle of the steam generator. Feed water is injected to the hot collector side of the steam generator, where the tube temperatures are higher. Hence the water level is higher on that side, Figure 4(b).

The transient caused by the loss of feed water pumps was first modelled with the Apros system code model of the Loviisa nuclear power plant in order to get the boundary conditions for the more detailed Apros model of the steam generator. The time-dependent inflow and outflow boundary conditions for the Fluent model were achieved from the Apros plant model and the time-dependent temperature boundary conditions for the tube bundles from the detailed Apros steam generator model.

Summary and discussion

Numerical methods have been developed for modelling transients in steam generators. The primary side of the steam generator is calculated using a one-dimensional Apros model. Three-dimensional modelling of the secondary side is performed by using the commercial ANSYS Fluent CFD code. The geometry of the secondary side is not described in detail, but the tubes of the primary circuit are modelled as a porous media, for which the pressure losses, mass exchange rates and enthalpy sources are defined explicitly. One-way coupling is used between the two code counterparts.

The models are used for simulating PWR PACTEL and VVER-440 steam generators. Stationary states of the steam generators have been resolved and the results have been compared to available experimental data. In addition, transient situations have been calculated. Steam tables of the Apros code were implemented in Fluent by using the user-defined real gas model of Fluent for modelling the pressure transients. Pressure drop and pressure rise on the secondary side of the PWR PACTEL steam generator has been simulated. Loss of feed water transient in a VVER-440 steam generator is calculated.

The present modelling techniques can also be applied to other devices, besides steam generators, that are of interest in nuclear safety analysis.

Acknowledgement

References

1. Kouhia, V., Purhonen, H., Riikonen, V., Puustinen, M., Kyrki-Rajamäki, R., Vihavainen, J. PACTEL and PWR PACTEL Test Facilities for Versatile LWR Applications. Science and Technology of Nuclear Installations, Volume 2012, Article ID 548513.

2. Stosic, Z.V., Stevanovic, V.D. Advanced Three-Dimensional Two-Fluid Porous Media Method for Transient Two-Phase Flow Thermal-Hydraulics in Complex Geometries. Numerical Heat Transfer, B 41(2002), 263–289.

3. Apros, Homepage of the Apros Process Simulation Software, 28.1.2013. www.apros.fi.

4. ANSYS, ANSYS Fluent 14.0 User's Guide, Ansys Inc., USA, 2011.

5. Pättikangas, T.J.H., Niemi, J., Hovi, Toppila, V.T., Rämä, T. Three-Dimensional Porous Media Model of a Horizontal Steam Generator. CFD for Nuclear Reactor Safety Applications (CFD4NRS-3) Workshop, Bethesda, MD, USA, 14–16 September 2010. 12 p.

6. Simovic, Z.R., Ocokoljic, S., Stevanovic, V.D. Interfacial Friction Correlations for the Two-Phase Flow across Tube Bundle. International Journal of Multiphase Flow 33(2007), 217–226.

7. Pättikangas, T.J.H., Niemi, J., Laine, J., Puustinen M., Purhonen, H. CFD modelling of condensation of vapour in the pressurized PPOOLEX facility. CFD for Nuclear Reactor Safety Applications (CFD4NRS-3) Workshop, Bethesda, MD, USA, 14–16 September 2010. 12 p.

5.8 Uncertainty evaluation for best estimate analyses (UBEA / BEPUE)

Joona Kurki, Torsti Alku, Ismo Karppinen

VTT Technical Research Centre of Finland
Tietotie 3, P.O. Box 1000, FI-02044 Espoo

Introduction

Best Estimate Plus Uncertainty approach to deterministic safety analyses is maturing to be a viable option for the licensing needs of nuclear power installations. Unlike in the conventional, so-called *conservative* approach, effort is put into modelling all physical phenomena and initial and boundary conditions of the simulations as realistically as possible, avoiding conservative assumptions to the largest possible extent. Fulfilment of the required safety margins are demonstrated by calculating bounding uncertainty curves for the output parameters of interest through statistical techniques.

A Best Estimate Plus Uncertainty analysis requires first of all a best estimate code, and secondly quantification of the uncertainties of all the parameters influential to the simulation. These influential parameters include coefficients in the physical phenomena models within the best estimate code, initial state variables within

the simulation model representing the nuclear installation, and other parameters used as boundary and initial conditions within the model. While the quantification of the uncertainties related to the boundary and initial conditions should be relatively easily available from plant data, the uncertainties related to the physical modelling within the simulation code are often more difficult to quantify: some of the physical models are based on simple separate effect tests (SETs) in which case the quantification of the model uncertainty should in most cases be quite straight forward. On the other hand, some phenomena cannot be measured directly from separate effect tests, such as is the case for most of the physical models dealing with interfacial phenomena, and the physical models describing these phenomena within the simulation codes are typically based on measurement of the secondary effects. In these cases, the quantification of the associated uncertainties has to be deduced from comparisons between simulation results and experimental data of integral tests. Methods aiming at accomplishing this task are studied in the currently-on-going OECD/NEA PREMIUM benchmark exercise.

The name of the SAFIR2014 subproject dealing with Best Estimate Plus Uncertainty approach was originally BEPUE (application of Best Estimate Plus Uncertainty Evaluation method) but was changed to UBEA (Uncertainty evaluation for Best Estimate Analyses) in the beginning of year 2012 to better reflect the focus of the project: research related to the quantification of the uncertainties needed in a BEPU analysis, instead of mere application of the BEPU approach.

The Best-Estimate Plus Uncertainty approach to safety analyses

There are several ways to practically implement the Best Estimate Plus Uncertainty approach, including CSAU (Code Scaling, Applicability and Uncertainty) developed by the U.S Nuclear Regulatory Commission, UMAE (Uncertainty Method based on Accuracy Extrapolation) proposed by the University of Pisa, and the "GRS method" developed at the Gesellschaft für Anlagen- und Reactorscherheit [1]. Due to its simplicity, and the fact that the computational complexity is independent of the number of uncertain parameters, the "GRS method" is probably the most widely used of the available methods.

In the "GRS method" all uncertain parameters are associated with a predefined probability density function (PDF). The analysed scenario is then simulated multiple times, with randomly sampling the values of all the uncertain parameters from their specific PDF's at the beginning of each simulation. The number of required simulations depends only on the desired confidence level, and can be deduced using the well-known Wilks' formula:

$$1 - na^{n-1} - (1-n)a^n \geq b,$$

where n is the number of required simulation runs and a is the probability that all the results will be enveloped with the confidence level b. With the de facto standard 95%/95% probability and confidence level, the required number of simulation runs becomes 93, which may take a considerable amount of time depending on

the analysed scenario, and the computer system used to run the simulations. As a result of the simulation a family of curves is obtained for all output parameters, from which the bounding curves can be calculated.

After completing the simulations, statistical correlation coefficients can be calculated between the varied input parameters and the output parameters obtained as result of the simulation runs, in order to identify and to rank the parameters most influential to specific output effects; the correlation coefficients can be used to prune out uninfluential parameters, and for example to see which varied parameter has largest influence on the peak cladding temperature attained during the course of the simulation. This kind of information may be valuable when determining which physical models used in a simulation code need improvement.

Applications of the BEPU approach

While best estimate thermal-hydraulic system codes have been applied to safety analyses at the VTT Technical Research Centre of Finland for decades, the simulations have still been of the conservative type due to the use of conservative values for initial and boundary conditions. The study of the application of the BEPU approach has been properly started only within the BEPUE/UBEA project. To gain insight on the method, and to develop the required tools and knowledge, a few best estimate plus uncertainty analyses were first carried out within the project.

Simulation of loss-of-coolant accident at a APR1400 power plant

The first analysed scenario was a large-break loss-of-coolant accident in one of the cold legs of a Korean APR1400 power reactor. [2]

For the needs of the BEPU study, a generic model of the APR1400 reactor system was created based on publicly-available data, and a previously created simulation model of the ATLAS[2] test facility. Because all details of the reactor system were not available, the model is not an accurate representation of the actual reactor system, but rather a generic model similar to the APR1400.

The list of varied parameters was created based on findings of the international BEMUSE programme, and included parameters such as the coefficient of critical flow limitation, initial pressures and temperatures in various parts of the reactor coolant system, maximum power of the hottest fuel assembly, and the coefficient of critical heat flux. All of the parameters suggested in the BEMUSE reports could not be varied because there was no variables for them in APROS.

An uncertainty analysis tool [3] developed earlier at Fortum as a module of the Testing Station software was utilized to carry out the best estimate plus uncertainty analyses, and to calculate the bounding curves and sensitivity measures.

---

[2] ATLAS itself is an integral test facility representing the APR1400 reactor at a scaled-down geometry.

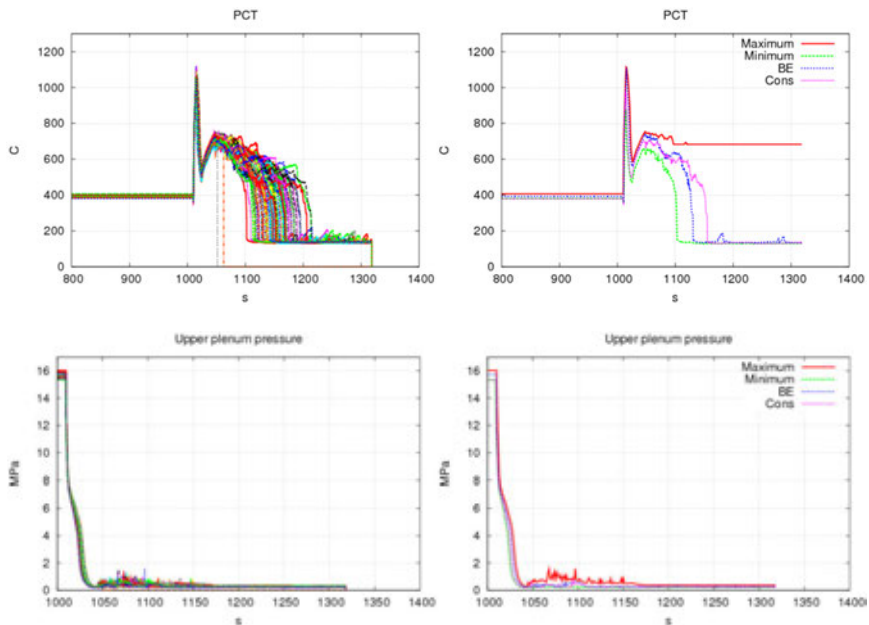Some results of the analysis are presented in Figure 1.

Figure 1. Some results from the BEPU analysis of the LOCA at an APR1400 power reactor: the peak cladding temperature (top) and the pressure in the upper plenum (bottom). On left side all the 93 output curves, and on the right side the calculated bounding curves, with the best estimate curve and the conservative curve.

As a result of the study some development needs were identified; namely the importance of parallelization, and the accessibility to some physical model coefficients within the code.

Simulation of the International Standard Problem number 50

The next analysed case was the International Standard Problem number 50 (ISP-50), which had previously been calculated with APROS at the VTT Technical Research Centre of Finland. [4, 5]

Because the otherwise very convenient uncertainty analysis tool of the Testing Station software was unable to parallelize the simulation runs, simple Python scripts were written specifically for the purpose of arranging the best estimate plus uncertainty analyses with APROS, using all the available computer cores on a single desktop computer. This enabled local parallelization to the four computer cores available on a typical desktop PC, which was deemed adequate for the present needs. Also at the same time, effort was put into adding the possibility to

vary the most important physical model parameters within APROS, which were not available for the APR1400 simulations.

The list of varied parameters was again created based on the recommendation of the BEMUSE project, but this time a longer list of varied parameters could be considered thanks to the code improvements. The BEPU analysis of 93 runs was applied three times to the transient scenario to provide for internal comparison of the method and the achieved results. The output parameter variations in the BEPU analyses were all in accordance with one another and no dramatic differences were found in this respect. Figure 2 shows comparison of some of the results in the three cases.
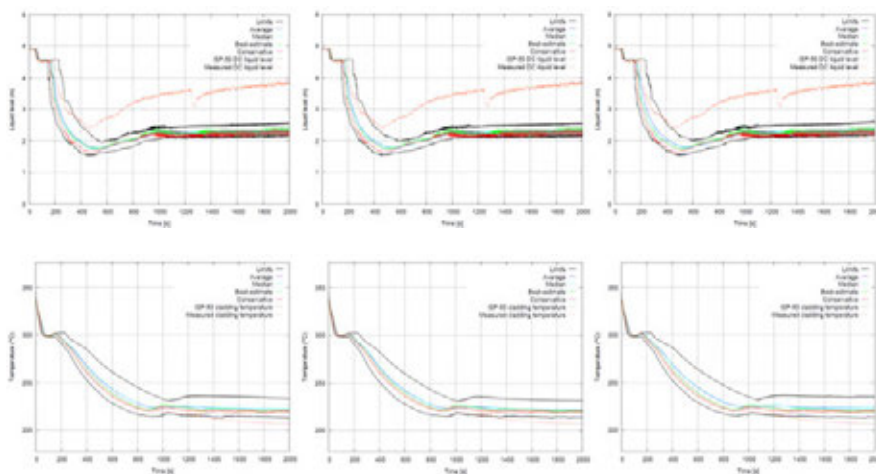
Figure 2. Some results from the three BEPU analyses of the ISP-50: the downcomer liquid level (top) and the cladding temperature (bottom). Portrayed are the bounding curves, the best estimate curve, the conservative curve, the average and median curves, along with the experimental results and previous ISP-50 analysis results for comparison.

Sensitivity studies were performed in the form of limit runs where each input parameter was varied on the ranges of their PDF's. Also, statistical correlation coefficients were applied to the results of the BEPU analyses for input parameter sensitivity analysis purposes. Contrary to the similarity of the BEPU analyses results the sensitivity analyses provided conflicting results to some degree, but this was to be expected with the ratio of the amount of input parameters to simulation runs being so high (26/93). Because of the unreliability of the sensitivity studies only parameters with very high influence were revealed, even with a ranking table that integrated all the different sensitivity analyses.

The ISP-50 analysis provided a basis for future research into best-estimate methods using APROS and laid out the general workflow for a BEPU analysis. What was found out was that to achieve reliable results with the BEPU method it is extremely

important to use a model that is able to reproduce the real situation very precisely. A recommendation was made of applying the BEPU method to APROS validation cases to provide more information on the usage of the method with APROS.

Participation in the PREMIUM benchmark

OECD/NEA/WGAMA organizes the PREMIUM (Post BEMUSE Reflood Models Input Uncertainty Methods) benchmark exercise between the years 2012 and 2014. Focus of PREMIUM is the quantification of the uncertainties of the physical models in system thermal-hydraulic codes, related to modelling of the reactor reflooding scenario. Different methods for quantification of the uncertainties of the physical model parameters have been proposed, and within the PREMIUM benchmark these methods are put into use in calculation of reflooding tests from two separate test facilities: FEBA and PERICLES-2D.

VTT Technical Research Centre of Finland participates in the PREMIUM benchmark using the APROS code, within the UBEA project [6]. During the year 2012, the focus in the PREMIUM was to identify all the influential parameters that affect the outcome of a reflooding simulation of the FEBA facility [7].

FEBA reflooding simulations

The purpose of the Flooding Experiments with Blocked Array (FEBA) which were conducted in Germany in the 1980's was to gain information about the thermal-hydraulic phenomena taking place in a reactor reflooding situation after an LBLOCA. To investigate reflooding with core meltdown the scope of FEBA included testing different kinds of geometries for blockage in the reactor channel. To have a reference point reflooding was also tested without blockage and additionally the effect of grid spacers was tested by performing test series where a grid spacer was removed.

The FEBA experimental setup consisted of a 3.9 m long 5 x 5 electrically heated rod array enclosed in a 4.114 m long stainless steel housing. To minimize heat losses the housing was surrounded by Triton Kao Wool insulation. The idea of the housing was to simulate other rod arrays so as to simulate the rod array being a part of a larger reactor core. The rods were heated in the axial direction with a cosine-shaped power profile divided into seven discrete sections. Six grid spacers and a longer removable central grid spacer were also situated inside the housing.

An initial list of all parameters that could be influential to the main responses of interests such as cladding temperatures, rewetting time instant, quench front elevation and pressure distribution within the channel was first drafted. The initial list included practically all physical parameters of the experiment that have been modelled in the APROS code. Next, the overall influence of all parameters was evaluated by simulating the reflooding experiment numerous times, with varying a single uncertain parameter at a time, at the limits of its predetermined PDF. To determine which of the parameters on the initial list were influential, a set of crite-

ria related to the maximum cladding temperature and the rewet time variation, proposed in the benchmark specification, was applied. In the end 30 out of the 40 parameters on the initial list were pruned out.

With the initial quantification of the influential input parameters, the experimental results were not enveloped by the bounding curves obtained as a result of the BEPU simulation, and it seems that APROS underestimates the rise of the cladding temperatures, and the quench times. Examination on the probable cause for the observed behaviour suggested that the interfacial heat transfer and friction models used above the quench front are in their current form inadequate to properly describe the reflooding phenomena at least in the case of the FEBA experiment.

The work with the PREMIUM benchmark continues with proper quantification of the uncertainties of the identified influential parameters by calculation of more FEBA experiments, and finally with calculation of a PERICLES-2D experiment, which will be organized as a blind exercise.

References

[1] Glaeser, H. GRS Method for Uncertainty and Sensitivity Evaluation of Code Results and Applications. Science and Technology of Nuclear Installations, 2008. Article ID 798901. 7 p. Doi:10.1155/2008/798901.

[2] Luukka, J. LOCA epävarmuusanalyysi APROS Testing Station -ohjelmistolla, Tutkimusraportti VTT-R-00782-12, Teknologian tutkimuskeskus VTT, 2012. (In Finnish)

[3] Peltokorpi, L. Developing of Uncertainty Analysis System for APROS Safety Simulation Environment. Master's Thesis, Helsinki University of Technology, Faculty of Information and Natural Sciences, 2009.

[4] Alku, T. Best-Estimate Plus Uncertainty Analysis of the ISP-50 Problem, Research Report VTT-R-08027-12, VTT Technical Research Centre of Finland, 2012.

[5] Inkinen, P. Simulation of ISP-50 with APROS. Research Report VTT-R-00749-11, VTT Technical Research Centre of Finland, 2011.

[6] Alku, T. Identification of Influential uncertain parameters of PREMIUM benchmark. Research Report VTT-R-08026-12, VTT Technical Research Centre of Finland, 2012.

[7] Ihle, P., Rust, K., FEBA – Flooding Experiments with Blocked Arrays: Evaluation Report, KfK 3657, Kernforschungzentrum Karlsruhe, 1984.

6. Severe Accidents

6.1 Core debris coolability and environmental consequence analysis (COOLOCE and COOLOCE-E)

Eveliina Takasuo, Tuomo Kinnunen, Stefan Holmström, Pekka H. Pankakoski,
Taru Lehtikuusi, Ville Hovi, Mikko Ilvonen, Veikko Taivassalo

VTT Technical Research Centre of Finland
P.O. Box 1000, FI-02044 Espoo

Introduction

At the Finnish BWRs in Olkiluoto, the flooding of the lower drywell of the containment is an important part of the severe accident management strategy. In the course of a core melt accident, corium is discharged from the reactor pressure vessel into a deep water pool in the lower drywell of the containment. Corium is fragmented and it is expected to form a porous debris bed from which decay heat must be removed in order to prevent re-melting of the material. Boiling and water infiltration into the particle bed interior play key roles in the heat removal. VTT has an active experimental programme of ex-vessel debris coolability, along with analytical activities aiming for the validation and development of simulation codes. The objective of the experiments is to measure the heat flux which results in local dryout (loss of coolant) within the porous bed. Then, the critical heat fluxes, or power densities, may be compared to realistic values of residual power in accident scenarios.

The first experimental facility for coolability studies at VTT was STYX which was active between 2001–2008 [1, 2]. The depth and pressure range in the experiments characterized the conditions expected in the Olkiluoto containments during a core melt accident and irregular gravel was used as the debris simulant material. STYX experiments examined dryout heat flux in one-dimensionally flooded setups, i.e. assuming that debris is evenly distributed in the spreading area. In realistic accident scenarios, however, heap-like (conical), mound-like or highly non-homogenous debris beds are possible as shown by experiments and particle

sedimentation models [3–5]. In heap-like debris beds, water infiltration is multi-dimensional which means that coolant infiltration occurs through other surfaces than top or bottom.

Compared to top flooding only, multi-dimensional flooding tends to increase dryout heat flux and improve coolability. On the other hand, a heap-like particle bed is higher than a flat-shaped cylindrical bed of the same volume and base diameter. This implies that the accumulated mass flux of steam is greater near the top of the heap which may reduce the heating power leading to local dryout, i.e. the coolability may be reduced for non-flat geometries regardless of the multi-dimensional flooding. Top and bottom flooding have been the topic of many studies (based on which dryout heat flux models and correlations have been developed) but only a few studies have investigated other flow configurations. To the knowledge of the authors, no experimental studies existed of dryout in conical or mound-like debris beds.

In order to fill in this gap of knowledge and address the debris bed geometry, the COOLOCE test facility was designed and built in 2009–2010. The experiments that compared the coolability of a top-flooded cylindrical bed and a conical (heap-like) bed were performed in 2011. As a result, it was experimentally verified that the higher of the geometries, the conical bed, has relatively poor coolability [6]. In addition, it was seen that 2D models for fluid flow and heat transfer in porous medium are capable of predicting the relative coolability difference with reasonably good accuracy [7]. Starting from 2012, the experimental programme was extended to include other representative debris bed geometries: a cylindrical bed with lateral flooding (top and sidewalls open) and cylinder with closed top, simulating an agglomerate of solidified corium that would block the flow through the top surface. In addition, an experiment for comparing two simulant materials has been made.

Simulations of the experiments using dedicated severe accident codes and other suitable codes, e.g. computational fluid dynamics (CFD), are an integral part of the project. The availability of simulation codes capable of assessing coolability in reactor scenarios has to be maintained and verified based on latest knowledge of what type of debris configurations are expected in reactor scenarios. The main computational tools used in the COOLOCE-E project for analyzing the particle bed coolability are the MEWA 2D code (developed by the IKE institute of Stuttgart University [8]) and the in-house 3D code PORFLO by VTT. All the COOLOCE experiments are modeled with the simulation codes for the purposes of code development, verification and validation. The analytical work includes (1) direct comparisons of the experimental and simulation results and (2) in-depth investigation of the performance of the different codes and models by code-to-code comparisons (flow fields, temperatures, grid effects etc.).

The research at VTT focuses on finding out the coolability limits in certain, well-defined representative conditions. However, it is important to observe that the debris bed configuration as well as its coolability depends on the melt discharge, and is determined by processes which include many uncertainties starting from the uncertainties inherent in the in-vessel accident progression. New data on the key physical phenomena of the debris bed formation which defines the spatial

configuration, porosity, particle morphology and size distribution of the bed is produced by KTH (Royal Institute of Technology) in the APRI-8 project in Sweden. A joint effort to reduce the uncertainties in coolability is conducted by VTT and KTH within the DECOSE project financed by NKS. The project facilitates information exchange and co-operation between the organizations so that the experimental and analytical activities in both APRI-8 and SAFIR2014 projects are "synchronized" for maximum benefit to the both participants, end-users and the scientific community.

Experiments

The main components of the COOLOCE test facility are the pressure vessel which contains the particle bed section with its heating arrangement, the feed water system and the steam removal system. The test vessel has a volume of 270 dm^3 with the outer diameter of 613 mm and a design pressure of 7 bar. The conical and cylindrical test beds are 500 mm and 310 mm in diameter, respectively. The decay heat is simulated by electrical resistance heaters arranged in a vertical configuration which aims for a volumetrically uniform power distribution within the test bed. The total maximum power is approximately 55 kW. The pressure vessel is equipped with sightglasses that have been used for visual observations of boiling in the fluid volume (by a video recorder).

The conical and cylindrical test beds have their own bottom plates, making it possible to change between configurations with relative ease. The debris simulant material was small, spherical beads in all the geometry comparison experiments. In the experiments investigating the effect of particle material, irregularly shaped and sized gravel particles were used (the same material as in STYX). These experiments also serve to distinguish the possible facility-specific differences since the results of COOLOCE and STYX can be compared. The experiments are listed in Table 1 with the main specifications of each set-up. The four different test beds in the experiments are shown in Figure 1.

Table 1. Summary of the COOLOCE experiments.

Experiment	Test bed	Flow configuration	Particle material	Pressure range [bar]
COOLOCE-1 – 2	Conical	Multi-dimensional	Spherical beads	1.6–2.0
COOLOCE-3 – 5	Cylindrical	Top flooding	Spherical beads	1.0–7.0
COOLOCE-6 – 7	Conical	Multi-dimensional	Spherical beads	1.0–3.0
COOLOCE-8	Cylindrical	Top flooding	Irregular gravel	1.0–7.0
COOLOCE-9	Cylindrical	Top flooding*	Irregular gravel	1.0
COOLOCE-10	Cylindrical	Lateral and top flooding	Spherical beads	1.3–3.0

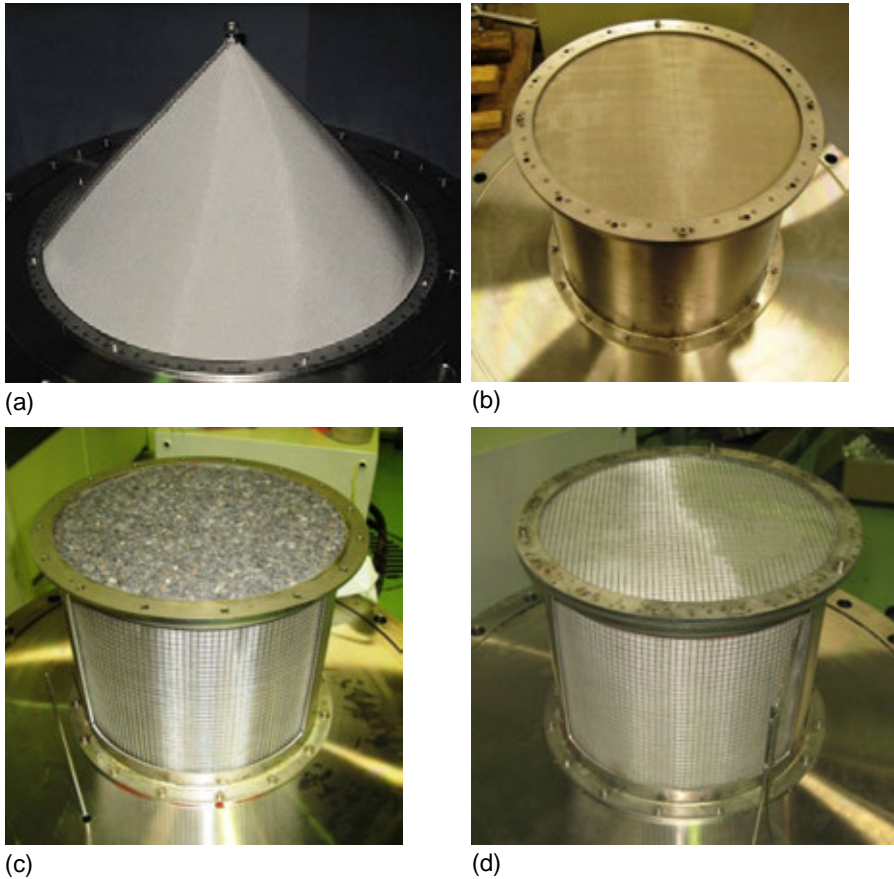*Initially subcooled water pool, saturated pool in all other experiments*

Figure 1. Test beds in the experiments: (a) Conical filled with beads, (b) cylindrical with top-flooding only and filled with beads, (c) cylindrical with top flooding and filled with gravel and (d) cylindrical with top and lateral flooding filled with beads. Note that in (c) the sidewalls are not yet attached.

Results of the geometry comparisons experiments

The most important result of the experiments thus far is the clarification of the relative coolability of the conical and cylindrical debris beds in the experiments COOLOCE-1–7. The measured dryout power levels suggest that the coolability of a conical debris bed is reduced by 47–51% compared to a cylindrical debris bed of equal diameter and volume. This is explained by the greater height of the conical debris bed configuration. In a homogenously heated debris bed, the heat flux through a cross-sectional surface increases with increasing height causing dryout in the upper part of the geometry when a critical steam flux (high enough to fully replace water) is reached. In case the height difference between the heap-like and

the flat-shaped cylindrical configurations is great enough, the heap-like configuration reaches dryout at a lower power (or power density) than the flat-shaped geometry, regardless of the multi-dimensional flooding which is expected to increases coolability compared to top flooding.

It was not possible to directly measure the dryout power in a flat-shaped cylinder and a cone three times higher than the cylinder (as is the case when the radius and volume are assumed equal). This would have resulted in an impractically low cylindrical test bed. Thus, the aforementioned result is obtained by a simple scaling process based on heat flux being independent of geometry in one-dimensionally flooded beds, see a detailed description in [6] and [7]. Indeed, the experiments also directly suggest that if the two debris beds have equal height, the coolability of the cone is better by 50–60% compared to the cylinder due to lateral flooding.

The series of geometry comparisons was continued in the COOLOCE-10 experiments in which a cylinder with water infiltration through all the surfaces (except bottom) was made possible. It was found that the dryout heat flux is increased by more than 50% compared to the top-flooded cylinder.

Results with different simulant materials

The COOLOCE-8 experiment conducted with irregular alumina gravel clarified the uncertainties related to the simulant material and the measurements by two test facilities with different types of heating arrangements and test vessels. It was found that the dryout heat flux measured for the alumina gravel was low compared to the experiments with spherical beads and slightly lower compared to the earlier experiments with the STYX facility.

The difference between the spherical beads and the gravel is mostly explained by the greater average size of the beads which yields a lower particle-fluid drag and thus increased coolability. For the gravel bed, the important physical parameters to which the dryout heat flux is very sensitive (particle diameter and porosity) are not well known compared to spherical particles. It is possible that the packing of particles has initially been different in COOLOCE and STYX. The test bed may even shift during the experiments as smaller particles fill the pores between larger ones and interlock with them. By combining the experimental observations with simulation including parameter variations, it was shown that the actual effect of the heating arrangement (if any) is obscured by uncertainty in the test bed properties. It is expected that the facility-specific uncertainties will be clarified by the comparison of COOLOCE and POMECO-HT (at KTH) experiments. Spherical beads will be used in these test runs to better eliminate the material-related uncertainty.

The COOLOCE-9 experiment was run after COOLOCE-8, without changing the particle material. The experiment was started with no heat-up sequence so that the water volume outside the debris bed remained subcooled. The results are preliminary but they strongly suggest that the subcooling increases dryout heat flux and increase coolability.

Modelling of dryout power

The objectives of the MEWA simulations, the main task in the analytical part of the project, are to predict the dryout power and the dryout zone location for direct comparisons of the experimental and simulation results and to elucidate the flow field in the debris bed by means of 2D models. MEWA solves the pressure loss in porous medium based on the two-phase extension of the well-known Ergun's equation [9]. Energy conservation equations are solved for the three phases (gas, liquid, solid) and mass conservation for gas and liquid. Homogenous heating is assumed in all the basic simulations as would be the case in reactor scenarios. Scoping simulations in which the heaters are modelled have been performed with PORFLO [10].

The agreement between simulation results and experiments varies from very good to reasonable in the examined flow configurations. The pressure loss in the two simulant materials was measured in a separate test facility at KTH in order to obtain the "effective" particle diameter to be used in calculations. It was found that the pressure-dependent dryout power in the MEWA calculations is in a close agreement with the experimental one in the case of top-flooded cylindrical bed filled with beads. In case of the gravel bed, the discrepancy between the simulations with the effective particle diameter and the experiments was larger. However, as already mentioned in the previous chapter, the packing of the bed is vulnerable to shifting, causing the porosity to differ from the assumption used in the simulation. According to sensitivity studies, particle diameter and porosity greatly affect the dryout power. The problem is easy to grasp by considering the porous matrix formed by hard, spherical particles in contrast to gravel: once packed densely, the nearly uniform spheres do not shift or compress like the gravel might.

For the conical bed, the direct comparison of simulated and experimental dryout power suggests that the coolability is somewhat underestimated by the models. The discrepancy, however, has a logical explanation: due to the co-current flow of water and steam in the conical bed, the mechanism of dryout formation is different from that of the top-flooded bed. The formation of first dry zone has been taken as coolability limit in both simulations and experiments. The simulations show that dryout first occurs as an extremely small zero-saturation volume near the tip of the cone where the accumulated steam flux is greatest. In simulations, this type of dryout can be detected as accurately as the density of the computational grid. It is not realistic to expect to detect dryout with the same accuracy in experiments because of limited number of thermocouples and non-homogenous heating (the heaters do not quite reach the highest part of the cone).

In this case, rather than pin-pointing the dryout power with several power levels, it is more feasible to take the experimental dryout power as the starting point in the simulations and compare the size and locations of the dry zone to the experimental observations. This way, the simulations results are in a better agreement with the experiments [6]. However, it should be mentioned that so far only a few this type of 2D simulations that attempt to exactly reproduce the experimental

sequence have been made. Also, the formation of the first local dryout as the coolability limit may be questioned. According to the simulations, the steam flow can maintain post-dryout steady-states in which the temperature increase is not drastic enough to pose a risk of re-melting of the solid.

2D and 3D simulations

The goal of the 3D modelling is to complement the 2D approach so that the effects of possible non-homogeneity of the debris bed can be taken into account. In general, the simulations aim for a more mechanistic, CFD type approach to the problem of internally heated porous bed in a water pool. The closure models for friction and heat transfer suitable for flows in porous media have been implemented into the in-house code PORFLO, of which a new version that utilizes unstructured grids and parallelization has been taken into use [11]. The models programmed for PORFLO were also included as user-defined functions in the widely-used commercial CFD solver FLUENT. The specific goal of this was to verify the implementation of the physical models in the different codes and to otherwise test the performance of the codes to e.g. sort out numerical problems.

Results of the 3D simulations with FLUENT and 2D simulations with MEWA are illustrated in Figure 2 which shows the void fraction distributions in a conical debris bed before and after dryout (pre- and post-dryout conditions). Quarter of the geometry has been modelled in 3D. Both simulations show that highest void fraction is formed near the top of the bed where dryout occurs when the critical power level is reached. In general, the void distributions in the 2D and 3D cases are reasonably similar. However, in FLUENT simulations the distribution is not as smooth as in MEWA: variations resembling a checkerboard are seen especially near the surface of the cone (at the interface of the pool and porous region) in pre- and post-dryout conditions. In addition, a larger part of the geometry has dried out in the FLUENT simulation.
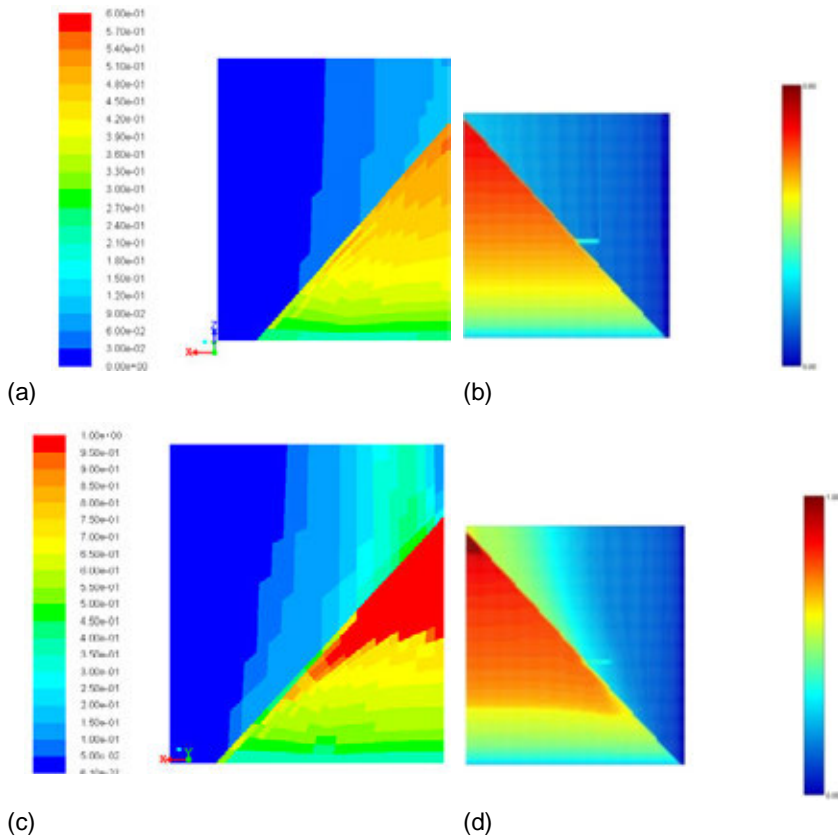
Figure 2. Void fraction distribution in simulations of conical debris bed: (a) FLUENT with 4 kW heating, (b) MEWA with 4 kW heating, (c) FLUENT with 30 kW heating, (d) MEWA with 30 kW heating.

Void fraction distribution in a PORFLO simulation is presented in Figure 3. This model too correctly predicts that the void fraction increases with increasing height. The grid is the same as the one used in the FLUENT calculations. Differences compared to the FLUENT results are that the large cells in the pool also show uneven void fractions and the high-void cells seen at the tip of the cone. This is probably a result of the uneven variable fields at the interface of the debris bed and the pool region, the effect of which is extended into the pool area. In addition, the pool region models are different: PORFLO models the pool region as a type of high-porosity porous zone with no-separate free-flow models (similarly to MEWA) whereas FLUENT applies the *k-ε* turbulence model for the free-flow.

The region at the interface between the porous bed and the free-flow in the pool is apparently problematic in the CFD solution. Previously, it was speculated

that too coarse grids (unstructured or Cartesian) might be the reason behind the checkerboard distributions. However, after running several test simulations this does not seem to be the case as even a 2D simulation in FLUENT with the same dense grid as in MEWA calculation showed uneven void fractions at the outermost cells of the conical region. This suggests that the results are related to other issues in the solution. A main difference between the CFD simulations and the 2D approach of MEWA is that the CFD codes solve the full momentum equations (Navier-Stokes equations) with temporal and spatial derivatives. In MEWA, the momentum equations are simplified to the time-independent pressure loss equations in porous media [8]. The difficulties may be related to the rather complicated calculation of the derivatives near the geometrical and/or modelling boundaries (e.g. a sudden change in porosity). Different numerical schemes might help to avoid the problem, or a transition region with gradually changing porosity at the pool interface.
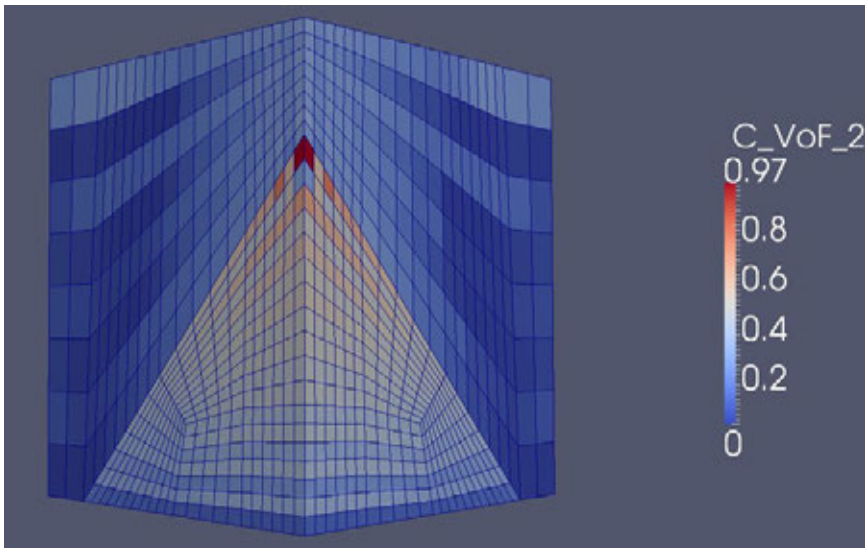
Figure 3. Void fraction in a PORFLO simulation of the conical debris bed, 4 kW heating power.

Summary

The research performed in COOLOCE and COOLOCE-E project combines an experimental programme of thermal hydraulic experiments investigating core debris coolability to analytical work and in-house code development. Dryout power has been measured for the following debris bed geometries: conical (heap-like), cylindrical with top flooding (evenly distributed) and cylindrical with lateral flooding (mound-like). The experiments have been modelled with the MEWA code which

solves heat transfer and fluid flow in the debris bed based on well-known porous media models. The agreement between simulations and experimental results ranges from very good to reasonable.

In addition to the MEWA simulations, 3D calculations of the flow behaviour of debris beds in pre- and post-dryout conditions have been performed with the in-house code PORFLO as well as FLUENT. The objective is to complement the 2D models by a more detailed approach which could better take into account irregularities in the debris bed properties. Even though the CFD modelling capabilities are not yet ready for systematic prediction of dryout power in different cases, the 3D modelling has provided valuable training and insight into the physical phenomena relevant to coolability as well as to the modelling principles.

References

1. Lindholm, I., Holmström, S., Miettinen, J., Lestinen, V., Hyvärinen, J., Panka-koski, P., Sjövall, H. 2006. Dryout Heat Flux Experiments with Deep Heterogeneous Particle Bed. Nuclear Engineering and Design, 236(2006), 2060–2074.

2. Takasuo, E., Holmström, S., Kinnunen, T., Pankakoski, P.H., Hosio, E., Lindholm, I. 2010. The effect of lateral flooding on the coolability of ir-regular core debris beds. Nuclear Engineering and Design (2010). Doi:10.1016/j.nucengdes.2010.04.033.

3. Karbojian, A., Ma, W.M., Kudinov, P., Davydov, M., Dinh, T.N. A Scoping Study of Debris Formation in DEFOR Experimental Facility. 15th Inter-national Conference on Nuclear Engineering (ICONE-15), Nagoya, Ja-pan, April 22–26, 2007.

4. Yakush, S., Kudinov, P. 2011. Effects of Water Pool Subcooling on the De-bris Bed Spreading by Coolant Flow. Proceedings of ICAPP 2011, Nice, France, May 2–5, 2011. Paper 11416.

5. Takasuo, E., Holmström, S., Kinnunen, T., Pankakoski, P.H., Hovi, V., Ilvo-nen, M., Rahman, S., Bürger, M., Buck, M., Pohlner, G. 2012. Experi-mental and computational studies of the coolability of heap-like and cy-lindrical debris beds. 5th European Review Meeting on Severe Accident Research (ERMSAR-2012), Cologne (Germany), March 21–23, 2012.

6. Takasuo, E., Holmström, S., Kinnunen, T., Pankakoski, P.H. 2012. The COOLOCE experiments investigating the dryout power in debris beds of heap-like and cylindrical geometries. Nuclear Engineering and Design, 250(2012), 687–700.

7. Takasuo, E., Hovi, V. Ilvonen, M., Holmström, S. 2012. Modeling of Dryout in Core Debris Beds of Conical and Cylindrical Geometries. Proceedings of the 20th International Conference on Nuclear Engineering, Anaheim, California, USA, July 30 – August 3, 2012. ICONE20-54159.

8. Bürger, M., Buck, M., Schmidt, W., Widmann, W. Validation and application of the WABE code: Investigations of constitutive laws and 2D effects on debris coolability. Nuclear Engineering and Design, 236(2006), 2164–2188.

9. Ergun, S. 1952. Fluid flow through packed columns. Chemical Engineering Progress 48, 89–94.

10. Takasuo, E., Hovi, V., Ilvonen, M., Holmström, S. 2012. Modeling of dryout in core debris beds of conical and cylindrical geometries. Proceedings of the 20th International Conference on Nuclear Engineering, July 30– August 3, 2012, Anaheim, California, USA. ICONE20-54159.

11. Hovi, V. 2012. New PORFLO version with unstructured grids and parallelization. VTT Research Report VTT-R-01143-12. Espoo, 2012. 27 p.

6.2 Chemistry of fission products (FISKE)

Tommi Kekki, Karri Penttilä, Suvi Lamminmäki, Niina Könönen, Jukka Rossi

VTT Technical Research Centre of Finland
Otakaari 3 K, P.O. Box 1000, 02044 VTT

Abstract

FISKE project investigated the chemistry of fission products inside a NPP containment. ChemPool is a new program to be used with MELCOR to calculate the equilibrium composition and the pH values of the pools. In this program the production of nitric acid during high dose rates is calculated which was also studied experimentally in this project. In addition, the behaviour of low volatile fission products (etc. Sr, Ba, La and Ru) during corium/concrete interactions were investigated using GEMINI2 and ChemSheet codes. CSFoam tool was used to calculate the viscosity of corium/concrete mixture at various temperatures and compositions. CSFoam tool contains correlations to calculate the viscosity, the surface tension and the density of molten oxide system.

Introduction

In the event of a severe accident, some fission products could be released from the fuel and become in the reactor containment. Volatile iodine will be adsorbed at and desorbed from surfaces above the sump area. From a safety perspective, painted surfaces are among the most important especially for those plants with small sump volumes but with very large containment painted surface areas; their action on iodine behaviour is two-fold: they act as a sink for I2 and as a source for volatile organic iodine. Radiation plays a strongly enhancing role, as it induces fast radiochemical reactions between iodine and the paints or paint components.

Nitric acid formation with irradiation has previously been studied in ORNL by Beahm et al. (1992) NUREG/CR-5950. However, very little further studies have been performed although NUREG/CR-5950 formulas are applied in plant evaluation and pool pH estimation e.g. in USA. The previous study by ORNL does not address HNO3 production in all severe accident conditions, like in water pools a top molten corium-concrete pool or in sump water with real solution composition. Consideration of additional HNO3 formation contributes to estimation of pool pH and thus should be evaluated in connection with iodine source term.

Molten core materials, when flowing out of the reactor vessel, may interact with the concrete of the reactor building. Experiments of corium-concrete interactions have been performed. The interpretation of such experiments was though to require the knowledge of different properties of corium-concrete mixtures such as viscosity in the solidus-liquidus temperature range. The models estimated that 100% of highly volatile fission products would be released but that release fraction for low-volatility fission products, e.g. Ba, La, Ru, Sr, would be in the range 0.001 to 0.5. The behaviour of low-volatility fission products in these interactions is important to know.

Main objectives

Currently MELCOR code is not able to consider aqueous species and how they affect the pH in the pools. In VTT ChemSheet has been coupled with MELCOR to calculate the equilibrium composition and the pH of the pools. A work for a new pool chemistry simulation model, ChemPool, has been objective. It is a standalone program using ChemApp thermodynamic library directly for equilibrium calculation. ChemPool will then automatically calculate the chemical conditions like pH values in the pools by using the saved results from the MELCOR simulation.

Project also follows-up the OECD/BIP2 project investigating the behaviour of iodine in support of source term evaluation in case of severe accident in a nuclear reactor. This project main objective is mechanistic understanding of iodine adsorption/desorption on painted containment surfaces.

Earlier advanced containment experiments (ACE) project shows that there might be the fission product release during corium and concrete interactions. The behaviour of fission products (etc. Sr, Ba, La and Ru) during corium/concrete

interactions are investigated using GEMINI2 and ChemSheet codes modelling the ACE experiments data.

ChemSheet has been used in different several accident cases earlier (modelling fission products I and Cs chemistry and sump pH). At the moment there is not NUCLEA database available in ChemSheet calculations in VTT. To upgrade ChemSheet code it is important to have the same NUCLEA database that is used in GEMINI2. It is planned to utilize this database in ChemSheet models and also to add viscosity calculation. The model will be used to calculate the viscosity in all HECLA tests done in previous COMESTA project.

Pool pH and nitric acid formation

In severe accident scenario the water vaporized by the melting core flows through compartments where it condenses again. Hydrochloric acid can be formed from organic materials containing chlorine. Cesium hydroxide and cesium iodine are formed from released fission products. Controlling the pH in the containment is important as in acidic conditions radioactive iodine could be formed and released into atmosphere. Injected buffer solutions can be used to keep the pH neutral or alkaline in the pools. Currently MELCOR code is not able to consider aqueous species and how they affect the pH in the pools. ChemPool is a new program to be used with MELCOR to calculate the equilibrium composition and the pH values of the pools. After MELCOR simulation the results from MELCOR are exported to external datafile containing the temperatures, the pressures and the compositions of the pools at each time steps. The estimated formation rates of acids and dissolved salts from fission products are then coupled with these and the equilibrium compositions and the pH values of the pools are calculated with ChemPool. Internally ChemPool uses thermodynamic programming library, ChemApp®, for calculating the equilibrium composition of a thermodynamic system (gas, aqueous water and solids like fission products) by minimizing the Gibbs energy of the system. ChemPool is an easy to use tool for adding simulation of pH chemistry to a MELCOR simulation.

The formation of nitric acid is estimated inside a NPP containment after severe accident using Olkiluoto 1 and 2 BWR as an example plant. Firstly, the selected severe accident progression and some boundary conditions were calculated with the MELCOR 1.8.6 code. The investigated accident scenario was a basic LOCA scenario with a break in the main steam line. Accident sequence was followed until core debris melted a hole in the reactor cavity. Secondly, radioactivity and doses of the most significant radioisotopes in the containment gas phase and water pools were calculated using ORIGEN2 code. Finally, the nitric acid formation and the amount of HCl released were calculated and pHs of water pools were calculated using a new developed ChemPool program. The formation of nitric acid in pedestal pool was 5.6 kg and in wetwell pool 8.7 kg. In water pool of pedestal most of the acid is coming from cables in form of HCl, 117.5 kg. Due this the pH drops rapidly to 2, Figure 1. The influence of nitric acid is small about 5%.

Also in wetwell the formation of nitric acid is small and the pH of wetwell pool stays alkaline due to CsOH. In these results only the formation of nitric acid in water phases was calculated using NUREG/CR-5950 formulas. This formation is very small and it is calculated that the dissolved nitrogen in water phase will be enough and do not limit this reaction.
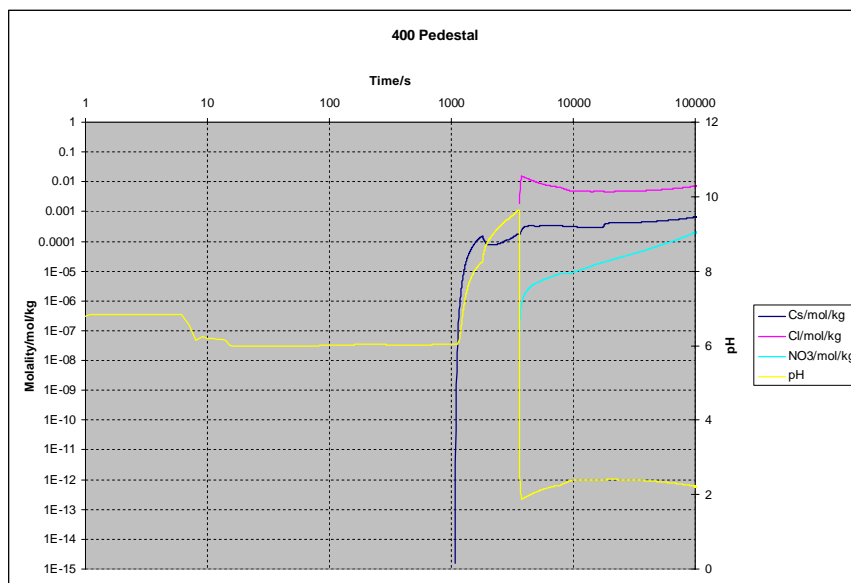

Figure 1. Cesium (CsOH), Chlorium (HCl), Nitrate ion (HNO3) and pH in Pedestal.

To get more data of the nitric acid formation the experimental work has started. The experiments will join gammacell and pool pH assessment capabilities at VTT and Chalmers. First series of tests were performed with a small amount of distilled water and air irradiated in a closed vessel. The first scoping measurements have been carried out at VTT's aged gammacell that does not allow measurements at dose rates expected in containment during severe accidents. The fresh gammacell at Chalmers will facilitate reaching dose rates close to those anticipated in severe accidents. Further, the test will concentrate for sump water compositions specific in Nordic reactors for use in severe accident plant evaluations. The chemical yield (G-value) for a species during the radiolysis of water may vary as a function of several factors in an irradiation system.

Molten corium concrete interactions

Seven molten corium concrete interaction experiments were conducted in the Advanced Containment Experiment (ACE) project in the 1990's. The tests were

made with different concrete types. Ablation rates for the concretes as well as the release fractions for low-volatile fission products and control materials were measured. Test results were compared to calculations of releases made with computer models. The release fractions of low-volatile fission products were significantly lower than the predictions made with the computer calculations. Thermodynamic databases have evolved much since the ACE-experiments were conducted. Under more specific examination are lanthanum, barium, strontium and ruthenium, which the models used in the ACE-experiments had particular problems with.

GEMINI2 software and NUCLEA database (NUCLEA-10_1.GEM) were used to model the ACE-experiments L1 and L6. Experiment L1 was made with limestone/common sand concrete. The initial oxidation of Zr was 70% and the corium mixture was of that used in PWR- plants. Experiment L6 was made with siliceous concrete. The initial oxidation of Zr was 30% and the corium mixture was of that used in PWR- plants.

According to the Gemini- calculations in test L1 it seems that only Ba and Sr, of the elements under special observation, have gaseous species in the temperature range of the tests. However, the calculated amounts of gaseous species are significantly lower than the collected aerosol samples indicate. According to the Gemini- calculations none of the elements under special observation, have gaseous species in the temperature range of the test L6, Figure 2. In the collected aerosol samples Sr, Ba, La and Ru were observed in small amounts. The amounts were lower than those observed in test L1.
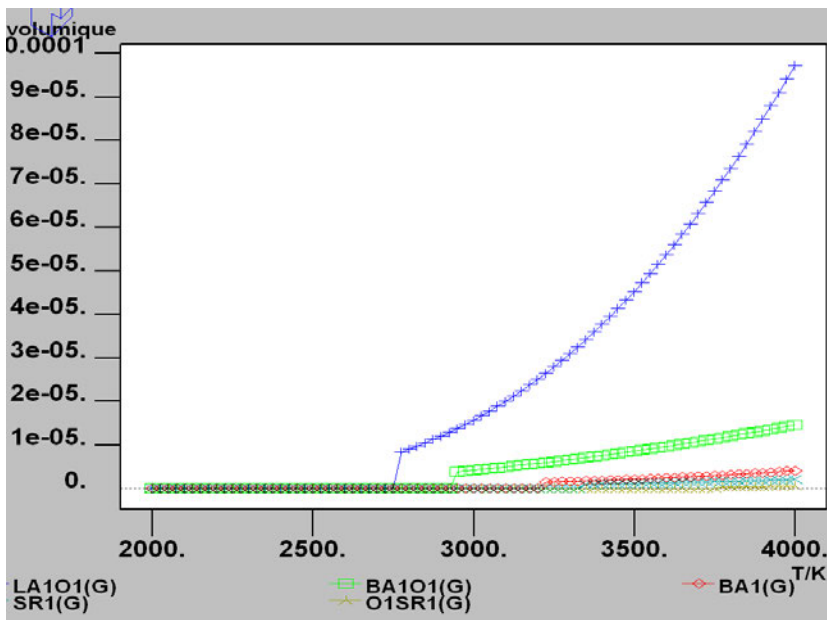
Figure 2. Amounts of gaseous species of La, Ba and Sr on the modelled L6 test.

The viscosity of molten corium

In a severe accident in a nuclear power plant, the core of the reactor melts forming corium, also called lava-like fuel containing material (LFCM). It consists of nuclear fuel, fission products, control rods, structural materials from the affected parts of the reactor, products of their chemical reaction with air, water and steam. If the molten corium cannot be cooled inside the reactor, it will penetrate the reactor pressure vessel and flow into the concrete cavity under the reactor. This causes a molten core – concrete interaction (MCCI). The concrete in the floor and sidewalls of the cavity starts to melt. The process is driven by the high initial temperature of the molten corium and the decay heat that is generated inside the melt by the radioactive decay of the fission products.

The phase composition of the corium at varying temperatures and amounts of steel and concrete can be studied with suitable thermodynamic databases and calculation tools. Since 1990 some people were interested in the assessment of thermodynamical data for a number of compounds of reactor materials and fission products based on the recommendations of a specialists meeting held at JRC-Ispra, Italy in 1990. Critical assessments have been made on a very large number of compounds and systems. NUCLEA is a Thermodynamic Database built for collecting all this knowledge. NUCLEA database is available from ThermoData in France and it is used in GEMINI2 program. NUCLEA database is also available for FactSage version 6.2 database program (TDNucl/2005). FactSage can be used to create a thermodynamic system of selected elements and phases that can be saved as a data-file, and this can then be used with ChemSheet tool in Excel. In this project the thermodynamic calculations of corium system were done with ChemSheet version 1.84.

NUCLEA database (TDNucl/2005) for in- and ex-vessel applications containing 18 + 2 elements was acquired for FactSage database program. A thermodynamic system of selected elements and phases was created from this database for calculations with ChemSheet tool in Excel. First melting temperatures of different concretes were calculated (from HECLA project experiments). Then melting behaviour of corium with different amount of steel and concrete were calculated at different temperatures. In the reactor pressure vessel the molten corium forms two immiscible liquid phases, the lighter oxide rich phase is formed on top and the heavier metal-rich phase on bottom. Then these hot molten phases will penetrate the steel wall of the reactor vessel and flow to concrete cavity causing concrete ablation. CSFoam tool was used to calculate the viscosity of this mixture at various temperatures and compositions. CSFoam tool contains correlations to calculate the viscosity, the surface tension and the density of molten oxide system. The calculation of the viscosity is based on the bonding state of oxygen in molten silicate and the flow mechanism of melts with a network structure. The needed viscosity parameters for uranium oxide (UO_2) and zirconium oxide (ZrO_2) were assessed and added to CSFoam tool. Viscosity model (without UO_2 and ZrO_2) has been validated with chromium and non-chromium containing slags for steel making.

Figure 3 shows the calculated viscosities for HECLA experiments. These have been calculated for the LIQUID#1 phase composition that was earlier calculated

with ChemSheet. In most cases LIQUID#2 phase also existed at equilibrium but its mass fraction was much less than that of LIQUID#1. Viscosities were calculated so that the volume fraction of solid phases was taken into account (although in this case it was probably not needed as the concrete that was still solid didn't exist as precipitated particles). Viscosity for HECLA2 experiment shows very high values compared to others. It has the highest SiO_2 and lowest Fe_2O_3 content and the viscosity is very dependent especially on the silica content, but it still might be out of valid range of the model and in that case the result is not reliable.

Calculated viscosities in HECLA experiments
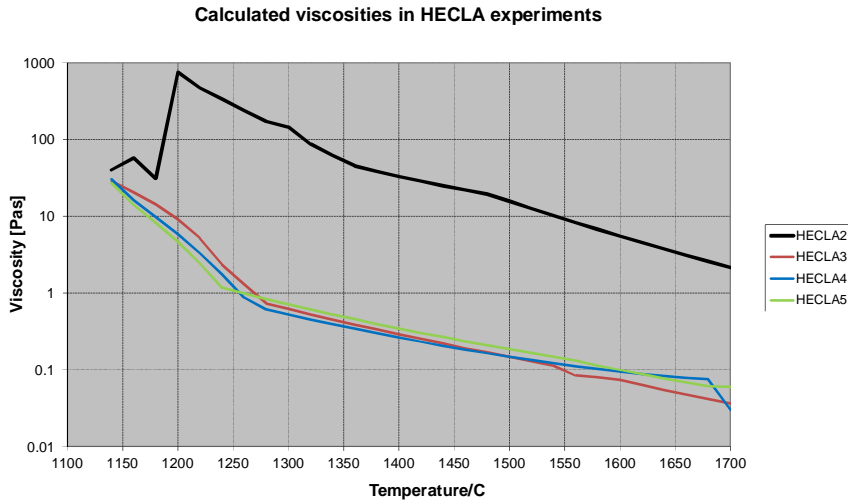
Figure 3. Viscosities in HECLA experiments: calculated with CSFoam using the composition of LIQUID#1 phase calculated by ChemSheet.

Conclusions

ChemPool is a new program to be used with MELCOR to calculate the equilibrium composition and the pH values of the pools. After MELCOR simulation the results from MELCOR are exported to external datafile containing the temperatures, the pressures and the compositions of the pools at each time steps. The estimated formation rates of acids and dissolved salts from fission products are then coupled with these and the equilibrium compositions and the pH values of the pools are calculated with ChemPool. ChemPool is an easy to use tool for adding simulation of pH chemistry to a MELCOR simulation. It is now tested for typical BWR case using Olkiluoto NPP as an example plant. In 2012 the code has upgraded and PWR case calculations have been made for Loviisa NPP.

Gemini- calculations for the ACE-test cases show that the amounts of gaseous Sr, Ba, La and Ru are very small or non-existent; the amounts of species actually observed in aerosol samples were slightly higher. The calculations made in the

ACE-project on the other hand predicted higher amounts of Sr, Ba, La and Ru than were actually measured.

ChemSheet with NUCLEA database and CSFoam are very efficient tools to calculate and study different severe accident scenarios that involve the melting of the core and the formation of different partly molten oxide and metals phases.

References

Beahm, E.C., Lorenz, R.A., Weber, C.F. Iodine Evolution and pH control. NUREG/CR-5950, Oak Ridge National Laboratory. December 1992.

Related publications

Penttilä, K. Chempool, Research report VTT-R-00900-12.

Könönen, N., Rossi, J., Penttilä, K. The formation of nitric acid inside a BWR containment after severe accident, Research report VTT-R-01408-12.

Penttilä, K. Molten corium and concrete thermodynamics and viscosity, Research report VTT-R-01441-12.

Lamminmäki, S. Molten corium concrete interactions – Gemini calculations based on the ACE-project, Research report VTT-R-01532-12.

6.3 Thermal hydraulics of severe accidents (TERMOSAN)

Tuomo Sevón, Anna Nieminen

VTT Technical Research Centre of Finland
Tietotie 3, P.O. Box 1000, FI-02044 Espoo

Introduction

The objective of the project was to improve modeling capabilities on severe accident thermal hydraulics. MELCOR is Finland's main severe accident analysis tool. MELCOR license for Finnish nuclear energy organizations is obtained from the U.S. NRC with the CSARP agreement in the frame of the TERMOSAN project. MELCOR was used for developing a model of the Fukushima accident and for modeling of passive containment cooling systems. The integral code ASTEC has

been adopted in the frame of the project to augment VTT's capabilities to provide a larger variety of independent tools for severe accident studies. Two international OECD NEA research programs, THAI-2 and SERENA-2, were participated in the frame of this project.

MELCOR modeling of Fukushima Unit 1 accident

The Fukushima accident was the world's first severe accident in a BWR. In addition, it was the first time when a severe accident progressed to the ex-vessel phase[3] in a light water reactor of western design. Even though unfortunate, the accident offers a unique opportunity for learning. Current understanding of severe accident phenomena, especially related to BWRs and to ex-vessel events, are based on small-scale experiments. With the help of information from the Fukushima accident, computer models of severe accidents can be tested, improved and validated.

In the TERMOSAN project the first version of VTT's MELCOR model of Fukushima Daiichi unit 1 accident was developed (Sevón 2013). The new MELCOR version 2.1 was used. This was the first full-plant model developed with the new code version at VTT. Until now the previous 1.8.6 version had been used in all VTT's full-plant calculations, but some experiments had been modeled with the new code version. Unit 1 was chosen as the starting point of Fukushima modeling because it is the simplest of the three accidents. All cooling systems were lost due to the tsunami, and the core melting progressed rapidly. At units 2 and 3 turbine-driven pumps injected water to the reactor for some time after the tsunami, and this complicates the modeling of those units' accidents. It is intended to attempt modeling the unit 2 and 3 accidents later.

Available plant data about the Fukushima plant is scarce at the moment. Information was collected from various Japanese publications. Missing pieces of plant data were taken mainly from the Peach Bottom plant in Pennsylvania in the United States. While similar to the Fukushima plant, Peach Bottom is larger: its electric power is 1112 MW, compared with 460 MW at the Fukushima unit 1. Therefore the Peach Bottom data could not be used directly, but it required some scaling, which inevitably increases uncertainties. The Peach Bottom plant has been used as a pilot plant in several American reactor safety analysis projects, lately in the State-of-the-Art Reactor Consequence Analyses (SOARCA) project (Chang et al. 2012). Therefore extensive public information about the Peach Bottom plant is available. Some details about Peach Bottom were not found. These parts of the model are based on crude estimates or guessing. It is intended to update the model when more plant data becomes available.

The accident started with the earthquake at 14:46 Japanese time on March 11, 2011. This was set as time zero in the calculations. The earthquake triggered a

---

[3] Fuel discharge to the containment has not yet been directly confirmed, but it probably happened at least in some of the three units.

reactor scram. At the same time offsite power was lost because the power lines collapsed. Emergency diesel generators were started automatically, and the reactor was cooled with the isolation condenser. 51 minutes after the earthquake the tsunami inundated the site, submerging the emergency diesel generators and much of the emergency power distribution systems, causing a total loss of AC and DC power.

In order to simplify this first version of the MELCOR model, the calculation starts at the time of tsunami arrival. This eliminates the need to simulate the isolation condenser. In order to get the first version of the model finished in a reasonable time, level of detail in the model is somewhat simpler than what the code developers recommend. For example, the reactor core is modeled with three rings (plus bypass) (Figure 1), while the code developers recommend five rings. In total there are 16 control volumes in the reactor coolant system, 5 control volumes in the containment and 4 control volumes in the reactor building.
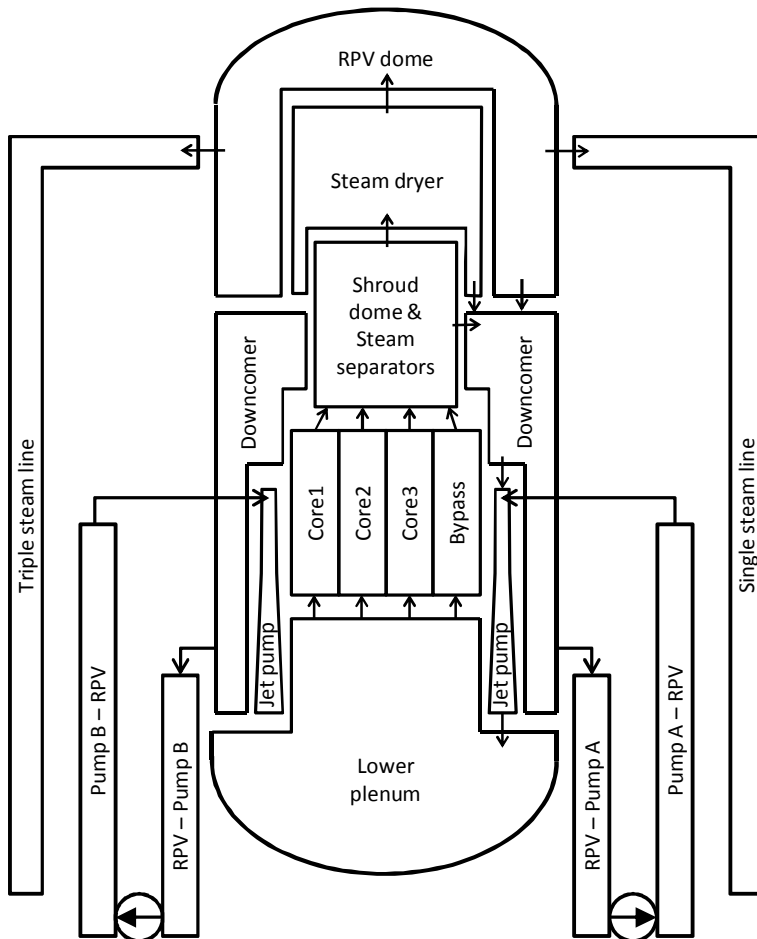
Figure 1. Nodalization of the Fukushima reactor and recirculation and steam lines.

The calculated water level in the reactor is shown in Figure 2. The core uncovery starts 2 h 35 min after the earthquake, and the water level is below bottom of active fuel at 4 h 23 min. The fission product release begins at 3 h 59 min when the peak cladding temperature exceeds 900°C, MELCOR's default temperature for gap release. The core degradation begins at 5 h 15 min, when the control rods start to collapse. The first fuel rod collapse occurs at 5 h 37 min, and eight minutes later there is a major fuel relocation to the lower plenum, causing vigorous boiling and a rapid decrease of the water level in the lower plenum. At 6 h 19 min all water has evaporated from the RPV, and the RPV lower head failure is calculated to occur at 9 h 35 min. State of the reactor at four instants of time is illustrated in Figure 3. The fuel rods in the innermost ring collapse first because the decay heat power is highest in the center of the core.
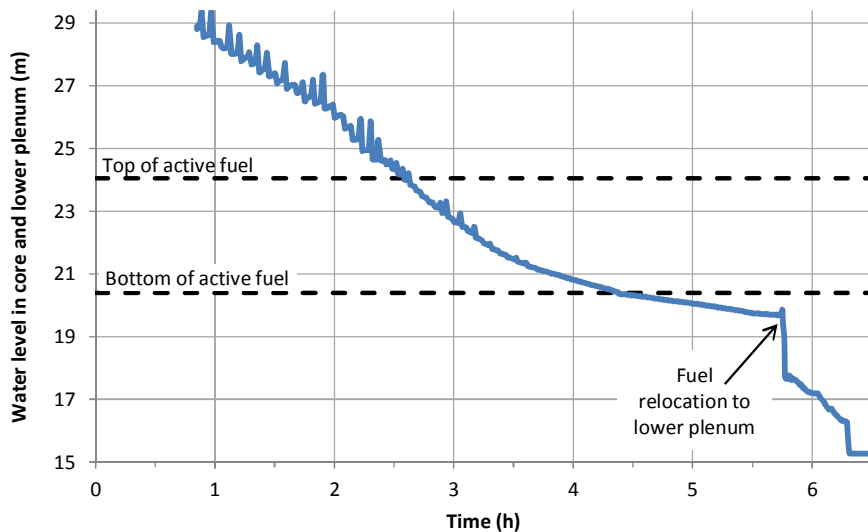
Figure 2. Water level in the core and lower plenum.
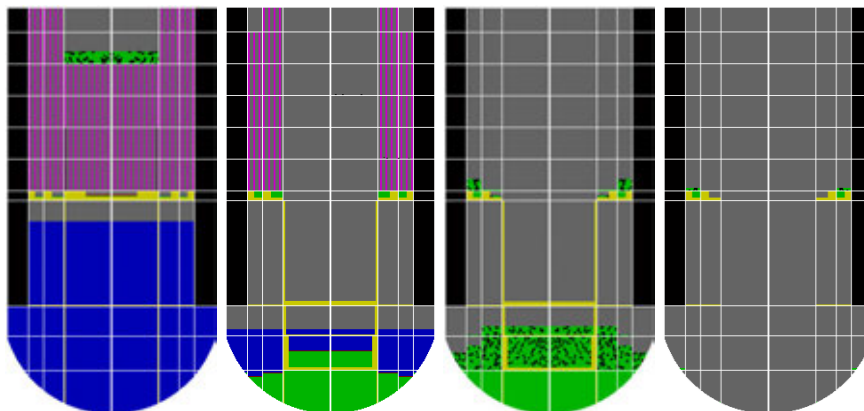
Figure 3. State of the Fukushima reactor at four instants of time: 5 h 38 min, 6 h, 6 h 25 min, and 10 h.

The most important operator actions during the accident were water injection to the reactor and containment venting. The fresh water injection started 15 h after the earthquake. In the beginning the injection rate was very small because the workers had to transfer the water by driving back and forth with the fire engine. After a few hours the workers managed to establish a continuous water injection. At 24 h 7 min the fire protection tank ran out of water and the water injection stopped. 80 000 L of water had been injected by this time. The explosion in the reactor building at 24 h 50 min complicated the efforts to restart water injection. Seawater injection was started at 28 h 18 min. The containment venting was started at about 23 h 30 min and stopped at 24 h 24 min.

The reactor pressure is plotted in Figure 4. In the beginning the pressure is controlled by the safety valve. After the RPV failure the reactor is at about the same pressure as the containment. The containment pressure in Figure 5 is the most interesting variable because it can be readily compared with the measurements. The pressure increases rapidly when the RPV fails at high pressure at 9.6 h, and the match with the two measurement points at that time is good. At 12 h the pressure is underestimated by 0.17 MPa. After 15 h the calculated pressure matches very well with the measurement because the containment leak model and the venting flow path were tuned for that purpose.
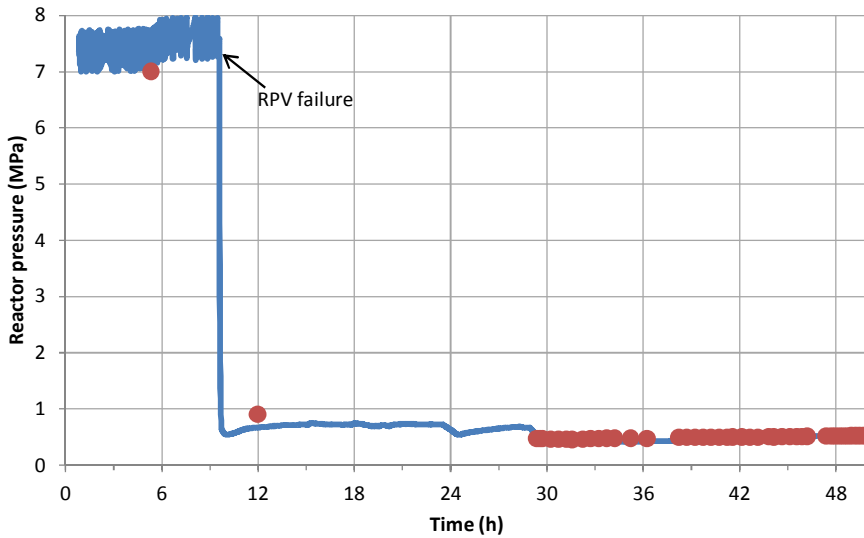
Figure 4. Reactor pressure. The red dots are measurement data, and the blue line is the calculation result.
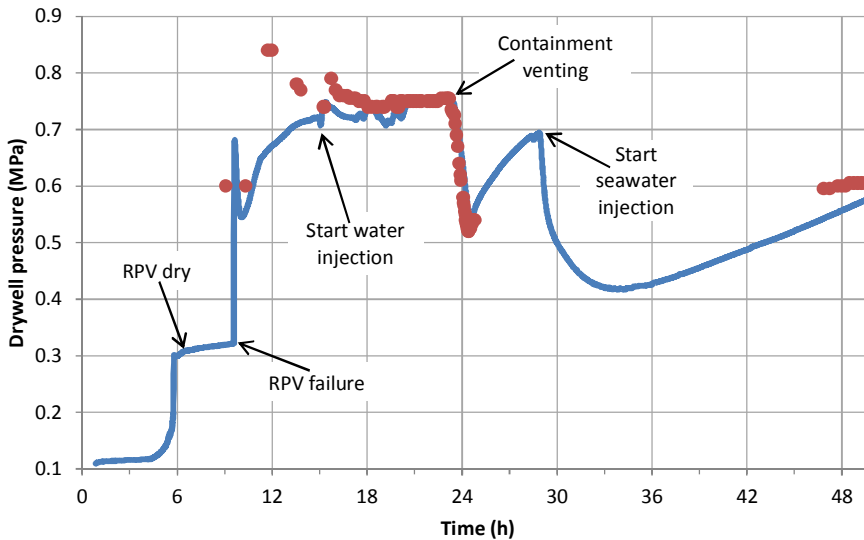

Figure 5. Containment pressure. The dots are measurement data, and the line is the calculation result.

After the RPV failure molten corium is discharged to the containment and the concrete basemat begins to melt. The calculation gives about 1.2 m concrete

ablation at 50 h, and the ablation still continues. Uncertainties at this phase of the accident are so large that this value is little more than a guess.

The calculation gives 19% hydrogen concentration in the top floor of the reactor building at the time of the explosion. This is clearly an explosive concentration, but again the uncertainties of the calculation are very large. Also the radioactive releases to the environment were calculated. It is estimated that, during 50 h, the release fraction was 4E−1 of core inventory for noble gases and 3E−4 of core inventory for cesium. Uncertainties in these numbers are larger than factor of ten.

MELCOR modeling of passive containment cooling systems

Modeling passive containment cooling systems with the MELCOR code was investigated (Sevón 2012). First a literature review of passive containment condenser experiments was performed. Two experiments were selected for MELCOR 2.1 calculations. Simple experiments on condensation and aerosol deposition in a vertical tube (Lehtinen et al. 2002) were used for validation calculations of MELCOR's condensation and deposition models. The calculated condensation rates were within 8% of the measurements. The calculated aerosol deposition was within 10 percentage units from the measurements.

PANDA T1.1 experiment (Paladino et al. 2003), which was conducted at PSI in Switzerland and investigated the ESBWR containment behavior in a severe accident, was calculated with MELCOR. It was found out that careful modeling of drainage of the condensed water in the passive containment condenser is important. With default treatment, the water formed tiny levitating pools inside the condenser. This caused numerical difficulties and serious oscillation to the results. Guiding the condensed water directly out of the condenser eliminated this problem. There was some uncertainty in the amount of helium injected to the PANDA facility. The calculations were made with 75 kg of helium. This amount was inferred from mass spectrometer measurements. According to the test report, 92 kg of helium was injected, but this appears to be an overestimation. It is concluded that MELCOR was able to calculate the condenser performance in the PANDA experiment with 7% accuracy. This is sufficient for using the model in full plant calculations. The calculated pressure is compared with the measurement in Figure 6.
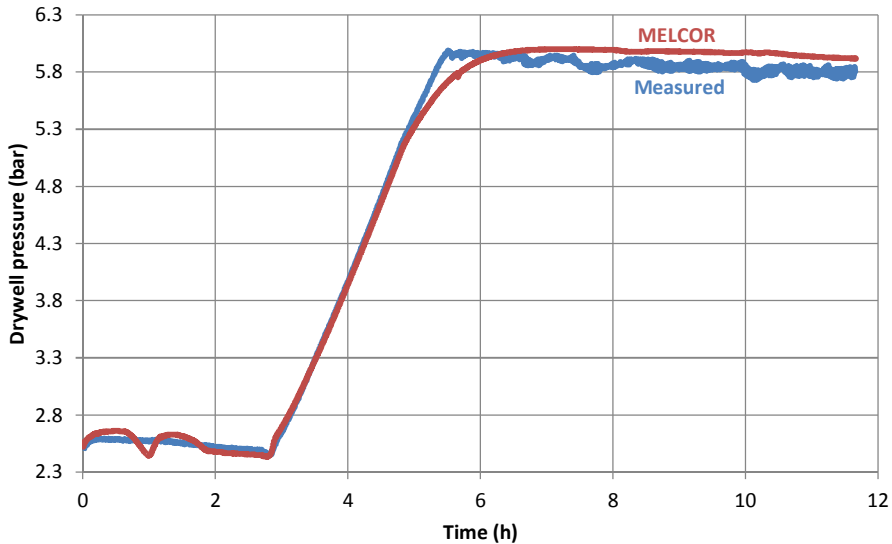
Figure 6. Drywell pressure in PANDA T1.1 experiment. A comparison between measurement and MELCOR calculation.

ASTEC analyses

ASTEC (Accident Source Term Evaluation Code) is an integral code to assess the complete scenario of a hypothetical severe accident in a water-cooled nuclear reactor. The aim of the code is to simulate an entire severe accident sequence from the initiating event through to release of radioactive elements out of the containment. The European ASTEC code is developed since 1996 mainly by the French IRSN and German GRS.

Modeling of melt pool in bottom of reactor pressure vessel

A master's thesis on core-melt behavior inside the reactor pressure vessel during the late-phase of a severe accident was written (Nieminen 2012). The purpose of the study was to evaluate the effects of the accident scenario and the melt composition – in terms of chemical form and melt layering – into the reactor pressure vessel rupture. The study brings the information obtained in the international experimental research program MASCA to the reactor scale. The tool used for the analyses is the ASTEC code. The chemical equilibrium studies for core melt were performed with ChemSheet. It was found that the initial chemical composition of the melt, depending on the accident scenario, has only a minor effect. The melt layer arrangement (Figure 7) was discovered to be the key point when considering the vessel failure and especially the place of rupture.
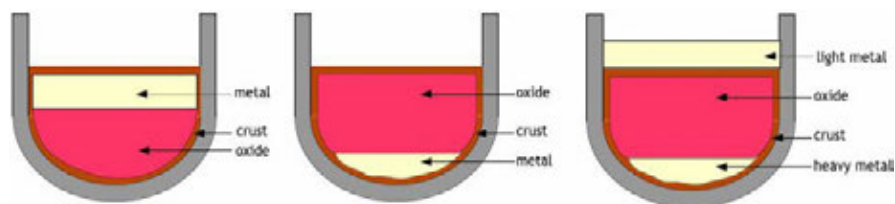
Figure 7. Three possible melt pool configurations in the reactor lower head (Chatelard et al. 2009).

Modeling of PPOOLEX PCCS facility

PPOOLEX test facility, designed and constructed by the Nuclear Safety Research Unit at Lappeenranta University of Technology, is designed for BWR containment and especially condensation studies. Since PCCSs (Passive Containment Cooling Systems) are becoming more common in the next generation BWR concepts, a need for experimental data of the thermohydraulic behaviour of the passive condensers arose for code validation purposes. A PCCS part to the PPOOLEX facility was designed by LUT.

In the frame of the TERMOSAN project, an ASTEC input deck for the PPOOLEX PCCS test facility was created. The purpose was in the first phase to validate the thermohydraulic models for BWR containment against a selected experiment, and then to clarify if it is possible to model a horizontal condenser with a model designed for reactor primary and secondary circuit analyses.

The results on CPA (Containment Part of ASTEC) module validation (Nieminen 2013) were promising. The temperature evolution in the pool and atmosphere were reasonably reproduced by ASTEC. There is an example of the results in Figure 8. The pressure evolution was slightly overestimated by ASTEC, but the difference was small and on the conservative side.

The CPA input deck was then extended with modelling the PCCS condenser with the CESAR module and creating a coupling between these two modules. Also the results produced by the coupled model will be validated against experimental data in the future. The results of the exercise encourage further development of the generated ASTEC model for applications for the future LUT PCCS tests.
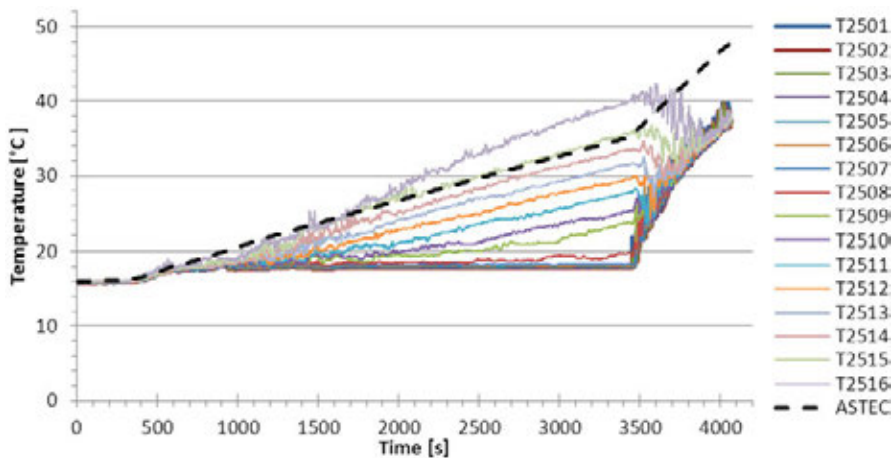
Figure 8. Temperature evolution in the wetwell pool. In the reference experiment there were several measurements points at different levels of the wetwell pool. Since ASTEC is a lumped-parameter code and the pool is modelled as single volume, ASTEC is able to produce only one uniform result for the pool.

International research programs

U.S.NRC CSARP

MELCOR is an integral severe accident analysis code, developed by Sandia National Laboratories. In the frame of the TERMOSAN project, Finland participates in U.S.NRC CSARP (Co-operative Severe Accident Research Program). This provides Finnish nuclear energy organizations with a license for latest versions of MELCOR and the right to participate in the annual CSARP/MCAP meeting.

OECD THAI-2

In the frame of the TERMOSAN project, Finland participates in THAI-2 program. It is an international research program that investigates aerosol and iodine issues and hydrogen behavior. The program is coordinated by OECD NEA, and there are 11 participating countries. The experiment facility is located in Eschborn, Germany, and operated by Becker Technologies. Experiments are performed in four categories:

1. Iodine deposition on aerosol particles. According to current iodine models, a large part of gaseous elemental iodine would be quickly removed from containment air by adsorption on painted surfaces. However, some iodine could deposit on aerosol particles that may remain airborne longer than gaseous iodine. If the containment fails, iodine could be released to the environment along with these aerosols. In the THAI-2 experiments, gaseous

iodine and aerosols are injected into a vessel, and iodine concentration in gaseous and aerosol form is measured.

2. Hydrogen recombiner operation in low oxygen concentration. In the late phase of a severe accident the oxygen concentration in the containment may be low because hydrogen oxidation by burning or in passive autocatalytic recombiners has consumed oxygen. In the THAI-2 program, efficiency of recombiners in low oxygen concentration is investigated.

3. Hydrogen combustion during spray operation. Containment spray condenses steam in the containment atmosphere. This can increase the risk of a hydrogen burn. The spray droplets may slow down the burning by reducing the temperature, or the droplets may accelerate the burning by causing turbulence. This issue is investigated by experiments in the THAI-2 program. These experiments are being calculated with the Fluent code at VTT.

4. Release of gaseous iodine from a flashing jet. If iodine-containing water is released into lower pressure, some of the water evaporates and gaseous iodine may be generated. This phenomenon is related especially to steam generator tube rupture, where iodine could be released from the primary circuit directly to the environment. The amount of gaseous iodine released in the flashing process is measured in the THAI-2 program.

OECD SERENA-2

In the frame of the TERMOSAN project, Finland participated in SERENA-2 program. It was an international research program that investigated steam explosions. The program was coordinated by OECD NEA, and there were 11 participating countries. Seven experiments were performed in the TROI facility in Korea and five experiments in the KROTOS facility in France. They provided experiment data of steam explosions with prototypic corium. The program was finished in 2012.

References

Chang, R. et al. 2012. State-of-the-Art Reactor Consequence Analyses (SOARCA) Report. Draft report for comment. U.S.NRC. (NUREG-1935.) http://pbadupws.nrc.gov/docs/ML1202/ML120250406.pdf.

Chatelard, P. et al. 2009. ASTEC V2 code ICARE physical modelling. IRSN Institut de radioprotection et de sûreté nucléaire, Direction de la prevention des accidents majeurs. (SEMCA-2009-148.)

Lehtinen, K.E.J. et al. 2002. Studies on steam condensation and particle diffusiophoresis in a heat exchanger tube. Nuclear Engineering and Design, 213, 67–77.

Nieminen, A. 2012. Core-melt behaviour inside the reactor pressure vessel during the late-phase of a severe accident. Master's Thesis, Aalto University School of Engineering.

Nieminen, A. 2013. Modelling of PPOOLEX PCCS facility with ASTEC. Research report VTT-R-00386-13.

Paladino, D. et al. 2003. Investigation of light gas effects on passive containment cooling system in ALWR. International Topical Meeting on Nuclear Reactor Thermal Hydraulics (NURETH-10), Seoul, Korea, 5–9 October 2003. Paper F00206.

Sevón, T. 2012. MELCOR Modeling of a Passive Containment Cooling System Experiment PANDA T1.1. Research report VTT-R-01433-12. http://www.vtt.fi/inf/julkaisut/muut/2012/VTT-R-01433-12.pdf.

Sevón, T. 2013. Status Report of MELCOR Modeling of Fukushima Daiichi 1 Accident. Research report VTT-R-00215-13.

6.4 Transport and chemistry of fission products (TRAFI)

Teemu Kärkelä, Ari Auvinen, Jarmo Kalilainen, Pekka Rantanen

VTT Technical Research Centre of Finland
Biologinkuja 7, P.O. Box 1000, FI-02044 Espoo

Introduction

In Fukushima Daiichi nuclear plant cooling of the reactor cores at units 1, 2 and 3 was lost due station black out. Since the cooling could not be restored in time, fuel damage took place in all three reactors and fission products were partly released from the core. As expected in a such severe accident, the highest contribution to the source term to the environment was from iodine isotopes.

Iodine activity in typical reactor core is roughly 750 million Curies. Traditionally, it has been assumed that in a severe accident most iodine would be released from the fuel. Release to the containment would take place mostly as aerosol particles with gaseous fraction of about 5%. Particulate iodine is expected to be removed from the gas phase of the containment by engineered safety systems as well as by natural aerosol processes like settling and diffusiophoresis. Particulate and gaseous iodine would finally end up in sump waters and remain there if alkaline

conditions are maintained. However, most iodides (except AgI, TlI and CuI) are very water soluble. Unfortunately, iodine water chemistry is also very complicated as it is one of the few elements that can assume any of the 8 different oxidation states. In case of acidification of the water from nitric acid formation and other radiolytic processes, molecular iodine would partition back to the atmosphere. It might also form volatile organic iodides. Rate of release from water would increase as the sump temperature would approach the boiling point.

Phébus FP program provided opportunity to test these expectations in iodine chemistry with realistic configurations and chemical environment. In Phébus FP tests iodine was indeed mostly released to the model containment as aerosol particles with gaseous iodine species making up few percent of the overall release. The release rate of iodine as well as aerosol sedimentation were also consistent with current severe accident modelling. Contrary to the expectations, gaseous iodine depleted from the atmosphere much faster than expected in the early phase of the tests. More alarmingly, a steady-state concentration of iodine in containment atmosphere was reached in all Phébus FP tests. The sump pH did not seem to influence the iodine partition in the gas phase. In addition, iodine concentration in the gas phase increased when the sump was condensing and decreased when it was evaporating. One would expect exactly opposite behaviour, if the source of the iodine is from the sump. In addition, silver iodide precipitated in the sump, when AIC control rod was applied in the tests. With B_4C control rod most iodine released in the model containment was in gaseous form.

Based on the results from Phébus FP program a number of hypothesis on iodine behaviour were formulated [1]. It was suggested that:

1) Either the painted surface or the steel walls acted as the source of the persistent gas phase iodine species in the tests.

2) Radiolytic processes destroyed gas phase molecular iodine and organic iodide to form iodine oxide or iodine nitroxe particles. These particles further coagulated and settled or were removed by other natural processes.

3) The source of gaseous iodine from the circuit was either chemical reactions on the gas stream or on the surfaces of the tube walls.

TRAFI-project was launched in SAFIR2014 program in order to test the hypothesized mechanisms. Only by mechanistic understanding of iodine behaviour the consequences of a severe accident can efficiently be mitigated.

Primary circuit chemistry of iodine

It was assumed that chemical reactions either on the gas phase or on primary circuit surfaces may modify the amount, composition and timing of fission product release to the containment. The gas phase reactions are studied at IRSN within ISTP and OECD STEM programs. At VTT the work has concentrated on quantifying the effect of surface reactions on gaseous iodine release from the circuit. The

possible influence of surface reactions on iodine speciation has a direct effect on nuclear safety. At the moment, they are not considered at all in the analysis of severe accidents.

Primary circuit experiments done in years 2011–2012 featured also silver precursor in addition to cesium iodide, molybdenum and boron used in the previous experiments within CHEMPC project. Silver could be present at severe accident conditions since it is one of the widely used control rod materials. Previous studies have also indicated that silver could play a major role in transport of iodine during severe nuclear accidents [2]. Also, previous experiments [3] showed that when CsI reacted with molybdenum species, gaseous iodine would be released at lower temperatures than 650°C. For this reason, some tests in 2011–2012 experiment set were conducted at lower temperatures, such as 400°C or 550°C. The list of 2011–2012 primary circuit experiments is shown in Table 1.

Table 1. List of primary circuit experiments done in 2011–2012.

Experiment	Precursor	Crucible material	Temperature [°C]
1	CsI	alumina (Al_2O_3)	650
2	CsI	alumina (Al_2O_3)	550
3	CsI + MoO_3	alumina (Al_2O_3)	650
4	CsI + Ag	alumina (Al_2O_3)	650
5	CsI + Ag	alumina (Al_2O_3)	400
6	CsI + Ag + MoO_3	alumina (Al_2O_3)	400
7	CsI + B_2O_3	alumina (Al_2O_3)	650
8	CsI + Ag	oxidized AISI 304	650
9	CsI + Ag	oxidized AISI 304	400
10	CsI + B_2O_3	oxidized AISI 304	650
11	CsI + B_2O_3	oxidized AISI 304	400
12	AgI	oxidized AISI 304	650
13	AgI	oxidized AISI 304	400

The experimental work was done using the updated EXSI PC facility [3]. The crucible containing the precursors was heated in the reaction furnace. The furnace tube used in the experiments was oxidized stainless steel (AISI 304). The reaction product particles were collected in PTFE filters with 5 μm pore size, and the gaseous reaction products were trapped in two consecutive bubbling bottles, situated downstream from the aerosol filters. Bubbling bottles contained 0.2 M NaOH and 0.02 M $Na_2S_2O_3$ water solution. The elemental composition of the bubbling bottle and filter samples were analyzed with Thermo Fisher Scientific HR-ICP-MS Element2 Inductively Coupled Plasma Mass Spectrometer. After each experiment, the facility was washed with the bubbling solution and a sample from the wall deposits was collected for the ICP-MS analysis. Experiments contained three different atmosphere conditions, with different fractions of steam, argon and hydrogen, shown in Table 2.

Table 2. Gas flow rates and volume fractions to the reaction furnace, used in the primary circuit experiments (NTP conditions 0°C and 1013 mbar).

		Condition		
		A	**B**	**C**
Argon	Flow rate [l/min] (NTP)	3.3	3.2	2.9
	Gas vol-%	90	88.3	79.2
Steam	Mass flow rate [g/min]	0.2	0.2	0.2
	Gas vol-%	10	10	10
Hydrogen	Flow rate [l/min](NTP)	0	0.1	0.4
	Gas vol-%	0	2.7	10.8

When the temperature of the furnace was dropped from 650°C to 550°C with CsI precursor in experiments 1 and 2, the release of iodine containing aerosol particles decreased significantly. At 550°C, a small amount of gaseous iodine was released but the overall release of iodine was significantly lower in experiment 2 than in experiment 1.

Experiments 4 and 5 featured CsI and silver precursor with furnace temperatures 650°C and 400°C, respectively. In experiment 4, the overall release of CsI aerosol particles was in same level and overall gaseous iodine release was less than observed experiment 1. Also, a small amount of silver was found in aerosol form, probably transported to the filter as AgI. In experiment 5, the gaseous iodine release was much higher compared to the previous higher-temperature experiment and almost no iodine containing aerosol particles were formed, since the lower furnace temperature significantly reduced vaporization of Cs, I and Ag compounds. Similar behaviour to experiment 5 was seen as MoO_3 was added to the precursor in 400°C temperature in experiment 6.

Experiments 8 and 9 featured same precursors as experiments 4 and 5 with the exception the chronological order of athmospheric conditions in the reaction furnace was reversed (from C to A). Mass concentrations experiments 8 and 9, obtained from the bubbling bottle and filter samples, are shown in Figure 1. When the temperature of the reaction furnace is lowered from 650°C to 400°C CsI particles are no longer found from the aerosol filters but a significant fraction of iodine is still released in gaseous form. Similar effect was also observed when CsI + MoO3 precursor was tested at 400°C [3]. The trends of iodine release in experiments 4, 5, 7 and 8 were similar with the exception of higher mass concentration of CsI particles observed in experiment 8 than in experiment 4. The mass concentration of gaseous iodine was also higher in experiment 5 than in experiment 9.

The release with CsI + B_2O_3 at 650°C in experiment 10 coincided with the result form previous experiment [4] with identical initial conditions. Also, cesium borate glass surface was again formed to the reaction crucible surface. High gaseous iodine fraction was caused by boron trapping most of the cesium to the reaction crucible, which was also seen in the previous experiment [4]. When the reaction

furnace temperature was lowered to 400°C in experiment 11, the gaseous iodine release was increased significantly.
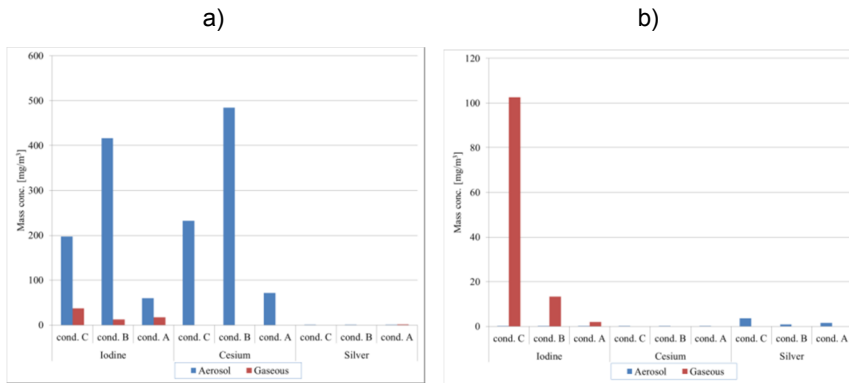
a)   b)

Figure 1. Iodine, cesium and silver mass concentrations in experiment 8 (a) and 9 (b), calculated from aerosol filter and bubbling bottle ICP-MS data. Condition A has Ar H_2O atmosphere where conditions B and C contain also H_2. Iodine was released in gaseous form.

Containment chemistry of iodine

One of the most surprising results of the Phébus FP program was the observed fast destruction of gaseous iodine within the containment atmosphere. It was assumed that radiolytical processes may lead to formation of iodine oxide particles. This has been studied in the previous CHEMPC project (SAFIR2010) by exposing gaseous organic iodine to gamma radiation [5]. Several complementary test were also conducted where inorganic and organic iodine were exposed to ozone and UV (c-type) radiation [6, 7]. The focus in TRAFI has been on the radiolytical oxidation of iodine by beta radiation, which causes the highest fraction of absorbed dose in the gas phase of containment [8]. Another task has been to find out the speciation of iodine oxide particles on various containment materials (paints, metals) after reacting with the surface and the desorption of iodine from iodine oxide deposits on the surfaces. This has been studied in collaboration with Chalmers University of Technology within SAFIR2014 and Nordic Research on Nuclear Safety (NKS-R) programs. The basic studies on iodine oxidation at VTT have already lead to a new filtration system, which can be applied to trap both gaseous elemental iodine as well as organic iodides. The efficiency of the system is currently evaluated in EU PASSAM project, which aims at demonstrating the ability of innovative systems to achieve larger source term attenuation.

Radiolytical oxidation of gaseous iodine by beta radiation

The first experiments on the radiolytical oxidation of gaseous iodine were conducted within a new test facility – built at VTT. The reaction chamber was made of

glass and a source of beta radiation (P-32, activity 5 mCi) was placed at the bottom. The residence time of the gaseous sample in the radiation field, the composition of the gas flow and the temperature of the facility could be adjusted. In the experiments, gaseous methyl iodide (CH_3I) was exposed to beta radiation in various mixtures of oxygen and nitrogen. The results of the experiments at 20°C revealed that as an outcome of radiolytical oxidation the nucleation of particles took place and the diameter of particles was very small, c.a. 10–50 nm. However, particles seemed to react with the humidity of air and dissolve/decompose very rapidly. A Scanning Electron Microscopy micrograph of solid, partially dissolved and dissolved particles on a nickel/carbon grid is presented in Figure 2. Since the formed particles were highly water soluble and volatile, it was very difficult to analyse their properties with SEM-EDX.
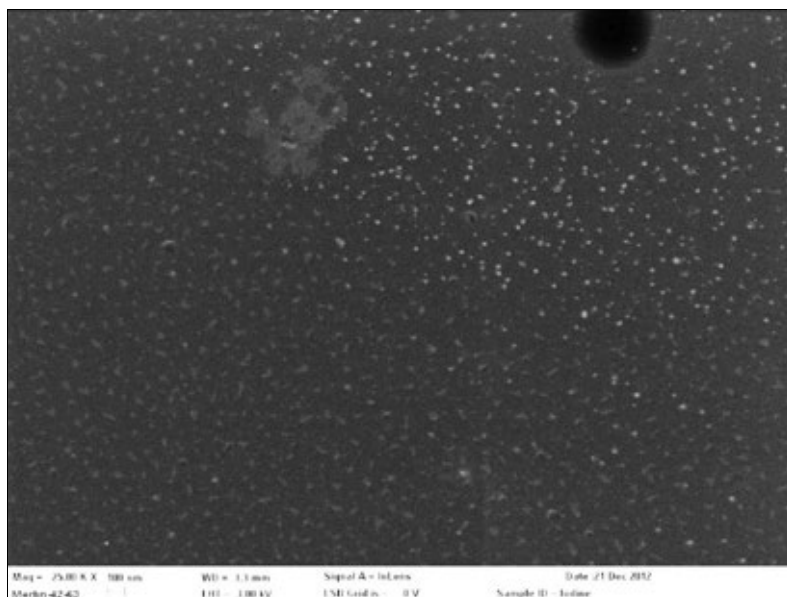
Figure 2. A SEM micrograph of solid, partially dissolved and dissolved iodine oxide particles collected directly from a gas phase on a nickel/carbon grid.

Analysis of iodine oxide deposits on containment surface materials

In order to validate the source of gasous iodine in the containment samples were prepared for iodine desorption studies. If iodine is assumed to form iodine oxide particles within the containment atmosphere, representative samples should be prepared by depositing the said particles on the substrates.

A set-up to produce iodine oxide particles and to deposit them on surface samples (15 mm x 15 mm x 0.25–1 mm) was designed and built. The surfaces exposed to IOx particles were paint (Teknopox Aqua V A), stainless steel (316),

copper, zinc and aluminium. The iodine oxide particles in the gas phase, produced by the reaction of ozone and gaseous elemental iodine, were mainly in the chemical forms of I_2O_4 and I_4O_9 when the reaction temperature was below 100°C. This conclusion is supported by the yellow colour of the particles on the filter sample. Both iodine oxides decompose to I_2O_5 and I_2 upon heating, which were observed in the Raman spectra. Therefore, the iodine oxide particles on the filter sample were originally most likely I_2O_4 or a mixture of I_2O_4 and I_2O_5. The particles for deposition on the surface materials were synthesized at 120°C. At this temperature, the formation of I_2O_5 is more likely especially as both other oxides decompose to I_2O_5. The deposit on the samples also had a lighter colour than of those collected on a filter sample. When I_2O_4 and I_4O_9 particles react with humidity they form HIO_3 and I_2. After exposure to humid air, I_2O_5 is rapidly converted to its partially hydrated form $I_2O_5 \cdot HIO_3$, also defined as HI_3O_8. On the other hand, the same product is formed when HIO_3 is partially dehydrated. The observed decomposition reaction was faster than reported in the literature [9] and is assumed to be caused by a smaller diameter of the iodine oxide particles.

With Raman and XPS analysis no chemical reactions of iodine oxides with the stainless steel surface and painted surfaces could be identified. According to the recorded Raman spectra the form of iodine seemed to be partially hydrated $I_2O_5 \cdot HIO_3$ on steel and painted surfaces. In addition, both Raman and XPS analysis found molecular iodine (I_2), which is likely to be formed due to decomposition of I_2O_4 and I_4O_9 particles on the surfaces. The iodine deposit on the aluminium surface was only studied with Scanning Electron Microscopy coupled with Energy Dispersive X-ray analyzator (SEM-EDX). There was no obvious reaction with the aluminium surface detectable.

On copper and zinc samples the peaks of solid HIO_3 and molecular iodine were detected in the Raman spectra. The results of the XPS analyses also suggested reactions between the iodine oxide deposit and the surface on both samples. This may relate to the fact that zinc forms water soluble iodide (ZnI_2). In contrast copper forms water insoluble iodide (CuI). The reaction seemed to be more extensive on the zinc surface, for which no chemical form of oxidised iodine could be identified with XPS. The analysis of elemental concentration of the deposition showed that zinc has reacted all through the deposit layer. Whereas a small amount of copper can also be found in the centre of the deposition indicating that the iodine oxide deposit has partially reacted with the copper surface. The differences between the Raman and XPS results may be caused by the fact that the signal for XPS comes from a layer that is only a few nanometres deeper than the surface. The SEM-EDX analysis of the copper sample (see Figure 3) suggested that, when the deposit layer was thin, areas with CuI crystals (spot analysis #2) were mixed with areas with HIO_3 formation (spot analysis #1). As the deposit layers became thicker these two compounds seem to have formed a rather homogeneous grain-like structure.
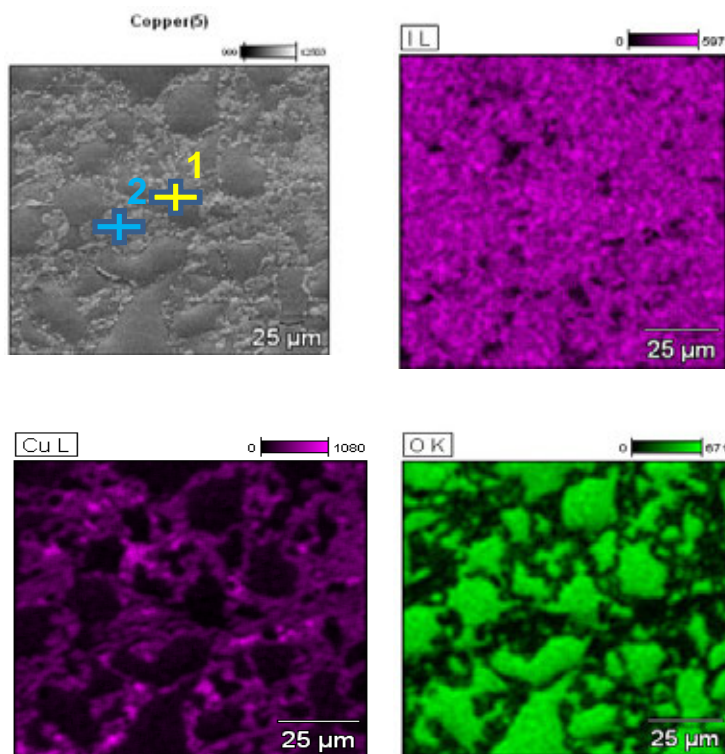
Figure 3. A SEM micrograph with two EDX spot analyses locations and an EDX map of iodine oxide deposition on copper sample in the area of crystalline deposit with pool-like structures.

The desorption of iodine from ^{131}I labelled iodine oxide deposits on paint and metal surfaces was observed to take place when the samples were exposed to heat, humidity and gamma irradiation. Humidity was shown to be the major factor for the revaporisation. The release rate of iodine seemed to be rather similar on all the surfaces. Therefore, it was obvious that the iodine desorption observed was mainly encountering on outer layers of multi-layer deposits and the effect of surface on the reaction remained unclear. This will be examined with mono-layer deposition samples in future.

Turbulent deposition of fission products

The deposition of fission products on the walls was significantly higher than expected in Phébus FP program. One hypothesis to explain the high deposition was that turbulent flow might have increased the fraction of wall deposition within the

model containment. The effect of turbulence on particle deposition is tested at PSI by modelling the flow using DNS and LES tools. These models are validated against experiments carried out at TRAFI –project. Similar turbulent natural convection flows will develop in real containment building due to temperature gradients.

The phenomenon of particle deposition in a cubic cavity with turbulent natural convective flow has been investigated at Paul Scherrer Institut using Direct Numerical Simulations (DNS) [10] and Large Eddy Simulations (LES) [11]. The main aim of this investigation is to experimentally determine the fluid motion, temperature fields, and particle motion inside a differentially heated cavity. Special emphasis is to enable validation of models used in LES, as well as enable comparison with earlier computational work using DNS.

DIfferentially heated cavity with **A**erosol in turbulent **NA**tural convection (**DIANA**) facility was constructed for measurements of particle depositions on a turbulent natural convection. The facility was designed to allow flow field measurements with Particle Image Velocimeter (PIV) as well as inside gas temperature measurements. Also in the future work, on-line aerosol devices can be used for particle concentration measurements. DIANA facility is a cubic with heated and cooled vertical walls with constant temperatures and top bottom and lateral walls with close to adiabatic boundary conditions. DIANA facility was designed to allow measurements using $Ra = 10^9$, which was also used in the simulation works [10, 11].

Gas temperature measurements were done using a K-type thermal couple with wire diameter 50 μm. The front glass walls of the cavity were replaced with two polyurethane sheets with a slit at desired measurement height. The thermal couple was inserted to the cavity through the slit. Translation stages were used to move the thermal couple. Wall temperatures were measured with 0.13 mm K-type thermal couples. Particle Image Velocimetry (PIV) was used for the gas flow velocity measurements. In PIV, the flow field is determined from the movement of large number of particles following the flow. The fluid velocity is computed from two successive images, taken from the illuminated portion of the flow, using a cross-correlation method. Particle or droplet feeding to the cavity is done from the bottom of the cavity. Copper tube with 10 mm diameter is inserted to the cavity through a hole in the glass at 350 mm from the front glass and 100 mm from the hot wall.
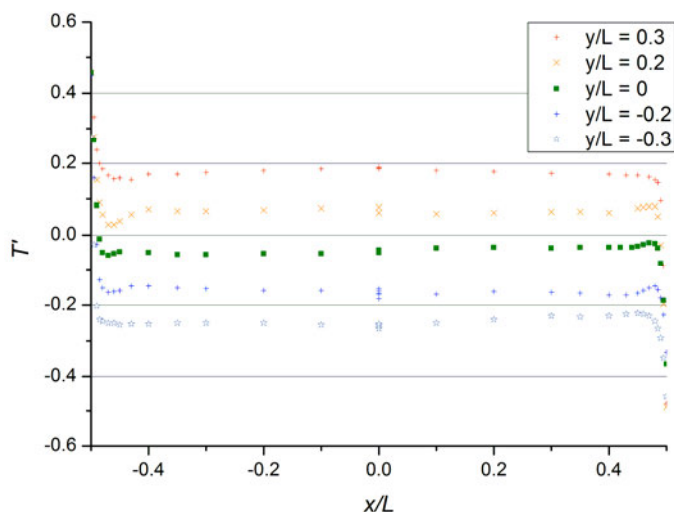
Figure 4. Horizontal temperature profiles, measured at five different heights of the DIANA cavity.

Figure 4 shows the average temperatures measured at five different heights from the DIANA cavity. Two or more measurements were done at the horizontal midpoint ($x/L = 0$) in every height to insure that the average temperatures in each measurement point remained nearly constant throughout the measurement. The temperatures at the cavity core are almost stratified. Significant changes to the temperatures at the specific profile only appear near the isothermal walls.

The temperature measurements differed significantly from the DNS results [10] obtained in the previous DHC work. The scoping studies made with Ansys Fluent 14.0 software suggested that the thermal radiations heat transfer should be taken into account in the DHC simulations. Future work will contain a more accurate Fluent simulations aiming to produce data that can be compared with the measurements.

The velocity measurements showed that the highest average velocities in the DIANA cavity are found near the hot and cold walls. The flow is pressed closer to the walls near the vertical boundaries, while at the horizontal walls, the slower moving flow stretches further to cavity centre. Also, recirculating flows are present at the horizontal walls, nearer to the cavity centre. The average velocities at the x-y plane of the DIANA cavity combined from all PIV measurements, are shown in Figure 5. The core of the cavity is almost stagnated compared to the circulating flow near the horizontal and isothermal walls.
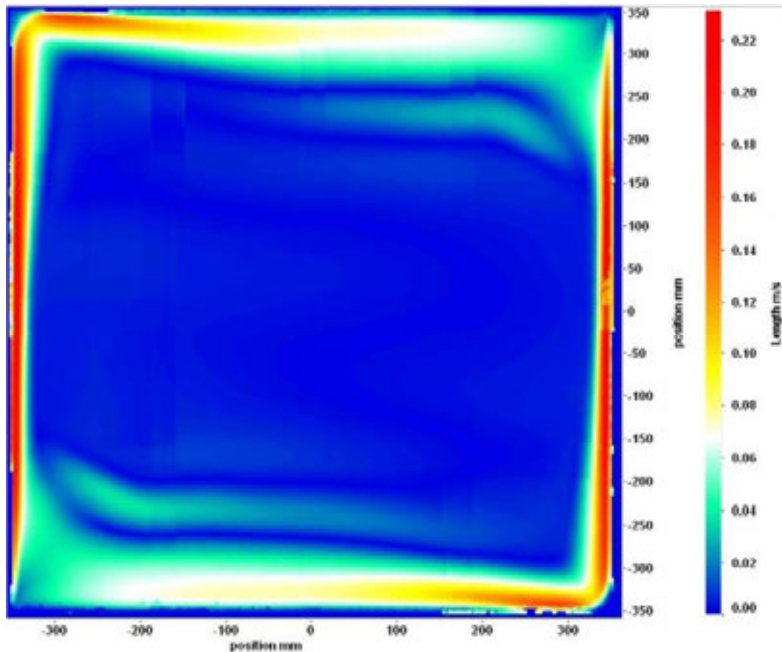
Figure 5. Average velocities at the x-y plane at 330 mm from the front adiabatic wall of the DIANA cavity.

Conclusions

Phébus FP program raised a number of questions that could not be answered by the current severe accident analysis tools. Based on the experimental observations several hypothesis e.g. on iodine behaviour in the primary circuit as well as within the containment were formulated. These hypothesis must be experimentally tested and not just parameterized.

Some of these hypotheses have been experimentally verified in TRAFI project. One of the uncertainties was the effect of reactions on primary circuit surfaces on the fraction and timing of iodine release into the containment atmosphere. In the experiments at VTT, a difference in the release of iodine in the primary circuit conditions at 400°C, 550°C and 650°C temperatures was detected. Iodine seemed to be released almost completely in gaseous form at lower temperature despite the used precursor mixtures. This suprising observation suggests that the FP deposits on the surfaces of primary circuit may act as a source of volatile iodine for a long period since the beginning of severe accident.

Preliminary results on the radiolytical oxidation of gaseous organic iodine by beta radiation, and previous complementary experiments with ozone, gamma and UV radiation within CHEMPC project, verified the formation of aerosol particles, which was one of the formulated hypothesis after Phébus FP experiments. The

diameter of nucleated particles ranged from c.a. 10 nm to 50 nm. These very small particles were highly water soluble and volatile.

The results on the analysis of iodine oxide particles behaviour in the containment conditions suggested that air radiolysis and following oxidation of gaseous iodine would most likely lead to a formation of I_2O_4, I_4O_9 and I_2O_5 particles depending on the reaction temperature. Since the humidity of atmosphere would be high due to water from the evaporating containment pools and containment sprays, these iodine oxides would decompose to a mixture of HIO_3 and $I_2O_5 \cdot HIO_3$ particles and I_2. In case iodine oxide particles react with metal surfaces, metal iodides could be formed as is suggested in this study. Also, organic ingredients of paint films can react with iodine and form strong bonds with iodine aerosols. The desorption of iodine from ^{131}I labelled iodine oxide deposits on paint and metal surfaces was observed to take place when the samples were exposed to heat, humidity and gamma irradiation. Humidity was shown to be the major factor for the iodine desorption.

The studies on the deposition of FP aerosol particles on the walls of containment by natural turbulent convective flows are on-going. A novel DIANA facility equipped with a PIV laser was built and the flow and temperature fields inside the facility are determined. In the next phase, the deposition of particles will be examined. DNS and LES models will be validated with the data gathered and CFD correlations will be prepared.

The experiments conducted in TRAFI project have produced new information on the chemistry and transport of iodine in severe accident conditions. These results are needed e.g. in order to explain the observed behaviour of iodine in the experiments of Phébus FP program. However, the most important impact of these results will be on the development of severe accident analysis codes. Previously, the lack of information has prevented to taking into consideration the FP deposits on primary circuit surfaces and iodine oxide particles both in the containment gas phase and on the containment surfaces as a short and long term source of volatile iodine.

The information on the iodine chemistry developed in CHEMPC and TRAFI projects have been utilized e.g. in the development of electric filtration technique for gaseous iodine species. The efficiency of this Finnish innovation is currently evaluated in EU PASSAM project.

References

1. Lee, R.Y., Salay, M. 2008. Phébus-FP Findings on Iodine Behaviour in Design Basis and Severe Accidents, Presented to the Advisory Committee on Reactor Safeguards 8.5.2008, U.S.NRC.

2. Girault, N., Dickinson, S., Funke, F., Auvinen, A., Herranz, L., Krausmann, E. 2006. Iodine behaviour under LWR accident Condition: Lessons learnt from analyses of the two Phebus FP tests. Nuclear Engineering and Design 236(12), 1293–1208.

3. Kalilainen, J., Kärkelä, T., Rantanen, P., Forsman, J., Auvinen, A., Tapper, U., 2011. Primary circuit chemistry of iodine. SAFIR2010, The Finnish Research Programme on Nuclear Power Plant Safety 2007–2010, Final report. VTT Technical research Centre of Finland, Finland. Pp. 312–320.

4. Kalilainen, J., Kärkelä, T., Zilliacus, R., Tapper, U., Auvinen, A., Jokiniemi, J. Chemical reactions on primary circuit surfaces and their effect on fission product transport in a severe nuclear accidents. Submitted to Nuclear Engineering and Design.

5. Kärkelä, T., Holm, J., Auvinen, A., Kajolinna, T., Glänneskog, H., Ekberg, C., Jokiniemi, J. 2011. EXSI facility – Experiments on radiolytical oxidation of CH_3I by gamma radiation. VTT-R-00527-11.

6. Kärkelä, T., Holm, J., Auvinen, A., Ekberg, C., Glänneskog, H., Tapper, U., Zilliacus, R. 2009. Gas phase oxid ation of elemental iodine in containment conditions, 17th International Conference on Nuclear Engineering, ICONE17. Brussels, 12–16 July 2009. ASME. Vol. 2. Pp. 719–727.

7. Holm, J., Kärkelä, T., Auvinen, A., Glänneskog, H., Ekberg, C. 2010. Experimental study on iodine chemistry (EXSI) – Containment experiments with methyl iodide, NKS-220.

8. Bosland, L., Cantrel, L., Girault, N. 2010. Evaluation of the dose rate inhomogeneities in PHEBUS containment during FPT1 and FPT3 tests, 31th CCIC meeting.

9. Vikis, A.C., Macfarlane, R. 1985. Reaction of iodine with ozone in the gas phase. J. Phys. Chem. 89, 812–815.

10. Puragliesi, R. 2010. Numerical Investigation of Particle-Laden Thermally Driven Turbulent Flows in Enclosure. Ph.D. Thesis, Eo: 4600, Ecole Polytechnique Federale de Lausanne, Lausanne.

11. Bosshard, C. Large Eddy Simulation of Particle Dynamics Inside a Differentially Heated Cavity. 2012. Ph.D Thesis, Eo: 5297, Ecole Polytechnique Federale de Lausanne, Lausanne.

6.5 Reactor vessel failures, vapour explosions and spent fuel pool accidents (VESPA)

Niina Könönen[1], Kari Ikonen[1], Mikko Patalainen[2]

[1]VTT Technical Research Centre of Finland
Tietotie 3, P.O. Box 1000, FI-02044 Espoo

[2]VTT Technical Research Centre of Finland
Kemistintie 3, P.O. Box 1000, FI-02044 Espoo

Introduction

VESPA (Reactor Vessel failures, vapour Explosions and Spent fuel Pool Accidents) project binds together three different fields of nuclear safety and severe accident management: Structural integrity, steam explosions and spent fuel pool accidents. The project itself consists of three main tasks.

One of the goals was to investigate the applicability of a commercial code Abaqus for modelling reactor pressure vessel lower head failures. The aim was to compare the results with a specific code PASULA developed at VTT. An additional objective was the knowledge transfer from senior scientists in training a new expert to mechanical analyses of RPV lower head under severe accident conditions.

The second task was to evaluate steam explosion loads for PWR and BWR cavities with TEXAS V and MC3D codes. A target was to train a new code user and expert on vapour explosion area. This task of VESPA project was connected to several international programs, such as EU SARNET2 WP 7.1 project and currently on-going OECD/SERENA2 project. Furthermore, VESPA project provided the Finnish contribution to the Task 8 of the NKS project DECOSE (Debris Coolability and Steam Explosions) in 2012.

The third purpose of the project was to develop an analysis tool for studies of loss of cooling accidents in spent fuel pools in the reactor building. The work in this task was concentrated in the development of the PANAMA code. Also the applicability of MELCOR code to spent fuel pool accidents was being assessed. MELCOR was used for modelling several different spent fuel pool accident scenarios for a Nordic BWR.

Benchmarking Abaqus against PASULA code

In this task the applicability of a commercial finite element code (Abaqus) for modelling large deformations of a reactor pressure vessel at high temperature was studied. The first aim was to compare the results obtained with the commercial code with the specific code (PASULA) developed at VTT. The PASULA code was

developed to estimate the large deformations and possible failure time of the RPV during a severe nuclear accident and other similar cases.

The Abaqus code was utilised to simulate a core melt scenario of a small scale pressure vessel that was experimentally tested in the Sandia OLHF-1 experiment. The OLHF-1 experiment was chosen as a benchmark case for the simulation of the pressure vessel rupture during nuclear accident. The PASULA code was utilised in that benchmark as well and was used in this work as a reference for the result comparison. Also the results obtained by the other participants of the benchmark were compared within the limitations of the available data provided in literature.

An axisymmetric FE-model was generated in the current computation according to the geometrical details from the OLHF-1 experiment. Temperature dependent material properties provided in the OLHF-1 benchmark specifications were utilised in the simulation. The thermal loading was modelled using measured temperature data which was interpolated to the nodes of the FE-model using a specific Fortran subroutine. Internal pressure and gravity load were also utilised in the model.

The results of the simulation indicated that the pressure vessel is exposed to high thermal stresses that are caused by the temperature difference between the internal and the external wall surfaces. Even small changes in the temperature difference caused stress peaks in the structure. The integrity of the vessel was maintained well until about 150 minutes. Prior to the rupture the non-reversible deformations of the vessel begun to occur with increasing rate until the rupture was reached in the simulation after 174 minutes. In the experiment the rupture occurred after 192 minutes.

The main result of the current simulations was the vertical displacement of the lower head bottom, which was computed relatively well by Abaqus prior to the rupture (Figure 1). The vertical displacement result obtained in this work fits well in the variety of the OLHF-1 benchmark calculated and measured results as well as the results from the PASULA simulation. In conclusion, commercial finite element code Abaqus is suitable for modelling large deformation at high temperature. The results are highly dependent on the utilised material parameters that need to be verified by experimental test data.

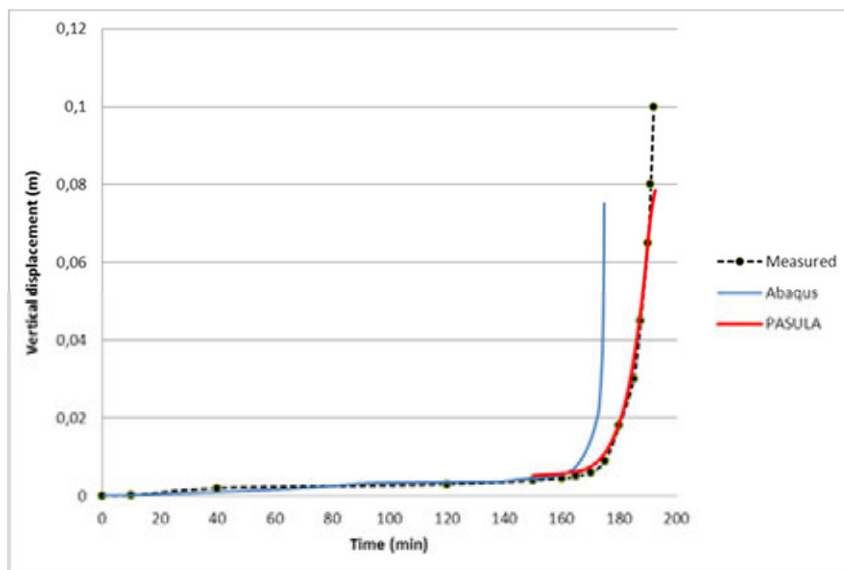Results from this task were reported as VTT research report [1].

Figure 1. Vertical displacement of the pressure vessel lower head. Figure shows the measured values as well as the simulated values for Abaqus and PASULA codes.

Vapour explosion analysis with TEXAS V

This task of VESPA/SAFIR2014 project concentrated on the use of a FCI code TEXAS-V. Co-operation was done with Swedish KTH during the project. In November 2012 a visit was organised at the KTH facility in Stockholm. The goal of the visit was to learn the use of the code and discuss upcoming issues. During the visit a post-processing script was written and three different reference cases were determined for calculations.

From the calculations it was concluded that with the predetermined reference case parameters steam explosions can occur in the simulation. The maximum explosion was obtained in the CRGT Failure scenario with a melt jet diameter of 0.07 m (Figure 2). At the distance of 3.68 m from the centre of the cavity the maximum detected pressure was 257 bar and the maximum impulse was 51.5 kPas (Figure 3). An extrapolation method is still needed for evaluating the loads on cavity walls.
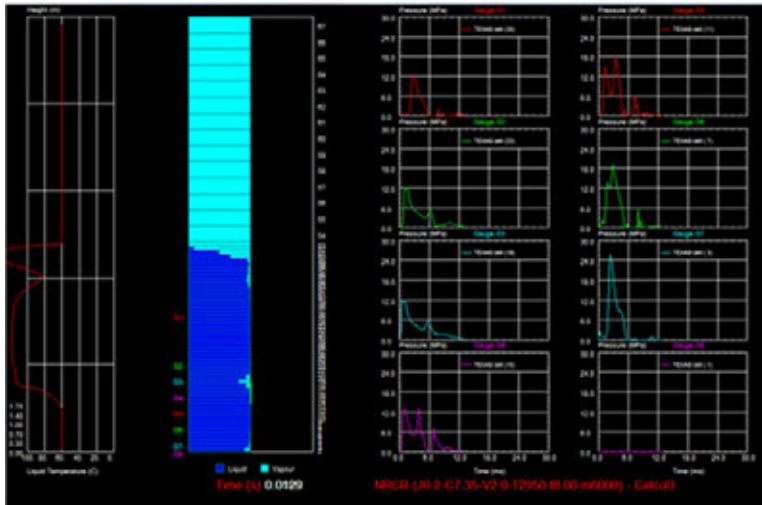
Figure 2. End of explosion phase in TEXAS-V for CRGT failure scenario.
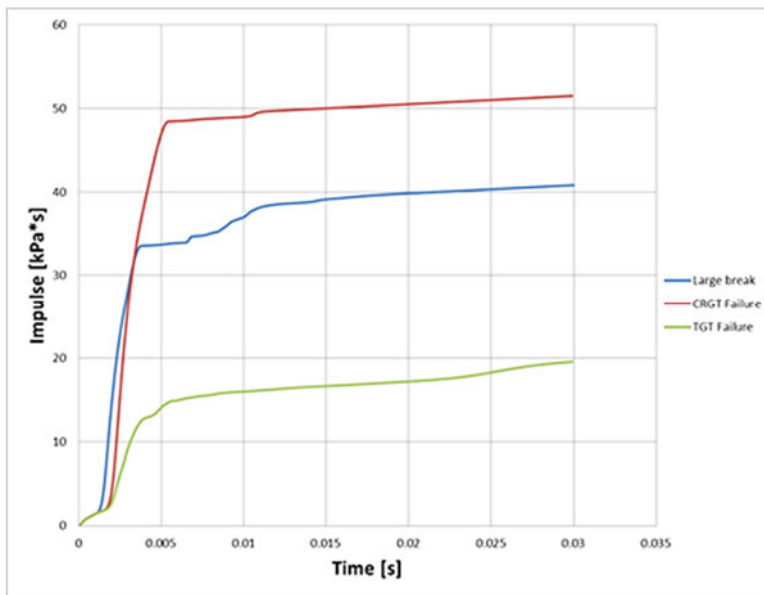
Figure 3. Maximum impulses obtained in different steam explosion scenarios.

The work done with TEXAS-V has been extremely useful and educational. TEXAS-V is in theory a simple code to use. Generating a basic input is simple and the graphic interface is very helpful during the constant iterating. For a steam explosions novice this is a good program to start with. However, there are many

modelling related things you need to know before using TEXAS-V. Luckily, many of these problems were solved during this work and the use of TEXAS-V has become more straight-forward.

Results were reported as VTT research report [2].

Development of PANAMA

Accidents leading to loss of coolant in the spent fuel storage plant have gained international interest during the recent years. Later the events at Fukushima plants in Japan have increased this interest. There is a need to study related phenomena in a more detailed way. Thermal-mechanical behaviour of steel and concrete structures may have impact on accident progression.

The objective of this work is to develop calculational methods to evaluate the heat-up of the spent fuel and surrounding structures in a hypothetical accident of loss of water coolant in water cooled interim storages. There is a question of very complicated heat transfer phenomena. Heat is transferred by conduction, convection by steam flows and irradiation between hot surfaces. Thermal heat radiation transfer is very essential heat transferring mechanism at high temperatures. Thermal deformations of structures due to thermal expansion may change heat transfer conditions. The strength of concrete structures is lost at about 400–600°C and this temperature can be reached quite easily in certain cases. Quite different types of analysis are needed and a group of special type of separate computer programs. The group of these codes is called PANAMA, which has been developed at VTT. Since there is no stationary state in heat-up of a spent fuel storage, long computing times are easily expected in CFD type analysis. That is why different ways to make the computation efficient has been studied. Validation at high temperatures is an essential subtask. Mesh density is also an important factor.

A special mesh generator has been developed to model the gap area and other parts of the racks and walls. Figure 4 below shows an example to model of the gap area between the concrete wall and racks.
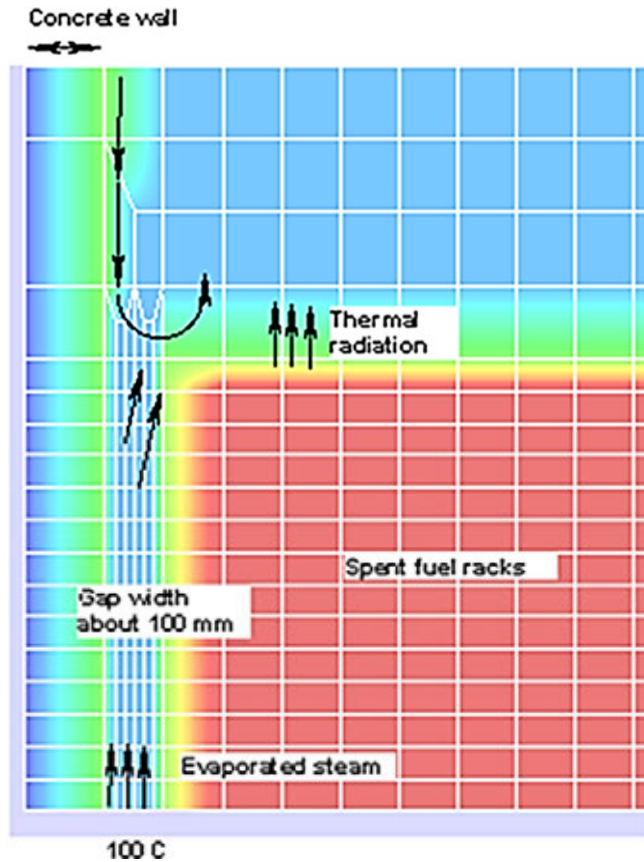
Results were reported as a VTT research report [3].

Figure 4. An example of a model for detailed analysis of a gap between the concrete wall and racks.

Spent fuel pool analysis with MELCOR

In this task of VESPA –project, the loss of pool cooling accidents at the spent fuel pools in the reactor hall of a Nordic BWR have been studied using the MELCOR 1.8.6 code. Studies were carried out with several different calculation nodalizations. Other investigated variables were the total decay heat power of fuel assemblies in the pool, the initiator of the accident (loss of pool cooling or loss of coolant from the pool), the LOCA leak elevation, the alignment of the re-flooding injection and the use of a lid on top of the pool.

From the results it was observed that ensuring natural circulation of air in the fuel is essential in preventing fuel damages. In cases where the air flow is prevented (loss of pool cooling, wall LOCA or a lid on top of the pool), the fuel is damaged in nearly all the cases (Figure 5). Only with the pool decay power being below 2227 kW, the melt of the fuel was prevented.
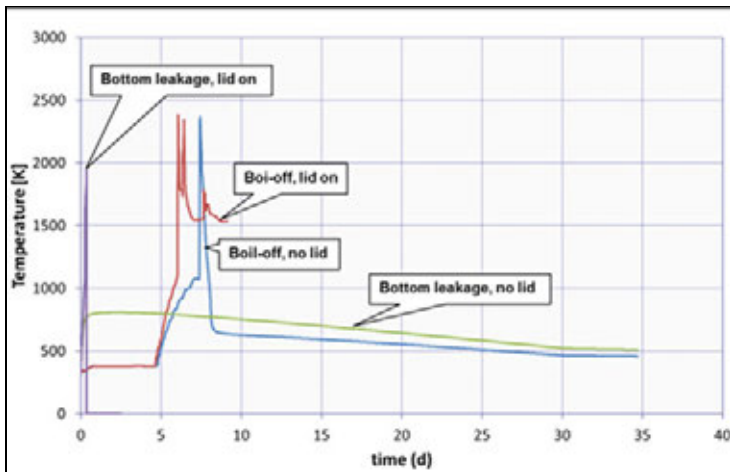
Figure 5. Maximum fuel temperatures in boil-off and bottom leakage scenarios, with and without a lid.

If water injection to the SFP is started before the fuel temperature reaches the cladding failure criterion (1173 K), the rewetting of fuel assemblies is successful and the fuel temperatures will quickly drop and the assemblies will remain intact (Figure 6). Re-flooding of already damaged fuel assemblies will also cool the fuel rods and reduce the radioactive releases to the environment. However, it may result in greater hydrogen releases.
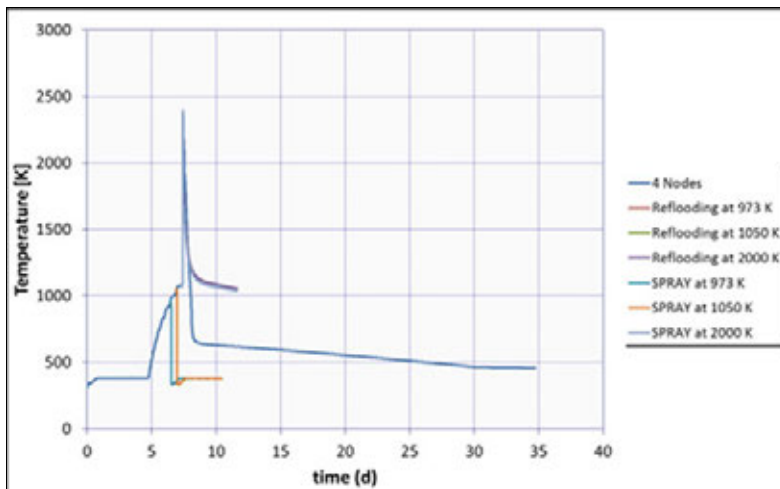
Figure 6. Maximum fuel temperatures for re-flooding scenarios.

The results of this MELCOR task were reported as a VTT research report [4]. A draft paper was also submitted to ICONE21 conference in July 2013.

References

1. Patalainen, M. Preliminary studies on high temperature failure of a pressure vessel lower head. VTT Espoo, 2013, VTT Research Report. VTT-R-00428-13.

2. Könönen, N. Tackling TEXAS-V. VTT Espoo, 2013, VTT Research Report. VTT-R-00706-13.

3. Ikonen, K. Status of PANAMA computing methods for analysing heating of interim spent fuel storage. VTT Espoo, 2013, VTT Research Report. VTT-R-00692-13.

4. Könönen, N. Spent Fuel Pool Accidents in a Nordic BWR. VTT Espoo, 2012, VTT Research Report. VTT-R-06461-12.

7. Structural Safety of Reactor Circuits

7.1 Environmental influence on cracking susceptibility and ageing of nuclear materials (ENVIS)

Ulla Ehrnstén[1], Janne Pakarinen[2], Wade Karlsen[1], Hannu Hänninen[3], Roman Mouginot[3], Erno Soinila[3], Matias Ahonen[1], Juha-Matti Autio[1], Pertti Aaltonen[1], Tapio Saukkonen[3]

[1]VTT Technical Research Centre of Finland
Tekniikantie 2, P.O. Box 1000, FI-02044 Espoo

[2]University of Wisconsin-Madison,
Department of Engineering Physics Madison, WI, 53706, USA

[3]Aalto University
P.O. Box 11000, FI-00076 AALTO

Abstract

The objective of the joint VTT – Aalto ENVIS project is to support safe operation of NPP's through increased understanding of the influence of light water reactor environments on the ageing and environmentally-assisted cracking (EAC) suscep-tibility of nuclear reactor materials. To meet these goals, several tasks are pursued dealing with irradiation assisted cracking, thermal ageing, dynamic strain ageing of stainless steels, characteristics of austenitic nuclear materials etc. International co-operation is important as a tool to bring the latest knowledge to Finland. Knowledge transfer and continuous education will secure uninterrupted availability of high-quality expertise for ageing management.

Selected results from the ENVIS project are briefly presented in this article, with the main emphasis on IASCC, which has been one focus area during the first two years of the project.

Introduction

The objective of the joint VTT – Aalto ENVIS project is to support safe operation of NPP's through increased understanding of the influence of light water reactor environments on the ageing and environmentally-assisted cracking (EAC) suscep-tibility of nuclear reactor materials. To meet the goals, several tasks are pursued, i.e. crack initiation and its precursors are investigated using super-slow strain tests in simulated NPP environments followed by detailed characterisation of the test specimens [1]. Mock-ups and nuclear components are characterised to increase the knowledge of the characteristics of such material conditions. Understanding irradiation-assisted cracking (IASCC) is increased through characterisation of irradiated stainless steel materials including field samples. The effect of environ-ment on the fracture behaviour is measured for nickel-based materials in hydro-genated water. The role of thermal ageing of different nuclear materials is ex-plored starting with a literature review [2] and continuing with characterisation of aged austenitic-ferritic materials. Fuel clad research capabilities are improved by development of testing capabilities for biaxial creep testing, enabling investigations on irradiation creep [3]. Knowledge transfer to the young generation is performed through everyday mentoring, teaching, updating the digital report archive, and by giving the project personnel possibilities to learn by doing. The knowledge achieved in the project is utilised also in customer assignments. The latest interna-tional knowledge is brought to Finland through active participation in international projects and networks, and by delivering detailed travel reports.

Selected results from the ENVIS project are briefly presented in this article, with the main emphasis on IASCC, which has been one focus area during the first two years of the project.

Summary of results from selected ENVIS topics

Characterisation of mock-ups

Two types of mock-ups have been characterised in the ENVIS project, i.e., 1) a low-alloy steel (LAS) – Alloy 52/152 – stainless steel (SS) 316L dissimilar metal weld mock-up received from KAIST, Korea and 2) a number of nickel-based dis-similar metal welds received from EPRI (Electric Power Research Institute), USA and Aalto University. The investigations of the LAS – Alloy 52/152 – SS 316L V-groove weld with Alloy 52 butter revealed strong dilution of chromium and nick-el, and enrichment of iron in the Alloy 52 butter, and to a lesser extent, in the Alloy 52 weld root. No major dilution was measured in the V-groove weld, where the composition was in accordance with the nominal composition of Alloy 152. A mar-tensite-like layer was observed locally in the butter close to the LAS fusion line, Figure 1. High hardness values, up to 270 HV0.1, were measured in this area [4]. As the local microstructures and their characteristics have an influence on the

fracture mechanical properties, the same weld is also used in the SAFIR2014 FRAS project for determination of local mechanical properties.
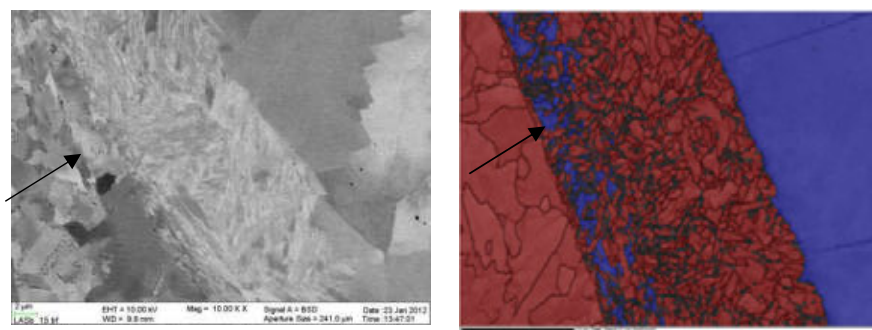

Figure 1. FEG-SEM-pictures of the LAS – Alloy 52 butter fusion line, at a location where a thin layer with an appearance resembling martensite, with a crystal structure similar to the LAS, is seen. The assumed location of the LAS – butter fusion line is indicated in the pictures.

Totally eight nickel-based dissimilar metal weld samples were characterised within a Master of Science work [5]. A narrow-gap Alloy 52 mock-up manufactured in the Tekes SINI-project was studied in the as-welded condition and after post-weld heat treatment (PWHT). It showed that PWHT resulted in increased carbon depletion in the LAS side and in an extensive chromium carbide precipitation in the weld metal, which was also responsible for a sharp hardness peak in the weld metal. Samples from EPRI were characterised, showing different weld configurations involving Alloy 690 as base metal and Inconel 52, 152 and 52M as filler metals. Differences in the behaviour of the filler metals were observed. Higher hardness was found in Inconel 52M, followed by Inconel 152 and 52, respectively. Inconel 152 showed different behaviour than Inconel 52 concerning carbon migration. The microstructure of Alloy 690 was characterised and was found to correspond to literature data, Figure 2 (a). Different microstructures were observed depending on the product form. Hot-rolled plates and forged plates showed extensive carbide banding, associated with smaller grain size, Figure 2 (b). Extruded Alloy 690 showed no carbide or grain size banding. Alloy 690 HAZ showed hardness increase due to increasing residual strains towards the weld interface, Figure 2 (c).
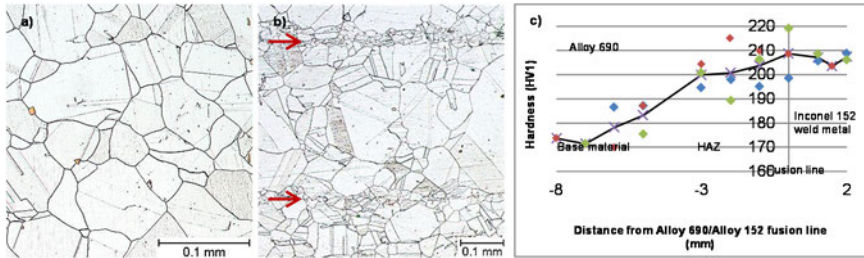
Figure 2. Characterisation of Alloy 690, with (a) microstructure showing twinning, intra-granular carbides and TiN particles, (b) carbide banding in Alloy 690 hot-rolled plate and (c) hardness measurement at Alloy 690 / Inconel 152 weld metal interface showing hardness increase in the Alloy 690 HAZ.

Influence of the strain rate and environment on fracture toughness properties of austenitic materials

The effect of hydrogenated PWR primary water on the Low Temperature Crack Propagation (LTCP) susceptibility of nickel-based weld metals Alloy 182, 152 and 52 has been studied [6]. The fracture resistance (J-R) test results show that Alloy 182 is the most susceptible to LTCP of the tested materials, Figure 3. The average fracture toughness (J_Q) of Alloy 182 reduces 69% (182 $\rightarrow$ 56 kJ/m^2) and tearing modulus (T) 39% (212 $\rightarrow$ 129) in hydrogenated water (30 cm^3/kg H_2O) compared to air values. Results indicate a slight restoration of Alloy 182 fracture toughness after 30 days pre-exposure to hydrogenated water at 300°C. Alloy 152 is less susceptible to LTCP than Alloy 182. The average fracture toughness (J_Q) values decrease slightly (151 $\rightarrow$ 135 kJ/m^2), when hydrogen content increases in low temperature water (0$\rightarrow$30 cm^3/kg H_2O), but they still remain considerably high. The measured bulk hydrogen content was found to be lower after the 30 days pre-exposure than in as-welded state, which supports the essential role of hydrogen in the LTCP phenomenon. Alloy 52 has so far been tested at hydrogen content 30 cm^3/kg H_2O where the material retained its remarkably high toughness.
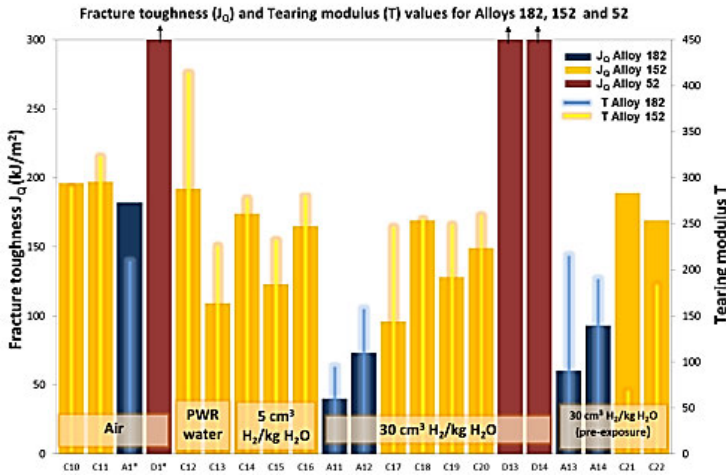
Figure 3. Fracture toughness and tearing modulus values for Alloys 182, 152 and 52 tested in various environments.

Ageing of nuclear materials

Thermal ageing of duplex stainless steel materials, with a composition close to those of nuclear welds, received from KAPL, USA was investigated using instrumented indentation with small forces, i.e., nanoindentation technique. The measurements were performed as a pattern and the hit phases we recorded to compile the information in Figure 4, showing much less hardness increase in the 2101 with a Cr_{eq} of 23.6 than in the 2209 steel with a Cr_{eq} of 26.0. This result suggests that the grade 2101 can be used for significantly longer times than the reference weld metal before significant embrittlement occurs.
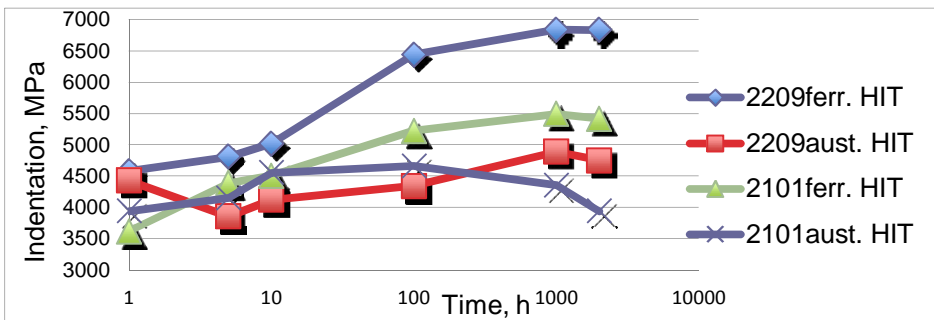
Figure 4. Instrumented indentation hardness (HIT, MPa) results as a function of exposure time (h) at 427ºC. (Berkovich diamond tip, Oliver & Pharr, 5 mN indentation force, Poisson's ratio 0.30).

272

Co-based hard-facing alloy Stellite 6 from a main steam gate valve guidance pis-ton, which had been in operation about 30 years before cracking was observed, has been investigated in the ENVIS project. Metallurgical examinations using optical microscopy, SEM, EBSD and X-ray analysis of the aged hard-facing alloy has revealed a microstructure containing sigma phase, Figure 5, which is known the be brittle. Also the mechanical properties have probably suffered from the thermal ageing. A room temperature impact energy value of only 0.5 J was meas-ured from the aged material [7].
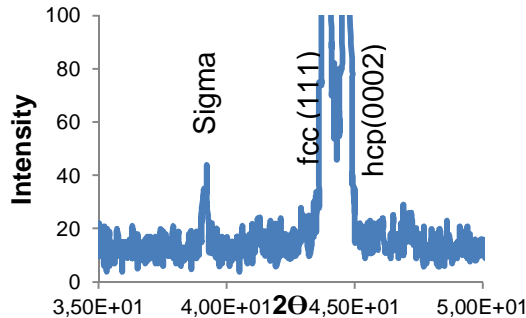
Figure 5. XRD-results of the aged Stellite 6 material.

International co-operation and education

International co-operation plays an important role in the field of nuclear materials degradation. Participating in international projects, conferences and networks gives access to the latest knowledge in this field, which is utilised in customer assignments and R&D. The ENVIS project represents STUK in the OECD/NEA Component Operational Experience, Degradation and Ageing Programme (CODAP) project, which is a NEA project in which a knowledge base is established and information is collected on various degradation modes. We also participate in the EPRI MRP Alloy 690/52/152 Expert Panel which deals with modern nickel based materials (used e.g. in OL3) and their behaviour. Knowledge transfer and continu-ous education is also important. The main part of the work in the ENVIS project is performed by the YG, thus enabling learning by doing. An advanced course in nuclear materials was arranged by professor H. Hänninen/Aalto University in 2012 with about 40 participants followed by a seminar with published papers [8].

Irradiation-assisted stress corrosion cracking

Field failures of irradiated stainless steel internals have been observed both in BWR and PWR environments. Plant experience and laboratory investigations indicate that the risk for irradiation-assisted stress corrosion cracking, IASCC, of austenitic stainless steels increases in boiling water reactor environment above a

fluence of about 1 dpa (displacement per atom), while the dose level for an increased IASCC risk is higher in non-oxidizing pressurized water environment, about 3 dpa. While in an oxidizing BWR environment the role of environment is obviously important, in a low-potential hydrogen-containing PWR environment the role of environment should not be as critical. Based on operational experience and laboratory investigations concerning baffle bolts cracked in French PWR's, where the bolts are made of cold-worked Type 316 stainless steels, a threshold of 4 dpa has been proposed. Stress corrosion cracking is, however, a result of a combination of a susceptible material, an aggressive environment and a tensile stress. Thus, an apparent threshold level concerning one parameter only (such as the dose) is applicable only when the two other parameters can be considered constant.

Neutron irradiation in light water power plant conditions causes hardening of the stainless steel material through formation of lattice defects. Simultaneously the ductility of stainless steels decreases, as does both the fracture toughness and the elongation to fracture. Irradiation causes also segregation, resulting in grain boundary depletion of chromium and molybdenum and enrichment of nickel, iron and silicon. VTT has been characterising irradiated materials for the OECD Halden project for several years (since 2011 as a part of the ENVIS project), increasing the knowledge and available literature data on radiation induced segregation and defect structures of different stainless steels. [9, 10, 11, 12, 13]

Non-destructive examinations (NDE) at the Loviisa NPP revealed indications in four core basket bolts made of solution-annealed Ti-stabilized stainless steel. These bolts were replaced after 31 years of operation and three of them were subjected to destructive failure analysis to reveal the reason for the indications. Further investigations were performed in the ENVIS project on one bolt using transmission electron microscopy (TEM) to clarify the detailed microstructure and finite-element (FE) modelling to evaluate the stress distribution in the bolt.

The failure analysis

The structure of the core basket and the shielding plate is seen in Figure 6. The bolts fasten the shielding plate to the core basket. To prevent unscrewing of the bolts during plant operation, the bolts are welded to the washers. The bolts are M12 x 29 mm bolts with a flat slot. They are made of solution-annealed titanium-stabilized stainless steel of type 0X18H10T, corresponding to Type 321 stainless steel. When bolt #1 was removed, an unintentional spot weld was observed between the washer and the shielding plate. This and two additional bolts with indications were subjected to a failure investigation as a customer assignment to determine the reason for the reported indications.

Bolt #1 had two cracks, one at the bolt shoulder, and one at the mid-length, Figure 7. Both cracks were intergranular, which is typical for stress corrosion cracking. A local region with branching was seen at the crack in the middle of the bolt length. Increased hardness values compared to typical values of solution-annealed SS (< 200 HV), in average 328 HV0.1, were measured from the bolt

material showing irradiation-induced hardening. Cracking was only observed in this bolt with an accumulated dose of 1.9×10^{21} n/cm^2 (2.9 dpa). The reason for the NDE indications in the other two bolts, with higher accumulated doses of 1.6×10^{21} (2.4 dpa) and 5.1×10^{21} n/cm^2 (7.7 dpa), respectively, was incomplete filling of the slot space when welding the bolt to the washer, leaving a cavity in the slot. [14]
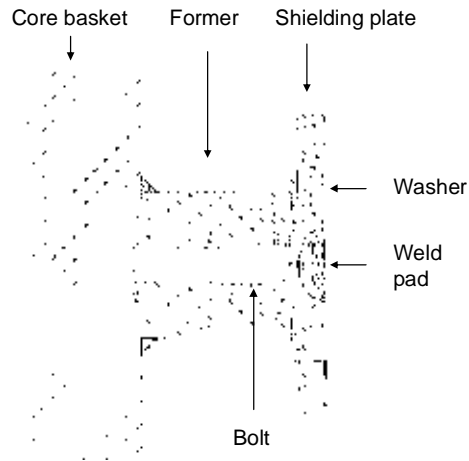

Figure 6. Schematic drawing of the shielding plate and core basket assembly.
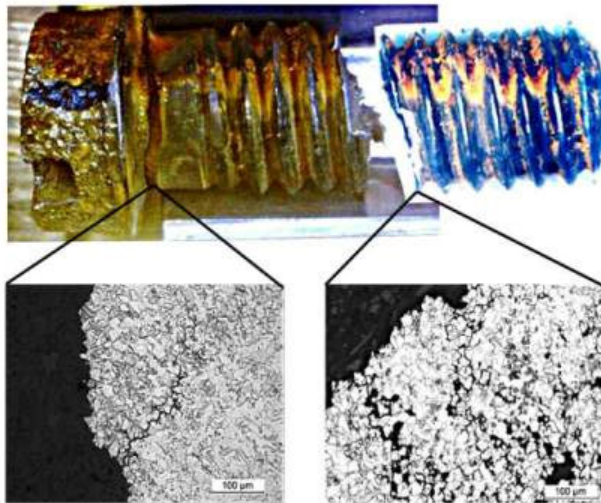
Figure 7. Optical micrographs of the intergranular cracking at the bolt shoulder and at mid-length, where the cracking was heavily branched within a certain area.

Further investigations

A Philips CM200 analytical field-emission gun (FEG) scanning transmission electron microscope (STEM) operating at 200 kV was used for the investigations of general microstructures, irradiation damage, and the composition of grain boundaries and precipitates [15].

FE modelling was performed using Abaqus 6.11-1 program package. In the modelling, symmetry conditions were assumed and one half of the structure including one bolt was modelled, Figure 8. The model included the bolt, former, washer and part of the shielding plate. The effect of irradiation was taken into account in the yield strength of the material, selecting a value of 620 MPa. The isotropic hardening plasticity model was utilized. Contact conditions were modelled between all the relevant surfaces and between the threads. The friction coefficient was assumed to be 0.15, and the preload of the bolt 10.5 kN. The primary loading was the vertical movement of the shielding plate, and its maximum value was assumed to be 0.7 mm. The computation was performed with and without the spot welding of the washer to the shielding plate. The spot welding was modelled by fixing the washer to the shielding plate at a certain area [16].
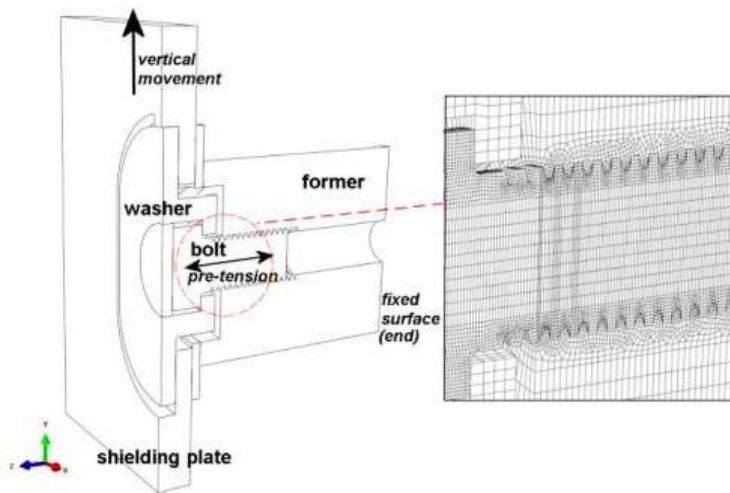

Figure 8. The FE model. One half of the structure and part of the shielding plate was modelled.

Results from FEG-(S)TEM investigations

The overall microstructure of the bolt material was characteristic of an annealed stainless steel that has been neutron irradiated; linear bands originating from extended stacking faults traversed the grains on the (111) planes and some planar dislocations were observed, Figure 9 (a) and (b). The dislocation and stacking fault

densities tended to be higher at the mid-length of the bolt, which indicates a higher degree of deformation. A distinct distribution of black dots populated the matrix, Figure 9 (c). Dislocation loops were quantified by the rel-rod method accompanied by weak beam dark field imaging (WBDF). Loop densities and average loop sizes for the bolt shoulder radius and mid-length are plotted in Figure 10 (a) together with values reported in the literature. The loop density values were in line with the literature, but the loops size was systematically smaller in both examined locations.

(a)

(b)

(c)

(d)
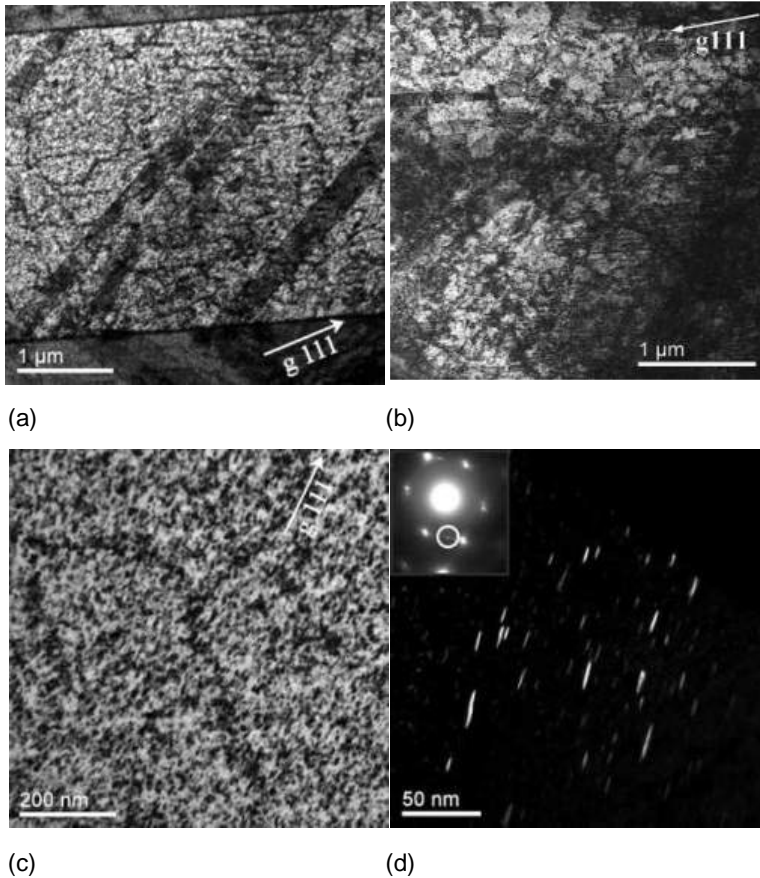
Figure 9. Band-like linear features on the (111) planes were the main deformation microstructure observed at the close proximity of the bolt shoulder (a) and bolt mid-length (b) cracks. (c) The matrix showed a small density of dislocations accompanied by a distinct distribution of irradiation-induced black dots. (d) Edge-on dislocation loops were quantified by using the rel-rod conditions (inset) and weak beam dark field imaging.

The grain boundary analyses were recorded using a converged beam with nominal spot size of 1 nm in TEM mode. A clear GB-RIS, i.e., depletion of chromium and iron and enrichment of nickel and silicon was observed. The minimum observed chromium content was as low as 13.6 wt% at the bolt shoulder section and 15.5 wt% at the mid-length. While the measured Cr wt% at the grain boundaries were in good agreement with the literature data, Figure 10 (b), the Si wt% was clearly higher than previously reported for irradiated stainless steels, Figure 9 (c). No traces of elements from the environment that could have increased the SCC risk, such as Cl or S, were found from the GBs close to the shoulder crack.
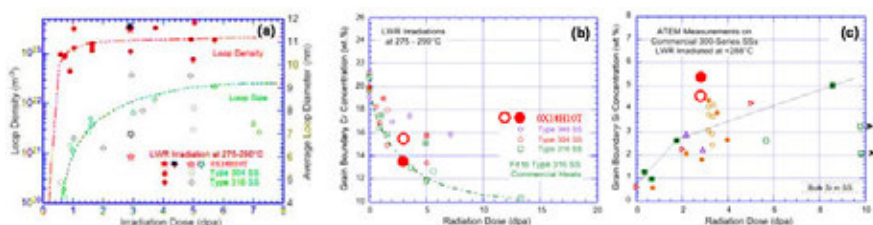

Figure 10. (a) The determined dislocation loop densities (solid symbols) and sizes (open symbols) compared with literature data. The stars with point down (up) show the obtained values for the bolt mid-length (shoulder). (b) Cr and (c) Si wt % of the current examination (red circles) compared with the values found from the literature. Solid (open) circles show the values from the head (radius) section of the bolt. The pictures are modified from literature data.

Computational (FE) results

The computed deformations are shown in Figure 11 for the un-welded and spot-welded case. The deformations of the spot-welded case show clearly bending of the bolt caused by the spot welding.
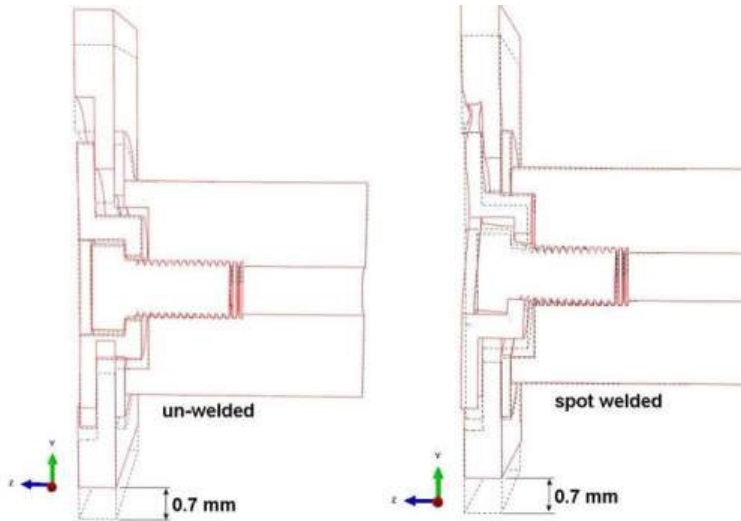
Figure 11. The computed deformations (enlarged by a factor of 10) for the un-welded and spot-welded case. The thermal deformation is 0.7 mm.
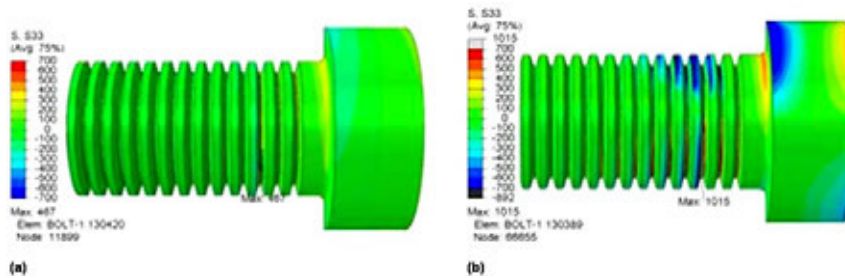

Figure 12. The computed axial stress in the bolt for the (a) un-welded case and (b) for the spot-welded case. The thermal deformation is 0.7 mm.

Figure 12 show the computed axial stress in the bolt in the case of maximum thermal deformation, 0.7 mm. The results show that bolt stresses in the spot-welded case are clearly higher. The maximum stress occurs at the root of the first effective thread. High stresses occur also in the roots of the other threads until the bolt mid-length, and also in the bolt head shoulder in the opposite position of the circumference. The results are in very good correlation with the findings from the failure analysis.

Discussion

The conclusion of the failure investigation was that the reason for two intergranular cracks in bolt #1, made from solution-annealed Ti-stabilized stainless steel, with an accumulated dose of 1.9 x 10^{21} (2.9 dpa), is stress corrosion cracking. The stress corrosion cracking can be a combination of intergranular stress corrosion cracking, IGSCC and irradiation-assisted stress corrosion cracking IASCC, which are both caused by a combination of a susceptible material, a tensile stress and an aggressive environment, although the role of the environment is considered to be less decisive for IASCC, especially in non-oxidising VVER conditions.

It is known, that molybdenum disulphide containing grease, which decomposes and creates an environment which increases the risk for SCC, may have been used during installation of the bolts. The FEG-STEM investigations showed no signs of sulphur, nor any other harmful elements, which could have increased the SCC susceptibility. Thus, the role of the environment is not considered to abnormal nor being the main cause for the cracking.

The analytical TEM observations from the bolt showed that there was a clear GB-RIS present at both crack locations. The amount of Si was higher (5.4 wt% Si max) than what is generally observed in stainless steels with a similar dose and the Cr wt% showed a clear reduction from the bulk value. It was concluded that GB-RIS most probably have increased the cracking susceptibility, but was not the main reason for the failure at the lowest dose reported for IASCC up to date. The amount of irradiation-induced dislocation loops was in line with the literature and the measured hardness values of the bolt.

The washer of this bolt had been welded to the shielding plate, which had resulted in unintentionally high stresses during plant start-up and operation as shown by the FE modelling. The FEM results are in good correlation with the observed findings. The exceptionally high stresses in bolt #1 with cracking, but a relatively low dose (2.9 dpa), while the bolt with the highest dose (7.7 dpa) had not suffered from cracking is a good manifestation that IASCC and IGSCC are a combination of material, environment and stress. [17]

Acknowledgements

References

1. Saukkonen, T. et al. Plastic strain and residual stress distributions in an AISI 304 stainless steel BWR pipe weld. 15th Symposium on Environmental Degradation of Materials in Nuclear Power Systems – rWater Reactors. 7–12.8.2011. Colorado Springs, CO, USA.

2. Ehrnstén, U., Aaltonen, P. Literature report on thermal ageing of selected nuclear materials. VTT-R-00431-12.

3. Tähtinen, S. Literature study on irradiation creep. VTT Research Report VTT-R-02354-12.

4. Ehrnstén, U., Autio, J-M., Saukkonen T. Characterisation of a LAS – 52/152 – SS dissimilar metal weld. VTT Research Report VTT-R-00036-12, 16.2.2011.

5. Mouginot, R. Microstructures of nickel-base alloy dissimilar metal welds. Aalto University, School of Engineering, Department of Engineering Design and Production, Engineering Materials, Master thesis, Kon-67, 5.12, 2012. 186 p.

6. Ahonen, M. Collation of LTCP test results obtained at VTT in years 2008–2012. VTT-R-00491-13, 2013.

7. Aaltonen, P. Ageing degradation of a hard-facing alloy after long-term exposure to BWR conditions. VTT Research Report VTT-R-00216-13.

8. Materials Science and technology – nuclear material, advanced course. Postgraduate seminar on engineering materials, seminar papers, Kon-67.5100, September 5–6, 2012. Ed. J. Hänninen and T. Kiesi. Aalto University, Department of Engineering Design and Production.

9. Karlsen, W. The role of non-monotonic loading in EAC – ra literature review. VTT Research Report VTT-R-00867-12, 17.2.2012.

10. Karlsen, W. Grain Boundary Segregation in a 24 dpa 304 stainless steel after post-irradiation annealing. Enlarged Halden Programme Group Meeting 2011. 3–7.10.2011, Sandefjord, Norway.

11. Karlsen, W. Grain boundary segregation in a 24 dpa 304 stainless steel after post-irradiation annealing. VTT Research Report VTT-R-03033-11, 16.2.2012. 27 p.

12. Pakarinen, J. TEM examination of the effect of post-irradiation annealing on 7.7 dpa AISI 304 stainless steel. VTT-R-05228-12, 4.10.2012.

13. Pakarinen, J. ATEM characterization of a slice from a 15 dpa AISI 316 stainless steel baffle bolt. VTT-R-05229-12, 8.10.2012.

14. Ehrnstén, U., Kytömäki, O., Hietanen, O. Investigation on core basket bolts from a VVER 440 power plant. 15th Symposium on Environmental Degradation of Materials in Nuclear Power Systems – Water Reactors. 7–12.8.2010. Colorado Springs, CO, USA.

15. Pakarinen, J. ATEM characterization of a failed core basket bolt removed from Loviisa NPP Unit 1, Parts I and II. VTT-R-00647-12, 27.3.2012 and VTT-R-05230-12, 6.10.2012.

16. Keinänen, H. Stress analysis of core basket bolt. VTT-R-00443-13.

17. Ehrnstén, U. et al. Investigations on core basket bolts from a VVER 440 power plant. Submitted to JNM, to be published.

7.2 Fracture assessment of reactor circuit (FAR)

Päivi Karjalainen-Roikonen, Juha Kuutti, Kalle Kaunisto Heikki Keinänen,
Tom Andersson, Tapio Planman, Pekka Nevasmaa

VTT Technical Research Centre of Finland
Tekniikantie 2, P.O. Box 1000, FI-02044 Espoo

Abstract

The FAR project (Fracture assessment of reactor circuit) project aims at (i) Develop and evaluate numerical structural integrity assessment methods such as crack growth dependent submodelling technique and extended finite element method (XFEM); (ii) Study applicability and limitations of leak-before-break (LBB) approach including requirements for material input data, tearing instability, effect of ageing and special features of LBB for narrow gap welds and dissimilar metal welds (DMW); (iii) Evaluate growth and criticality of real cracks with shallow or irregular shape in structures and develop low-constraint fracture mechanical testing methods as well as develop transferability to structures and advanced numerical methods. (iv) Develop structural integrity assessment procedure for dissimilar metal weld (DMW) based on realistic failure criteria of DMWs, and develop practice with which the

zones that are most critical for fracture can be identified and their fracture toughness and mechanical strength can be determined reliably. This report summarises the results of the FAR project after two years (2011–2012) of the four year project.

Introduction

For fracture risk assessment of nuclear components it is essential to know loads, operational conditions, material properties and their changes due to ageing or environment as well as fracture mechanisms. Both experimental material data and validated numerical assessment methods are needed for qualitative assessment of fracture risk. New material and structural solutions such as narrow gap welds set specific requirements for structural analysis and development of numerical and fracture mechanical testing methods.

Recent development in **fracture assessment methods** has been in the field of numerical modelling. Development in applying numerical methods in assessing component integrity was made during the previous SAFIR2010 program but suitable tools for the end-user are yet to be employed in large scale. Also uncertainties have been a concern in the nuclear field and many design approaches therefore yield to overconservative results. These uncertainties may be due to not precise input data of loadings or material parameters. The state of the art in numerical fracture mechanics methods needs to be assessed and suitable methods selected for assessing integrity of nuclear related components. Numerical tools are often required in assessing crack growth in complex cases such as leak before break analyses or unsymmetrical crack criticality analyses. An example of these advanced numerical methods is crack growth dependent submodelling technique. Other recently developed method for modelling crack growth is the extended finite element method (**XFEM**). Suitability and appropriate parameters in nuclear applications need to be evaluated for both of these methods. More simplistic engineering tools provide a way of verifying advanced numerical methods but they can also be applied directly in assessing component integrity. Uncertainties and conservatisms of fracture mechanics analysis methods will be evaluated using parametric analyses. The applicability of available fracture mechanics analysis software in nuclear applications needs to be evaluated.

Leak before break (LBB) is based on the assumption that a crack like flaw in a wall of a pressurised component will be detected via leakage long before the crack becomes structurally critical. Use of LBB approach requires information and methods of fracture mechanics (simple and numerical methods), material properties (stress/strain, fracture toughness), fluid mechanics (leak size, leak rate) and leak detection systems. The LBB approach stems from operating experiences showing extremely low probability of breaks in primary circuit piping. Prior to applying any of the levels of the LBB assessment methodology, there needs to be a general screening criteria set to preclude its application to cases for which LBB is not applicable. LBB is already included in nuclear safety authority codes in many countries. In Finland it is included in the design of new plants and is also a part of

Finnish nuclear safety YVL codes. In the past (1995), a survey of the LBB procedures has been made in Finland [1]. Since that no significant Finnish research directly regarding to LBB has been performed in the nuclear area. Recent development of LBB is based on R6 and has been developed in European non-nuclear projects (e.g. FITNET). Thus, updated state-of-the-art of LBB is needed. Further, applicability and limitations of LBB approach concerning effect of ageing on material fracture properties, different crack shapes, tearing instability and welded structures (narrow gap welds, dissimilar metal welds, DMW) as well as special loading cases such as earth quake loads should be studied.

Low constraint i.e. lower stress triaxiality which prevails in a tip of shallow crack is less severe for fracture than the stress caused by a deep crack. Fracture mechanical input data for structural analysis is usually based on deep crack fracture toughness. This leads easily also for extra safety margins in structural assessment. For more realistic integrity assessment of the structure with irregular shape / shallow cracks, especially in weld seam region, further development of analysis and experimental methods is needed.

For **dissimilar metal welds** such as safe end structures, research is needed especially for a successful control of the metallurgical properties in bimetallic weld joints. It is noteworthy that the potential flaws forming typically on the bimetallic joint interfaces are difficult to detect. New welding methods, e.g. narrow gap welding, particularly require mastery of the correlations between the mixing of the base material, the alloying element gradients, the microstructures formed and degradation and failure phenomena. Chemical composition and material properties may vary greatly in a narrow zone close to the weld fusion line, which makes it difficult to determine the relevant zone-specific material properties experimentally. In practice, it requires the use of miniature specimen techniques. Another essential aspect is the transferability of test specimen scale results to the integrity analyses of genuine structural components. The localisation of the asymmetrical deformation typical to bimetallic welds and the presence of an uneven crack front require the use of modern modelling techniques (such as XFEM) in estimating crack growth. Metallurgical discontinuity also causes a complex loading and stress-strain state, which may cause residual stress and stresses due to thermal loading.

Objective

The objective of the 4-year project is to develop and to validate numerical and experimental methods for reliable reactor circuit structural integrity assessment. Especially, to

- Develop and evaluate numerical structural integrity assessment methods; evaluate and further develop advanced methods – such as crack growth dependent submodelling technique and extended finite element method (XFEM) – for nuclear structural integrity assessment. Evaluate uncertainties and conservatisms of fracture mechanical structural analysis methods.

Applicability of more simple engineering structural assessment tools and numerical software will be studied.

- Study applicability and limitations of leak-before-break (LBB) approach; Limiting factors, requirements for material input data, tearing instability, effect of ageing, special features of LBB for narrow gap welds and dissimilar metal welds (DMW) will be considered. Experimental and analytical methods for LBB will be developed.

- Evaluate growth and criticality of real cracks with shallow or irregular shape in structures; low-constraint fracture mechanical testing methods, transferability to structures and advanced numerical methods will be developed.

- Develop structural integrity assessment procedure for dissimilar metal weld (DMW) based on realistic failure criteria of DMWs, and develop practice with which the zones that are most critical for fracture can be identified and their fracture toughness and mechanical strength can be determined reliably.

Advanced numerical structural integrity assessment methods, XFEM

A recent advancement in numerical fracture mechanics is the extended finite element method (XFEM) that allows defining mesh-independent cracks in the analysis model. Popular FE-software package Abaqus has included an XFEM implementation in its more recent versions. Although the implementation has some limitations, generally it is currently the easiest way of carrying out XFEM fracture analyses.

The applicability of the XFEM implementation in Abaqus was studied [2]. A very comprehensive overview on the same topic is given recently [3] obtaining a good stress intensity factor agreement for benchmark cases with errors less than 10 per cent. The reported drawback was that the acceptable accuracy requires very dense mesh in the crack tip. The proposed element size is from 0.8 per cent to 13 per cent, depending on desired accuracy. The analysis models had several hundred thousand elements most of which located at the crack region. Also, best accuracy was obtained when the mesh was designed to coincide with the crack boundaries. This is not practical if the crack location needs to be varied or is unknown. It was found that the mesh in the crack location most affects the accuracy of the stress intensity factors [2, 3]. However, the verification cases in Abaqus manuals utilize relatively coarse mesh indicating that good results can be obtained also with a coarse mesh if the crack is placed correctly with respect to element edges.

When the location of the flaw is not explicitly known or the critical areas need to be determined for design purposes building traditional FE-models with cracks is extremely laborious. The XFEM approach simplifies this task notably. Only one uncracked mesh of the component needs to be built and all desired crack locations, shapes and sizes can be analysed with the built mesh. The automated crack generation procedure introduced in this work allows the user to generate multiple analysis models by defining the location and size of the crack.

The procedure was demonstrated for simple cases to show what kind of results can be obtained using a single FE-model and multiple analysis runs [4]. The procedure is implemented for elliptical axial and circumferential surface cracks for demonstrative purposes, see Figure 1.

The agreement with the obtained stress intensity factors with reference results was reasonable at its best. The results demonstrated the fact [3] that accurate evaluation of stress intensity factors requires very dense mesh in the crack region. The developed procedure is usable with any element size but carrying out multiple XFEM analysis with a very dense mesh would take weeks of computing time. Therefore, it is recommended that the critical locations are first screened using a coarse mesh and then selected cases are analysed with a denser mesh.

The procedure can later be developed for crack growth modelling by creating a propagated crack based on the results obtained from an earlier analysis and a crack growth law such as the Paris law as was manually demonstrated [4]. Utilizing submodels for defining a dense mesh around the crack region provides an attractive and flexible option for modelling cracks in various locations. This approach will be studied in the next phase of the sub project.
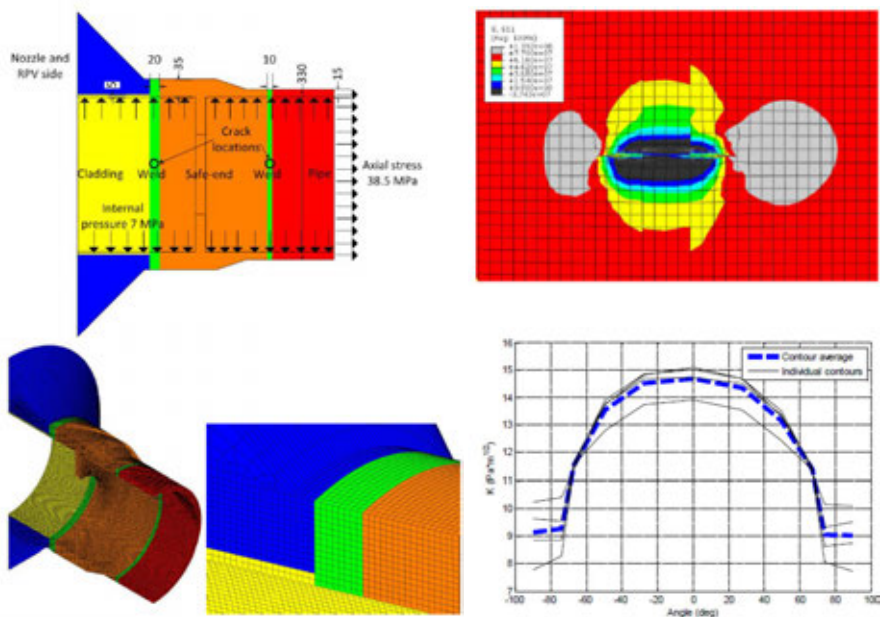

Figure 1. Example: RPV nozzle, cracks in welds. Axial crack in pipe-safe-end weld.

LBB

Deterministic LBB procedures have been developed and are being used in several European and other countries operating nuclear power plants. A review of state of

the art of LBB was done [5]. In Finland, the main source of information on LBB for nuclear power plant (NPP) components is Radiation and Nuclear Safety Authority (STUK). On a national level, not much is published in Finland concerning LBB analysis practices, however the main references on the subject are the YVL Guide 3.5 [6], and YVL Guide 2.6 [6] (regulatory requirements). The former one of these can be considered as the main source concerning the Finnish LBB practices, whereas the latter guide covers only the special case of an earthquake.

Two LBB case studies were examined [8]. The first case study deals with a circumferential crack in pipe bend of a BWR piping and the second case with a straight pipe. Of the case study concerning a circumferential crack in boiling water reactor (BWR) piping, the dimensions, loading and boundary conditions of the modelled pipe bend are shown in Figure 2. The material of the pipe is AISI 304 austenitic stainless steel. At the operating temperature of 286°C the value of the Young's modulus is assumed to be 180 GPa, and Poisson's ratio 0.3. Yield stress is 120 MPa, ultimate stress 380 MPa and elongation 40%. The stress strain properties were defined with the Ramber-Osgood parameters.

The length (2Θ) of the circumferential through-wall crack varied in the analyses from 60° to 160° using approximately 20° increments. The assumed crack fronts were straight, and perpendicular to the component surfaces. The crack growth phase was not considered in the analyses, thus the analyses with different crack sizes were performed separately.
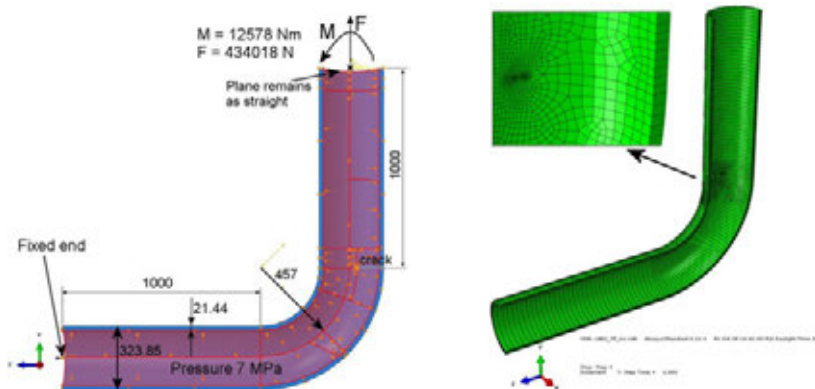

Figure 2. Studied case of a through-wall crack at the extrados of a BWR pipe bend. Half of the structure is shown. (left) The finite element model in the case crack length (2Θ) is 150°. (right)

Abaqus finite element code was used in the computations. Figure 2 shows the uncracked finite element model, which was utilised to define the deformation values. One half of the structure was modelled with symmetry boundary conditions. In one either end force and moment or displacements and rotations were applied. The other end was rigidly fixed.

The LBB evaluation procedure presented in reference [1] was applied. This follows the in-service inspection practice having a safety margin of 2 between critical crack size and leakage crack size. The requirements for LBB are following: A leakage of 10 GPM (gallons per minute) is assumed to be detectable during normal operation; The crack, which size is large enough to cause detectable leakage, should remain stable even if 1.4 times the normal loading is applied; A safety margin of 2 between critical crack size and leakage crack size is required.

J-integral was computed using six paths around the crack tip. A check was made for the path independency of the J-integral. A mean value of paths 3…5 was utilised to compute the stress intensity factor values. Figure 3 shows the computed stress intensity factors for different crack lengths (2Θ) in the inner and outer surface as well as in the middle of the wall. The results are shown for the force load case and for the displacement load case. As could be expected, the stress intensity factor values for the latter case are lower. Leak area was approximately computed using the crack opening displacements along the crack length. For leak rate determination with SQUIRT2 code, an approximate mean value of the crack gap (crack opening displacement, COD) was computed along the crack length. Concerning other parameters, e.g. surface roughness, the default values of the SQUIRT2 code were utilised. Leak rate was computed for different crack lengths (2Θ).

A detectable leak rate of 10 gal/min results if the crack length is approximately 105° for the force load case and 115° for the displacement load case. On the basis of the previous results [5], crack having a length of 210° is not stable due to plastic collapse in the force load case. A critical crack length concerning gross plasticity is approximately 190° in the force load case, which gives a safety factor of 1.8 for the detectable crack size with respect to the critical crack size. This is less than the required safety factor of 2. Thus the requirements of the LBB concept are not fulfilled in the force load case.

Figure 6 shows comparison of computed von Mises stress [MPa] and deformations for two crack lengths in the displacement load case. The results show, that the crack and corresponding cross section loading is reduced in the case of larger crack. Thus it is clear that the requirements of the LBB concept are fulfilled in the displacement load case.

On the basis of the results, in the force/moment load case of the pipe bend the requirements of the LBB concept were not fulfilled. In the displacement/rotation load case the requirements of the LBB concept were fulfilled. The second computed case, a straight pipe, showed similar behaviour as the pipe bend.

The condition in a real pipeline or pipe bend is probably somewhere between the force and displacement load case and should be thus evaluated case by case basis using the actual pipeline and boundary conditions.
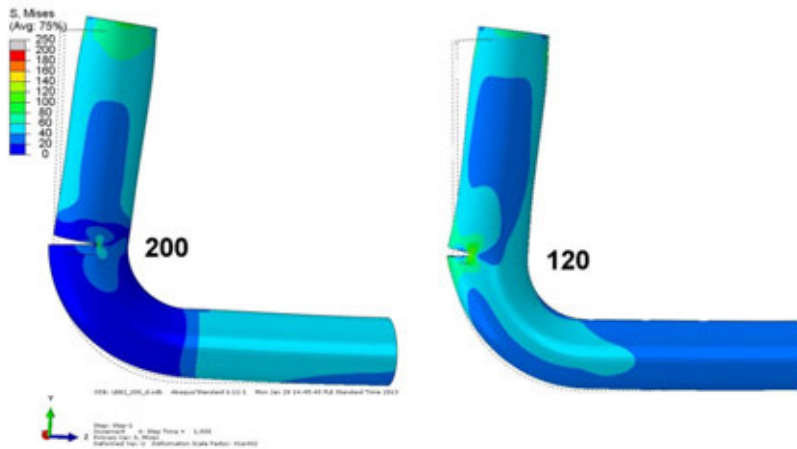
Figure 3. Comparison of computed von Mises stress [MPa] and deformations for two crack lengths (2Θ = 200°, 2Θ = 120°) in the displacement load case.

In addition to numerical LBB analysis, tearing instability of long crack was studied [9].

Low constraint

The constraint and biaxial effect and their interaction in combination with the effect of warm pre-stressing (WPS) have been investigated. FEM-model of a WPS case was made [10].

The warm pre-stress (WPS) effect resulting from various loading transients and constraint have been studied very intensively during the past decades. The effect itself has been well verified for different transients. One of the first models to take into account the WPS effect, is based mainly on the loadcool-fracture and load-unload-cool-fracture type transient cases [11]. A simpler but equally accurate model, together with a comprehensive review of data and methodologies, was presented in 2003 by Wallin [12]. A model based on the modified Beremin model is presented in [13]. Constraint as well as some other advanced procedures and correction parameters have already been included in assessment procedures (e.g. R6, FITNET and SINTAP). Inhomogeneity Screening Criterion for the ASTM E1921 T0 Estimate Based on the SINTAP Lower-Tail Methodology has been published [14]. Also, the WPS consideration is being occasionally applied and may have been included in national procedures or guides, but so far there is no commonly approved/applied approach. Further verification of the aforementioned procedure and Master Curve developments (the re-analysis [15], constraint Tstress correction to T0, and the WPS estimation with Master Curve) will be performed.

Ductile tearing (J-R curve) behavior of low constraint level single-edge-cracked tension SE(T) specimen was compared to that of obtained using standard deep crcked SE(N) specimens [16]. The SE(T) specimen geometry and loading mode is

designed to produce a level of crack-tip constraint in the test that is similar to the constraint experienced in service for a surface circumferential flaw in a pipe under tension or bending load.

DMW

This state-of-the-art review report [17] concerns the influence of welding residual stress (WRS) distributions on the integrity analyses of nuclear power plant (NPP reactor circuit component dissimilar metal welds (DMWs). The specific characteristics of DMWs are presented and explained from the metallurgical and microstructural standpoint, with connection to their stress-strain behaviour and the resulting effects to structural integrity. The covered WRS procedures in the structural integrity analyses of NPP reactor circuit component are: ASME recommendations, British Standard BS 7910: 1999, R6 Method Rev. 4, SINTAP, API 579, and FITNET. Recent WRS solutions for welds in the as-welded condition and subjected to PWHT, as well as for repair welds in the as-welded and the PWHT condition have been included. Additionally, recent recommendations given by the SSM Handbook particularly for real butt-welded bi-metallic pipes are briefly presented.

The investigation demonstrates a substantial scatter in the calculated WRS distributions between the various applied procedures. In comparison to the as-welded condition, the PWHT appears to remarkably decrease the WRS level of the piping welds; the same applies to repair welds subjected to the PWHT. Of the covered WRS recommendations, only the SSM Handbook provides WRS distributions also for a selection of real dissimilar (bi-metallic) weld types. In the case of the other covered WRS procedures, the applied distributions are calculated applying different formulae derived separately for ferritic steel and austenitic stainless steel. Further validation of the SSM Handbook WRS distribution solutions for DMWs of various metallurgical concepts and flaw locations & orientations will therefore be of utmost importance in the future, both by using experimental work and numerical computations, coupled with modelling of the actual welding sequence and its thermal history 'pass-by-pass'.

References

1. Ikonen, K., Raiko, H., Keskinen, R. Leak-before-break evaluation procedures for piping components. STUK-YTO-TR 83. December 1995. ISBN 951-712-088-5.

2. Kuutti, J., Kaunisto, K. Utilizing XFEM in fracture mechanics analyses. VTT Research Report VTT-R-00779-12.

3. Levén, M., Rickert, D. 2012. Stationary 3D crack analysis with Abaqus XFEM for integrity assessment of subsea equipment. Master's Thesis 2012:35, Applied Mechanics. Chalmers University of Technology, Göteborg, Sweden.

4. Kaunisto, K., Kuutti, J. Parametric XFEM crack analysis procedure. VTT Research Report VTT-R-00155-13.

5. Keinänen, H., Cronvall, O. Pipe break analysis: An updated state-of-the-art review of LBB procedures. VTT Research Report VTT-R-00299-12.

6. YVL Guide 3.5 – Ensuring the strength of pressure vessels of a NPP. Finland, 5 April 2002. 21 p. (in Finnish only.)

7. YVL Guide 3.6 – Seismic events and nuclear power plants. Finland, 5 April 2002. 21 p. (in Finnish only.)

8. Keinänen, H. Leak Before Break analysis of a pipe bend and a straight pipe. VTT Research Report VTT-R-00634-13.

9. Karjalainen-Roikonen, P. Tearing instability of long crack. VTT Research Report VTT-R-00xxx-13.

10. Planman, T. (ed.), Andersson, T and Laukkanen, A. Validation of WPS - benchmark on CABINET project Case 1. VTT Research Report VTT-R-00840-13.

11. Chell, G.G. Some fracture mechanics applications of warm pre-stressing to pressure vessels. In: Proceedings of the 4th International Conference on Pressure Vessel Technology. Inst Mech Eng, Paper C22, 1980. Pp. 117–24.

12. Wallin, K. Master Curve implementation of the warm pre-stress effect. Engineering Fracture Mechanics, 70 (2003), 2587–2602.

13. Lefevre, W., Barbier, G., Masson, R., Rousselier, G. A modified Beremin model to simulate the warm pre-stress effect. Nuclear Engineering and Design 216(2002), 27–42.

14. Wallin, K. Inhomogeneity Screening Criterion for the ASTM E1921 T0 Estimate Based on the SINTAP Lower-Tail Methodology, Journal of Testing and Evaluation 40(2012)6.

15. Wallin, K. Distribution free statistical assessment of scatter and size effects in the Euro fracture toughness data set. Engineering Fracture Mechanics 2012. (In press, available online.)

16. Karjalainen-Roikonen, P. Low constraint tearing resistance. VTT Research Report VTT-R-00xxx-13.

17. Nevasmaa P., Cronvall, O. State-of-the-Art in residual stress assessment in dissimilar metal welds (DMWs) VTT Research Report VTT-R-00669-13.

7.3 Monitoring of the structural integrity of materials and components in reactor circuit (MAKOMON)

Tarja Jäppinen, Ari Koskinen, Esa Leskelä, Antti Tuhti,
Jonne Haapalainen, Stefan Sandlin

VTT Technical Research Centre of Finland
Kemistintie 3, P.O. Box 1000, FI-02044 Espoo

Introduction

Non-destructive testing (NDT) techniques are used to monitor the condition of the structures of reactor circuit during the operation of nuclear power plants. The in-service inspections (ISI) are normally performed during the revision with tight time schedule.

The objectives of the SAFIR2014 MAKOMON project is to develop more reliable and more efficient ways to use non-destructive testing techniques for monitoring the structural integrity of the primary circuit components. The main methods used in the MAKOMON project are different ultrasonic applications and ultrasonic simulation, eddy current and radiography.

NDE subtasks in MAKOMON project

MAKOMON project 2011–2012 consisted of five subtasks. One task compares the indications received from different types of defects in ultrasonic evaluation. It was found out that EDM notches produced significantly stronger indications than the same size fatigue cracks [1, 2]. This comparison continued with different fatigue cracks and these results are presented in this article.

Ultrasonic simulation can be used to optimize the inspection techniques, and to see the restrictions of the inspection. The aim in the project is also to calculate probability-of-detection curves from simulated defects [3, 4]. New methods, nonlinear ultrasound and laser ultrasound, are also reviewed for new possibilities of detecting early stages of material degradation. The state-of-the-art review reports have been prepared for nonlinear ultrasound [5] and laser ultrasonics.

Development of eddy current method to detect the magnetite piles in the steam generation tubing is an area of interest that continues in this project. Magnetite on the steam generator tubing is well detected and to certain limit, the thickness of the magnetite can be measured. [6, 7]

The potentials for replacing X-ray film with digital detectors in nuclear environment have been studied in the project. The research is concentrated on pointing out the advantages of the digital radiography in the nuclear industry. [8, 9]

Differences in NDE reflectors using mechanical and thermal fatigue cracks

This study was done to compare two different types of artificial defects and to test and study the influence of different reflector properties on indications. The aim was to produce new data on artificial reflectors for the needs of qualification as well as inspection.

There are many ways to produce artificial defects in steel. Different flaws have different responses when they are inspected and it is crucial for the reliability to know how well artificial defects corresponds to the ISI defects. Fatigue defects can nowadays be produced using thermal fatigue or mechanical fatigue. In this study thermal fatigue and mechanical fatigue defects were produced in two test specimens. These artificial defects were inspected first with conventional ultrasonic transducers with mechanised scanner and secondly with phased array ultrasonic method. Also scanning acoustic microscope (SAM) and radiographic inspections were made. The results will be presented in a separate VTT research reports.

In 2013 more inspections will be made using eddy current inspection (ET) and time of flight diffraction (TOFD). After NDE, the specimens will be investigated with destructive methods to gain the real size and characteristics information. Final analysis of the NDE results and comparison between two different artificial fatigue defects will be done after the destructive investigation is completed.

Fatigue defect specimen

Two different fatigue specimens were studied. Both specimens were made of austenitic stainless steel 316L (ASTM) plate with thickness of 25 mm. Specimens were butt welded from two pieces and the defects were produced on the root side along the solidification line (Figure 1). The dimensions of the defects in both specimens were targeted to be 15 mm in length and 5 mm in depth. These dimensions will be confirmed after the final destructive investigation in 2013. The crack made in the other specimen is thermal fatigue and in the other specimen there are two mechanical fatigue cracks.
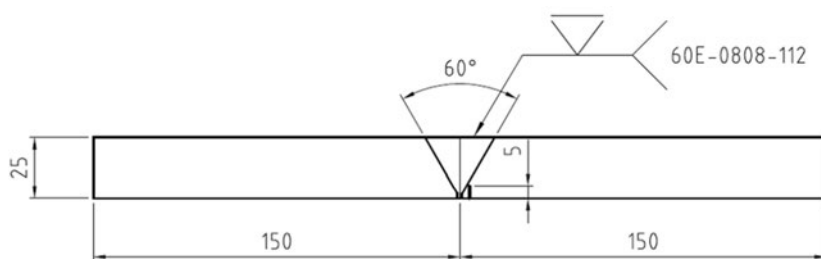
Figure 1. Schematic picture of the specimen.

Conventional ultrasonic inspection

Inspections using conventional ultrasonic technique were carried out using Om-niScan ultrasonic device with a motorized scanner (SPIDER) with software control by UltraVision. UltraVision software was used for evaluation of inspection results. Probes, angles and wave forms used can be seen in Table 1. Scanning was performed from both sides of the weld on weld face side using water as couplant.

Table 1. Conventional ultrasonic inspection details.

Probe	Wave mode	Angle	Frequency (MHz)	Focus (mm)	Transducer size (mm)
MWB45-2	Transverse	45°	2	-	8x9
MWB55-2	Transverse	55°	2	-	8x9
MWB70-2	Transverse	70°	2	-	8x9
MWK45-2	Transverse	45°	2	-	8x9
MWK55-2	Transverse	55°	2	-	8x9
MWK70-2	Transverse	70°	2	-	8x9
MWK45-4	Transverse	45°	4	-	8x9
MWK55-4	Transverse	55°	4	-	8x9
MWK70-4	Transverse	70°	4	-	8x9
TRL45-2	Longitudinal	45°	2	~30	2(8x14)
TRL60-2	Longitudinal	60°	2	~25	2(8x14)
TRL70-2	Longitudinal	70°	2	~25	2(8x14)

Conventional ultrasonic inspection results

Signal to noise ratios (SNR) for all 12 probes for transverse wave conventional pulse echo ultrasonic inspection are shown for mechanical fatigue defects (MF15x5A and MF15x5B) and for thermal fatigue defect (TF15x5) in Figure 2.

In scanning direction 90 (e.g. MWB45-2 90) the defect MF15x5A is at the probe side of the well, whereas MF15x5B and TF15x5 are scanned through the weld. On the contrary, in scanning direction 270 (e.g. MWB45-2 270) the defects MF15x5B and TF15x5 are on the probe side, and MF15x5A is scanned through the weld. Typically the SNR was better when the scanning was done on the defect side of

the weld. Only in four cases the defect SNR is higher for the defect inspected through the weld (MWB55-2 90, MWB70-2 90, MWB70-2 270 and MWK70-2 270). MWK type probes seem to be more efficient when inspecting from the defect side.
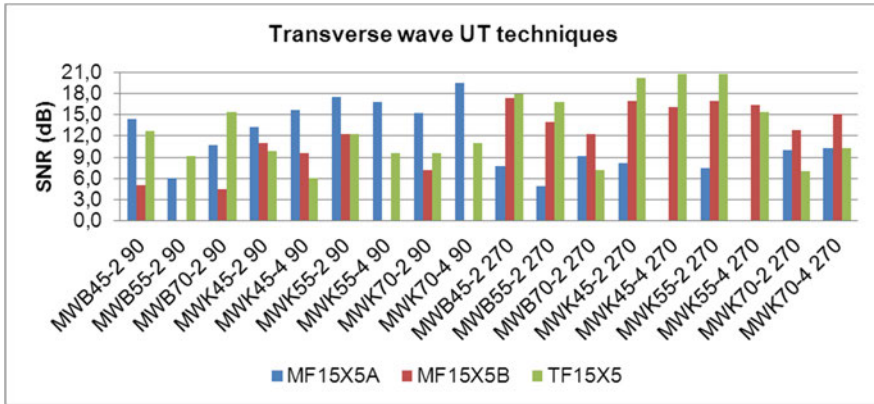

Figure 2. Conventional ultrasonic inspection results for transverse wave.

In Figure 3 longitudinal wave transmit/receive (TR) inspection result for conventional ultrasound shows that the 45 degree probe is the most efficient for both inspection from the defect side and from the opposite side of the weld. Results show that if probe angle increases the SNR decreases significantly in all cases.
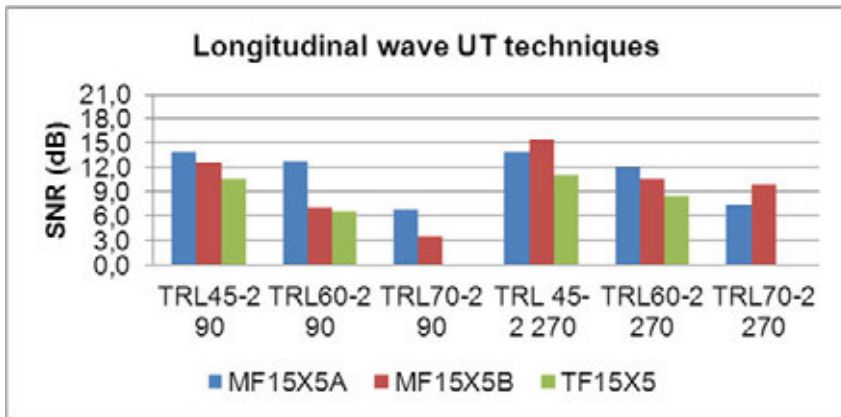
Figure 3. Conventional ultrasonic inspection results for longitudinal wave.

Phased array ultrasonic inspection

Phased array testing was carried out with three different techniques. Technique PA-1 was carried out using OmniScan 16/128PR. PA testing with techniques PA-2 and PA-3 was performed using Dynaray Lite 64/64PR. Scanning in all three techniques was carried out using Zetec's Manual Pipe Scanner anddata acquisition was controlled with UltraVision software. More detailed inspection parameters information can be seen in Table 2 and more detailed probe parameters in Table 3.

Table 2. Phased array inspection details.

Technique	Description
PA-1	Scanning from weld face side using dual matrix phased array probes with sectorial scan. Scanning was performed from both sides of the weld using manual encoded scanner with several scan lines along the weld. Technique is qualified to be used in in-service inspections of piping welds in nuclear power plants in the USA. Procedure: Zetec OmniScanPA01 rev. C.
PA-2	Scanning from weld face side using single linear phased array probes with sectorial scan. Scanning with resolution of 1 mm was performed from both sides of the weld using manual encoded scanner with several scan lines with index resolution of 5 mm.
PA-3	Scanning from weld face side using single linear phased array probe with linear electronic scan. Scanning with resolution of 1 mm was performed from both sides of the weld using manual encoded scanner with several scan lines with index resolution of 10 mm

Table 3. Phased array probe parameters.

Technique	Probe	Wedge	Wavemode	Angles	Frequency (MHz)	Focus (mm)	Aperture (mm)
PA-1	1.5M5x3E17.5-9	ADUX576A	Transverse	40–70°	1.5	25 TD	2x(9x17.5)
	1.5M5x3E17.5-9	ADUX582A	Longitudinal	40–70°	1.5	25 TD	2x(9x17.5)
PA-2	2L16A10	SA10-N55S	Transverse	40–70°	2.25	25 TD	9.6x10
	5L32A11	SA11-N55S	Transverse	40–70°	5	25 TD	11.4x10
PA-3	5L32A11	SA11-N55S	Transverse	45°, 55°, 70°	5	25 TD	11.4x10

Phased array ultrasonic inspection results

The test results for PA-1 tests are presented in Figure 4. For both mechanical fatigue defects the highest SNR values were detected when the inspection was performed from the defect side (90 for MF15x5A and 270 for MF15x5B). The difference between the mechanical fatigue defects was that MF15X5A received the highest SNR value with longitudinal wave PA probe, whereas MF15X5B received the highest SNR value with transverse wave PA probe. With TF15X5 defect the

two highest SNR values were detected with transverse wave PA probe and sur-prisingly the highest SNR value for TF15X5 defect was detected when inspection was performed through the weld.
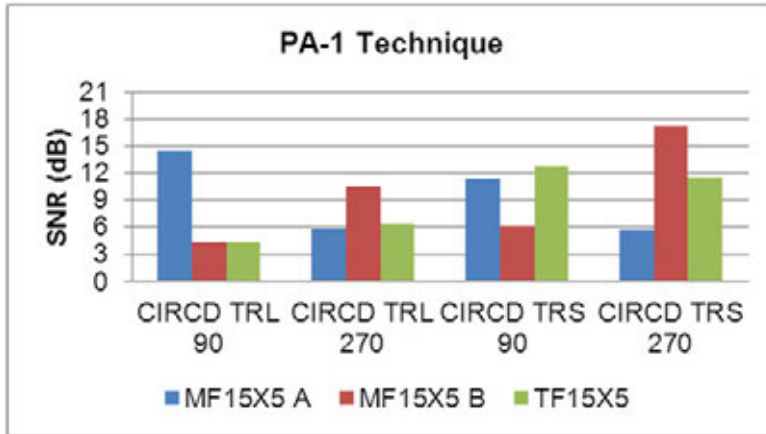

Figure 4. Phased array inspection from weld face side using dual matrix phased array probes with sectorial scan.

With PA-2 technique only transverse wave mode PA probes were used with two different frequencies 2.25 MHz and 5 MHz (Figure 5). MF15X5A and MF15X5B defects were detected only from the defect side of the weld (90 for MF15X5A and 270 for MF15X5B). TF15X5 defect was detected both from the defect side (90) and through the weld (270). It seems that there is no significant difference in SNR between the two different frequencies when inspection was performed from the defect side.
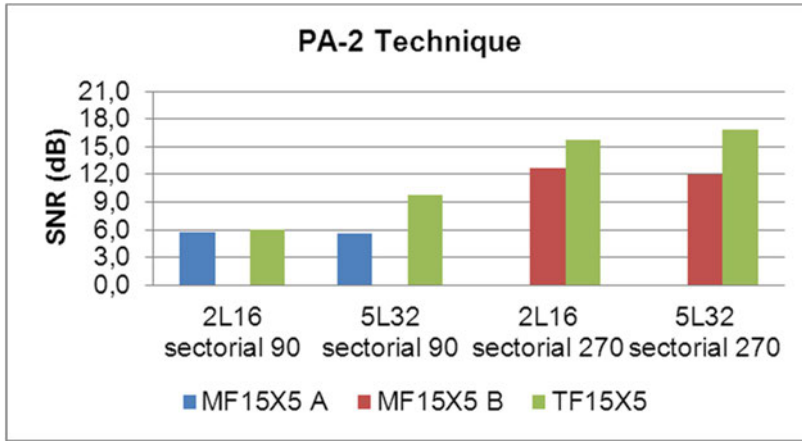
Figure 5. Phased array inspection from weld face side using single linear phased array probes with sectorial scan.

In PA-3 technique tests almost similar results were obtained as in PA-2 tests as can be seen in Figure 6. Both mechanical fatigue defects MF15X5A and MF15X5B were detected only from the defect side. Thermal fatigue defect TF15X5 was detected from the defect side as well as from the opposite side with one exception. With 70 degree angle and inspecting through the weld, TF15X5 defect was not detected.
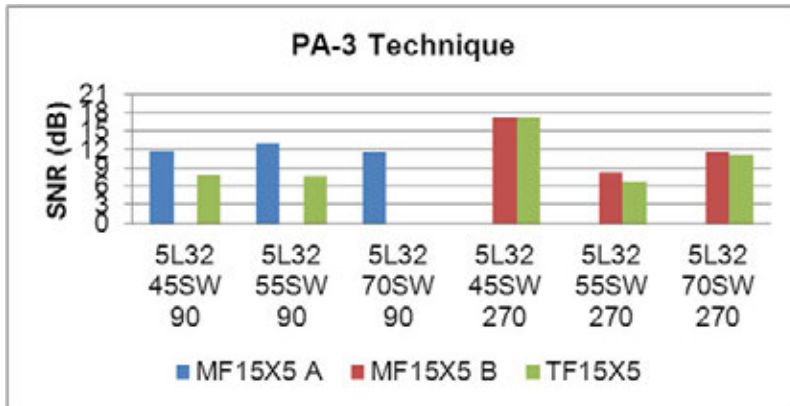
Figure 6. Phased array inspection from the weld face side using single linear phased array probe with linear electronic scan.

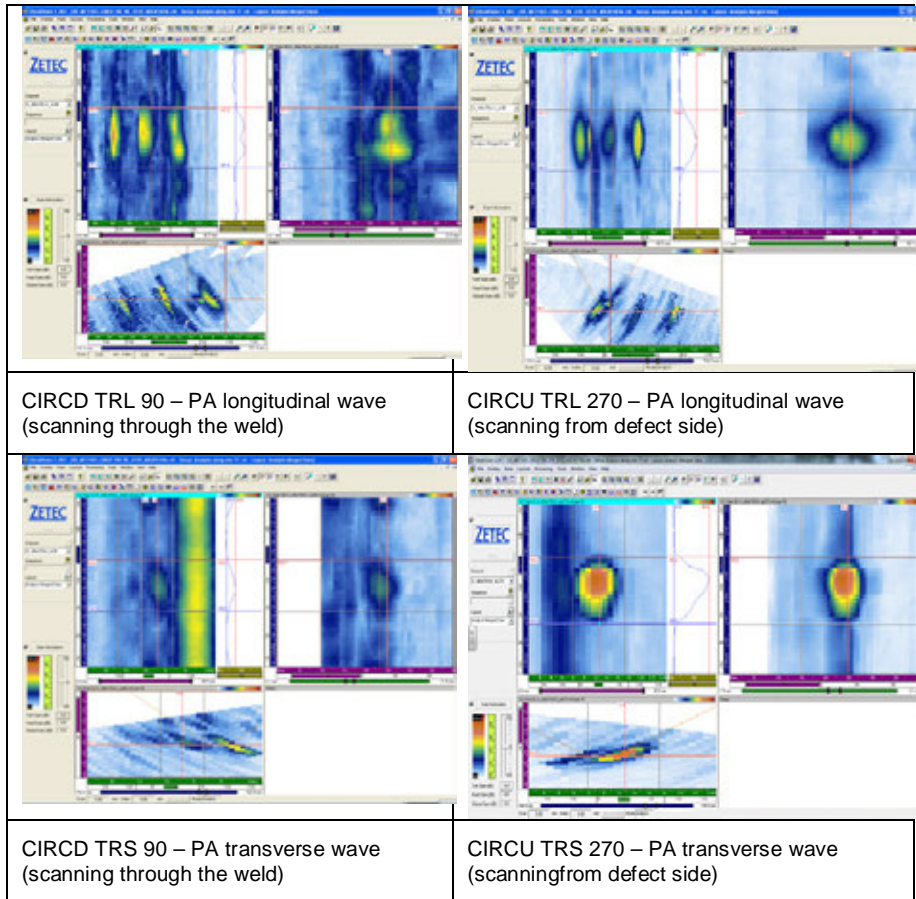|	
CIRCD TRL 90 – PA longitudinal wave (scanning through the weld)	CIRCU TRL 270 – PA longitudinal wave (scanning from defect side)
CIRCD TRS 90 – PA transverse wave (scanning through the weld)	CIRCU TRS 270 – PA transverse wave (scanningfrom defect side)

Figure 7. Phased array ultrasonic inspection of MF15x5B defect.

In Figures 7 (MF15x5B) and 8 (TF15x5) there is a significant difference between longitudinal and transverse wave inspections. In these two cases, the transverse wave inspection produced the best indication when the inspection was performed from the defect side. When the inspection was performed through the weld, longitudinal wave produced clearer indication in MF15x5B (Figure 7) whereas in TF15x5 clearer indication was produced by transverse wave (Figure 8).
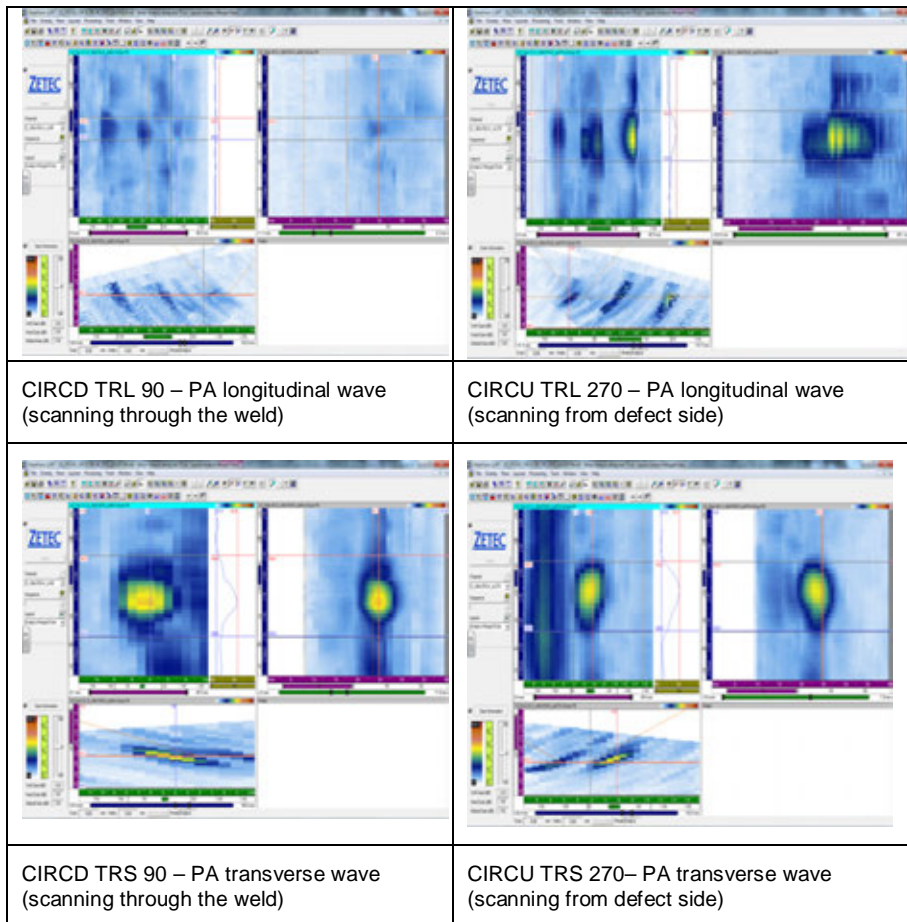
CIRCD TRL 90 – PA longitudinal wave (scanning through the weld)	CIRCU TRL 270 – PA longitudinal wave (scanning from defect side)
CIRCD TRS 90 – PA transverse wave (scanning through the weld)	CIRCU TRS 270– PA transverse wave (scanning from defect side)

Figure 8. Phased array ultrasonic inspection of TF15x5 defect.

Conclusions

In this paper first results of the differences in ultrasonic NDE reflectors were briefly presented. Even in these results it is clearly seen that the defect characteristics have a significant impact on ultrasonic indications. Not only between different types of fatigue defects but also between two mechanical fatigue defects. These results presented in this paper encourage studying this subject more during 2013. More precise analysis will be performed on the results already gained and simulation will also be made using the results of the ultrasonic tests. After the destructive inspection and evaluation, more knowledge on defect characteristics is gained and final results will be presented.

The MAKOMON project will continue in SAFIR2014 and the results already gained will carry the research forwards into the following years.

References

1. Koskinen, A., Haapalainen, J., Virkkunen, I., Kemppainen, M. Differences in Ultrasonic Indications – Thermal Fatigue Cracks and EDM Notches. 18th World Conference on Nondestructive Testing, 16–20 April 2012, Durban, South Africa.

2. Koskinen, A. Ultrasonic reflectors in ultrasonic inspections for primary circuit components – work report, VTT Research Report VTT-R-00538-12. 13 p.

3. Haapalainen, J., Leskelä, E. Probability of Detection Simulations for Ultrasonic Pulse-echo Testing. 18th World Conference on Nondestructive Testing, 16–20 April 2012, Durban, South Africa.

4. Haapalainen, J. Ultrasonic simulation and simulation verification in demanding inspection applications, VTT Research Report VTT-R-01326-12. 8 p.

5. Sandlin, S. Evolving ultrasonic NDE techniques for detecting fatigue damage and partially closed cracks, VTT Research Report VTT-R-08878-11. 45 p.

6. Jäppinen, T., Lahdenperä, K., Ala-Kleme, S. Locating Magnetite on the Steam Generator Tubes with Eddy Current. 18th World Conference on Nondestructive Testing, 16–20 April 2012, Durban, South Africa.

7. Jäppinen, T. Eddy Current Inspections to Detect Magnetite Depositions on 16x1,5 mm 316Ti tubes – Work Report, VTT Research Report VTT-R-01263-12. 8 p.

8. Haapalainen, J. Digital Radiography in Power Generation Industry, VTT Research Report VTT-R-00965-12. 29 p.

7.4 RI-ISI analyses and inspection reliability of piping systems (RAIPSYS)

Otso Cronvall[1], Jouni Alhainen[1], Kalle Kaunisto[1], Ilkka Männistö[2],
Taneli Silvonen[2], Ari Vepsä[1]

[1]VTT Technical Research Centre of Finland
Kemistintie 2, P.O. Box 1000, FI-02044 Espoo

[2]VTT Technical Research Centre of Finland
Vuorimiehentie 2, P.O. Box 1000, FI-02044 Espoo

Introduction

The overall objective of the RAIPSYS project is to support the implementation of risk informed in-service inspection (RI-ISI) at Finnish nuclear power plants (NPPs) by studying and further developing relevant issues related to RI-ISI. The main objectives are:

- the development of structural reliability methods for quantification of piping leak and break probabilities,

- further development of methods for evaluating inspection capability,

- further development of RI-ISI analysis methods, and

- strengthening inter-disciplinary readiness to combine structural integrity, non-destructive testing (NDT) and probabilistic safety analysis (PSA) expertise in Finland.

The project includes international activities, the most important being the participation in the European Network for inspection and Qualification (ENIQ), especially in the work of its Task Group on Risk.

RI-ISI aims at rational in-service inspection management by taking into account the results of plant-specific risk analyses in defining the inspection programme and focusing the inspections efforts to the most risk significant locations. Ideally, this can lead to improved safety and availability, reduced doses and reduced inspection costs.

Even though RI-ISI has been widely applied in the US, European utilities and safety authorities think that several issues need further research. Furthermore, the US RI-ISI approaches cannot always be adopted as such since they have been originally developed to the US regulatory environment, and do not comply as such with national regulations and different standards in many European countries.

In Finland, the use of risk-informed methodology in planning new ISI programmes is a regulatory requirement, and both domestic utilities are developing RI-ISI programmes for the existing plants. The ISI programme for the new EPR unit will also consider risk insights.

Evaluation of piping failure potential

There are alternative ways to assess the probability of failure, ranging from purely qualitative assessment to quantification with either statistical analysis of service data or structural reliability models. The disadvantage of a qualitative approach is that the relative importance/severity of the degradation potential is not addressed, and quantitative comparison of e.g. alternative inspection strategies cannot be done. In RAIPSYS project, methods and tools for quantification of piping failure probabilities are developed. This necessitates methods and tools for computation of leak and break probabilities due to various degradation mechanisms. This is carried out by further developing structural reliability approaches and probabilistic fracture mechanics (PFM) procedures.

In particular, the PFM procedures allow taking into account in a realistic quantitative way piping component geometry, material properties, loads and inspection strategies. Rather than considering the computed probability of failure (POF) results to represent some form of true or absolute value, they much better serve in quantifying relative POF differences between the piping components. The accuracy of the POF results can be improved by using statistical estimates based on both plant specific and global databases in order to provide anchoring/calibrating points for single POF results, in relation to which they could be improved in other locations as well. Quantitative approaches can also be used to conduct sensitivity studies, for instance to assess the impact of inspection capability and interval on the POF results.

Probabilistic analysis methods for estimating pipe component failures

Research work on structural reliability analysis methods at VTT has resulted in further development of a PFM tool. This tool is an expanded version of fracture mechanistic analysis code VTTBESIT, developed by the Fraunhofer-Institut für Werkstoffmechanik (IWM), Germany and by VTT. With the VTTBESIT code it is possible to quickly compute the stress intensity factor values along the crack front and, based on this, simulate the crack growth. VTTBESIT was expanded by adding probabilistic capabilities to the code, which was originally intended for deterministic fracture mechanics based crack growth analyses.

The accuracy of VTTBESIT was improved by developing and implementing a more accurate crack growth increment computation procedure [1]. This procedure takes into account the crack growth potential in all computation points along the crack front, whereas the earlier procedures considered it only in one or two crack front points. When simulating a crack growth increment with the new procedure, the semi-elliptic area corresponding to the next crack size is computed first, by taking into account all crack growth vectors along the crack front, see Figure 1. Then, the shape of the area is determined from the relation of the through wall and parallel to wall surface components of the crack growth vectors. According to

application computations, the results agree quite well with those obtained with finite element (FE) analysis code Zencrack in an earlier SAFIR2010 project FRAS. On the other hand, the agreement is very good with results computed with such procedure which takes into account the crack growth vectors only from the crack surface and tip points.

Another achievement concerning crack growth computation procedure was the addition of plasticity correction factor [2]. This allows taking into account the locally confined elastic-plastic stress concentration surrounding the crack front. In most NPP piping analysis cases this stress concentration region is very small as compared to the other relevant dimensions, and thus its effect is practically negligible. However, in cases with relatively large cracks and severe loading, taking into account the plasticity correction can improve the accuracy of the crack growth computations. As for the relevant degradation mechanisms concerning NPP piping components, the plasticity correction can be applied both to stress corrosion cracking (SCC) and fatigue induced crack growth computations.

VTTBESIT code uses Latin hypercube simulation (LHS) in the probabilistic simulation. In order to investigate possible computationally more efficient probabilistic methods, a case study concerning importance sampling (IS) was performed. This sampling method is a variance reduction method that can be used to enhance the plain Monte Carlo simulation (MCS) method. With IS the sampling is concentrated near the values of the random variables which are the most important with regard to the probability to be estimated. When this probability decreases, the resulting values usually concentrate increasingly more on the tails of their corresponding density functions. According to the analysis results, if the procedure is to be repeated often, and if less conservative assumptions are used for lower transfer probabilities, the IS is a useful alternative probabilistic simulation procedure [1].
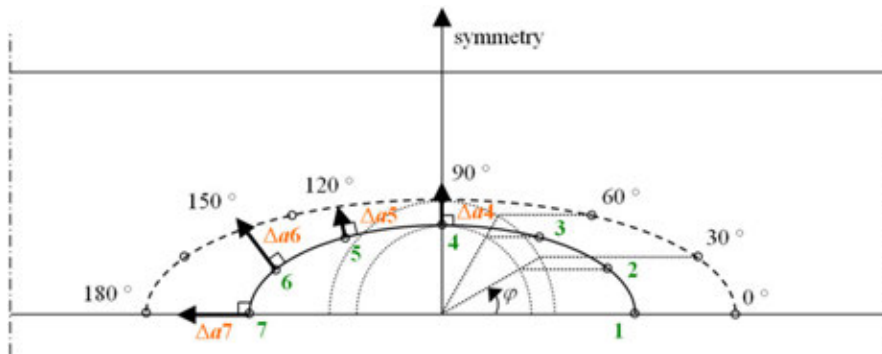

Figure 1. Crack postulate with local crack growth vectors [1].

Database applications

A study on the estimation of crack initiation and leak frequencies concerning NPP piping components by using NPP piping degradation databases was performed [3]. This included also the OECD Pipe Failure Database OPDE which is for the time being arguably the most significant database on NPP piping component degradation and failures. In particular, OPDE was utilized in failure initiation rate and leak frequency estimation for boiling water reactor (BWR) and pressurized water reactor (PWR) primary circuit piping welds, while the considered degradation mechanism was stress corrosion cracking (SCC). The analysis approach covered also the effect of inspections.

As OPDE does not contain any piping component or weld population data, the population data from Swedish NPP unit Barsebäck-1 were used for the BWR cases, and corresponding data obtained from NUREG/CR-4407 report for the PWR cases.

The applied computational procedure was based on a Markov model, which uses a differential equation to take into account the degradation. In a Markov model, the transition rates between the degradation states are placed into a transition matrix, and the probabilities that a given state is occupied in a certain component follow from matrix multiplication.

It was concluded that the applied approach for computation of flaw initiation and leak frequencies, the latter considered here as failure probabilities, is feasible for practical analysis purposes. The study includes also the programming of the used approach. However, without more detailed input data the usefulness of the obtained results is somewhat limited. In practical applications, piping component and weld population data from actual NPP units would be used. However, the accuracy of the analysis results would remain limited if no data concerning smaller detected cracks/flaws are made available. An analysis result example concerning one BWR primary circuit weld is shown in Figure 2.
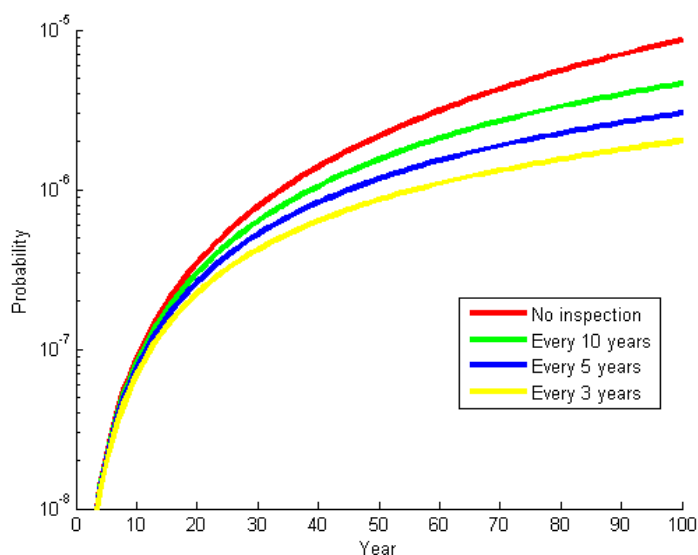
Figure 2. For three different inspection intervals and case of no inspections, the probability of failure for one BWR primary circuit pipe weld over 100 years [3].

RI-ISI methodologies

The research work on RI-ISI methodologies concerns issues related to risk ranking, selection of inspection sites and acceptance criteria of a RI-ISI program. As the main criterion for the acceptance of a RI-ISI program is that the risk will not increase when replacing the earlier ISI program with the risk informed equivalent, one research subject is the robust quantification of the change in risk. Another issue is to provide both development and application guidance concerning quantitative RI-ISI methodology. As a supporting approach, the benefits and applicability of risk informed safety margin characterisation (RISMC) approach to RI-ISI analyses were examined. The international co-operation and connections concern mainly participation to activities of ENIQ.

ENIQ Task Group Risk activities

VTT has actively participated in the work of the Task Group Risk (TGR) of ENIQ. The TGR works towards developing European best practices for RI-ISI methodologies. The participation to TGR work includes contributing to ENIQ consensus documents, position/discussion documents and technical reports as well as attending the ENIQ TGR meetings. More recently, ENIQ activities include also the follow-up of development of and adaptation to ENIQ, as in 2012 it has become a part of the NUGENIA Association. This far the main reporting contribution by VTT

has been to ENIQ TGR discussion document: RI-ISI – Lessons Learned from Application to European Nuclear Power Plants.

Effect of initial flaw and load assumptions on risk estimate changes

This study, spanning altogether three years, concerns the effect of initial flaw and load assumptions on risk estimate changes [4]. In addition, the effect of inspections is also taken into account. The performed analyses are summarised, to provide the most suitable way to present the achieved results. As the main criterion for the acceptance of a RI-ISI program is that the risk shall not increase when moving from the earlier ISI program to the risk informed one, means for robust quantification of the change in risk are needed.

The performed degradation potential and risk analyses concern a representative selection of NPP piping welds. Worldwide several initial flaw distribution assumptions for NPP pipe welds have been published. The main load component concerning welds is most often the welding process induced residual stresses (WRSs), and also for them several distribution assumptions have been published. Of the degradation mechanisms encountered in the NPP environments, the WRSs affect especially SCC. To describe the accuracy of the NDT to find cracks, applicable probability of detection (POD) functions were used.

The scope of this study covers:

- three representative BWR pipe weld cross-section sizes with the weld material similar to austenitic stainless steel, see Table 1,

- SCC as the considered degradation mechanism, with the considered flaw postulate being a semi-elliptic circumferentially oriented crack opening to inner surface,

- operational BWR conditions as the considered process loads, with pressure of 70 bar and temperature of 286°C,

- three sets of probability density distributions for sizes of initial cracks, one of which has been developed within this study, see Table 1,

- three distributions for the WRSs as well as the case of no WRSs, see Table 1,

- inspection intervals of 3 and 10 years as well as the case of no inspections.

Table 1. Input data used in performed degradation potential and risk analyses.

Pipe size	Outer diameter [mm]	Wall thickness [mm]	Reference
Small	60	4.0	[4]
Medium	170	11.0	[4]
Large	310	26.0	[4]
Initial crack sizes by	**Cause for crack initiation**	**Median crack depth [mm]**	**Reference**
Simonen & Khaleel	fabrication	1.4 … 2.7 (*)	[5]
NURBIT distribution	SCC	1.0	[6]
VTT distribution	SCC	0.5	[4]
WRSs by/from	**Maximum value [MPa]**	**Minimum value [MPa]**	**Reference**
ASME	200, 210, 210 (**)	-200, -210, -210 (**)	[7]
R6 Method, Rev. 4	320, 320, 320 (**)	30, 30, 120 (**)	[8]
SSM handbook	200, 260, 50 (**)	-200, -170, -50 (**)	[9]
POD from	**Scope**	**NDT quality options**	**Reference**
NUREG/CR-3869	intergranular SCC, austenitic stainless steels and ferritic steels	advanced, good, poor	[10]
CCDP value	**No. of degradation states**	**Time in operation [years]**	**Reference**
0.00001	10	60	[4]

(*) depends on wall thickness,

(**) for Small, Medium and Large pipe weld cross-sections, respectively.

In the VTT application for degradation potential and risk analyses, the crack growth through the pipe wall is quantified with discrete degradation states. This approach allows the use of Markov process simulations to calculate the leak and failure probabilities for piping components. The transition probabilities are assessed using the results from the PFM simulations, which are performed with the probabilistic VTTBESIT code. In the VTTBESIT simulations the sizes of the initial cracks are taken randomly from the respective probability density functions, while all other input data variables are considered as deterministic. VTTBESIT results are used to construct a degradation matrix for the Markov process, in which crack growth leads into more degraded states, while inspections and subsequent repairs/replacements lead into less degraded states. For transition probabilities into less degraded states, POD functions are used. They are applied in the computations in the form of inspection matrices. Figure 3 illustrates a four state Markov model for pipe degradation and inspections with repairs.
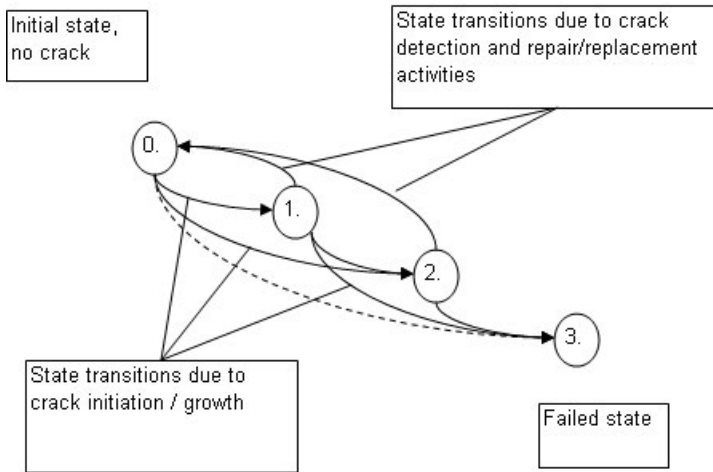
Figure 3. Four state Markov model for pipe degradation and inspections with repairs [4].

A set of leak probability results is shown in Figure 4 and a set of risk results in Figure 5, respectively. To summarise, the effect of initial flaw and load assumptions as well as inspections on risk estimate changes is remarkable. At the start and early phase of operation the initial crack sizes dominate the POF and risk results. In general, the highest POF and risk values were obtained with fabrication cracks, while the lowest POF and risk values were achieved with SCC induced initial cracks developed within this study. Towards the end of operation the effect of initial crack sizes to POF and risk results decreases remarkably, while the effect of loads increases considerably. Of the three used WRS distributions, i.e. those given in R6 Method, Rev. 4, ASME recommendations and SSM handbook, the first one provides the highest WRS values in the tensile side. Towards the end of operation the POF and risk curves for the cases with the R6 Method WRSs climb to the highest positions. The inspections remarkably decrease the POF and risk values, but after inspection they soon start to climb higher again.
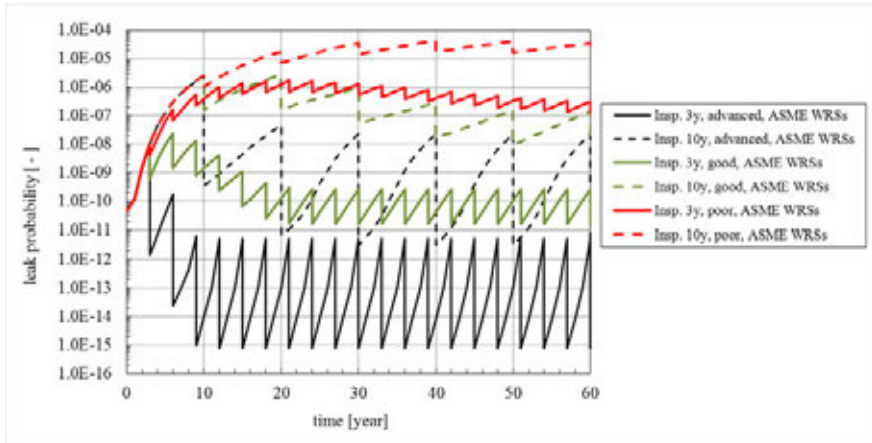
Figure 4. Leak probability results for Medium weld cross-section with fabrication flaws as initial cracks [4].
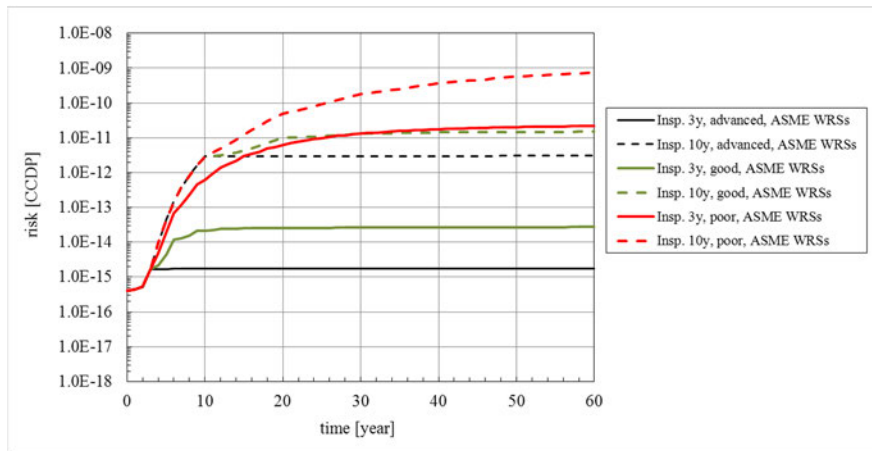

Figure 5. Risk results for Medium weld cross-section with fabrication flaws as initial cracks [4].

Scientific and academic publications

Scientific journal article: Assessment of Initial Cracks for RI-ISI Analysis Purposes [11]. The article concerns quantitative assessment of initial cracks. Two developed approaches to recursively calculate estimates for the sizes of the initial cracks are described. The application example presents the impact of different initial crack sizes on POF results.

Scientific journal article: A study on the effect of flaw detection probability assumptions on risk reduction achieved by non-destructive inspection [12]. The article summarises the results of a study on the effect of piping inspection reliability assumptions on failure probability using structural reliability models. The main interest was to investigate whether it is justifiable to use a simplified POD curve. Further, the study compared various structural reliability calculation approaches for a set of analysis cases. The results indicate that the use of a simplified POD could be justifiable in RI-ISI applications.

Scientific VTT publication: Structural lifetime, reliability and risk analysis approaches for power plant components and systems [13]. The publication begins with an overview of power plant environments and a description of the various degradation mechanisms affecting the power plant systems and components. Then, deterministic structural analysis methods are described. Several probabilistic analysis procedures and risk analysis methods are presented. The modelling methods for various degradation (or ageing) mechanisms are described. As for the analysis applications, a wide selection of probabilistic system/component degradation and risk analysis software tools is presented. The computational application concerns probabilistic failure and lifetime analyses to a representative set of NPP piping components with probabilistic analysis codes VTTBESIT and PIFRAP. The publication ends with a summary and suggestions for future research.

Licentiate in technology thesis: Structural lifetime, reliability and risk analysis approaches for power plant components and systems [14]. The above mentioned scientific VTT publication is based on this thesis.

References

1. Cronvall, O., Vepsä, A. Further development and validation of probabilistic analysis application VTTBESIT. Research Report VTT-R-01837-12, Technical Research Centre of Finland (VTT), Espoo, Finland, March 2012. 49 p. + app. 7 p.

2. Alhainen, J., Kaunisto, K., Vepsä, A. Further development and validation of probabilistic analysis application VTTBESIT: the work carried out in 2012. VTT Research Report VTT-R-08803-122, Technical Research Centre of Finland (VTT), Espoo, Finland, 2013.

3. Kaunisto, K., Männistö, I. Estimation of crack initiation and leak frequencies using NPP piping degradation databases. Research Report VTT-R-00078-12, Technical Research Centre of Finland (VTT), Espoo, Finland, March 2012. 25 p.

4. Cronvall, O., Kaunisto, K. Second phase of a study – rEffect of initial flaw and load assumptions on risk estimate changes. VTT Research Report

VTT-R-08805-12, Technical Research Centre of Finland (VTT), Espoo, Finland, 2013.

5. Khaleel, M., A., Simonen, F., A. Effects of alternative inspection strategies on piping reliability. Nuclear Engineering and Design 197 (2000) 115–140.

6. Brickstad, B. The Use of Risk Based Methods for Establishing ISI-Priorities for Piping Components at Oskarshamn 1 Nuclear Power Station. SAQ/FoU-Report 99/5, SAQ Control AB, Sweden, 1999. 83 p.

7. Section XI Task Group for Piping Flaw Evaluation, ASME Code. Evaluation of Flaws in Austenitic Steel Piping. Journal of Pressure Vessel Technology, 108(1986), 352–366.

8. R6 Method; Assessment of the Integrity of Structures containing Defects, Revision 4. 2004 update of 2001 edition. British Energy (BE).

9. Dillström, P. et al. 2008. A Combined Deterministic and Probabilistic Proce-dure for Safety Assessment of Components with Cracks – Handbook. SSM Research Report 2008:01, Swedish Radiation Safety Authority (Strålsäkerhetsmyndigheten, SSM). Stockholm, Sweden, 2008. 27 + 196 p.

10. Simonen, F., A., Woo, H., H. Analyses of the Impact of Inservice Inspection Using a Piping Reliability Model. NUREG/CR-3869, Topical Report. U.S. Nuclear Regulatory Commission (USNRC), July 1984. 59 p.

11. Cronvall, O., Männistö, I., Alhainen, J. On Assessment of Initial Cracks for RI-ISI Analysis Purposes. Journal of Materials Science and Engineering B1(2011), 296–307.

12. Cronvall, O., Simola, K., Männistö, I., Gunnars, J., Alverlind, L., Dillström, P., Gandossi, L. A study on the effect of flaw detection probability assump-tions on risk reduction achieved by non-destructive inspection. Reliability Engineering & System Safety 105(2012), 90–96.

13. Cronvall, O. Structural lifetime, reliability and risk analysis approaches for power plant components and systems. VTT Publications 775. 264 p. http://www.vtt.fi/inf/pdf/publications/2011/P775.pdf

14. Cronvall, O. Structural lifetime, reliability and risk analysis approaches for power plant components and systems. Aalto University School of Science and Technology, December 2011. 193 p.

7.5 Advanced surveillance technique and embrittlement modelling (SURVIVE)

Matti Valo, Petteri Lappalainen, Tuomo Lyytikäinen, Jari Lydman, Marko Paasila

VTT Technical Research Centre of Finland
Tekniikantie 2, P.O. Box 1000, FI-02044 Espoo

Introduction

The target of SURVIVE project is to understand irradiation embrittlement, annealing and re-irradiation behaviour of pressure vessel steels in order to base safety assessment of the pressure vessels on sound physical knowledge. Good understanding requires mechanical test data, understanding of the effect of irradiation, annealing and re-irradiation on microstructure and modelling, which shall link microstructure to mechanical properties. The modelling chain is long and it has been described up to now only to limited extent and qualitatively. SURVIVE focuses on high impurity VVER440 steels, which are not studied e.g. in EU framework programmes. High impurity VVER440 pressure vessels are in use in Russia, Finland and Ukraina. Cleaner VVER440 pressure vessels are operated in addition in Czech Republic, Hungary and Slovakia.

Mechanical test data is created by small specimens and hence acceptability and applicability of small specimen data is one focus in SURVIVE. During the reporting period specimen reconstitution performed with the new electron been welding system has been validated [1]. The dependence of the value of the Master Curve T0 on specimen geometry is also under study in SURVIVE. Comparative test with small CT-specimens and three point bend specimens are under way and the same subject is studied in a CRIEPI/Japan co-ordinated research programme, where several Japanese partners, VTT, UJV, EPRI, ORNL and Westinghouse participate. Small specimen studies are not further described in the current review.

Modelling work is currently focused on cleavage fracture of real materials [2] and a software package to include multi-crystalline structure into the model has been completed. The modelling work continues. It is also essential to describe mechanical properties behaviour as a function of neutron fluence, fluence rate and copper and phosphorus contents. The simplest way is to perform curve fits and create best fit trend curves [3]. The evolution of microstructural changes should be reflected in the trend curves. Modelling is not further discussed in this review.

The microstructures formed during irradiation have the size of few nanometers and the only powerful analysing method is atom probe tomography (APT), which is able to identify as well as to localize single atoms in the structure. Small angle neutron scattering (SANS) is also a sound physical method, which can measure size distributions of microstructural formations in material. Positron annihilation (PA) is sensitive to volume type defects and it can form localized states in copper based formations. With coincident doppler broading (CDB) technique the physical

surrounding of the annihilated positron can be identified. APT, SANS and PA are performed as co-operation with foreign partners. Currently the main co-operation partners are Helmholz Zentrum Dresden-Rossendorf (HZDR), Tohoku University and CRIEPI/Japan.

Annealing is in principle a powerful tool for identifying embrittlement mechanisms, if multiple mechanisms are available, the idea being that annealing depends on activation energy of the formation and hence different formations anneal separately from each other. Resistivity as well as hardness measurements are performed as a function of annealing treatment. Microstructural studies are further discussed below.

Microstructure of steels

Microstructural studies on weld 501, which is the surveillance material for vessel annealing in Loviisa, were initiated some years ago and new data has emerged recently. This data is described in some detail. The surveillance programme is schematically shown in Figure 1 and the irradiation parameters are given in Table 1. Material representing several irradiation-annealing conditions in the matrix has been sent to HZRD and to Tohoku University.
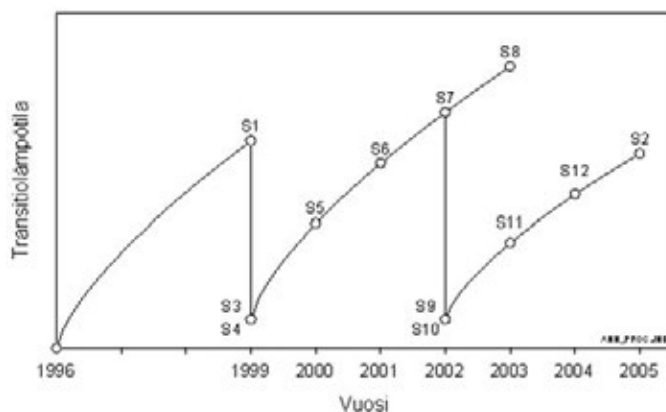
Figure 1. Surveillance programme for vessel annealing realized with weld 501. Transition temperature on y-axis and irradiation time (year) on x-axis.

Table 1. The irradiation conditions and phosphorus content of weld 501. Copper content is constant Cu = 0,14 wt-%.

Capsule	State	P	I	IAI	IAIAI
		wt-%	*	*	*
-	ref	0.028	0	-	-
1S1	I	0.038	2.5	-	-
1S3	IA	0.040	2.5	0	-
1S5	IAI_1	0.032	2.5	0.9	-
1S6	IAI_2	0.034	2.5	1.8	-
1S7	IAI_3	0.039	2.5	2.7	-
1S8	IAI_4	0.038	2.5	3.6	-
1S9	IAI_3A	0.038	2.5	2.7	0
1S11	IAI_3AI_1	0.034	2.5	2.7	0.9
1S12	IAI_3AI_2	0.030	2.5	2.7	1.8
1S2	IAI_3AI_3	0.039	2.5	2.7	2.7

*10^{19} n/cm^2, E > 1 MeV

Small angle neutron scattering data from HZRD

Small angle neutron scattering (SANS) data [4] was measured by HZDR with the neutron beams in Saclay and in Berlin research reactors. The measurements were performed before atom probe tomography data (APT), i.e. data on chemical contents of the formations, was available. With SANS the size distribution of clusters can be determined reliably but SANS is relatively poor in identifying the chemical contents of the formations. Hence the measured size distributions are reliable but volume fractions and number densities, which correlate with mechanical properties, shall be reanalysed based on the new APT data. The assumed iron content of the copper rich formations is key parameter for determining the volume fractions. Size distributions of the clusters in the un-irradiated, irradiated and irradiated-annealed conditions are shown in Figure 2.
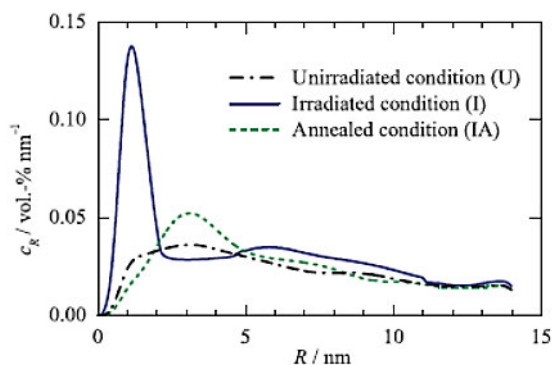
Figure 2. Size distributions of scattering formations in the un-irradiated, irradiated and irradiated-annealed conditions measured by SANS.

In the un-irradiated condition broad distribution of low volume fraction formations are observed. In the irradiated condition a very clear and narrow peak of approximately 1 nm formations is seen. In the irradiated-annealed condition the peak has shifted approximately to 3 nm and it has broadened. Data on re-irradiation behaviour is shown in Figure 3.
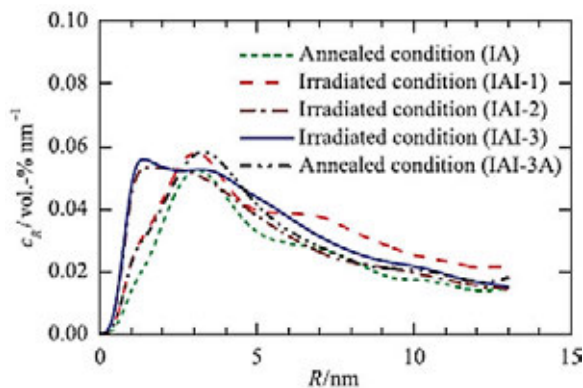

Figure 3. Size distributions of scattering formations in the annealed condition, in the re-irradiated conditions IAI1, IAI2, IAI3 and in the re-annealed condition IAI3-A.

Size distribution of the microstructural formations in the first re-irradiated condition IAI (I=0.9) is nearly the same as the distribution in the annealed condition IA. Slight increase in the number of formations of size 1nm and of size 7nm is observed compared to annealed condition IA. In the second re-irradiated condition IAI (I=1.8) a clear and strong increase in the number of 1nm formations is noticed. In the third re-irradiated condition IAI (I=2.7) the number of the 1nm formation has

not increased further and an apparent saturation is observed. In the second time annealed condition IAIA the size distribution of the formations is nearly the same as in the first annealed condition except that some amount of 1nm formations may remain in the structure. The scattering ratio A (ratio of magnetic scattering to nuclear scattering) was not easy to fit to the assumed chemistry of the formation but APT data was not available at that time. Re-analysis may clarify the situation.

Atom probe tomography (APT) and positron annihilation data

The APT measurements were performed by Tohiku University [5] with same material as the SANS measurements by HZRD. Figure 4 shows the distribution of atoms measured for the unirradiated condition. Vanadium and iron carbides are visible but no clustering of copper or other atoms is seen. Figure 6 shows the distributions of atoms in the irradiated condition, Figure 7 the distribution of atoms in the IA-condition and Figure 8 the distribution of atoms in the IAI-condition.

In the un-irradiated condition iron and vanadium carbides are seen but no other atoms show clustering. In the irradiated condition large number of copper rich formations are seen and in addition vanadium and iron carbides. In the irradiated-annealed condition few large copper rich formations are seen with some amount of Si, Mn, Ni, P and V in them. In the irradiated-annealed-reirradiated condition few large copper rich formations remain with some amount of Si, Mn, Ni, P and V in them but also new small copper rich clusters are observed. Notice that the re-irradiation fluence is small, i.e. I=0.9, compared to the initial fluence I=2.5 and hence the number of small copper formation in I- and IAI-conditions should not be directly compared.
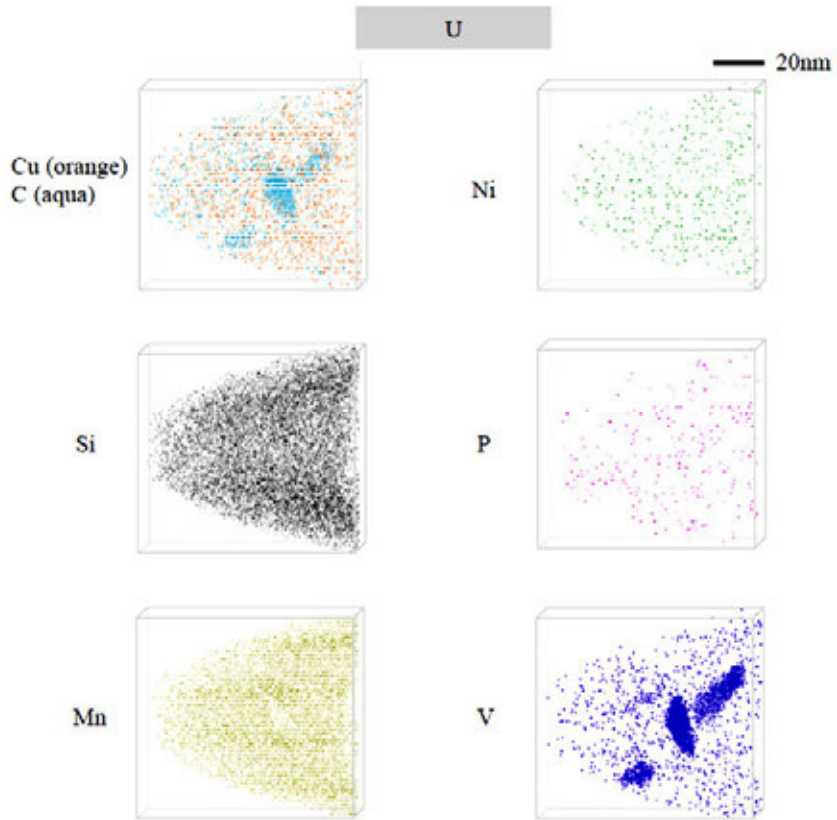
Figure 4. Distribution of atoms in the un-irradiated condition of weld 501. Iron and vanadium carbides are observed but no other atoms show clustering.
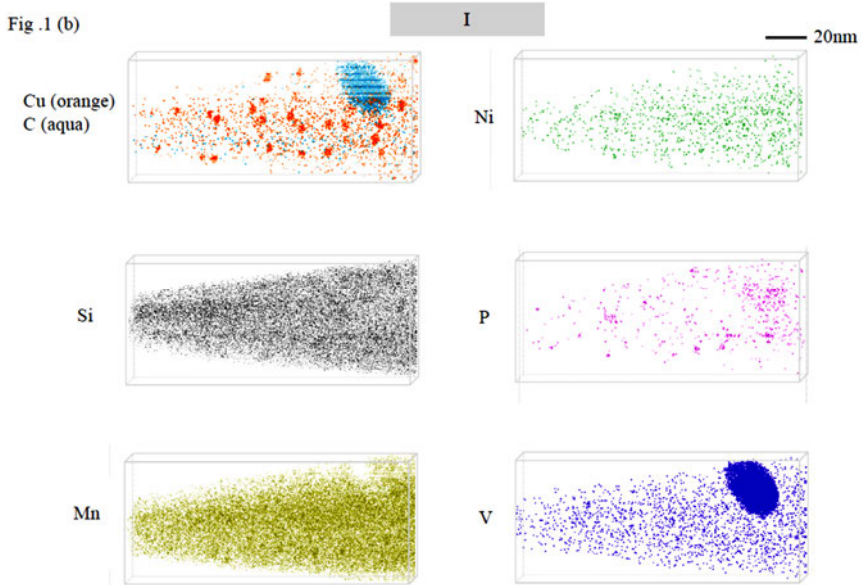
Figure 5. Distribution of atoms in the irradiated condition of weld 501. Large number of small copper rich formations are seen. In addition vanadium and iron carbides.
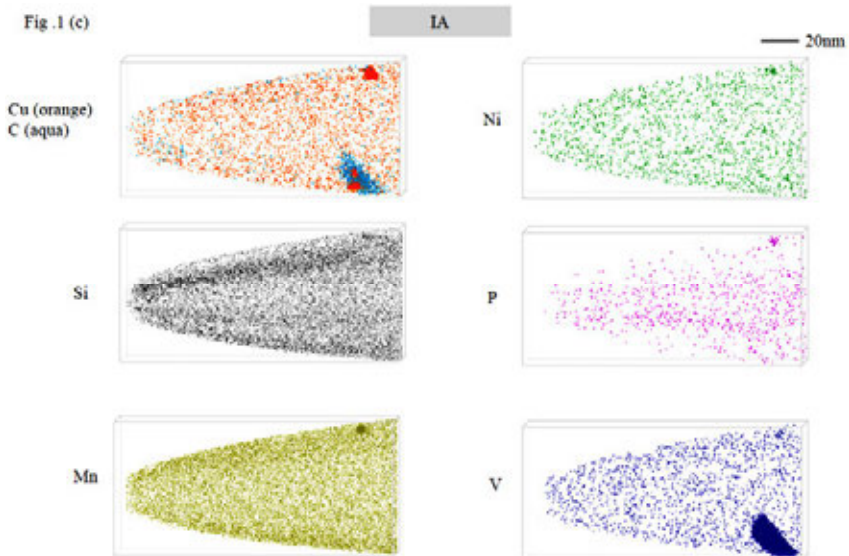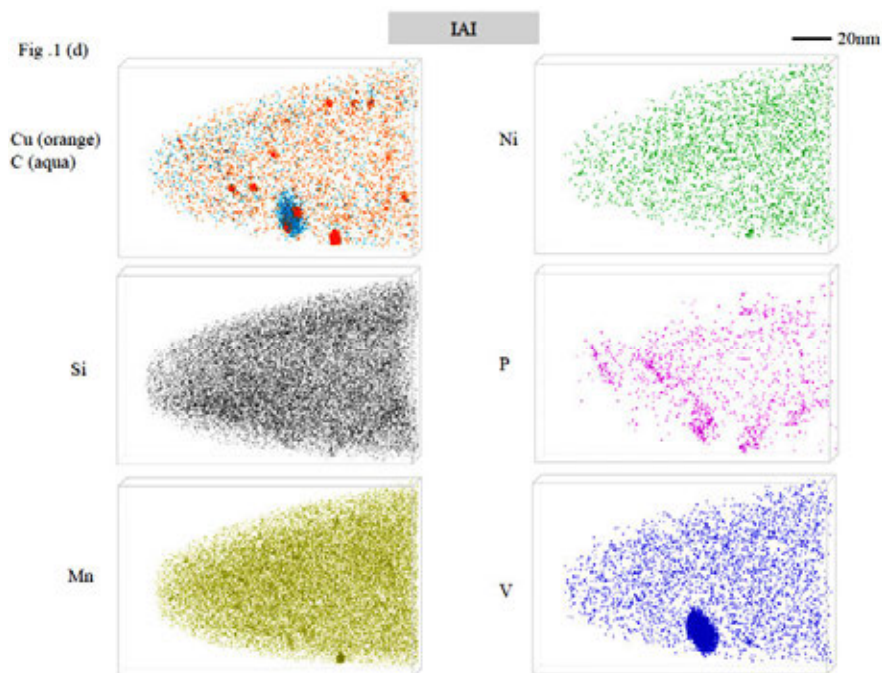

Figure 6. Distribution of atoms in the irradiated-annealed condition of weld 501. Some large copper rich formations are seen with some amount of Si, Mn, Ni, P and V constituents.

Figure 7. Distribution of atoms in the irradiated-annealed-reirradiated condition of weld 501. Some large copper rich formations are observed with some amount of Si, Mn, Ni, P and V and in addition new small copper rich clusters. Notice that the re-irradiation fluence is small, i.e. I=0.9, compared to the initial fluence I=2.5.

A closer look at the vanadium carbides and the nearby atoms is show in Figure 8. Copper and phosphorus atoms have been clustered on the carbide surface and these formations do not resolve to the matrix during annealing. A closer look at atoms near the dislocations is shown in Figure 9. The measurement reveals that phosphorus and copper atoms have been located in dislocations. Composition of clusters as a function of cluster size is shown in Figure 10. Copper content is proportionally larger in large clusters than in small clusters. Ni, Mn and Si contents of the cluster decrease when the cluster size increases. Composition of clusters is summarized in Figure 11, where the composition of small and large copper rich clusters is given in the I-, IA- and IAI-conditions. The composition of small clusters is the same in the I- and IAI-conditions. Practically no phosphorus is observed in the clusters in IA- condition.
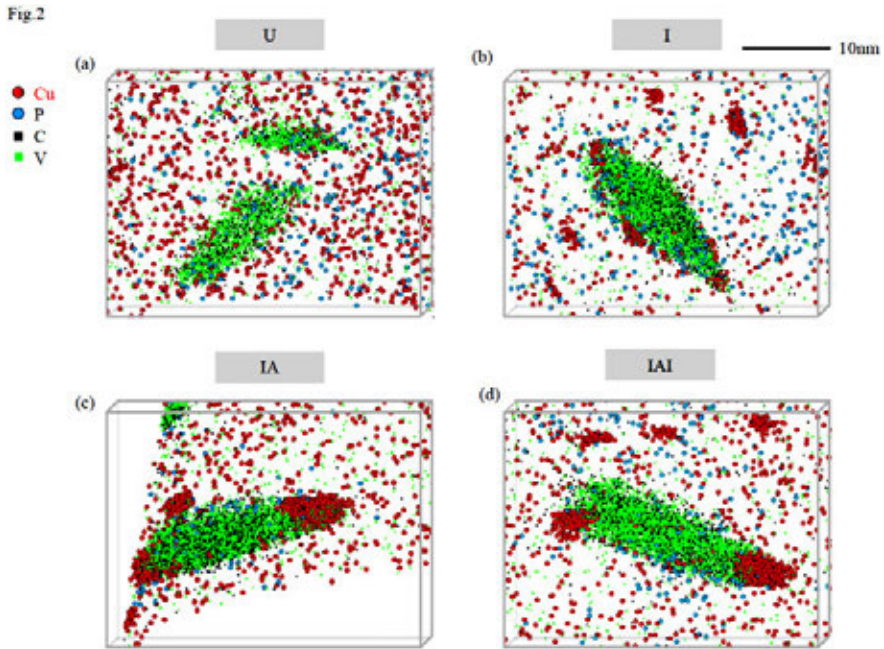
Fig.2

Figure 8. Distribution of atoms near a vanadium carbide in various irradiation-annealing conditions. Copper and phosphorus will cluster on the surface of the carbide during irradiation and re-irradiation and these atoms will not dissolve into matrix during an annealing treatment.
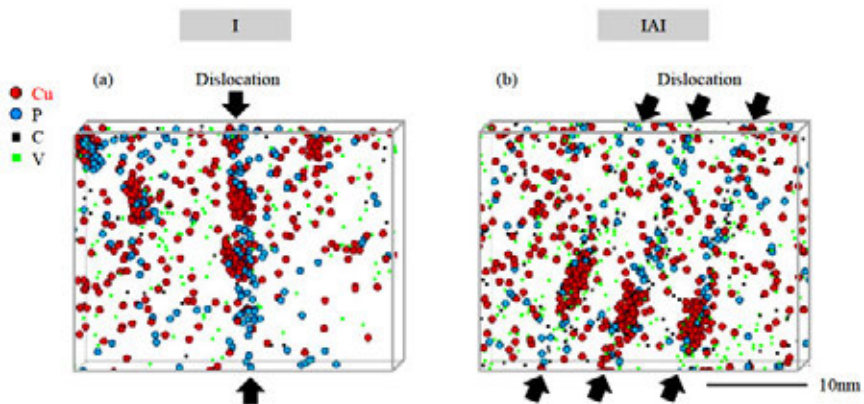

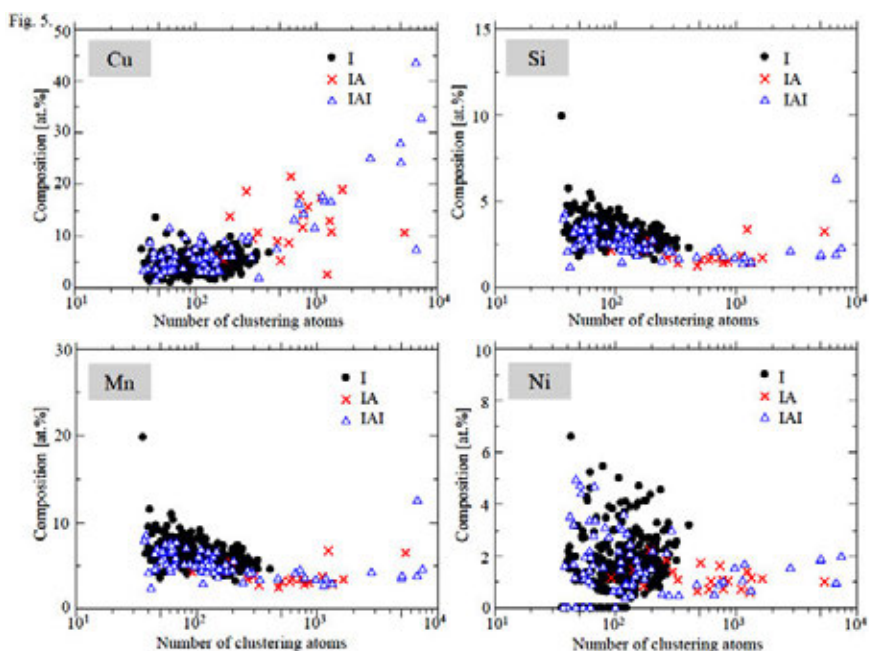**Figure 9.** Decoration of dislocation by copper and phosphorus atoms.

Figure 10. Composition of clusters as a function of cluster size. It is seen that copper concentration in a cluster increases as function of cluster size. Concentration of other atoms, i.e. Si, Mn and Ni, decrease, when the cluster size increases.
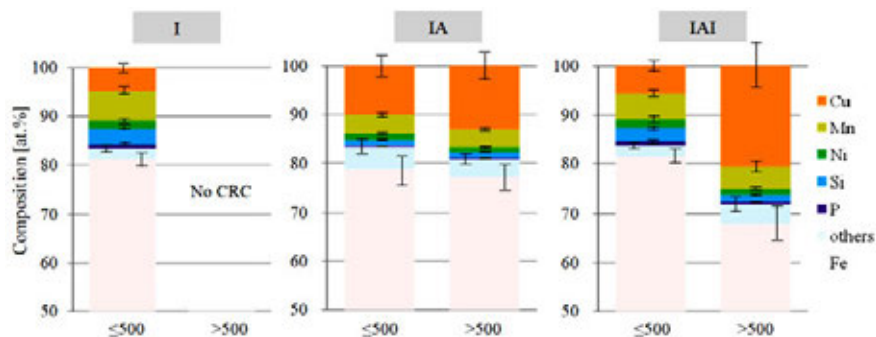

Figure 11. Composition of small and large clusters in I-, IA- and IAI-conditions. The small clusters in I- and IAI-conditions have the same composition. Large clusters have proportionally more copper than the small clusters. The clusters in IA-condition have practically no phosphorus.

Summary

SANS and APT data is very consistent with each other. Analysis of SANS data will benefit from the composition data measured by ATP but this reanalysis has not yet been made.

Tohoku University performed also positron annihilation measurements, which are not discussed here. Positrons are sensitive to open volume defects, which APT cannot detect. Scattering ratio A is sensitive to vacancy type defects and hence PA can further support the analysis of SANS data.

Hardness of the samples was measured and the hardening response of the clusters identified by APT was estimated by the Russell-Brown model. It was observed that material hardening during the first irradiation can be well explained by the model. The calculated hardening during re-irradiation, however, was only 50% of the measured hardening. Hence other hardening mechanisms should be active.

In the Russian norm the chemistry factor in embrittlement formula is $800*(P+0.07*Cu)$ and in high impurity welds like weld 501 phosphorus accounts for approximately 75% of the embrittlement shift and copper only for 25%. The dominating role of phosphorus is not explained by the current data, i.e. new experiments and ideas are required.

References

1. Valo, M., Lappalainen, P., Lydman, J., Lyytikäinen, T. Physical bases of specimen reconstitution. VTT-R-00508-12, 2012.

2. Laukkanen, A. Library and wrapper for microstructures of polycrystalline and composite materials. VTT-R-00214-12.

3. Valo, M. Irradiation embrittlement trend curves of VVER 440 weld and base metals based on Charpy-V surveillance data, TUO73-043591, 2004.

4. Ulbricht, A., Bergner, F., Böhmert, J., Valo, M., Mathon M.-H., Heinemann, A. SANS response of VVER440-type weld material after neutron irradiation, post-irradiation annealing and re-irradiation. Philosophical Magazine, 87(12), 21 April 2007, 1855–1870.

5. Kuramoto, A., Toyama, T., Nagai, Y., Inoue, K., Nozawa, Y., Hasegawa, M., Valo, M. Microstructural changes in VVER440-type weld material after neutron irradiation, post-irradiation annealing and reirradiation studied by atom probe tomography and positron annihilation spectroscopy. To be submitted to Acta Materialia.

7.6 Water chemistry and plant operating reliability (WAPA)

Martin Bojinov[2], Petri Kinnunen[1], Timo Saario[1], Saija Väisänen[1]

[1]VTT Technical Research Centre of Finland
Tekniikantie 2, P.O. Box 1000, FI-02044 Espoo

[2]University of Chemical Technology and Metallurgy
Kl. Ohridski Boulevard 8, 1756 Sofia, Bulgaria

Introduction

The main focus in the project "Water chemistry and plant operating reliability" is to study the role of water chemistry in preventing degradation of the components both in the primary and secondary side of NPPs.

The primary circuit of a new PWR reactor is passivated (preoxidised) before loading the first fuel. This procedure is called Hot Conditioning which is part of the Hot Functional Testing (HFT). The main purpose of the preoxidation is to minimise the concentration of corrosion products in the coolant during future power cycles, and thus minimise corrosion damage and activity build-up at the plant. There is no international consensus on the best available procedure for HFT. Open questions exist on the minimum length of passivation time, the optimal concentration of Li, and the use of boric acid. Answers to these questions were sought after within this project and are reported in this paper.

In the secondary circuit, a major factor influencing the lifetime and reliability of the steam generator and some other components is degradation caused by magnetite deposition. In this project, the main focus has been to develop understanding of and a model for dissolution, deposition and re-entrainment of magnetite and soluble iron species in the secondary circuit conditions. The parameters include effects from water chemistry, hydrodynamical conditions and thermal gradient. A set of focused experimental methods need to be developed to determine some model parameters (e.g. surface charge / zeta potential) and their dependence on water chemistry. The present paper gives an update of the progress in this area.

Optimisation of the HFT water chemistry

The first target in determining the optimal water chemistry for HFT period of a new plant was to develop and verify the techniques necessary for the task. An opportunity for this appeared as part of the co-operation between VTT and Bhabha Atomic Research Centre (BARC) in India. The main reactor type in India is pressurised heavy water reactor (PHWR) which has carbon steel as the primary ciruit tubing material and lithiated (LiOH) water with pH = 10…10.5 as primary coolant.

The pre-passivation in PHWRs is normally studied using stringers of coupons which are exposed to water during the pre-passivation in a flow through chamber. After pre-determined exposure times a few coupons at a time are withdrawn and analysed for the thickness and structure of the formed magnetite film.

An alternative technique allowing for in situ online determination of the properties and protectiveness of such a film is electrochemical impedance spectroscopy (EIS). Figure 1 shows the conventional data gained for coupons exposed to PHWR water during Hot Conditioning at Rajasthan Atomic Power Plant (RAPP-5). The disadvantage of the conventional coupon measurements is that the data gained does not give a direct measure of the protectiveness of the formed layer against corrosion.
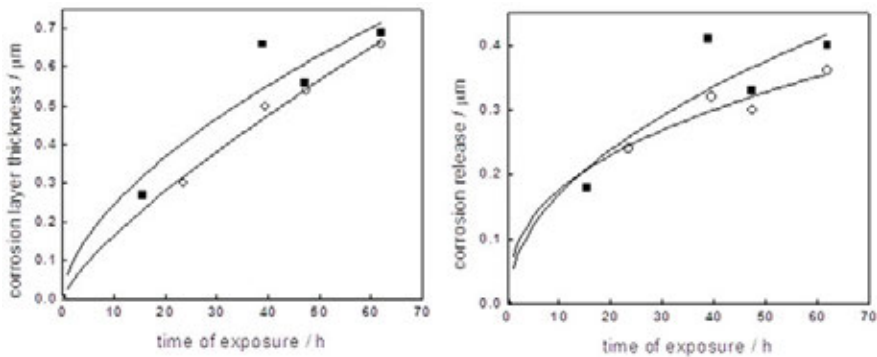

Figure 1. Corrosion layer thickness and corrosion release as measured from coupons exposed during the pre-passivation of Rajasthan Atomic Power Plant (RAPP-5) [1].
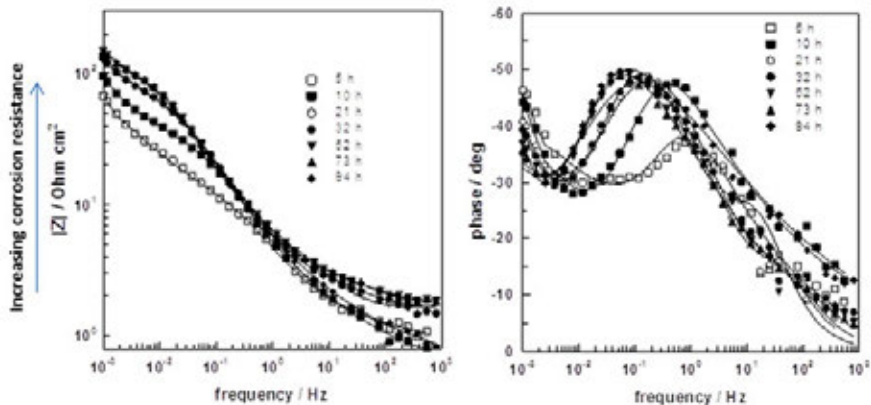

Figure 2. In-situ impedance spectra (magnitude on left, phase angle on right) during exposure to simulated hot conditioning water chemistry at 250 °C at open circuit as depending on exposure time [1].

Figure 2 shows the in-situ electrochemical impedance spectra of carbon steel exposed to simulated PHWR hot conditioning water chemistry at 250°C. The spectra was analysed according to the Mixed Conduction Model (MCM) [1]. The electric and transport properties of the oxide formed on carbon steel in simulated PHWR hot conditioning water chemistry change with the oxidation time and stabilise after ca. 30–40 h of exposure. This was in line with the observations at the RAPP-5 plant as well as the conventional coupon studies [1–2].

After verifying the applicability of the in situ EIS technique for determination of the quality of the oxide film forming on carbon steel during pre-passivation of a PHWR plant, the same approach was used to study the pre-passivation of Alloy 690 under simulated pressurised water reactor (PWR) hot functioning water chemistry conditions. Alloy 690 is typically used as steam generator (SG) tubing in PWR new builds. Steam generator tubing forms a major part of the surface area (70%) exposed to the primary coolant in a PWR plant and thus governs the release of corrosion products into the primary circuit. Optimisation of the PWR hot conditioning water chemistry mainly aims at forming the most corrosion resistant oxide layer on the SG tubing.

Electrochemical impedance spectra measured for Alloy 690 in simulated PWR Hot Conditioning water (1 ppm Li as LiOH, 30 cc/kgH$_2$O H$_2$, T = 290°C) is shown in Figure 3. The spectra stabilises in less than 20 hrs, indicating that the oxide film forming on Alloy 690 gains its protective capabilities very soon during the exposure. The corrosion resistance (impedance magnitude) of Alloy 690 is about 10x higher than that of carbon steel shown in Figure 2 under roughly similar water chemistry conditions. The effect of lithium (as lithium hydroxide LiOH) on Alloy 690 passivation was studied in the range 1…2 ppm and that of boric acid (H$_3$BO$_3$) in the range 0…1200 ppm. Figure 4 shows a compilation of the data for Alloy 690. Increasing lithium concentration is seen to decrease the corrosion resistance markedly. Addition of boric acid can counteract the detrimental effect of lithium to some extent. The optimal water chemistry for pre-passivation of a PWR new build, based on these results, would be Li = 0.5…1.0 and H$_3$BO$_3$ = 200…600 ppm. Here, the function of boric acid is both to buffer the pH elevating effect of lithium hydroxide and to aid in passivation of the surface of Alloy 690 [3–4].
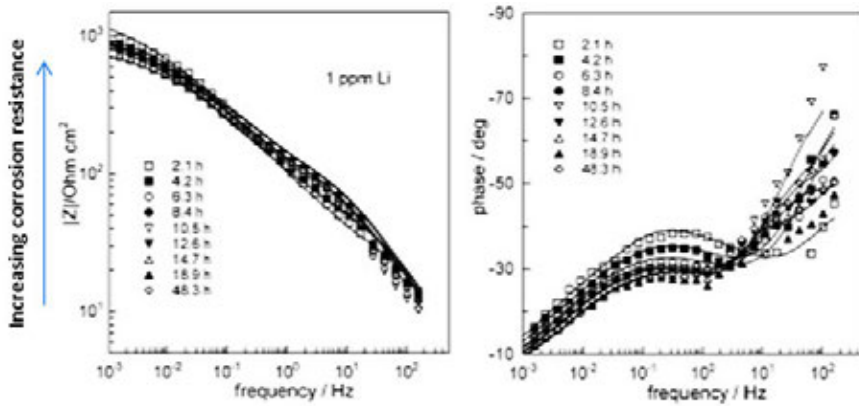
Figure 3. Impedance magnitude (left) and phase angle (right) of Alloy 690 during exposure to PWR Hot Conditioning water (1 ppm Li, 30 cc/kgH$_2$O H$_2$, T = 290°C) [3].
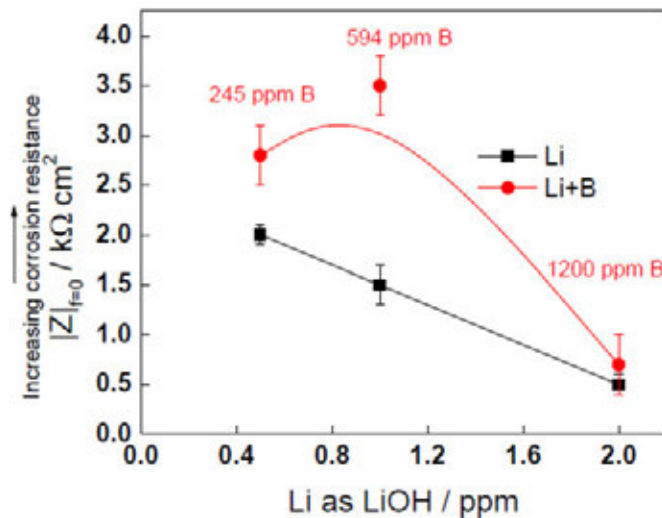

Figure 4. Dependence of the corrosion/oxidation rate of Alloy 690 steam generator tubing on the water chemistry conditions during HFT [4].

Experimental determination of surface charge of magnetite particles

Magnetite (Fe$_3$O$_4$) is formed in the pressurised water reactor secondary circuit mainly from corrosion of carbon steel tubing and other carbon steel components. Magnetite particles originating from the corrosion process are transported with the flow through the feed water line and deposit e.g. in the flow holes/crevices be-

tween the steam generator tubes and tube support plate and on the tube sheet creating flow and corrosion problems.

In aqueous solutions, colloidal magnetite particles usually have a surface charge, the sign and magnitude of which depends on the water chemistry conditions (e.g. pH and chemicals used to adjust pH). Direct measurement of the surface charge is, however, not possible. Information on the electrical state of the surface can be obtained with zeta potential measurements.

A charged particle surface in an aqueous solution is surrounded by oppositely charged species. The distribution of the charged species is not uniform but it is a function of distance from the particle surface; the species are packed closer together the closer they are to the surface. The region where the charge lies is called electrical double layer. It can be divided into sublayers depending on how tightly the charged species are bound to the surface. The plane between the charge fixed to the particle surface and the species distributed more or less diffusely within the solution in contact with the particle is called hydrodynamic shear plane or slipping plane because no hydrodynamic movement exists between this plane and the surface. Zeta potential is the potential at this plane. A schematic representation of zeta potential is shown in Figure 5. Zeta potential can be used in evaluation of the stability of colloidal magnetite particles because the electrical interaction between the particles depends on the magnitude of the zeta potential. In principle, the smaller the zeta potential, the easier it is for the magnetite particles to coagulate (less repelling force) and deposit. In case the surface film forming on the substrate (e.g. SG tubing or tube support plate) has a zeta potential opposite to that of the magnetite particles, electrostatic interaction will aid deposition.
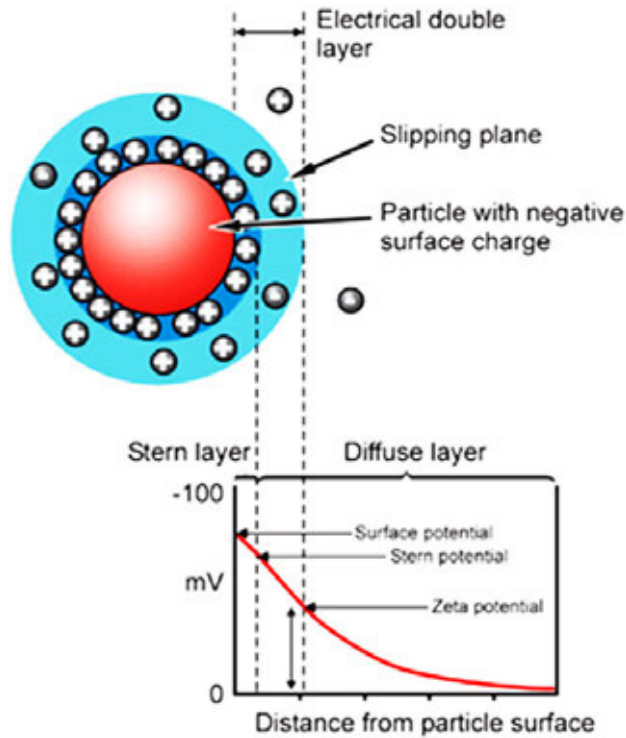
Figure 5. Schematic representation of the definition of zeta potential [5].

Several techniques exist for experimental determination of zeta potential, namely electro-osmosis, electrophoresis, sedimentation potential, streaming current and streaming potential. The streaming potential technique was chosen for this work. This technique is based on the measurement of the electrical potential created by the movement of electrolyte solution relative to the charged surface of colloidal particles. The movement is created by a pressure difference across the colloidal particles packed into a column. Zeta potential of the particles can be calculated from the ratio of the potential and the pressure differences across the sample column according to the following equation

$$\zeta = \frac{\Delta U}{\Delta P} * \frac{4\eta l}{E_0 D r^2 R},$$

where ΔU and ΔP are potential and pressure differences across the column, R is resistance, r radius and l length of the column, E_0 permittivity of free space, D dielectric constant of water and η viscosity of water.

The experimental arrangement developed for the streaming potential measurements is shown in Figure 6. The arrangement is in principle a small-size once-through feed water line simulator.
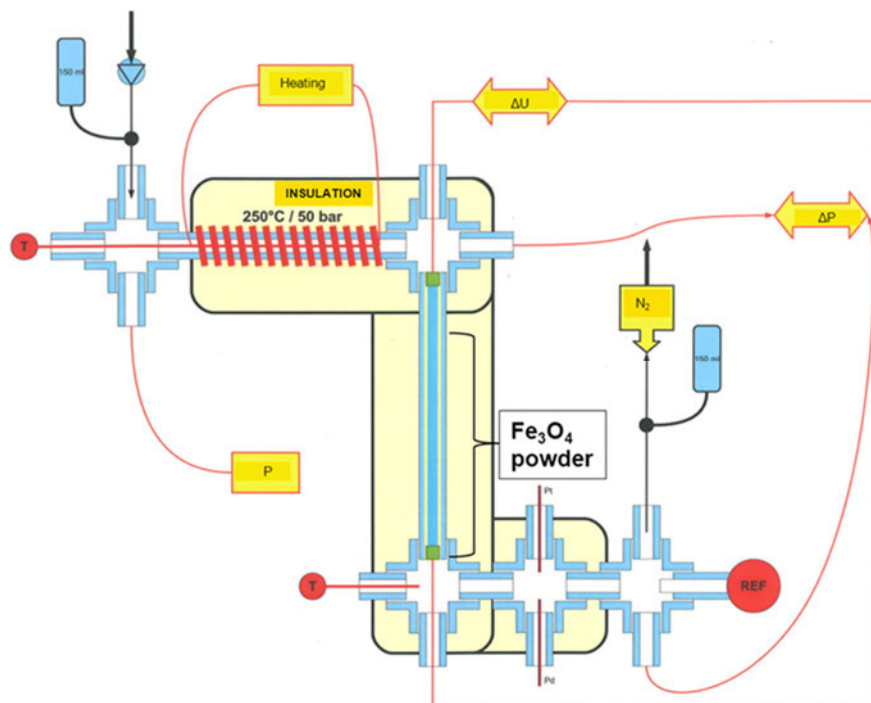

Figure 6. Scheme of the experimental arrangement constructed for magnetite zeta potential measurements [6].

The feed water was fed through a heating unit and then led through the magnetite column. The magnetite column was resting on a ceramic filter and surrounded by a PTFE-tube which was assembled inside a stainless steel housing. After passing through the magnetite column and the ceramic filter the feed water was led through chambers equipped with Pt- and Pd-electrodes as well as a Ag/AgCl-reference electrode, through a cooling jacket, a room temperature pH and conductivity cell and then to drain. Pt-electrodes at the upper and lower ends of the magnetite column were used to monitor the potential difference ΔU across the column, and a pressure difference meter was used to measure the corresponding pressure difference. To keep the feed water from boiling during the experiment a back pressure of 5 MPa was typically applied using nitrogen gas. A minimum set of three different flow rates were used in zeta-potential measurements at each temperature and chemistry condition.

The correct functioning of the experimental arrangement shown in Figure 6 was verified by comparing the results of zeta-potential measurements with those gained with a commercial system, namely Malvern Zetasizer. The results of the two systems are reasonably well comparable, Figure 7, taking into account that the results are based on two fundamentally different measurement techniques. The disadvantage of the commercial system is that it can only be used in temperatures up to T = 60°C. Increasing temperature was found to decrease the magnitude of the zeta-potential in water with ammonia (Figure 8) and ethanolamine, but not in water with morpholine. Thus, increasing temperature tends to promote the deposition tendency of colloidal magnetite particles in PWR secondary side water conditioned with ammonia and ethanolamine. The future work in this area is directed in determination of the zeta-potential (surface charge) of the SG tube support plate and tube sheet materials as well. In addition, effect of different water chemistry options on the deposition rate of magnetite will be determined in situ using on line activity (OLA) technique with radiated magnetite having ^{59}Fe isotope.
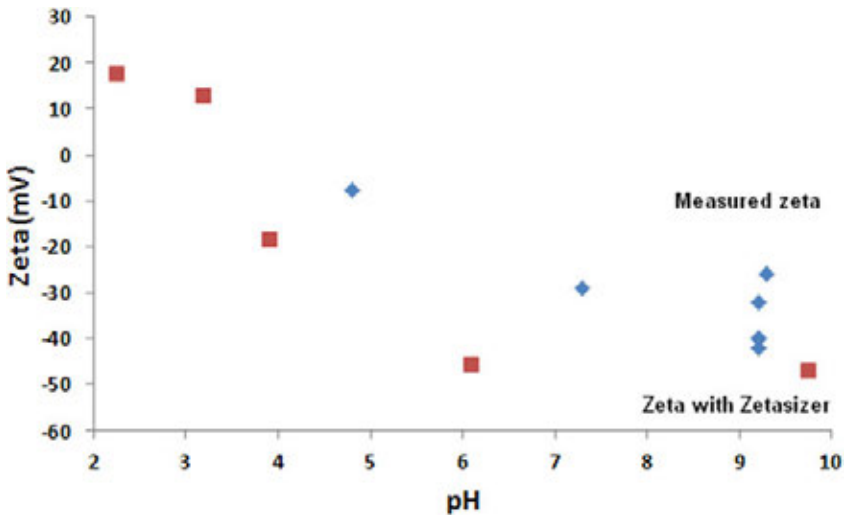

Figure 7. Effect of pH on magnetite zeta potential at room temperature. Red symbols represent the zeta potential values measured with Malvern Zetasizer and the zeta potential values based on the streaming potential measurements are marked with blue symbols [7].
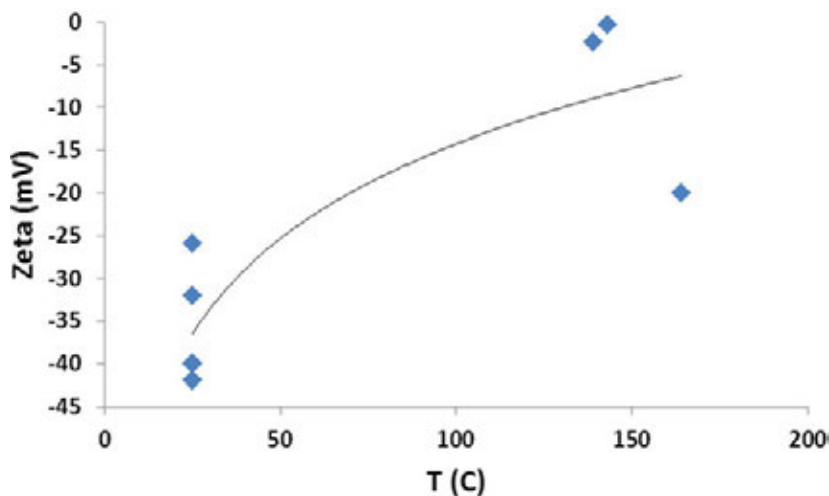
Figure 8. Effect of temperature on magnetite zeta potential when pH is adjusted with ammonia [7].

Conclusions

The pre-passivation (Hot Conditioning) of a PWR new build is performed during the Hot Functional Testing period before loading the first fuel in the core. In this project, optimal water chemistry for the Hot Conditioning was investigated experimentally. Increasing lithium concentration (in the range 1 to 2 ppm as LiOH) was found to decrease the corrosion resistance of the oxide layer forming on Alloy 690 with a factor of roughly three. Boric acid addition to lithiated water was found to be beneficial at all investigated lithium concentrations. The best corrosion resistance for Alloy 690 was found in water containing 0.5…1 ppm Li with 200…600 ppm boric acid. The time to reach a stable oxide film was less than 30 hours.

The experimental arrangement, based on streaming potential measurement, developed for determination of the zeta-potential (surface charge) of colloidal magnetite particles was shown to provide similar results at room temperature to those generated with a commercial equipment, based on electrophoretic light scattering. Increasing temperature was found to decrease the magnitude of the zeta-potential in water with ammonia and ethanolamine, but not in water with morpholine. Thus, increasing temperature tends to promote the deposition tendency of colloidal magnetite particles in PWR secondary side water conditioned with ammonia and ethanolamine.

References

1. Bojinov, M., Gaonkar, K., Ghosh, S., Kain, V., Kumar, K., Saario, T. Characterisation of the oxide layer on carbon steel during hot conditioning of primary heat transport systems in heavy-water reactors. Corrosion Science 51(2009) 5, 1146–1156. Doi: 10.1016/j.corsci.2009.02.006.

2. Kumar, K., Gaonkar, K., Ghosh, S., Kain, V., Bojinov, M., Saario, T. Optimisation of the hot conditioning of carbon steel surfaces of primary heat transport system of Pressurized Heavy Water Reactors using electrochemical impedance spectroscopy. Journal of Nuclear Materials 401(2011)1–3, 46–54. Doi: 10.1016/j.jnucmat.2010.03. 017.

3. Betova, I., Bojinov, M., Karastoyanov, V., Kinnunen, P., Saario, T. Effect of water chemistry on the oxide film on Alloy 690 during simulated hot functional testing of a pressurised water reactor. Corrosion Science 58(2012), 20–32. Doi: 10.1016/j.corsci.2012.01.002.

4. Betova, I., Bojinov, M., Karastoyanov, V., Kinnunen, P., Saario, T. Optimisation of the water chemistry regarding stability of the oxide film on alloy 690 during simulated hot functional testing of a pressurised water reactor. Nuclear Plant Chemistry Conference NPC 2012, Paris 23–27 September 2012 (2012).

5. Malvern Instruments Ltd. Zeta potential measurement using laser Doppler electrophoresis (LDE). http://www.malvern.com/labeng/technology/zeta_potential/zeta_potential_lde.htm (accessed 14 Jan 2013).

6. Väisänen, S. Zeta Potential of Magnetite under PWR Secondary Circuit Conditions. Master of Science Thesis, 74 pages, 12 Appendix pages. March 2012, Tampere University of Technology. (In Finnish.)

7. Ikäläinen, T., Lehtikuusi, T., Peltonen, S., Saario, T., Väisänen, S. Effect of ammonia, morpholine and ethanolamine on zeta potential of magnetite – results in 2012. VTT Research Report VTT-R-00211-13, January 2013.

7.7 Fatigue affected by residual stresses, environment and thermal fluctuations (FRESH)

Michael Chauhan, Antti Timperi, Heikki Keinänen

VTT Technical Research Centre of Finland
Kemistintie 3, P.O. Box 1000, FI-02044 Espoo

Introduction

The FRESH project aims at expanding and deepening understanding of fatigue behaviour experienced by NPP pressure boundary components under realistic loads and environment. The following topics were studied durig the first year of the project:

- stresses in a weld prior to NPP operation (weld residual stresses),

- sensitivity of the F_{en}-factor to variation in the loads,

- determination of the realistic loads caused by turbulent mixing,

- clarification of stress component categorization for numerical fatigue analyses, and

- weld overlay as a long term repair method.

The two last topics are not treated here.

A mock-up of a pipe containing multiple butt-welds was manufactured in on-going MACY-project. Residual stresses are measured with multiple methods and the results will be reported in future. Computational simulation of welding will provide one more independent result for the residual stress distribution, and also the computational analyses will be validated.

The sensitivity of the environmental fatigue correction factor (F_{en}) was studied with actual boiling water reactor (BWR) nuclear power plant (NPP) load events. This was executed by computation of the F_{en}-factor values and fatigue usage factor values at selected locations of feed water system using design load data and actual measured temperature and flow rate data, this way varying the temperature range and strain rate from transient to another. The computation of the F_{en}-factor is based on the equation present in NUREG/CR-6909 (ref. [1)] for austenitc stainless steels. The computation was performed using FPIPE program, created by FEMdata, and its ASME NB3650M output handler [2]. The ASME NB3650M output handler uses the methodology developed by FEMdata and TVO, and is validated by VTT. It allows the computation of the F_{en} values for realistic NPP load transients, taking into account the actual stress state and directions of the involved stress and strain components. The computation procedures are described in more detail in ref. [2].

Thermal fatigue caused by turbulent mixing is a relevant damage mechanism in the piping and components of NPPs. Prediction of this fatigue phenomenon is difficult, particularly for determining the thermal load for the structure. In this work, the loads in a mixing Tee are simulated by coupled CFD-FEM calculations. The studied case is the experiment performed by Vattenfall Research and Development for validation of CFD calculations [3]. For later fatigue studies, the plexiglass pipe of the experiment is replaced with a stainless steel one and the temperature difference is scaled up.

Computation of welding residual stresses in a multi-pass welded mock-up pipe

Geometry, materials and computational models

The mock-up pipe outer diameter was 323.85 mm and wall thickness was 17.45 mm. The length of the mock-up was 400 mm consisting of two pipes of 200 mm length which were welded together. The pipe materials were austenitic steel SA 376 TP 304, and weld material AISI 318L. The welding was performed by nine passes. The first three passes were welded using gas tungsten arc (TIG) welding and the rest of the passes were welded using manual metal arc welding.

The computation of welding process was performed as follows:

- Specifically tailored finite element (Abaqus [4]) analyses were performed;

- The welding was modelled by pass-by-pass basis. Thermal and mechanical analyses were performed separately;

- The non-linear characteristics of the material including temperature dependency and plasticity were taken into account.

The material properties of Eshete 1250, which is a fully austenitic chromium-nickel steel having a rather similar chemical composition as AISI 304 steel, were utilised. The temperature dependent material properties include also the material parameters for combined isotropic/kinematic hardening material model of Abaqus [4]. An anneal temperature of 1000°C was utilised in the mechanical analysis. The anneal procedure simulates the relaxation of stresses and plastic strains.

Pass by pass modelling was performed adding the corresponding elements to the model utilising 'model change, add'- option of Abaqus code. Pass lumping was performed between the first and ninth pass so that welding sequence shown in Figure 1 was obtained.
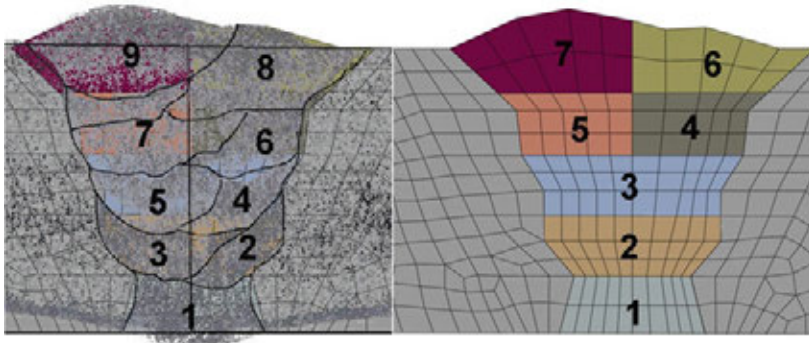
Figure 1. Real welding process sequence (left figure), and the sequence in the three dimensional FE analysis (right figure).

Results

In the thermal analysis the heat input was modelled using uniform internal heat generation and an exponential time function. A reduced 90 degree model was utilised in the three dimensional computation. The element side length varied between 0.6…2.2 mm in the weld area. For comparison the analyses were performed also using an axisymmetric model. In the axisymmetric model the welding is assumed to be performed instantaneously around the circumference.

Figure 2 shows computed temperatures during the welding of bead 4. The molten (grey) area is visible in the Figure.
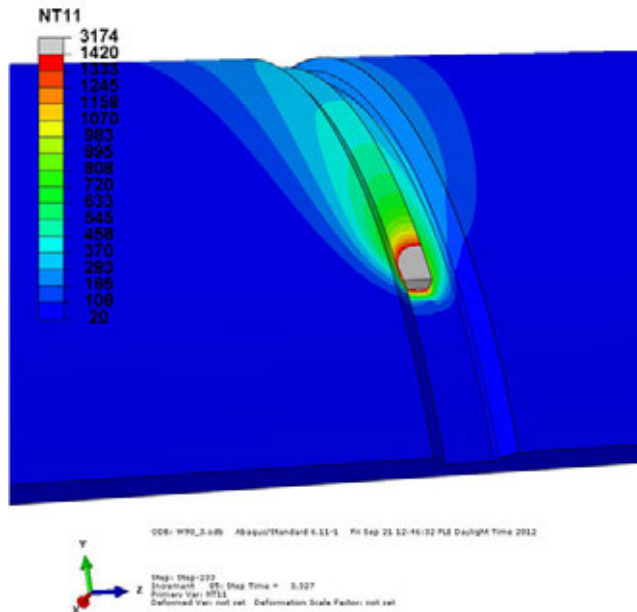
Figure 2. Computed temperatures during the welding of bead 4.

The computed maximum deformation in the middle of the weld is approximately 2 mm. The computed deformed shape is basically similar to that of the mockup. Figure 3 shows the computed through-wall stress distributions at the middle of the weld. The differences between the three dimensional and axisymmetric circumferential (hoop) stress results are clearly visible near the inner surface. Larger tensile stresses were obtained with the axisymmetric model in the weld area near the inner surface.
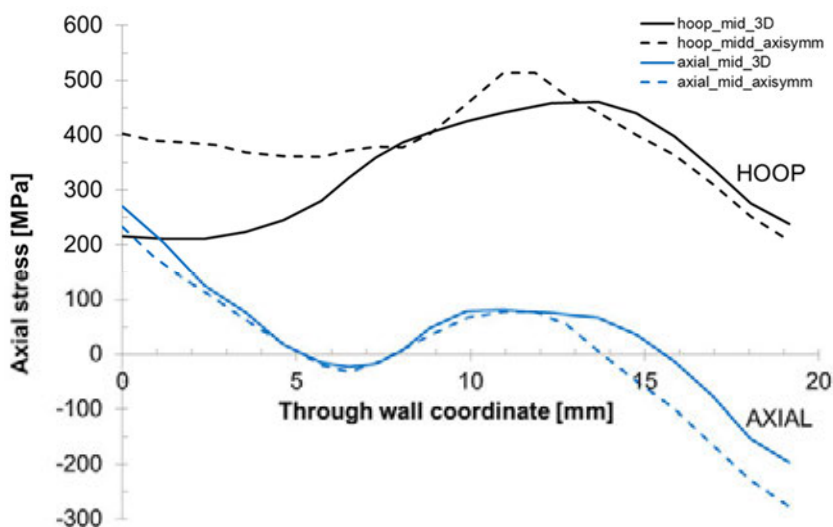
Figure 3. Computed axial and circumferential (hoop) residual stress (MPa) after welding at the middle of the weld. Three dimensional and axisymmetric results are shown. Pipe inner surface corresponds to coordinate value of 0 mm.

Computational sensitivity analysis on environmental fatigue

Description of the loads

Selected load transients for the sensitivity analysis were 1a, 10a and 6sa, which are labels for cold start-up, cold shutdown and manual pumping with system 312 during hot stand by (HBS), correspondingly. Transient 6sa forms a full cycle in itself i.e. the event includes temperature drop and rise, but transients 1a and 10a have to be combined in order to form a cycle. The selected load transients have different characteristics and were therefore selected for this study. Transient 6sa is a rapid thermal shock whereas the duration of temperature rise and drop of transients 1a and 10a is measured in hours.

The measured transients were selected from measured data between years 2000 and 2011 so that they represent the extremes in terms of duration and temperature variation. Altogether seven measured cycles were seeked and used as loading. The determined cases for transient 6sa were:fast (shortest duration), slow (longest duration), large dT (largest temperature difference) and small dT (smallest temperature difference). For transients 1a+10a, the following cases were determined: fast (shortest durations), slow (longest durations) and median (representing median durations for both transients). The selected measured 6sa transients are presented in Figure 4.
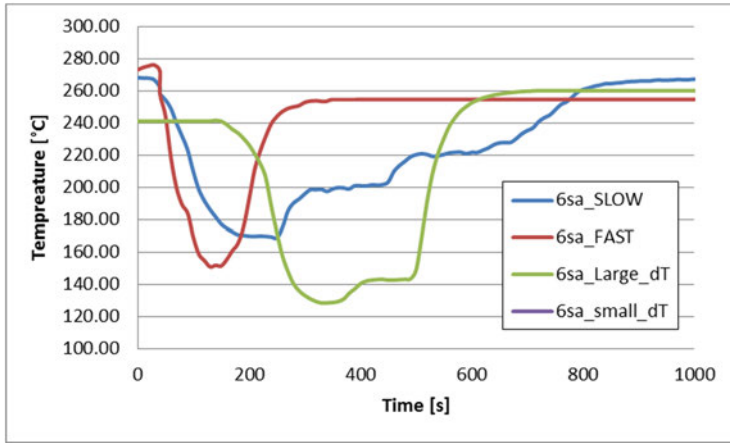
Figure 4. The selected measured 6sa transients.

Results

The comparison between the usage and F_{en}-factors obtained with the design and measured loads showed that at the selected locations the design transients are mostly conservative in terms of fatigue even when the environmental effect is taken into account. The product of the F_{en} –factor and the usage factor was higher only in few cases for the measured transients. In most cases the product was equal or higher for the design transients. The product of usage and F_{en}-factor produced at maximum 1% higher usage factor values in cases where the measured transient induced more fatigue, whereas the design transient produced up to 12% higher products of usage and F_{en}-factor values in some cases. In many cases the strain amplitude for measured transients was below the threshold value, 0,1%, in which case the F_{en}-factor is set to value 1, as in accordance with ref. [1]. Example of this kind of situation is presented in Figure 5, where the computed axial strains during the measured transients for location 2 of node 41 are presented. Variation in the F_{en}-factor obtained for different measured transients was found to be negligible. All in all, it was found that both the measured and the design transients induce very little fatigue.
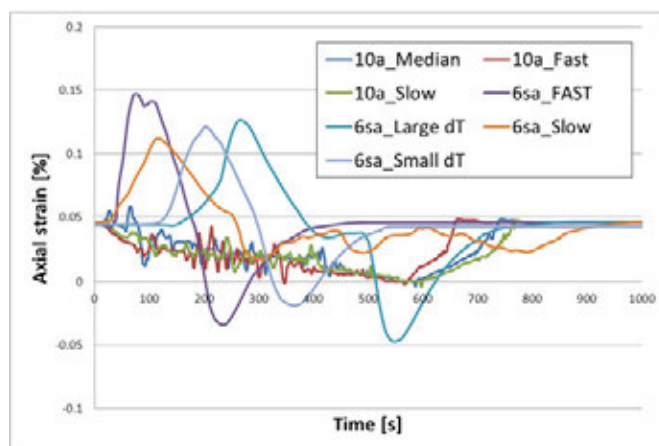
Figure 5. Axial strain at location 2 (point angle 90°) of node 41 during measured transients. The duration of transients 1a+10a is scaled for visual reasons, thus the time scale for them is not realistic.

Thermal loads caused by turbulent mixing

The coupled CFD-FEM calculations were performed by using the Star-CD v4 and Abaqus v6.9 codes, while the thermal loads were transferred with an in-house code. The Smagorinsky turbulence model was used for Large-Eddy Simulation (LES) of the temperature fluctuations. Results by using two different inlet boundary conditions were compared: steady inlets and turbulent inlets by using the vortex method. LES with the steady inlets were performed earlier in the EC FP7 project STYLE.

Contour plots of root-mean-squared (rms) temperature are shown at the pipe inner surface in Figure 6. The turbulent inlets show generally lower temperature fluctuations than the steady inlets, the difference being most visible at the corner where the highest fluctuations are obtained with the steady inlets. The fluctuations are somewhat lower with the turbulent inlets also downstream of the T-junction.

Profiles of mean and rms temperature are compared with the experiment in Figure 7. For the mean temperature, the both inlets yield fairly similar results and agreement with the experiment is good. For the rms temperature, the turbulent inlets yield generally slightly lower values than the steady inlets, except at $x = 2D$ at the sides of the pipe, where the turbulent inlets yield higher values. Agreement with the experiment is generally quite good also for the rms temperature. For temperature spectra, the both inlets and the experiment showed fairly similar results.

Mean velocity and Reynolds stresses are compared in Figure 8. The turbulent inlets seem to yield slightly better agreement with the experiment compared to the steady inlets. The difference between the two boundary conditions is most visible in cross-stream mean velocity and in the Reynolds stresses near walls. In the bulk of the flow, the differences in the Reynolds stresses are generally small.

Preliminary analysis of stresses and fatigue at the pipe inner surface shows that while the results are fairly similar after the T-junction, there are significant differences at the corner where the steady inlets yield higher fatigue. The results indicate that the realistic turbulent inlets should be included in the studied flow case, where the highest fatigue occurs near the T-junction.

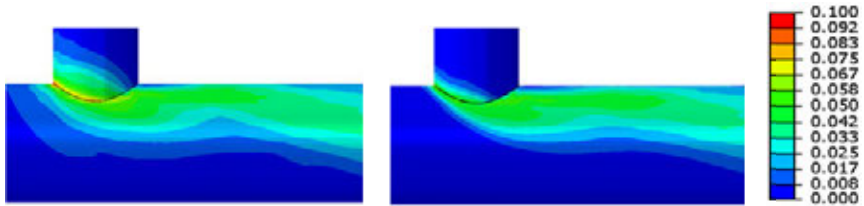**Figure 6.** Normalized rms temperature at pipe inner surface with steady (left) and turbulent (right) inlets.
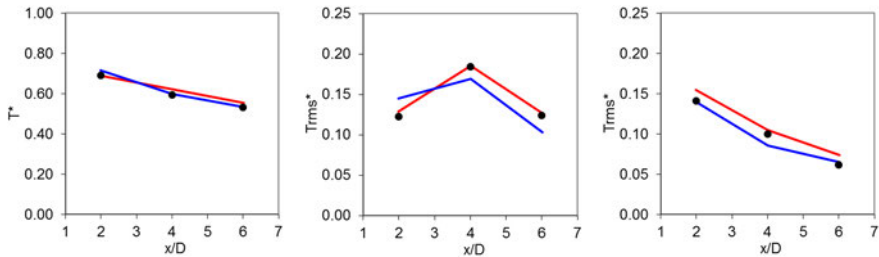

Figure 7. Normalized mean and rms temperature 1 mm from wall along the main pipe. (— Steady inlets, — Turbulent inlets, ● Experiment)
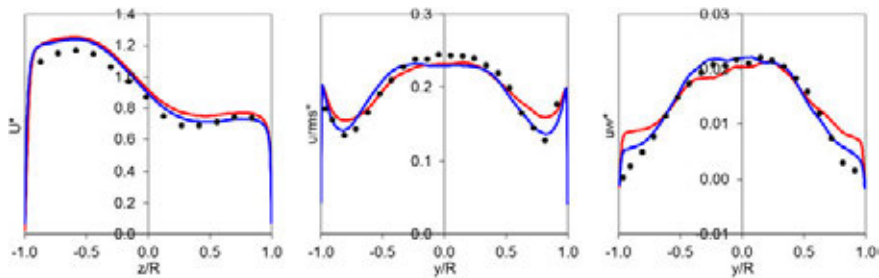

Figure 8. Normalized mean velocity and Reynolds stress profiles at cross-section x = 2.6D. (— Steady inlets, — Turbulent inlets, ● Experiment)

Conclusions

In on-going MACY-project residual stresses are measured from a multi-pass welded mock-up pipe. Computational simulation of welding will provide one independent result for the residual distribution. The computation was performed with the Abaqus FE code. Both axisymmetric and three dimensional model were utilised. The non-linear characteristics of the material including temperature dependency and plasticity were taken into account. Considering the computation of the welding, the weld pass lumping was a powerful method to simplify the computation procedure. However, the final weld passes were individually modelled to get adequate results. The computed size of the fusion zone is reasonable, which is verification for the thermal results. The computed axisymmetric and three dimensional stresses show a formal agreement with each other. The axisymmetric model gave higher circumferential stresses near the inner surface. This is most probably partly due to thermal results and partly due to the lack of capability of the axisymmetric model to model the movement of welding torch in the circumferential direction and deformations in front of and behind the torch. A comprehensive comparison of the computational results to the measured ones will be performed in future.

The fatigue usage factors and F_{en} –factors were computed for a number of load transients as based on design load data as well as on measured temperature and flow fluctuations, provided by the plant personnel. The sensitivity of the F_{en} –factor values was studied by varying the loading. The design transients are mostly conservative in terms of fatigue also when the environmental effect is taken into account. The product of usage and F_{en}-factor produced at maximum 1% higher usage factor value in few cases where the measured transient induced more fatigue, whereas the design transient produced up to 12% higher products of usage and F_{en}-factor values in some cases. Large variation between the F_{en}-factors for the measured transients is obtained only if the strain amplitude threshold (0,1%) is exceeded during one transient but not during the other. Otherwise the variation is low. All in all, both the measured and design transients induce very little fatigue.

Thermal mixing in the Vattenfall experiment was studied by LES. Comparison of steady and turbulent inlet boundary conditions showed that these have generally fairly small effect in the bulk of the flow, while the effects are non-negligible near the walls, especially near the T-junction where the highest temperature fluctuations are obtained. The turbulent inlets resulted in somewhat lower temperature fluctuations at the pipe inner surface. In the bulk of the flow, the mean and fluctuating components of velocity and temperature were overall in good agreement with the experiment with the both inlets. The turbulent inlets resulted in slightly better agreement with the experiment in mean velocities and Reynolds stresses, but the agreement was worse in rms temperature at one location. The both inlets and the experiment showed fairly similar temperature spectra.

References

1. Chopra, O.K., Shack, W.J. 2007. Effect of LWR Coolant Environments on the Fatigue Life of Reactor Materials, Final Report, NUREG/CR-6909, ANL-06/08, US Nuclear Regulatory Commission.

2. FPIPE ASME, FPIPE-ohjelman ASME NB jälkikäsittelijä referenssimanuaali. 2011. Insinööritoimisto FEMdata Oy. (In Finnish)

3. Andersson, U., Westin, J., Eriksson, J. 2006. Thermal mixing in a T-junction. Model tests 2006. Report U 06:66, Vattenfall Research and Development. 43 p. + app. 25 p.

4. Abaqus Theory Manual, version 6.11-1. Dassault Systemes, 2011.

8. Construction Safety

8.1 Impact 2014 (IMPACT2014) and structural mechanics analyses of soft and hard impacts (SMASH)

Ilkka Hakola[1], Arja Saarenheimo[1], Ari Vepsä [1], Kim Calonius[1], Simo Hostikka[1], Juha Kuutti[1], Ari Silde[1], Topi Sikanen[1], Markku Tuomala[2]

[1]VTT Technical Research Centre of Finland
Kemistintie 3, P.O. Box 1000, FI-02044 Espoo

[2]Tampere University of Technology
P.O. Box 600, FI-33101 Tampere

Introduction

The total number of tests carried out within IMPACT project during 2011–2012 is 37. Ten force plate tests were carried out, some of them with water filled missiles. The number of the impact tests with reinforced concrete target is 25. The target structure is a simply supported square slab. Additionally, two static four point bending tests were conducted.

Numerical methods and models are being developed in SMASH project. In fact, the whole idea behind testing is to obtain reliable and relevant data against which numerical methods and models can be verified so that they can be used with confidence in more challenging problems encountered in practical applications. Numerical analyses are also needed in designing the tests. Numerical studies on so called combined bending and punching test are presented here.

The DETO code has been developed at VTT to calculate values of shock wave parameters induced by chemical explosions. The code also includes a tool to couple the time dependent pressure loads with the FE program Abaqus. A typical explosion case was simulated using cohesive surface methodology that allows modelling large scale material fragmentation and interaction of fracmented particles.

Experiments with liquid-filled missiles were carried out to measure the liquid spray properties, serving as input and validation for CFD simulations. Droplet measurements were made using high-speed digital cameras with back-light laser illumination. Plant-scale impact fire simulations were then carried out to examine the physical extent of the flame and smoke influence, and the time it takes for a flame to reach the critical locations.

Impact tests

Tests carried out within IMPACT project during 2012 are listed primarily in order of test type and secondarily in chronological order in Table 1 with some main characteristics. In IMPACT project, there are three main types of impact tests against reinforced concrete slabs: Punching, bending and combined bending and punching tests. IMPACT test facility is described in detail in [1]. The target in all impact tests is a two-way simply supported reinforced concrete slab with span dimensions of 2 m and thickness of either 150 mm or 250 mm. The last four columns show the impact velocity of the missile, v_0 the total mass of the missile, m_m, the missile material and pipe thickness and total length, l_0. Finally, some results are given for some of the tests. Water missile tests carried out with force plate are summarized in Table 3.

In addition to the tests described in Table 1, almost every test slab was tested with an impact hammer and accelerometers to assess its dynamic properties with varying boundary conditions.

Table 1. Tests conducted within IMPACT project in 2012 with main data.

Code	Type	Target	v_0 [m/s]	m_m [kg]	Missile material	l_0 [mm]
F1	bending	150 mm, 6 mm closed stirrups	144	50.2	st. steel 2 mm	2361
P1	punching	250 mm, 12 mm hooked stirrups	102	47.4	steel 12.5 mm	640
P2	punching	250 mm, prestressed and grouted tendons	123	47.5	steel 12.5 mm	640
P3	punching	250 mm, increased bending reinf.	140	47.5	steel 12.5 mm	640
P4	punching	250 mm, increased bending reinf.	120	47.5	steel 12.5 mm	640
P5	punching	250 mm, tendons without prestress	121	47.5	steel 12.5 mm	640
P6	punching	250 mm, 10 mm T-headed bars	111	47.5	steel 12.5 mm	640
X1	combined	250 mm, 6 mm closed stirrups	166	50.1	st. steel 3 mm	1811
X2	combined	250 mm, 6 mm closed stirrups	165	50.1	st. steel 3 mm	1811
1	static	150 mm, narrow (600 mm)	-	-	-	-
2	static	150 mm, narrow (600 mm)	-	-	-	-

Punching tests

Six punching test were conducted in 2012. Results of the first and last ones are considered here. The main difference between these tests was in the missile impact velocity and type of shear reinforcement. Hooked stirrups were used in P1, while T-headed bars were used in P6. The amount of shear reinforcement was higher in P1. The strength of concrete was somewhat higher in P6. Perforation took place in both tests with residual velocities of the missile of 17 m/s and 5 m/s in P1 and P6, respectively. Back surfaces of both slabs are shown in Figure 1. In case of P6, the cracks are highlighted. The scabbed area was wider when T-headed shear reinforcement was used. Based on the earlier studies [2], the higher strength of concrete effectively reduces the residual velocity. This is in agreement with these test observations.
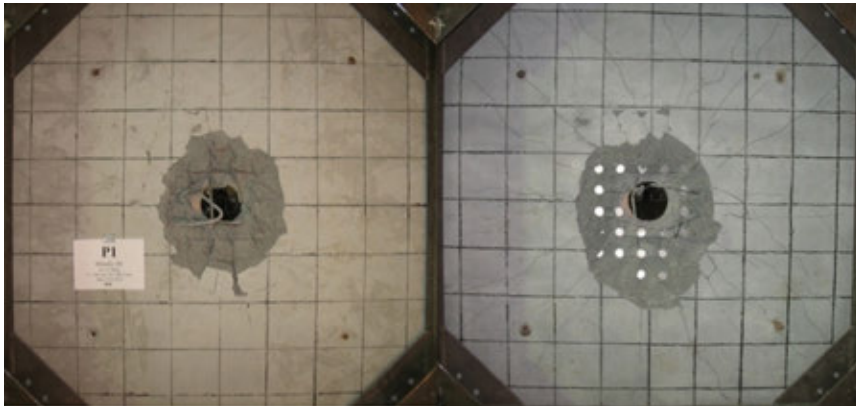
Figure 1. Back surface of the slab after the test P1 (left) and P6 (right).

Combined bending and punching tests

Two tests, X1 and X2, have been conducted, where the main aim is to cause both bending and punching shear damage to the slab. The amount of shear reinforcement was lower in test X2. The results were nearly identical. Numerical studies on test X1 are described in Chapter "Numerical studies on combined bending and punching test X1".

Vertical (left) and horizontal (right) cross-sections sawn through the centre-lines of the X1 slab are shown in Figure 2. They show clearly that no clear punching (shear) failure occurred but an incipient shear cone formation can be seen.

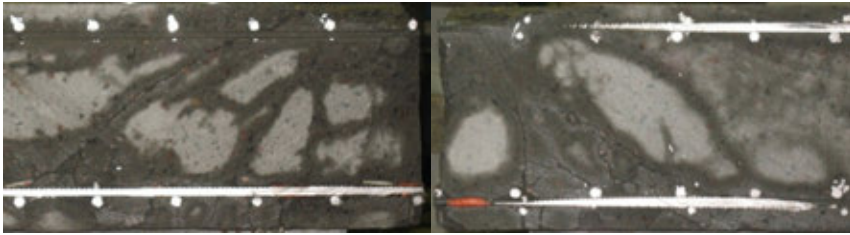**Figure 2.** Vertical (left) and horizontal (right) cross-sections sawn through the centre-lines of the X1 slab.

Static bending tests

Two narrow, reinforced concrete slabs were tested both statically for 4-point bending and also with an impact hammer for dynamic properties. The slabs are otherwise almost identical to the thin slabs used in impact tests with bending as the main deformation mode, but the width was only 600 mm. The static tests were carried out by loading and unloading the slab by cyclic test, increasing the maximum load slightly for each new cycle. Finally the slabs were loaded up to rupture. The dynamic properties of the slab were tested first before the loading was applied and then after each loading cycle excluding the ruptured state.
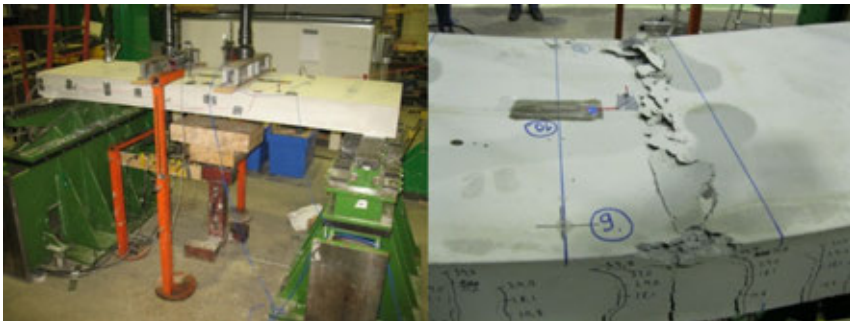
Figure 3. Static test slab during the beginning (left) and after the test (right).

The slabs were instrumented with optical fibres fixed in the reinforcement, strain gauges glued on the bending reinforcement, displacement sensors and accelerometers on the upper surface of the slab. In addition, the applied force and the maximum width and depth of the cracks after each loading cycle were measured.

The main goal was to validate the behaviour of the optical fibres that were used to measure the strains on the reinforcement rebars during the tests. An additional goal was to study how the damage changes dynamic properties of the slab. These goals were successfully reached, though these optical fibres were not adequate

for this test type. The numerical calculation methods and models can also be verified against these test results.

Water-filled missile tests

Six impact tests with 1.5 mm thick stainless steel missiles, of which five were filled with water, some only partly, and one (SFP6) was empty, were conducted. The missiles were shot against a force plate in order to measure the impact force. The main goal was to video record the dispersal of the water released as the water tanks of the missiles were ruptured. This video material was used to determine the relative dimensions of the droplets flying in the air at different times and the propagation velocity of the droplet spray front (described in Chapter "Jet fuel dispersion"). This data was further used as input data in the spray and fire simulations belonging to the SMASH project. One additional goal of the test series was to define the force-time-histories with different missile types. These goals were successfully reached. Figure 4 shows the high frame rate video footage taken during test SFP5. Also the impact forces were recorded during these tests.
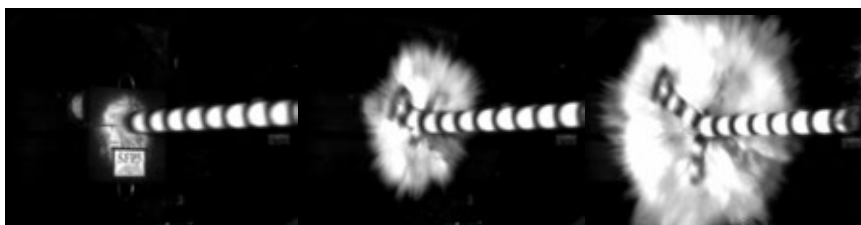

Figure 4. The high frame rate video footage taken during test SFP5. The presented frames are taken 4 ms apart from the beginning of the impact.

Numerical studies on combined bending and punching test X1

The considered test case, named X1, is called combined bending and punching test because due to rather heavy impact load and the plate geometry, besides global bending response also local punching failure is possible to occur. However, no clear punching failure took place in this test. This behavior is verified also by the numerical analyses presented here.

The dimensions of the two-way simply supported slab used in the dry stainless steel missile impact test X1 are: the span $l = 2.0$ m, the thickness $h = 0.25$ m and the effective thickness $h_e = 0.225$ m (assuming a concrete cover of 20 mm and a rebar diameter of 10 mm). The properties of reinforcement are: the modulus of elasticity $E_s = 210$ GPa, the yield stress $\sigma_y = 500$ MPa, the ultimate stress $\sigma_u = 600$ MPa, reached at a strain value of $\varepsilon_u = 0.1$. The bending reinforcement consisted of bars with a diameter of 10 mm and a spacing of 90 mm and the shear

reinforcement was made with 6 mm closed stirrups with spacings of 90 mm and 180 mm in two orthogonal directions.

The material properties of the concrete slab used in computations are: the modulus of elasticity of concrete is $E_c = 23.425$ GPa, the Poisson ratio is $\vartheta = 0.2$, the compressive cubic strength of concrete is $f_c = 40.6$ MPa and the tensile strength of concrete is $f_t = 3.03$ MPa.

An experimentally observed frequency of bending vibration of the damaged slab was $f = 43$ 1/s.

Prediction of loading function due to missile impact

The missile fuselage in test X1 is made of stainless steel pipe with an outer diameter $d_0 = 0.256$ m and a wall thickness of 3 mm. The mass of a steel pipe with a length of 1.7 m assuming a density of 7850 kg/m^3 is about 31.82 kg. By adding a front cap and some steel parts at the rear end of the missile the total mass increases to the desired 50 kg. The total length of the missile is 1811 mm (pipe 1700 mm, front cap 86 mm and steel plate at the rear end 25 mm). The impact velocity of the missile in the analysed test is 166 m/s. An average yield strength of 480 MPa is assumed for the missile material. Due to rather stiff missile, the maximum impact load is in this case over 1 MN.

The impact load is calculated with the Riera method. The crushing force term is obtained with a visco-plastic folding model. Two methods are used. In both methods the missile material is assumed rigid visco-plastic. In the simpler method the crushing force is calculated with a folding visco-plastic mechanism in an average sense (denoted fvp). In the more accurate, true, folding model (denoted fold) the actual formation of folds is followed. In both cases visco-plastic material parameter values $D = 1522$ 1/s and $q = 5.13$, suitable for stainless steel, for the adopted Cowper-Symonds model are used [3]. In this true folding model bending and stretching energies are calculated. The bending deformation varies linearly in the missile wall thickness direction, and numerical integration becomes necessary when considering the effects of strain rate sensitivity and strain hardening of missile material. In the present case a five point Simpson integration is performed in the wall thickness direction similarly as is usually done with axially symmetric shell finite elements.

Figure 5 shows load functions for the missile with an impact velocity of 166 m/s obtained with different methods. The finite element (FE) model is an accurate representation of the missile. Ower 14000 shell elements were used to model one quarter of the missile in 3D with Abaqus/Explicit code [4]. Figure 6 shows deformed shape of missile at the end of impact photographed after the test (left), obtained with the true folding model and simulated with the FE model (right). In the applications the effect of the fluctuating impact force of the true folding model on the plate response is considered. The deformed shapes correspond quite well with each other and are in agreement with the experimental deformed shape of the missile. The fluctuating force curves are the contact force histories which are diffi-

cult to record in tests. In fact, the experimental force histories are recorded behind the force plates at the measuring transducers.
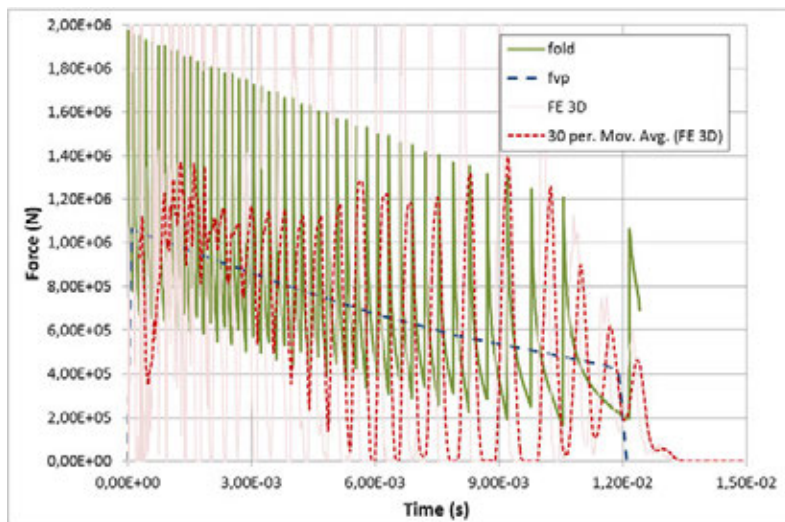

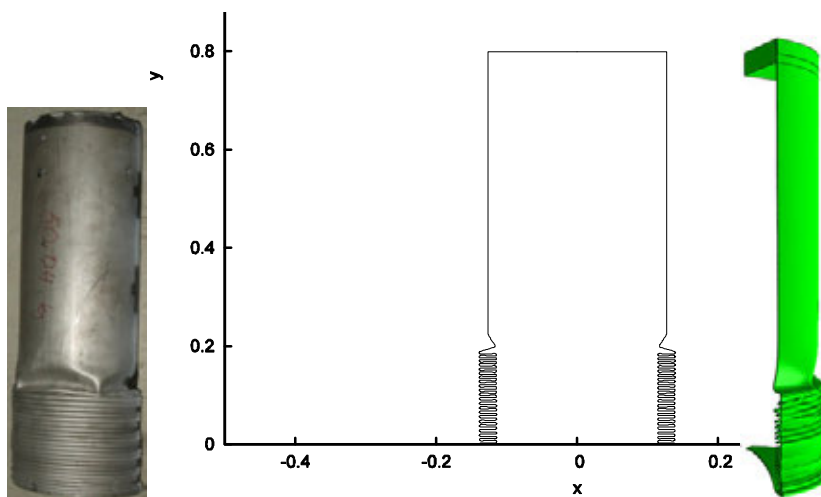**Figure 5.** Load functions for plate X1 with an impact velocity of 166 m/s.

Figure 6. Deformed shape of missile at the end of impact in test X1 photographed after the test (left), obtained with the true folding model (fold) and simulated with quarter FE shell model (right).

Structural integrity studies on reinforced concrete slab

The simplest model used is a two-degree of freedom (TDOF) elasto-plastic oscillator, which is, however, capable of predicting the bending behavior of plate structures subjected to impact load but also suitable for predicting the possible local failure of plates. In TDOF calculations Rayleigh damping with a damping ratio of 0.07 at frequency 40 Hz was assumed.

Two finite element codes, Abaqus/Explicit [4] and a special purpose finite element program, are used in calculating the responses of the present test plates.

Abaqus code and its use are described in earlier reports, e.g. [5]. Nonlinear behaviour of concrete was modelled with a so called concrete damaged plasticity material model. In the Abaqus model one quarter of plate is divided into a mesh of 20 by 20 elements. Four noded shell elements with reduced integration were used. Bending reinforcement was modelled as layers and shear reinforcement was not taken into consideraton. The impact load is applied on plate middle surface by assuming a load spreading angle of 45°. In Abaqus calculations damping is due to nonlinear material properties.

For the sake of comparison, alternative numerical results are computed also with a different finite element program. The used Bogner-Fox-Schmidt (BFS) plate element is based on third order polynomial deflection interpolation and it has 16 degrees of freedom. Due to nonlinearities, numerical Gaussian integration is used in obtaining the internal load vectors of elements. The BFS element is based on Kirchhoff plate theory. A resultant formulation is adopted in which the material nonlinearities of concrete and reinforcement are formulated in terms of the stress resultants and curvatures. At each integration point in the element the principal curvatures are calculated from the deflection and then the principal moments (or their increments) are calculated based on the curvatures and the moment curvature relation for the reinforced concrete cross section at hand. In reverse motion, cracked state stiffness is assumed. In this formulation, integration through the plate thickness is avoided making the method simple and effective. The central difference (CD) time integration method is used in integrating the equations of motion. The curvatures and moments are calculated and updated after every time step in the step by step analysis. A 10 by 10 element mesh is used with BFS element model and the load is applied on plate middle surface as described above. A damping ratio of 0.05 at 40 Hz was used in these calculations.

In the figures, curves with label FEKR are obtained with the finite element program using the BFS elements combined with the stress resultant formulation.

Calculations were carried out by using these three different methods and applying two different types of loading functions shown in Figure 5. Calculated displacements are compared with the experimental recordings in Figure 7a and b. The horizontal distance from the slab centre to the displacement sensor D5 is 400 mm.
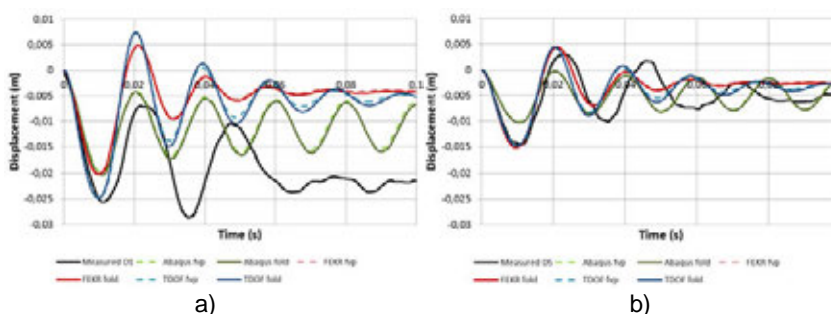
a)   b)

Figure 7. Displacements as a functions of time at the centre of the wall: a) at the centre and b) at the displacement sensor location D5.

Maximum displacement at the center of the wall and maximum displacement at the displacement sensor location D5 were predicted with reasonable accuracy by the used methods. The simple stress resultant formulation gives reasonable accurate results when compared with experimental recordings. The vibration frequency obtained with the numerical methods is somewhat higher than that observed in test. Maximun deflections calculated with TDOF method and Abaqus FE code underestimated the maximum displacement somewhat but the permanent deflection of the Abaqus model is near the observed one. The shape of the loading function is not affecting the results.

Explosions

Shock pressure loads from external explosions

The DETO code has been developed at VTT to calculate values of shock wave parameters induced by chemical explosions, [6] and [7]. The code also includes a tool to couple the time dependent pressure loads with the FE program Abaqus. This means that the pressure loads calculated by DETO are converted into a form that is directly readable as input for the Abaqus program. The coupling is one-directional i.e. there is no feedback from Abaqus to DETO.

In DETO, the explosion energy is given as equivalent mass of TNT and the energy is released instantaneously in a small origin. A local explosion induces a spherical shock wave, which propagates freely at certain velocity through gas medium (Figure 8). As the spherical shock impacts a planar vertical wall, a shock reflection from the wall occurs. The reflected shock pressure may be much higher than the pressure of the incident shock. The reflection phenomena may be normal, oblique or Mach stem formation depending on the angle of incident between the shock plane and a wall (Figure 9).
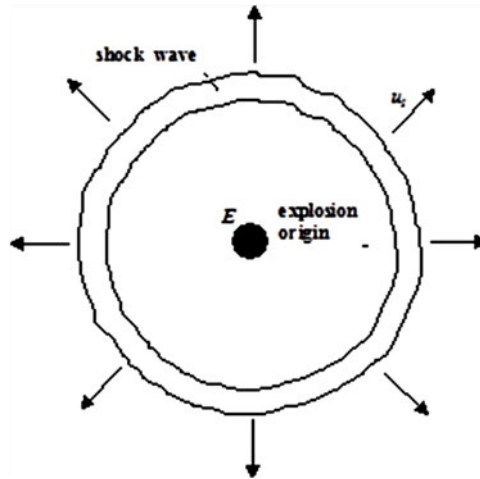
Figure 8. Schematic drawing of strong explosion with induced shock wave.
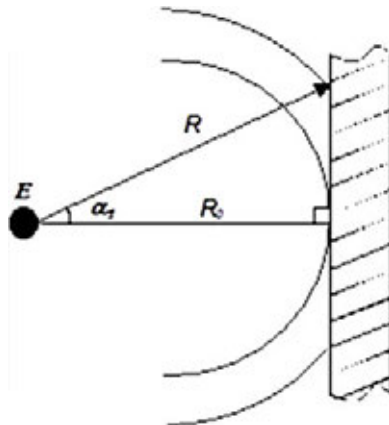
Figure 9. Distance of explosion centre (E) from a wall and impact angle of shock plane with a wall.

The basic model of DETO estimates the parameters of incident shock wave with the experimental correlations presented by Kinney and Graham [7], who give the tabulated values in scaled distances from 0.053 m/kg$^{1/3}$ to 500 m/kg$^{1/3}$. Two explosions with different energy can be expected to give identical blast waves, if the scaled distances are similar. The scaled distance is

(scaled distance) = (actual distance) / $W^{1/3}$ (1)

where W is the equivalent mass of TNT.

Effects of normal and oblique shock reflection, and Mach stem formation are calculated according to the theoretical considerations by Kinney and Graham [8].

The basic theory used in DETO treats air as a diatomic ideal gas. When the peak side-on pressure exceeds about 10 bar (corresponding values of scaled distance are lower than 1.0 m/kg$^{1/3}$), the shock temperature is so high that air molecules dissociate and ionise [9]. In this near range, the model based on the ideal gas assumption underestimates reflected pressure and is not more valid. Therefore, a new approach, which is suitable also in the near range (scaled distance ≤ 1 m/kg$^{1/3}$) has been developed and implemented in the DETO code v4.0. The new approach is based on two sets of curves presented by the handbook [10] for reflected pressure and specific impulse when a spherical or a plane shock is reflected from a planar wall surface. The former curves are only used to calculate approximate values. These curves have been parameterised by Lautkaski [9] and implemented in the DETO code. The new methods are suitable for cases, where scaled distance is greater or equal to 0.119 m/kg$^{1/3}$ and less than 1 m/kg$^{1/3}$. When the scaled (normal) distance is larger than 1 m/kg$^{1/3}$, use of the basic model based on the experimental data and theory presented by Kinney and Graham is recommended.

Structural integrity assessment by cohesive surface methodology

Simulation models for shock wave effects on structures were calibrated in 2011 in SAFIR2014 project SMASH. Spalling and breaching of concrete walls was simulated using explicit FE analysis with traditional element erosion technique. In 2012 a new simulation method called cohesive surface methodology was applied in simulating similar cases. In the methodology, each bulk element in the model is surrounded with thin cohesive elements that are able to damage and fail due to loading. No solid element deletion that violates the conservation of mass and creates empty voids in the model is needed. The method allows modelling large scale material fragmentation and interaction of fragmented particles as it produces free surfaces after cracking. The cohesive elements model the fracture process zone using a cohesive material law to relate the stress over the crack with crack opening. The cohesive law is simply a stress-displacement diagram representing the relation between the forces acting between the crack faces and the separation of the faces. The most important cohesive material parameters are fracture stress and fracture energy. Typically, the cohesive response is linear prior to initial failure at which point the tractions over the crack plane start to decrease as fracture initiates. As the loading is continued crack planes separate more still decreasing the cohesive stresses. Finally stresses have decreased to zero and the crack is thought to be fully open. In brittle crack growth the load decrease is nearly instantaneous and occurs rapidly after initial failure.

In the cohesive surface methodology explicit cracking is a natural solution of the mathematical model without any assumptions on crack trajectories. Global response of the model is anisotropic due to different crack orientations although

the local softening model for individual cohesive element is isotropic. A single cohesive element carries only compressive and tensile loads normal to element plane and in-plane shear loads. Loading in other directions is carried by the bulk elements and other cohesive elements with different orientations. The mesh orientation effects are avoided by using an unstructured mesh.

In this example the cohesive surface methodology is applied in simulating fracture of cylindrical concrete slabs with radius 2 m and thickness 0.5 m or 1.0 m under shock wave loads. Two wall thicknesses were studied with three explosion loads. Shock wave pressure-time functions corresponding to 50 kg, 100 kg or 200 kg equivalent TNT masses were applied as loading. The loads are determined using the DETO code version 4.0. The pressures applied to the slab are visualized in Figure 10 together with the pressure-time functions for 100 kg TNT loads.
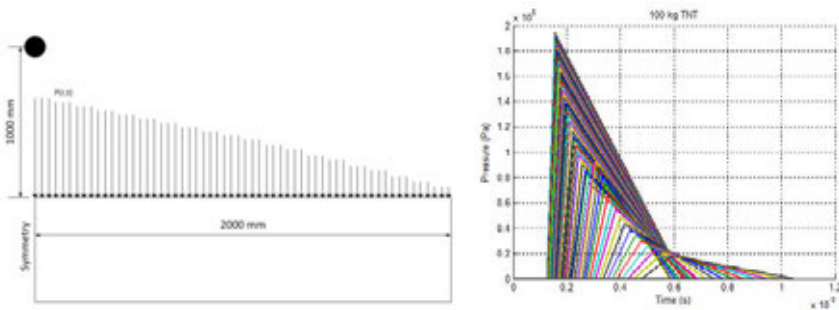
Figure 10. Pressure loads applied to the slab top surface. The pressures dependent on both time and radius were defined by DETO code v4.0.

The case is analysed with axisymmetric FE model shown in Figure 11 for the 0.5 m thick slab. The mesh in the 1.0 m slab is very similar. The models present plain homogeneous concrete slabs without rebars. Cohesive elements between the bulk elements are too small to be seen in the figure.
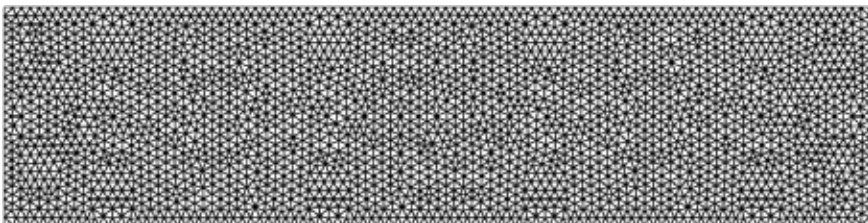
Figure 11. Axisymmetric model of the 0.5 m thick concrete slab.

Typical concrete material properties (i.e. elastic modulus 31 GPa, tensile strength of 2 MPa and fracture energy of 100 J/m^2) were applied in the simulations. A plastic-type traction separation law for the cohesive elements was utilized. Strain-rate

dependency for the tensile stress was specified based on CEB-FIB design code. The cohesive elements model the tensile failure and the compressive failure is captured with the bulk elements using traditional von Mises model.

The simulated slab deformation, cracking and plastic strains in the bulk elements are shown for all cases in Figure 12. Only the final deformed shapes are shown for all simulations. The end time of the simulation was set to 0.01 seconds. This is 10 times larger than the duration of the pressure load functions. The colouring of the figure indicates cumulated equivalent plastic strain in the bulk elements that is mostly caused by compressive stresses. The tensile damage in the cohesive elements can be evaluated based on the visible cracks. The results show shear cone formation, back surface spalling and some through-thickness cracking. Largest plastic strains are located on the top surface directly below the explosive location but the largest cracking occurs near the midplane of the slab. Spalling and breaching is caused mainly by tensile cracking that separates debris and pieces from rest of the slab. The simulations are unable to capture the crater formation on the top surface due to simplified modelling of compressive failure.
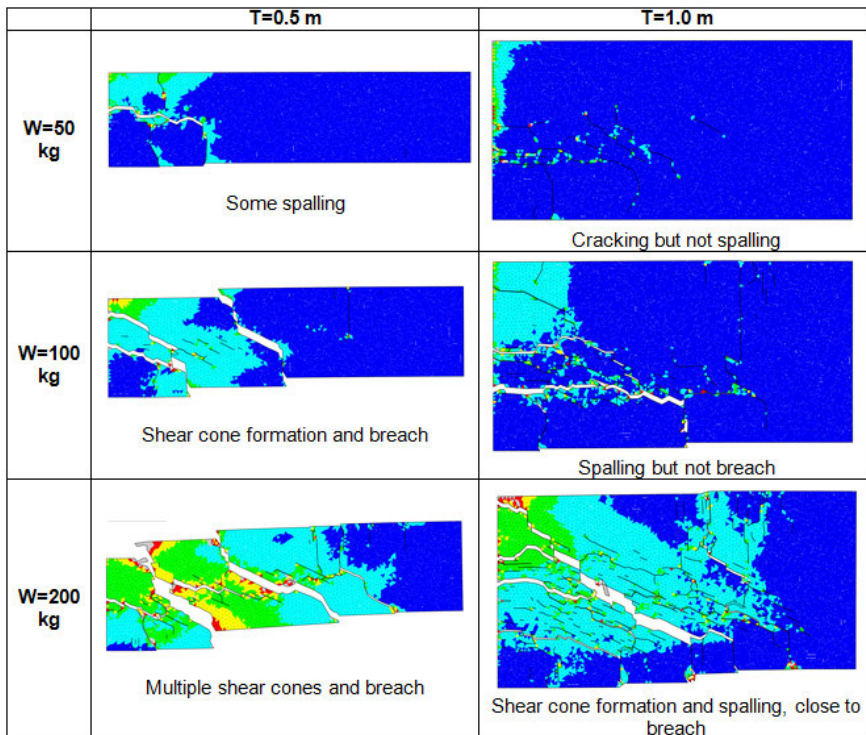

Figure 12. Final deformed shapes for all simulated cases. Contour color indicates magnitude of equivalent plastic strain with grey areas over 3%.

Jet fuel dispersion

Overview

The research on the jet fuel dispersion has three main focus areas: (1) impact experiments on liquid filled missiles for the determination of the simulation input parameters and production of validation data; (2) development and validation of the CFD simulation tool (FDS) for the spreading of high-speed liquids; and (3) application of the FDS model in plant-scale simulations of the aircraft impact fires. Areas (1) and (3) are here shortly summarized.

Liquid experiments

Over the years, some of the impact tests have been made using water-filled missiles. These experiments have provided data on the overall spray form, speed and deceleration of the spray front, spreading pattern, and to some extent the droplet sizes. During 2012, five tests were carried out with water-filled missiles, applying a new technique for measuring the droplet size, velocity and flux. The missiles were made of stainless steel, and they were 0.154 m in diameter, 2.13 m long, and had a wall thickness of 1.5 mm. The tests are summarized in Table 2.

Table 2. Liquid impact tests in 2012.

Test	Total mass (kg)	Water mass (kg)	Tank fillling	Water tank length (m)	Impact speed (m/s)
SFP1	50.4	37.0	100%	2.13	96.3
SFP2	50.5	37.1	100%	2.13	97.3
SFP3	38.1	24.7	67%	2.13	96.6
SFP4	38.4	24.8	100%	1.37	98.7
SFP5	38.4	24.7	100%	1.37	99.3

Droplet measurements were made using high-speed digital cameras recording images of flying droplets. Back-light illumination was utilized to record images of silhouettes (i.e. shadows) of droplets on a bright background. Figure 13 shows the measurement setup with camera, back-light and flying droplets that cross the measuring volume. An example of an obtained image of droplets is shown on right. The measurements were carried out by Pixact Oy using two Photron Fastcam cameras (SA-1.1 and SA-5). Frame rates from 50 000 to 100 000 fps were utilized at image resolutions from 640x224 to 512x112 pixels. Droplets as small as 6 µm in diameter could be detected. Cavilux HF lasers (810 nm) were used to illuminate the images with 300 ns long light pulses.

Resulting droplet size distributions are illustrated in Figure 14 for test SFP4. The resulting data could be roughly classified in two groups: the early spray front with very large water fragments and possibly unfinished break-up process, and the residual mist. The analyzed droplet size distributions for the spray front showed mostly unimodal shape, but the distribution of the residual mist indicated bi-modal shape. The bi-modal distribution can be explained as a result of the bag break-up process, where small child droplets are detached from the surface of each larger droplet. In the analysis of the results, the bimodal distribution was represented as a sum of two uni-modal distributions:

$$G(d, \boldsymbol{d_m}, \sigma) = \lambda F_1\big(d, d_m^1, \sigma^1\big) + (1 - \lambda)F_2\big(d, d_m^2, \sigma^2\big) \tag{2}$$

Here F_1 and F_2 are the cumulative distribution functions for particle classes 1 and 2 respectively. Parameters d_m and σ are the size distribution parameters to be estimated, and parameter $\lambda \in [0 \ldots 1]$. The resulting size distribution parameters are summarized in Table 3.
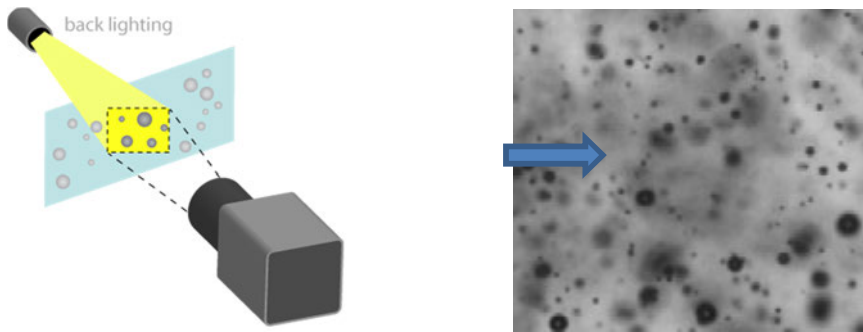

Figure 13. Measurement setup for high-speed imaging of droplets with back-light illumination and an example of the obtained image of fast moving droplets.
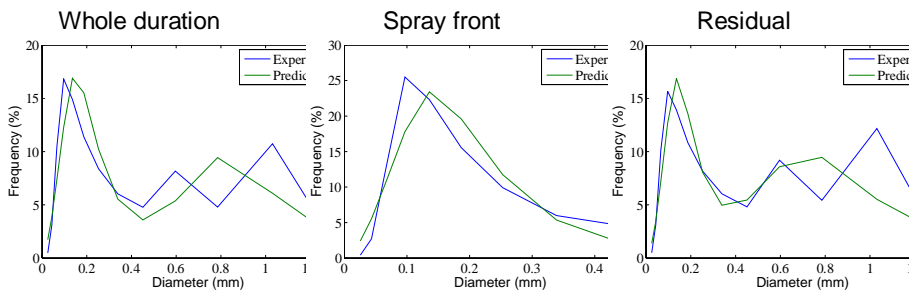

Figure 14. Experimentally observed and fitted droplet size distributions for test SFP4.

Table 3. Estimated droplet size distribution parameters for two Rosin-Rammler distributions.

Experiment		Distribution 1		Distribution 2		λ
		d_m (mm)	γ	d_m (mm)	γ	
SFP3	All	0.15	2.57	0.56	3.65	0.70
	Front	0.32	2.25	0.82	9.36	0.74
	Residual	0.15	2.59	0.55	4.32	0.78
SFP4	All	0.13	2.35	0.69	3.35	0.68
	Front	0.86	1.83	0.48	0.97	0
	Residual	0.13	2.27	0.72	3.61	0.66
SFP5	All	0.17	1.48	1.44	9.77	0.79
	Front	0.83	1.77	0.48	1.06	0
	Residual	0.17	1.38	1.44	10	0.77

Liquid simulations

Previous simulation studies on the impact fires within the SAFIR programmes have investigated the thermal impact on the buildings and the fuel behaviour, i.e. whether the fuel burns in the fire ball or is collected as pools on the bottom of the reactor building wall. In SMASH project, we focused on the physical extent of the flame and smoke effects in a scale that covers the whole reactor building and most of the neighbouring buildings. An example of the simulation is shown in Figure 15. The impact scenario was a horizontal impact at height of 35 m from the ground at speed 125 m/s, releasing 10 tons of jet fuel. Five different impact positions were considered. Both still and windy conditions were studied, assuming eight different wind directions. From the simulation, statistics were collected for the presence of flames or smoke in eight different monitoring positions around the plant. Two different bi-modal droplet size distributions were used, denoted here as "large" and "small". Comparison of the observed peak gas temperatures and the times from the impact to the flame arrival, observed with small and large droplets, are shown in Figure 16. Finally, a rough estimate of the threatened region around the reactor building was made, as shown in Figure 17.

Time: 2.01   Time: 4.0
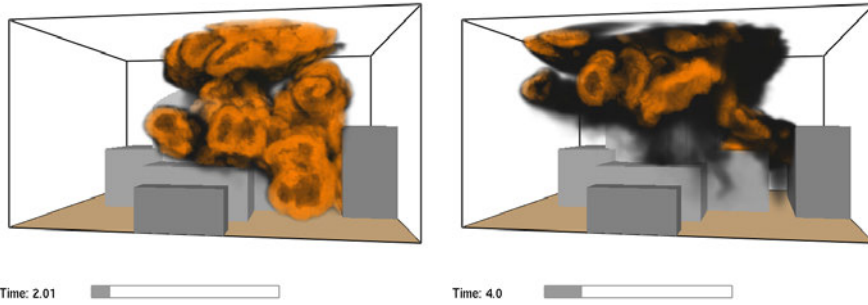
Figure 15. Instantaneous flame and smoke shapes from one of the plant-scale simulations.
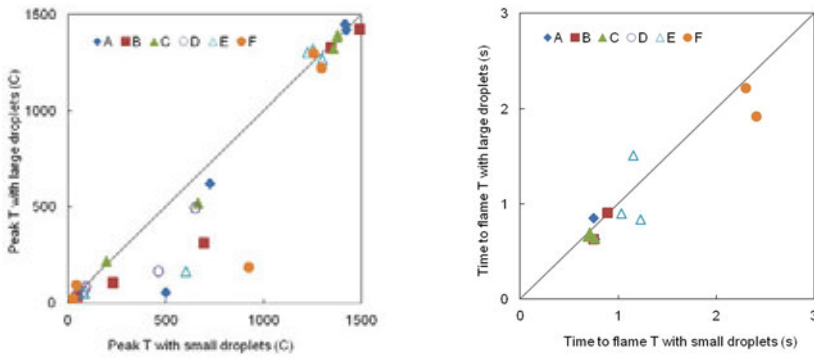

Figure 16. Comparison of gas temperature results obtained with large and small droplets. Peak values on the left and times to reach 700 °C on the right.
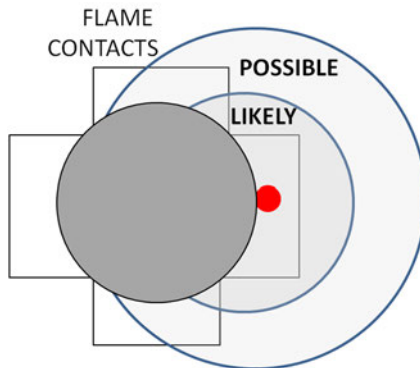

Figure 17. The possible and likely regions of aircraft impact flame contact around the NPP reactor building.

Conclusions

Several tests have been carried out within IMPACT project during 2011–2012. All the tests were carried out as planned. Also the measurements were mainly successful. The measurement system is being improved and developed continuously.

The impact load due to a deformable missile impact was calculated with the Riera method and using a FE model. Also a more accurate folding model was used in which the actual formation of folds is taken into consideration. Two finite element codes, Abaqus and a special purpose finite element program, are used in calculating the responses of the present test plates. Additionally a TDOF model is used for structural response studies. Displacements calculated with three different methods applying two different loading functions were compared with the experimental recordings. The shape of the loading function did not significantly affect the results in the considered case. Maximum deflections obtained by Abaqus and TDOF model were somewhat underestimated. It should be noted that these results are very sensitive to the material property assumptions. Also, the applied damping value affects the bending vibration behaviour. Damping values for nonlinear analyses on reinforced concrete structures can not be found in the literature. Experimental research is needed to obtain relevant data on damping for numerical analyses.

The DETO code has been developed at VTT to calculate values of shock wave parameters induced by chemical explosions. The calculated pressure transients can be further used in FE code as a loading.

A new simulation method called cohesive surface methodology was applied in simulating spalling and breaching of concrete walls due to shock waves.

Experiments with liquid-filled missiles were carried out to measure the liquid spray properties, serving as input and validation for CFD simulations. Droplet measurements were made using high-speed digital cameras with back-light laser illumination. Smallest observed droplets had diameters of about 10 μm. Bi-modal droplet size distributions were observed with median diameters in the ranges 0.13…0.17 mm and 0.56…1.44 mm, respectively. To our knowledge, this is the first time when the size distribution of the flying droplets has been successfully measured from a full-scale impact experiment.

The liquid measurements were used in the plant-scale impact fire simulation examining the physical extent of the flame and smoke influence, as well as the times required from the flames and smoke to reach different parts of the NPP construct. The results indicated that the flame resulting from a 10 ton release of jet fuel will very likely reach about one quarter of the reactor building perimeter. It took 0.5 … 3 s from the impact for the flame to reach the monitoring positions in the simulations.

References

1. Vepsä, A., Saarenheimo, A., Tarallo, F., Rambach, J.-M., and Orbovic, N. Impact Tests for IRIS_2010 Benchmark Exercise. Journal of Disaster Research, Vol 7 No. 5, 2012.

2. Tuomala M., Calonius, K., Kuutti, J., Saarenheimo A., Välikangas, P. Sensitivity studies on a punching wall of IRIS_2010 benchmark exercise. Journal of Disaster Research, Vol 7 No. 6, 2012.

3. Schleyer, G.K., Langdon, G.S. 2003. Pulse pressure testing of 1/4 scale blast wall panels with connections. Department of Engineering. Impact Research Centre. Liverpool University. Research Report 124, ISBN 0 7176 2706 3.

4. Abaqus Theory Manual. 2012. Version 6.12-3. Dassault systems.

5. Saarenheimo, A., Calonius, K., Tuomala, M. Sensitivity studies on reinforced concrete walls impacted by soft and hard missiles. VTT Research Report VTT-R-00859-12. 41 p.

6. Silde, A., Lindholm, I. On detonation dynamics in hydrogen-air-steam mixtures: theory and application to Olkiluoto reactor building. NKS-9, ISBN 87-7893-058-8. Feb 2000. 83 p.

7. Silde, A. The DETO 4.0 code: shock pressure loads from external explosions, User's Guide. VTT Research report VTT-R-07572-12. 23.11.2012. 45 p.

8. Kinney, G.F., Graham, K.J. 1985. Explosive shocks in air. Second edition. Berlin: Springer. ISBN 0-387-15147-8. 282 p.

9. Lautkaski, R. Blast waveform. VTT Research Report VTT-R-07690-12. 14.11.2012. 70 p.

10. UFC 2008. Structures to resist the effects of accidental explosions. Chapter 2. Washington, DC: Departments of Defence. (UFC 3-340-02) http://www.wbdg.org/ccb/DOD/UFC/ufc_3_340_02.pdf

8.2 Ageing management of concrete structures in nuclear power plants (MANAGE)

Rui Miguel Ferreira[1], Erkki Vesikari E[1], Mikko Tuomisto, Olli Stenlund[1],
Petr Hradil[1], Fahim Al-Neshawy[2], Esko Sistonen[2]

[1]VTT Technical Research Centre of Finland
Tekniikantie 2, P.O. Box 1000, FI-02044 Espoo

[2]Aalto University
P.O. Box 11000, FI-00076 AALTO

Introduction

Finlands first nuclear reactor came into operation in 1977. Within three years another 3 reactors were operational. Since these nuclear power plants (NPP) have been designed for a service life of approximately 40 years, they are reaching the end of their licensed operating service life. The ageing management of the NPP, especially the concrete structures, has become an important issue. Therefore the NPP companies are interested in developing Ageing management systems to avoid premature degradation of NPP facilities and to be able to extend their operating service life.

In response to this need the "MANAGE project – Ageing Management of Concrete Structures in Nuclear Power Plants", funded by SAFIR 2014 (The Finnish Research Programme on Nuclear. Power Plant Safety 2011–2014) [1], was initiated in 2011.

The ageing management system developed by the project consists of the central database and a group of analysing and planning tools which access data from the database. The database together with the analysing and planning tools can be used during different phases in the lifetime of a NPP: design, operation, inspection, monitoring, maintenance and repair of structures. The implementation of an ageing management system in practice guarantees a safe and uninterrupted use of the NPP for the whole intended lifetime.

This paper describes the development of an ageing management system software for the NPP concrete structures undertaken within the Manage project.

The ageing management system platform

According to STUK (Radiation and Nuclear Safety Authority Finland) guideline YVL 1.0 [2], in "NPP design, the service life and the effect of their ageing on the safety of all safety significant structures, components and materials shall be assessed using sufficient safety margins. Furthermore, provision shall be made for the surveillance of their ageing and, if necessary, their replacement or repair."

Furthermore, the guideline YVL 1.4 [3] states that " a management system shall be planned and implemented to incorporate all the operations of an organisation, and it shall be continuously maintained and improved. … The management system shall contain procedures to identify, assess and MANAGE safety risks relating to the operation of the nuclear facility."

Based on the IAEA Safety Guide NS-G-2.12 [4] for ageing management systems addresses both physical ageing of structures, systems and components (degradation of their performance), and their obsolescence. Effective ageing management is in practice accomplished by coordinating existing programmes, including maintenance, in-service inspection and surveillance, as well as operations, technical support programmes (including analysis of any ageing mechanisms) and external programmes such as research and development. This requires the use of a systematic approach to manAgeing ageing that provides a framework for coordinating all programmes and activities relating to the understanding, control, monitoring and mitigation of ageing effects of the plant component or structure [5].

In context with applying an extension to a plant operating license it is especially important for the NPP to know the current condition state of concrete structures. That is only possible by continuous inspection of structures and through a management system which is able to store and treat the inspection reports in a systematic way. Also, to be able to make provisions for the ageing of a nuclear facility, predictive methods are necessary to evaluate the future performance of structures and to make a maintenance strategy for the prolonged life time of a plant. An applicant of a licence shall be able to present a comprehensive ageing management programme with a description on how the design and qualification of the components and structures, their operation and operating experience, in-service inspections and tests, and maintenance are integrated logically and systematically [6].

However, massive concrete structures (i.e. foundations and containment structures) are not intended to be renewed and cannot be economically renovated. The final service life of NPP facilities may be dependent on the service life of the concrete structures in the facilities.

The premises and aims of the MANAGE project's ageing management system are the same as those presented in the YVL Guides and in the IAEA Safety Guide NS-G-2.12. The goal of the MANAGE system is to build up a platform that provides access to the structural, material and environmental information and to a package of various applications with appropriate methodologies and optimisation processes, which will assist the designers and maintainers of a NPP.

The MANAGE ageing management system will assist to implement the ageing management activities at different phases of the service life of a power plant. It will provide systematic methods for planning, surveillance, inspection, monitoring, condition assessment, maintenance and repair of structures.
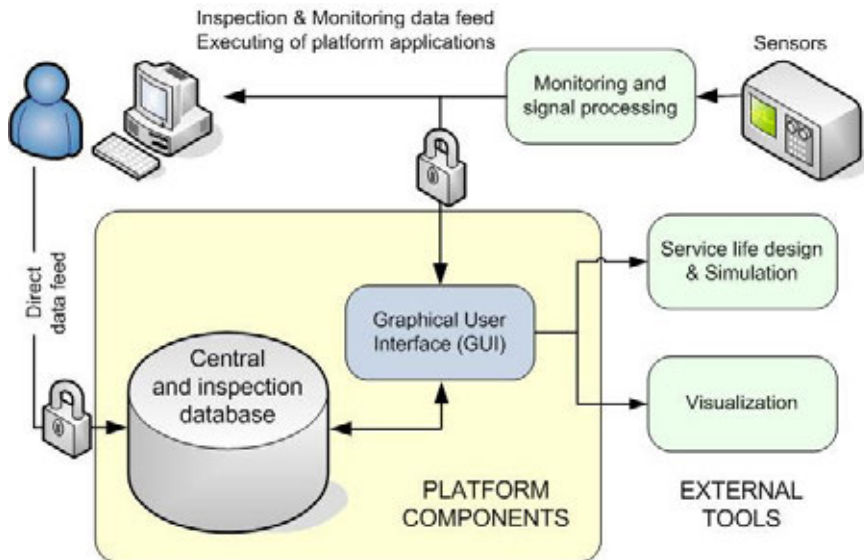
Figure 1. Conceptual view of the ageing management system platform.

From a conceptual point of view (Figure 1), the ageing management system platform is built around a central database with various applications. Access to the platform is through the Graphic User Interface (GUI) which connects the user to the various applications and the central database.

The Graphic User Interface (GUI)

The interface provides the user with access to the central database and the applications. The GUI is a point of interaction between components, and is applicable at the level of both hardware and software. The ageing management system platform has evolved since its initial concept in 2011. The applications iinitially considered are: ServiceMan, Visualization, Inspection database, and Monitoring (not implemented). Due to technical reasons and time constraints some of the application would not be implemented in this current project.

Users access to the GUI from server is by using a web browser. Web browser facilitates user access because there is no need to install any applications to a user's computer. GUI is programmed by using Visual Basic and it is on top of .NET environment. Both Visual Basic and .NET are widley known technologies.

The Central Database

The ageing management system's central database is the core of the platform. It assembles and systematically organizes the information gathered from all applications [7, 8]. The goals and objectives of the central database are to (1) collect the essential and up-to-date data of the condition and the performance of the NPP concrete structures, (2) store and update these data effectively, (3) allow sophisticated search strategies, (4) produce detailed reports automatically for the condition and the performance of the NPP concrete structures and (5) enable data transfer to other software for further analysis: for example act as a data source for estimation of the service life of the NPP concrete structures.

The components of the ageing management system's central database are organized into a series of sub databases relating to the Ageing management system of the nuclear power plants concrete structures, as shown in Figure 2. These sub-databases are:

- User's management database for user's data and their authorized limits.

- Visualisation database for dealing with the geometrical input and out for the visualisation tool.

- Service life management database for the input and output data for the service life calculation application (ServiceMan).

- Structural database for storing information about the structural types and components of the NPPs concrete structures.

- Inspection database for the data gathered from the investigation and the diagnosis of the NPPs concrete structures.

- Monitoring database for monitoring and simulating the performance of the NPPs concrete structures.

The authorized users of MANAGE central database come in two levels: the database administrators, and end users. Administrators are responsible for manAgeing the database system and have full access to modify the database code and design. The end users are the persons that use the database for querying, updating, generating reports, etc.

This database is developed to run on the NPP computers systems which are running on Oracle database management system. Therefore, the database was developed with ORACLE 11gR2 Express Edition software. A user interface is provided in the form of edit screens of the inspection database. The user interface was developed using Oracle Application Express. The use of the Oracle Application Express simplifies the deployment process because it is built-in oracle database and develope a web based database applications.
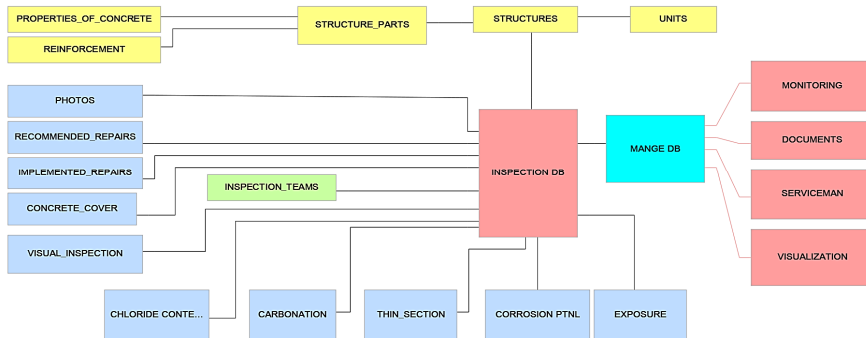
Figure 2. Conceptual design of the ageing management system's central database [8].

Figure 3. View of the front sheet of the ServiceMan tool.

The ServiceMan application

ServiceMan is a service life management tool for life cycle planning of concrete structures in nuclear power plants. It is able to predict the degradation of concrete structures and to evaluate the timing of necessary maintenance and repair actions over the remaining licensed life time of the plant or longer (extended life time). The tool can also be used for planning, organizing and optimizing the maintenance strategy of concrete structures in NPPs. A detailed description of the ServiceMan tool is presented in [9, 10].

The system was programmed based on Microsoft Excel. Macros, such as the user interface, were coded using Visual Basic for Applications. The actual service life management system includes the database and tool for service life management. The service life management tool includes prediction of degradation in structures, guarding of safety limits, timing of condition assessments, timing and specification of MR&R actions, and evaluation of life cycle costs and environmental impacts. In-service operations of the service life management system are condition assessment for structures, maintenance, repair and rehabilitation (MR&R) actions, and, updating the degradation models.

An interface between ServiceMan's Excel and the ageing management system's central database is done through the GUI. The application can read from and write to the database and make calculations using ServiceMan tool. Calculation results can also be stored back in the central database.

The Inspection database

The ageing management system's inspection database is part of the central database which includes all the NPP condition survey data. New inspection data is transferred to an electronic form then stored in the inspection database. The data consists of observations during both periodical inspections and special inspections. The design process of the inspection database is similar to the design of the central database. The structure of inspection database includes four main tables:

- Electronic documents and digital photos
- Visual investigation and diagnosis
- Non-destructive tests
- Destructive and laboratory tests.

The logical design of the inspection database describes the condition survey data in as much detail as possible, without regard to how they will be physical implemented in the database. The logical design of the inspection database is presented in Figure 4.
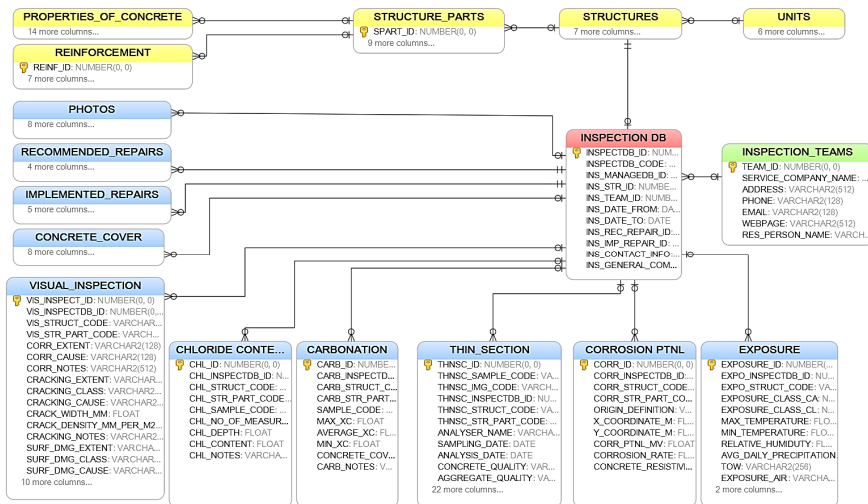
Figure 4. Example of the logical design of the inspection database [8].

The visualization application

The objective of the visualization application module is to propose an interactive system for visualization of data and documents related to the concrete structures of NPP. The proposed visualization environment is able to provide visual representations of the database content. It is also able to provide direct access to all the digital content, both in terms of physical access to the structural data files as well as in terms of searching and retrieving information.

The visualization interface can be used to import the geometrical data of the structures and report the in-service condition of these parts as attached notes to the geometry drawings. The application is currently using a simple procedure of visualization of all document types in their native format by external visualization software (e.g. AutoVue) that is able to interpret the data. Any kind of original (DWG, DXF, PDF, JPG, TIFF, etc.) can be stored in the central database and linked to the structure it represents. The platform interface will enable users to download process the drawing in an external application and then save the processing results and the original file in the MANAGE central database.

Visualization data is stored in a local Oracle database that consists of 4 tables. Visualization document data is stored in the first table and there are tables for possible unit, structure and module numbers also. Visualization document files are not stored in the database, just the path of the files. Each document is linked to only one unit, structure and module number. These numbers are stored in the Visualizations table example of search screen for specific document is given in Figure 5.
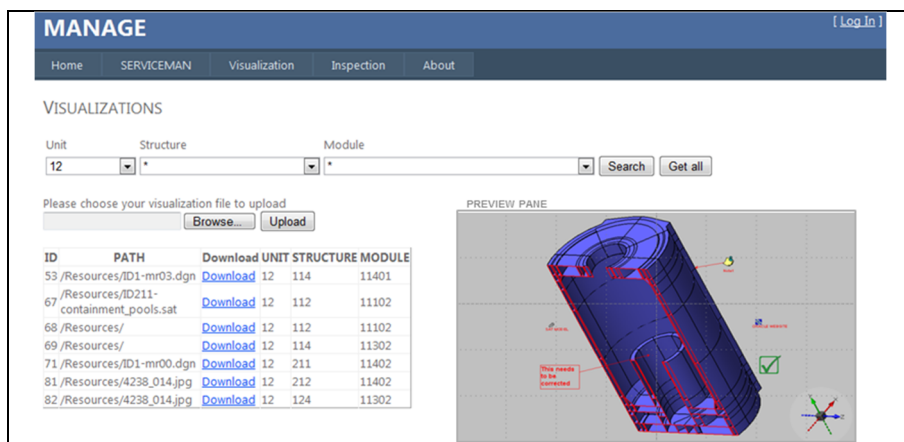
Figure 5. Screenshot of the GUI showing the Visualization interface.

Complementary analyses

Within the first two years of the MANAGE project several complementary studies/analyses have been performed to provide additional insight into the ageing management of NPP:

- Condition assessment of cooling water channels in Finnish Nuclear Power Plants (VTT-R-00342-11) – The objective was to evaluate the condition of cooling water channels in Olkiluoto 1 and Loviisa 1 NPP. The research was based on concrete samples taken from the structures at three levels: above the water level, at the range of the water level and below the water level [11].

- Condition assessment of cooling water channels in Finnish Nuclear Power Plants – Based on sample tests in 2011 (VTT-R-08960-11) – In all identical to the previous assessment but with different locations for specimen extraction in the cooling water channels of Olkiluoto 2 and Loviisa 1 [12].

- Half-cell potential measurements in Loviisa 1 cooling water chambers (AALTO-R-001-12 2012) – The goal was to measure half-cell potential values of the reinforced concrete structures of the cooling water chambers in Loviisa 1 NPP to verify the state of corrosion of the reinforcement. The half-cell measurements were performed at the same positions in the cooling water chambers as with the condition assessment carried out in 2010 [13].

- Structural failure analysis of post-tensioned containment building of Olkiluoto 2 NPP (VTT-R-00327-11) – The main goal of this report is to conduct structural failure analyses which help to evaluate the above mentioned probability. The intent is to calculate how possible tendon breaks affect the structural integrity of the whole containment building, and to be more precise, how the stress state of the containment wall changes and whether

there is an underlying mechanism by which the degradation propagates further in the structure to concrete, adjacent tendons and liner. To evaluate damage in the concrete induced by tendon breaks and/or pressure tests, supplementary cracking analyses are also conducted [14].

- Condition assessment of pre-stressing tendons by NDT inspection techniques (Ramboll Report) – The aim is to verify the suitability of non destructive test methods (NDT), for example by Ultrasound MIRA 3D Tomographer system, for detection of voids in grouted pre-stressed structures tendon ducts. In addition, other NDT techniques were used for general evaluation of concrete structures: the Impact – Echo DOCter system, the Surfer System, and the Impulse – Response s'MASH system. The structure chosen for the investigation task was the protective concrete structure of the containment structure of Olkiluoto 2 NPP [15].

Summary

This paper briefly presents the approach to the development of an ageing management system for concrete structures of Finnish NPP.

The ageing management system consists of the central database and a group of analysing and planning tools which access data from the database. The database together with the analysing and planning tools can be used during different phases in the lifetime of a NPP: design, operation, inspection, monitoring, maintenance and repair of structures.

The implementation of an ageing management system in practice guarantees a safe and uninterrupted use of the NPP for the whole intended lifetime.

References

1. SAFIR 2014 Framework Plan. National Nuclear Power Plant Safety Research 2011–2014. 2010. 102 p.

2. YVL 1.0. Safety criteria for design of nuclear power plants, Finnish Centre for Radiation and Nuclear Safety (STUK). 1996.

3. YVL 1.4. Management systems for nuclear facilities. Finnish Centre for Radiation and Nuclear Safety (STUK). 2008.

4. NS-G-2.12. Ageing Management for Nuclear Power Plants, IAEA Safety Guide, International Atomic Energy Agency, 2009.

5. Vesikari, E., Tuomisto, M., Hradil, P., Calonius, K., Al-Neshawy, F., Sistonen, E. Working plan for the Ageing Management System of concrete structures

in Finnish Nuclear Power Plants. Research Report VTT-R-08738-11. 2011. 63 p.

6. YVL 1.1. Regulatory control of safety at nuclear facilities, Finnish Centre for Radiation and Nuclear Safety (STUK). 2006.

7. Al-Neshawy, F., Sistonen, E., Piironen, J., Huovinen, S. Design of database based on condition survey of concrete facades. CONSEC'07, Concrete under severe conditions: Environment and loading, Tours, France, June 4–6, 2007. Pp. 1799–1806. (2007).

8. Al-Neshawy, F., Sistonen, E., Piironen J., Vesikari, E., Ferreira, R.M. Development of database for the in-service inspection of the concrete structures of the Finnish Nuclear Power Plants, IABSE Workshop on Safety, Failures and Robustness of Large Structures. February 14–15, 2013. Tuusula, Finland. (Submitted.)

9. Vesikari, E. Service life management system ServiceMan – User Manual. The Finnish Research Programme on Nuclear Power Plant Safety 2007–2010. Research Report VTT-R-00450-11. 41 p. (2011)

10. Vesikari, E. Service life management system of concrete structures in nuclear power plants. VTT Technical research Centre of Finland. VTT Publications 648. 82 p. http://www.vtt.fi/inf/pdf/pub-lications /2007/P648.pdf (2007).

11. Vesikari, E. Condition assessment of cooling water channels in Finnish Nuclear Power Plants. VTT Technical research Centre of Finland. VTT-R-00342-11. 2011. 51 p.

12. Vesikari, E., Ferreira, RM. Condition assessment of cooling water channels in Finnish Nuclear Power Plants – Based on sample tests in 2011. VTT Technical research Centre of Finland. VTT-R-08960-11. 2012. 44 p.

13. Piironen, J., Sistonen, E. Corrosion Measurements in Loviisa 1 Cooling Water Chambers. Aalto University. Espoo: Research Report AALTO-R-001-12 2012. 26 p.

14. Calonius, K., Fortino, S., Patalainen, M. Structural failure analysis of post-tensioned containment building of Olkiluoto 2 NPP. VTT Technical research Centre of Finland. VTT-R-00327-11. 2011. 83 p.

15. Rapaport, G. Condition assessment of pre-stressing tendons by NDT inspection techniques. Ramboll Report. 44 p.

8.3   Seismic safety of nuclear power plants: targets for research and education (SESA)

Ludovik Fülöp[4], Ilmari Smedberg[1], Timo Tiira[1], Päivi Mäntyniemi[1], Pekka Heikkinen[1], Marianne Malm[2],Niko Leso[2], Jouni Saari[2], Jari Puttonen[3], Vilho Jussila[4]

[1]Institute of Seismology, University of Helsink
P.O. Box 68, FI-00014, University of Helsinki, Finland

[2]ÅF-Consult Ltd
Bertel Jungin aukio 9, FI-02600 Espoo, Finland

[3]Aalto University
P.O. Box 11000, FI-00076 AALTO

[4]VTT Technical Research Centre of Finland
P.O. Box 1000, FI-02044 VTT, Finland

Introduction

Finland is located in one of the most stable continental regions, the Fennoscandian Shield. Due to low seismicity and sparse seismic networks in the area in the past, it has not been easy to find suitable strong seismic events which could be used for determining local attenuation functions, crucial in hazard assessment. Thus it has been necessary to use functions from geologically similar stable areas like Canada. Since the seismicity studies conducted in 1980's, when the present nuclear power plants (NPP) were constructed, quite a development has also occurred in the methodological side too. The decisions to build new nuclear power plants in Finland, and especially the positioning of one NPP in the northern Finland, calls for reassessing the potential effect of earthquakes on plant safety requirements. This is a challenging task since ordinary buildings are exempted from seismic design in Finland, and therefore the seismic engineering community is small and fragmented in several organizations.

A further complication is that two schools of seismic design exist, one group of professionals exclusively concentrating on NPP's and the more general practice of designing ordinary buildings in earthquakes. While, the different sophistication of the design methods and the philosophy behind the design goals often justify such differentiation, there is more and more interaction between the two areas. The construction industry of a country is serving both ordinary and NPP applications, obviously with different quality standards. New technologies and materials penetrate the field of ordinary buildings more easily; and in the area of predicting the resistance side, modern design codes in the field of ordinary buildings (e.g. Eurocodes) have made tremendous progress. The effort to run in parallel two design

code systems is pressing for unified procedures – e.g. in the non-NPP AISC 360-10 and its NPP "supplement" N690-06, but also the code KTA–GS-78, being examples in this direction.

In the SESA project we focus on the seismic qualification process and identify uncertainties which reflect and cumulate to qualification of systems, structures and components (SSC's) against seismic hazards. So far, the project contributed to a refined understanding of the seismic hazard and the related uncertainties in Finland, by adding and interpreting new measurement data in the continuously increasing bank of observations from earthquakes. A search for a suitable hazard analysis software is conducted within the SESA project. We also developed understanding of the participants in the design of the NPP of the consequences of increased seismic demands compared to the existing experience, particularly by exploiting finite element modeling (FEM) of buildings. Component qualification is the next, yet unexplored, element in the chain of building up understanding of uncertainties of seismic qualification procedure.

Updating the earthquake databank for Finland

One of the goals was to update and to improve the attenuation functions used in the hazard analysis in Finland. For this purpose we have started to collect recordings of strong local events in an earthquake databank. Before the year 2000 almost all seismic stations were short-period instruments with a sampling rate of 20 Hz. Since then the number of stations in the Fennoscandian area has increased and the instruments have been modernized. Nowadays almost all instruments are broadband sensors with a 100 Hz sampling rate.

One of the problems in building up the databank is that different institutions often use different data formats. For example, the data from the Institute of Seismology seismograms are in the so-called CSS-format, University of Uppsala uses (mini-) SEED-format and data from the Norwegian Seisweb can be downloaded in either SEISAN-format or GSE-format. All recordings have now been converted and the databank has velocity seismograms except few accelerograms from smaller events.

Figure 1 shows the epicentral distances vs. magnitudes of the events with magnitudes (Helsinki University magnitude scale MLHEL) between 1.8–5.0. Most of these have epicentral distances less than 100 km from the nearest station. The events have occurred in the depth range of 0–30 kilometres. Only displacement recordings with known instrument response functions are included. The figure contain 1184 recordings from 102 different seismic events. Most of the recordings are in distance range 200–500 kilometres and there are not many recordings with short epicentral distances. Three large events stand out, the two Kaliningrad earthquakes, MLHEL = 4.8 and 5.0 in 21.09.2004 and Ystad earthquake, MLHEL = 4.9 in 16.12.2008.
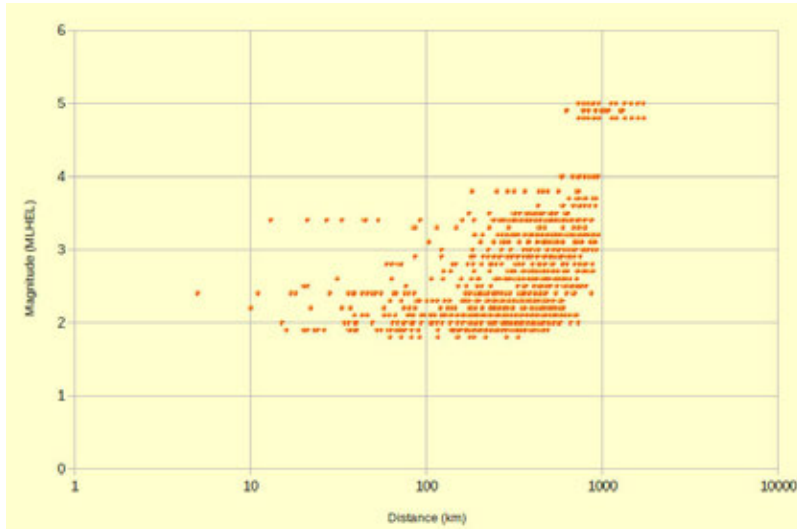
Figure 1. Epicentral distances vs magnitudes of the events in the data bank.

The geographical distribution of seismic events collected to the databank and the magnitudes of these events is shown in Figure 2. The bigger events of Ystad and Kaliningrad are clearly seen in the south. There are also few events in the Oslo Fjord where earthquakes occurred in 1904. The events in the Kola mining area as well as the earthquakes in the South-western Finland are usually shallow events in the depth range of 0–5 kilometres. Kuusamo area earthquakes usually occur much deeper with hypocentres at depths of 10–30 kilometres. Majority of the events are located in the Lapland, Tornio River Valley in the Swedish-Finnish border zone and in the Bothnian Bay Region.

In the databank there are 27 seismic events of magnitude 3 or greater. These seismic events are earthquakes, mining induced seismic events and rockbursts. As can be seen in Figure 1, there are not many recordings from the largest events at short distances. For many events the closest station is few hundred kilometres away. Figure 2 (right) displays the seismic events of magnitude 3 or greater. Five of these epicentres are located in the Bothnian Bay Region which is the area of importance in the future in seismic hazard and risk assessment in Finland. Only one of the events occurred in Finland, an earthquake of magnitude 3.5 in Kuusamo in 2000.

Figure 2. Epicenters of the events in the databank. The right panel shows events with magnitude 3 or greater, left panel shows all events (MLHEL > 1.8).
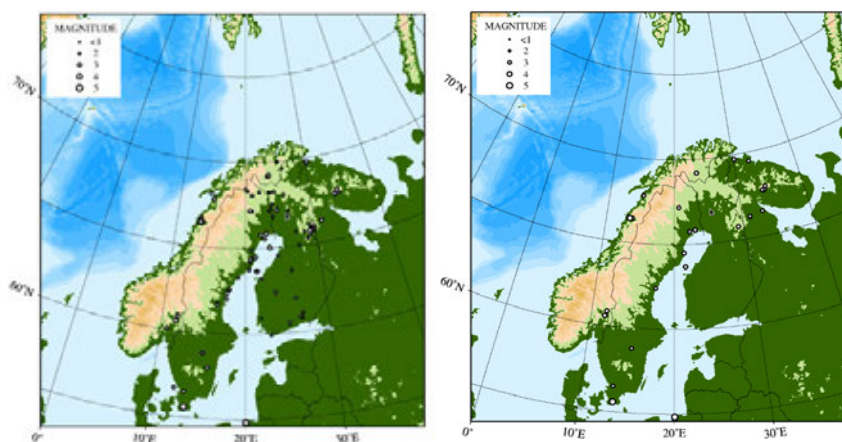
The Kouvola swarm and the Kotka earthquake

The ML 2.8 EQ 01.12.2011 triggered earthquake swarm at Kouvola area. On 19.–20.12.2011 four broad-band sensors were installed on source area with sampling rate 250 Hz, recording the 22.12.2011 ML 2.6 earthquake event in the distance range of 1–9 km (Figure 3). Further valuable data resulted from the ML2.0 Earthquake in Kotka, 27.04.2012. The event was recorded at distances 35, 59, 113, 144, 181, 215 km by 80–100 Hz instruments, but also by the 4 temporary 250 Hz broad-band stations with epicentral distances of 40–50 km.

Preliminary analysis of these events show frequencies up to 100 Hz and over near-to-site, and that small earthquakes at shallow depths may generate large accelerations (Figure 4). The content of high frequencies from broad-band stations hint to the need to use only recordings with sample rate 100 Hz or more in attenuation studies. On the other hand, the effect on SSC's of the high frequency content of the earthquake shaking is not fully settled (EPRI, 2007), and investigations in this direction are on-going.

It can be noted that the Kouvola and Kotka data nicely complemented the existing dataset (Figure 1) in the short distance range for small magnitudes. The data from all Finnish stations and stations available in Sweden, Norway, Estonia, Latvia and Russia was processed calculating characteristics of the signal PGA, PGV, those of the spectra (sPGA, sPGV) and the corresponding predominant periods.

By including events with smaller magnitudes the number of events in the data bank has been increased. At the moment the data bank contains 32782 three-component recordings from 1381 seismic events, with sampling rate > 80Hz, used to formulate an attenuation relationship for small magnitude earthquakes in Finland. The regional seismic events are usually characterized using local magnitude ML whereas attenuation relations are given as a function of the moment magnitude Mw.

Using the events of the data bank, it has been possible to determine the relation between ML and Mw for regional events in Fennoscandia.

Review of software platforms for hazard analysis

One of the objectives of the project for 2012 was to find suitable probabilistic seismic hazard analysis software and test it with Finnish data set. Given the development in direction of proposing attenuation relationships based on Finnish data sets, one important condition for the software platform was to flexibly incorporate user defined attenuation functions.

Component	Distance	Azimuthal	PGD	PGV	PGA
Z / N / E	km	direction	micrometer	mm/s	m/s^2
Z	1	35	123,46	1,45	0,843
N	1	35	123,02	2,37	1,031
E	1	35	116,51	1,47	1,565
Z	7	156	9,53	0,24	0,192
N	7	156	14,24	0,30	0,181
E	7	156	11,97	0,34	0,302
Z	8	40	3,34	0,12	0,12
N	8	40	3,97	0,29	0,286
E	8	40	6,41	0,41	0,443
Z	9	299	7,81	0,15	0,218
N	9	299	1,72	0,10	0,246
E	9	299	5,81	0,14	0,257
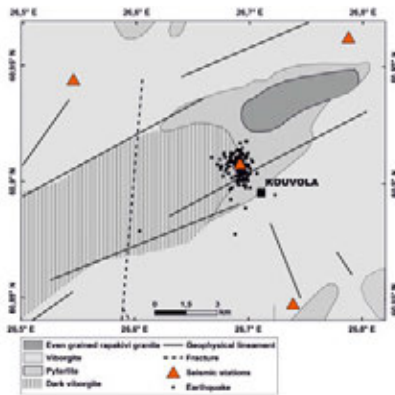
Figure 3. Location of the 145 swarm events analysed for the study.

Figure 4. Peak ground displacement (PDG), velocity (PGV) and acceleration (PGA) of the ML2.6 near the source for vertical (Z) and horizontal (N/E) components at different azimuthal directions (degrees).

Several software programs (CRISIS 2007, FRISK88M, OpenSHA, EqHaz, Open-Quake and EZ-FRISK) were tested or inspected and EZ-FRISK was chosen as best option. Test calculations were made with OpenQuake also, but it turned out to be quite complicated to use and not able to incorporate user defined attenuation functions. The results from OpenQuake were compared with ones from SEISRISK III to estimate how similar results are obtained with two different programs. Also, short reviews of OpenSHA and OpenQuake programs were conducted.

Based on the review and testing, it was decided that EZ-FRISK will be used as reference software with the Finnish data sets, once the attenuation equation suitable for Finnish geological conditions is finalized.

Design philosophy for structures

There is always considerable randomness in phenomena related to earthquakes. As shown in the previous section this is amplified by uncertainty in a low seismicity area like Finland, because of the scarcity of earthquake data. From the point of view of the loading arriving to structures the main particularities identified so far are (1) the general uncertainty of the load prediction in terms of PGA and (2) the potential effect of high frequency shaking being stronger than presumed.

In order to respond to the uncertainty from loading side, the base of the design philosophy for earthquake resistant buildings is to create buildings insensitive to deviation of the loads. The performance objectives of the designer have to be well understood and followed.

Regular buildings are traditionally designed with two performance objectives, human lives are to be protected and damage must be limited. Nuclear seismic design codes (e.g. YVL 2.6, 2001) focus on functionality of structures important for safety. The designed structure must maintain its function during and/or after the seismic event. By default, or stated explicitly, functionality also means integrity. While on declarative level design targets are clear, the difficult engineering task is assigning measureable criteria to performance target, which are necessary for the designer to evaluate the state of the SSC's.

The load levels at which the different performance objectives are to be reached are also important. Nuclear codes usually operate with two basic levels on the loading side – the Operating Basis Earthquake Ground Motion (OBE) is the vibratory ground motion for which all features of the NPP necessary for continued operation will remain functional; the Safe Shutdown Earthquake Ground Motion (SSE) is the vibratory ground motion for which certain structures, systems and components important to nuclear safety must be designed to remain functional.

The annual probability of exceedance, or return period is the usual way to define the different levels of design seismic action. Conventional structures are usually designed for 10% probability of exceedance in 50 years (return period of 475 years) for the life-safe objectives. Nuclear codes – due to the potentially high consequences of damage to NPP's will push return period for OBE and especially SSE very high (e.g. T_{NRC}=100 000 years in YVL 2.6). Even in these conditions, because of uncertainty related to load prediction, beyond design basis events are investigated.

Exploratory modelling of a reactor building

The FE modelling of a complex model of a generic reactor building started in 2012 (Figure 5). The mesh of the model has been received from Fennovoima. The loading considered correspond to the YVL 2.6 guide loads, and a second proposal with a broader frequency content spectra having a sPSA plateau between 4Hz and 40Hz.

The basic FE model has: (a) plan dimensions 61x58m; (b) elevation 55.76m to edge of the dome; (c) total mass 216 000 tons; (d) prevailing mesh size ~0.67m; (e) all material properties limited to elastic. Two spent fuel tanks and the pressure vessel were later added to the model, hence increasing the mass to 222 500 tons.

The aim of the modelling has been exploratory so far. The aim is to explore the bounds of the expected response, in terms of floor spectra, by using the two loading scenarios. The modelling is conducted at higher level of sophistication than expected in current design in order to answer research questions concerning expected behaviour beyond design basis loads. Particularly, in certain model versions the liquid in the pools have been modelled to take into account sloshing and vibration transmitted by the liquid (Abaqus coupled Euler-Lagrangian domain simulation with water material model defined with Mie-Grunesein equation of state (EOS), density, viscosity and specific heat). Also, in later modelling stages, the aim is to extend material behaviour into the non-linear range to a limited extent. The reasonable limits of studying the non-linear range of response is currently being investigated.

(a) (b)
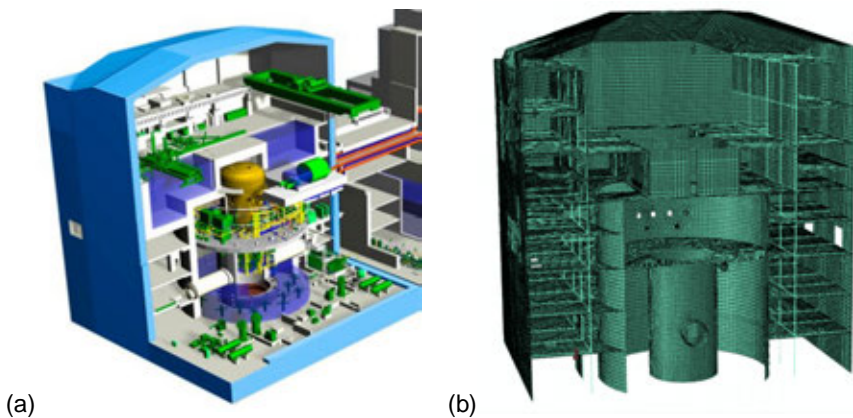
Figure 5. Reactor building analysed in this study (a) general view[4] (b) FE model (structural Axis 5).

University course about earthquakes and seismic loading on structures

In 2012 the project facilitated the organizing of a course on earthquakes, seismic hazard assessment and seismic design of SSC's by Aalto University. Teaching tasks were shared between personnel from Aalto University, the University of Helsinki and VTT. With 26 hours lectures and 80 hours independent work, the

---

[4] http://yle.fi/uutiset/fennovoima_calls_for_reactor_tenders/5384376#

course had about 50 participants, more than half practicing engineers from all areas of the Finnish industry working with seismic issues in their practice. The course material generated by this exercise is a valuable asset supporting dissemination in the future.

Conclusions

As the project is at mid-term, and we have not covered the full path of SSC qualification process, only some preliminary assessments can be presented as conclusions.

On the Finnish bedrock very high values of acceleration can be expected at small distances from even small magnitude earthquakes. We believe that the predominant frequency range includes also very high frequencies. This aspect is being further investigated. One particular focus of the study is also to what extent this high frequency components are able to affect SSC's.

Important results of the project after mid-term are the development of software for automatic determination of PGA (PGV) values necessary for calculating the attenuation relationships and formulation of the first versions of these relationships for small magnitude earthquakes based on locally measured data. This attenuation function will be tested with EZ-FRISK software.

The high uncertainty of earthquake load prediction in Finland calls for the investigation of beyond design basic load effects on SSC's. At the moment the project is focusing on exceedence of PGA values and presence of high frequency components in the acceleration signal. Generally, buildings should be configured to be insensitivity to beyond design basis loading scenarios.

The general acceptance of using Eurocodes in predicting the strength of components in the construction sector, and the superiority of strength models in this code over older models, calls for seeking bridges and clarifying limitations when using this codes in NPP context. In Europe the recommendation KTA–GS-78 is attempting to address consistently this question, and the further development to this direction will be monitored in the project.

Related publications

Smedberg, I. et al. 2012. Intraplate earthquake swarm in Kouvola, southeastern Finland, EGU2012 Vienna.

Smedberg, I., Malm, M., Saari, J., Heikkinen, P. SESA SP1 – Earthquake Hazard Assessment, Progress report 2011. Institute of Seismology, University of Helsinki & ÅF-Consult Ltd.

Seismic Design and Qualification for Nuclear Power Plants. Vienna: IAEA, 2003.

Considerations for NPP Equipment and Structures Subjected to Response Levels Caused by High Frequency Ground Motions. EPRI, Palo Alto, CA:2007.

KTA–GS-78 – Recommendations regarding the application of KTA safety standards considering current structural engineering standards (Progress report 2005).

YVL 2.6 – Maanjäristysten huomioon ottaminen ydinvoimalaitoksissa. STUK, 2001.

Differences in Approach between Nuclear and Conventional Seismic Standards with Regards to Hazard Definition. NEA Committee on the Safety of Nuclear Installations, 2008.

Fülöp, L. Seismic design of NPP's versus practice for ordinary structures; Research Rep. VTT-R-08439-11.

ABAQUS CAE/ Version 6.12 User's Manual.

9. Probabilistic Risk Analysis (PRA)

9.1 Extreme weather and nuclear power plants (EXWE)

Pauli Jokinen, Hilkka Pellikka, Milla Johansson, Seppo Saku, Matti Lahtinen, Hilppa Gregow, Kimmo Ruosteenoja, Ari Venäläinen, Kirsti Jylhä, Jenni Rauhala, Kimmo Kahma, Hanna Boman, Anu Karjalainen, Katri Leinonen

FMI Finnish Meteorological Institute
Erik Palmenin aukio 1, P.O. Box 503, FI-00100 HELSINKI

Abstract

The very rare weather phenomena that trigger sudden or prolonged sea level variations, abundant freezing rain or excess snowfall as well as extremely cold and warm episodes need to be included in the risk calculations of the nuclear power plants. We studied these extremes by investigating the observed quality controlled datasets of the Finnish Meteorological Institute, archives of non-digitized data, as well as reanalyzed weather data sets and global scale climate models.

The freezing rain and snowfall extremes have not caused catastrophes in Finland although in Sweden and Russia these events have been severe at some locations, in Canada even catastrophic. The extreme freezing rain situations in Finland can potentially be approximately 20 mm during a freezing rain episode whereas in Canada the highest observed amount is around 100 mm in a multi-day event. Similarly the "lake effect snow" which can take place in Finland is not of the same severity as those of Sweden. Still according to the Millennium-climate model simulations the snowfall could be around 100 kg/m^2 in the course of a few days. The peaks of extremely cold air masses could last for over three days but the conditions supporting extremely high temperatures did not last long in the simulations (less than a day). The changes in storm tracks and intensities in the last 200 years were visible in the ensemble mean of the Millennium climate model simulations. In southern Finland the simulated strongest winds showed an increase of approximately 3% most likely due to anthropogenic effects.

Meteotsunamis, which are long tsunami-like waves caused by meteorological phenomena, were found to be more common on the Finnish coast than they were assumed to be. The strongest known meteotsunamis on the Finnish and Swedish coasts are about 1–1.5 meters high, and it seems that these oscillations are included in distributions of sea level extremes. The worst situation would develop if a meteotsunami would occur after a winter storm that has first pushed the water level high along the coast like during the storm Gudrun 9th of January in 2005. Research on these important topics will continue and more cases and models with higher resolution will be used in the next steps.

Wind-related changes in sea level behavior on the Finnish coast

Based on Johansson (2013) the sea level variations in the Baltic Sea ranging from hours to decades are to a large degree wind driven. The correlation between the monthly mean zonal geostrophic wind over the southern Baltic Sea and the monthly mean sea level on the Finnish coast explains 82–88% of the interannual sea level variability, and 76–81% of the intra-annual month-to-month variability. Due to the slow response of the total water volume in the Baltic Sea to the water transport in the Danish Straits, the correlation has a time lag: the monthly mean sea levels correlate with the same month's as well as previous month's zonal geostrophic wind.

The correlation can be utilized to construct an estimate for the monthly wind-induced sea level component. Changes in this wind-induced component were compared with observed changes in sea level behavior to estimate the role of wind behind the observed changes. An increase in the zonal wind contributed an increasing trend of 0.5–1.2 mm/yr in the sea levels during the 20th century. The accelerating mean sea level trend since 1990s is however not related to regional wind conditions.

The annual sea level maxima on the Finnish coast have increased by 20–30 cm from the 1930s. The increase is partially explained by changes in monthly mean wind conditions, and the changes in wind conditions also explain changes in seasonal sea level variability. High sea levels that are exceeded a few weeks per year or less have increased, especially in winter (January–March).

The correlation between wind conditions and sea level, together with geostrophic wind scenarios from global circulation models, can be used to estimate future sea level changes. On average, the changes in wind conditions will result in 6–7 cm higher sea levels in the end of this century than in the present climate, the full scenario range extending from a 4 cm decline to a 19 cm increase. Combined with estimates for land uplift and the regional effects of global-scale sea level rise, these yield scenarios for the relative sea level change on the Finnish coast. In the Gulf of Finland, rising relative sea levels will result, in contrast to the past declining trend. In the Gulf of Bothnia, stronger land uplift balances the sea level rise according to the average scenario. The highest scenarios project sea level rise everywhere on the Finnish coast.

Occurrence of meteotsunamis in the Baltic Sea

Meteotsunamis are long waves in the tsunami frequency band caused by mesoscale atmospheric disturbances, such as thunderstorms, squall lines and other air pressure anomalies, moving above the sea at a resonant speed (Monserrat et al. 2006). In addition, shoaling, focusing by refraction as well as harbor resonance effects are required to amplify the small open sea waves into sizeable waves at the shoreline. These waves occur more or less regularly in some areas of the world ocean, where conditions favor their formation, and under certain conditions the waves can reach destructive dimensions.

The meteotsunami phenomenon is known on the Swedish and Finnish coasts under the name *sjösprång*, and strongest known meteotsunamis have been 1–1.5 m high (Renqvist 1926, Pellikka 2013). These types of unexpected and inexplicable high waves have long been known among the coastal residents of the Baltic Sea. There are several historical references of very strong, destructive waves of unknown origin on the present-day Polish coast in the 15th and 18th centuries. These waves are reported to occur under clear and calm weather, but sometimes they are accompanied by high winds or a sound of thunder. As the seismic activity of the region is low, it seems unlikely that these waves could have been of seismic origin.

Three meteotsunami cases were reported by eyewitnesses on the Finnish coast in 2010 and 2011: rapid sea level fluctuations of up to 1 m and strong currents with varying direction (Pellikka et al. 2013). Sea level measurements at the Finnish tide gauges confirm these observations, although with considerably smaller amplitude, as the strength of a meteotsunami strongly depends on coastal bathymetry (Figure 1). The meteorological origin of these events was confirmed using radar data and coastal observations. All three cases occurred during a passage of a cold front type of boundaries (squall lines, gust fronts) moving at a speed close to the long wave velocity in the sea, thus enabling efficient energy transfer from the atmospheric disturbance to the sea wave it generates (Figure 2). In the coastal air pressure observations, the meteotsunamis are shown as sudden peaks or jumps of a few hPa arriving approximately at the same time with the sea level oscillations.
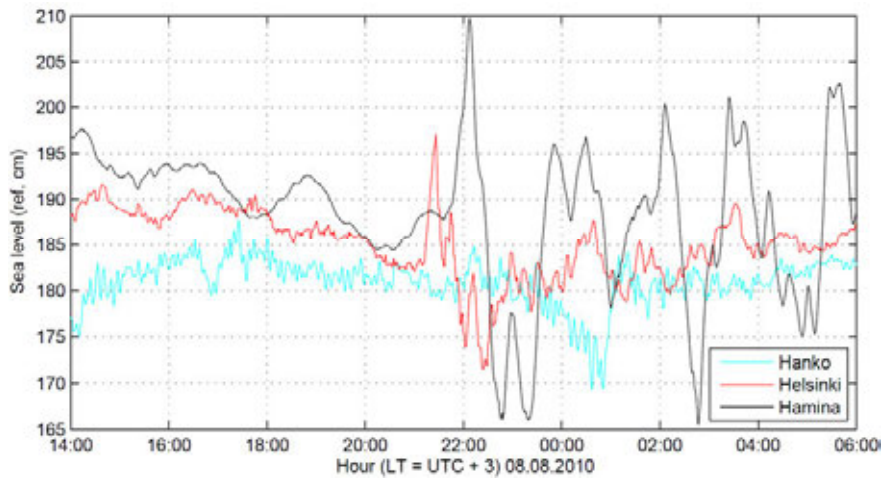
Figure 1. Sea level observations with a 1-minute time resolution at the Gulf of Finland tide gauges on 8 August 2010, showing a small meteotsunami.
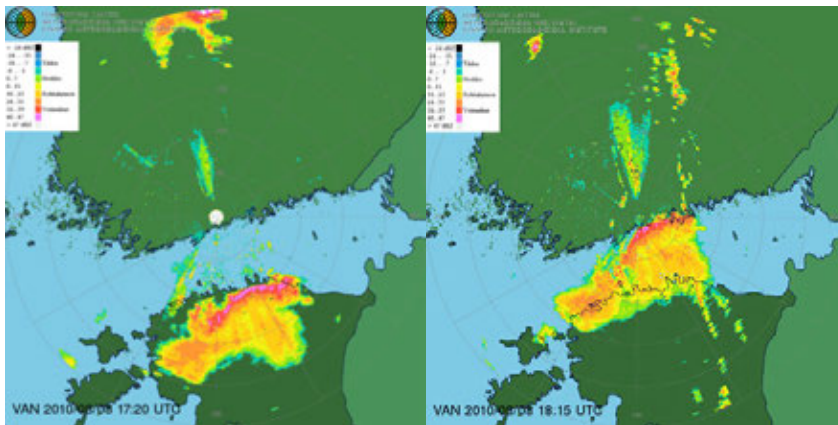
Figure 2. Squall line movement over the Gulf of Finland on 8 August 2010, causing the exceptional sea level fluctuations.

We have developed methods that allow us to recognize meteotsunamis from sea level and meteorological time series and to obtain data of meteotsunami frequency for statistical analysis. Preliminary results indicate that small meteotsunamis with a height of 10–40 cm are not frequent but occur occasionally on the Finnish coast. It seems possible that the frequency of rapid sea level oscillations has increased during the past decades. The meteotsunamis are probably included in the distributions of sea level maxima at least to some extent, which gives credibility to the previously conducted sea level studies concerning sea level extremes.

385

Analysis of the success of earlier mean sea level scenarios

Considerable number of scenarios of sea level rise have been published during the last 30 years. The first scenarios with starting point at 1980 or 1985 have significant differences already at 2012. In this report these early scenarios were compared with the estimates of global sea level. Four estimates were used: two estimates based on satellite data and two based on tide gauge from the Permanent Service of Mean Sea Level. While these estimates have some differences they agree more than an order of magnitude better that the scenarios.

The scenarios were first compared in the format they were presented in the literature review Kahma et al. (1990). In this comparison the estimated global sea level was smaller than most of the scenarios following the first quartile. i.e 75% of the scenarios were higher at the year 2012 than the actual sea level. This is an overestimate of the difference between the measured and the predicted value, as the scenarios contain only values for certain years and linear interpolation was used for the years in between. In some cases the scenario gave the sea level only for one year, for example 2100, which resulted in a very high growth already at 2012.
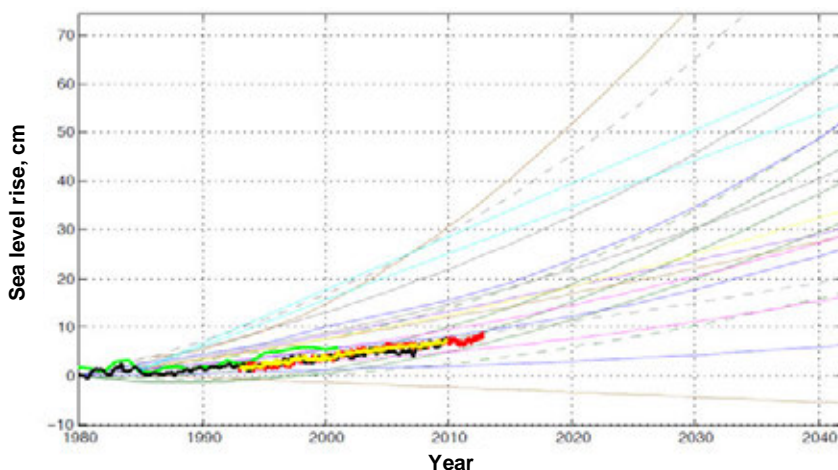
Figure 3. The comparison between observed sea level and scenarios made before 1990.

For the second comparison curved sea level scenarios were constructed following the intrepolation methods applied e.g. in Johansson (2013). In the cases where the original scenarios did contain only the end value (e.g. year 2100) the curvature was constructed from global temperature scenario following as closely as possible the method which was used in the original paper. The results in Figure 3 show considerably less deviation from high scenarios but the observations still follow the first quartile of the scenarios.

Theoretically possible weather extremes in Finland

The climate of the past 1200 years has been simulated with the fully coupled Max Planck Institute Earth System Model (MPI-ESM) climate model ("Millennium") in order to determine the conditions in which extreme temperatures, heavy "lake-effect" snowstorms and freezing precipitation events occur around the Loviisa area. The monthly and annual distributions as well as persistence of these events have been investigated (Jokinen et al. 2013). In addition, the return periods of extreme temperatures have been estimated with the aid of the Millennium-data.

The results indicate that the inclusion of Millennium-data significantly narrows the confidence limits of the return period estimates. The return levels have changed by several degrees especially for the longer return periods. For example the best estimates of the 1000 year return level extreme temperatures in Loviisa are +34.0°C and -38°C (compared to the values based on observations only, +32.1°C and -40.9°C, respectively).

There are no known cases of severe ice storms in Finland even though freezing drizzle/rain has been observed in the past. The Millennium-dataset indicates that conditions potentially resulting in over 20 mm of freezing precipitation in a day can occur in southern Finland (Figure 4). This kind of an event could be regarded as an ice storm with fairly significant local impacts. The potential freezing precipitation conditions lasted up to 66 hours (~almost three days) in the simulations. Most of the significant simulated events occurred in the autumn and spring months. There were no clear signals in the simulations that severe freezing precipitation events would become more frequent in southern Finland due to climate change.
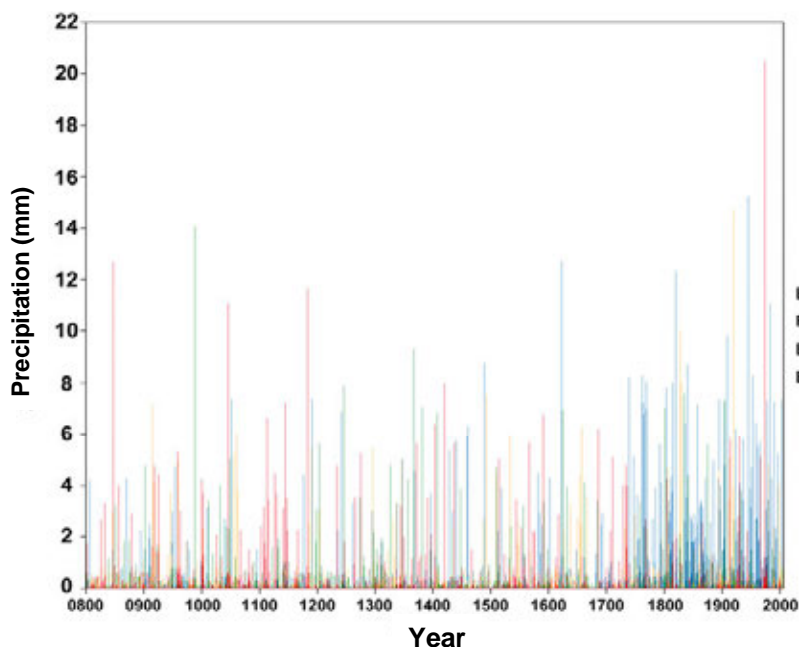
Figure 4. The daily running freezing precipitation sum based on the Millennium-simulations (mm). The values depict the theoretical highest amount. The four different ensemble members are colored (Jokinen et al. 2013).

"Lake-effect" snow is a phenomenon where intense snow showers are formed over relatively warm waters that then get advected to the coast, sometimes resulting in a long-duration heavy snowfall. The worst cases around the Baltic Sea have occurred on the coasts of Sweden and Denmark. In some events the snow depth has increased over a meter in a few days. The Millennium-dataset shows that similar snow intensities are possible on the southern coast of Finland, but the events are more likely to last for a shorter period than in Sweden or Denmark. However, the worst case scenario in Finland could bring approximately 80–110 kg/m^2 of snow in a few days. The most ideal conditions for heavy lake-effect snows exist in November and December.

Storm track changes based on observations and 1000-year climate simulations

Several international studies about the effects of climate change on storm tracks and storm intensities have been made with many different global and regional climate models (e.g., Gregow et al. 2012 and references therein). The main conclusion is still that storminess is expected to increase in Northern Europe. Yet the observed Finnish storms don't match their counterparts in Central- and Western

Europe, either in terms of their intensity or impacts. Therefore it is important to study whether such storms could theoretically be possible even in Finland.

Data of actual wind speed measurements and storm damage is not available of all storms. In the first part of our work (Gregow et al. 2013a) we limited the analyses to the last 50 years and the available forest damage reports (EFIATLANTIC) and reanalyzed meteorological datasets ERA-40 (Uppala et al. 2005) and ERA-Interim (Dee et al. 2011). With this data a comparison between the worst Finnish and European storms was made. Based on the reanalyzed dataset and the wind speed calculations, the wind gusts in the worst Finnish storms ranged from 33 ms^{-1} to 36 ms^{-1} whereas the significant storms in the rest of Europe typically had wind gusts stronger than 37 ms^{-1} in large areas.

Climate model studies of the past 1200 years were used to study how storm tracks and intensities might have changed in a very long time scale (Gregow et al. 2013b). The effects due to changes in the anthropogenic forcing were studied. In addition the typical weather patterns, durations as well as monthly and annual distributions of extreme Finnish storms were analyzed.

The simulations showed a statistically significant change in the average intensity of the strongest storms in large parts of Central-Europe during the last 200 years compared to the previous centuries. This result is shown in Figure 5. The same simulated signal exists in Southern Finland.

The Millennium-simulations as well as observations from the past 50 years show that the strongest winds in Southern Finland are typically from the southwest although a few northwesterly cases were found as well. The latter are potentially the worst on land areas due to significant turbulence in the lower part of the atmosphere.

The return period calculations of the mean winds showed that a once-in-a-millennium event in the middle of Gulf of Finland is approximately 32–34 ms^{-1} based on the Millennium-data similar to what was observed during the storm "Gudrun" (9.1.2005). However, this result does not take into account small, but very intense low pressure systems that the model cannot simulate due to its coarse resolution. Being prepared for the storms like "Gudrun" is therefore assumed to be wise. Future studies should be carried out with spatially and temporally more accurate climate models to minimize the uncertainty in the results.
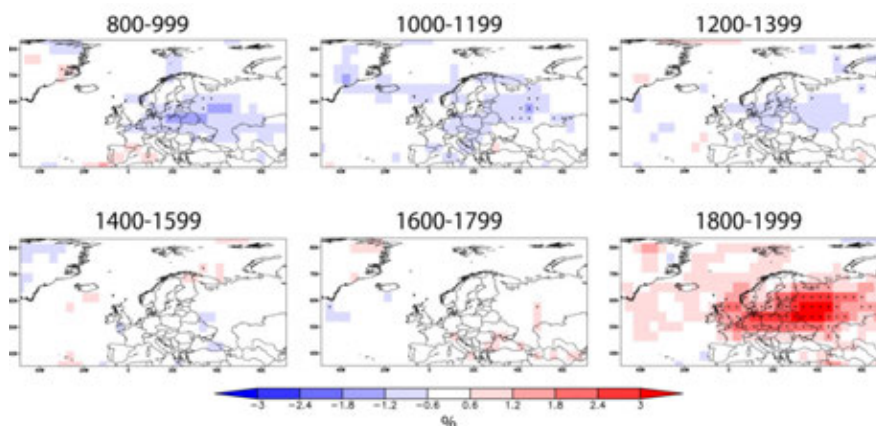
Figure 5. The 200-year anomalies of the annual maximum geostrophic wind speeds (shaded, %) based on the mean of the entire 1200 year simulations. An ensemble mean of five simulations is used. The dots depict grid points where the anomaly is statistically significant (95% confidence limit) (Gregow et al. 2013b).

Conclusions

- The changes in storm tracks and intensities in the last 200 years were visible in the ensemble mean of the Millennium climate model simulations in central and northern Europe in accordance with other international storm related studies

- In Finland, the "once-in-a-millennium -storm" based on the simulations is considered to be of same magnitude as the storm Gudrun in Sweden in 9.1.2005 – however the coarse resolution may give too low estimates meaning the return period can be less – the uncertainty can be minimized by using higher resolution models in the future work

- The annual sea level maxima on the Finnish coast have increased by 20–30 cm from the 1930s

- The average changes in wind conditions will result in 6–7 cm higher sea levels by 2100 compared to the current climate – the full scenario range extending from a 4 cm decline to a 19 cm increase

- The sea level rise observations still follow the first quartile of the scenarios

- The strongest known meteotsunamis on the Finnish and Swedish coasts are about 1–1.5 meters high and these oscillations are included in distributions of sea level extremes

- It appears that the frequency of rapid sea level oscillations has increased during the past decades

- The theoretically possible extreme freezing rain in Finland may reach 20 mm during a freezing rain episode. The limit 30 mm of freezing rain is known to cause damage to infrastructure

- The theoretically possible extreme "lake effect snow" according to the Millennium-climate model simulations could in Finland cause around 100 kg/m^2 snow loads in 1–3 days.

References

Dee, D.P. et al. 2011. The ERA-Interim reanalysis: configuration and performance of the data assimilation system. Q. J. Roy. Meteor. Soc. 137, 553–597. Doi: 10.1002/qj.828.

Gregow, H., Ruosteenoja, K., Pimenoff, N., Jylhä, K. 2012. Changes in the mean and extreme geostrophic wind speeds in Northern Europe until 2100 based on nine global climate models. Int. J. Climatol. 32, 1834–1846.

Gregow, H., Jokinen, P., Venäläinen, A., Laaksonen, A. 2013a. Estimating windstorm related forest damages in Europe in 1960–2010 by the geostrophic and ageostrophic isallobaric winds. Submitted to International Journal of Climatology 30.1.2013 (# JOC-13-0053).

Gregow, H., Jokinen, P., Lahtinen, M., 2013b. Occurrence of storms based on 1000-year climate simulations. (In Finnish) SAFIR2014/EXWE report, 31.1.2013, Finnish Meteorological Institute.

Johansson, M.M. 2013. Wind-related changes in sea level behavior on the Finnish coast. PhD thesis (manuscript in approval process), University of Helsinki.

Jokinen, P., Lahtinen, M., Saku, S., Venäläinen, A., Gregow, H. 2013. The observed and unobserved extreme weather phenomena in Finland (In Finnish). SAFIR2014/EXWE report, 31.1.2013. Finnish Meteorological Institute.

Kahma, K., Alenius, P., Boman, H., Vuorinen, I. 1990. Meriveden korkeus, aallokko, lämpötila, suolaisuus ja biologinen kasvusto Loviisan rannikolla seuraavinen 20–50 vuoden aikana. Merentutkimuslaitos. (In Finnish)

Monserrat, S., Vilibić, I., Rabinovich, A.B. 2006. Meteotsunamis: atmospherically induced destructive ocean waves in the tsunami frequency band. Natural Hazards and Earth System Sciences 6, 1035–1051.

Pellikka, H. 2013. Meteotsunamit: esiintyminen, syntymekanismit ja riskit Suomen rannikolla [Meteotsunamis: occurrence, formation mechanisms and risks

on the Finnish coast]. SAFIR2014/EXWE report, 31.1.2013, Finnish Meteorological Institute.

Pellikka, H., Rauhala, J., Aalto, J., Boman, H., Gregow, H., Kahma, K. 2013. Meteotsunamis on the Finnish coast. SAFIR2014/EXWE report, 31.1.2013. Finnish Meteorological Institute.

Renqvist, H. 1926. Ein Seebär in Finnland. Zur Frage Nach der Entstehung der Seebären. Geografiska Annaler 8, 230–236.

Uppala, S. et al. 2005. The ERA-40 reanalysis, Quart. J. Roy. Meteor. Soc. 131, 2961–3012. Doi: 10.1256/qj.04.176.

9.2 Risk assessment of large fire loads (LARGO)

Simo Hostikka, Terhi Kling, Johan Mangs, Anna Matala, Antti Paajanen,
Topi Sikanen

VTT Technical Research Centre of Finland
Kemistintie 3, P.O. Box 1000, FI-02044 Espoo

Introduction

The computational assessment of the NPP fire consequences is currently possible for prescribed fires within the compartment of fire origin. Significant steps towards the prediction of fire size have been taken during the last decade. Probabilistic methods to account for the uncertainty associated with the initial and boundary conditions have also been developed and applied on paired-redundancy problems. These studies have been limited to the problems considering only one fire compartment. The issue of fire spreading outside the compartment has not been covered, except for the smoke spreading through the ventilation network covered roughly in the late 1990's. The simulation of fire penetration through structural barriers is currently beyond the validated capabilities of fire simulation programs. In addition, the knowledge about the response of electrical and mechanical devices on heat and smoke is currently limited to the traditional technology, leaving a plenty of open questions for those dealing with the digital automation under and after fire exposures.

The main objective of the project is the assessment of risks associated with large industrial fire loads within NPPs, such as oil or electrical cables. The project should develop tools for the assessment of the defence-in-depth fulfilment in fire protection. The work includes the development of fire simulation methods towards a validated capability to predict fire size under ventilation controlled conditions and

suppression, and development of a software tool for the interoperability of state-of-the-art fire and structural simulation models. The capability to evaluate the efficiency of counter measures by plant personnel will be examined by further development and practical application of the new stochastic operation time model (fire-HRA). Methods to evaluate the failure of digital automation under smoke and heat are also studied. The objective of the response studies is the estimation of safe shutdown success probability.

Evaluation of the fire compartmentation

To support the evaluation of fire defense-in-depth (DID), a new method for the assessment of the performance of passive fire barriers is suggested. According to the codes and requirements, fire-separating building elements and the associated equipment and fittings must be made so that the spread of fire from one department to another within a specified period of time will be prevented. The fire rating of the parts of the building is the time in minutes that the part can fulfill the required criteria when exposed to the standard time-temperature curve (ISO 834). Using the fire rating in the DID evaluation has a few problems: (1) How much the existing fire rating correlates to the probability of fullfilling the requirement? (2) The standard curve can be overly conservative or optimistic, depending on the application. (3) What if the fire exposure is longer than the fire rating?

Based on the basic ideas of EPRESSI-method (Gautier et al., 2010) we suggest a new method that can be used to evaluate the performance of the compartmentation in real fires. The method is based on three main steps:

1. Determine the performance curves of the barrier components.

   Calibrated models are used to forecast the resistance of the components for time-temperature curves (test loads) that are different than the standard ISO 834 curve.

2. Determine the real temperature load curves in the compartment

   The real (realizable) temperature curves are determined by Monte Carlo fire simulations.

3. Test how well the components resist the fire loads

   We assume that the component withstands a real load if some of the test loads is higher than the real load for the whole time period of the fire. The probability of succesfull compartmentation is calculated as fraction of all real temperature loads for which the above condition is true.

Figure 1 shows the performance tree of the compartmentation and a typical test load. The method is tested using the existing Monte Carlo simulations of the TVO cable room. From the simulations, different types of test loads were identified. Most of them could be evaluated using the family of existing test loads, but some

new types of time-temperature curves were found. These curves were results of fires that extended in space and time (traveling fires).
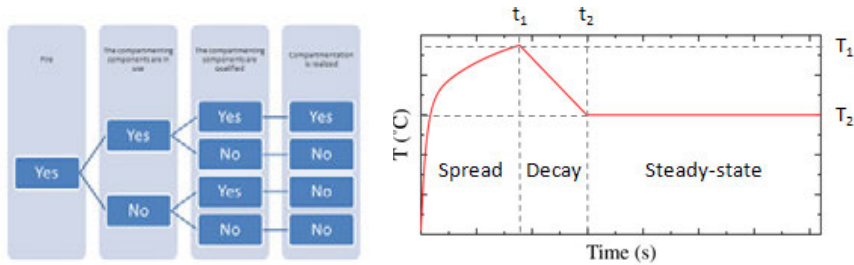

Figure 1. Performance tree of the compartmentation and a typical test load of a component.

Response to fire: stochastic simulation of fire and human operations

Deterministic fire simulations are used in the fire PRA to connect random initial and boundary conditions to the fire consequences. The most typical consequence of interest is a thermally induced failure in a device or cable. Often, the fire brigade intervention has not been examined because it has not been credited in the fire-PRA. How conservative this simplifaction is, has not been known. A new stochastic operation time model was developed for the calculation of the probability of fire suppression by plant fire brigade before the fire causes unwanted effects. The model is implemented as a flowchart describing the chronological order of human actions and the transversal connections between the parties. The main assumption of the model is that each of the human operations can be described as a time delay and a possible additional delay due to the human errors or unfavourable circumstances. The model is evaluated using the Monte Carlo method, and the result is the distribution of the total time delay from fire ignition to the successful fire suppression. Comparing the result to the simulated failure time distribution gives the overall failure probability. The model also reveals the most important factors contributing to the total fire fighting time.

As an application of the developed method a fire scenario was simulated, where a fire was ignited in the cable room of the NPP (Figure 2). The location and other properties of the initial fire, as well as many of the material properties were selected at random. With the sprinkler system operational, none of the fires resulted in cable failures in the target system. In the non-sprinkled simulations, about 65% of the fires caused cable failures in the target system.

Stochastic operation time simulations (1000 iterations) were carried out for all (100) fires. The times of the fire brigade interventions were compared with the failure times to calculate the final failure probability. Two different scenarios were identified depending on if the voltage cut-off is needed before the fire brigade

intervention. According to the simulation results (Figure 3) of the non-sprinkled cases, the fire brigade success probabilities were < 1% and 25% for the cases with and without the voltage cut-off, respectively. The corresponding conditional failure probabilities (sprinklers not in use) became 65.5% and 49.4%.
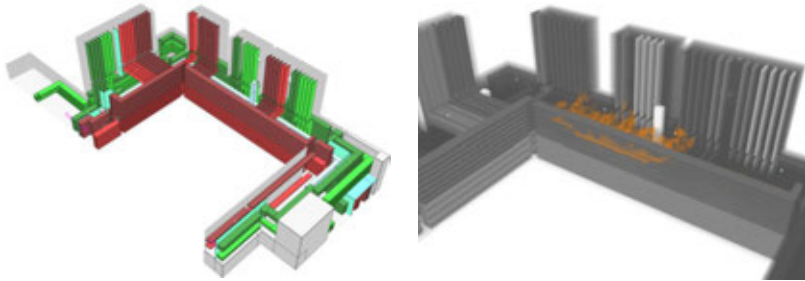
Figure 2. Simulation of a fire in the cable room.
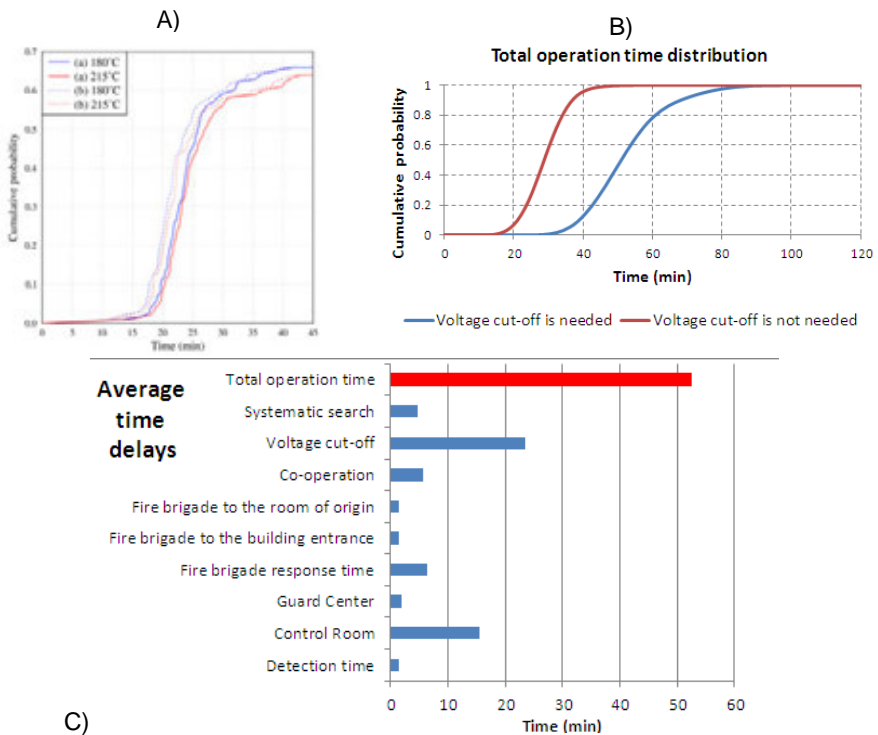
Figure 3. A) Time-to-failure measured from (a) ignition and (b) smoke detector activation, B) total operation time distribution of the plant fire brigade and C) average time delays of human actions.

CFD simulation of large fire loads

Analytical techniques for Micro-Scale Combustion Calorimeter

Over the last few years, methods have been developed for the estimation of pyrolysis model parameters from small and bench scale experiments. Micro-Scale Combustion Calorimeter (MCC) is a technique for measuring the heat release potential of a material. In this project, two methods were developed for combining MCC and TGA analysis for the calculation of the reaction-specific heats of combustions. Method 1 provides a simple engineering solution while Method 2 enables more complicated reaction paths (see Figure 4). The methods were verified using a fictitious material and validated using PVC cable data from the U.S.NRC CHRISTIFIRE project. Figure 5 shows measured and predicted data for TGA, MCC and cone calorimeter.
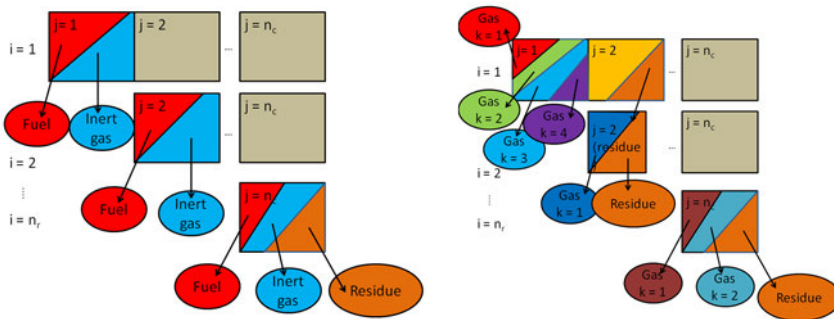
Figure 4. Reaction paths for the MCC-TGA analysis methods 1 (left) and 2 (right).
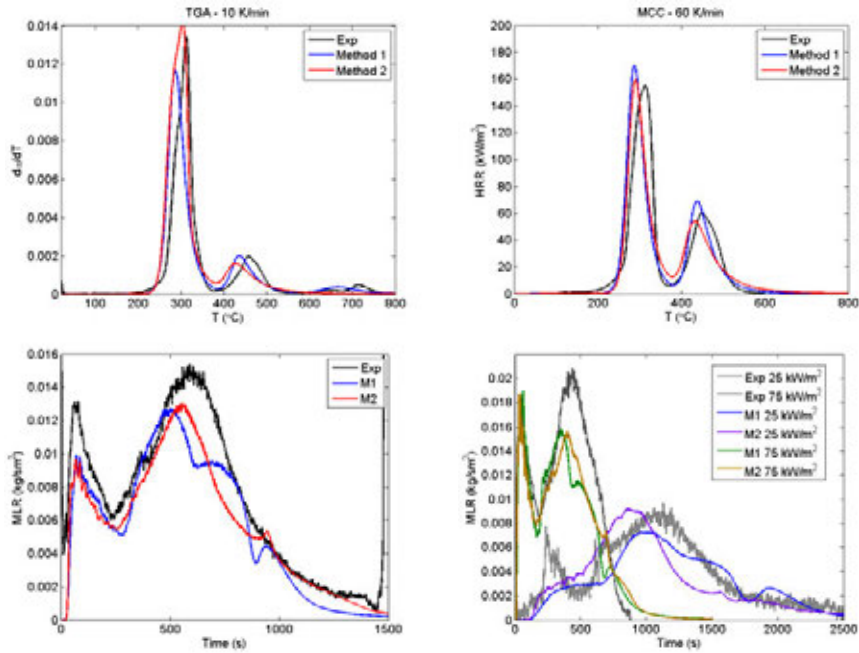
Figure 5. Experimental and model simulations for PVC cable. Up: small scale. Down: Mass loss rates (MLR) in cone calorimeter.

Sub-grid scale models for burning cables

In fire-CFD, all the solid fuels, including cables, have traditionally been modelled using obstacles that are limited by the resolution of the CFD mesh. A new approach has been developed for modelling solid fuels as Lagrangian particles to increase the flexibility in modelling complicated fuels and non-rectangular objects, such as cables. The drawback can be the increased calculation time in some applications. The model was implemented in the Fire Dynamics Simulator program. The validation of the model is going on using the OECD PRISME vertical cable experiments (Figure 6).
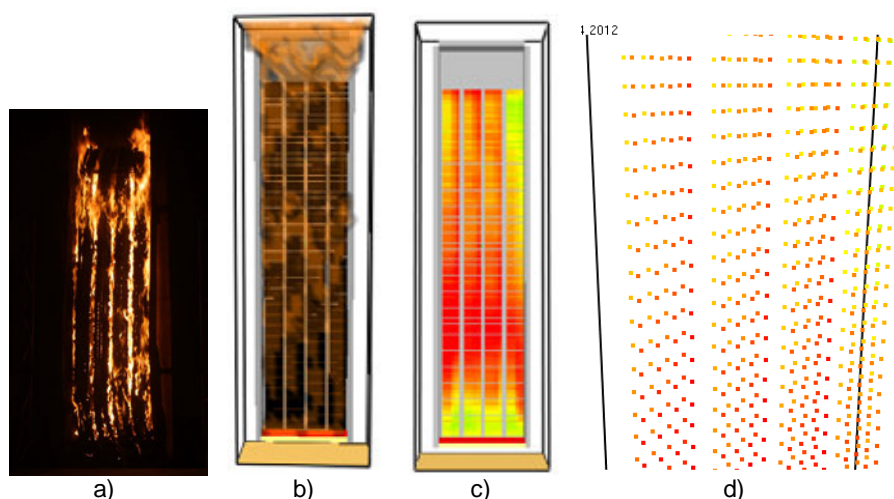
Figure 6. OECD PRISME vertical cable experiment. a) Experiment in full fire. b) Simulation in full fire. c) Cable temperatures in full fire. d) Zoomed in cable bundles.

Characterization of cables for the OECD PRISME experiments

Within the OECD PRISME2 project, full scale experiments of the cable flame spread on horizontal cable trays are performed with cables provided by the project partners. One of these cables is MCMK 3x2.5 mm^2 PVC cable that is used at the TVO nuclear power plants in Finland. The cable is similar to but not identical with cables studied in earlier SAFIR-projects [Matala & Hostikka 2011]. Experimental characterization of the cable was carried out to provide basis for the numerical simulations of the PRISME experiments and to determine the applicability of earlier (2009) results. The structure of the cable is presented in Figure 7.

The characterization was carried out using Simultaneous Thermal Analysis (STA), flame spread experiments, and cone calorimeter. The chemical composition of the cable materials was investigated using Fourier transformed infra-red spectroscopy (FTIR), gas chromatography combined with mass spectrometry (GC-MS), X-ray fluorescence analysis (XRF), X-ray diffraction (XRD) and calcination.

From the TGA results, three main decomposition steps were identified: (1) 200…320°C, (2) 430…530°C, and (3) > 660°C. Figure 7 shows the DSC results of the cable sheath, indicating endothermic first reaction and exothermic second reaction. Also shown are the heat release rates from the cone calorimeter. The only significant difference in the cone calorimeter was the ignition time, which is shorter for the "2009" cable. The vertical flame spread rates at ambient temperatures 20… 176°C were measured with the VTT 2 m apparatus [Mangs 2009]. The observed flame spread rates are presented on the bottom of Figure 7, showing slightly higher rates for the "2009" cable. According to the results, the "2009" and

"2012" cable samples are very similar in terms of fire characteristics, which is good for the applicability of the results.
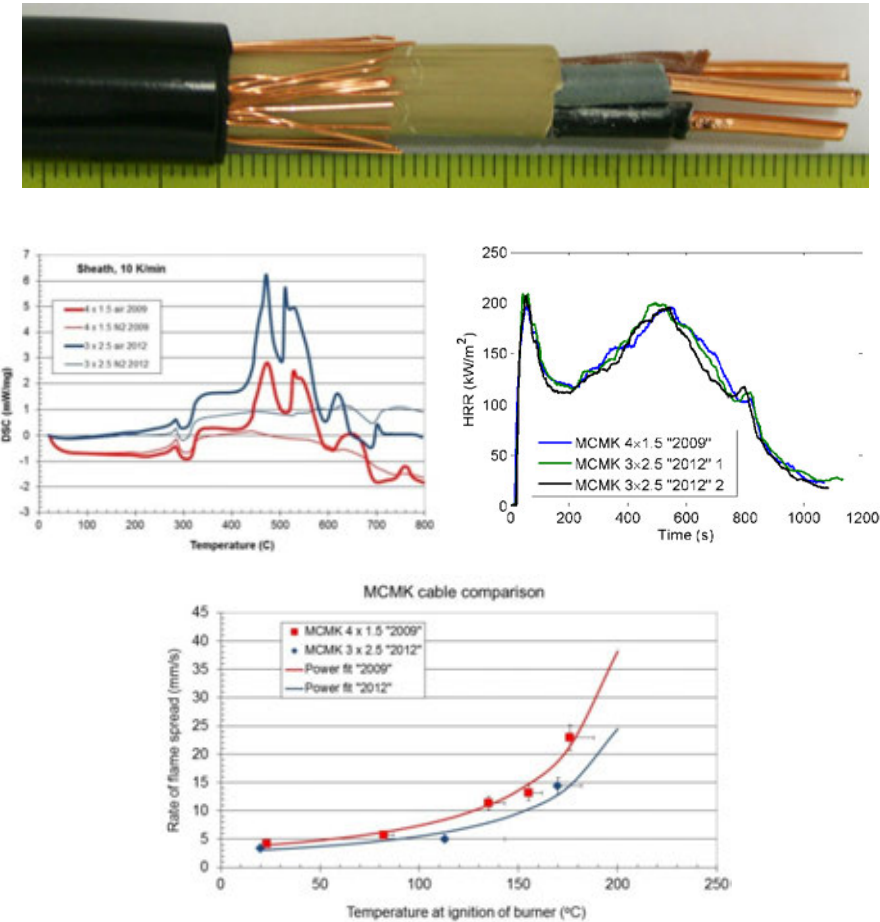
Figure 7. MCMK 3x2.5 mm^2 "2012" structure (Top). DSC results for 2009 and 2012 cable sheat (Middle left) and cone calorimeter heat release rate (Middle right), flame spread rate results (Bottom).

Simulation of liquid pool fires

A new evaporation model has been implemented in the FDS to reduce the grid dependence of the pool burning rate predictions. In the new evaporation model, the problem of the unresolved concentration boundary layer near the pool surface is solved by using a mass transfer correlation

$$\dot{m}'' = h_m \rho_f \, \log\!\left(\frac{X_G - 1}{X_f - 1} \right) \qquad\qquad (1)$$

where h_m = (Sh μ_a / Sc Δx) is the mass transfer coefficient and ρ_f and X_G are the fuel vapour density and volume fraction in the grid cell adjacent to the pool surface. The Schmidt number Sc = 1, Sh is the Sherwood numer.

The model was first validated using the data from SFPE Handbook (Figure 8) [Gottuk and White 2002]. In average, the predicted burning rates are lower than the experimental values but the overall uncertainty is not high. Further validation using the OECD PRISME data for well- and under-ventilated room fires was performed. The model uncertainties for various output quantities were first determined by carrying out simulations with prescribed burning rates (Figure 9). Then the predictive simulations of the pool fires were carried out (Figure 10). Finer grids produce lower (and better) estimates of HRR. However, the grid sensitivity is weaker than with the old, equilibriuim vapor pressure based model.
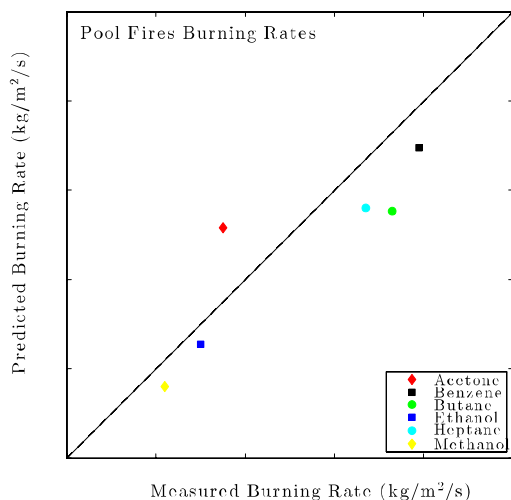
Figure 8. Comparison of FDS predictions with experimental data on maximum burning rates of large hydrocarbon pool fires.
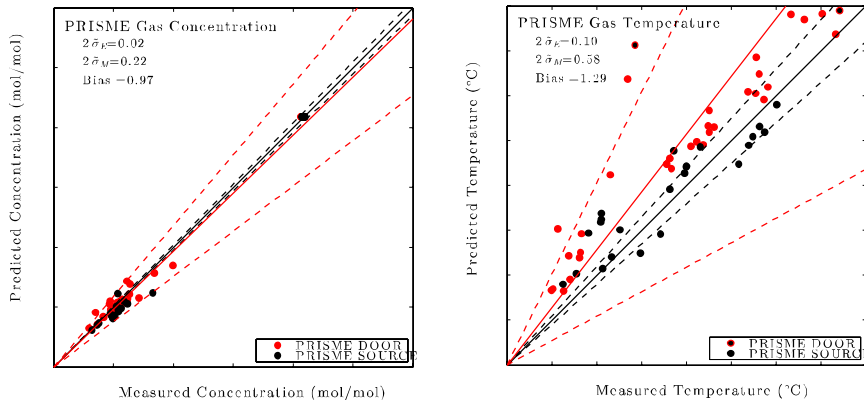
Figure 9. Measured vs. predicted quantities in the PRISME SOURCE and PRISME DOOR test series. Simulations with prescribed HRR.
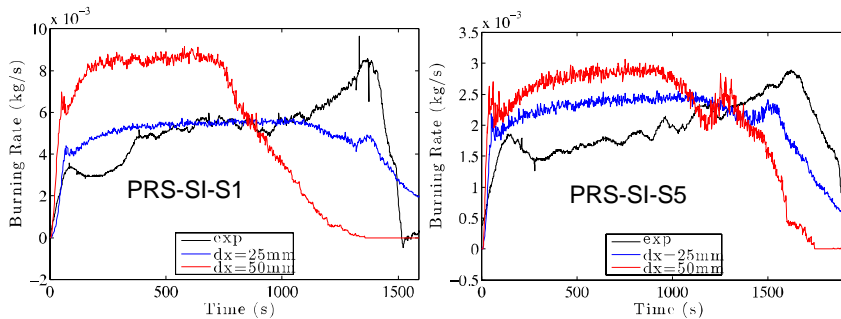
Figure 10. Comparison of experimental and simulated pool burning rates in two of the PRISME tests.

References

Gautier, B., Mosse, M., Eynard, O. 2010. EPRESSI Method – Justification of the Fire Partitioning Elements. Sixth International Seminar on Fire and Explosion Hazards, Weetwood Hall, Leeds, UK, April 11th to 16th, 2010. Compartment Fires 2.

Gottuk, D.T., White D.A. 2002. Liquid Fuel Fires. In: SFPE Handbook of Fire Protection Engineering. 3rd Ed. National Fire Protection Association, Quincy, MA. USA.

Matala, A., Hostikka, S. 2011. Pyrolysis Modelling of PVC Cable Materials. Fire Safety Science 10: 917-930. Doi: 10.3801/IAFSS.FSS.10-917.

Mangs, J. 2009. A new apparatus for flame spread experiments. VTT Working Papers 112. Espoo. 51 p. + app. 28 p. http://www.vtt.fi/inf/pdf/working papers/2009/W112.pdf.

9.3 PRA development and application (PRADA)

Jan-Erik Holmberg[1], Kristiina Hukki[1], Ilkka Karanta[1], Taneli Silvonen[1], Antti Toppila[2]

[1]VTT Technical Research Centre of Finland
Tekniikantie 2, P.O. Box 1000, FI-02044 Espoo

[2]Aalto University
P.O. Box 11000, FI-00076 AALTO

Introduction

The aim of the PRADA (PRA Development and Application) is to develop tools and use of probabilistic risk analysis (PRA). A central challenge in PRA is to extensively identify and assess quantitatively processes, events, factors and phenomena related to nuclear safety. Due to the complexity of the systems analysed, PRA involves multidisciplinary approaches and handling different kinds of uncertainties, with widely varying empirical datai. The General goals of the PRADA project are to:

- Improve and develop methods for risk-informed decision making to support strategic and operative plant management

- Improve and develop PRA methods in terms of uncertainties and critical areas

- Develop PRA knowledge and expertise in Finland

- Foster international co-operation and import the best practices of the field into Finland.

The project is divided into four independent and mutually complementary tasks: human reliability analysis, passive systems reliability, level 2 and 3 PSA (including dynamic PSA), the handling of imprecise probabilities in reliability analysi, and risk communication. Handling of imprecise probabilities is carried out by Aalto University, all the other tasks by VTT.

Human reliability analysis

In nuclear power plants, humans have a major role in maintaining the plant in a safe state as well as, in certain scenarios, bringing the plant back to a safe state. Human

reliability analysis (HRA) is an important tool for assessing the human contribution to failures, given the surrounding environment in which the humans operate.

EXAM-HRA

In PRADA, the main activity in the HRA area has been to participate in EXAM-HRA, which is an ongoing Nordic and German collaboration project, in which existing HRA applications are assessed and compared in order to identify areas for plant improvement. The main goal of the project is to produce a guideline for a state of the art HRA for PSA purposes, based on performed assessments, ensuring that plant specific properties are properly taken into account in the HRA [1].

The project is performed in several consecutive phases, including the following main parts:

- Survey of operator actions in existing HRAs

- Development of an evaluation guide for assessment and comparison of operator actions

- Assessment of operator actions

- Reassessment of operator actions

- Conclusions for plant improvement

- Guidance for HRA applications.

The evaluation format that has been developed within the EXAM-HRA project have been found useful and the assessments of actions performed in the case studies has resulted in findings regarding plant features as well as features of the HRA and PSA applications. Some findings that deserve to be highlighted are:

- Difference in plant feature: In some plant, restoration of residual heat removal function involves manually triggering a low pressure scenario by triggering a reactor protection system permission. This was found to be a complex action, especially in some plants, which should be reflected in the HRA as well as the estimation of the HEP.

- Difference in HRA application: The level of detail varies, both in the HRA documentation and the analysis itself. The assessments have resulted in findings concerning the use of simplified methods, which sometimes results in less conservative methods, contradictory to the intention. On the other hand, the more detailed the HEP assessment is, the more conservative the result tends to be. It should consequently be discussed whether it is possible to define an appropriate level of detail in order to achieve a realistic value, which is neither too conservative nor not conservative enough.

- Difference in PSA application: In some PSAs, no manual actions are modelled as part of the flooding scenarios. In others, significant operator ac-

tions are identified, which are credited in flooding isolation in order to avoid degradation of safety components.

The aim of the EXAM-HRA project is both to provide guidance for a state of the art HRA for PSA purposes, in order to ensure that plant specific properties are properly taken into account in the HRA and to give insights for potential plant improvements. Formulating the guidance for a state of the art HRA is part of the upcoming work, which will use existing experiences and insights as a basis. There is a potential for both increases in efficiency and in preciseness of HRA analysis by accounting the lessons learnt from comparison and from plant specific reassessments.

Enhanced Bayesian THERP method development

The Enhanced Bayesian THERP is a human reliability analysis method developed initially from similar methods used at Olkiluoto and Forsmark probabilistic risk assessment methods. In PRADA, the method has been developed further, based on experience and insights gained from recent cooperative projects on human reliability analysis, the International HRA Empirical Study [5] and the EXAM-HRA project. [2]

One of the areas that is still outside the development is the connection of the performance shaping factors to probability. The PSF framework requires additional work and empirical data to increase the performance of the model. While the development steps in this report increase the methods capability for modelling the action context, the extent of the effect of context on performance remains an open question until further empirical data is available. Further development needs for the Enhanced Bayesian THERP method are in the quantitative side of the PSF framework.

Another weakness identified in the EXAM-HRA study is the use of the time correlation curve itself. The curve does not lend itself well into long time window actions. In level 2 PRA there are more cases that have long time windows, and the use of a limit value is not satisfactory, especially in a dynamic PRA models where the available time window is not static.

The way the expert judges work is also a topic of interest. Currently the method utilizes experts that work independently. Experts working in a panel is a more commonly used approach. To improve the modelling of context for the operator actions a closer look at the expert judgment work and performance shaping factor definitions would be needed.

Digital HRA

More widespread use of digital technology is expected in the existing nuclear power plant control rooms upgrades and the new NPP builds. Practically all safety functions will be controlled by digital I&C systems, including the human system interfaces in the main control room.

Advances in automation present a new modeling environment for the HRA practitioner. Existing HRA methods to quantify the human actions were developed

during a time when no computer-based procedures or digital I&C existed in the operating nuclear power plants. These impacts, whether positive or negative, on the operator performances from the use of digital I&C need to be investigated and reflected in the HRA quantification.

In PRADA, a literature review on challenges of HRA in the digitalization of nuclear power plant control rooms has been prepared. The aim has been to present, on the basis of selected literature, what kind of aspects have been brought out concerning HRA as support to risk assessments and HRA as a design tool.

The literature on the subject is scarce. The findings concerning HRA as part of PSA consist of considerations on needs and ways of taking account the control room changes in the analysis of influencing contextual factors in HRA. The findings related to HRA as a design tool consider integration of HRA with human factors design activities in the early phase of the design process.

Passive systems reliability analysis

Passive safety systems do not need any external input such as mechanical or electrical power to operate. Instead, they are reliant on natural laws, internally stored energy and material properties. The concept of passivity is considered in terms of four categories defined by the IAEA, i.e. there are different levels of passivity. Higher categories are at issue when all components of a safety system can be classified passive. Advantages of passive systems include simplicity, reduction of the need of human interaction and external power. In future, passive systems will be increasingly used because they are regarded more reliable and simpler than their active counterparts. Thermal-hydraulic passive systems, i.e. natural circulation systems are an important example of passive systems.

To assess the reliability of passive systems is especially challenging due to their reliance on physical principles, which complicate modeling. Significant amount of uncertainty related to passive systems, both of aleatory and epistemic kind, pose further difficulties. The measures which determine failure states of passive systems are typically continuous, e.g. a percentage value of nominal performance. The choice of failure criteria is therefore not an unambiguous task. Also there is often lack of information and reliability data, and many decisions made in the analysis must be based on expert judgements and simulations.

A case study on passive autocatalytic hydrogen recombiners

In PRADA, the majority of research within the passive systems reliability analysis subtask was conducted in conjunction with a Master's Thesis [13]. The objective of the Thesis was to perform reliability assessment for Passive Autocatalytic hydrogen Recombiner (PAR) system and incorporate it into a level 2 PRA study. The methods presented were implemented in a case study, which employed the Loviisa nuclear power plant whose hydrogen management strategy includes PARs.

During an accident progression, hydrogen is produced primarily as a result of heated zirconium reacting with steam. The hydrogen production, distribution and combustion are very complex and highly plant- and scenario-specific phenomena. Given an ignition source, hydrogen can combust in several ways depending on hydrogen concentration and the containment atmospheric composition. There are analytical ways, such as Shapiro diagram, to determine the combustion mode which can be e.g. a deflagration or a direct detonation. A hydrogen explosion can cause the loss of containment integrity and failures of safety systems. In addition to PARs, other hydrogen management measures include for instance enhancement of mixing, deliberate ignition and post-accident inerting.

PARs are rather simple devices designed to remove hydrogen from the containment atmosphere during an accident sequence. They consist of catalyst surfaces arranged in open ended enclosures. In the presence of hydrogen, a catalytic reaction involving hydrogen and oxygen and producing steam occurs spontaneously at the catalyst surface. The heat of the reaction produces natural convection through the enclosure, thus ensuring continuous gas supply. Being passively operating devices, PARs do not need any external input to function.

PARs are prone to poisoning of the catalyst sheets by fission products, aerosols and reactor structure materials. Also an oxygen starvation can lead to a drop in PAR performance. A PAR failure is best understood as impaired performance, i.e. decrease in recombination rate, whereas a complete inoperability is not considered that probable. A simplified Failure Modes and Effects Analysis (FMEA) was performed for a PAR unit, and the analysis is summarized in Table 1. The failures were divided into catalyst sheet related failures and into those failures which are due to difficulties with respect to natural phenomena required for the system to function as desired. Additionally, the failures were divided into on-demand and standby failures, although the eventual PAR reliability model dealt only with on-demand issues.

Table 1. A simplified failure modes and effects analysis for a PAR system. Some failure causes occur when the system is in standby (S) but some take place only during an accident progression when the system is on-demand (D).

Component or function	Failure mode	Failure cause	Consequence	Identification in advance
Catalyst sheets	Degraded capacity	Poisoning (S,D)	Less H_2 processed	Performance tests
	Sheets destroyed or unavailable	Unintended ignition (D), External cause (S,D)	Unit not operational	Visual inspections
Natural phenomena	Degraded capacity	Oxygen starvation (D), Impaired gas inlet (S, D)	Less H_2 processed	Performance tests

The FMEA served as the basis for the actual PAR reliability analysis. In addition to passivity, the concept of redundancy was chosen to characterize PAR operation. The total PAR performance was divided into 10% portions, and the portions were assumed to exhibit common cause failures (CCF), i.e. the analysis focused on the total performance of the system as a whole instead of statuses of single units. Thereby the PAR failure rate could be evaluated by using Alpha Factor Model and Extended Common Load Model (ECLM). In order to determine the failure criterion, deterministic MELCOR simulations of accident progression were performed. The simulations aimed to determine the effect of performance degradations on the combustibility of the containment atmosphere. There was no real data on PAR operation, and the reliability assessment was entirely reliant on analyst judgement and simulations.

The reliability analysis results were intended to be utilized in a level 2 PRA study. Hence a general framework to combine reliability analysis with containment event tree (CET) modeling was developed. The method is depicted in Figure 1. The left branch concentrates on the safety system and its goal is to obtain an estimate for the reliability of the system. The right branch focuses on issues not directly related to the particular safety system being investigated, although also these aspects are at least implicitly present. The right branch predominantly deals with case-specific and phenomenal issues instead. The framework should be applicable for any safety device, not only for PARs or other passive and redundant systems.
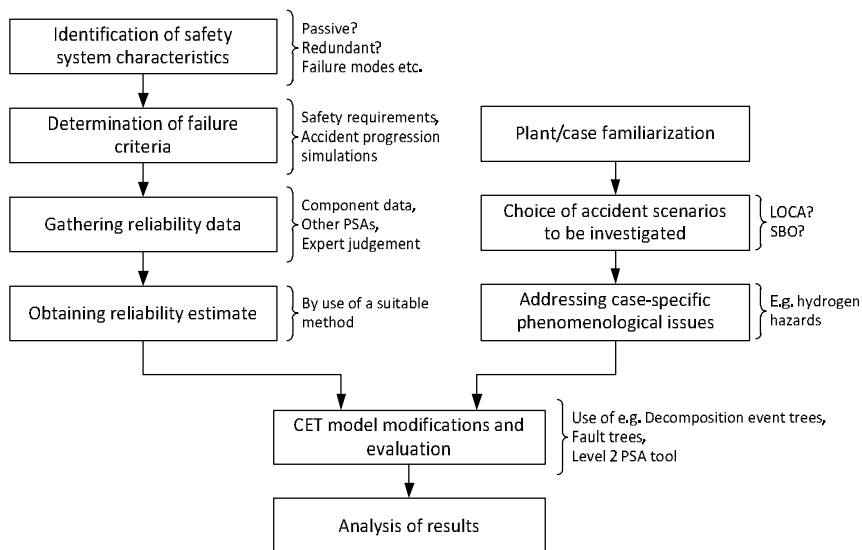

Figure 1. An illustrative scheme of how to conduct a reliability assessment of a safety system and implement it in a CET analysis.

The containment event tree of the Loviisa nuclear power plant for full-power operation was modeled by using SPSA code developed by STUK, the radiation and nuclear safety authority of Finland. SPSA is developed for full scope PRA modeling and it provides an integrated level 1 and level 2 methodologies.

The most important Loviisa CET heading questions regarding hydrogen issues are whether ice condenser doors can be forced open, whether core reflood takes place in critical time window and does hydrogen management succeed. More attention was paid to the latter two questions, whereas other questions in the CET were handled in a more simplified way. The modeling of hydrogen management branch was entirely based on results obtained from PAR reliability assessment, and the effect of igniters was not explicitly taken into consideration. Thus the model does not strictly speaking represent Loviisa hydrogen management strategy. The influence of igniters can, however, be thought to be included in the rather conservative hydrogen management failure probabilities.

The objective of the CET analysis was to conduct source term analysis, but in a highly simplified manner, without treating all the radionuclide groups. Moreover, no complex models for e.g. core heat up or melting were attempted although a model for fission product transport was included. Most important parameters affecting the severity of the release were the timing of the containment failure, size of the leakage and whether the reactor pressure vessel breaches. Because of the restricted CET modeling, the analysis is nowhere near a full scale level 2 PRA study. Instead, the model and its results should be considered exemplary.

SPSA is essentially based on a Monte Carlo methodology, and 10000 simulations were run to analyse the Loviisa CET. Source terms were quantified as fractions of core inventory. The containment event tree sequences were binned into release categories according to the similarity of accident sequence characteristics, and sequences where hydrogen management fails belong to 'early containment failure' bin. The results show the importance of accident sequences binned into this category. Thus the mitigation of accident consequences is easiest done by concentrating on these sequences. Especially, by raising the success probability of hydrogen management, significant improvements in the overall PRA results could be achieved. In general, the results with respect to the relative severity of accident sequences were in good accordance with some reference results.

The CET model developed here for Loviisa NPP is simple, but it would be easy to extend it, if needed. In this case study there was only a single containment event tree investigated, i.e. there was no data from level1 PRA. If different initiating events were to be included, some modifications to the CET would be required in order to achieve high enough correspondence between the model and actual accident progression. Also the dependence on physical quantities, such as pressures and temperatures, could be increased. Given the limited scope (M.Sc. Thesis), the results can be regarded satisfactory.

Integrated Deterministic and Probabilistic Safety Assessment

Ongoing in Nordic countries programs on modernisation and power uprates of old plants, ageing management, and construction of new nuclear facilities require adequate safety analysis tools which can reveal potentially dangerous subtle time-dependent interactions between deterministic and stochastic natures of plant components, physical processes, plant control systems and operator actions. The effects of the modernizations on severe accident phenomena and management are of special importance with respect to the potentially hazardous impact on the environment. Development of combined Dynamic Deterministic/Probabilistic Safety Assessment tools is imperative for performing comprehensive safety analysis which can tackle with multifaceted complexity of the powers plants.

Integrated Deterministic and Probabilistic Safety Assessment (IDPSA) is a framework referring to the variety of different approaches and tools developed for combined probabilistic and deterministic analysis during the last decades. IDPSA is a family of methods which use tightly coupled probabilistic and deterministic approaches to address aleatory (stochastic aspects of scenario) and epistemic (modelling) uncertainties in a consistent manner. For example, what has been referred to in the past as Dynamic PSA (DPSA) belongs to the family of IDPSA methods. A European and US network has been established to promote the IDPSA concept [3, 4].

Level 3 PRA

A proposed interface between PSA levels 2 and 3 has been defined. The interface specifies, on an abstract level, the information needs of level 3 from level 2, and thus, the information that level 2 analysis results should contain. The interface may be implemented for example as a relational database or an XML file/files. Also consequence modeling has been considered from a software architecture point of view. Alternatives for conducting level 3 analyses, based on level 2 results given by the SPSA program, have been outlined. The main two alternatives that have emerged are to stick to established, dedicated level 3 analysis codes (such as ARANO), and to utilize a set of tools developed for specific task, such as atmospheric dispersion simulation, uncertainty analysis and visualization. The latter alternative has some merits to it, such as flexibility and the ability to use the best available tool for each task.

A project proposal has been prepared to NKS/NPSAG jointly with Scandpower, Risk Pilot and ES-konsult for 2013-14 work. The proposal was accepted by NKS. The project will define appropriate risk metrics for level 3, based on a literature review and survey of existing regulation, guides and standards. The main results will be a guidance document and a pilot application.

Imprecise probabilities

In this subtask, we have developed [6] a computational framework for analyzing the impact of epistemic uncertainty on the prioritization induced by risk importance measures [7]. The framework is based on lower and upper bounds that define intervals within which the probabilities vary. For example, instaed of stating that the failure probability of a component is 0.02, it could be stated that a probability is within an interval [0.01, 0.03]. These types of intervals for probablities araise in many methods for analyzing epistemic uncertainty about probabilities, such as in interval-probabilities [8], coherent lower and upper probabilities [9], imprecise reliability [10], alpha-cuts of fuzzy probabilities [11], and bound for sensitivity analysis [5].

Conclusions in our method are based on the analysis of the the concept of dominance, which we define as follows: Event E1 dominates event E2 based on the risk importance measure I if and only if

   a) I(E1,p)>= I(E2,p) for all probabilities p within the intervals and
   b) I(E1,p)> I(E2,p) for some probabilities p within the intervals,

where I(E,p) is the value of risk importance measure I of event E using probabilities p.

Dominance is a conservative approach for comparing the risk importance of events. If an ordinary fault tree analysis were to be conducted by using event probabilities that belong to the intervals, a dominated event would not have a higher risk importance than an event that dominates it and moreover, for some probabilities within the intervals, it would have a strictly lower risk importance. In spirit of probabilistic risk assessment, providing conservative results is a good feature of the concept of dominance.

Illustrative case study

We applied our method to analyze the fault tree that represents a residual heat removal system (RHRS) of a nuclear reactor. The structure and failure probabilities of this fault tree are representative of existing reactors. The RHRS fault tree has 31 events and 147 minimal cut sets. The standard 90% confidence intervals for the probability estimates are employed as the lower and upper bounds on the probabilities. The events are labeled based on their ranking with regard to the Fussell-Vesely measure, which makes it easy to compare the results with traditional Fussell-Vesely risk importance measure analysis.
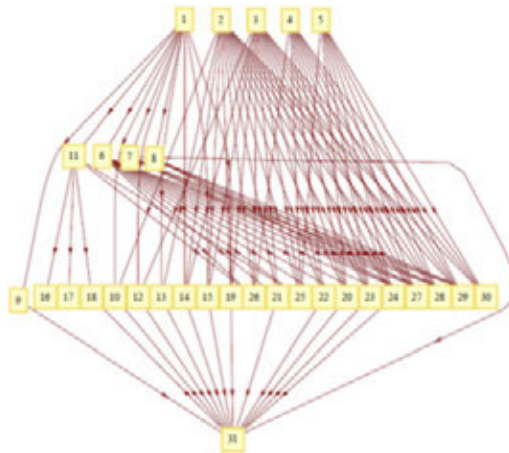
Figure 2. Dominance graph of the residual heat removal system.

In the Fussell-Vesely dominance graph in Figure 2, the first five events are non-dominated and thus they should receive the highest priority. That events 1 and 5 should both be prioritized the highest may be considered counterintuitive, because FV1 = 0.57 and FV5 = 0.06, wherefore their risk importance measures have almost tenfold difference. However, because neither dominates the other, there exist probabilities within the intervals for which event 5 has higher Fussell-Vesely importance measure than event 1. Thus, the uncertainties about the probabilities are large enough to reject a definitive priority between events 1 and 5.

Even if the layout of the graph would suggest that there are three classes of events that do not dominate each other, this is not the case. For instance, the non-dominated events 1–5 do not dominate all the other events. Event 1 dominates events 6–31, event 2 dominates events 10, 13, 14, 15, 19–31, event 3 dominates 12, 14, 15, 19–31, event 4 dominates 20, 22, 23–31 and event 5 dominates 20, 23–25,27–31. The parallel argument applies to event 31, which is at the bottom of the graph: Even if it does not dominate any other event, it is still not dominated by all events (that is events 16, 17, 25–30). In fact, all events dominate, or are themselves dominated by, different sets of events.

An upper bound for the highest ranking (1 = highest priority, 31 = lowest priority) that an event may have is given by the number of events that dominate the event plus one. Similarly, a lower bound is given by 31 minus the number of events that the event dominates. These bounds may or may not be the tightest possible (that is, these bounds are based on the dominance graph alone). Let us compute the highest and lowest priorities for the non-dominated events: The ranking of event 1 is in the set {1,...,5}, event 2 in {1,...,15}, event 3 in {1,...,16}, event 4 in {1,...,21}, event 5 in {1,...,24}. Thus, based on this, the non-dominated events should not automatically be considered as the highest priorities, because there may be significant uncertainty about their ranking. However, because these ranking intervals may not be tight, this analysis may overemphasize the impact of uncertainty.

Application to modeling uncertainty in reliability parameters

An other application of this method is to modeling parameter uncertainty. In the example in Figure 3, each components 1,...,7 in th system are modeled with a Weibull-distribution with known characteristic life but unkown aging parameter. In Figure 4 are two examples of how component failure probabilities may vary when time passes by. The figure shows that the uncertainty about the failure probability may become narrower or wider as time proceeds, although the uncertainty about the aging parameter (that is the lower and upper bounds for the parameter) remains the same. If there where uncertainty about the characteristic life as well, then these intervals would be wider. This changing uncertainty about parameter values has an impact on the importance and uncertainty about the dominance structure.

In Figure 5 are dominance graphs at different time steps. Noteworthy is that how the impact of epistemic uncertainty about the parameters change. At times 0, 1 and 2, the uncertainty about the prioirities among the components is the larger compared to time steps 3, 4 and 5, where the prioritization among the componets is almost complete.

Computational aspects

The algorithm developed for solving the dominance is a Branch-and Bound algorithm, that sets probabilites to their lower or upper bound. It is guaranteed to find all dominace relations. It can be applied for resolving dominance with respect to any risk importance measure that can be expressed (possibly scaled) sums and differences of (un)conditional reliability functions. This is true for all widely used risk importance measure such as Fussell-Vesely, Birnbaum, Critical Importance, and risk achievment worth.

Using our algorithm, computing the dominances in the residual heat removal system case lasted about 15 seconds with our Mathematica implementation of this algorithm on a regular laptop PC (Intel(R) Core(TM)2 Duo CPU T5870 @ 2.00GHz processor and 4 GB RAM). The visualizations are also made using Mathematica.

The theoretical worst case computational effort of our algorithm can be exponential in problem size. However, the algorithm is exponential only with respect to the number of events in the multilinear function that is derived from the risk importance measure under consideration. This means that the required computational effort does not grow significantly when the number of minimal cut sets increase, and consequently systems with a complicated structure function can be analyzed.

Conclusions

We have developed a method for analyzing the impact of epistemic uncertainty about event probabilities in fault tree analysis. This uncertainty is captured through interval-valued probabilities, and its implications for the relative priorities of events are explored by considering commonly used risk importance measures and by

establishing dominance relations for the events based on these measures. The dominance relations can be displayed with the help of directed graphs, which gives an easy-to-understand way of illustrating the results. These graphs show which events deserve highest priority, in view of the uncertainties that are accommodated by the probability intervals.

We have also applied this method to examine the fault tree of complex system that represents the residual heat removal system of a nuclear power plant. Specifically, this application showed that the relative priorities of events can change significantly when the probabilities are allowed to vary within their respective probability intervals, and that despite these variability, we can still make definitive conclusions about the priorities among the event. From this perspective, our method can also be seen as a means of conducting global sensitivity analyses ex post. Technically, it is possible to introduce also other kinds of constraints on the probabilities, even if a greater computational effort may be needed to derive dominance results.

$$F_i(T|\tau) = 1 - \exp\left[-\left(\frac{T+\tau}{\beta_i}\right)^{\alpha_i} - \left(\frac{\tau}{\beta_i}\right)^{\alpha_i}\right]$$

- Characteristic life $\beta_i = 15, i = 1,\ldots,7$
- $\underline{\alpha} = \{0.6, 0.5, 1.2, 3, 2, 0.8, 1\}$
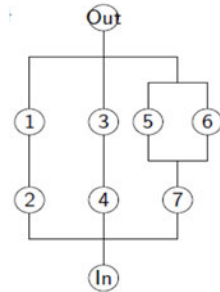- $\overline{\alpha} = \{0.8, 0.6, 0.5, 4, 3, 1.2, 1\}$

Figure 3. Example system with aging components that have uncertain aging parameter alpha.
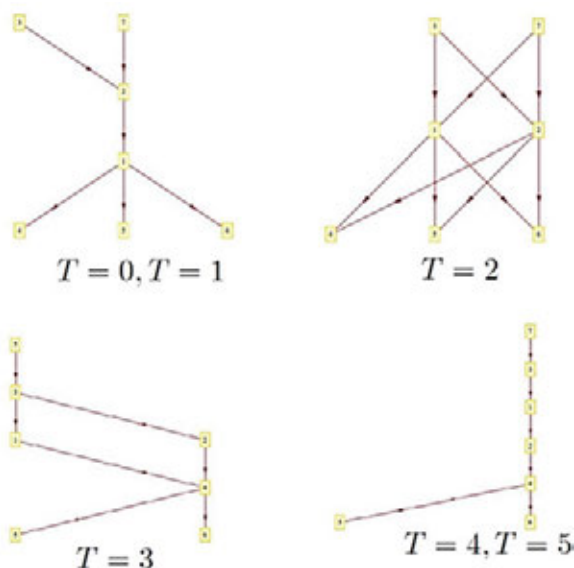
Figure 4. Uncertainty of the failure probability of components 1 and 6 with respect to time.

Risk communication

The objective of risk assessment is to support decision-making. Therefore, the way of communicating risk information related to probabilistic risk assessment (PRA) to the different stakeholders is very important. There are plenty of studies dealing with communication on risk information to the public but less attention has been paid to communication to the other parties.

In PRADA, a report [12] has been written focusing on the risk analysts' communication to decision-makers and domain experts. A special attention has been paid to the significance of *transparency* for the effectiveness of information in PRA related risk communication.

The aim has been 1) to find out, on the basis of selected literature, a) what kind of issues are currently regarded as improving PRA related risk communication and, b) what kind of conceptions of communication problems, resulting from the risk analysts' differing views on PRA, the analysts themselves have brought out, and 2) in the discussion to consider, on the basis of the presented conceptions, the challenges of improving risk communication by enhancing the transparency of risk information and mutual understanding between the different parties.

It is concluded, in the report, that especially the complexity and the inherent subjectivity of PRA and the differences in the ways of thinking between the different disciplines, and even within one discipline, pose requirements for the transparency of risk information. There is need for enhancing mutual understanding among the risk analysts, between the risk analysts and the deterministic safety

assessment experts and, in expert judgment elicitations, between the risk analysts and the domain experts.

References

1. Fritzson, L., Becker, G., Bladh, K., Johanson, G., Karlsson, A., Männistö, I., Olsson, A., Tunturivuori, L. EXAM-HRA – Evaluation of Existing Applications and Guidance on Methods for HRA. Proc. of 11th International Probabilistic Safety Assessment & Management Conference, PSAM 11, Helsinki, June 25–29, 2012.

2. Männistö, I., Hukki, K. Enhanced Bayesian THERP HRA Method Development, VTT Research Report VTT-R-02059-12, 2012, Espoo.

3. Adolfsson, Y., Holmberg, J.-E., Hultqvist, G., Kudinov, P., Männistö, I. Proceedings of the Deterministic/probabilistic safety analysis workshop October 2011, VTT Research Report VTT-R-07266-11, 2011, Espoo.

4. Adolfsson, Y., Holmberg, J.-E., Karanta, I., Kudinov, P. Proceedings of the IDPSA-2012 Integrated Deterministic-Probabilistic Safety Analysis Workshop November 2012, VTT Research Report VTT-R-08589-12, 2012, Espoo.

5. Holmberg, J.-E., Kent Bladh, K., Oxtrand, J., Pyy, P. Enhanced Bayesian THERP – Lessons learnt from HRA benchmarking. Proc. of PSAM 10 – International Probabilistic Safety Assessment & Management Conference, 7–11 June 2010, Seattle, Washington, USA, IAPSAM – International Association of Probabilistic Safety Assessment and Management, paper 52.

6. Toppila, A., Salo, A. Prioritizing Failure Events in Fault Tree Analysis Using Interval-valued Probability Estimates Proceedings of the International Conference on Probabilistic Safety Assessment and Management & Annual European Safety and Reliability Conference, 25–29 June 2012, Helsinki, Finland (to appear).

7. Apostolakis, G. The concept of probability in safety assessments of technological systems. Science 250, 1359–1364, 1990.

8. Weichselberger, K. The theory of interval-probability as a unifying concept for uncertainty, International Journal of Approximate Reasoning 24(2–3), 149–170, 2000.

9. Walley, P. Statistical Reasoning with Imprecise Probabilities, Monographs in Statistics and Applied Probability 42, Chapman and Hall, 1991.

10. Utkin, L., Coolen, F. Imprecise reliability: An introductory overview, in: G. Levitin (ed.) Intelligence in Reliability Engineering, Studies in Computational Intelligence, 40, 261–306, 2007.

11. Buckley, J. Fuzzy probabilities: New approach and applications, 115, Physica-Verlag, 2003.

12. Hukki, K., Männistö, I. Communication on PRA Related Risk Information to Domain Experts and Decision-Makers, VTT Research Report VTT-R-02060-12, 2012, Espoo.

13. Silvonen, T. Reliability analysis for passive autocatalytic hydrogen recombiners of a nuclear power plant, MSc Thesis, Aalto University, Espoo, 2012.

9.4 FinPSA knowledge transfer (FINPSA-TRANSFER)

Teemu Mätäsniemi[1], Ilkka Niemelä[2], Tero Tyrväinen[3], Kim Björkman [3]

[1]VTT Technical Research Centre of Finland
Tekniikankatu 1, P.O. Box 1300, FI-33101 Tampere

[2]STUK – Radiation and Nuclear Safety Authority
P.O. Box 14, FI-00881 Helsinki

[3]VTT Technical Research Centre of Finland
Vuorimiehentie 3, P.O. Box 1000, FI-02044 VTT

Introduction

FinPSA and its predecessor SPSA are unique software tools developed by the Finnish Centre for Radiation Safety (STUK) for carrying out probabilistic risk analyses (PRA). STUK started the development of SPSA in 1988 and the trial usage of level 1 part started in 1991. Level 2 part of the code was completed in early 1993. After validation and pilot modelling, the TVO power company completed the first level 2 PRA in 1997. The development of FinPSA was started in 2000 and the software was launched to customers in 2005. The current version of FinPSA supports only level 1 analysis.

In order to support FinPSA and SPSA software end users in the future, an agreement was made to move maintenance and development of these software from STUK to VTT Technical Research Centre of Finland. A new project, FinPSA knowledge transfer (2012–2014), was started. Ensuring the support and development of these tools was stated to the main objective of the project. In addition, a more general objective was stated to develop and demonstrate practice and skills in the development of software products critical to safety. This paper introduces the software tools, identifies the initial situation of the project and represents the selected strategies and achievements of the first project year.

Tools for level 1 and level 2 analysis

SPSA

SPSA is a Microsoft DOS based software tool for integrated level 1 and 2 PRAs. Level 1 part of the code is based on standard event tree – fault tree approach. Level 2 part implements dynamic Containment Event Trees (CET), where special CET programming Language (CETL) allows modelling of causal dependencies and time-dependencies of complex phenomena and interactions occurring in severe accidents. The modeling methodology combines probabilistic computations with parametric dynamic models to describe plant and accident behavior. The interface between levels 1 and 2 is transparent and bi-directional, transferring a large amount of information between levels. It has been implemented as a rule-based system, which uses the event tree logic to classify end states of sequences to Plant Damage States (PDS). The output of the interface is cut set files leading to different PDSs, including accident sequence descriptors, which can be utilized in level 2 CETs. In this way, level 2 models and results can be expressed in terms of level 1. The risk integrator manages the execution of a level 2 PRA and it automatically detects modified CETs to take care of combining distributions of individual CETs. The result analysis part provides information in several formats and on several levels, in order to reveal dependencies, uncertainties and correlations. A typical CET model may produce thousands of distributions, scatter plots and correlation analyses, which can be viewed with built-in interactive viewer.

FinPSA

FinPSA is a comprehensive risk and reliability analysis teamwork tool intended for full scope PRA modeling. As a Microsoft Windows multithread application it has been designed to support easy model creation, efficient, parallel and versatile analysis, good traceability, flexible reporting and information exchange with typical office tools. Almost every item like database tables, fault trees and event trees in the model can be imported and exported. Special attention has been paid to traceability in order to track back the origin of each minimal cut to event tree and

accident sequence. Also, failure propagation can be visualized in a fault tree. Hazard table and I&C model are new features of FinPSA. Hazard table presents the propagation of failures due to hazards and there is no need to modify system fault trees or to use house events. I&C model implements task-oriented modelling of control systems and allows the compact and convenient expression of large systems isolated from fault trees by a clear interface. The modeling of partial diversity is supported by asymmetric CCF models. All these features make possible to maintain living PSA in plant assessment and operational modifications.

Challenges and identification of initial situation

Since the main application area of FinPSA and SPSA is PRA for nuclear power plants, a long lifetime is an essential feature of the software. This fact emphasises the role of development resources, software processes and their contributions to the qualities of the software. FinPSA and SPSA are in this context in different positions as illustrated in the following figure. The needs for future development are consequently quite different.
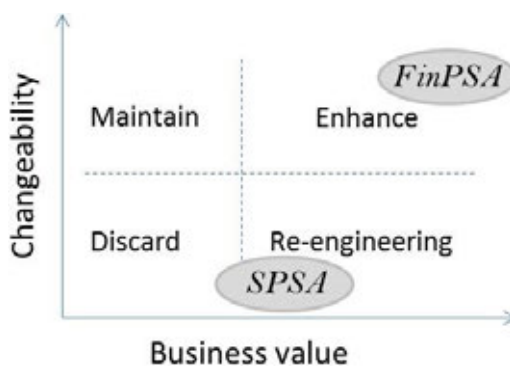
Figure 1. Decision matrix (Jacobson and Lindström 1991), what to do with FinPSA and SPSA.

FinPSA has been developed and maintained with the newest software development tools and it is one of the most powerful PRA tool in the market. In addition, its implementation utilizes several design patterns and algorithms which are already tested in the predecessor (SPSA) software. The user interface of FinPSA is user friendly, it provides clear modelling concepts to an analyser and it has numerous new capabilities compared to SPSA. So, the maintenance of the software is quite easy and it has a high business value. Thus, it is realistic to assign FinPSA to enhance category and to continue its development and maintenance.

On the other hand, SPSA has been developed with Borland's Turbo Pascal 6.0 compiler which do not operate in the newest operating systems because the compiler have 16-bit architecture and todays operating systems support only 32-bit or

higher applications. In addition, restructuring of the code with a newer compiler is not realistic originating from the lack of documentation. However, SPSA has very attractive modelling environment which allows modelling of causal dependencies and time-dependencies of complex phenomena and interactions needed in the level 2 analysis. Thus, SPSA's type code has some business value which can even be increased by integrating the similar functionality with a level 1 software. So, SPSA is assigned between re-engineering and discard categories as shown in the Figure 1.

The both software have been developed by few experts with little resources for documentation. This has led to a situation in which traceability to and validation of requirements have only been partly done or documentation has been forgot totally. In consequence, it is challenging to prove the quality of the software to unfamiliar audience, to prove the correctness of analysis results and to show that the software satisfy requirements stated by international standards.

Software processes

The identified challenges of the previous section showed that new type of software development and maintenance processes are needed and the different kinds of strategies have to be applied to FinPSA and SPSA. Before the selected strategies are introduced basic terms and processes are clarified. This material is based on the work of Harsu (2003) and Chikofsky and Cross II (1990).
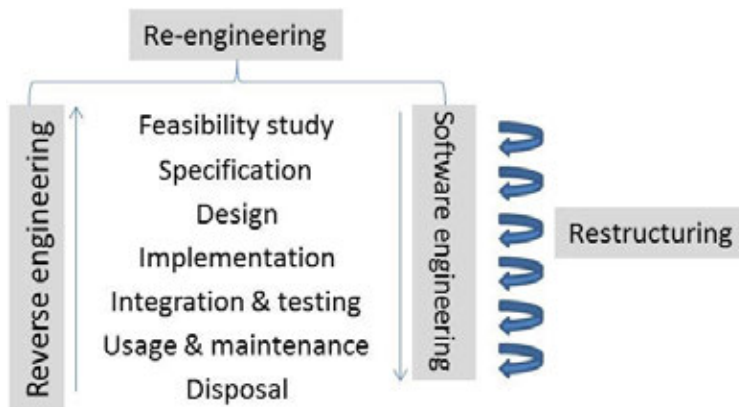
Figure 2. Terms and processes related to software lifecycle.

Typically, software lifecycle consists of phases as feasibility study, requirement specification, design, implementation etc. (Figure 2). The most often mentioned process is a software engineering (ohjelmistotuotanto in Finnish) or forward engineering which includes the all activities of the lifecycle needed to produce an executable program. Of course, the software engineering process has iterative and

recursive nature although it is presented quite linear according to its progression direction. The related documentation describes software by more concrete representations while software engineering process goes on.

On the other hand, more abstract models of software are produced or checked during a reverse engineering process (takaisinmallinnus in Finnish). The reverse engineering process studies and analyses existing software and other available material with general knowledge about the problem and application domain in order to extract, abstract and check information but the process modifies nothing. The reverse engineering is used, for example, to recover missing design decisions and rationales, to gain a sufficient design-level understanding, to elicit original product and end user requirements or just to support redocumentation. The objective of the process is to increase the overall comprehensibility of the software for both maintenance and new development. Typical methods applied in the reverse engineering are code structure and logic visualizations or interviews of end users and earlier maintainers and developers.

As noticed, during software engineering and reverse engineering processes the abstraction level of software descriptions are changed. If modifications and changes lie at one abstraction level only, it is talked about a restructuring (uudelleen rakentaminen in Finnish). During the restructuring process a representation form or a coding language of software can change but the system's external behaviour remains.

Re-engineering (uudistaminen in Finnish) couples actions from both forward engineering and reverse-engineering processes but it is not a supertype of these two. Re-engineering covers changes and alterations in functionality, semantics, implementation techniques or some combination of these three.

Objectives, strategies and approach

The main objective of our project is to ensure the support and development of FinPSA and SPSA. In addition, our general objective is to develop and demonstrate practices and skills in the development of software products critical to safety. According to these objectives and the challenges identified in the section 0 the different strategies have been selected for the tools.

Figure 3. Approach for FinPSA and related activities.

Approach for FinPSA and related activities have been represented in the Figure 3. To continue maintenance and development a sufficient design-level understanding for new developers have to be achieved. This means at least that design rationales have to be recovered and re-documented (arrow 1). Only after that the new developers have possibilities to continue their work. Design recovery and re-documentation cover fields like architecture description, database and unit designs. Most program units have been re-documented, but the recovery of complex algorithms has been the out of scope in the first project year (2012). In addition, organization of some education is essential in order to study the most critical parts of the designs and to speed up adoption of things. The study has also included a little new development and correction of deficiencies. This kind of approach familiarizes also new developers to usage of new tools and gives some experiences about the quality related issues of software processes.

The validation of requirements and the satisfaction of requirements stated by the international standards need the identification and specification of these requirements before it can be go on (arrows 2 and 3). To collect an initial requirement set the standards have been studied and end users have been interviewed. After these, the requirements have been documented, analysed and harmonized together and with current design of FinPSA. The results of these processes are represented in the next section.

To prove correctness of FinPSA behaviour in the PRA model creation and analysis VTT started elicitation and re-documentation of the needed test cases (arrow 4). The elicitation of the cases was done by interviewing PRA experts and studying the usage of the PRA tool. VTT's main focus was on system level tests but different modelling aspects were separated. In addition, possibilities to validate the results of test runs have been initially studied. To achieve also an addition value for FinPSA end users the automatic execution of test runs was settled to a new requirement (arrow 5). Thus, the end users can also execute their analysis as batch runs.

SPSA was assigned to the middle of discard and re-engineering categories because it is hard to maintain the current implementation with new operating systems. In addition, level 2 implementation would have better business value if its functionality works together with the newest level 1 software. However, a direct re-implementation was not selected to the approach since SPSA contains also functionalities like CETL that can be implemented partly by commonly used open source packets which were not available in the time of original SPSA development. Thus, the software engineering strategy is selected for the new version production. The developers studied also the best ideas of the old version, level 2 modelling principles and provided functionalities to possible reuse them. The work was started by the feasibility study of the level 2 related standard as in the level 1 case.

Results

During 2012 end user experiences from using FinPSA were collected. Additionally, end user requirements were documented, analysed, classified, and prioritized.

FinPSA level 1 (Niemelä and Björkman 2013) and level 2 (Björkman 2013) requirement specifications were prepared. The goal was to demonstrate that FinPSA conforms to related international standards and to link FinPSA specific requirements to framework represented in the standards. Level 1 requirements specification covers level 1 and interface between levels 1 and 2. The specification contains two viewpoints:

- Generic requirements for PSA level 1 and PSA level 1 software as presented in (IAEA SSG-3 2010).

- Software-specific requirements, which follow IAEA generic requirements. IAEA generic requirements are expressed first, and software specific requirements that serve the attainment of the generic requirements follow.

For level 1 requirements specification about 280 requirements have been specified. Of the requirements about 60 originated from end user requirements. FinPSA seems to fulfil all of the requirements obtained from IAEA SSG-3 except a few that mainly relates to verification and validation of the software.

FinPSA level 2 requirements specification lists necessary requirements the level 2 code shall fulfil so that level 2 PSA can be carried out according to (IAEA SSG-4 2010). For level 2 about 30 requirements were specified. The considerable difference between the amount of level 1 and level 2 requirements depends on the lifecycle phase of the computer codes. FinPSA level 1 code is a ready product in use, whereas the level 2 code is planned to develop. Thus, level 2 requirements are on a much higher abstraction level.

The experiences from developing requirements specification demonstrated that obtaining a necessary set of requirements for a PRA computer code is not a trivial task and that managing requirements specification is an iterative process. During each iteration, the level of detail of the requirements increases. IAEA-SSG-3/4 safety guides contains only a few recommendations that relates directly to PRA computer codes. Deriving relevant requirements requires interpretation of the safety guides and reasonable interpretation without a structured process and tool support requires extensive knowledge of PRA analysis and PRA computer codes in general.

During design recovery and re-documentation the documentation of FinPSA was divided into two documents (Niemelä and Mätäsniemi 2013a, 2013b): 1) main units including architecture description and 2) supporting units. In 2012, supporting unit documentation was finished, and the most of main units documentation was performed. Of course, documentation of algorithms in the following years can change this division when amount of information is increasing.

Already in the early phase, it was understood that the testing of the level 1 software has to be planned and performed carefully because of its importance to nuclear safety and its complexity. For testing purpose (Tyrväinen and Mätäsniemi 2013a) over fifty properties of the software were identified and their testing history was studied and reported briefly. Test case specifications were planned and documented for the most of the properties and the testing can be performed according

to those specifications in the next years. It was concluded that the main focus of the testing should be on generation of minimal cut sets, numerical calculations and performance testing. It is also noticed as preferable to exploit the models of the end users in testing as much as possible. As described, a long term plan is to make the testing as automatic as possible. It was concluded that the testing could be automated using task files of the software and script files that are launched outside the software. It was also discussed about the kinds of commands required for the testing of different properties. For few properties, an alternative would be to use the unit testing approach instead of the external command files.

A quality assurance study of safety related software was started by a literature survey (Tyrväinen and Mätäsniemi 2013b) in which both PRA standards and software quality assurance standards were examined. PRA standards address computer codes only briefly. The most common requirement was that PRA computer codes have to be validated and verified. A moderate set of general requirements and guidelines could be constructed by putting findings from different sources together. A set of overall requirements was constructed based on software quality assurance standards. Both quality of the development process and quality of the software product were addressed. Overall quality requirements have been set for verification, validation, documentation and different areas of the development process as well as software design and source code. Only one quality assurance guide had been specifically written for safety analysis software, but it was concluded that also other general quality assurance principles in the standards and guides can very well be applied to safety analysis software.

References

Björkman, K. 2013. FinPSA – Software requirements – Level 2 documentation. Version 1.0. 18 p. Espoo. VTT Technical Research Centre of Finland. VTT Research Report VTT-R-00364-13. Limited Distribution.

Chikofsky, E.J., Cross II, J.H. 1990. Reverses Engineering and Design Recovery: A taxonomy. IEEE Software 7(1), 13–17. Doi 10.1109/52.43044.

Harsu, M. 2003. Ohjelmien ylläpito ja uudistaminen. Talentum Media Oy. Helsinki. ISBN 951-762-829-3. (In Finnish)

IAEA SSG-3. 2010. Development and application of level 1 probabilistic safety assessment for nuclear power plants: specific safety guide. In: IAEA safety standards series. Vienna. International Atomic Energy Agency. ISBN 978–92–0–114509–3.

IAEA SSG-4. 2010. Development and application of level 2 probabilistic safety assessment for nuclear power plants: specific safety guide. In: IAEA

safety standards series. Vienna. International Atomic Energy Agency. ISBN 978–92–0–102210–3.

Jacobson, I., Lindström, F. 1991. Re-engineering of old systems to an object-oriented architecture. In: ACM SIGPLAN, Proceeding OOPSLA '91 Conference proceedings on Object-oriented programming systems, languages, and applications. New York, USA. Pp. 340–350. ISBN 0-201-55417-8.

Niemelä, I., Björkman, K. 2013. FinPSA – Software requirements – Level 1 documentation. Version 1.0. 52 p. Espoo. VTT Technical Research Centre of Finland. VTT Research Report VTT-R-00447-13. Limited Distribution.

Niemelä, I., Mätäsniemi, T. 2013a. FinPSA – Software design – Main unit documentation. Version 1.0. 197 p. Espoo. VTT Technical Research Centre of Finland. VTT Research Report VTT-R-00353-13. Limited Distribution.

Niemelä, I., Mätäsniemi, T. 2013b. FinPSA – Software design – Supporting unit documentation. Version 1.0. 95 p. Espoo. VTT Technical Research Centre of Finland. VTT Research Report VTT-R-00351-13. Limited Distribution.

Tyrväinen, T. and Mätäsniemi, T. 2013a. FinPSA – Software testing – Test plan. Version 1.0. 77 p. Espoo. VTT Technical Research Centre of Finland. VTT Research Report VTT-R-00430-13. Limited Distribution.

Tyrväinen, T., Mätäsniemi, T. 2013b. Quality assurance of a safety analysis software. Version 1.0. 16 p. Espoo. VTT Technical Research Centre of Finland. VTT Research Report VTT-R-00241-13.

10. Development of Research Infrastructure

10.1 Enhancement of Lappeenranta instrumentation of nuclear safety experiments (ELAINE)

Antti Räsänen, Heikki Purhonen, Jani Laine, Lauri Pyy

Lappeenranta University of Technology
Skinnarilankatu 34, P.O. Box 20, FI-53851 Lappeenranta

Introduction

The ultimate goal of the nuclear safety thermal hydraulic experiments is to enhance the reliability of the computer codes in predicting the behavior of the reactors and their safety systems. This can be done using facilities that can produce sufficient conditions for the phenomena or the action of the system studied. Lappeenranta University of Technology (LUT) has conducted experiments on thermal hydraulics of nuclear power plants and related subsystems for decades. The facilities have grown and become much more complex. And so have the computer codes.

Instead of recording few temperatures, pressures and flow rates in an experiment, the development and validation of computational fluid dynamics (CFD) codes as well as modern system codes require accurate, extensive set of data with high spatial and temporal resolution from the test facilities.

In order to ensure the availability of high quality data from the experiments ELAINE project was proposed for SAFIR2014 research programme to start in 2011. The main goals of the project were listed as follows:

- to improve the measuring capabilities of Nuclear Safety Research Unit at Lappeenranta University of Technology by acquiring novel measuring devices

- to ensure the availability of data storage and safe method for distributing the archived experimental data by developing an archiving software

- to improve the reliability of data gathering and measurement infrastructyre by purchasing suitable measuring hardware to provide sufficient on-site inventory for measurement needs in the foreseeable future.

In the plan for 2012 the above goals were updated and installation of the main circulation pumps to PWR PACTEL was introduced in ELAINE with the following goals:

- to purchase the main circulation pumps
- to prepare for the installation of the pumps.

Equipment related to the pumps were identified, such as power feeds, drives, safety automation and mounting pedestials. Also the plans for the support structures and primary piping modifications are to be made.

Measuring capabilities

The safety research of nuclear energy is based on infrastructure capable of sufficiently representing the studied system of a nuclear power plant (NPP) and close connection with computational studies. Research methods, test facilities and devices and research infrastructure in general has to be up-to-date. This is true especially when the special requirements for the research of the new NPP concepts and the ageing of the operating units are taken into account. Improving the measuring capabilities by developing the existing or taking into use new instruments and methods to achieve extensive experimental data for the validation of the analytical methods using CFD codes is an important research goal as such [1].

Capturing the physical phenomena taking place in the experiments and converting it to numerical form is one of the main challenges of experimental research. The quality and usefulness of the recorded information depends on the equipment in use. Recently the requirements for the quality of data and also for the quantity have increased due to the use of CFD codes in safety analyses of NPPs.

The applicability of sophisticated measuring devices have to be studied first and, if they are found to be useful, they are purchased. As the first device, a Particle Image Velocimetry (PIV) system was purchased and commissioned in 2011. The system was first applied in the EXCOP project during 2012. Wire mesh sensor (WMS) devices were also investigated and purchased in 2012.

Particle Image Velocimetry (PIV)

The technical requirements of the PIV system were decided after the research staff had familiarized with similar PIV applications on a visit to Paul Scherrer Institut (PSI) in Switzerland in March 2011. Extensive presentations on the basics of the PIV, boundary conditions in different applications as well as the technical requirements for cameras and lasers were held by the personnel of PSI. PSI also gave support in resolving the questions that rose later in the project.

Based on the defined technical requirements a procurement process was initiated obeying the rules for this kind of purchase. Before the deadline of the public announcement one offer was received from LaVisionUK. The system was ordered based on this offer.

Main components of the PIV system were received in late October 2011. The original goal for the delivery was late September, but confusion with the terminology in the supply agreement caused some delay.

The commissioning itself was carried out as a master's thesis work [2]. The thesis includes an extensive description of the related topics; general introduction to PIV systems, tracer particles, lasers as light sources, light sheet optics, digital image recording and the basics of the image evaluation. The PIV system is applied first in two research configurations: the PPOOLEX facility in the laboratory of the Nuclear Safety Research Unit and the centrifugal compressor test station in the laboratory of Fluid Dynamics at LUT Energy.

The thesis describes the components of the acquired PIV system including lasers (Figure 1), laser accessories, light sheet optics, cameras (Figure 1), camera accessories, system computer and software and seeding.

The thesis serves as a user manual in these two applications, including issues from the positioning to the laser safety aspects. Applying the PIV in the PPOOLEX experiments is described step by step including the experimental set-up, image processing and the results.

Figure 1. Laser (left) and camera (right) of the PIV system.

Examples of the images of the exit of the blowdown pipe in PPOOLEX are shown in Figures 2–4. The figures show few phases of the PIV data processing. The blowdown pipe outlet is visible in Figure 2 and Figure 3.
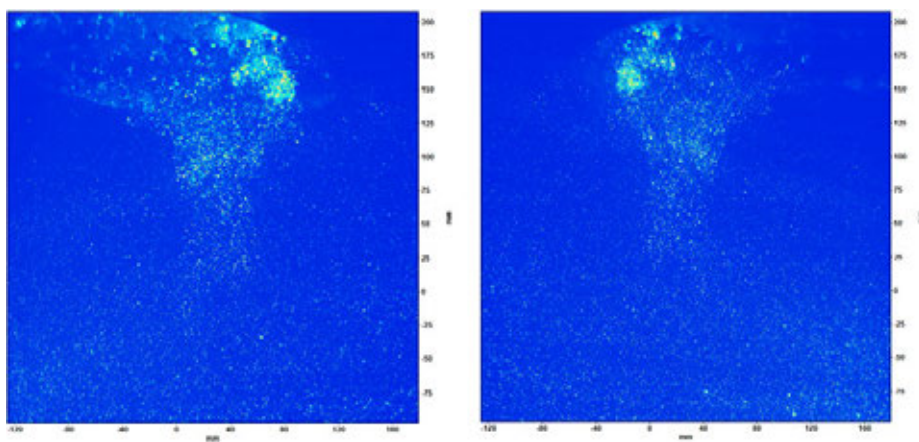
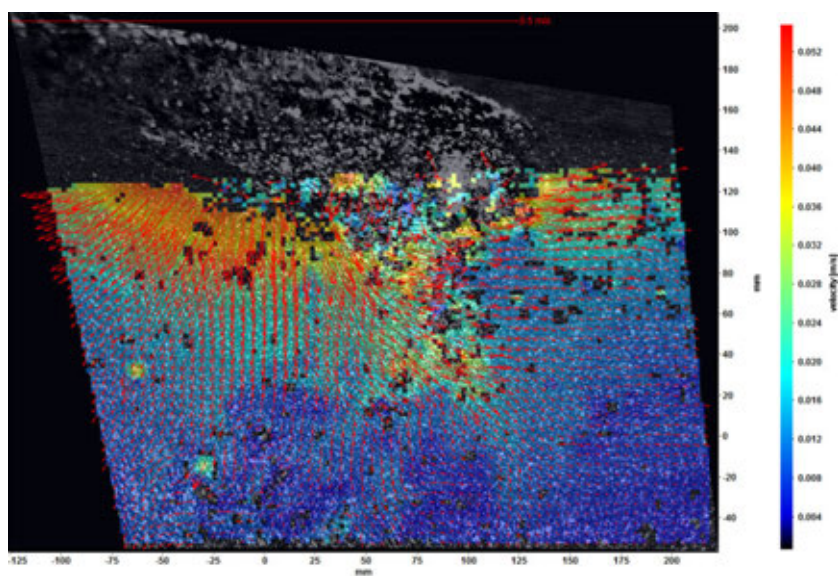**Figure 2.** A background raw image with seeding for camera 1 (left) and 2 (right).

Figure 3. The velocity field of the outflow phase with a background image.
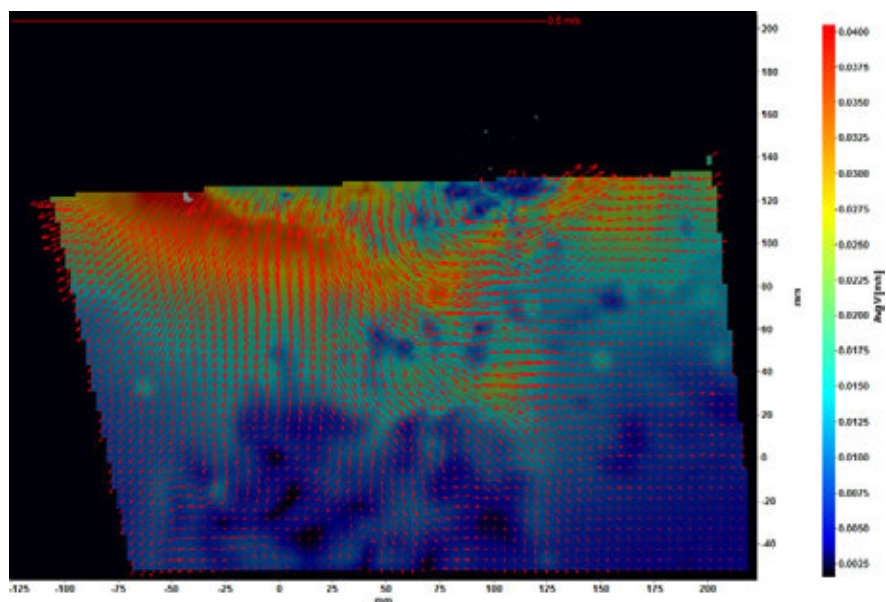
Figure 4. The averaged velocity field of the outflow phase.

Wire Mesh Sensor (WMS)

The applicability of a wire mesh sensor (WMS) and the availability of the components have been studied in respect of the usefulness for different purposes. The most expensive component of the system is the electronics that measures the signals from the wire mesh sensor.

Nuclear safety research unit familiarized with some of the WMS applications in Paul Scherrer Institute (PSI) in Switzerland. The system can be used for measuring various quantities that are directly or indirectly related to electric properties of the substance such as impedance. The wire mesh sensors can also be constructed in such a way that the temperature sensors between the two sets of wires can be used for temperature field measurements.

Based on the survey of the wire mesh sensors, the wire mesh electronics unit was purchased from Teletronic Rossendorf GmbH in 2012. The electronics is capable of simultaneously acquiring the signals of two 128x128 sensors with temporal resolution of 1 ms.

The sensors themselves are not very expensive, and they can be built on site in the laboratory in case they are used at atmospheric pressure. Sensors aimed to be used at higher pressures bring additional requirements for the manufacturing process, naturally.

According to current plans, the use of the system starts in 2013 by applying the wire mesh sensors in a separate simple low pressure test facility where the signal processing and other features can be tested. Later, sensors suitable for more

challenging applications (in high pressure) can be purchased from manufacturers like Helmholz Zentrum Dresden Rossendorf (HZDR), or construct by LUT after more experience has been gained.

Data storage and distribution software

After a successful experiment, the acquired numerical results has to be postprossessed and finally stored safely. Also the distribution of the data has to be controlled. In the CERTA EU project a network of STRESA databases was introduced and the operation was demonstrated. The STRESA database system was developed by JRC Ispra in Italy. In CERTA several research institutes prepared few data sets to be installed in local STRESA servers. The security of the system was specially taken into account. As a result of CERTA project the functionality of STRESA was proved and the system was adopted at LUT as a tool for storing and distributing the experimental data and documents. However, the support for the development of STRESA by JRC was reduced after the hosting of STRESA was moved to JRC Petten. After some years the new Windows based software libraries did not work anymore with all features of STRESA, and new versions of the database were not launched. As the usability of the database was already seen at LUT, a decision to program an own version of the software was made. The new software utilizes the same data formats and has the same functions available as in STRESA. The new database software was named Experiment Data Storage (EDS), Figure 5. In 2012 EDS was opened for internal and external use and both user and administrator manuals were written. In addition to the new software, the hardware in the form of the WWW server was replaced and equipped with an UPS-power feed.

Figure 5. Home page of the EDS database.

Instruments, substitutive components and other devices

This subproject aims at ensuring the operability of the test facilities in all conditions. The process control system used in the PACTEL and PPOOLEX facilities has been installed and coded in a new platform. A license for operating the test facilities using the updated control system has been granted by Inspecta. The operating manual of the control system has been written [3].

Components such as measuring units for the data acquisition systems, pressure and differential pressure transmitters, thermocouples and flow meters have been purchased partly as spare parts for reserve to prepare for component failures, since the delivery times of certain components can be unexpectedly long. Components have also been purchased to avoid the swapping of the devices from one test facility to another. Swapping can be time consuming and there is always a danger to damage the devices. Also devices, that help and make the use of the new laboratory and the installation of the devices into the test facilities safer, have been bought.

Main circulation pumps for the PWR PACTEL facility

This subproject aims at acquiring and installing the main circulation pumps to the PWR PACTEL facility. The pumps will widen the range of possible experiments and help in the heat up process of the facility. They also make it a lot easier to remove non-condensable gases from the facility. After the installation is finished, the pumps will be tested and characterization tests (pressure and heat losses) will be carried out in the PAX project and test reports will be written.

Purchase of the pumps and assorted equipment, such as power feeds, drives, safety automation and mounting pedestals was completed in 2012.

Preparation for the installation of the pumps and the assorted equipment to the PWR PACTEL facility was also done in 2012. The installation plans have been finished. Power feeds have been installed, and the automation system has been upgraded so that the pump controls can be integrated to the system. Pedestals, piping etc. have been designed, and ordered from an outside contractor.

Installation of the pumps is scheduled for 2013.

Conclusions

The goals of the ELAINE project for 2011 and 2012 have been achieved. The quality and the quantity of the measured data have increased remarkably with the commissioning of the PIV system. The first application with the PPOOLEX facility as a part of the commissioning phase of PIV has been successful. Although the utilization of the system has just been started, the potential of the system has been proved. As a logical continuation for the commissioning of the PIV system is the study on wire mesh sensor (WMS) applications. Technical requirements have been defined and the procurement of the measurement system finished. Installation and testing of the WMS is planned for 2013.

To ensure the fluent availability of the experimental and simulation data generated through nuclear safety research at LUTalso in the future new data archiving and distribution software was developed to replace the STRESA database. The Experiment Data Storage (EDS) has been opened for internal and external use.

To take the full advantage of introducing novel measuring techniques, also the traditional control and measuring infrastructure has to be up to date. Thus, the essential replacement components have to be available on-site. Components and devices have been replaced with newer ones to meet the modern standards, and spare components have been bought. Long delivery times or even the discontinuance of manufacturing the important components may cause unexpected delays in research projects. Moving the instruments back and forth between the test facilities is not effective.

To widen the range of PWR PACTEL experiments the main circulation pumps were purchased in 2012. The installation of the pumps is scheduled for 2013.

References

1. National Nuclear Power Plant Safety Research 2011–2014. SAFIR2014 Framework Plan. Publications of the ministry of Employment and the Economy, Energy and climate, 50/2010.

2. Pyy, L. Utilization of particle image velocimetry in PPOOLEX condensation experiments. Master's thesis. Lappeenranta University of Technology, 2012.

3. Kotro, E. Pactel-laitteiston prosessiohjausjärjestelmän käyttöohje, Report ELAINE 2/2011, Lappeenranta University of Technology, 2012.

10.2 Renewal of hot-cell infrastructure (REHOT)

Irina Aho-Mantila, Ulla Ehrnstén, Tarja Jäppinen, Wade Karlsen, Petteri Lappalainen, Jari Lydman, Tuomo Lyytikäinen, Marketta Mattila, Marko Paasila, Aki Toivonen, Seppo Tähtinen, Matti Valo

VTT Technical Research Centre of Finland
Tekniikantie 2, P.O. Box 1000, FI-02044 Espoo

Background

Many critical issues concerning plant life management for operating nuclear power plants are related to materials. Present plans for concurrent lifetime extension, power upgrading, and construction of new plants that may employ new materials in new conditions will require investigating and solving problems related to components and structural integrity. Degradation related to the ageing of structures and components is an important aspect of power plant safety, and ageing management requires activities related to the utilization, inspection, surveillance, testing, examination, and degradation mitigation of materials. This drives the on-going effort to better understand the effects of the reactor environment and operating conditions on the strength and integrity of components and structures. With particular regard to materials that have become activated or contaminated by irradiation-related processes, the ALARA principle requires the utilization of hot-cell facilities for conducting fracture mechanical and mechanical testing, metallography, analytical microscopy, autoclave testing, etc. as well as the associated material handling and specimen fabrication and preparation facilities for those techniques.

A national research capability is a basic requirement of the safe use of nuclear power in Finland, and significantly contributes to making the exploitation of nuclear

energy economical and efficient. A key component of this is hot-cell facilities for the handling, testing and examination of activated nuclear power plant structural materials. However, the current domestic research infrastructure requires renewal.

VTT has been hosting the national hot laboratory infrastructure since it was first constructed and equipped in the 1970's. However, the current hot labs are neither technically up to date nor adequate to all present research requirements, in addition to being housed in a building that is being renovated by its new owners. As such, during 2009–2010 VTT and Senaatti-kiinteistöt (actual building owner) carried out the conceptual design and the first draft design phases for the construction of a new building, to bring together all the nuclear research areas at VTT. In 2011 Senaatti-kiinteistöt subcontracted ISS Proko Oy to additionally make a survey of alternative strategies to achieve the needed level of infrastructure renewal. Several options were evaluated, but deemed to offer little advantage over the original proposal for a new facility housing hot laboratories and office space for about 150 persons. In November 2011 VTT made the decision to go forward with the effort to have such a facility built, by agreeing to rent the facility. The facility will be called the Centre for Nuclear Safety (CNS). In August 2012 the second draft design phase of the CNS was launched, with A-Insinöörit as the primary construction supervisor. With its conclusion in January 2013, Senaatti-kiinteistöt is poised to make their final decision regarding whether or not to go forward with having the facility built for VTT to rent.

Profile of the new Centre for Nuclear Safety

In its current rendition the CNS is comprised of a 3,300 m^2 office wing and a 2,360 m^2 laboratory wing. The office wing includes a ground-level conference center, above which are three floors of modern, flexible office space for 150 people. The office wing is intended to serve nuclear sector researchers in areas such as computerized fluid dynamics, process modelling (APROS), fusion plasma computations, severe accidents, core-computations, waste-management and safety assessments, as well as the staff working in the laboratory wing. The laboratory wing includes a basement level and two floors of laboratory space. The laboratory space is arranged around the main high-bay, which houses the hot-cells proper, while the basement is primarily intended for storage and handling of radioactive materials and waste. The laboratory activities include radiochemistry, nuclear waste, dosimetry, failure analysis as well as mechanical and microstructural characterisation of structural materials.

Figure 1. Architect's rendition of the Centre for Nuclear Safety (SARC Arkkitehti-toimisto).

Hot-laboratory facilities

The hot-laboratory facilities of the laboratory wing are arranged in three main zones, according to the level and nature of radioactivity intended to be handled, which dictates the safety features required in the facility. The C-laboratory has the least requirements, and is dedicated primarily to radiochemistry and nuclear waste experiments. The B-laboratory has a moderate level of requirements, and in addition to radiochemistry and nuclear waste, it includes an iodine laboratory and microscopy of structural materials of low activity. The A-laboratory includes the hot-cell proper, and is primarily dedicated to the testing and examination of irradiated reactor structural materials, including reactor pressure vessel steel, stainless steel and nickel base internals materials, and fuel cladding. Irradiated nuclear fuel itself is NOT researched in the facilities. Besides the laboratories, the transport, handling and storage of radioactive materials is a key function of the hot-laboratory facilities.

The REHOT project

The primary objective of the four year REHOT project is to plan and execute the hot-cell portion of the infrastructure renewal, including the planning and making of critical equipment investments for the hot-cell facility, and training of the technical personnel that will be staffing the facility. The project is divided into three closely-related subprojects:

Subproject 1 is dedicated to the hot-cell design and construction project, which will define and guide the technical construction of the hot laboratory portion of the new building in tandem with the engineering design of the CNS. Central to this are the shielding cells themselves, to be constructed of suitable materials and equipped with appropriated manipulators and devices to provide protection against human radiation exposure in line with the ALARA principle, designed utilizing an external engineering design consultant. This subproject includes the collecting and describing of procedures to be employed in conducting specific tests and processes within the cells remotely by utilizing manipulators, jigs, tools and other in-cell devices.

Subproject 2 focuses on procurement of research equipment to be installed in the hot-cells, and includes designing the investment schedule and installation parameters in conjunction with the facility construction, and executing the competitive bidding process for each item. The equipment is of three main categories: those that can be directly moved from existing facilities with minimal adaptation, those that can be moved from existing facilities with some modifications necessary to meet the ALARA principle, and finally, new procurements. This sub-project also includes the training needed for the new equipment.

Subproject 3 is to assure continuous exchange of information between the VTT project team and the engineering design team carrying out the design and construction work of the building itself, as it pertains to the aspects involving the interface between the building systems and the hot laboratory and hot-cells facilities (structural, electrical, ventilation, fire protection, security, etc.)

A-laboratory and hot-cell facilities

The main focus of the REHOT project is the A-laboratory and the hot-cell facilities. The facilities must enable a wide variety of research-related activities proper, as well as provide the supporting handling, storage and maintenance infrastructure. A schematic example of a hot-cell facility, with manipulator equipped shielded cells, is shown in Figure 2. Many of the preparation, test and characterization activities must take place inside the shielded cells. A number of the activities included in the CNS hot-cells is briefly described in the following sections.
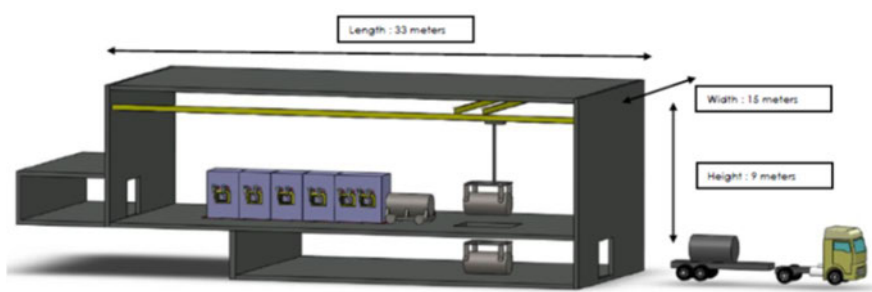

Figure 2. Schematic example of a row of shielding cells in a high-bay. (ROBATEL)

Active material receiving and shipping

Active materials are shipped from elsewhere, and are generally returned to the customer following the testing and examination activities. A person receiving an active shipment has to always have an operative safety authorization. Active material is shipped in different type of shielded shipping casks in different kind of vehicles. Maximum weight for a cask is about 10 tons. Before unloading and storage, a surface contamination measurement is done for the shipment casks and racks. With this measurement, cleanliness is assured and spreading of contamination into the hot-lab is prevented.

Casks can be quite heavy. The manipulation of the casks for moving, tipping up-right, and in the case of large casks, removal of lids can be done using mechanical devices. Big and heavy A-type shipping casks can be lifted from the shipping vehicle on the loading dock and further into the A-laboratory with e.g., a big fork-lift truck, a lorry having strong hoist or with a bridge crane type structure. Casks whose max weight is about 1 000 kg can be moved and lifted by electrical truck, pump cart or by other auxiliary devices.

There is a small chance that casks bearing radioactive materials can become contaminated due to corrosion deposits flaking off, activated liquid residues rubbing off etc. It is a requirement for shipping that the casks first be decontaminated before returning or reusing. For this purpose a means for decontaminating them is required. Alternatives include water washing, chemical washing, wiping, etc.

Nondestructive examination (NDE)

One of the needs for NDE or nondestructive testing (NDT) is finding the exact location of a defect before crack evaluation. Another application for NDE is to estimate the defect size or cladding layer thickness without breaking the specimen.

The place for the NDE is e.g. right after capsule opening. Considering the restrictions in the hot-cell the most suitable set of NDE methods are eddy current inspection (ET) for surface cracks and layer thickness measurements and ultrasonic inspections (UT) for defects inside the inspected material.

NDE in a hot-cell environment is most commonly considered as eddy current, x-ray, gamma activity and visual inspection by cameras. The NDE methods used previously at VTT for irradiated material testing have been ultrasonic and penetrant testing. Also some eddy current testing has been performed for bolts using a special probe with a thread.

NDT in the hot-cell environment has special restrictions considering the probe handling with telemanipulators. The grib of the mechanical arm on a small probe is not firm. To have stable measurement, the probe needs to be attached in a special cassette that is designed for the application. The tests can be performed by moving either the specimen or the probe. A more stable set up might be reached by anchoring the probe and moving the specimen on a test bench.

Test specimen preparation

The hot-cells can be used for a number of different kinds of mechanical tests, including tensile, impact, bending, and compact-tension (CT), and test specimens may need to be fabricated from delivered materials. For metallographic examinations, resizing procedures may be required for reducing the volume of radioactivity and/or fitting into a SEM, enabling mounting in plastic for cross-sections, or for subsequent TEM specimen fabrication. In general these procedures require a capability for sawing and machining.

Sawing methods

Dry sawing methods include band saws and circular saws. Conventional toothed band saws are useful for larger pieces of relatively soft materials, but produce chips that must be collected. The need for such a saw would primarily be with respect to large blocks of RPV material. Wire mechanical saws can utilize diamond-bearing wires for precision cutting of hard materials, but are generally limited to small pieces, and the wires are susceptible to breaking. Circular saws can utilize diamond-bearing blades to cut hard materials, and while the blades are more robust than wires, they may be susceptible to heating up, which limits the feed rates in the absence of a coolant. Wet mechanical sawing methods include all of the above methods, but with the addition of a liquid coolant/lubricant to produce more efficient cutting with less impact on the microstructure adjacent to the cut. Naturally the involvement of water or cutting oil presents the disadvantage of producing more contaminated waste. In addition, abrasive cut-off saws enable high-speed, coarse cutting for high throughput, but are dependent on a high degree of liquid cooling that can be quite messy, even when enclosed.

Machining methods

Test specimens are often prepared from materials supplied. Mechanical test-bars generally have simple geometries, with either round or rectangular cross-sections, and they are often symmetrical along their axis. The simplest are impact or bending specimens, which generally have straight, parallel faces on all sides, but require a V-notch to be produced in a manner that retains the original material microstructure at the apex of the notch. Flat and square tensile test bars generally have straight, parallel lines, but require an ample radius at the transition between the test gauge region and the grip region. The grips themselves may require holes for retaining pins, or other specific geometries to enable securing them in the test machine grips. Round bars for SSRT and CL tests may have particularly complex geometries along their axis. In addition to the gauge region and a transition radius from the gauge to the grip region, there may be specific features for engaging extensometers, DC potential drop devices, etc. The most demanding specimens may be CT specimens, which may have flat, parallel sides, but also have specific

features such as a notch, side-grooves, features to engage mouth-opening displacement measurement devices, etc.

Electric discharge machining (EDM)

An EDM wire saw can not only saw, but can produce complex 2-D geometries by computerized control of the feeding, enabling some "pre-machining" steps to be carried out. An EDM is used for separating specimen from bigger blocks of material, preparing specimen for testing/inspection and reconstructing tested specimen for retesting. An EDM is capable of doing almost all of the metal machining of a hot-cell. However EDM machining takes a lot of time for big pieces, and historically being the bottleneck of specimen reconstruction, it should be supplemented with a machine more suitable for rough cutting. EDMs are also large equipment that require a significant amount of liquid (water) for operation, and so can be quite messy (contaminated).

Supporting the reconstitution method

To enable more efficient use of the limited amount of irradiated surveillance material available, the reconstitution method has been developed. In the method, the two halves of a broken Charpy test specimen are reconstituted into two new specimens. To do this, the fracture surfaces are first cut off, then stubs of non-irradiated material are welded onto each end of the remaining pieces of irradiated test material, after which a new groove is machined and the new specimen can be tested.

   Utilization of the reconstitution method is essential in the new hot laboratory, but also requires specific facilities. In addition to an EDM, a key piece of equipment is an electron beam welder (EBW), which requires a large power-supply that can be external to the EBW head itself. In the case of space limitations, the power supply can be located at a short distance from the rest of the instrument, for example elevated on a dedicated support structure above the welder.

10.2.1 Mechanical testing

It is necessary to be able to carry out several different kinds of mechanical tests on irradiated RPV and internals materials. Equipment for mechanical testing include servohydraulic testing machines, servomechanical testing machines, instrumented Charpy-V impact hammer, small instrumented impact hammer, and bellows-operated devices. Mechanical testing may be done in room temperature air, but also at reduced or elevated temperatures, and in particular liquid environments (using autoclaves). In general, if the specimen activity level is high, special precautions are required, so testing must be done in a shielded facility. Large specimens are normally needed only for valid crack arrest testing, so whenever possible, smaller specimens are used.

Impact testing

Impact testing is an essential part of RPV surveillance programs. The tests made by impact hammer are Charpy-V and dynamic FT. Testing starts with the measurements of dimensions. The dimensions should be measured in a separate cell under a microscope or a camera using manipulators. Before the impacts, the hammer is checked and two test specimens are struck. Equipment to be controlled (impact angle display unit, feed voltage of load strain gauge bridge, preamplifier of strain gauge bridge) should be outside the cell. After the impact test, lateral expansion is measured and the fracture surface is photographed. The specimens which are struck at higher temperatures do not necessarily break through, so then they are cooled in liquid nitrogen and then broken the rest of the way. One of the problems of the impact hammer is that specimen halves can fly in any direction after the test. First it can be challenging to detect the halves, and second they should somehow be recovered.

Fracture mechanics testing

Fracture mechanics testing utilizes pre-cracked specimens to determine key material parameters relevant to the fracture mechanics approach to structural integrity. These include parameters such as K-values. Tests are conducted using a servohydraulic or servomechanical test machine. An important test for RPV materials is the T_0 test, in which the Master curve is generated for a particular material through a series of bending tests of pre-cracked Charpy type specimens at different temperatures. Fracture mechanics testing specimen must be centralised according to the loading tools. In this, magnets, wedges, jigs and other means are necessary. Often a clip measuring crack opening must be assembled to the specimen. Calibration of clip gauge and LVDT occurs before every series, and currently often requires access by hand. Load cell calibration is done less frequently, but still once per year.

Tensile testing

Standard tensile testing of RPV materials is carried out to determine basic material properties (strength, elongation and reduction in area). Tensile testing at room temperature requires using a servohydraulic or servomechanical test machine. For testing at elevated temperature, a test chamber is also required. Routine tensile testing is often made using small flat specimens. Elongation is measured by two symmetrically located, freely hanging extensometers from the ends of the specimen. It is also possible that the elongation must be measured from the gauge length.

Cyclic loading

An important material parameter particularly for internals materials is that of fatigue resistance. Fracture mechanics tests also require a pre-cracked specimen, which is generally made by pre-fatiguing. The challenges presented by tensile testing in a hot-cell environment are similar for fatigue testing, but generally the relatively low deformation and long duration of fatigue tests makes accurate extension measurement a key procedure.

10.2.1.1 Hardness testing

Hardness is a material mechanical property, describing the ability to resist deformation. Hardness is measured by several different ways, of which the most important are Rockwell, Brinell and Vickers hardness. Hardness measurement is used e.g. to determine if a material fulfils the requirements, or to determine effects of different heat treatments, and of irradiation. The equipment is calibrated annually and checked before each measurement work and after all repairs and other changes. The equipment must be protected against impacts and vibrations during testing. The specimen is not allowed to move during the measurement and sometimes an anchorage is necessary.

Hardness measurement is normally made for a surface which is smooth and flat, without oxide scales and other substances and especially clean of lubricants. The surface quality must be good enough, in order to be able to measure the indent diagonals accurately. Surface is prepared so that the surface hardness is changed as little as possible e.g. due to heating or cold deformation. Polishing suitable for the material in question is recommended. For rounded surfaces, standard SFS-EN ISO 6507-1 Appendix B gives correction coefficients for hardness calculation.

Bellows devices for fuel cladding tests

During normal and incidental operation of LWRs, fission gas release and Pellet-Cladding Interaction combine to impose to the fuel cladding a non-monotonic, multi-axial, thermo-mechanical loading sequence. The continuous push for better agility and for higher burn-up operation without reduction of safety margins drives the research for higher performance clad materials, and hence the need for reliable experimental data on their behaviour under irradiation, when subjected to a multi-axial stress. Indeed, the modelling of LWR fuel performance is complicated by the fact that zirconium alloys of industrial interest are strongly anisotropic, not only due to their hexagonal crystal structure, but also due to the texture induced by the manufacturing process.

By biaxial stress control on a tubular cladding sample, an axial stress and a circumferential ("hoop") stress can be applied to the sample in an independent way. Full-control of stress and bi-axiality is performed by three independent high-

pressure gas circuits, e.g., one to pressurize the sample and two to pressurize the bellows of a push-pull system able to generate a positive or negative axial stress for the sample. Specification for this kind of system is the ability to cover a bi-axiality ratio a between 0 and 1.

The experimental facility for controlled bi-axial stress experiments is comprised of a pressurised gas production and gas circuit based on a gas compressor, pressure control of loading bellows based on servo controlled by-pass circuit, a sample holder including axial loading bellows, pressurized specimen and both axial and diameter strain measurement devices, (either LVDT or laser based), and a furnace able to accommodate the sample holder at temperatures up to about 600 to 700°C in vacuum or a shielding gas. For implementation in a hot-cell, the pressure control circuit can be outside the shielding and only the furnace and sample holder is inside the shielding chamber.

Environmental testing

Particularly for internals materials, it is important to also test the materials' susceptibility to environmental attack, particularly in conjunction with a load (i.e. stress corrosion cracking susceptibility). Testing in simulated NPP environments (generation 1–3 light water reactors) involves high temperature water and a pressurized system, which is achieved by the use of autoclaves. The desired test environment in the autoclave is maintained with water recirculation systems described below. Typically the test temperature is between $250^{o}C$ and $360^{o}C$. At the highest operating temperature the autoclave pressure is > 20 MPa. The recirculation water is either purified BWR water or PWR water with boric acid and lithium hydroxide (western NPPs) or boric acid with potassium hydroxide (VVER plants). The recirculation water can also contain small amounts of desired impurities.

The hot-cell must contain manipulators for specimen handling and installation into the autoclaves. For the same reason, closure of the autoclaves must be possible from a distance. The closure may be done using an electric mechanism for raising and lowering the autoclave lid (or the autoclave itself). Hermetic sealing of the lid can be done using bolt tightening combined with a hydraulic wrench. Another possibility is to use a bayonet mount type sealing mechanism.

Control of specific simulated NPP environments is achieved through a recirculation system. Such recirculation systems require the use of a large amount of piping, which must withstand high pressure use and must not leak. Nonetheless, the facilities must include back-up features in case failures occur. The recirculation loop(s) can be outside of the hot-cell that contains the autoclave(s). However, in some operating situations the circulated water may contain small amounts of dissolved radioactive elements. These dissolved elements are filtered with de-ionizers. Because of this feature, the loop(s) should be located in a shielded place. The role of the shielding is to prevent the spreading of contamination in case of leaks in the piping so a light shielding is sufficient.

The easiest way to realise the installation of the specimen into the autoclave is to use open specimen loading grips in which the specimen can be inserted with the manipulator. However, if the specimen must be instrumented, the instrumentation is easier to be done in a separate shielded working bench. After instrumentation, the specimen should be installed in a cassette, which can be inserted into the loading grips of the autoclave. The shielded bench can also be used for handling (e.g. assembly and disassembly) of contaminated internal components of the materials testing autoclaves.

Metallographic characterization of materials

Dimension measurement

An important aspect of various studies on both RPV and internals materials included precise measurement of dimensions. This includes the precise measurement of test bars dimensions (gauge lengths, gauge widths/diameters both before and after tests), of fracture surface partitioning by crack path (i.e. intergranular, transgranular and ductile portions), crack lengths, etc. Geometrical measures are traditionally done by hand-held tools (micrometres, calipers), but for irradiated materials it can be more desirable to utilize remote methods, which typically include optical methods in conjunction with motorized x-y stages. Particularly with more radioactive specimens, remote optical dimensioning is desirable. Verification is important.

Preparation of metallographic specimens

In order to better understand the contribution of a materials microstructure to its performance or failure, metallographic cross-sections must be made. A suitably-sized specimen for metallography is on the order of no more than a few centimeters on a side, and the region of interest should be as flat as possible. Thus, prior to specimen mounting a bigger piece or a rounded piece must be cut to the appropriate geometry for mounting. The cut specimen is washed carefully in acetone and dried with hot-air drier. If the surface of the specimen is oxidized, oxide removal liquid can be used, followed by washing with alcohol and drying.

To assure a flat surface for examination, to protect a brittle or cladded material and to produce good sharp edge areas, the piece must first be embedded in an appropriate mounting medium. The mounted specimen is then subjected to a series of every-finer grinding and polishing steps to produce a mirror-like surface finish. Numerous types of manual, semi-automated and automatic equipment are available with a variety of different grinding and polishing solutions, but generally all utilize a motor-driven rotating plate bearing the grinding or polishing media, and in semi- or fully-automated systems, a motorized holder that moves one or several mounts with a planetary motion across the grinding media. Polishing generally

uses different kinds of soft fabric textures bearing diamond paste or abrasive slurries, or else finer versions of the embedded particles. A key issue with regards to grinding and polishing is that both are material removal processes, and so by definition they produce debris that, in the case of radioactive specimens, must be contained, recovered, and placed with the other waste for shipping back to the source.

After polishing, the specimen is etched for microscopic examinations. In etching, the details of the microstructure (e.g. grain and phase boundaries) are revealed. In etching, the specimen is dipped in etching media, washed in ethanol and dried by hot-air dryer. General etching media are based on e.g. HNO_3, HCl and FeCl. The use of HF should be avoided; it is a toxic waste. In electrolytic etching, one could use less strong acids than in the immersion etching. The specimen should be stored in air tight place in order to keep it unchanged. Suitable storage place would be e.g. vacuum desiccator, in which there are water-free (orange) silica gel crystals on the bottom.

Optical microscopy and microhardness testing

The microscopic facilities include optical, inverted and stereo microscopes, motorized objective table, objective revolver, digital camera and recording and analyzing programs. With new equipment there is also a possibility to cover macro and microhardness measurement with one equipment. In the laboratory facilities there are electron microscopes TEM, SEM and optical microscopes. With optical and SEM, whole test specimen halves are examined. Optical microscopes are small and they can be located in a lead-shielded chamber. It is desirable to locate SEM and TEM instruments in their own rooms with appropriate isolation from vibration and electromagnetic interference.

Scanning Electron Microscopy (SEM) and microanalysis

The SEM-specimens foreseen to be subject for investigations in the CNS include a wide range, including fracture surfaces of fracture mechanical specimens (measurement of crack growth and identification of fracture modes), fracture surfaces of cracks from failure cases (identification of initiation points, factors affecting initiation and crack growth, determination of fracture modes, determination of corrosion products, determination of the surface quality etc.), microstructural investigations of cross-sections (determination of the general features of the microstructure, identification of secondary phases and determination of crack path within the microstructure), as well as other kinds of specimens.

A hot-cell SEM should be equipped with an energy dispersive x-ray analyzer (EDS), which is essential particularly for failure analyses, but also when identifying microstructural features at initiation sites of, e.g. RPV materials. In addition to EDS, electron back-scattered detectors (EBSD) enables evaluation of anisotropy, local residual strains, etc.

Both the SEM operator and other people must be radiologically protected. Additionally the SEM requires maintenance at least once a year, which require access to the equipment and a low level of equipment contamination. These requirements can be fulfilled by putting the SEM into a hot-cell, a glove box, adapting local shielding of the specimen in the SEM, adapting local shielding between the SEM-chamber and the operator and increasing the distance between the SEM-chamber and the operator.

Transmission Electron Microscopy (TEM) and microanalysis

Transmission electron microscopy (TEM) and microanalysis is a powerful microstructural characterization technique particularly for irradiated materials, because many of the effects of irradiation on the microstructure, microchemistry and material deformation behavior are manifested on a scale requiring very high magnification observations. Besides the unique imaging possible with a transmitted electron beam, TEM enables local crystallographic information to be extracted, and when equipped with an analyzer, measurement of elemental distributions on a fine scale. A well-tuned TEM instrument can achieve atomic level resolution in imaging, and microchemistry analysis to about 1 nm resolution. Typical features of interest in a TEM investigation of irradiated structural materials include dislocation distributions, radiation induced stacking-fault tetrahedra, black spot and dislocation loop populations, radiation induced precipitate populations, and in deformed material, the presence of cleared channels and deformation-induced phase transformations such as austenite to martensite. Other topics of interest include aerosols of radioactive particles, scrapings of corrosion or crud products, and of course oxide layers, dissimilar metal weld fusion lines, and stress corrosion cracks, but the range of potential topics is not limited.

TEM examination of irradiated materials does not differ markedly from examination of non-irradiated materials, with the exception of precautions necessary when preparing specimens, storing and transporting them, and special considerations when conducting energy dispersive x-ray spectroscopy (EDS) analyses. In the case of TEM specimen preparation, most of the challenges are common to those also presented by metallographic specimen preparation, i.e. delicate handling of radioactive materials is required, and fine solid radioactive waste produced from cutting and grinding stages must be captured and isolated, while radioactive chemical waste must also be handled. Specimen storage and transport must naturally be done in a methodical manner that maintains the inventory, and retains appropriate identification of the parent material, in particular with cognizance of its radioactivity. With regards to EDS analyses, on the other hand, it is the interference with the detector by the specimen's self-irradiation that is a problem.

Waste management, sorting and packaging

Good and operative specimen storage is necessary in contract work. Often valuable research material is stored in specimen storage for several years for additional examinations and tests. Nonetheless both specimens and waste are ultimately only stored temporarily, because VTT has no final repository resource of its own, and so must return everything to the source. The principle feature is proper indentification and tracking of the materials throughout their lifecycle, from their reception through to their return.

Active material, which is not any more used as research material, is classified as waste. Waste is sorted with activity measurement to non-active and active waste. According to the activity waste is classified as low, mid or high active waste. Waste in typically either solid or liquid. Active waste is always sent back to the customer. It is therefore necessary to sort and separate waste as properly as possible.

Solid waste

Non-active and low active waste is typically waste produced by normal laboratory work, cleaning, and protective clothing (e.g. cleaning cloths, gloves, paper wipes). Solid waste is sorted immediately after use by measuring the activity level and putting waste according to the measurement either into non-active or low active waste bins. Waste is typically packaged into 200 litre barrels, and can be compressed for better package density. According to the transport rules, the surface activity is a limited to 2 msv/h. If the activity is below 100 kBq/kg and total activity below 1 GBq, waste can go to a dump or be burned. Low activity waste exceeding this level is always shipped back to the customer.

Moderately active waste originates mainly from radiated pressure vessel material or samples taken from failed primary circuit components. It includes active particles in the cutting or grinding liquids used in the mechanical machining, small active pieces formed in the cutting (fracture surfaces, unusable pieces), and debris formed in wire and band sawing and in different grinding and polishing processes. It also includes the acid residues from EDM sawing fluid, dissolved ions from specimen preparation and solvents and washing and rinsing liquids. Mechanical filters / filter fabrics (wire and band saws, grinding machine) and ion exchange resins (autoclaves) also fall into this category. Highly active waste mainly originates from stainless steel radiation capsules, their parts and machining waste, all reactor internal materials and all materials activated in a reactor core. These waste forms can be isolated by various separation processes, and then packaged for shipping either in normal or lined 200 l barrels, or if necessary in a transport cask, such that the shipping package has a surface activity of less than the 2 msv/h limit. Moderately and highly active waste is always shipped back to the customer.

Liquid wastes containing active species

Liquids may have activated solids suspended in them, or ions dissolved in them. Mechanical filtering enables impurities or materials in suspension to be separated from the liquid. If active solid material is magnetic, solid particles can be removed from the liquid by using magnetism. Alternatively, a centrifuge can be used to separate the suspended species based on its mass. Once solids are removed, the non-active liquid can be vaporized either at room temperature in e.g. a fume hood, or by heating or even distilling. In these cases active residues are generally still left, but can then be placed with the other solid waste. Alternatively, with selective ion exchange, it is possible to remove only certain substances from active water. Good selectivity for certain ions makes it possible to use the ion exchange material effectively and economically.

Title	**SAFIR2014** **The Finnish Research Programme on Nuclear Power Plant Safety 2011–2014** Interim Report
Author(s)	Kaisa Simola (ed.)
Abstract	The Finnish Nuclear Power Plant Safety Research Programme 2011–2014, SAFIR2014, is a 4-year publicly funded national technical and scientific research programme on the safety of nuclear power plants. The programme is funded by the State Nuclear Waste Management Fund (VYR), as well as other key organisations operating in the area of nuclear energy. The programme provides the necessary conditions for retaining knowledge needed for ensuring the continuance of safe use of nuclear power, for developing new know-how and for participation in international co-operation. The SAFIR2014 Steering Group, responsible of the strategic alignements of the programme, consists of representatives of the Finnish Nuclear Safety Authority (STUK), Ministry of Employment and the Economy (MEE), Technical Research Centre of Finland (VTT), Teollisuuden Voima Oyj (TVO), Fortum Power and Heat Oy (Fortum), Fennovoima Oy, Lappeenranta University of Technology (LUT), Aalto University (Aalto), Finnish Funding Agency for Technology and Innovation (Tekes), Finnish Institution of Occupational Health (TTL) and the Swedish Radiation Safety Authority (SSM). The research programme is divided into nine areas: Man, organisation and society, Automation and control room, Fuel research and reactor analysis, Thermal hydraulics, Severe accidents, Structural safety of reactor circuits, Construction safety, Probabilistic risk analysis (PRA), and Development of research infrastructure. A reference group is assigned to each of these areas to respond for the strategic planning and to supervise the projects in its respective field. Research projects are selected annually based on a public call for proposals. Most of the projects are planned for the entire duration of the programme, but there can also be shorter one- or two-year projects. The annual volume of the SAFIR2014 programme in 2011–2012 has been 9,5–9,9 M€. Main funding organisations were the State Nuclear Waste Management Fund (VYR) with over 5 M€ and VTT with nearly 3 M€ annually. In 2011 research was carried out in 38 projects, and in 2012 the number of research projects was 42. The research in SAFIR2014 has been carried out primarily by VTT. Other research organisations involved in research activites are Lappeenranta University of Technology, Aalto University, Finnish Institution of Occupational Health, Finnish Meteorological Institute, Finnish Software Measurement Association FiSMA, Fortumn Power and Heat Oy, and Helsinki University. In addition, some subcontractors have contributed to the work in some projects. This report gives an overview of the SAFIR2014 programme and a summary of the scientific and technical results of the research activities in 2011–2012.
ISBN, ISSN	
Date	February 2013
Language	English
Pages	447 p.
Name of the project	The Finnish Nuclear Power Plant Safety Research Programme 2011–2014, SAFIR2014
Commissioned by	MEE
Keywords	nuclear safety, safety management, nuclear power plants, human factors, safety culture, automation systems, control room, nuclear fuels, reactor physics, core transient analysis, thermal hydraulics, modelling, severe accidents, structural safety, construction safety, risk assessment, research infrastructure
Publisher	

SAFIR2014
The Finnish Research Programme on Nuclear Power Plant Safety 2011–2014
Interim Report

The Finnish Nuclear Power Plant Safety Research Programme 2011–2014, SAFIR2014, is a 4-year publicly funded national technical and scientific research programme on the safety of nuclear power plants. The programme provides the necessary conditions for retaining knowledge needed for ensuring the continuance of safe use of nuclear power, for developing new know-how and for participation in international co-operation. More than half of the research programme funding is secured by a separate reserve of the State Waste Management Fund (VYR) which consists of annual fees collected from Finnish nuclear facility operators. The second major funding organisation is VTT with a share of nearly 30 % of the programme volume.

The research programme is divided into nine areas: Man, organisation and society, Automation and control room, Fuel research and reactor analysis, Thermal hydraulics, Severe accidents, Structural safety of reactor circuits, Construction safety, Probabilistic risk analysis (PRA), and Development of research infrastructure.

Research projects are selected annually based on a public call for proposals. The annual volume of the SAFIR2014 programme in 2011–2012 has been 9,5–9,9 M. In 2011 research was carried out in 38 projects, and in 2012 the number of research projects was 42.

The research in SAFIR2014 has been carried out primarily by VTT. Other research organisations involved in research activities are Lappeenranta University of Technology, Aalto University, Finnish Institute of Occupational Health, Finnish Meteorological Institute, Finnish Software Measurement Association FiSMA, Fortum Power and Heat Oy, and Helsinki University. In addition, some subcontractors have contributed to the work in some projects.

This report gives an overview of the SAFIR2014 programme and a summary of the scientific and technical results of the research activities in 2011–2012.